ORDOVICIAN VOLCANISM AND MINERALIZATION IN THE WILD BIGHT GROUP, CENTRAL NEWFOUNDLAND: A GEOLOGICAL, PETROLOGICAL, GEOCHEMICAL AND ISOTOPIC STUDY

HAROLD SCOTT SWINDEN

ORDOVICIAN VOLCANISM AND MINERALIZATION IN THE WILD BIGHT GROUP,
CENTRAL NEWFOUNDLAND: A GEOLOGICAL, PETROLOGICAL,
GEOCHEMICAL AND ISOTOPIC STUDY

BY

© Harold Scott Swinden, B.Sc. (Hons.), M.Sc.

A thesis submitted to the School of Graduate

Studies in partial fulfillment of the

requirements for the degree of

Doctor of Philosophy

Department of Earth Sciences

Memorial University of Newfoundland

St. John's, Newfoundland

October, 1987

ABSTRACT

The Wild Bight Group, part of the Newfoundland Dunnage Zone or Central Mobile Belt, is a thick (probably more than 8 km.) sequence of dominantly epiclastic (~75%) and lesser volcanic (~25%) rocks which outcrops in and to the south of central Notre Dame Bay. The base of the group is not exposed. It passes conformably upward into fossiliferous shale with a Caradocian (Middle Ordovician) graptolite fauna. On this basis, it is considered as Early to Middle Ordovician in age.

Volcanic rocks occur throughout the stratigraphic section of the Wild Bight Group. Eleven separate volcanic sequences are identified and sampled, most of which comprise dominantly or wholly mafic pillow lava. Less commonly, massive basalt or pillow breccia and associated mafic pyroclastic rocks are the dominant lithology. Felsic volcanic rocks occur in five of these sequences and volcanogenic sulphide deposits or prospects in four of them. The entire assemblage is intruded by fine to medium grained mafic sills and, less commonly, dykes, which are interpreted on field and geochemical evidence to be subvolcanic.

The mafic volcanic rocks exhibit a greenschist facies metamorphic assemblage of chlorite - albite - quartz - epidote ± (actinolite, sphene, magnetite and calcite). The only primary mineral remaining is clinopyroxene. Comparison of secondary mineral chemistry with ancient and modern oceanic rocks and with experimental results are consistent with metamorphism at temperatures in the range 200° C to 280° C and low water / rock ratios. The local presence of secondary amphibole is interpreted to reflect slightly higher temperatures.

Major and trace element whole rock analyses of volcanic and subvolcanic rocks, as well as clinopyroxene mineral chemistry, reveal a complex geochemical association. Two broad paleotectonic environments can be identified using high field strength elements; volcanic rocks in the lower and middle parts of the group have a clear island arc geochemical signature (negative Ta and Nb and positive Th with respect to La on a chondrite-normalized basis) whereas those in the upper parts of the group generally do not. However, basalts of both affinities occur together

ii

In one sequence at the top of the group, suggesting that magmatism of island arc and non-arc affinity overlapped in time.

Within these two environments, further variations can be recognized. Rocks with an island arc geochemical signature include both LREE-depleted and LREE-enriched island arc tholeiites as well as a group of very incompatible element-depleted tholeiites which are interpreted to represent partial melting of refractory sources. Rocks lacking the island arc geochemical signature range from slightly LREE-enriched basalts to alkalic basalts and include a group of basalts that have geochemical characteristics transitional between the two end members. Mafic subvolcanic rocks represent all of these eruptive types.

Felsic volcanic rocks are Low - K, high - SiO_2 rhyolite. They occur only in the central stratigraphic parts of the group and are associated with mafic rocks of island arc affinity.

Petrogenetic modelling of the Wild Bight Group volcanic rocks, using a comprehensive suite of Nd isotope analyses on selected whole rocks, allows further interpretation of their origin. Rocks of island arc affinity, for the most part, have epsilon$_{Nd}$ in the range -1.2 to +4.8, indicating the involvement of enriched mantle sources in the magmas. Negative Nb and Ta and positive Th anomalies with respect to the LREE indicate that this component was most likely a continental crustal source from the subducting slab. The island arc tholeiites can be modelled as resulting from mixing of this crustal source and normal depleted mantle followed by varying amounts of partial melting. However, the melting history of the depleted tholeiites must be more complex, as suggested by a strong negative correlation between epsilon$_{Nd}$ and both Sm/Nd and atomic Mg/(Mg+Fe) (Mg#). All rocks that lack the island arc geochemical signature have epsilon$_{Nd}$ in the range +4 to +7 and are interpreted to have resulted from varying degrees of partial melting of an ocean island basalt - type source, locally mixed with normal depleted mantle.

The geochemical and isotopic data, and comparisons with modern oceanic environments such as Fiji and the Mariana Trough, suggest a four-stage conceptual model for the geological development of the Wild Bight Group. Stage 1, the bottom of the group, records the last phases

iii

of volcanic activity in what may have been an originally more extensive island arc terrane. Stage two records the fragmentation of the arc, with attendant hydrous partial melting of both refractory mantle sources and basal arc crust. Stage three records an early stage of back-arc magmatism with the eruption of alkalic and transitional alkalic/tholeiitic basalts, respectively formed by increasing amounts of partial melting of an oceanic island basalt-type source. Stage four records a more mature stage of back-arc volcanism with advanced partial melting of oceanic island basalt sources and possibly mixing with normal depleted mantle sources. The continued eruption of arc tholeiites at this stage indicates that the back-arc basin was not very wide, and even in the latter stages was still broadly in a "supra-subduction zone' environment.

The four volcanogenic sulphide deposits in the Wild Bight Group include both massive sulphides and stockwork deposits formed during Stage 2, probably as a result of increased fracturing, heat flow and hydrothermal circulation accompanying breakup of the arc.

Comparison of geochemical data from the Wild Bight group with nearby, approximately coeval, volcanic sequences suggests that the environments can be recognized throughout central and eastern Notre Dame Bay and in south-central Newfoundland. Lead isotope studies of volcanogenic sulphide deposits throughout central Newfoundland suggest that deposits in the Wild Bight Group arc had similar lead sources to those in an earlier island arc of late Cambrian age that is represented throughout south central Newfoundland and Notre Dame Bay. This suggests a tectonostratigraphic relationship between them and it is possible that the earlier arc was the basement upon which the later arc was built. Lead isotopes in these sequences are relatively radiogenic and contrast sharply with those in most of the western Dunnage Zone deposits, where relatively non-radiogenic lead is prevalent. This contrast suggests that a major structural boundary may be present along the eastern side of the Buchans - Robert's Arm belt. Sequences on either side of this boundary may represent different tectonostratigraphic terranes, juxtaposed during the late Ordovician or early Silurian.

ACKNOWLEDGEMENTS

LIST OF ABBREVIATIONS

AA	- atomic absorption spectrometry
al	- albite
am	- amphibole
BABV	-back-arc basin volcanic rocks
bi	- biotite
ca	- calcite
CAB	-calc alkalic basalt
ch	- chlorite
cpx	- clinopyroxene
crptx	- cryptocrystalline material
DM	- depleted mantle
DSDP	- Deep Sea Drilling Project
E-MORB	- enriched mid-ocean ridge basalt
En	- enstatite
ep	- epidote
ES	- enriched source
Fe#	- atomic Fe/[Fe+Mg]
Fs	- ferrosilite
glx	- glomerocryst
G.S.C.	- Geological Survey of Canada
gt	- garnet
HDM	- highly depleted mantle
HFSE	- high field strength elements
hm	- hematite
IAD group	- 'island arc depleted' group
IAI group	- 'island arc intermediate' group
IAT	- island arc tholeiite
ICP-MS	- Inductively coupled plasma mass spectrometry
ID	- isotope dilution
il	- ilmenite
INAA	- instrumental neutron activation analysis
LFSE	- low field strength elements
L.O.I.	- loss on ignition
LREE	- light rare earth elements
MAR	- Mid-Atlantic Ridge
Max.	- maximum
Mg#	- atomic Mg/[Mg+Fe]
min.	- minimum
MORB	- mid-ocean ridge basalt
MREE	- middle rare earth elements
mt	- magnetite
M.U.N.	- Memorial University of Newfoundland

'n' subscripted (e.g. La$_n$) - concentration which has been chondrite-normalized

N.D.M.E.	- Newfoundland Department of Mines and Energy
N-MORB	- normal mid-ocean ridge basalt
NAE	- 'non-arc enriched' group
NAI	- 'non-arc intermediate' group
NAT	- 'non-arc transitional' group
Nd IC	- Neodymium isotopic composition
N.T.S.	- National Topographic System
OIB	- oceanic island basalt

ol	- olivine
opq	- opaque minerals
opx	- orthopyroxene
pl	- plagioclase
ppm	- parts per million
qz	- quartz
REE	- rare earth elements
ser	- sericite
sp	- sphene
SPSS-PC	- statistical package for the Social Sciences for personal computer
St. Dev.	- standard deviation

't' superscripted with an iron oxide (e.g. FeO^t) - total iron

T-MORB	- transitional mid-ocean ridge basalt
VAB	- volcanic arc basalt
Wo	- wollastonite
WPB	- within plate basalt
WPT	- within plate tholeiite
WPA	- within plate alkali basalt
w / r	- water / rock ratio
XRF	- X-ray fluorescence

TABLE OF CONTENTS

CHAPTER 1
INTRODUCTION

CHAPTER 2
GEOLOGY AND PETROLOGY OF THE WILD BIGHT GROUP VOLCANIC AND SUBVOLCANIC ROCKS

CHAPTER 3
GEOCHEMISTRY OF VOLCANIC AND SUBVOLCANIC ROCKS IN THE WILD BIGHT GROUP

CHAPTER 4
Nd ISOTOPES AND PETROGENESIS OF THE WILD BIGHT GROUP VOLCANIC AND SUBVOLCANIC ROCKS

CHAPTER 5
GEOLOGICAL AND PALEOTECTONIC DEVELOPMENT OF THE WILD BIGHT GROUP; MODERN ANALOGUES AND ANCIENT CORRELATIVES

CHAPTER 6
VOLCANOGENIC SULPHIDE MINERALIZATION: FIELD RELATIONSHIPS, PALEOTECTONIC SETTING AND LEAD ISOTOPES

CHAPTER 7
SUMMARY AND PRINCIPAL CONCLUSIONS OF THE THESIS

xiii

LIST OF FIGURES

xiv

LIST OF TABLES

LIST OF PLATES

CHAPTER 1

INTRODUCTION

1.1 Subject and Scope of Thesis

The Wild Bight Group comprises a sequence of early and middle Ordovician volcaniclastic, volcanic and subvolcanic rocks-outcropping in the central part of Notre Dame Bay, north-central Newfoundland. It forms part of an extensive tract of dominantly pre-middle Ordovician, oceanic, stratified (dominantly volcanic and volcaniclastic) rocks that outcrops throughout Central Newfoundland and defines the "Central Mobile (or Volcanic) Belt" (Figure 1.1). The thick sequences of volcanic and volcaniclastic rocks in this tract have been widely interpreted as the products of island arc volcanism and sedimentation accompanying the closure of the Iapetus Ocean (e.g. Wilson, 1966; Bird and Dewey, 1970; Williams et al., 1974; Strong, 1977; Williams, 1979; Dewey et al., 1983).

The broad outlines of the stratigraphy of the Wild Bight Group were first described by Heyl (1938) and further refined by later reconnaissance studies (Williams. 1964; Horne and Helwig, 1969; Dean and Strong, 1976; Dean, 1978, among others). However, few detailed data regarding the distribution and stratigraphic setting of the volcanic rocks have been published. Likewise, there are no geochemical or isotopic data on which to interpret the magmatic and paleotectonic history of volcanic rocks in the group and the interpretation of this sequence as products of island arc tectonism remains unsubstantiated.

This lack is particularly significant in view of the fact that the Wild Bight Group hosts four volcanogenic sulphide deposits including the Point Leamington deposit, the largest massive sulphide deposit in the Canadian Appalachians outside the Bathurst area. Pre-Middle Ordovician volcanogenic depositsare widespread in Central Newfoundland, have historically been a major source of base and precious metals and continue to be a major target for exploration efforts. Despite this, there is little documentation of the specific types of volcanic rocks associated with mineralization or the paleotectonic environments in which they formed.

Figure 1.1: Tectonostratigraphic subdivision of Newfoundland. Wild Bight Group indicated by dark stipple. Other Cambrian to Ordovician volcanic and volcaniclastic rocks indicated by light stipple, ophiolites by black shading.
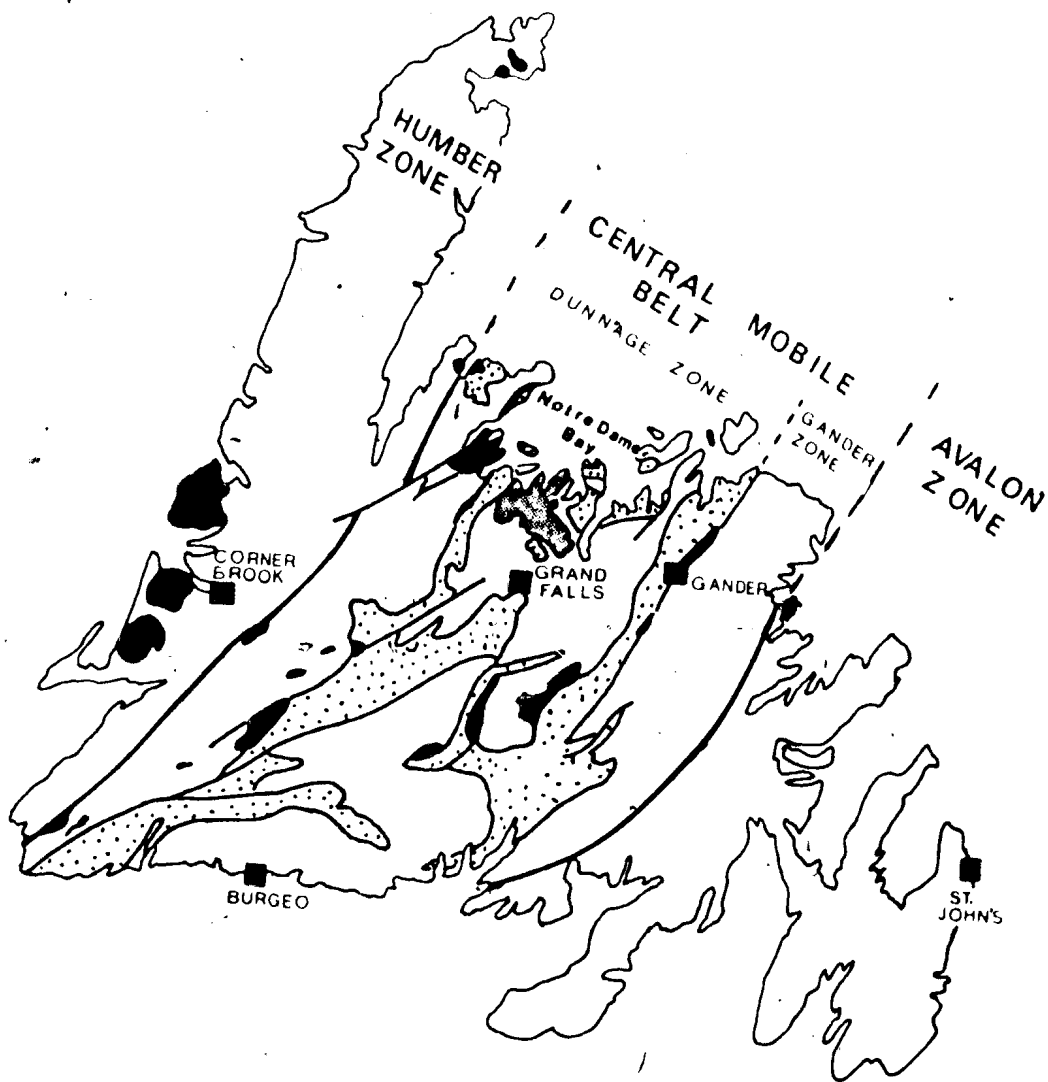
HUMBER
ZONE

CENTRAL MOBILE
BELT

DUNNAGE ZONE

Notre Dame Bay

GANDER
ZONE

AVALON
ZONE

CORNER
BROOK

GRAND
FALLS

GANDER

BURGEO

ST.
JOHN'S

This thesis presents the results of a detailed geological, petrological, geochemical and isotopic study of volcanic and subvolcanic rocks in the Wild Bight Group. The aims and principal objectives of the study are:

1) to document the geological settings and petrological characteristics of volcanic and subvolcanic rocks in the Wild Bight Group;

2) to identify and document the geochemical variation in volcanic and subvolcanic rocks in the Wild Bight Group, and to interpret these characteristics in terms of the petrogenetic history of the magmatic rocks and the paleotectonic environments in which they might have formed.

3) to define the geological setting of volcanogenic mineralization in the Wild Bight Group, to interpret this setting in terms of possible paleotectonic environments and to refine genetic models for the mineralization based on this understanding of their paleotectonic setting;

4) to integrate this study in the wider reference frame of the geology and paleotectonic history of Central Newfoundland, in order to further our understanding of the pre-Middle Ordovician geological development of the Central Mobile Belt.

The Wild Bight Group has several characteristics that make it particularly amenable to such a study:

1) adequate geological control at a scale of 1:50,000 is provided by the geological compilations of Dean and Strong (1976);

2) volcanic rocks are widespread in the succession and occur at virtually all stratigraphic levels;

3) the Wild Bight Group outcrops along (and generally strikes into) more than 80 km of deeply indented coastline, providing excellent access to the complete stratigraphy and good exposures of many critical stratigraphic and structural relationships;

4) no geochemical or whole rock isotopic data were previously available;

5) like many other volcanic units in north-central Newfoundland, it is overlain by a widespread fossiliferous unit, the "Caradocian shale" (Dean, 1978), which provides a compelling stratigraphic link and permits conclusions reached in the Wild Bight Group to be applied over a

broad area;

6) the Wild Bight Group contains four volcanogenic sulphide deposits, and, therefore, provides an excellent opportunity to investigate the relationship between genesis of the volcanic rocks and the presence (or absence) of mineralization.

Chapter 2 presents detailed descriptions of the geological settings of the volcanic and subvolcanic rocks from field data collected by detailed traversing of all volcanic sequences including examination of all contact and internal stratigraphic relationships where exposed, detailed traversing of all coastal exposures to examine regional lithological and stratigraphic relationships, and systematic inland traverses to examine regional relationships not exposed on the coastline. These data are supplimented by petrographic studies of the volcanic and subvolcanic rocks and electron microprobe analyses of selected secondary mineral phases.

Whole rock samples were analysed for major and trace elements and selected samples were analysed for additional high field strength elements (HFSE) and rare earth elements (REE). These analyses are presented in Chapter 3 with preliminary interpretations of the nature of the magmatism and the possible tectonic environment(s) that the rocks represent. Electron microprobe analyses of clinopyroxene in mafic rocks further contribute to the discussion.

Whole rock Nd isotopic studies, presented in Chapter 4, allow further comparison of the magmatic history of the Wild Bight Group, by helping to constrain the nature of the magmatic source area(s). Isotopic and geochemical data are integrated in a synthesis and interpretation of the petrogenesis(es) of the various magmatic rocks at the end of this chapter.

In Chapter 5, the geological, petrological, geochemical and isotopic data are compared with modern oceanic environments that are interpreted as good analogues for the Wild Bight Group. These form the basis for a model of the paleotectonic development of the Wild Bight Group.

Volcanogenic sulphide deposits in the Wild Bight Group are described in Chapter 6 and their genesis interpreted in terms of the paleotectonic setting of the host rocks. Lead isotopic data from these and other deposits in Central Newfoundland are used to constrain further the

correlation of units across the Mobile Belt and to interpret further the tectonic history of the Central Mobile Belt.

Chapter 7 is a summary of the thesis and its principal conclusions.

1.2 Location and Access

The Wild Bight Group is centered at approximately $49°,20'$ N., $55°$, $30'$ W. and occupies parts of 1:50,000 map sheets 2E/3 (Botwood), 2E/4 (Hodges Hill), 2E/5 (Robert's Arm) and 2E/6 (Point Leamington). Most of the northern part of the Wild Bight Group is easily accessible by small boat from the shores of Badger Bay, Seal Bay and Osmonton Arm and from all weather gravel roads linking Point Leamington with Leading Tickles (Figure 2.1). The southeastern corner of the Wild Bight Group is crossed by highway 350 near Northern Arm and much of the area northwest of here is accessible via an extensive network of (mainly abandoned) bush roads and trails (now passable only to four-wheel drive and all-terrain vehicles) which connect with major highways at Point Leamington, Botwood and Grand Falls. Inland outcrops in the western part of the group are locally accessible via all-weather forest access roads which link with Highway 380 between South Brook and Robert's Arm. Access to remote areas throughout the southern part of the group is gained by canoe on the numerous lakes and rivers and by fixed and rotary winged aircraft.

1.3 Regional Setting of Pre-Middle Ordovician Stratified Rocks in the Central
Mobile Belt

The island of Newfoundland is the northeastern termination of the Appalachian Orogen (Williams et al., 1974; Williams, 1978). The orogen in Newfoundland is generally regarded as a "two-sided, symmetrical system" (Williams, 1964). Precambrian continental platforms (the Humber and Avalon Zones of Williams, 1978, or the Humber and Avalon Terranes of Williams and Hatcher, 1983) occur to the west and east, respectively (Figure 1.1). These are separated by an early Paleozoic mobile belt (the Dunnage and Gander Zones or Terranes, Williams, 1978; Williams and Hatcher, 1983) which records the formation, development and subsequent destruction of part of

an early Paleozoic oceanic terrane, commonly termed the "Proto-Atlantic" or "Iapetus" Ocean (Wilson, 1966; Harland and Gayer, 1972). The Dunnage Zone forms the western and northern part of the Mobile Belt and its pre-Silurian rocks record mostly intra-oceanic events. In the Gander Zone to the south and east, the pre-Silurian record contains quartzose clastic and felsic volcanic rocks which are interpreted to have been deposited at or near a sialic continental margin (Colman-Sadd, 1980; Colman-Sadd and Swinden, 1984).

A summary of stratigraphic relationships in the northern part of the Central Mobile Belt can be found in Dean (1978), to which the reader is referred for a comprehensive reference to previous work and the development of ideas concerning the geological history of this part of the orogen.

The analogy between pre-Middle Ordovician volcanic sequences of central Newfoundland and modern volcanic islands has been part of geologic thought for more than one hundred years. Wadsworth (1884) was one of the first to compare volcanic rocks of Notre Dame Bay with those in modern volcanic islands and Heyl (1936) also considered that volcanic and volcaniclastic rocks in central Notre Dame Bay (now assigned to the Exploits and Wild Bight Groups) probably represent ancient volcanic islands. The concept of an Ordovician chain of volcanic islands was also an integral part of geosynclinal theory applied to the Appalachians by, among others, Kay (1951).

Wilson (1966) pointed out that modern volcanic chains adjacent to continental margins were probably analogous to Ordovician volcanic-volcaniclastic sequences in the Appalachians and with the advent of plate tectonic theory, many authors were quick to note the similarity between the pre-Middle Ordovician sequences of central Newfoundland and modern island arcs. This geological comparison was the basis for the identification of an early to middle Ordovician island arc in regional syntheses by, for example, Bird and Dewey (1970), Mitchell and Reading (1971), Williams et al. (1972,1974), Kay, (1973), Kennedy (1975), Strong (1977), Dean (1978) and Dewey et al., (1983) and figured strongly in more detailed studies of individual sequences by Kean and Strong (1975, Cutwell Group), Strong and Payne (1973, Moreton's Harbour Group), DeGrace et al. (1976, Snooks Arm Group) and Tuach and Kennedy (1978, Pacquet Harbour

Group) among others.

These and other early models for Central Newfoundland geological and tectonic development assumed a simple stratigraphic succession from basal ophiolites to overlying island arc sequences interpreted as recording the Cambrian to early Ordovician opening of Iapetus (ophiolitic rocks) followed by its early to middle Ordovician closing (volcanic/volcaniclastic sequences interpreted as island arc-related). In each case, island arc volcanism was postulated on the basis of some or all of the following observations:

(1) the substantial thickness of some sequences (up to ten km), believed to be more characteristic of island arc than oceanic settings;

(2) the association of volcanic rocks with voluminous, volcanically - derived, clastic sedimentary rocks;

(3) the presence of felsic volcanic rocks in the sequences;

(4) the stratigraphic setting of these sequences above ophiolitic rocks which, following Church and Stevens (1971), were generally interpreted as ocean floor;

(5) geochemical data suggesting a broad calc alkalic affinity for many of the volcanic products.

However, more recent detailed geochemical and isotopic studies, and particularly geochronological work, have shown that such a simplified model is unfenable. Geochronological studies have shown, for example, that there are at least two generations of ophiolites (Dunning and Krogh, 1985), each of which locally contains evidence for magmatism in a supra subduction zone environment (the Pipestone Pond Complex at ~495 Ma, Swinden, in press; the Betts Cove Complex at ~ 488 Ma, Coish et al., 1982). Furthermore, at least three generations of island arc volcanic rocks have been identified (Dunning et al., 1986; 1987) spanning the time period from late Cambrian to middle Ordovician and geochemical studies have shown that within some of the thick volcanic-volcaniclastic sequences previously interpreted as arc-related, there are magmatic rocks that appear to be products of within-plate rather than island arc activity (e.g.,. Jenner and Fryer, 1980; Jacobi and Wasowski, 1985; Wasowski and Jacobi. 1985; see Section 1.4).

It is now clear that the Central Mobile Belt records a long and complex history, the details of which are equivocal. The present geological, geochemical and geochronological data base, however, suggests the general sequence of events summarized below (time scale according to van Eysinga, 1975):

1) ~505 to 520 Ma, late Cambrian: The oldest radiometrically-dated rocks in the Dunnage Zone are felsic volcanic rocks of the Tally Pond volcanics (~517 Ma, Dunning et al., 1986), The geology of this sequence (mafic pillow lavas and up to 35 percent felsic volcanic rocks) is indicative of an island arc origin (Kean and Jayasinghe, 1980). A somewhat younger U/Pb (zircon) date of 510(+17/-16) Ma has been obtained from the Twillingate trondhjemite (Williams et al., 1976), likewise interpreted as formed in an island arc environment (Payne and Strong, 1979). It is not known whether there is any direct relationship between these two old island arc terranes, but together they apparently constitute the earliest volcanic activity in the Dunnage Zone.

Most recently, a preliminary late Cambrian U/Pb (zircon) age has been recovered from the southernmost part of the Tulks Hill volcanics in the Victoria Lake Group (G.R. Dunning, pers. comm. 1987) and it now appears that at least part of this sequence may be approximately coeval with the late Cambrian arc.

2) ~495 Ma, Tremadocian: ophiolitic rocks of the Gander River Ultrabasic Belt (GRUB) represent the earliest period of ophiolite generation. Geochemical studies of the Coy Pond (Colman-Sadd, 1985) and Pipestone Pond (Swinden, in press) ophiolites suggest that they were, at least in part, supra-subduction zone ophiolites. There are no geological links between these and the slightly younger ophiolites of the western Dunnage Zone.

3) ~475 to 488 Ma, Arenigian: During this period, most of the western Newfoundland ophiolites (e.g. Betts Cove, Annieopsquotch, Bay of Islands) were generated (Dunning and Krogh, 1985). These mainly appear to represent oceanic crust generated in back arc basins (e.g. Upadhyay and Neale, 1979; Dunning and Chorlton, 1985) although geochemical and isotopic evidence suggests that the Betts Cove complex may represent the latter stages of an arc rifting event (Coish et al., 1982).

These ophiolites are locally conformably overlain by volcaniclastic and mafic volcanic rocks of oceanic island affinity (Jenner and Fryer, 1980).

4) ~475 Ma, late Arenigian: The Buchans and Robert's Arm groups were formed at this time (Dunning et al., 1987) as were nearby volcanic rocks of the Cutwell Group (G.R. Dunning, pers. comm. 1987). The extensive development of felsic volcanic rocks and data from detailed geochemical studies in the Buchans area suggest an island arc origin (Thurlow, 1981). Little detailed work on the petrogenesis of these rocks has been published to date although Bostock (1978) suggested on the basis of TiO_2 and P_2O_5 concentrations that parts of the Robert's Arm. Group contained volcanic rocks of both oceanic island and island arc affinity.

3) ~460 Ma, Llanvirnian to Caradocian: Felsic volcanic rocks in both the Dunnage and Gander Zones, have yielded dates of approximately 460 Ma at a number of localities in central and southern Newfoundland (Dunning et al., 1986). Volcanic sequences that have yielded these dates have previously been interpreted as of island arc affinity on the basis of geological and geochemical arguments (e.g. volcanic rocks in the northwestern part of the Victoria Lake Group, here termed the "Victoria Mine sequence", Kean and Jayasinghe, 1980; the Bay du Nord Group, Chorlton, 1980). However, recent work has also identified volcanic rocks with geochemical signatures of oceanic within plate environments in some of these sequences (e.g. Reusch, 1983; Jacobi and Wasowski, 1985; Wasowski and Jacobi, 1985). Locally, the volcanic rocks are interbedded with fossiliferous sedimentary rocks containing a Llanvirnian fauna (e.g. the Tulks Hill volcanics, Kean and Jayasinghe, 1982) and at several locations, are conformably overlain by fossiliferous Caradocian shale (Dean, 1978).

4) Caradocian to Silurian: Carbonaceous argillite, grey and red chert and local accumulations of calcareous argillite and siltstone overlie the volcaniclastic and volcanic sequences of Notre Dame Bay and south-Central Newfoundland (Kay, 1975; Dean and Strong, 1976; Dean, 1978; Dean and Meyer, 1982). This pelagic facies is overlain in most areas, by Late Ordovician to Silurian turbidites, consisting of greywacke and fine-grained conglomerate, assigned to the Sansom Formation, the Point Leamington greywacke and the Goldson

conglomerate. These were derived from a volcanic terrane to the north and northwest (Helwig, 1967; Helwig and Sarpi, 1969; Nelson and Casey, 1979) and detrital chromite grains in them

suggest a partially ophiolitic provenance (Nelson and Casey, 1979). An exception is found in the Cutwell Group on Long Island where Caradocian argillites are overlain by intermediate volcanic rocks of the Parson's Point Formation (Kean and Strong, 1975).

Volcanic activity resumed in the early-Silurian with the widespread eruption of terrestrial volcanic rocks accompanied by the deposition of fluviatile clastic sediments. Detailed studies of the Springdale Group and volcanic sequences on the Burlington Peninsula (Kontak and Strong, 1986; Coyle and Strong, 1987) indicate that these rocks were erupted in an epicontinental environment and are not related to subduction.

The post-Silurian history of Central Newfoundland involved mainly extensive granitoid plutonism spanning Silurian to Carboniferous time (Strong *et al.*, 1974a; Strong and Dickson, 1978; Bell *et al.*, 1977; 1979; Strong, 1980; Elias and Strong, 1982) and the opening of successor basins, beginning in the late Devonian, accompanied by clastic fluviatile sedimentation (Belt, 1969; Bradley, 1982).

1.4 Previous Geochemical Studies of Pre-Silurian Volcanic Rocks in Central

Newfoundland

There are a number of published and unpublished geochemical studies of pre-Silurian volcanic rocks in the Central Mobile Belt. These data have figured prominently in some paleotectonic models for the Central Mobile Belt and are particularly relevant to the results of the present study. A compilation of previous geochemical studies is presented in Table 1.1 and the brief discussion below highlights significant features of the studies.

Geochemical studies in the early 1970's relied heavily on interpretation of major element relationships (including alkali and alkaline earth elements without regard to possible effects of alteration) and a limited number of trace elements, usually including Ti, Zr, Y, Cr and Ni,

Table 1:1: Summary of previous geochemical studies of
pre-Silurian volcanic rocks in the Central Mobile Belt.

REFERENCE	UNIT(S)	DATA-DIAGRAMS	INTERPRETATIONS
Gale (1971; 1973)	Pacquet Harbour Gp.	major elements, limited trace elements	identified two basalt types based on Al_2O_3 and TiO_2 contents: 1) tholeiitic basalts with major and trace (Y,Zr) contents typical of ocean floor basalts; 2) "basaltic komatiites" enriched in MgO, Ni, Cr and depleted in incompatible elements
Strong (1973)	Robert's Arm Gp.	as above	volcanic rocks are a bimodal basalt-rhyolite assemblage with calc alkaline affinities related to island arc volcanic activity
Upadhyay (1973)	Snooks Arm Gp.	major elements only	concluded that chemistry of Snooks Arm Group basalts was not consistent with formation in an island arc
Kean (1973), Kean and Strong (1975)	Cutwell Gp.	major elements, traces including Cr, Ni, Rb, Sr, Zr.	used major element relationships and Ti-Zr diagram of Pearce and Cann (1973), suggested that island arc tholeiites at base give way to progressively more calc alkaline rocks upward. Interpreted as a transition from primitive to mature arc volcanism.
DeGrace et al. (1976)	Snooks Arm Gp.	as above	using alkali element relationships and Ti-Zr diagram (Pearce and Cann, 1973), concluded these rocks were broadly similar to rocks in modern island arcs
Thurlow (1973,1981), Thurlow et al. (1975)	Buchans Group	as above	Suggested calc-alkaline affinity and island arc origin for mafic volcanic rocks. Interpretations more concerned with changes related to mineralization than petrochemistry
Strong (1977)	compilation for northern Central Mobile Belt. New data for Snooks Arm and Moreton's Harbour groups	as above	using major element (alkali elements, SiO_2, FeO) relationships, suggested Snooks Arm and Moretons Harbour groups transitional alkalic-subalkalic. Noted Ti, Zr and Cr relationships not consistent with island arc origin and suggested diagrams might not have universal applicability.
Bostock (1978)	Robert's Arm Group	major and trace element data referred to but not presented	based on TiO_2 and P_2O_5 relationships, suggested island arc tholeiitic and calc alkaline basalts as well as oceanic island tholeiites present.
Chorlton (1980)	La Poile Group	as above	using major and trace element diagrams of Pearce and Cann (1973) and Winchester and Floyd (1976), concluded these rocks are subalkaline basalts and dacites with a calc alkaline affinity indicating an island arc environment.
Jenner and Fryer (1980)	Snook Arm Gp.	major and trace elements, REE	suggested these rocks to be LILE-enriched tholeiites indicative of an oceanic island or marginal basin environment.
Reusch (1983)	Summerford Gp.	major and trace elements, microprobe analyses of clinopyroxene	found basalts to be strongly tholeiitic with MORB affinities. Interpreted them as formed at an oceanic spreading center or in a back arc basin.
Jacobi and Wasowski (1985)	Summerford Gp.	major, trace elements, REE	using mainly Ti, Zr, Cr and Y relationships on a smaller data set than that of Reusch, interpreted these rocks as ocean island tholeiites and alkali basalts, representing Tremadocian to Llandeilian/Caradocian seamounts
Wasowski and Jacobi (1984) Wasowski (1985)	Exploits Gp.	major, trace elements, REE	concluded that volcanics in the upper part of the group are oceanic island basalts. Those in lower parts are extremely depleted and their similarity to boninites interpreted as suggesting a forearc setting
Wasowski and Jacobi (1985)	blocks in Dunnage melange	major, trace elements, REE	similar to Summerford and upper Exploits Groups

interpreted with reference to the discriminant diagrams of Pearce and Cann (1971; 1973). These data led to early recognition of probable island arc volcanic rocks in the Cutwell, Robert's Arm and Buchans Groups. However, they also led some workers to suggest that the chemistry of many of the volcanic rocks in the thick volcanic/volcaniclastic sequences in Notre Dame Bay might not be of island arc origin. Strong (1977), in particular, pointed out that although geological interpretations of the Snooks Arm and Moreton's Harbour groups indicated an island arc origin, they generally plotted in ocean floor fields on the Pearce and Cann diagrams. Bostock (1978) made a similar case for tholeiitic rocks at the base of the Robert's Arm Group (although without publishing his data) and suggested that this group was bipartite, with a lower volcanic sequence of oceanic island origin and an upper sequence formed in an island arc.

Jenner and Fryer (1981) were the first to present rare earth element (REE) data for any of these volcanic rocks in their analysis of the petrochemistry of the Snooks Arm Group. They showed that these volcanic rocks are dominantly large ion lithophile element (LILE) enriched tholeiites unlikely to have been generated in an island arc environment, supporting previous conclusions of Upadhyay (1973) and Strong (1977).

Geochemical studies in central and eastern Notre Dame Bay have not yielded much evidence of island arc volcanic activity. Both the Summerford Group (Reusch, 1983; Jacobi and Wasowski, 1985) and the upper part of the Exploits Group (Wasowski, 1984; Wasowski and Jacobi, 1985) have been found to contain mainly light rare earth element (LREE) enriched tholeiites indicative of oceanic island volcanics although incompatable-element depleted basalts in the lower Exploits Group were interpreted by Wasowski (1985) as possibly representing a forearc setting. The geochemical similarity of volcanic blocks in the Dunnage Melange to those in volcanic units in the nearby Summerford and Exploits groups (Wasowski and Jacobi, 1985) supports the contentions of Hibbard (1976) and Hibbard and Williams (1979) that the blocks are derived from the adjacent units.

In summary, although geochemical studies of volcanic rocks in the Central Mobile Belt have been carried out sporadically for over fifteen years, there are still few volcanic sequences

that have been adequately characterised geochemically. In particular, REE data are only available for three units (Snooks Arm, Exploits and Summerford groups) and the trace element data for many rocks which was gathered in the early to mid 1970's is of variable quality and in many cases does not include precise analyses for critical elements (in particular Nb and Y). There are no published data for the high field strength elements (HFSE) Ta or Hf. Clearly, the paleotectonic environments of most volcanic rocks in the Central Mobile Belt, interpreted on geological grounds, have yet to be confirmed by geochemical data.

1.5 Definition of Terms

This thesis deals with a large number of samples that have been subdivided in various ways (i.e. on the basis of geographic distribution, geochemical composition). For ease of reference when describing and discussing these different sample groupings, semantic terms have been assigned to the different types of subdivisions. These have a specific meaning with regard to the units being discussed and are defined as follows:

Suites: Sample combinations referred to as "suites" are groups of volcanic and subvolcanic rocks identified on the basis of their geographic distribution (e.g. the Glover's Harbour suite). The geographic areas are shown and labelled on Figure 2.1.

Groups: Combinations of samples that have been combined on the basis of similar geochemical characteristics are referred to as "groups" (e.g the "Ti-poor group"). They may include samples from more than one suite.

CHAPTER 2

GEOLOGY AND PETROLOGY OF THE WILD BIGHT GROUP VOLCANIC AND

SUBVOLCANIC ROCKS

2.1 Introduction

The Wild Bight Group underlies approximately 1000 km^2 and has been estimated by Dean (1978) to comprise a stratigraphic thickness in excess of 10 km. Approximately 75 percent of the sequence comprises epiclastic rocks, the remainder being mainly mafic and lesser felsic volcanic rocks. Mafic dykes and sills interpreted to be subvolcanic occur throughout the sequence.

Volcanic rocks occur only in the eastern and central parts of the Wild Bight Group. The distribution of lithologies and regional setting of the Wild Bight Group is illustrated in Figure 2.1 while the geological relationships in the eastern part of the group, particularly with respect to the setting of the volcanic members, are depicted in more detail in Figure 2.2.

2.2 Previous Work and Nomenclature

Early workers in Notre Dame Bay recognized the widespread outcrop of volcanic and epiclastic rocks (e.g. Murray and Howley, 1881; Wadsworth, 1884; Sampson, 1923; Snelgrove, 1928). However, Espenshade (1937) was the first to publish detailed descriptions of rocks presently assigned to the Wild Bight Group. Mapping in what is now considered as the western part of the Wild Bight Group, he considered the volcanic strata in Wild Bight-Badger Bay, which he termed the "Wild Bight volcanics" (the "Badger Bay basalt" of this thesis) to form the base of a west-facing stratigraphic sequence (the "Badger Bay Series") that included rocks now assigned to the Wild Bight Group, Shoal Arm formation (Caradocian shale), Sansom Greywacke and the Robert's Arm Group.

Previous to Espenshade's work, Heyl (1936) had described the geology of the Bay of Exploits area immediately east of the present Wild Bight Group. In 1937, he extended this work westwards in a reconnaissance fashion to the area between New Bay and Badger Bay (Heyl,

Figure 2.1: Generalized geological map of the Wild Bight Group (light and dark stipple) illustrating

the regional setting, contact relationships and distribution of lithologies . Volcanic rocks are in

dark stipple, epiclastic rocks in light stipple. Names in boxes are nomenclature for the volcanic

rock units (Section 2.5). Light stipple is dominantly Wild Bight Group epiclastic rocks. Crosses

indicate probable Acadian plutonic rocks, wavy lines are Caradocian shale and broken pattern the

South Lake Igneous Complex. Geology is shown in more detail in Figure 2.2.

Map showing Notre Dame Bay region with locations including Long I., Pilleys Island, Halls Bay, Springdale, Badger Bay, Seal Bay, New Bay, Leading Tickles, Point Leamington, North Twin Lake, South Twin Lake, Botwood. Scale 0-5-10 km. Tommys Arm Fault and Northern Arm Fault indicated. North arrow shown.
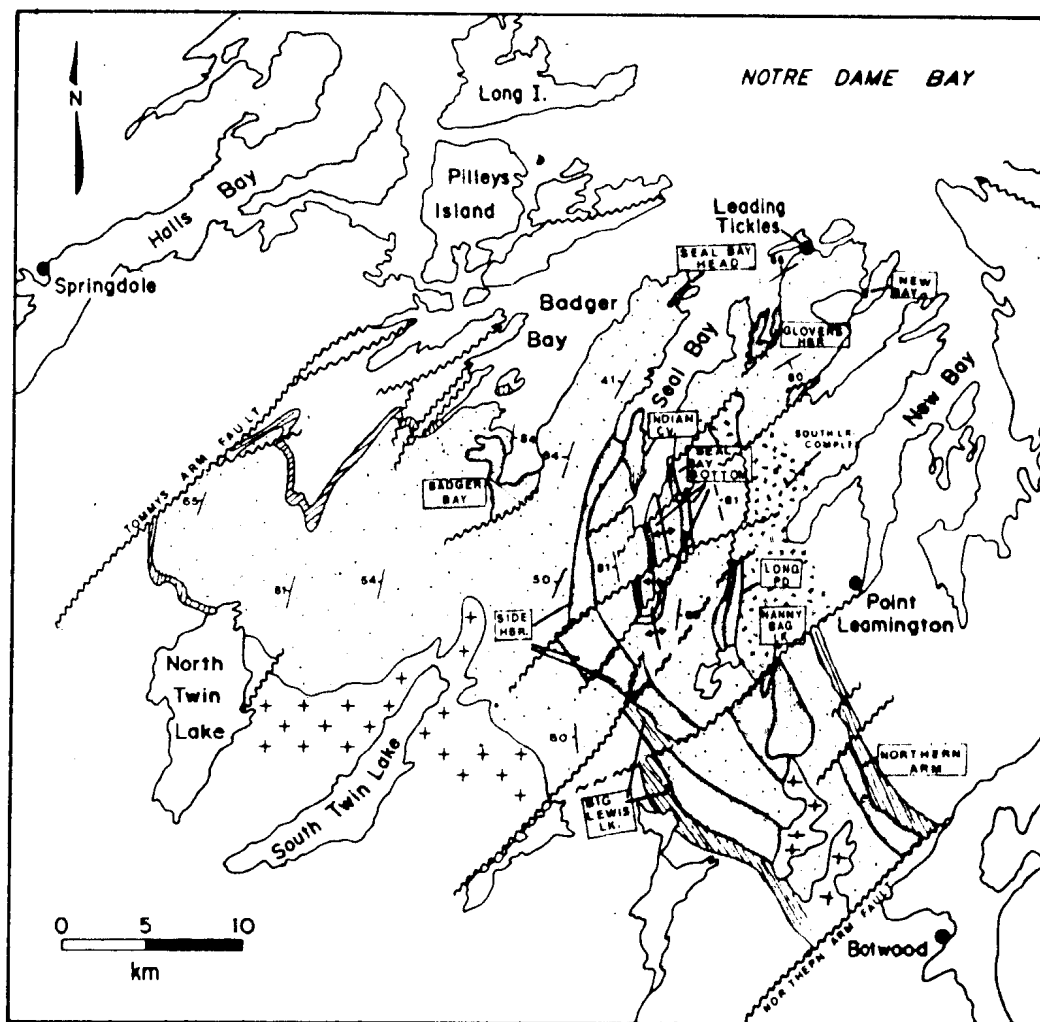
1938). In the process he examined much of the Wild Bight Group coastal exposure, assigning it to the Exploits Series which he had previously defined in the Bay of Exploits area. Unfortunately, much of Heyl's (1936) stratigraphy in the Bay of Exploits area was erroneous (see review in Dean, 1978) and these errors were propagated across the central part of the Notre Dame Bay area during his later work. Although most of Heyl's nomenclature has been discarded by later workers, it is of interest with respect to the present study that he was the first to assign a formal name to volcanic rocks in the western part of the Wild Bight Group (again, the "Badger Bay basalt" of this thesis) which he termed the "Wild Bight Formation".

Hayes (1951) mapped roughly the western third of the present Wild Bight Group, extending Espenshade's work inland to the southwest. However, he adopted Heyl's (1936) nomenclature, retaining the name "Wild Bight Formation" for volcanic rocks in Wild Bight, Badger Bay.

Williams (1963) was the first to define the Wild Bight Group in its present form. Recognizing the significance of the Shoal Arm Formation as a regional stratigraphic marker in western and central Notre Dame Bay, he included only rocks below this unit in the Wild Bight Group. He assigned an Ordovician age to the Wild Bight Group, correlating it with volcanic rocks on New World Island (now the Summerford Group) and the Fortune Harbour Peninsula (now the Moreton's Harbour and Cottrell's Cove groups).

Horne and Helwig (1969) retained Williams' (1963) nomenclature and proposed detailed correlations between the Wild Bight Group and the adjacent Exploits Group (as redefined by Helwig, 1969) to the east. They correlated volcanic rocks in Wild Bight, Badger Bay (near the top of the Wild Bight Group) with the basal unit of the Exploits Group (Tea Arm volcanics) implying that most of the Wild Bight Group is stratigraphically lower than the exposed base of the Exploits Group.

The 1:50,000 scale geological compilations of Dean and Strong (1976) were the first detailed published maps of the complete Wild Bight Group. Most of their data for this unit derived from previously cited workers, and from unpublished maps prepared by Noranda Mines Limited at

1"=1/4 mi., supplemented by field checking of critical localities. A stratigraphic synthesis based on these map compilations was later prepared by Dean (1978) who retained Williams' (1963) definition of the Wild Bight Group and further subdivided it into five formations (Figure 2.3). He showed that the group is disposed in a major anticline which he termed the "Seal Bay anticline", outlined the distribution of volcanic and epiclastic rocks throughout the group, and provided the first published account of rocks in the central and southern parts of the group.

Recent geological maps of the Wild Bight Group have drawn heavily upon Dean and Strong's (1976) compilations (e.g. Kean *et al.*, 1981), emphasizing the correlation of the Wild Bight Group with other pre-Caradocian volcanic and sedimentary sequences in central and southern Newfoundland.

Swinden (1984) published brief descriptions of the volcanic rocks and mineral deposits of the Wild Bight Group, reporting on field work that forms the basis of this thesis.

Geological mapping carried out during the present study, although not sufficiently comprehensive to attempt revision of Dean's (1978) nomenclature of the Wild Bight Group, does indicate that revision is necessary. The basal Omega Point Formation forms a distinctive and easily mappable unit. However, the overlying Sparrow Cove Point Formation, a thin basalt unit, does not outcrop on the point after which it is named, its place being taken by coarse-grained gabbro and epiclastic rocks (Figure 2.2). The Side Harbour Formation appears to be an appropriately named and subdivided unit but the Seal Bay Brook and Penny's Brook formations include a great variety of rock types, not all of which are stratigraphically or lithologically correlative. They are probably not useful subdivisions.

For descriptive purposes in this thesis, Dean's (1978) nomenclature is discarded in favour of a purely lithological subdivision of: a) sedimentary (epiclastic), b) volcanic and c) subvolcanic rocks. The epiclastic rocks are not subdivided but variations in sedimentary facies in different parts of the group are commented upon in Section 2.4. Eleven separate volcanic units are recognized and designated with informal names for ease of description in Section 2.5 (not all the

Figure 2.3: Distribution of formations in the Wild Bight Group according to Dean (1978). Base map is the same as Figure 2.1.

NOTRE DAME BAY

N

Long I.

Halls Bay

Pilleys Island

Leading Tickles

Springdale

Badger Bay

Seal Bay

New Bay

Point Leamington

North Twin Lake

South Twin Lake

Botwood

0   5   10
km

Pennys Bk Fm
Side Hbr Fm
Seal Bay Bk Fm
Sparrow Cove Pt. Fm
Omega Pt Fm
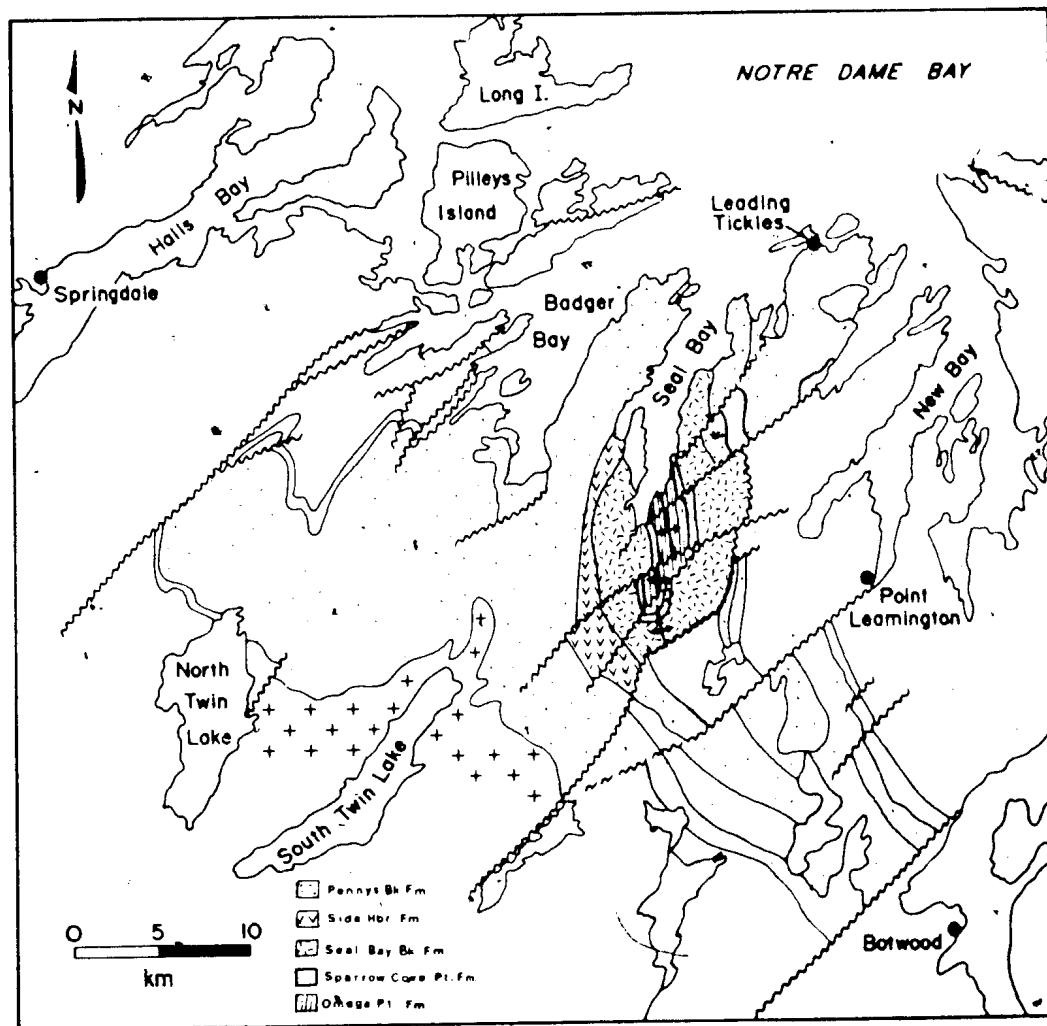
names are the same as those used by Swinden, 1984). Geological evidence for the stratigraphic positions and correlation of these volcanic units is presented in Section 2.5.2.

2.3 Geological Setting and Contact Relationships

The Wild Bight Group is generally considered to occupy a broad anticlinal structure (the Seal Bay anticline, Figure 2.1), the axis of which trends approximately north-south through the center of Seal Bay. This is undoubted an oversimplification of the actual case, particularly in the southwestern part of the group (see Section 2.7) but, nevertheless, provides a useful structural framework for stratigraphic reconstructions. Strata interpreted to be the exposed base of the sequence outcrop in Seal Bay Bottom in the core of this anticline. The stratigraphic succession on either side of the anticline faces generally outward, although in detail, there are many local facing reversals resultiong from minor folds. Despite these minor folds, the succession youngs more or less continuously to the east and west of the Seal Bay anticlinal axis and is interpreted to pass conformably on both limbs into the overlying fossiliferous shale and chert of the Caradocian Shoal Arm Formation (Figures 2.1, 2.2). The Shoal Arm Formation shale in the Badger Bay and Leading Tickles areas contains a graptolite fauna indicating a *Nemagraptus gracilis* zone (Llandello - Caradoc) age (Espenshade, 1937; Horne and Helwig, 1969; Dean, 1978) providing the only direct constraint on the age of the Wild Bight Group.

Dean's (1978) estimate of a stratigraphic thickness of more than 10 km. assumed an almost continuous, uninterrupted, more or less continuously younging, section from the core of the Seal Bay anticline to the Caradocian shale in Badger Bay. In view of the many minor folds and strike slip faults of indeterminate displacement in the area, this estimate should be viewed with caution. However, as an order of magnitude estimate, it is probably broadly correct. Construction of a structural cross - section from Seal Bay to Badger Bay, incorporating facing reversals dictated by folds shown on existing maps, yields an estimate of slightly more than 8 km of stratigraphic thickness for the sequence.

The Wild Bight Group is cut by numerous, northeast-trending, faults which show abundant

evidence for dextral strike-slip movement (e.g. Plate 2.1) and these faults locally modify the upper contact of the Wild Bight Group. For example, the Osmonton Arm Fault juxtaposes the upper Wild Bight Group with the Point Leamington greywacke southwest of Osmonton Arm. Further south, the Long Pond Fault brings similar strata against the Ordovician Frozen Ocean Group northeast of Frozen Ocean Lake and the western margin of the Wild Bight Group is faulted against the base of the Robert's Arm Group along the Tommy's Arm fault north of North Twin Lake (Figure 2.2). The eastern part of the Wild Bight Group is in part faulted against and in part intruded by granodioritic plutonic rocks of the South Pond Igneous Suite (Figure 2.2).

The southern contacts of the Wild Bight Group, are intruded by intermediate to mafic plutonic rocks of the Twin Lakes Complex and by leucocratic granitoid rocks of the Hodges Hill granite. These intrusive rocks have not been studied in detail but display complex intrusive relationships with each other and probably are part of a single intrusive suite. Mafic and intermediate rocks which are probably related to the Twin Lakes Complex intrude the southeastern corner of the Wild Bight Group west of Northern Arm.

The age of the Wild Bight Group is directly constrained only by the age of the overlying Caradocian shale. During the course of this study, several attempts were made to date different parts of the sequence directly. Five different 150 kg samples of felsic volcanic rock, representing all felsic volcanic units, were collected in an attempt to produce a U/Pb (zircon) age. None yielded sufficient zircon of suitable quality for dating (G.R. Dunning, pers. comm., 1986), although sampling was directed by early geochemical results to outcrops with the highest Zr concentrations. A single, 10 cm thick, limestone bed in the upper part of the Group was sampled and processed for microfossils but none was recovered (S. Stouge, written communication, 1985). Likewise, several attempts to recover graptolites from grey and black argillites in Seal Bay Bottom were unsuccessful.

COLOUR PHOTOGRAPHS SHOULD NOT BE USED. THEY WILL APPEAR AS GREY OR BLACK. WE RECOMMEND THAT THE COPY OF THE THESIS SUBMITTED FOR MICROFILMING INCLUDE BLACK AND WHITE PHOTOGRAPHS REPRINTED FROM THE COLOUR PHOTOGRAPHS BY A PHOTOGRAPHER IF NECESSARY.

LORSQUE MICROFILMEES, LES PHOTOGRAPHIES EN COULEUR PARAISSENT GRISES OU NOIRES. NOUS RECOMMANDONS QUE L'EXEMPLAIRE DE LA THESE A MICROFILMER SOIT ACCOMPAGNE PLUTOT DE PHOTOGRAPHIES EN NOIR ET BLANC PRODUITES A PARTIR DES PHOTOGRAPHIES EN COULEURS PAR UN PHOTOGRAPHE, SI NECESSAIRE.

Plate 2.1: The Winterhouse Cove Fault north of Glover's Harbour. Recessive rocks on right side of the photo are highly sheared, hematized, pillow lava of the Glover's Harbour suite. Those on the left are greywacke and siltstone in which the beds are dragged into the fault in a sense indicating dextral strike slip movement. The fault continues through the tickle in the upper-central part of the photo

Plate 2.2: Volcaniclastic rocks in southern Seal Bay. The lower sequence comprises laminated argillite and siltstone with minor chert. The upper sequence is chaotic, unsorted, matrix-supported, polylithic, volcaniclastic conglomerate.

2.4 Epiclastic Rocks

Epiclastic rocks are the dominant lithology in the Wild Bight Group, comprising up to 85% of the stratigraphic section. They were not mapped in detail during this study and a discussion of their sedimentology is beyond the scope of this thesis. However, observations made during the course of the field work do permit a general discussion of their nature and variations within the stratigraphic succession. For descriptive purposes, these rocks can be considered in terms of a tripartite subdivision: (1) a basal, fine grained clastic unit; (2) a central succession characterised by sandstone turbidites and debris flow conglomerates; and (3) an upper sequence of fine grained sandstone, siltstone and argillite.

The basal unit of the Wild Bight Group, at its present level of exposure, comprises up to 500 m of red and green argillite, chert and siltstone with lesser pebbly sandstone and minor fine-grained conglomerate which was assigned by Dean (1978) to the Omega Point Formation. This unit includes a single, six meter thick member of carbonaceous black argillite exposed on a small island in Seal Bay Bottom. Both the red argillite and the carbonaceous shale are unique to this unit in the Wild Bight Group.

The transition from the basal fine grained clastic unit to the overlying, coarser grained, epiclastic rocks is gradational. Dean (1978) placed the upper contact of the Omega Point formation at the base of a thin basalt flow which he termed the Sparrow Cove Point Formation (the Seal Bay Bottom basalt of this thesis). The basal part of the turbidite-debris flow unit, well exposed on the shore of Seal Bay north of Sparrow Cove Point, comprises rhythmically bedded, cyclic pairs of laminated sandstone/siltstone/chert and fine to medium grained, matrix-supported conglomerate (Plate 2.2). The sandstone/chert units are laminated to finely bedded, locally exhibit cross beds, current ripples, scour and fill structures and load casts. In many exposures, ABCD and BCD Bouma (1962) sequences can be recognized. The intervening conglomerate beds consist of angular to subrounded, poorly sorted clasts of locally-derived sedimentary and volcanic material, of which 60 to 70% are sedimentary and the remainder mafic volcanic with minor felsic volcanic rocks (i.e. the clasts reflect the proportions of the lithologies in the nearby

succession). The clasts generally show little or no preferred orientation, stratification or imbrication and the rocks are interpreted as debris flows.

The thickness and abundance of the debris flow units and the maximum and average size of the clasts increases steadily northeastwards (i.e. up section) along the east shore of Seal Bay. In the area north of Locks Harbour, 1 to 10 m intervals of fine grained, laminated siltstone and sandstone are typically separated by as much as 60 m of conglomerate. The conglomerates are typically structureless, generally display no imbrication or stratification, and have a sharp, unscoured base. Clasts are very poorly sorted, angular to subrounded, range in size from less than 5 cm to greater than 40 cm, and consist mainly of locally derived sedimentary and volcanic rocks. In thin section, angular to locally subrounded quartz, plagioclase and pyroxene crystals are seen to be common constituents of the fine grained part of the clast assemblage. These interbedded medium to coarse grained turbidites and debris flows form a major part of the sequence in exposures along the east shore of Seal Bay and are locally present although less abundant on the western shore of Seal Bay immediately north of Side Harbour.

The upper, fine grained, clastic facies of the Wild Bight Group is well exposed along the shores of Badger Bay, Leading Tickles and Wild Bight, New Bay. The transition with the underlying turbidite-debris flow unit is gradational. Epiclastic rocks in this upper sequence are generally finer grained than and lack the prominent debris flows of the underlying sequence. In Badger Bay, the dominant lithology is bedded, green greywacke and lesser siltstone, locally containing isolated pebble-sized clasts and more rarely, pebbly conglomerate beds. Similar lithologies dominate in Leading Tickles and New Bay but here, the section also contains a substantial amount of chert and siliceous argillite and a single 40 cm thick limestone bed was observed in the bottom of Wild Bight, New Bay.

2.5 Volcanic Rocks

2.5.1 Description and Field Relationships

Volcanic rocks occur mainly in the eastern and central parts of the Wild Bight Group. They

occur in eleven separate geographic areas and exhibit a considerable range in thickness, stratigraphic setting (summarized in Section 2.5.2) and lateral extent. The geological setting of these units is illustrated on Figure 2.2 and detailed maps of individual units are presented, where necessary, with the descriptive material in the sections below. Field relationships of each of the volcanic units are summarized in Table 2.1, Volcanogenic sulphide deposits are briefly mentioned in the context of the volcanic units in which they occur but detailed descriptions are presented in Chapter 6.

2.5.1.1 Seal Bay Bottom basalt

The Seal Bay Bottom basalt is best exposed on the coast near the mouth of Seal Bay Brook where contact relationships are well displayed. It can be traced in inland outcrops around the core of the Seal Bay anticline, although it is slightly offset by several northeast-trending faults (Figure 2.2).

The Seal Bay Bottom basalt attains a maximum thickness of approximately 600 m on the east limb of the Seal Bay anticline south of the Cramp Crazy Fault. However, it thins dramatically to both north and south to a minimum thickness of less than 200 m. The dominant lithology is moderately amygdaloidal, slightly plagioclase-phyric, pillow lava.

The Seal Bay Bottom basalt conformably overlies epiclastic rocks of Dean's (1978) Omega Point Formation; the contact is exposed on a small island on the west side of Seal Bay Bottom (Plate 2.3) and in inland outcrops southeast of Seal Bay Bottom where pillow lava is chilled and the underlying sediments are baked at the contact. The upper contact is not exposed but is interpreted as conformable.

2.5.1.2 Indian Cove volcanic unit

The Indian Cove volcanic unit, occurring on the east side of Seal Bay between Side Harbour and Mill Cove (Figure 2.2), comprises three stratigraphic subdivisions, a basal rhyolite dome, an intermediate unit of coarse felsic pyroclastic rocks and breccia with minor pillow lava, and

| UNIT NAME | THICKNESS | CONTACT RELATIONSHIPS | | PREVIOUS NOMENCLATURE | INTERBEDDED VOLCANI-CLASTIC ROCKS | MAFIC VOLCANIC ROCKS | | | | FELSIC VOLCANIC ROCKS | | VOLCANOGENIC SULPHIDE DEPOSITS |
		BOTTOM	TOP			%	LITHOLOGIES	PILLOW SIZE	AMYGDALOIDAL	%	LITHOLOGIES	
Seal Bay Bottom basalt	200 m to 800 m	conformable with volcaniclastic rocks (Omega Pt. Fm.)	conformable with volcaniclastic rocks	Sparrow Cove Point Fm. (Dean, 1978)	N/A	100	pillow lava	0.5 to 1 m	moderate	N/A	N/A	
Indian Cove volcanic unit	up to 800 m	not exposed	conformable with volcaniclastic rocks	Side Harbour Fm. (Dean, 1978)	5 to 10 %	< 5 %		< 0.5 m	abundant	> 85 %	quartz-feldspar porphyritic flows, porphyritic and aphanitic pyroclastic rocks	Indian Cove deposit
Glover's Harbour volcanic unit	maximum 1300 m	faulted in west, conformable with volcaniclastic rocks in east	not exposed	Penny's Brook Fm. (Dean, 1978)	~ 10 %	85 %	pillow lava	0.7 to 1.5 m	abundant	~ 5 %	quartz-feldspar crystal tuff	Lockport deposit
Nanny Bag Lake volcanic unit	> 2000 m	not exposed, probably conformable with volcaniclastic rocks	as for bottom	Penny's Brook Fm. (Dean, 1978)	< 5 %	50 %	massive flows, minor pillow lava	N/A	sparse	50 %	quartz-feldspar crystal tuff, possible subvolcanic porphyry	
Long Pond volcanic unit	< 500 m	faulted against South Lake Intrusive Suite	faulted against volcaniclastic rocks (Long Pond fault)	Penny's Brook Fm. (Dean, 1978)	20 %	< 5 %	pillow breccia	N/A		> 80 %	quartz-feldspar crystal tuff, silicic volcanic breccia	Long Pond prospect
Side Harbour volcanic unit	up to 2000 m	conformable with volcaniclastic rocks	as for bottom	Side Harbour Fm. (Dean, 1978)	< 5 %	85 %	mainly pillow lava, minor pillow breccia	0.3 to 0.5 m	sparse	< 15 %	quartz-feldspar crystal tuff, silicic volcanic breccia	Point Leamington deposit
Seal Bay Head basalt	< 100 m	conformable with volcaniclastic rocks	as for bottom	Penny's Brook Fm. (Dean, 1978)	none	100 %	pillow lava, lava tubes	up to 3 m diameter	sparse	N/A	N/A	
New Bay basalt	two flows, one ~ 3m, the other ~ 15 m	conformable with volcaniclastic rocks	as for bottom	Penny's Brook Fm. (Dean, 1978)	approximately 150 m between two flows	100 %	pillow lava	0.3 to 1.5 m	sparse	N/A	N/A	
Badger Bay basalt	> 1300 m	conformable with volcaniclastic rocks	as for bottom	Wild Bight volcanics (Espenshade, 1937), Wild Bight formation (Heyl, 1936), Pennys Bk. Fm. (Dean, 1978)	none	100 %	pillow breccia, lesser pillow lava	1 to 1.5 m	abundant	N/A	N/A	
Northern Arm basalt	~ 1000 m	conformable with volcaniclastic rocks	conformable with Caradocian shale	Penny's Brook Fm. (Dean, 1978)	none	100 %	pillow lava	1 to 1.5 m	moderate	N/A	N/A	
Big Lewis Lake basalt	up to 1300 m	conformable with volcaniclastic rocks	conformable with Caradocian shale	Penny's Brook Fm. (Dean, 1978)	< 10 %	100 %	pillow breccia, lesser pillow lava	1 to 1.5 m	moderate	N/A	N/A~	

Table 2.1: Summary of field relationships of volcanic rocks in the Wild Bight Group
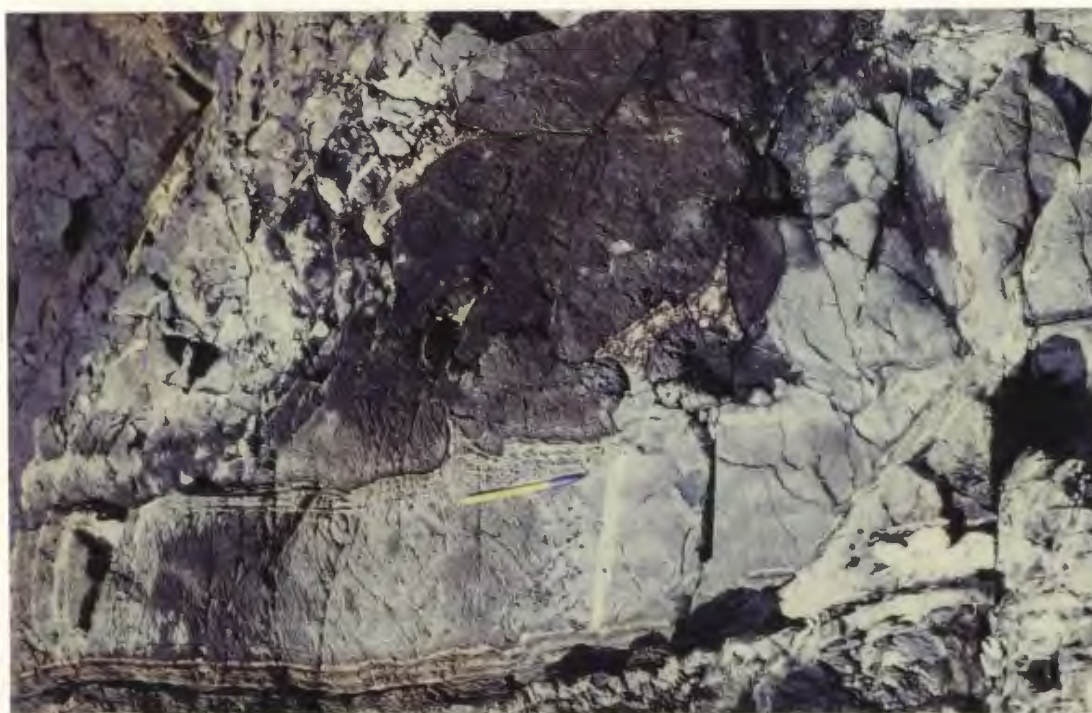
Plate 2.3: Conformable contact between Seal Bay Bottom pillow lava and underlying siltstone. Sediment above and to the right of the pen has been squeezed upward into pillow interstices while still in a plastic state.

an upper, laminated, commonly ferruginous, argillite. These units are disposed in a moderately open, north- to northeast-trending anticline, although in detail the distribution of lithologies is complicated by numerous east to northeast-trending faults (Figure 2.4). The maximum exposed thickness in the central part of the unit is approximately 600 m.

The stratigraphically lowest rocks in the Indian Cove unit consist of massive, buff to green rhyolite dome outcropping in and immediately west of Indian Cove. The rhyolite is extensively hydrothermally altered, locally exhibiting gas breccias and closely spaced fractures filled with epidote, hematite, and pyrite.

The basal rhyolite is overlain by coarse-grained pyroclastic rocks comprising angular and unsorted fragments of rhyolite, chert and lesser basalt fragments ranging in size from less than 1 cm to several 10's of centimeters set in a buff to dark green, felsic to intermediate matrix (Plate 2.4). The deposits are poorly stratified, exhibit very rapid lateral variations and are interpreted as pyroclastic fall deposits resulting from explosive volcanism at a nearby vent. Hydrothermal alteration, locally iron and/or base metal sulphide-bearing, is extensively developed in both the rhyolite dome and the overlying pyroclastic rocks.

The pyroclastic rocks are overlain by and grade laterally into spectacular megabreccias as much as 40 meters thick that contain unsorted, matrix-supported fragments and blocks ranging from 2 cm to 10 meters in diameter (Plate 2.5). These fragments and blocks consist of red chert, green siltstone and minor carbonate, which locally have the form of disrupted and plastically deformed, semi-coherent beds, and are chaotically distributed in a green to slightly reddish chloritic matrix. The megabreccias are interpreted as debris flows formed on the flanks of the volcanic complex.

The top of the Indian Cove unit consists of finely laminated red chert and argillite interbedded with green epiclastic siltstone and sandstone. A few dark grey to black argillite beds, up to 1.5 m thick and locally containing minor conformable massive pyrite beds as much as 10 mm thick, are locally interbedded with green and red argillite. The lowest bedded red chert is apparently stratigraphically equivalent to the debris flow megabreccias.

Figure 2.4: Geology of the Indian Cove volcanic unit. Star marks the location of the Indian Cove Prospect; subsidiary mineralized alteration zones are marked by solid triangles.

Legend: 1 - rhyolite flows; 2- felsic to intermediate, coarse- grained pyroclastic rocks; 3 - pillow lava; 4 - coarse slump breccia; 5 - bedded, green to black argillite and siltstone, ferruginous chert, minor carbonaceous, pyritic argillite; 6 - mafic intrusive rocks.

SEAL BAY

Side Hbr

Mill Cv

0   1
Km
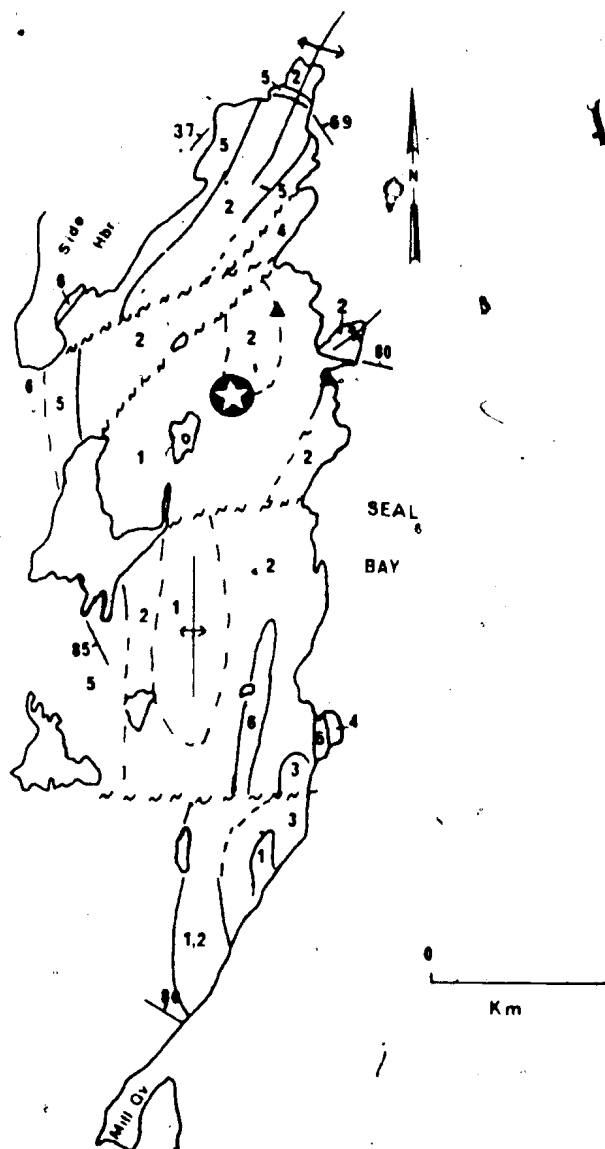
Plate 2.4 : Coarse volcanic breccia in the Indian Cove volcanic unit.

Plate 2.5: Coarse debris flow breccia near Corner Point. Large red fragments are ferruginous chert and argillite.

A single pillowed mafic flow, exposed on the coast south of Corner Point (Plate 2.7), contains the only mafic volcanic rocks in the Indian Cove unit. It is generally amygdaloidal and strongly cleaved; pillow top determinations and outcrop distribution suggest that it occupies the core of a minor anticline and is stratigraphically equivalent either to rhyolitic rocks that form the base of the unit or the lower part of the overlying pyroclastic unit.

Neither upper, nor lower contacts of the Indian Cove volcanic unit are exposed and rocks along strike to the north and south cannot be lithologically correlated with it. This may be a stratigraphic feature resulting from rapid facies changes along strike or non-deposition because of synvolcanic faulting. However, it is also possible that movement on northeast-trending faults through Mill Cove (the Winterhouse Cove Fault) and Side Harbour has removed stratigraphically equivalent rocks from adjacent positions. Almost continuous exposure along the Seal Bay shore between Corner Point and Mill Cove does not reveal any evidence of stratigraphic disruption and in this area, at least, a conformable stratigraphic succession from volcanic to overlying epiclastic rocks can reasonably be inferred.

2.5.1.3 Glover's Harbour volcanic unit

The Glover's Harbour volcanic unit, outcropping in and around Glover's Harbour (Figure 2.5), comprises dominantly mafic volcanic flows, consisting of 0.7 to 1.5 m long, bulbous to moderately flattened and highly amygdaloidal pillows. Most pillows have well developed rims, and minor hyaloclastic material occurs in the pillow interstices; amygdules are generally filled with chlorite, calcite and minor quartz (see also Section 2.7). Both basalts and andesites are present (Chapter 3) although the two rock types cannot be distinguished in the field. Pillow breccia and fine-grained hyaloclastites are common, particularly west of Glover's Harbour.

The pillow lava unit is bisected by up to 200 m of mafic pyroclastic and epiclastic rocks which outcrop on islands and headlands in the central and eastern parts of Glover's Harbour. The pillow lavas to the west and east of this epiclastic/pyroclastic interval are geochemically distinct and the relationship between the two types is further investigated in Chapters 3 and 4.

Figure 2.5: General geology of the Glover's Harbour volcanic unit. Star is location of Lockport Mine.

Legend: 1 - epiclastic sandstone, siltstone, lesser conglomerate, minor argillite; 2- pillow lava; 3 - mafic pyroclastic rocks; may include pillow breccia, local hyaloclastite; 4 - rhyolite; 5 - ferruginous chert
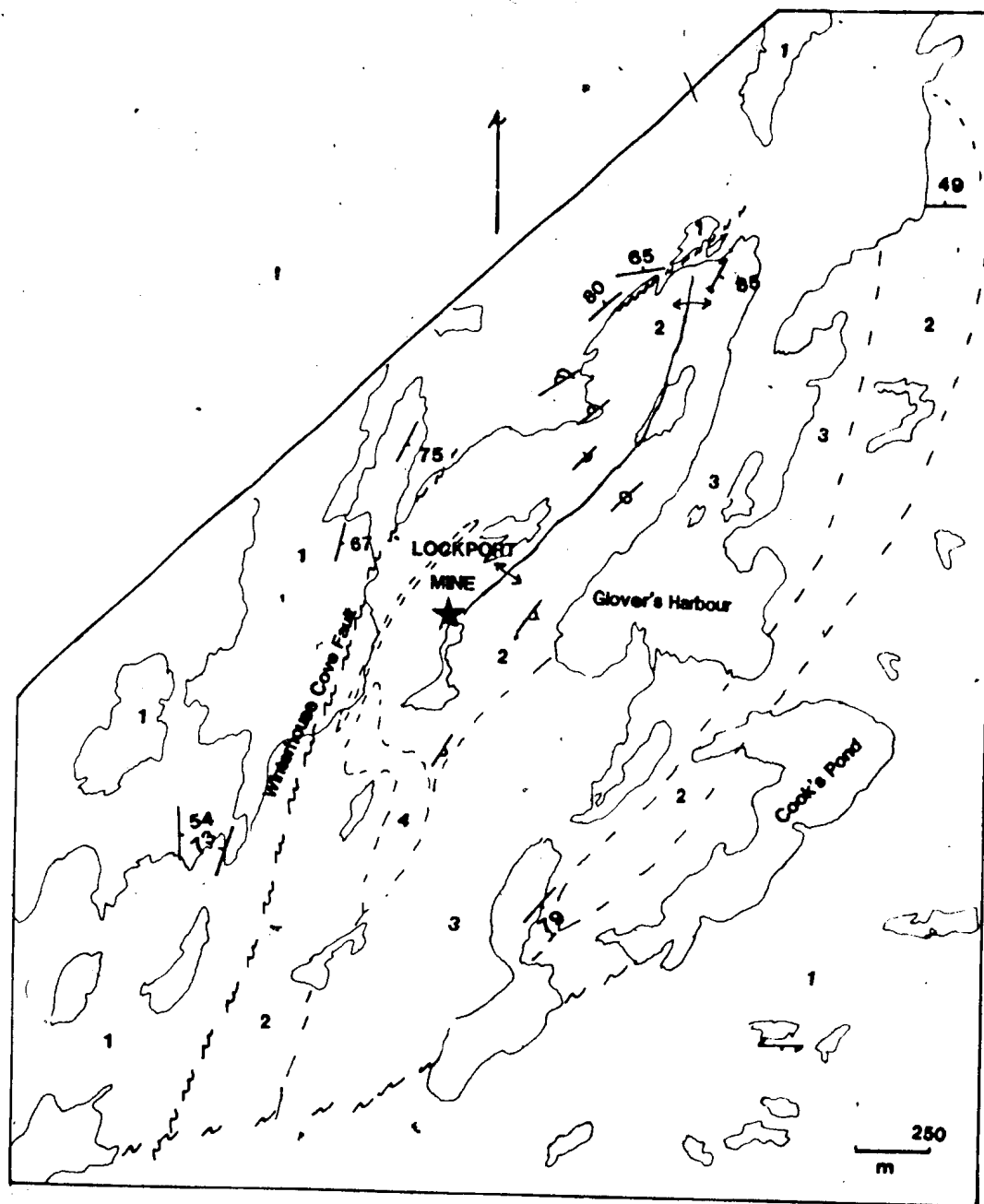
A single felsic volcanic member, consisting of grey to bluish, quartz-feldspar crystal tuff, outcrops on several rocky hills about 1500 m west of Glover's Harbour village. It appears to represent an single ash flow near the exposed base of the Glover's Harbour volcanic unit.

Pillow lavas west of Glover's Harbour host a volcanogenic sulphide deposit, the old Lockport deposit.

The northwest boundary of the Glover's Harbour volcanic unit is faulted against well bedded chert, argillite and sandstone along the Winterhouse Cove Fault, a dextral strike slip fault which is exposed on the coast northeast of Glover's Harbour Head and along the east shore of Winterhouse Cove (Plate 2.1). Adjacent to this fault, the basalts are intensely cleaved and hematized and face northwest. The eastern boundary, exposed on the coast between Glover's Harbour and Leading Tickles, is a conformable succession from volcanic rocks upward into coarse epiclastic conglomerate.

Pillow facing directions in the volcanic rocks suggest that they are disposed in a north-northeast trending anticline, the axis of which lies west of Glover's Harbour (Figure 2.5). A maximum of approximately 1300 m of volcanic and epiclastic rocks occupies the east limb of this fold between its axis and the conformable contact with overlying epiclastic rocks.

2.5.1.4 Nanny Bag Lake volcanic unit

The eastern part of this unit consists of an extensive felsic volcanic complex centered on the west end of Nanny Bag Lake (Figure 2.2). The principal lithology is pale blue rhyolite with minor quartz and feldspar microphenocrysts. Scattered outcrops of medium grained, intrusive, quartz-feldspar porphyry, interpreted as subvolcanic, occur within this felsic complex.

The felsic volcanics pass to the south and west into massive, sparsely- to non-amygdaloidal basalt. A few pillow lava outcrops were observed near the western contact but most of the sequence is composed of massive sheet flows. The basalt is separated from the felsic complex by a thin (less than 50 m) unit of epiclastic greywacke and conglomerate.

As a result of the present mapping, the revised map pattern of the Nanny Bag Lake unit

(Figure 2.2) differs from the compilations of Dean and Strong (1976) in the following particulars:

1) mafic rocks near the New Bay River south and southeast of the felsic center include coarse grained, feldspar-phyric phases, lack volcanic textures and locally have intrusive contacts. Although previously mapped as volcanic, they are here interpreted as intrusive, probably related to the Acadian mafic pluton centered northeast of New Bay Pond.

2) there are no mafic volcanic rocks immediately east of Nanny Bag Lake.

3) mafic (volcanic) rocks north of the Four Mile Lake Fault and east of Big Lewis Lake are reinterpreted as intrusive based on their medium-grained nature and lack of volcanic textures. They are believed to be part of the South Lake Intrusive Complex (Dean, 1978; Lorenz and Fountain, 1982).

There are no exposed stratigraphic contacts between this volcanic unit and the adjacent stratified rocks although clear intrusive contacts with younger mafic rocks are exposed southwest of Nanny Bag Lake. Scattered outcrops of epiclastic rocks within the unit provide the only bedding attitudes and these are generally approximately parallel to those in epiclastic rocks to the west and east. Scattered east-facing top determinations in sedimentary rocks adjacent to the volcanic complex provide the only evidence of facing directions and suggest that the felsic volcanic rocks occupy the stratigraphic top of the unit.

2.5.1.5 Long Pond rhyolite

The Long Pond rhyolite, outcropping in a narrow, north trending belt north of Lewis Lake, comprises dominantly white to buff quartz-feldspar crystal tuff and lesser silicic volcanic breccia. There is a thin (30 to 40 m) unit of highly altered basaltic pillow lava and pillow breccia in the middle of the unit that carries minor disseminated pyrite (the Long Pond prospect). The volcanic rocks are in contact to the west with laminated green chert and pebbly mudstone with minor reddish and black argillite. A prominent red argillite unit is exposed along the east shore of Long Pond and is succeeded to the west by epiclastic sandstone and fine grained conglomerate. Stratigraphic facing directions are not known.

The Long Pond rhyolite probably represents less than 500 m of stratigraphic section. It is fault-bounded on all sides; to the west against epiclastic rocks along the Long Pond Fault and to the east against the South Lake Intrusive Suite.

2.5.1.6 Side Harbour volcanic unit

This laterally extensive unit outcrops in a 15 km long arc between Side Harbour and the area north of Lewis Lake (Figure 2.2). Mafic volcanic flows consisting of moderately amygdaloidal, bulbous pillows 30 to 50 cm across are well exposed in isolated outcrops throughout this belt. Pillows are commonly west-facing and the unit attains a maximum thickness of more than 2000 m at the southern end of the outcrop area.

A small felsic volcanic unit consisting of quartz-feldspar crystal tuff and felsic volcanic breccia outcrops at the western side of the unit northwest of Big Lewis Lake. It is associated with a large volcanogenic massive sulphide deposit, the Point Leamington deposit, and has been traced in drill core for more than 1500 m along strike.

The Side Harbour volcanic unit is bounded above and below by epiclastic rocks. The contact between volcanic rocks and the overlying epiclastic rocks has been observed in drill core near the Point Leamington massive sulphide deposit and is conformable. Elsewhere, the contacts are inferred to be conformable based on parallelism of adjacent strata. The northern end of the belt outcrops in the bottom of Side Harbour but cannot be traced beyond this to the northeast. At its southern end, it is juxtaposed with the Big Lewis Lake basalt along a branch of the Long Pond Fault (Figure 2.2).

2.5.1.7 Seal Bay Head basalt

This unit comprises a thin lens of spectacular (up to 3 m in diameter) pillows and lava tubes in cliff exposures on Seal Bay Head and in the bottom of Wild Bight, Seal Bay (Plate 2.6). The volcanic rocks are only slightly amygdaloidal and little deformed. The entire unit is less than 100 m thick and is exposed along a strike length of slightly less than 2 km. Good three dimensional

Plate 2.6: Large pillows and lava tubes of the Seal Bay Head basalt.

exposures of pillows and lava tubes allow confident determination of westward facing directions.

Conformable contacts with underlying and overlying epiclastic rocks are exposed on the coast at Seal Bay Head and in Wild Bight, Seal Bay.

2.5.1.8 New Bay basalt

The New Bay basalt consists of two thin flows in the bottom of Gull Cove, Wild Bight, New Bay. Rocks in this cove were assigned to the Penny's Brook Formation by Dean (1978) although his map does not show any volcanic rocks in this area.

The upper (westernmost) flow is approximately 3 m thick and in conformable contact above and below with well bedded epiclastic greywacke. The lower flow, roughly 150 m to the southeast, is approximately 15 m thick and enclosed in somewhat finer grained sedimentary rocks, principally argillite. and chert. Both flows consist of slightly amygdaloidal pillow lava with bulbous pillows ranging from 30 to 50 cm in diameter.

2.5.1.9 Badger Bay basalt

This unit, outcropping on the bottom and eastern shores of Wild Bight, Badger Bay, comprises dominantly basaltic, highly amygdaloidal, pillow breccia in which pillow fragments range from 5 to 30 cm across and possess well developed rims on rounded surfaces. Thin pillowed flows make up approximately 20% of the sequence. Complete pillows are locally preserved within the breccias which range from clast-supported (>70% fragments) to matrix-supported (as little as 20% fragments) (Plate 2.7). Groundmass material consists of a fine chloritic (probably hyaloclastic) matrix with abundant small (2-20 mm), angular, basalt fragments. These rocks are interpreted as autobreccias formed on the tops and sides of moving flows, as slump deposits in which pillow debris was transported laterally from the flows into adjacent hyaloclastite and mud and perhaps, in the case of clast-supported facies, as talus on volcanic slopes.

The intact pillow lava flows are 10 to 30 m thick, consisting of 1 to 1.5 m long pillows which generally contain abundant calcite- and chlorite-filled amygdules. Locally pillow lava can be seen

Plate 2.7: Pillow breccia in the Badger Bay basalt. In the upper photo, pillow fragments make up less than 40 percent of the rocks and are supported by a hyaloclastite matrix. In the lower photo, pillow fragments make up more than 75 percent of the rock and the breccia is clast supported.

to grade upward into pillow breccia.

Contacts with adjacent epiclastic strata are not exposed. West of Wild Bight, contacts are interpreted to be conformable based on parallelism of strata; the volcanic rocks in this area are less than 300 m stratigraphically below the Caradocian shale (Shoal Arm Formation).

Existing maps of this area (e.g. Espenshade, 1937; Dean, 1978) show these volcanic rocks as extending up the east side of Badger Bay to the area of Little Cove. The present mapping has shown that this area is in fact underlain by massive to slightly pebbly, dark green epiclastic sandstone locally cut by thin mafic sills. No volcanic rocks were encountered in shoreline traverses of the eastern side of Badger Bay.

2.5.1.10 Northern Arm basalt

This unit outcrops in a northwest-trending band between Northern Arm and the New Bay River and is well exposed in roadcuts along highway 350 near the village of Northern Arm. The dominant lithology is moderately amygdaloidal pillow lava interbedded with minor epiclastic material. The basalts are locally weakly plagioclase-phyric and green chert is locally preserved in the pillow interstices.

The Northern Arm basalt is approximately 1000 m thick and forms an overturned, west-dipping, sequence which is interpreted to be overlain conformably to the northeast by the Caradocian shale (Shoal Arm Formation) and underlain to the southeast by epiclastic rocks of the upper part of the Wild Bight Group. The contacts are not exposed.

2.5.1.11 Big Lewis Lake basalt

The Big Lewis Lake basalt forms an extensive but very poorly exposed unit in the south-central part of the Wild Bight Group. It is juxtaposed with the Side Harbour volcanic unit across the Frozen Ocean Lake Fault but is distinguished from the Side Harbour unit in two respects:

1) It consists mainly of pillow breccia and basalt-bearing volcanic breccia with relatively little pillow lava;

2) It passes conformably up into Caradocian shale and chert of the Shoal Arm Formation and, therefore, occupies a higher stratigraphic position than the Side Harbour unit;

The Big Lewis Lake basalt has a maximum thickness of 1500 m and includes a considerable amount of interbedded epiclastic rocks; an accurate estimation of the proportions is hampered by poor exposure. The inferred distribution of the unit south of the Four Mile Lake Fault on Figure 2.2 differs considerably from that depicted by Dean (1978). Although constrained by only a few scattered outcrops, this distribution is consistent with both airborne magnetic and electromagnetic data and with additional outcrop data collected during the present mapping.

The upper contact of this unit with the Shoal Arm Formation is exposed on the shores of Big Lewis Lake and is conformable. The lower contact is not exposed but is inferred to be conformable with adjacent epiclastic rocks.

2.5.2 Stratigraphic Relationships

Field relationships allow the stratigraphic position of some of the volcanic rocks in the Wild Bight Group to be inferred with reasonable confidence. In other cases, however, structural disruption and the paucity of outcrops in critical areas render such interpretations uncertain. Stratigraphic relations inferred from field data are illustrated in Figure 2.6; units have been placed within the 8.5 km thick succession by inferring the thickness of strata interpreted to lie in stratigraphic continuity between them and either the Caradocian shale or the exposed base of the group in Seal Bay Bottom. These relationships, particularly with regard to correlation of units in light stipple, should be viewed with caution. Structural disruption of the sequence is not understood well enough to correlate stratigraphic units precisely and it is possible that there are major gaps in the stratigraphy between some units and the Caradocian shale; in particular, it is possible the significant portions of the stratigraphic column have been excised and/or repeated by northeast-trending faults, the movement on which is not well constrained (see Section 2.7).

Seal Bay Bottom	Indian Cove	Glovers Hbr.	Nanny Bag Lk	Long P	l.Side Hbr.	Seal Bay Hd.	New Bay	Badger Bay	N'thern Arm	Big Lewis Lk.

Caradocian Shale

No Data

~ 8.5 km

Exposed base of sequence
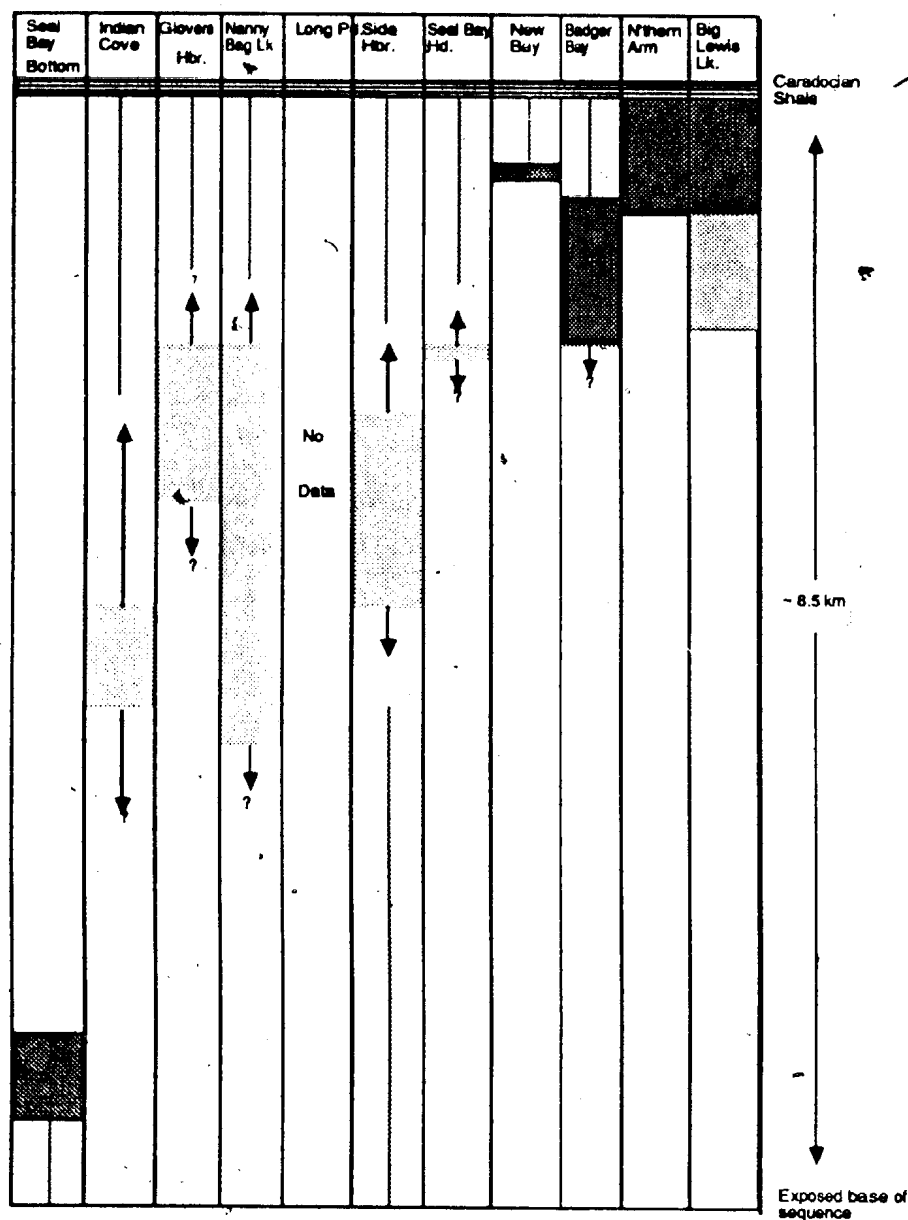
Figure 2.6: Schematic illustration of stratigraphic relationships of volcanic rocks in the Wild Bight Group inferred from field relationships. Observed and inferred stratigraphic ranges are indicated by heavy and light stipple respectively. Thicknesses are inferred maxima. Stratigraphic positions are interpreted from relationships with Caradocian shale and/or the exposed base of the sequence in Seal Bay Bottom. Dotted lines indicate which datum applies to each volcanic unit. Arrows indicate uncertainty in stratigraphic placement.

Although it is clear that most light stippled units occur in the intermediate part of the stratigraphy, the precise correlation of these units with each other, particularly across the Seal Bay Anticline or major faults, is by no means unequivocal. Furthermore, stratigraphic equivalence in this Figure should not be construed as time equivalence; deposition rates and facies may differ in different parts of the group. The evidence for the positioning of units in Figure 2.6 is summarized below.

1). The Seal Bay Bottom basalt is in stratigraphic continuity through an area of good exposure with the exposed base of the group in the core of the Seal Bay Anticline. It is the stratigraphically lowest volcanic unit in the group.

2) The Northern Arm and Big Lewis Lake basalts are apparently conformably overlain by the Shoal Arm Formation and so are interpreted to occur at the top of the Wild Bight Group. Although the contacts are not exposed, there is no evidence for structural breaks or stratigraphic unconformity. Elsewhere in the group, this stratigraphic position is occupied by epiclastic rocks which are interpreted as lateral equivalents of these uppermost volcanic members.

3) The Badger Bay basalt is overlain by approximately 800 m of typical Wild Bight Group epiclastic rocks (in an area of good exposure) and these pass upward into Caradocian shale of the Shoal Arm Formation. These volcanic rocks, therefore, occur close to the top of the Wild Bight Group. A correlation with at least part of the Big Lewis Lake basalt is suggested by stratigraphic position and supported by the lithological similarity between these units, both containing large amounts of basaltic hyaloclastite, volcanic breccia and pyroclastic rocks.

4) The Side Harbour volcanic unit is intermediate in the volcanic stratigraphy. There may be as much as 4 km of underlying epiclastic (and perhaps volcanic) rocks between it and the top of the Seal Bay Bottom basalt and it is probably over 1000 m below the base of the Badger Bay basalts. The top of this unit appears to be along strike with the Seal Bay Bottom basalt.

5) The Nanny Bag Lake volcanic unit is interpreted to be in stratigraphic continuity with the overlying Shoal Arm Formation and separated from it by up to 2000 m of epiclastic rocks. A similar thickness of epiclastic rocks separates the top of the Glover's Harbour volcanic unit from the Caradocian shale on Osmonton Arm.

6) The New Bay basalt is in stratigraphic continuity with and probably less than 1000 m below the Shoal Arm Formation in Leading Tickles. This is an area of good exposure and no major structural breaks have been recognized.

7) The stratigraphic position of the Long Pond volcanic unit cannot be inferred from field evidence as it is fault bounded to the east and west. Likewise, the position of the Indian Cove volcanic unit is enigmatic as the lower and upper contacts are not exposed and it does not appear to fit readily into the stratigraphic sequence along strike. If the western contact is conformable (suggested by the continuity of planar features across the contact) then the top of the Indian Cove volcanic unit is slightly lower in the section than the Side Harbour Formation.

In summary, although it is clear that volcanic activity is represented at several stratigraphic levels in the Wild Bight Group, the various volcanic units can not generally be precisely correlated on stratigraphic evidence. The position of the Seal Bay Bottom basalt near the bottom of the sequence and the Big Lewis Lake, Northern Arm and Badger Bay basalts near the top are well supported by field evidence. Other sequences occur at intermediate parts of the succession but their stratigraphic relationships to each other are less well defined. Geochemical data presented in Chapter 3 provide further evidence as to the precise correlation of these units.

2.5.3 Petrography of the Mafic Volcanic Rocks

Petrographic data for all thin sections are summarized in Appendix 1. Further details of the mineralogy, including electron microprobe data for amphibole, albite and chlorite, are presented in Section 2.8 and in Chapter 3.

Based on primary groundmass features, the mafic volcanic rocks can be subdivided into two classes: 1) rocks with a hyalocrystalline groundmass of randomly-oriented plagioclase laths, locally in subophitic intergrowth with clinopyroxene microcrysts, in an altered, glassy mesostasis; depending on the proportion of cryptocrystalline material, textures vary from intersertal to hyalopilitic, and 2) rocks with a holohyaline groundmass. The proportion of optically resolvable groundmass crystals in the hyalocrystalline mafic volcanic rocks generally varies from less than 5%

to as much as 90%.

The dominant crystalline phase is usually plagioclase, now completely altered to albite (Figure 2.7). The albite commonly occurs as lath-shaped, locally saussuritized, microlites from 0.25 mm to 1.5 mm long (Plates 2.8, 2.9).

Groundmass clinopyroxene (shown by electron microprobe analyses to comprise dominantly calcic augite with lesser endiopside, see Table 3.19) occurs in approximately 30% of the samples and is the only primary mineral phase preserved in the groundmass. It occurs as small (generally less than 0.5 mm in diameter) euhedral to subhedral crystals which commonly have reaction rims and are locally completely psuedomorphed by chlorite and/or amphibole.

The remainder of the groundmass consists of secondary alteration minerals. Chlorite (dominantly diabantite, pycnochlorite and brunsvigite, Figure 2.8) is the most abundant, commonly occurring as irregular plates and microcrystalline aggregates. Epidote is a common, although usually minor, groundmass constituent, occurring as euhedral, isolated crystals up to 0.25 mm in diameter, as slightly larger crystal aggregates and as microcrystalline aggregates. Secondary green amphibole is locally present, mainly in the Glover's Harbour and Nanny Bag Lake suites, occurring as isolated fibrous crystals and sheaves up to 4 mm long. Electron microprobe analyses show a range of compositions from ferro-hornblende to actinolite (Figure 2.8). Amphibole, where present, is generally a relatively late mineral, overgrowing both albite and chlorite but locally being overgrown by late chlorite. Calcite is less common as a groundmass phase; where present, it forms euhedral rhombic crystals and crystal masses which overgrow most other phases. Sphene is a ubiquitous but minor secondary phase. Other minor phases include opaque minerals (mainly magnetite and pyrite with minor ilmenite) and quartz.

Thin sections reveal no regional penetrative fabric and both platy and fibrous secondary minerals are commonly randomly oriented in the rock. The exceptions to this occur in samples taken near major ductile shear zones where all minerals have been realigned parallel to the shearing (Plate 2.10). There was apparently no static mineral growth postdating these shear zones.
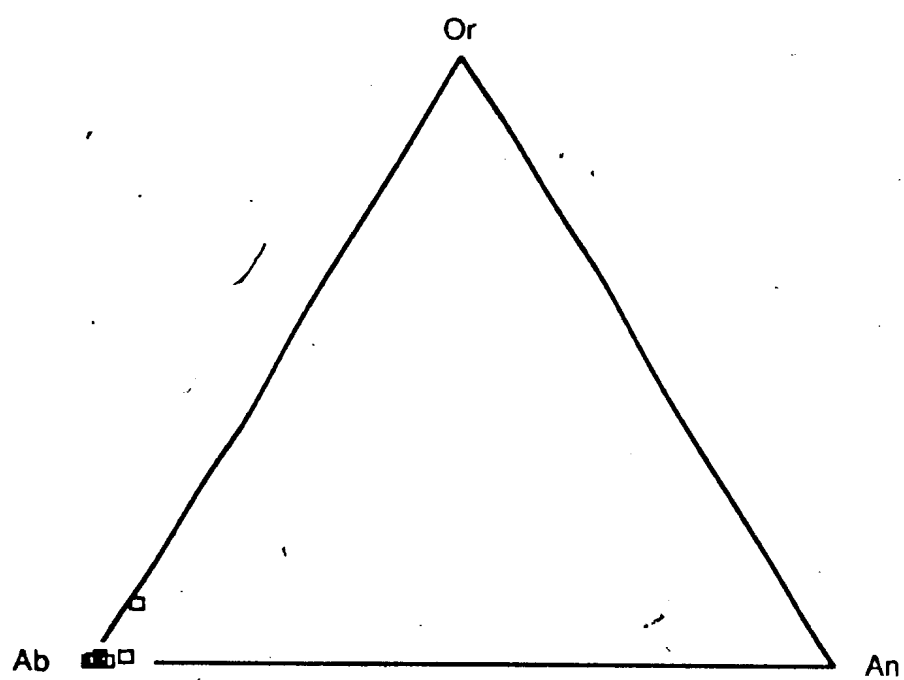
Figure 2.7: Ab-An-Or ternary diagram showing compositions of feldspars in mafic volcanic rocks.

A
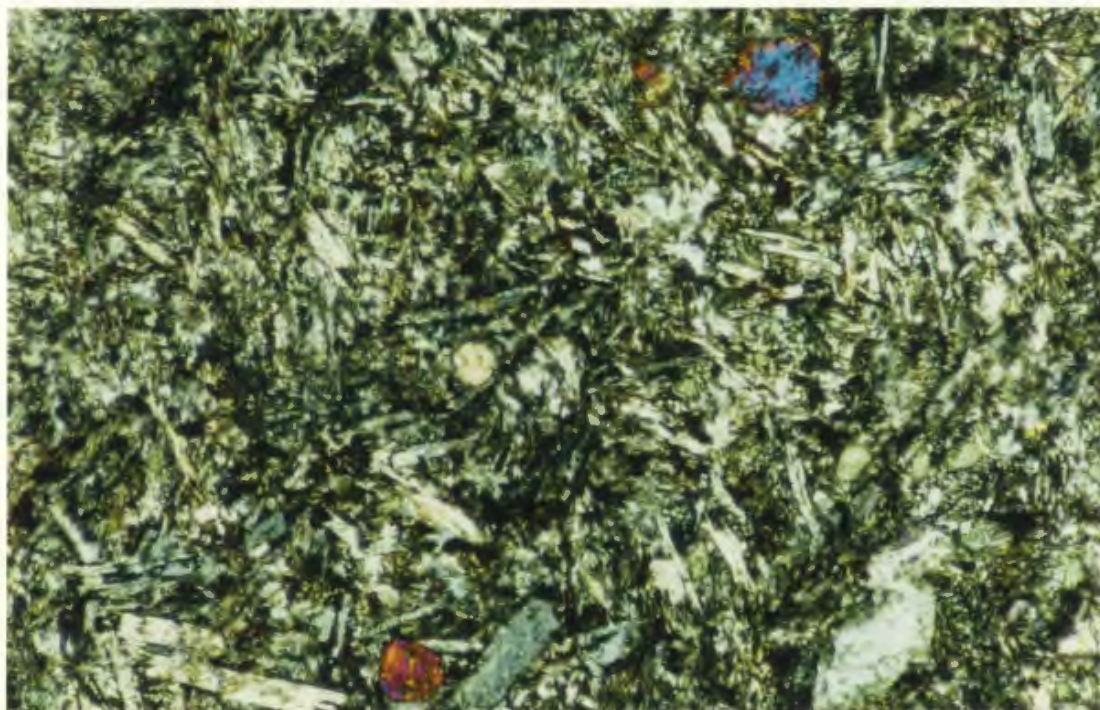
Plate 2.8: Textural variation in the mafic volcanic rocks.

In A, typical hyalocrystalline groundmass with abundant white albite microlites and rare groundmass clinopyroxene (two red and blue equant grains). Much of the material between feldspar grains is chlorite. There is a single, small, round, chlorite-filled, amygdule slightly left of the center of the photo. Crossed polars, field of view is 2.2 mm, sample no. 2140497.

In B, holohyaline groundmass with albite (al) and clinopyroxene (cpx) phenocrysts. Plane polarized light, field of view is 2.2 mm, sample no. 2140463.

In C, highly saussuritized feldspar microlites with groundmass clinopyroxene (small, equant, red/yellow/blue grains) and a single clinopyroxene phenocryst. crossed polars, field of view is 0.9 mm, sample no. 2140467.

B

C

A

B

Field of chlorite compositions in greenschist facies volcanic and plutonic rocks of the Del Puerto ophiolite (Evarts and Schiffman, 1983)

Field of chlorite compositions in greenschist facies volcanic and intrusive rocks penetrated by Hole 504B, DSDP Leg 83 (Alt et al., 1985)
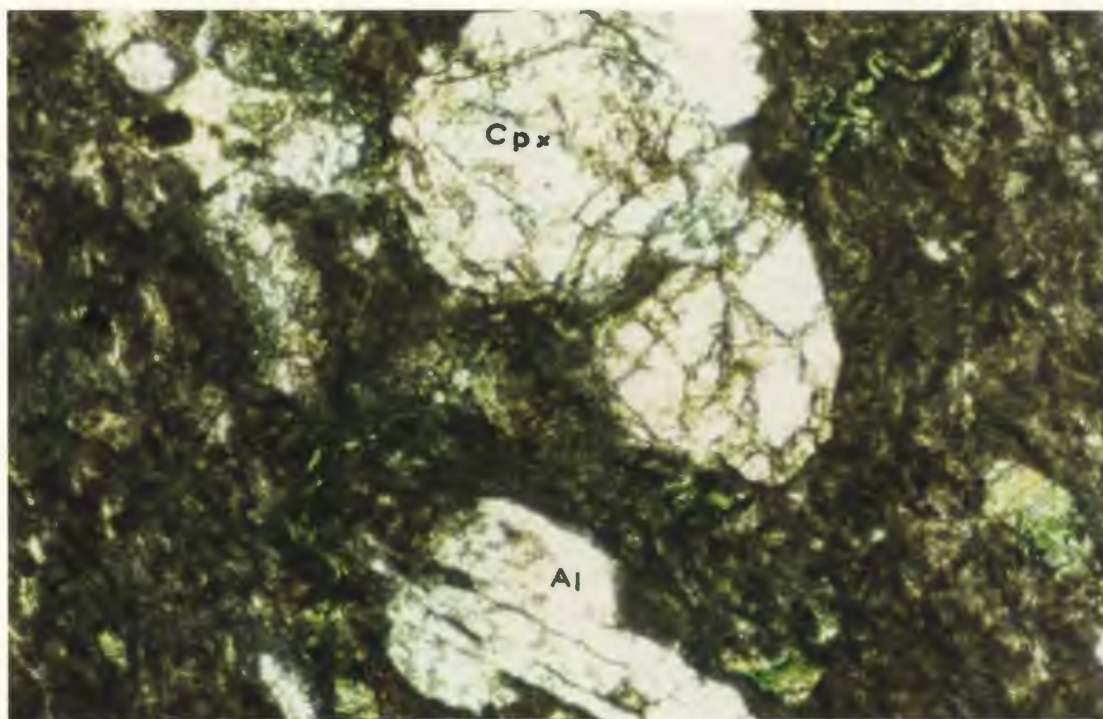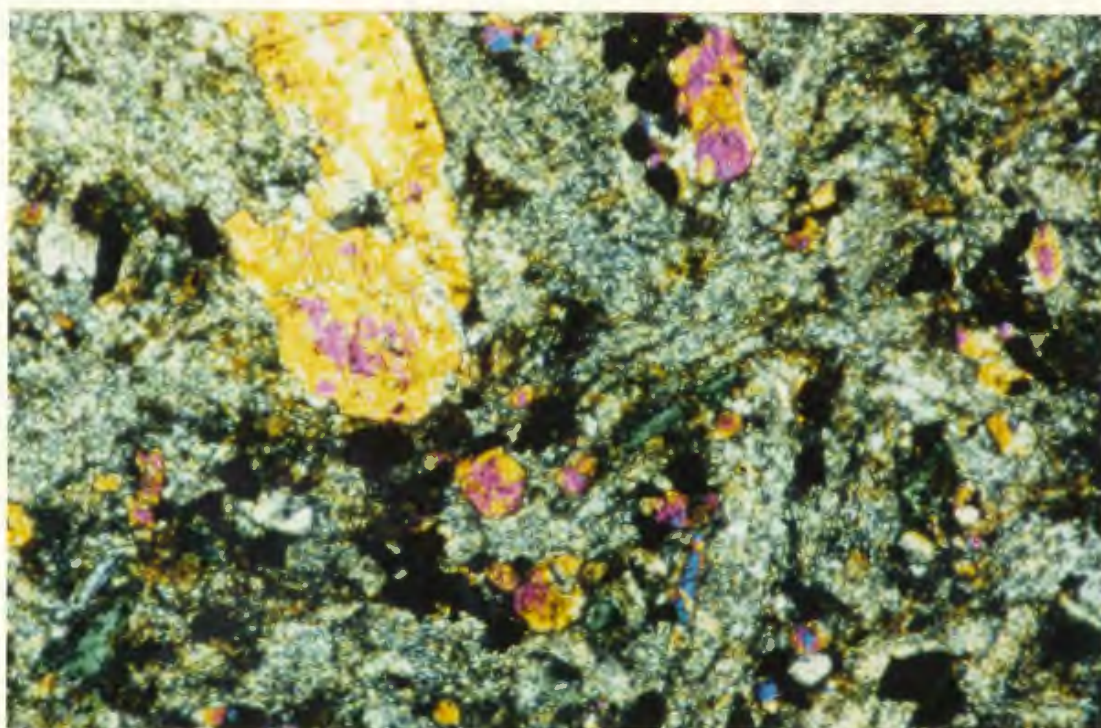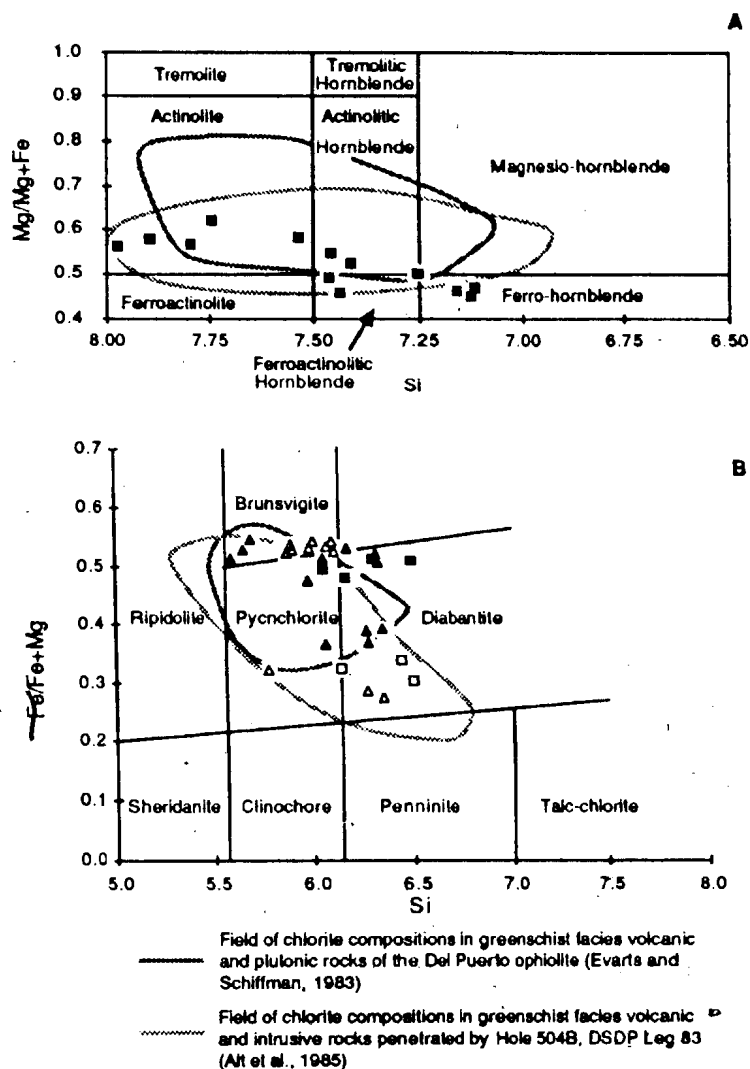
Figure 2.8: Comparison of secondary mineral compositions in Wild Bight Group mafic volcanic rocks with those formed by seafloor metamorphism of modern and ancient oceanic crust.
A - Microprobe analyses of secondary amphibole plotted on an amphibole classification diagram after Leake (1978);
B - Microprobe analyses of chlorite plotted on a classification diagram after Hey (1954). Squares are from groundmass, triangles from amygdules. Open and closed symbols from secondary amphibole-free and amphibole-bearing samples respectively.
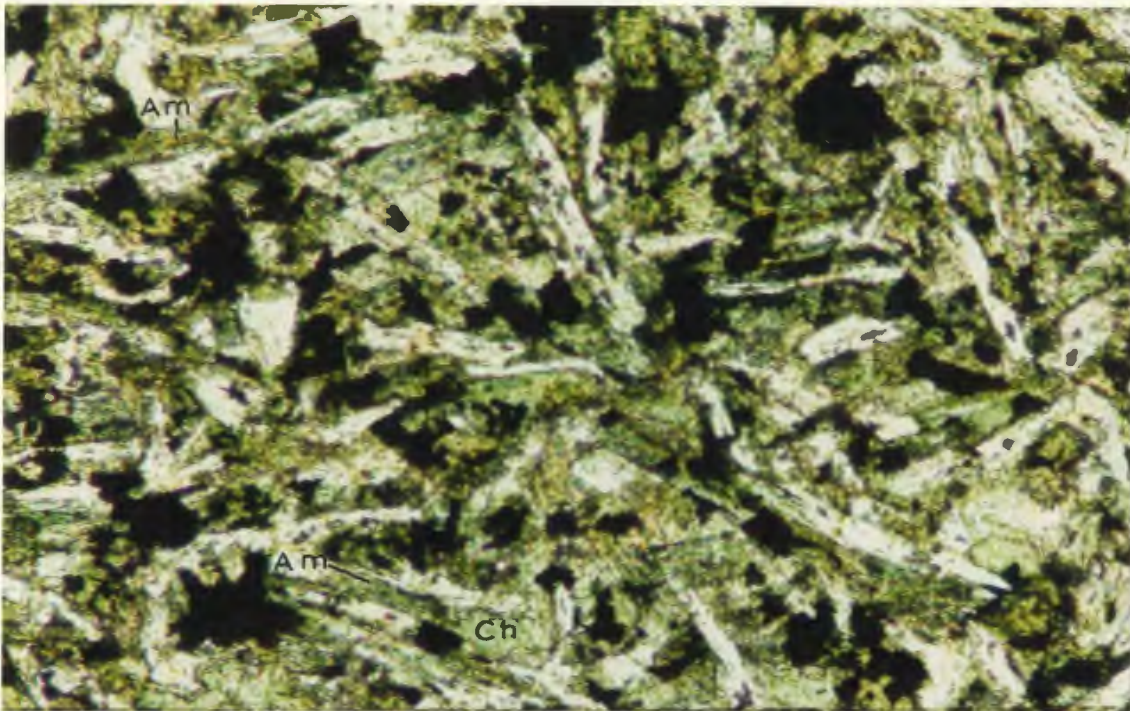
Plate 2.9: Secondary amphibole-bearing mafic volcanic rock. White feldspar laths are intergrown with green amphibole (am) and chlorite (ch). Plane polarized light, field of view is 0.9 mm, sample no. 2140532.
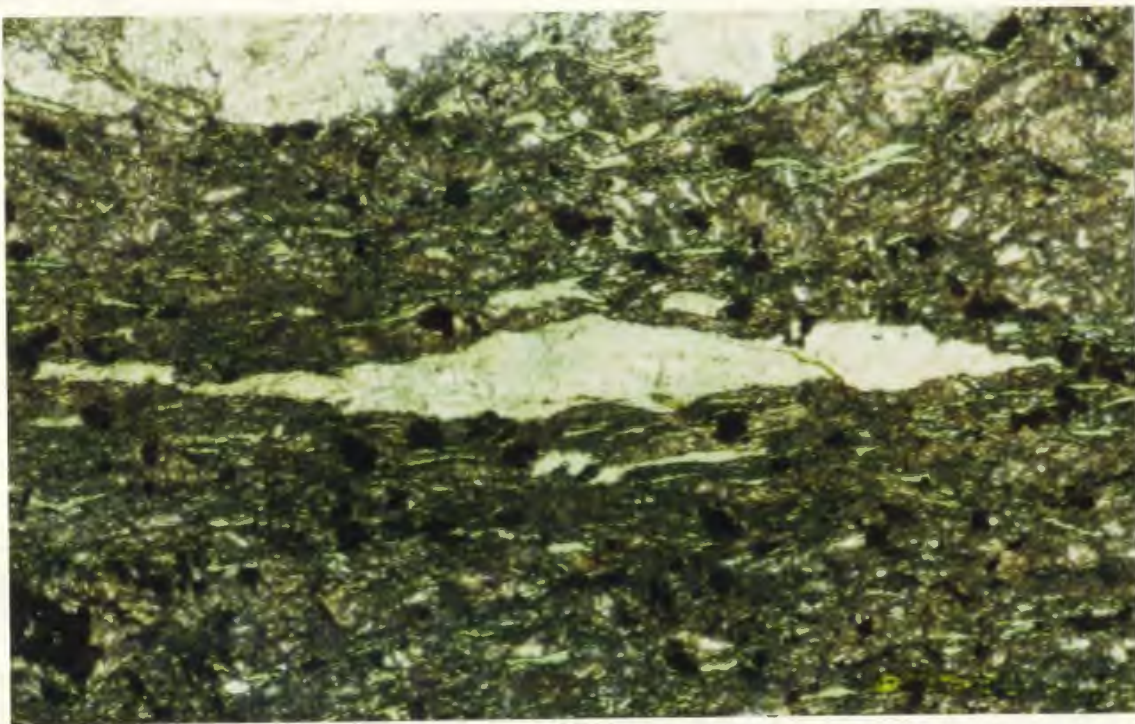
Plate 2.10: Mafic volcanic rocks from within a local shear zone. Chlorite-filled amygdule (center) is strongly flattened in the plane of the foliation defined by chlorite grains. Plane light, field of view is 2.2 mm, sample no. 2140480.

More than 85% of samples have at least one phenocryst phase. Plagioclase phenocrysts ranging from less than 0.5 mm to greater than 6 mm in their longest dimension are the most common. They are commonly euhedral to subhedral, equant to rectangular in outline and locally twinned. However, most are at least partly altered, most commonly to albite with development of checkerboard textures, or to an alteration assemblage including some or all of chlorite, epidote, calcite, amphibole and quartz.

Clinopyroxene phenocrysts, occurring in approximately 50% of samples, are rare in the absence of plagioclase phenocrysts and are generally both smaller and less abundant than plagioclase. Locally occurring in subophitic intergrowth with or poikilitically enclosed by plagioclase, they are typically equant euhedral to subhedral grains, 0.5 to 2 mm (although locally greater than 6 mm) across and locally twinned. Most have reaction coronas and locally they are psuedomorphed by actinolite.

Glomerocrysts up to 10 mm in diameter, consisting of plagioclase and clinopyroxene in approximate proportions of 3:1, were noted in three thin sections. Plagioclase is commonly the coarser phase. In some glomerocrysts, clinopyroxene is absent and in one case, two olivine crystals were noted, the only olivine identified in any of the samples.

More than half of the samples are amygdaloidal although the size and proportion of amygdules is highly variable. Amygdules range in size from less than 0.5 mm to greater than 10 mm and in abundance from less than 1% to greater than 35%. They are filled by a variety of minerals including chlorite, calcite, epidote and epidote group minerals, quartz, amphibole and magnetite in various combinations (see Appendix 1). Chlorite in the amygdules almost invarlably gives anomalous Berlin Blue interference colours, in contrast to the first order greys in the groundmass. Quartz, calcite, and chlorite are the only minerals observed to occur alone in individual amygdules. Where these minerals occur together, they follow a consistent sequence of deposition with quartz being the first, followed by chlorite and then calcite (Plate 2.11). Epidote and amphibole are generally late, overgrowing other mineral phases. This sequence of filling was also observed in the alteration veinlets present in approximately 40% of samples.
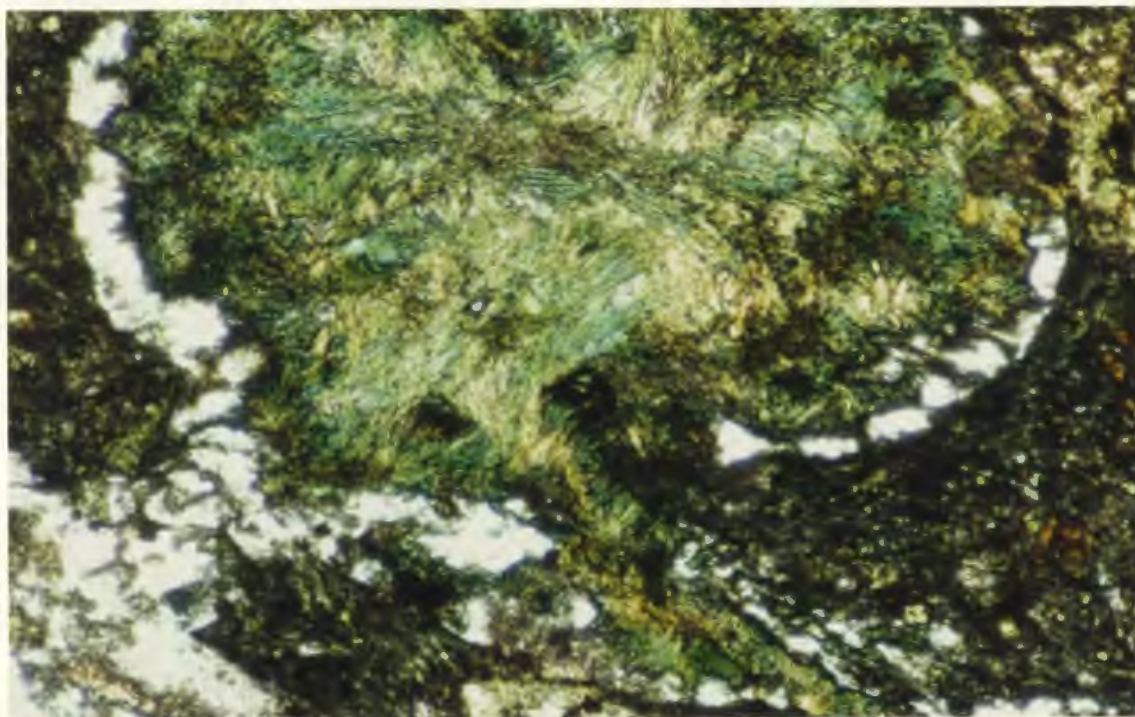
Plate 2.11: Illustration of the sequence of filling of amygdules in mafic volcanic rocks. Quartz in veinlet at lower left of photo also rims the amygdule. Chlorite veinlet in lower right cuts across the early quartz rim and fills the remainder of the amygdule with green fibrous chlorite. Plane polarized light, field of view is 2.2 mm, sample no. 2140460.
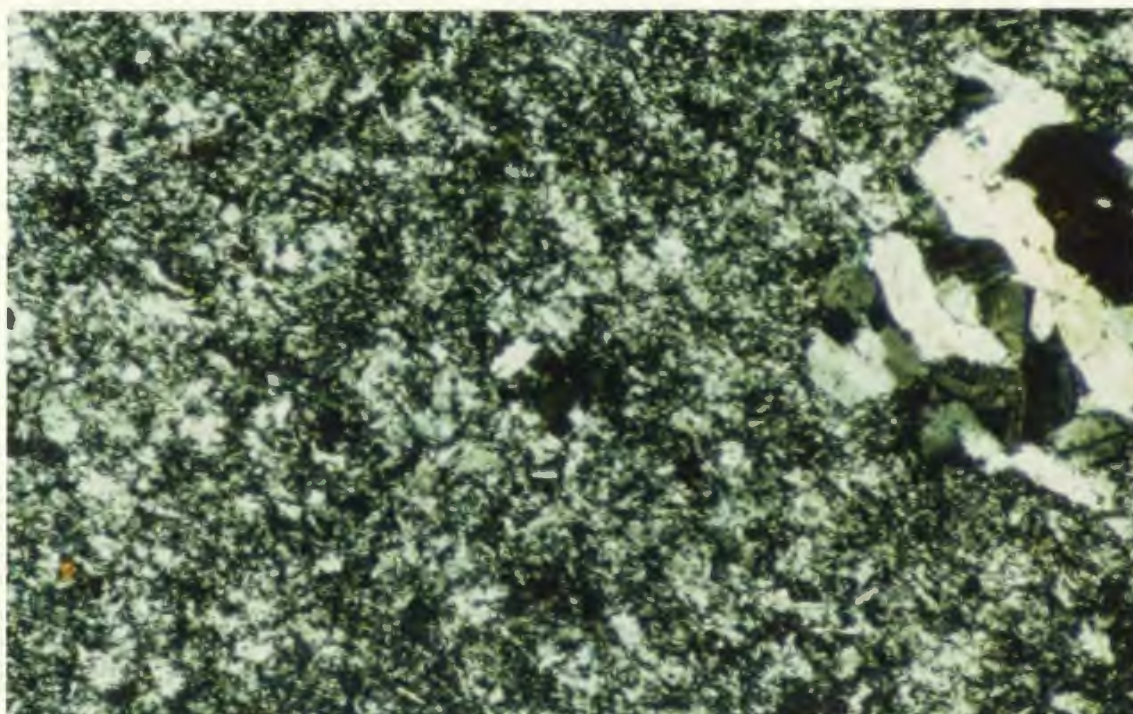
Plate 2.12: Groundmass of felsic volcanic rocks is a fine, quartzo-feldspathic mosaic. A single lithic grain is present in the upper right of the photo. Crossed polars, field of view is 2.2 mm, sample no. 2140490.

Mineralogical and textural features of the basalts exhibit some consistent variations between the geographical suites. Groundmass clinopyroxene is very common in the Side Harbour and Big Lewis Lake basalts and is present in one of two samples in both the Seal Bay Head and New Bay basalts; however, it is absent in other suites. Sphene is relatively abundant in the Side Harbour and Seal Bay Head basalts. Secondary amphibole is very common in the Nanny Bag Lake and the western part of the Glover's Harbour units but less so elsewhere.

Phenocryst sizes and abundances vary considerably within suites. Plagioclase phenocrysts are rare and small in the Nanny Bag Lake unit and absent in the Indian Cove unit but common elsewhere. Clinopyroxene is very rare as a phenocryst phase in the Nanny Bag Lake, Badger Bay and Big Lewis Lake basalts but very common elsewhere. In the Side Harbour volcanics, the feldspar-larger-than-pyroxene relationship is commonly reversed.

Samples from the Glover's Harbour suite (particularly the western part of the unit), as well as the Indian Cove and Badger Bay suites generally contain abundant amygdules. The Seal Bay Head, New Bay, Seal Bay Bottom and Nanny Bag Lake units are generally sparsely to non - amygdaloidal.

2.5.4 Petrography of the Felsic Volcanic Rocks

Most felsic volcanic rocks consist of varying proportions of three components, (1) groundmass, (2) veinlets, and (3) phenocrysts (or crystal fragments).

In almost all samples, most of the groundmass is too fine grained to be resolved optically. Locally, recrystallization has produced irregular quartz grains up to .25 mm across and patches of chlorite (which locally show Berlin Blue interference colours), epidote and, more rarely, calcite (Plate 2.12). Epidote is the most common resolvable groundmass alteration mineral in the Indian Cove suite while chlorite is more common in the Glover's Harbour suite. Sericite was identified in most samples where it commonly forms very small, randomly oriented laths in the groundmass. In a few samples, sericite occurs dominantly in microveinlets and concentrated at the margins of crystal fragments probably having formed in response to abnormally severe potassium
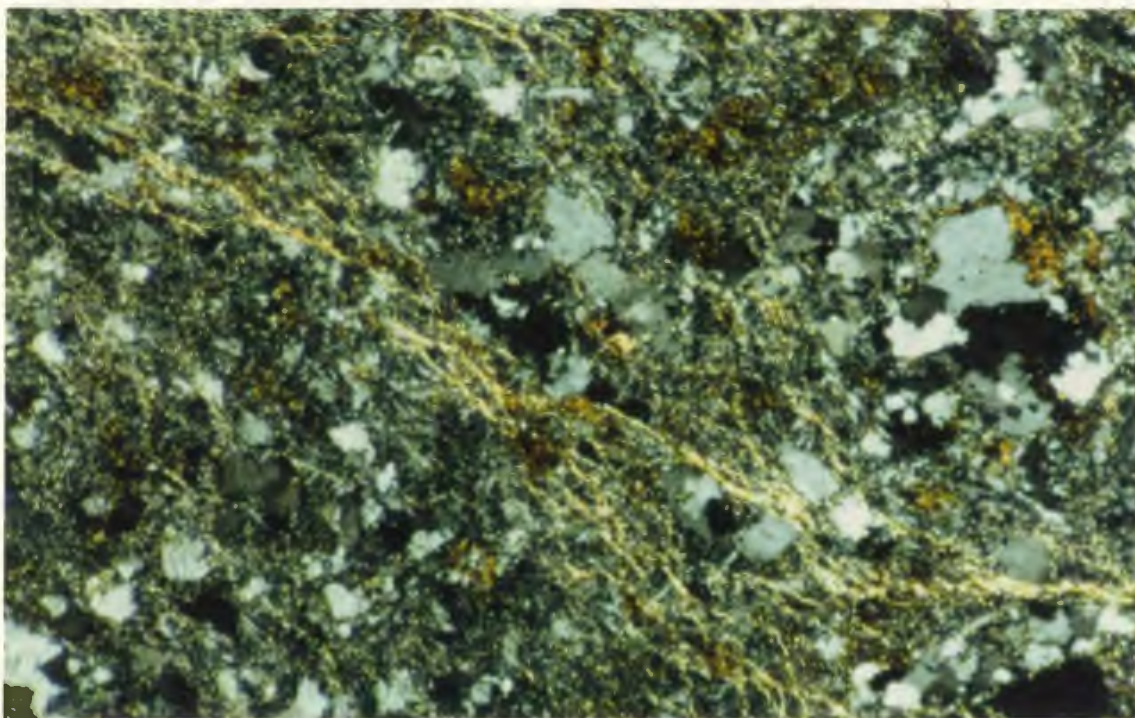
Plate 2.13: Petrographic evidence of potassium metasomatism of a K_2O-rich, rhyolitic tuff. Sericite is abundant in the groundmass (very fine grained yellow specks) and also forms microveinlets in the rock. Crossed polars, field of view is 2.2 mm, sample no. 2140538.
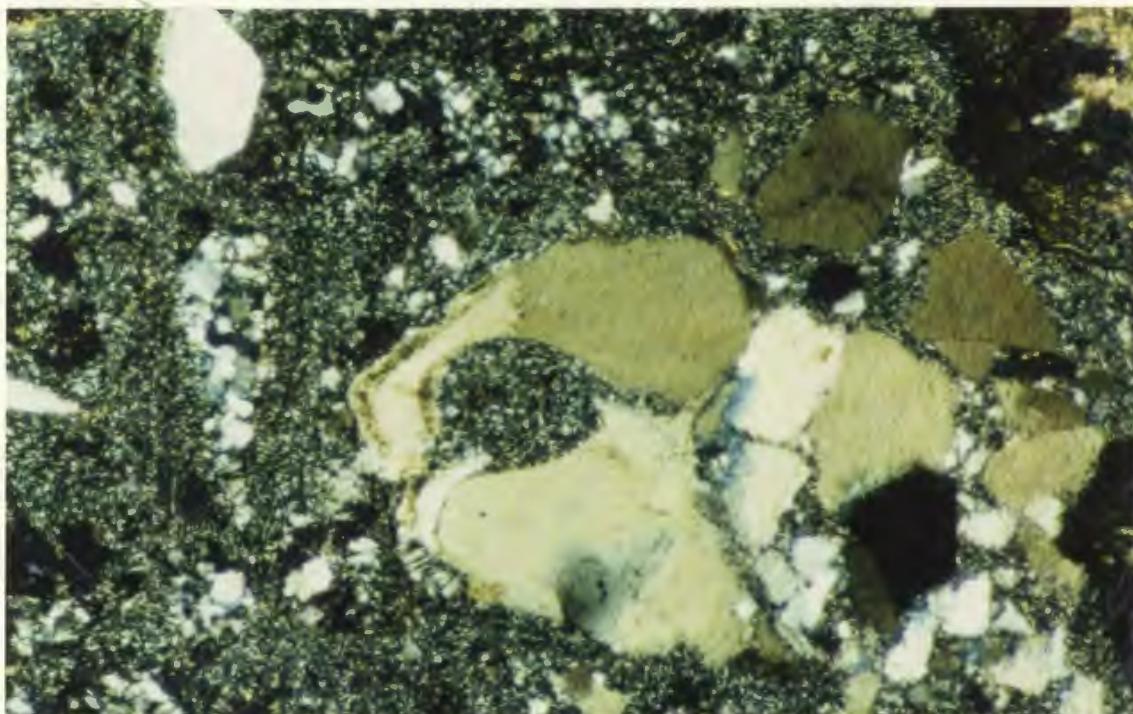
Plate 2.14: Photomicrograph showing rounded quartz crystals fragments with resorption embayments in a felsic volcanic rocks. Crossed polars, field of view is 2.2 mm, sample no. 2140525.

metasomatism (Plate 2.13).

Approximately 75 percent of the samples have phenocrysts or crystal fragments. They range widely in size, from less than 0.5 mm to more than 8 mm across. Plagioclase phenocrysts have been albitized and are generally larger than quartz. Both occur as subhedral to anhedral grains which locally are broken and/or show volcanic (resorption) embayments (Plate 2.14). Feldspar grains are generally cloudy and are locally completely saussuritized. Very rarely, rhyolitic lithic fragments are present.

Most of the samples show clear indications that they are of pyroclastic origin, including broken crystal fragments and the local presence of lithic clasts. However, rhyolitic rocks which form the core of the Indian Cove unit and which were interpreted on field evidence as a rhyolite dome, are generally aphanitic and phenocrysts are rare or absent (e.g. plate 2.12). These consist only of polygonized quartz and feldspar and minor sericite and are the most likely candidates for true rhyolite flows.

Secondary veinlets are not abundant in any samples but are present in all but two samples examined. In the Glover's Harbour, Long Pond and Nanny Bag Lake suites, they commonly comprise narrow quartz veinlets accompanied by minor amounts of other secondary minerals. However, in the Indian Cove samples, the veinlets reflect the pervasive hydrothermal alteration that has affected this unit and are rich in epidote and/or hematite. They are locally very abundant and produce gas breccias in the country rock (Plate 2.15).

2.6 Subvolcanic Mafic Intrusive Rocks

2.6.1 Description and Field Relationships

The Wild Bight Group is cut by numerous mafic sills and dykes, most of which consist either of fine-grained diabase dykes or sills or coarse-grained and/or porphyritic diorite and gabbro sills. Intrusions of intermediate grain size are present but not abundant.

Fine grained intrusions are commonly concordant to slightly discordant. They range from 30 cm to 10 m, but are generally less than 3 m thick. Chlorite- and calcite-filled amygdules are
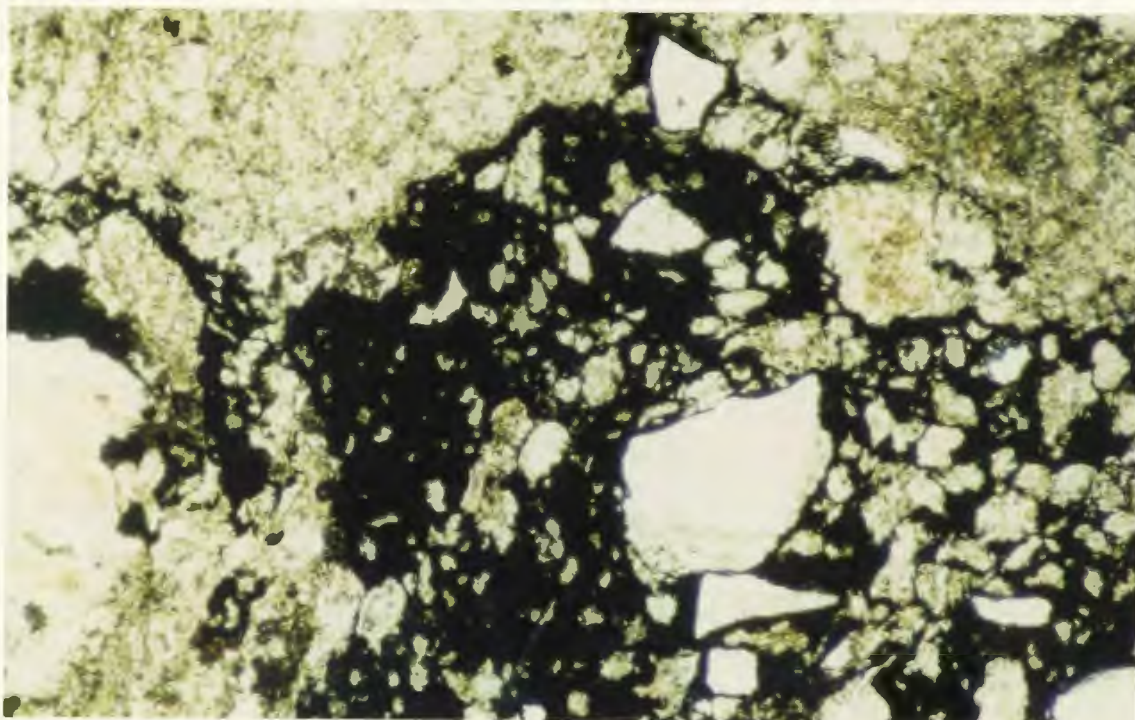
Plate 2.15: Hydrothermal gas brecciation in the Indian Cove rhyolite. In upper photo, dark veins cutting rhyolite consist of hematite, rhyolite fragments and cominuted rock grains. In lower photo, brecciation of rhyolite (white) in a hematite-filled breccia vein is seen in thin section. Plane light, field of view is 2.2 mm, sample no. 2140493.

generally present in amounts ranging from 5% to 25%. The intrusions have chilled margins and the interiors of some contain slightly coarser grained or feldspar-phyric phases.

Field relationships suggest that the fine grained mafic intrusions were intruded early in the history of the Wild Bight Group and are genetically related to the mafic volcanism. These include: (1) The intrusions are locally plastically deformed and broken and associated with numerous quartz and calcite veins suggesting intrusion into wet sediments (Plate 2:16); (2) Although fine grained intrusions have not been observed to feed pillow lavas directly, they do cut and locally terminate in the volcanic units; (3) Mafic intrusive rocks generally do not intrude the sequence stratigraphically above the highest pillow lavas. For example, southeast of Leading Tickles, there are no mafic intrusive rocks in the roughly 800 m of stratigraphic section between the New Bay basalt and the Caradocian shale. Elsewhere, where basalt occurs considerably higher in the section (e.g. below the Big Lewis Lake and the Badger Bay basalts), fine grained mafic intrusive rocks persist to the top of the group; (4) in all areas, the fine grained intrusions are deformed with the adjacent stratified rocks.

Gabbroic sills and lesser dykes are not as common as but generally thicker than the fine grained intrusive rocks, ranging up to several tens of metres. They are generally equigranular, although locally feldspar-phyric, and exhibit good chilled, locally discordant margins. The larger intrusions are commonly polyphase with coarse gabbro cut by fine grained dykes. Complex intrusive relationships indicate that these are phases of the same magmatic event. The fine grained phases are lithologically similar to the fine grained intrusions described above and are deformed with the enclosing rocks. Therefore, they are interpreted as related to the fine grained intrusions and to the volcanic activity.

Geochemical data allow a more detailed correlation of the subvolcanic intrusions and their extrusive counterparts; these data are presented in Chapters 3 and 4 where this relationship is further discussed.

Plate 2.16 Fine grained diabase dyke in red argillite near Omega Point. Dyke is plastically deformed, associated with abundant calcite and quartz veins, and is interpreted to have been intruded into wet sediment.

2.6.2 Petrography of the Fine Grained Intrusive Rocks

The fine grained dykes are generally hyalocrystalline, less commonly holocrystalline, and consist of variably altered plagioclase and lesser clinopyroxene associated with greenschist facies alteration minerals (some or all of epidote, sphene. magnetite, chlorite, rare sericite, quartz and biotite, see Appendix 1). The hyalocrystalline varieties are petrographically similar to the mafic volcanic rocks.

Variably altered, lath-shaped, plagioclase microlites are commonly the most abundant mineral in the groundmass; in some sections these are albitized but in most cases, the plagioclase is almost completely psuedomorphed by epidote, white mica, calcite and opaque minerals. Groundmass clinopyroxene is present in most sections, occurring as small, euhedral to subhedral, equant grains which are locally subophitically intergrown with plagioclase. Olivine, identified in two samples, occurs as small (<0.25 mm), subhedral crystals and is the only other primary phase preserved.

Secondary minerals, as in the mafic volcanic rocks, record a greenschist assemblage. Chlorite is the most common, optically resolvable, alteration mineral. It occurs in the groundmass as green, slightly pleochroic plates and microcrystalline aggregates and locally as crystal aggregates showing Berlin Blue interference colours. It is followed in abundance by epidote group minerals which commonly form cryptocrystalline crystal aggregates and less commonly small euhedral crystals, sphene and opaques (dominantly lath-like ilmenite and magnetite) which are generally the latest alteration products. Secondary amphibole is abundant in one sample.

' Remains of phenocrysts are present in two samples, although in both cases they are highly altered. Sample 2140461 contains 3% to 5% equant pyroxene grains up to 2 mm in diameter, now completely psuedomorphed by chlorite, sericite, sphene and epidote while sample 2140496 has 10% to 15% completely saussuritized plagioclase phenocrysts up to 3 mm long.

A few, very small, chlorite-filled amygdules occur in sample 2140496.

2.6.3 Petrography of the Coarse Grained Intrusive Rocks

. The coarse grained intrusions are generally, highly altered, holocrystalline rocks consisting of plagioclase and clinopyroxene with minor olivine and a variable assemblage of greenschist facies alteration minerals.

Plagioclase is the dominant, and usually coarsest-grained, phase, locally comprising as much as 60% of the rock and occurring as euhedral to subhedral grains up to 10 mm long. It is commonly highly altered; in plane light the grains have a dense, brown dusting that obliterates primary features and in polarized light they are opaque. This alteration is a fine grained mixture of epidote, clinozoisite and sericite and imparts a pale green tint to the feldspars in hand specimen.

Clinopyroxene commonly occurs as subhedral, equant to lath-shaped, unzoned grains which locally have reaction coronas and exsolution lamellae. In many thin sections, clinopyroxene is variably altered to chlorite and epidote and locally only ragged remnants of the original minerals remain. In some cases, clinopyroxene grains poikilitically enclose feldspar.

Olivine is a minor component of approximately 30% of samples typically occurring as fine (less than 1 mm in diameter) equant grains, locally psuedomorphed by a greenschist alteration assemblage.

Magnetite and pyrite are common minor phases and biotite was identified in one specimen. Other secondary minerals in approximately decreasing order of abundance are chlorite, albite, epidote, sericite.

2.7 Structure

Present knowledge of the structural geology of the Wild Bight Group is based mainly on the regional mapping of Espenshade (1937), Heyl (1938), Hayes (1951), Williams (1963) and Dean and Strong (1976). There have been no detailed structural studies in the Wild Bight Group and none were undertaken during the present study. Structural relationships shown on the previous maps were checked and confirmed at critical localities. Stratigraphic observations made during the course of this study point to the need for further, detailed structural work.

The earliest structures in the Wild Bight Group are upright, moderately tight to isoclinal, folds, the axes of which generally trend northerly to northeasterly and plunge northerly at more than 35°. An axial planar penetrative cleavage is inhomogeneously developed in silty and argillaceous sedimentary rocks and volcanic breccias but not in the igneous rocks.

The Seal Bay Anticline is of this fold generation. It is well exposed in Seal Bay Bottom and can be traced in outcrop southwards for approximately 6 km where it intersects the Frozen Ocean Lake Fault (Figure 2.2). South of this fault, strata cannot be correlated on opposite limbs of the fold and it is inferred that there are further complications as a result of unrecognized faulting in this area. South of the Long Pond Fault, the problems of correlation of rocks on opposite sides of this fold are even more pronounced. Although Caradocian shale outcrops on both the east and west sides of the Wild Bight Group in this region, apparently representing the top of respective east- and west-facing sequences and suggesting an anticlinal structure, the section is much attenuated and volcanic rocks below the Caradocian shale on opposite sides of the structure (the Big Lewis Lake and Nanny Bag Lake units) contrast strongly in field and petrographic characteristics (and in geochemistry, see Chapter 3). They clearly do not represent the same unit on opposite sides of a major anticline. Unrecognized structural complexity, possibly including northwesterly - trending faulting, appear to be necessary to explain the distribution of lithologies in this region.

Second generation folds are inhomogeneously developed and do not define a consistent regional structural pattern. These are commonly seen in two settings: 1) adjacent to northeast-trending strike slip faults (see below) where they define a dextral sense of shear and are interpreted to result from dragging of strata adjacent to the faults and; and 2) in shear zones in argillaceous and tuffaceous rocks where they similarly commonly define a dextral sense of shear. Penetrative fabrics related to this shearing are locally developed close to the shear zones.

The Wild Bight Group is cut by numerous northeast-trending rectilinear faults. In coastal outcrops, these are observed to be high angle faults with a dominant strike-slip component (Plate 2.1) and locally, they have significantly disrupted the stratigraphy.

The timing of structural events is not well constrained. However, the F_1 folds affect rocks at least as young as the overlying Sansom Greywacke (Lower Silurian) indicating that folding continued at least through this time (although it could have begun earlier). The F_2 folds are probably related to the northeast-trending faults which truncate and offset the earlier fold axes and are not folded by them. Furthermore, they locally juxtapose Wild Bight Group rocks with Acadian granitoid rocks of probable Devonian age (the Twin Lakes Complex and the Hodges Hill Granite) and, therefore, are probably late Acadian structures. Similar conclusions regarding timing of deformation were reached by Karlstrom *et al.* (1982) from their detailed structural studies of correlative rocks and structures in eastern Notre Dame Bay.

2.8 Metamorphism

' The groundmass mineralogy of the mafic volcanic rocks (albite - chlorite - sphene - magnetite $\pm$ epidote $\pm$ calcite $\pm$ actinolite) is a typical spilitic assemblage which records metamorphism in the greenschist facies. This metamorphism has undoubtedly resulted in some redistribution of elements in the rocks. An estimate of the conditions of metamorphism is necessary to help constrain the probable effects of this redistribution prior to the geochemical discussions in Chapter 3.

There is a voluminous literature concerning the development of greenschist facies metamorphic assemblages in mafic volcanic rocks. Early ideas held that greenschist facies metamorphism commonly resulted from deep burial ($P_{load} > 2$ kb) accompanied by sufficiently high temperatures to allow reactions to proceed (e.g. Gilluly, 1935; Vallance, 1965; Smith, 1968). However, more recent work has shown that hydrous reactions during hydrothermal convection under relatively shallow conditions ($P_{load} < 1.5$ kbars) can also account for the observed metamorphic effects (e.g. Spooner and Fyfe, 1973; Bonatti *et al.*, 1975; Seyfried *et al.*, 1978; Mottl, 1983). Evidence for the nature of these processes comes from a variety of sources including: (1) study of alteration in ophiolitic rocks interpreted to represent ancient oceanic crust

(e.g. Coish, 1977; Stern and Elthon, 1979; Liou and Ernst, 1979; Evarts and Schiffman, 1983); (2) observation of greenschist facies samples drilled or dredged from the seafloor along mid-ocean ridge systems (e.g. Melson et al., 1966; Melson and van Andel, 1966; Humphris and Thompson, 1978a,b; Alt et al., 1985); (3) experimental studies in which hydrothermal fluids are reacted with basalt under varying conditions of temperature and pressure (e.g. Ellis, 1968; Bischoff and Dickson, 1975; Hajash, 1975; Mottl and Seyfried, 1980; Mottl, 1983; Rosenbauer and Bischoff, 1984); and (4) analysis of hydrothermal discharges at sub-seafloor vents in order to infer the conditions existing at depth within the hydrothermal systems (e.g. Edmond et al., 1979; 1982; Craig et al., 1980).

Studies of ancient ophiolites have documented a downward - increasing metamorphism, ranging from sub-greenschist to greenschist facies, that can be interpreted on many lines of evidence as reflecting sub-seafloor hydrothermal alteration through reaction with sea water (Spooner et al., 1977; Liou and Ernst, 1979; Evarts and Schiffman, 1983). Recently, this interpretation has been incontrovertibly confirmed by evidence from Deep Sea Drilling Project (DSDP) Hole 504B in the Costa Rica rift, which cored 1075.5 m of pillow lava and mafic intrusive rocks, the deepest penetration of oceanic crust to date. Petrological and geochemical studies of metamorphism of the mafic volcanic and intrusive rocks in this hole (Alt et al., 1985; Alt and Emmermann, 1985) have demonstrated a continuously increasing grade of metamorphism characterised by sub-greenschist assemblages in the upper part of the hole, and a typical greenschist assemblage including albite - actinolite - chlorite - epidote - sphene below approximately 900 m. The pervasive greenschist alteration, characterised by generally incomplete recrystallization of primary phases, was estimated to have occurred under anoxic conditions through reaction with partially-reacted seawater at temperatures between 200° and $250^\circ C$ (Alt et al., 1985). The sequence of metamorphic changes is in good agreement with the observations of previously cited workers in ancient ophiolites.

Similar interpretations have resulted from experimental studies. For example, Mottl (1983), noting that the experimental studies had been notably successful in reproducing the chemical

changes of hydrothermal, greenschist facies alteration but generally unsuccessful in reproducing the mineralogy, modelled the expected metamorphic assemblages at $300^\circ C$, and 500 to 600 bars for a variety of water/rock ratios using natural assemblages as a guide. He showed that the composition of the alteration minerals, especially chlorite, would be sensitive to changing water/rock ratios during alteration, and that an increasing water/rock ratio should produce increasingly Mg-rich secondary minerals such as amphibole and chlorite.

The greenschist facies metamorphism observed in both mafic volcanic and subvolcanic rocks in the Wild Bight Group, is interpreted as resulting from sub-seafloor, hydrothermal activity that closely followed the volcanic activity. Several lines of evidence indicate this: (1) The abundant alteration veinlets carry the same mineralogy, and in the same filling sequence, as do the amygdules. Locally, the veinlets connect and appear to feed the amygdules (Plate 2.17). The veinlets probably served as conduits for fluids from which the amygdule fillings were precipitated. Evidence from modern seafloor basalts suggests that veinlet formation resulting from fracture- or amygdule-filling is usually an early event attributed to hydrothermal circulation closely following the extrusion of the rocks (e.g. Alt et al., 1985). Because the veinlets cut the spilitic assemblage in the groundmass in most samples, the spilitization must also be an early event; 2) epiclastic sediments in the Wild Bight Group contain mafic volcanic clasts which were spilitized prior to their incorporation in the sediments. This implies that they were altered relatively soon after deposition; 3) the presence of volcanogenic mineralization and relatively intense hydrothermal alteration in some sequences further attests to the circulation of hydrothermal fluids in the rock column during and shortly after the volcanic activity; (4) Compositions of the secondary minerals in the mafic volcanic rocks are consistent with those formed during well documented sea floor metamorphism of basaltic rocks. Plagioclase in the mafic volcanic rocks has been completely altered to albite (Appendix 3; Figure 2.7). Compositions of secondary amphibole and chlorite (Appendix 3) are similar to published examples from both modern and ancient oceanic crust (Figure 2.8).

As noted in Section 2.5.3, secondary amphibole is common in the Nanny Bag Lake and

Glover's Harbour suites but uncommon in other suites. Mottl (1983) showed that the presence or absence of actinolite may in some cases be related to the water/rock ratio during metamorphism, the presence of this mineral being favoured by water/rock ratios of less than 30. If the amphibole-bearing rocks in the Wild Bight Group were metamorphosed at a lower water/rock ratio than their amphibole-free counterparts, the associated chlorite should be more iron rich (Mottl, 1983). Chlorite analyses from amphibole-bearing and amphibole-free rocks are differentiated in Figure 2.8; there is no consistent relationship between chlorite composition and the presence or absence of secondary amphibole in the rocks. (This is not a completely satisfactory criterion. Chlorite compositions will also be influenced by primary Fe and Mg variation in the rocks which may overwhelm any variation resulting from changing water/rock ratios). However, in the absence of other evidence, the alternative interpretation, that the presence of amphibole in some suites reflects slightly higher temperatures during metamorphism, seems more plausible.

Estimates of water-rock ratios during alteration of ancient rocks are fraught with uncertainties. However, comparison with Mottl's (1983) models can yield some useful generalities in this regard. Mottl (1983) predicted from his models, and observed in natural systems, a positive correlation between the modal amount of quartz and chlorite in hydrothermally altered rocks. He recognized two types of metabasalt in studies of modern oceanic crust in the literature, a chlorite-quartz poor variety (chlorite ~ 1 to 25 modal percent, quartz ~ 0 to 3 modal percent) and a chlorite-quartz rich variety (chlorite ~ 42 to 70 modal percent, quartz ~ 3 to 30 modal percent) and suggested that they formed in response to low (W/R<3) and high (W/R>20) water/rock ratios, respectively. In terms of modal alteration mineral percentages, most of the Wild Bight Group rocks would fall in Mottl's chlorite-quartz poor group (see petrographic tables, Appendix 1), indicative of low water-rock ratios.

A low water/rock ratio is further suggested by comparison of the Wild Bight Group chlorite compositions with those for typical metabasalts and compositions predicted by Mottl's models at varying water/rock ratios (Figure 2.9). Most Wild Bight Group chlorites are more iron-rich than Mottl's "typical metabasalt" and many are more iron-rich than chlorite from DSDP Hole 504B. They

x - Calculated model composition of chlorite in mafic
metabasalt resulting from reactions at diffent water / rock
ratios after Mottl (1983).
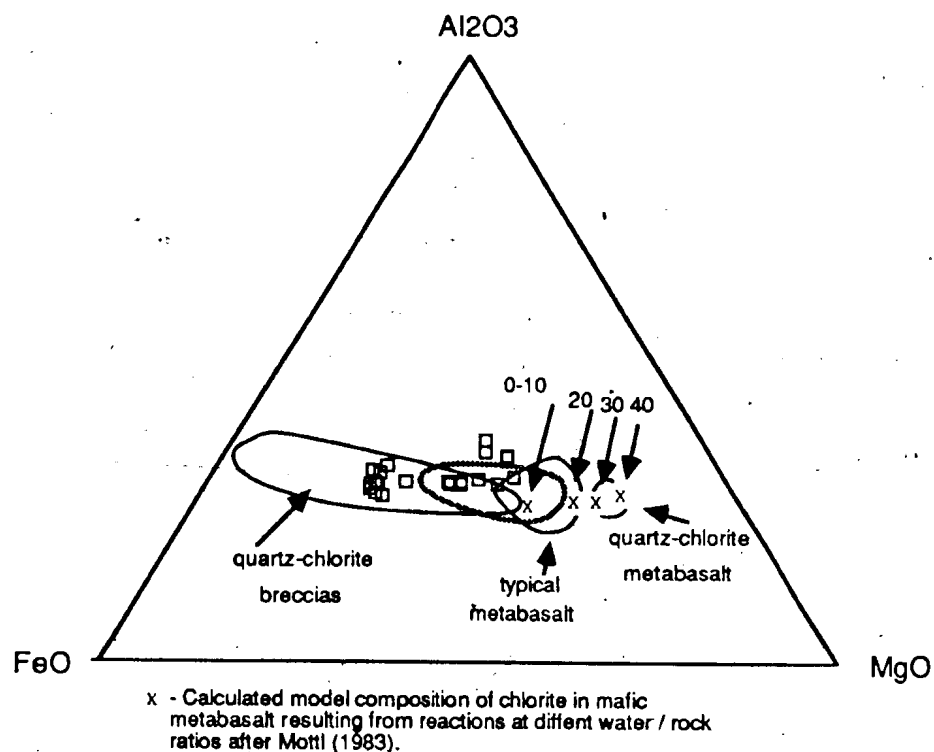
Figure 2.9: AFM diagram for chlorite in mafic volcanic rocks. Fields of
quartz-chlorite breccias, typical metabasalts and chlorite-quartz rich
basalts from Mottl (1983). Stippled line is field of chlorite in greenschist
facies basalt in DSDP Hole 504B (Alt et al., 1985)

clearly have not formed in response to the passage of large volumes of Mg-rich seawater (e.g. high water/rock ratios in the downflow zone of a hydrothermal cell). The postulated relationship between chlorite compositions and water/rock ratio is supported by the comparison of chlorite compositions in amygdules and groundmass in the same specimens (samples 2140477 and 2140510, Appendix 3). Amygdules and fractures in the rock would be expected to have seen a higher water/rock ratio than the adjacent rock because of their greater permeability. In both samples noted above, chlorites in the amygdules have lower Fe/(Fe+Mg) than those in the groundmass, consistent with the expected higher water/rock regime.

A relatively low water/rock ratio is also suggested by FeO/MgO ratios in secondary amphibole. Mottl's (1983) models predict that high water/rock ratios would also be accompanied by formation of MgO-rich actinolite (e.g. for water/rock=10, FeO/MgO>1.4). Examination of the data in Appendix 3 shows that Wild Bight Group amphiboles are considerably more iron rich than this, and are unlikely to reflect high water/rock ratios.

In summary, mineral compositions suggest that hydrothermal alteration of the Wild Bight Group volcanic rocks proceeded at low water/rock ratios and generally at temperatures slightly above the epidote and chlorite stability minimum (approximately 200 to 230°C; Tomasson and Kristmannsdottir, 1972) and below the actinolite stability field (approximately 280°C; Kristmannsdottir, 1976). Locally (e.g. in the Glover's Harbour and Nanny Bag Lake suites) temperatures apparently exceeded the actinolite minimum. These slightly higher temperatures may have resulted from an increase in the heat flow during eruption and subsequent alteration of these suites, a fact that is consistent with and may contribute to models for the development of the Wild Bight Group presented in Chapter 4.

2.9 Summary and Conclusions

The Wild Bight Group is a thick (probably >8 km) sequence of dominantly epiclastic (75%) and volcanic (25%) rocks. The lower contact is not exposed; the stratigraphically lowest rocks are found in Seal Bay Bottom in the core of the Seal Bay Anticline. The top of the sequence,

represented by epiclastic rocks in some areas and laterally equivalent mafic volcanic rocks in others, is conformably overlain by fossiliferous carbonaceous shale and chert of Caradocian age.

Sedimentary rocks at the bottom of the group are fine-grained, quiet water facies but above the first volcanic flows, they pass into a succession characterised by sandstone turbidites and coarse-grained debris flows. At the top of the group, relatively quiet water conditions are once again prevalent.

Volcanic rocks outcrop mainly in the eastern part of the group, occurring in eleven separate geographic areas and occupying various stratigraphic intervals. Mafic volcanic rocks include pillow lava, pillow breccia and fine grained hyaloclastite and massive sheet flows. Felsic volcanic rocks are locally present. Figure 2.10 summarizes the principal geological and petrological features that distinguish the different mafic volcanic units and highlights some points of comparison and contrast between them including:

(1) Mafic pillow lava is the dominant lithology in most volcanic units. Exceptions are the uppermost units in the western Wild Bight Group (the Badger Bay and Big Lewis Lake units) where pillow breccia is predominant and the Nanny Bag Lake unit in the southeastern part of the group where mafic volcanic rocks comprise mainly massive sheet flows. volcanic unit where they are associated with minor pillow lavas.

(2) Five of the volcanic units include felsic volcanic rocks and four of these have associated volcanogenic mineralization. All occur in the intermediate part of the stratigraphy.

(3) Secondary amphibole in mafic volcanic rocks is common only in the Nanny Bag Lake and Glover's Harbour areas.

(4) Plagioclase-phyric mafic volcanic rocks are widespread, except in the Nanny Bag Lake area. Clinopyroxene-phyric rocks are uncommon in the uppermost volcanic units but common in most other areas.

(5) The proportion of amygdules in the rocks varies widely. Quartz-bearing amygdules are common only in the Indian Cove and Glover's Harbour areas, in rocks that have both associated felsic volcanic rocks and volcanogenic mineralization.

Suite	Geological Features					Petrographic features of mafic volcanic rocks					
	Dominant mafic lithology			felsic volc.	mineral-ization	g'mas s cpx	amphi-bole	plag. pheno.	cpx. pheno.	amyg-dules	quartz-filled amyg.
	pillow lava	mass flows	pillow bx.								
Seal Bay Bottom	▨					▨		▨	▨		
Indian Cove	▨			▨	▨						▨
Glover's Harbour	▨			▨	▨		▨	▨	▨	▨	▨
Nanny Bag Lake		▨		▨			▨				
Long Pond			▨	▨	▨	N/A					
Side Harbour	▨			▨	▨	▨		▨	▨		
Seal Bay Head	▨							▨	▨		
New Bay	▨							▨	▨		
Badger Bay			▨					▨			
Northern Arm	▨							▨			
Big Lewis Lake			▨					▨			

Figure 2.10: Qualitative summary of geological and petrological features of the Wild Bight Group volcanic units. Intensity of stipple is proportional to relative abundance (except felsic volcanics and mineralization where stipple indicates presence, no stipple absence).

Stratified rocks throughout the group are cut by mafic subvolcanic sills and dykes of fine to medium grained diabase and coarse-grained gabbro. Several lines of geological evidence indicate that they are related to the Wild Bight Group mafic volcanic rocks.

Structural relationships in the Wild Bight Group are more complex than existing maps would indicate. In particular, the section is considerably attenuated in the southeastern part of the group and a considerable stratigraphic section is probably missing south of the Long Pond Fault. Major, northwest-trending faulting seems to be necessary to explain relationships in this area.

The mafic volcanic rocks are commonly altered to a spilitic assemblage including some or all of chlorite - albite - quartz - epidote ± actinolite, sphene, magnetite, and calcite. The metamorphism is interpreted as sub-seafloor hydrothermal alteration which probably occurred at very low seawater/rock ratios. Temperatures in the $200°$ to $280°C$ range are generally indicated although abundant secondary amphibole in the Nanny Bag Lake and Glover's Harbour suites may signal slightly higher temperatures in these areas.

CHAPTER 3

GEOCHEMISTRY OF VOLCANIC AND SUBVOLCANIC ROCKS IN THE WILD BIGHT GROUP

3.1 Introduction

Whole rock samples from mafic and felsic volcanic rocks representing all known volcanic accumulations in the Wild Bight Group as well as a representative collection of mafic subvolcanic rocks were analysed for major and standard trace elements. In addition, samples selected on the basis of initial results were further investigated through analysis for rare earth elements (REE) and selected high field strength elements (HFSE) and through microprobe analyses of primary clinopyroxene.

Sampling and sample preparation methods are described in detail in Appendix 4. In most cases, volcanic units were sampled so as to obtain a representative collection from throughout their areal extent, although in a few cases, systematic sampling at short intervals was carried out across strike in the volcanic members in order to test within-suite variability.

Sample locations are shown on Figure 3.1. Universal Transverse Mercator (UTM) grid coordinates, given in Appendix 5 for all sample locations, pinpoint the sample locations on the ground to ±50 m. Most mafic volcanic rock samples are from pillow lava, the exception being the Nanny Bag Lake suite which comprises dominantly massive basalt and contains only a few pillowed flows. Samples were taken from the crystalline interiors of pillows, and selected in order to minimize the effects of weathering, alteration and vesiculation.

Mafic subvolcanic rocks include both aphanitic to fine grained diabase and medium to coarse grained gabbro. Samples were taken from the interiors of dykes and sills and chosen to minimize alteration, vesiculation and weathering.

Representative samples were collected from felsic volcanic rocks at all localities where they outcrop and include samples of both quartz- and quartz-feldspar phyric crystal tuff as well as
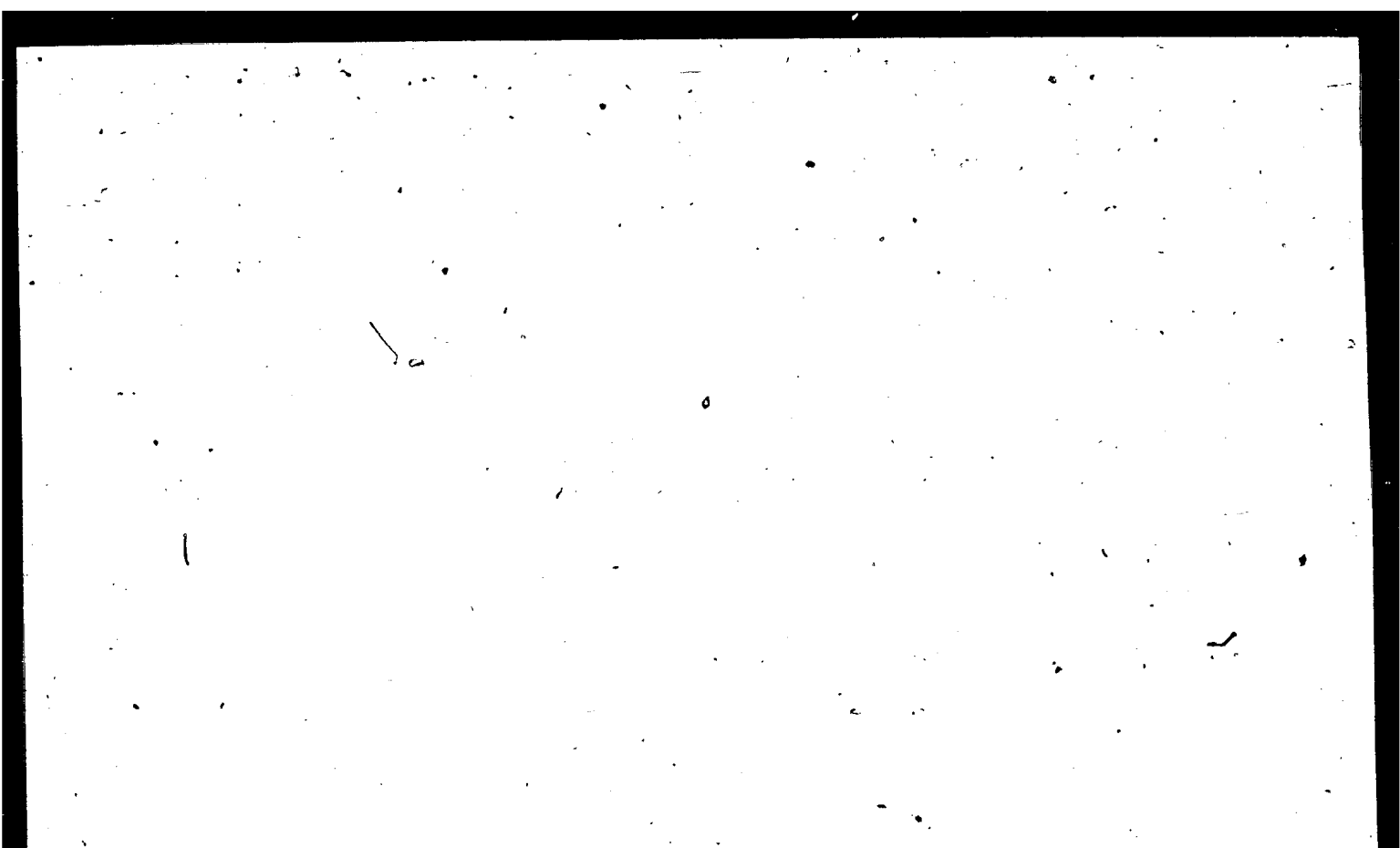
Figure 3.1: Location of geochemical samples. Squares are mafic volcanic rocks, triangles felsic volcanic rocks, circles mafic intrusive rocks. Sample numbers are the last three digits of seven-digit numbers used elsewhere in the thesis. Base map as for Figure 2.1.
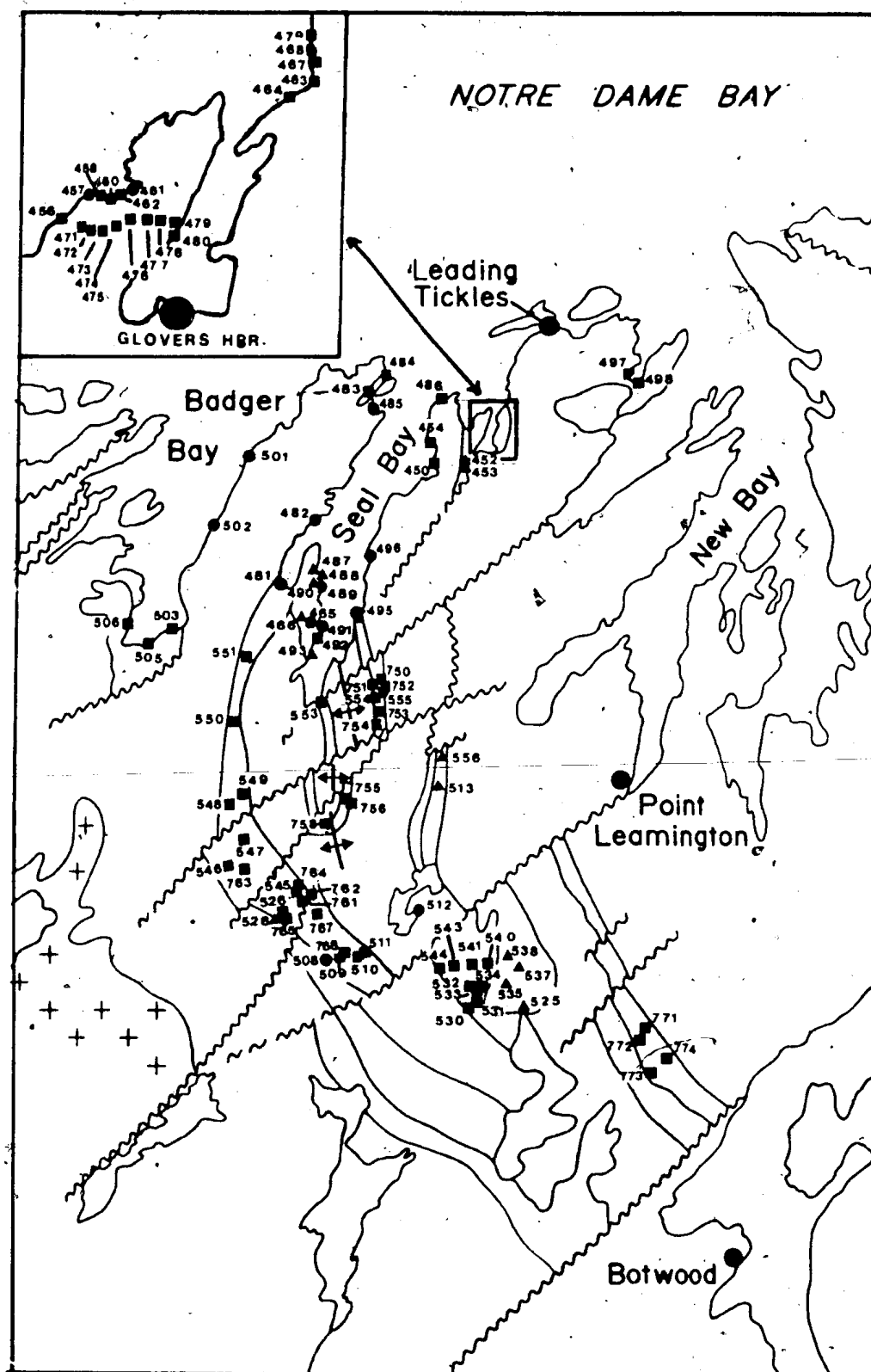
massive aphanitic flows. In the Indian Cove unit, where hydrothermal alteration is widespread, samples were selected to avoid zones where alteration effects were visible in outcrop.

Major elements as well as Cu, Zn and Ni were analysed at the Newfoundland Department of Mines and Energy laboratory by atomic absorption spectrometry. FeO was determined by titration with standard potassium dichromate. Loss on ignition (LOI) was determined by weighing a sample before and after heating to $1200°C$; gas compositions were not determined. The trace elements Rb, Sr, Y, Zr, Nb, Ba, V and Cr were determined at Memorial University by X-ray fluorescence analysis of pressed pellets. REE were determined on some samples at Memorial University by ion exchange chromatography and X-ray fluorescence according to the method of Robinson et al. (1986) and on other samples, along with Ta, Hf, Th, and Sc, by instrumental neutron activation analysis (INAA) by J. Hertogen at Universiteit Leuven, Leuven, Belgium. Details of analytical methods as well as estimates of precision and accuracy of the methods are presented in Appendix 6.

Sixty-nine mafic volcanic whole rocks were analysed for major and standard trace elements. In addition, 22 were analysed for REE and selected trace elements by INAA and a further 9 for REE by X-ray fluorescence. Whole rock analyses for major and trace elements are presented in Tables 3.2, 3.5, 3.8, 3.9, and 3.10.

Seventeen mafic subvolcanic whole rocks were analysed for major and standard trace elements and an additional 9 for REE and selected trace elements by INAA. Analytical results are presented in Table 3.13.

Fourteen felsic volcanic whole rocks were analysed for major and standard trace elements and an additional 3 for REE and selected trace elements by INAA. Analytical results are presented in Table 3.17.

Study of the chemical composition of the mafic volcanic rocks has shown that they represent a heterogeneous assemblage of magmatic rocks and probably record more than one tectonic environment. Any attempt to summarize the composition of these rocks at this point would, therefore, be difficult and premature. In the following Chapter, following a brief

assessment of the probable effects of alteration, a subdivision based on geochemical parameters is introduced and the rocks that define these classes are described. On all major element diagrams in this and subsequent Sections, elements have been recalculated to 100 percent anhydrous.

3.2 Effects of Alteration in the Mafic Rocks

The use of geochemical data to interpret the magmatic history of volcanic rocks is based on the assumption that some original geochemical characteristics of the rocks have been preserved. Field and petrographic evidence, however, clearly indicates that all mafic volcanic rocks in the Wild Bight Group have been metamorphosed in the greenschist facies. An assessment of the probable effects of this alteration on their composition is necessary as a prerequisite to discussing their geochemistry in detail.

There is a voluminous literature on the effects of alteration and metamorphism on the composition of igneous rocks, particularly directed towards the question of which elements remain essentially immobile. Various approaches to investigating this problem have been attempted including:

1) comparison of the chemical characteristics of relatively more and less altered rocks in order to establish element mobility vectors (e.g. Humphris and Thompson, 1978a; Ludden and Thompson, 1979; Schrader and Stow, 1983; Alt et al., 1985).

2) experimental studies on the reaction of seawater and basalt under greenschist conditions (e.g. Ellis, 1968; Bischoff and Dickson, 1975; Seyfried and Bischoff, 1981; Mottl, 1983);

3) study of the chemistry of hydrothermal fluids aimed at interpretation of the alteration conditions at depth in the hydrothermal system; (e.g. Arnorrson et al., 1978; Giggenbach, 1981.)

4) comparison of the stability of inter-element relationships, the nature of which can be inferred from observation or theory (e.g Pearce and Cann, 1973; Pearce and Norry, 1979; Stephens, 1982);

5) theoretical treatment of the mobility vectors of various elements during mineralogical change and fluid flux (e.g. Bird and Norton, 1981; Goff, 1984).

A complete review of studies of element mobility during alteration is beyond the scope of the present study. Such a review has recently been carried out by Goff (1984) and to a lesser degree by Stephens (1982). There is substantial agreement among most workers that many elements, including P, Ti, Y, Zr, Nb, Hf, Ta, Th and the heavy rare earth elements (HREE), are essentially immobile on hand specimen scale, during seafloor weathering and low grade hydrothermal alteration. In addition, Sc, V, Cr, Co, Ni and the light rare earth elements (LREE) may be sufficiently immobile under these conditions for use in petrogenetic interpretations (e.g. Miyashiro *et al.*, 1971; Humphris and Thompson, 1978a,b; Coish, 1977; Stephens, 1982; Goff, 1984). Al may be stable through low grade alteration but Fe, the alkali metals and the alkaline-earth metals are variably mobile and their absolute and relative abundances may be disturbed. Before using these elements, therefore, some assessment of the effects of alteration must be made.

The mobility of the alkali elements Na and K in mafic rocks can be assessed using the 'igneous spectrum' diagram of Hughes (1973), on which fields of normal igneous rocks, spilites and keratophyres are defined on a binary plot of two functions of K_2O and Na_2O. On this diagram, shown in Figure 3.2 with field boundaries after Stauffer *et al.* (1975), approximately 75 percent of mafic volcanic rocks plot outside the 'igneous spectrum'. Most of these plot in or near the 'spilite' field, suggesting substantial Na_2O addition and K_2O depletion although Na depletion is suggested in five samples that plot below the field. Samples that plot within the 'igneous spectrum' may be relatively unaltered; however, it is also possible that they have experienced K_2O and Na_2O addition in appropriate proportions to have moved their bulk compositions parallel to the field boundaries.

Mafic intrusive rocks, in contrast, do not show evidence of extensive alkali metasomatism. All except five of the analyses plot within the field of normal igneous rocks.

Calcium mobility is tested in Figure 3.3 with reference to a binary plot of Na_2O versus CaO
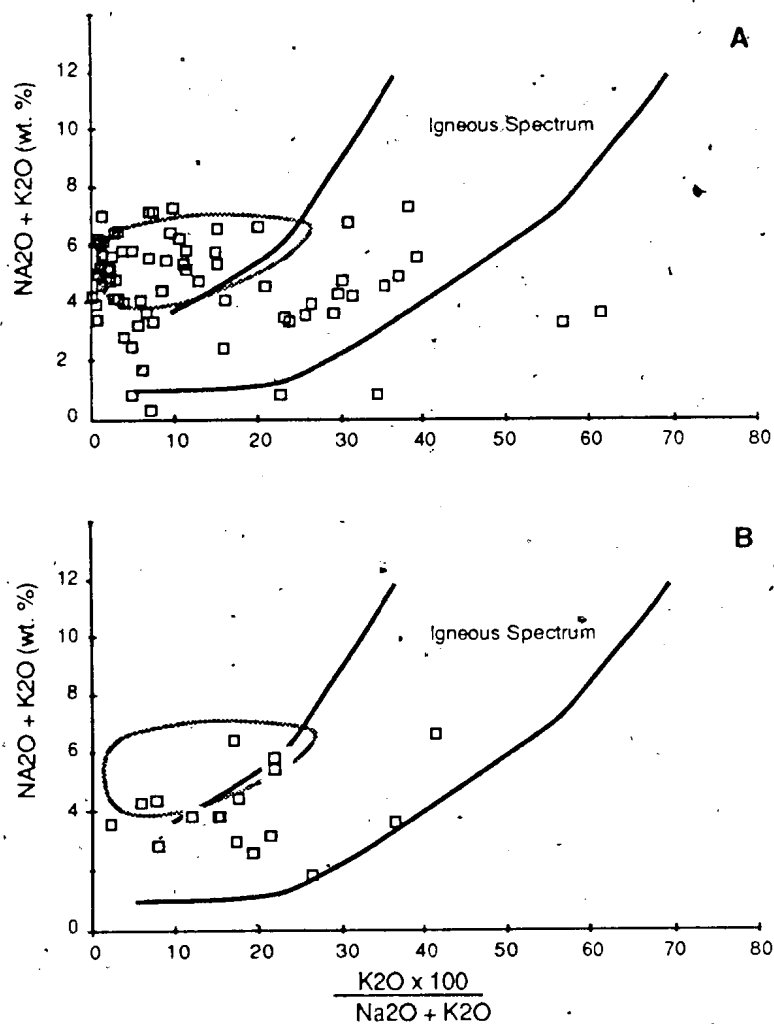
Figure 3.2: 'Igneous spectrum' diagrams for Wild Bight
Group mafic volcanic rocks (A) and mafic subvolcanic rocks
(B) after Hughes (1973) and Stauffer et al. (1975). More
than 70 percent of volcanic rocks are Na - metasomatized
and plot in the field of spilites (outlined by stippled line) while
more than 60 percent of subvolcanic rocks plot in the
igneous spectrum.
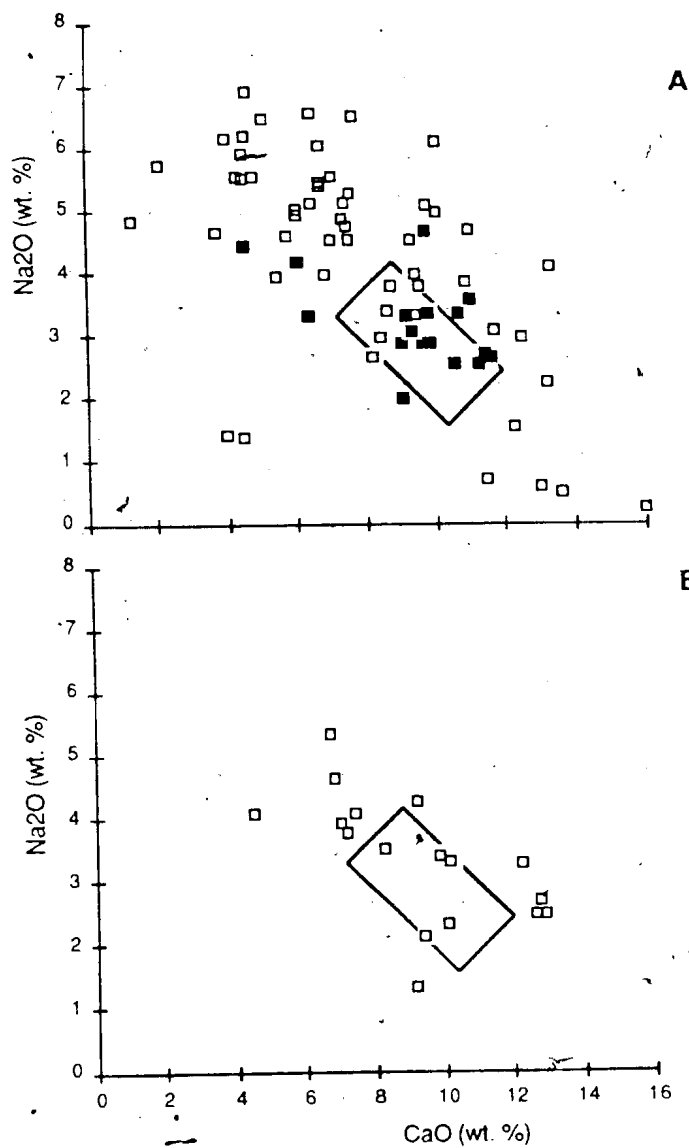
Figure 3.3: CaO-Na2O diagrams for Wild Bight Group mafic volcanic (A) and subvolcanic (B) rocks. Rectangular field outlines normal igneous mafic rock compositions (after Stephens, 1982). Solid symbols in A are samples that plot in the igneous spectrum field in Figure 3.2.

after Stephens (1982). Approximately 20 percent of the mafic volcanic rocks plot within the field of normal igneous compositions. Most of the remainder have apparently been depleted in CaO and enriched in Na_2O relative to normal igneous rocks. Samples with apparent enrichment in CaO are seen in thin section to contain an unusually large proportion of calcite-filled vesicles and veinlets. Samples that plot in the igneous spectrum in Figure 3.2 mostly plot in or close to the field of igneous compositions in Figure 3.3 supporting the conclusion that these rocks may preserve relatively unaltered igneous compositions.

Most intrusive rocks, particularly those that plot within the 'igneous spectrum' field (Figure 3.2B), plot in or near the igneous field on this diagram but with considerable scatter indicating some mobility of calcium.

The above discussion suggests that in the majority of volcanic rocks in the Wild Bight Group, Na_2O, K_2O and CaO have been substantially redistributed. By inference, most of the low field strength trace elements, (i.e. Rb, Ba and Sr) must also be considered suspect and caution should be exercised in their use for petrogenetic interpretations. As pointed out by Wood et al. (1979), Wood (1980) and Saunders et al. (1980), the one low field strength element (LFSE) that probably has only limited, if any, mobility during low grade hydrothermal alteration is Th. The stability of Th under these conditions has recently been documented by Merriman et al. (1986) in the hydrothermally altered margins of a dolerite intrusion in Wales.

Alkali and alkaline earth element mobility is less in evidence in the mafic intrusive rocks. This is additional indirect evidence that the metasomatism of the volcanic rocks resulted from sub-seafloor weathering and/or hydrothermal activity soon after eruption rather than a later burial metamorphism which should have had a similar effect on both intrusive and extrusive rocks.

The mobility of SiO_2 is of considerable interest as subdivision of mafic volcanic rocks into basalts, basaltic andesites, etc. is commonly done on the basis of SiO_2 contents. Experimental evidence clearly demonstrates that silica can be mobilized during low grade metamorphism (e.g. Mottl and Holland, 1978; Seyfried et al., 1978; Hajash and Archer, 1980) and studies in modern (Humphris and Thompson, 1978b) and ancient (Smith, 1968; Coish, 1977) environments have

confirmed that silica changes do accompany greenschist facies hydrothermal alteration. Silica is commonly taken up in seawater in these circumstances (demonstrated in the experimental studies referenced above) and, in most cases, increased hydrothermal alteration will result in a decrease in SiO_2 in the rock (Coish, 1977; Humphris and Thompson, 1978b)..However, local veining and filling of amygdules with quartz may locally result in an increase in silica contents during low grade metamorphism (Humphris and Thompson, 1978b). It is concluded that in the absence of free vein- and amygdule-filling quartz, the present silica content of a greenschist facies, hydrothermally-altered, mafic volcanic rock is best considered as a minimum estimate for its original concentration in the unaltered rock.

The relative mobility of iron and magnesium is of some importance in basalt petrogenesis as the fractionation of these elements is commonly used as a differentiation index. Later in this Chapter, extensive use is made of the atomic Mg/[Mg+Fe] (Mg number) and it is desirable to know the extent to which this number may have been affected by alteration. Many authors have shown both through experimental studies (e.g. Ellis, 1968; Bischoff and Dickson, 1975; Hajash, 1975; Mottl and Holland, 1978); Seyfried and Bischoff, 1981; Rosenbauer and Bischoff, 1984) and comparisons of altered pillow rims and less altered cores in submarine basalts (e.g. Cann, 1971; Coish, 1977; Humphris and Thompson, 1978a,b; Seyfried et al., 1978) that Mg is a major reactant in hydrothermal alteration of basalts. Mg from sea water is taken up by the basalt during chlorite-forming reactions while total iron is essentially conserved. The important factor in the amount of Mg uptake during alteration of basalt is apparently the effective water/rock ratio of the system, the amount of Mg-addition being directly correlated with the water/rock ratio (Seyfried et al., 1978; Mottl and Seyfried, 1980; Mottl, 1983).

Hydrothermal alteration of a pillow basalt pile will not be homogeneous. Spooner et al. (1977), pointing out that the bulk permeability of a pillowed sequence is probably several orders of magnitude greater than the permeability of unfractured basaltic rock, suggested that hydrothermal flow (and, therefore, mass transfer through the pile as a whole) principally occurs along pillow boundaries, fractures and cooling joints. In these areas, reactions may proceed

under high seawater/rock conditions. Mass transfer accompanying chemical reactions in the solid rock, on the other hand, occurs mainly by grain-boundary diffusion at low water/rock ratios.

Chemical changes during hydrothermal alteration are likely to be less severe in pillow cores than in the rims for two reasons: (1) pillow interiors contain more crystalline material from which elements are less easily mobilized than the glassy material at the rims; and (2) because of permeability differences as suggested above, they will see considerable less water during the life of the hydrothermal system. Data from Humphris and Thompson (1978a) and Coish (1977), plotted in Figure 3.4A and B, illustrate this. In both cases, the more altered rim is significantly enriched in Mg (i.e. has reacted under higher water/rock conditions and taken up more Mg) producing a significant shift to higher Mg# with higher water/rock ratios. Pillow rims should be avoided in geochemical studies of ancient rocks.

Data from two sources, however, suggest that in the solid rock, Mg# changes with respect to original rock compositions are not likely to be significantly large:

1) Alt and Emmermann (1985) have documented chemical changes with increasing metamorphic grade in DSDP Hole 504B (see Chapter 2). Mg# of their 'dark' basalt is plotted against depth in Figure 3.4C. There is no apparent consistent change in Mg# with depth and Mg# in all cases is within ±0.04 of their value for least altered basalts. These data show that at low water/rock ratios, there may be little change in the Mg# during the transition from fresh basalt to greenschist facies metabasalt.

2) Experimental data from Seyfried et al. (1978), plotted in Figure 3.4D, show the expected increase in Mg# with increasing water/rock ratio. Despite the fact that the reactant in this experiment was glass and not crystalline material, alteration at water/rock=10 produced a change of only +0.05 in the Mg#. Alteration at much lower water/rock ratios under natural conditions could be expected to produce even less change.

It is concluded that by confining sampling to pillow cores and by avoiding pillow rims and fractures with obvious alteration (e.g. calcite, chlorite, quartz-filled veins) most problems associated with using the Mg# as a differentiation index in these rocks should be obviated. This
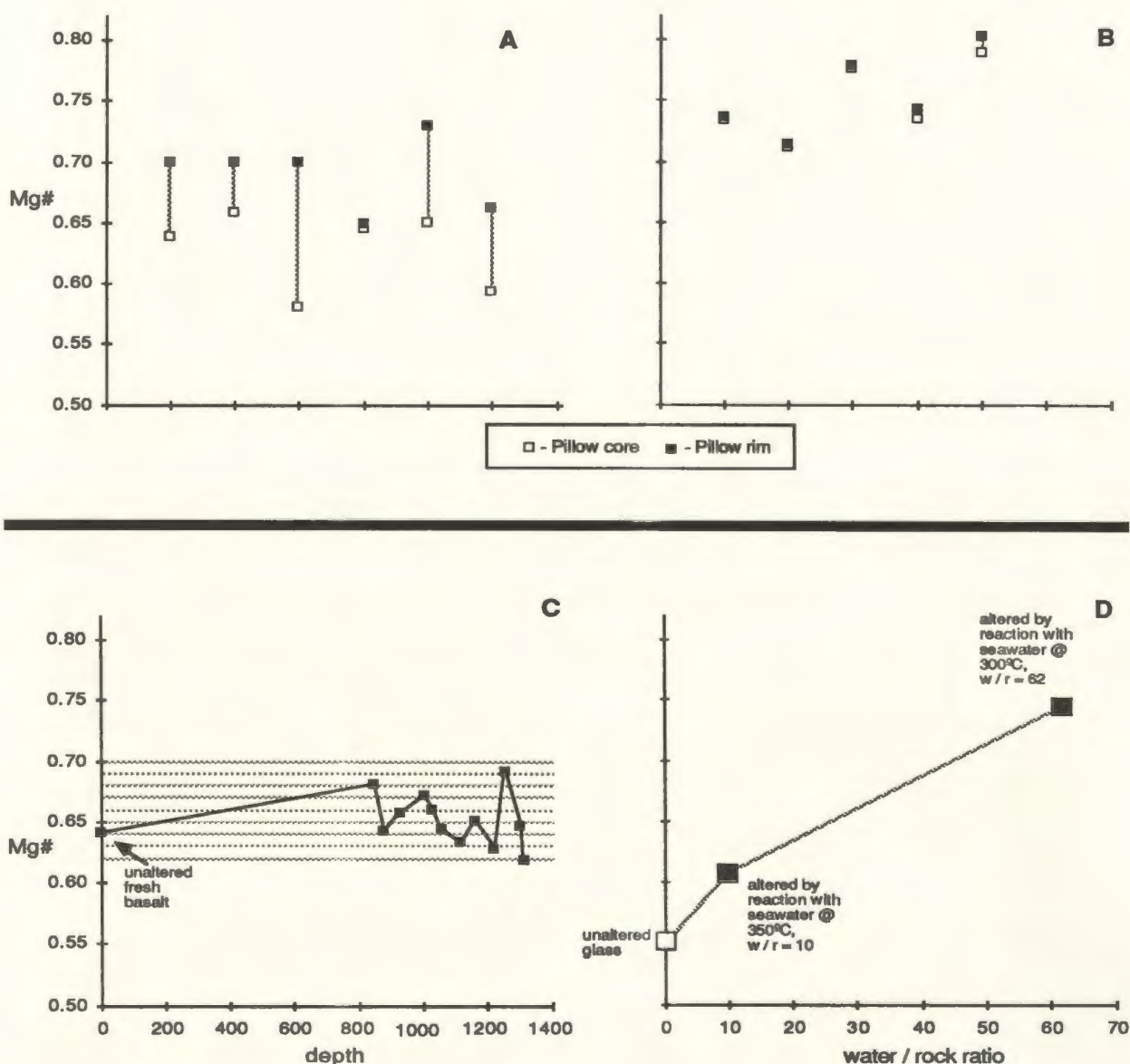
Figure 3.4: Change in Mg# resulting from sub-seafloor hydrothermal alteration. In A, change in Mg# from core to rim of individual mid-Atlantic ridge pillows from the data of Humphris and Thompson (1978a) and in B, in Ordovician basaltic pillows in the Betts Cove ophiolite from the data of Coish (1977). In both cases, Mg# increases from pillow core to pillow rim although the magnitude of the changes are generally greater in the former. In C, variation in Mg# with increasing depth and degree of metamorphism in DSDP Hole 504B (data from Alt and Emmermann, 1985). There is little systematic change from fresh compositions to greenschist facies at low water/rock ratios. In D, change in Mg# of basalt glass reacted with heated seawater under increasing water / rock ratios from the data of Seyfried et al., (1978).

conclusion is supported by data presented later in this Chapter where it will be seen that in petrogenetically related rock groups, although there is generally a consistent, linear relationship between Mg# and the immobile elements (c.f. Figures 3.15, 3.21, 3.34), no such relationship exists between Mg# and mobile elements (e.g. total alkalis, see Figures 3.15, 3.21, 3.34). Specific problems related to abnormal alteration of individual samples do exist, however, and will be noted where appropriate in the following discussion.

3.3 Subdivision of the Mafic Volcanic Rocks

3.3.1 General Statement

Mafic volcanic rocks in the Wild Bight Group, in terms of their SiO_2 content, span the compositional range of basalt and basaltic andesite (the basalt - basaltic andesite boundary is taken as 53 percent SiO_2, following the Basaltic Volcanism Study Project, 1981) and have a broadly bimodal distribution (Figure 3.5). However, from minor and trace element considerations, it is clear that these rocks are not a single, petrogenetically-related group. This is particularly apparent in the wide range of incompatible element abundances. For example, TiO_2 contents range from 0.35% to 3.87%, a compositional range that is unlikely to have resulted from a single parent by any simple fractionation process in the differentiation range of basalts and basic andesites. A similar argument holds for other incompatible elements such as P_2O_5 (< .01% to 1.4%), Zr (3 ppm to 414 ppm), Nb (< 0.5 ppm to 85 ppm), and Y (< 5 ppm to 57 ppm). Comparison of the relationships between compatible and incompatible elements further emphasizes the heterogeneous nature of these rocks. Cr and Ni are plotted against TiO_2 in Figure 3.6 and show no simple linear or curvilinear relationship which would suggest a common fractionation history. Furthermore, the heterogeneity of Nd isotopic compositions of volcanic rocks in the group, described in detail in Chapter 4, is a compelling argument that they represent a petrogenetically complex assemblage of volcanic rocks.

Before describing the geochemistry of the rocks or attempting to interpret their tectonic setting or petrogenesis, it is necessary to subdivide them into consistent and geologically
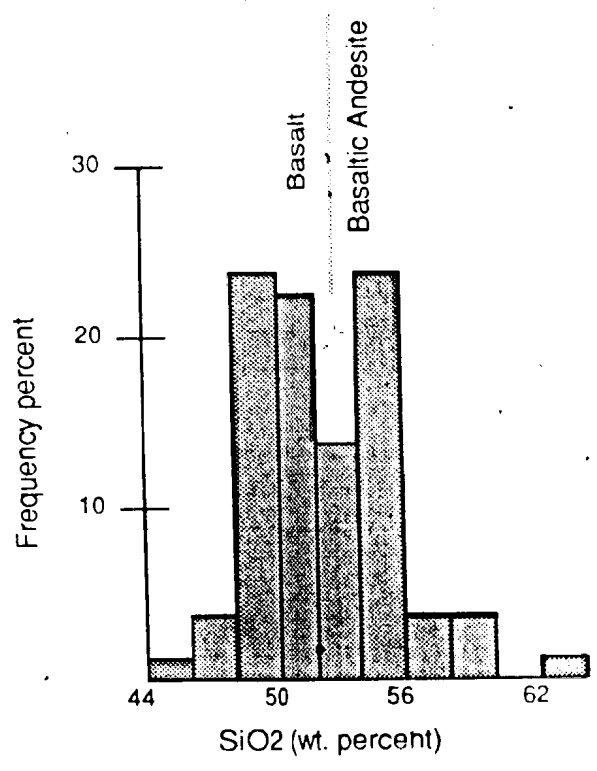
Figure 3.5: Histogram of SiO2 contents of
mafic volcanic rocks in the Wild Bight
Group. Basalt-andesite subdivision after
the Basaltic Volcanism Study Project
(1981).
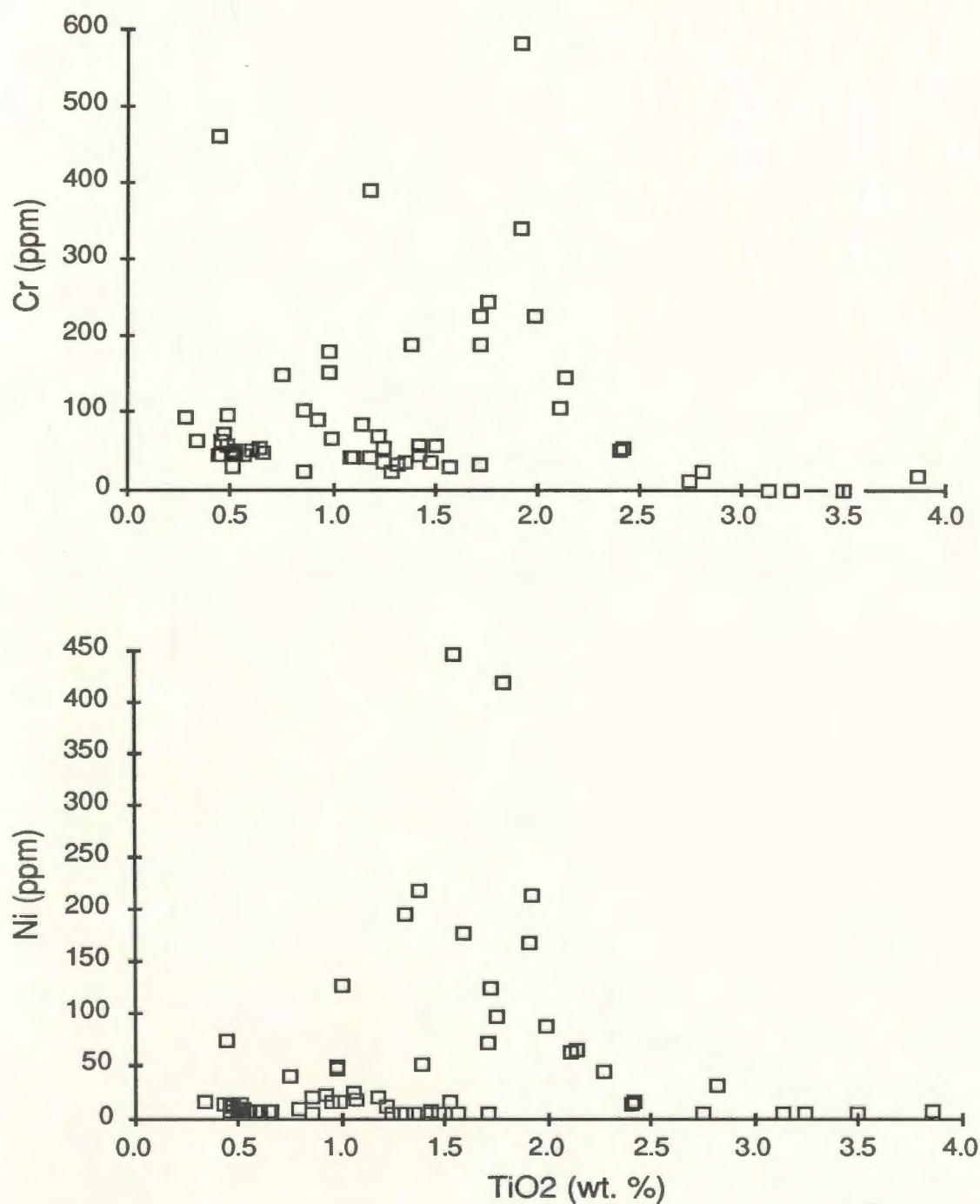
Figure 3.6: Cr and Ni versus TiO2 for all Wild Bight Group mafic volcanic samples. There is no simple linear or curvilinear relationship in either case suggesting that these samples comprise a heterogeneous assemblage that cannot all be related by a single, simple fractionation history.

meaningful groups. This subdivision procedure is a two-stage process and is outlined in detail in the following Sections. Geochemical groups are defined in Section 3.3.2 based on variations in incompatible element abundances within and between the geographically defined suites. The subdivision is refined and final assignment of samples to the various geochemical groups is made based on relationships between high field strength elements (HFSE), low field strength elements (LILE) and rare earth elements (REE) in Section 3.3.3. In Section 3.3.4, the subdivision is tested statistically by discriminant function analysis.

3.3.2 Identification of Geochemical Groups Based on Incompatible Element Abundances

The initial subdivision of the Wild Bight Group is based on the recognition that the various geographic suites (and in some cases, parts of these suites) form coherent groups according to their incompatible element contents. In Figure 3.7, binary incompatible element relationships, represented by Zr and TiO_2, exhibit a rather diffuse positive trend. However, with three exceptions (see below), each geographic suite has a restricted and relatively homogeneous incompatible element composition on this diagram, suggesting that rocks in each suite are genetically related. Four classes of mafic volcanic rocks can be defined based on increasing incompatible element concentration, termed for convenience, 'depleted', 'intermediate', 'transitional' and 'enriched' (Figure 3.7). Each class includes two or more suites or subsuites. There is very little overlap between these classes. Although they are defined in this case on the basis of Zr and TiO_2, binary plots using other incompatible elements (e.g. P_2O_5, Nb, Y) yield similar results.

The distribution of samples from the individual suites in this framework is shown in Figure 3.8 where it can be seen that the Glover's Harbour, Side Harbour and Big Lewis Lake suites are inhomogeneous and probably composite. The Glover's Harbour suite contains two clear subsuites, one with 'depleted' and the other with 'intermediate' incompatible element concentrations; respectively, these represent the western and eastern (stratigraphically lower
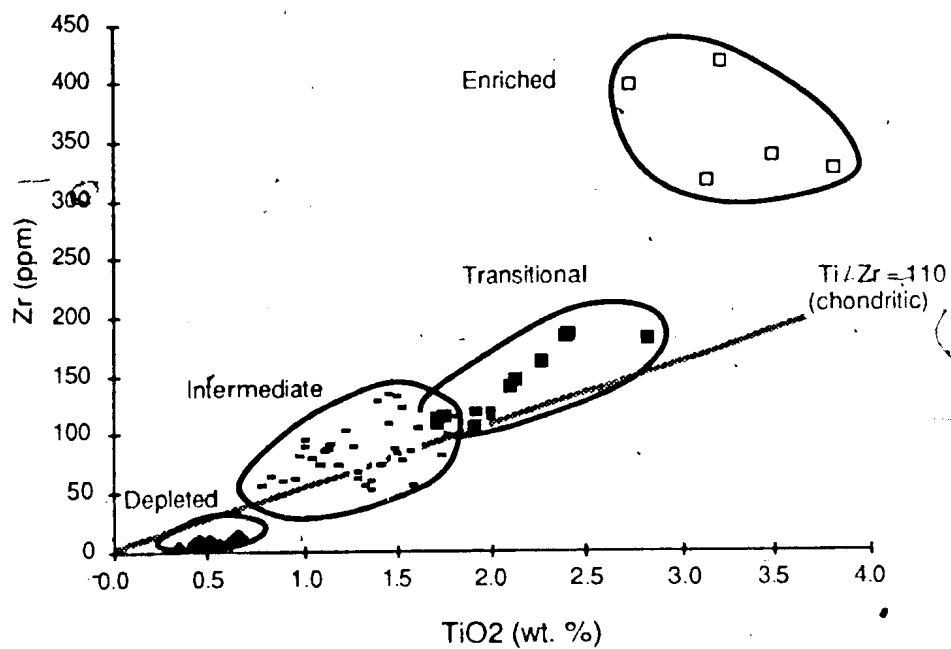
Figure 3.7: TiO2-Zr plot for all Wild Bight Group mafic volcanic rocks. Geographically-defined suites and subsuites can be combined in four geochemical classes of different incompatible element concentrations.
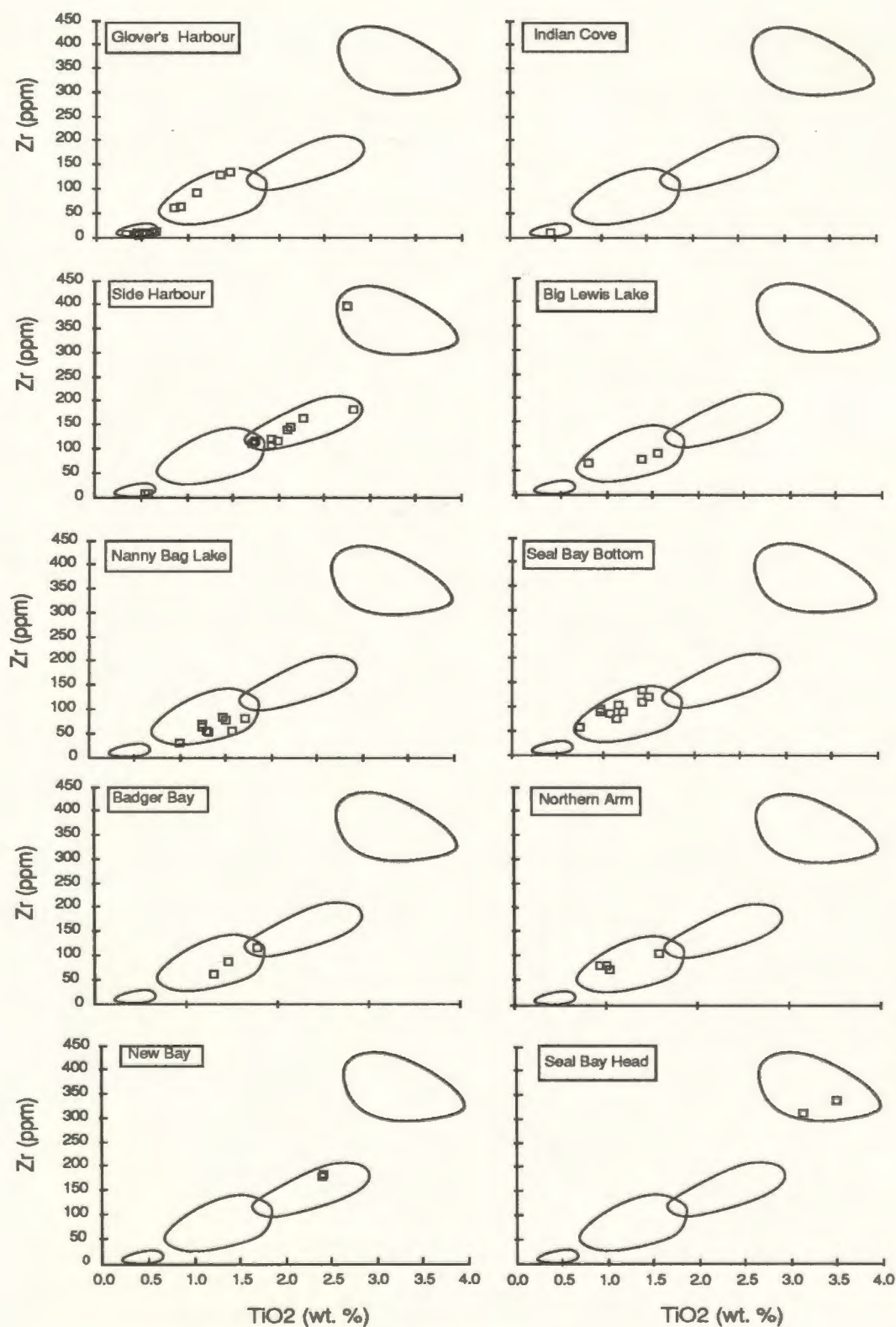
Figure 3.8: TiO2 versus Zr plots illustrating the classification of samples (open squares) in the individual geographic suites. Solid lines outline fields defined in Figure 3.7.

and upper) portions of this volcanic unit. No stratigraphic or structural break has previously been

recognized between these rocks although they are separated by approximately 200 m of mafic

pyroclastic and/or epiclastic rocks (Figure 2.5) Hereafter, they are referred to as the 'Glover's

Harbour West ' and 'Glover's Harbour East' suites. The Side Harbour suite contains three

subtypes. The two 'depleted' samples come from the southwestern part of the volcanic unit less

than 300 m below the Point Leamington massive sulphide deposit. 'Transitional' rocks form the

rest of this suite except for the one 'enriched' sample which is interbedded with 'transitional' rocks

north of Big Lewis Lake. The Big Lewis Lake suite contains two subsuites of 'intermediate' and

'enriched' composition which are interbedded with each other on outcrop scale on the north

shore of Big Lewis Lake.

3.3.3 Paleotectonic Affinities of the Geochemical Groups and Further

Refinement of the Subdivision

A full discussion of the tectonic settings represented by the Wild Bight Group volcanic

rocks is premature at this point. However, it is necessary to introduce the topic as it is precisely the

geochemical features that are commonly used to discriminate paleotectonic environments which

provide the key to the second stage subdivision of the Wild Bight Group volcanic rocks.

Relationships between HFSE and REE on a partial extended rare earth plot (e.g. Wood,

1979; Wood et al., 1979; Sun, 1980; Briqueau et al., 1984), presented in Figures 3.9 to 3.11.

and between Ti, Y and Zr on a ternary plot after Pearce and Cann (1973), presented in Figure

3.12, are used to accomplish this subdivision. Further evidence in support of the preliminary

interpretations advanced in this Section is presented in later discussions of whole rock

geochemistry (Section 3.7), primary mineral chemistry (Section 3.11), Nd isotopic studies and

petrogenetic calculations (Chapter 4).

Wood et al. (1979) and Sun (1980) were among the first to point out that volcanic rocks

erupted in island arc settings show a distinctive underabundance of the HFSE Ta and Nb with

respect to REE of similar ionic character. They further pointed out that relative overabundance of
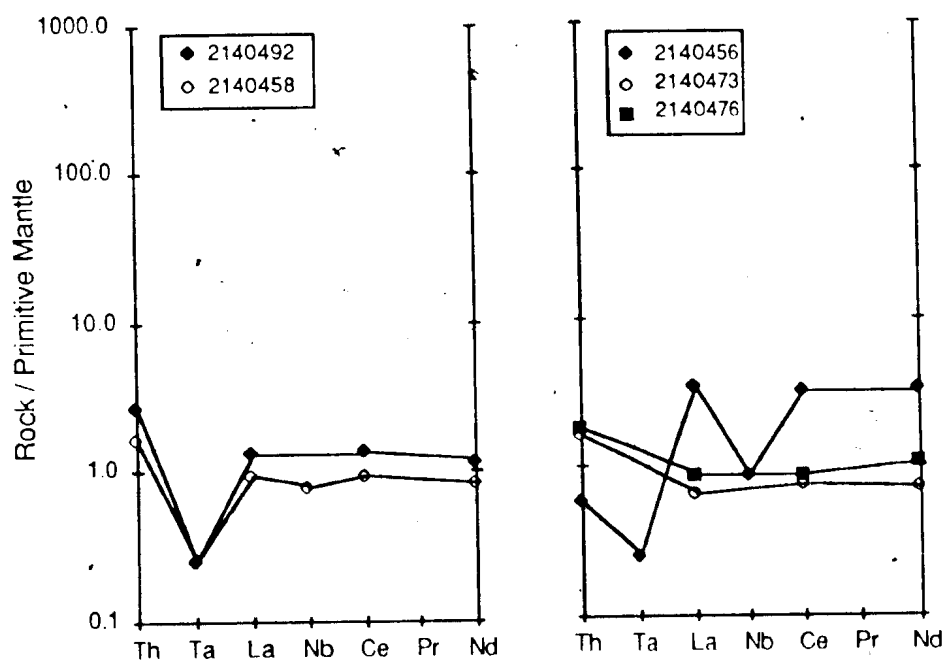
Figure 3.9: Partial extended REE plot for 'depleted' mafic volcanic rocks. All have negative Ta anomalies. Nb is below detection limits in most samples. Primitive mantle normalizing values given are in Appendix 7.
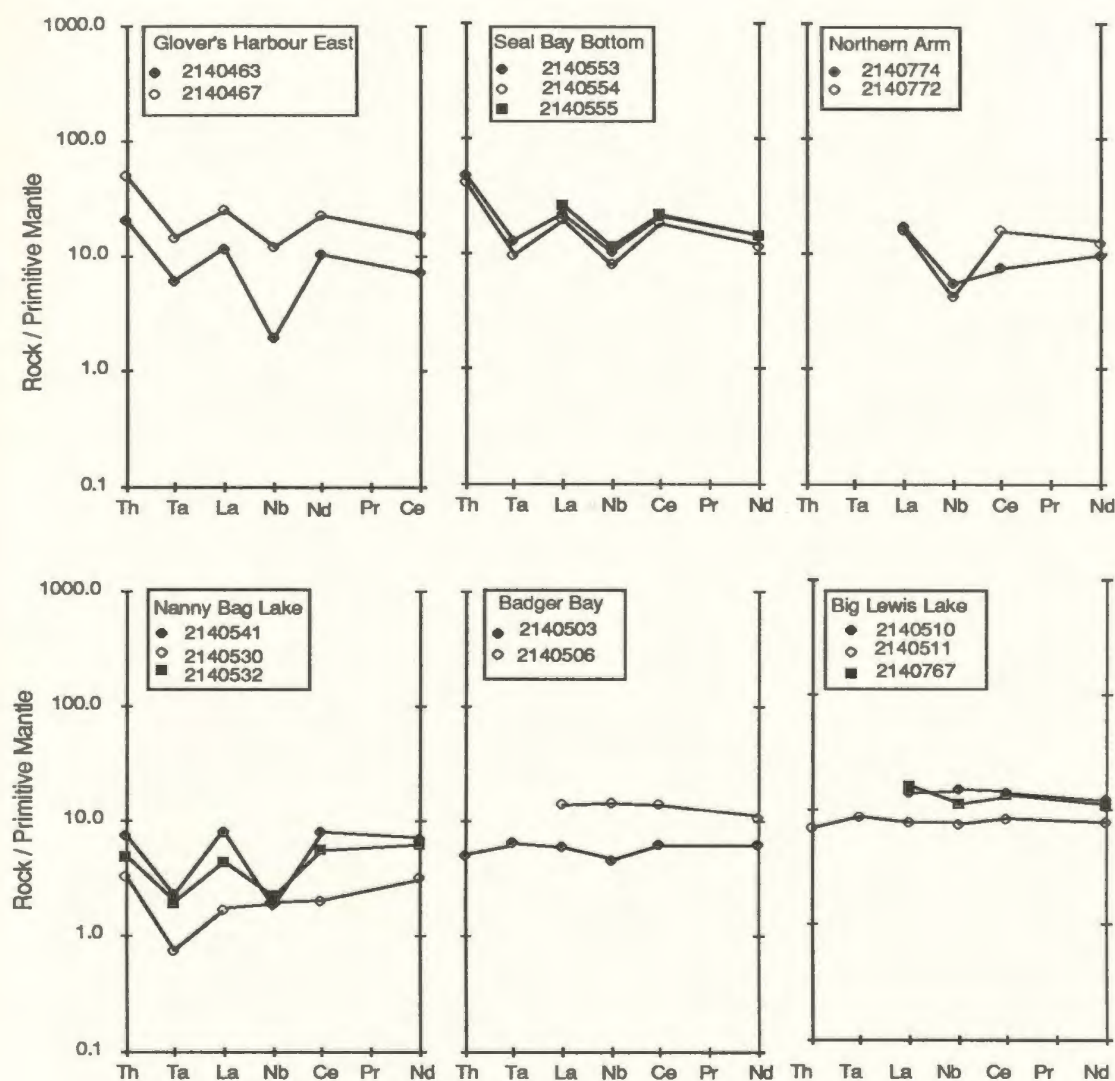
Figure 3.10: Partial extended REE plots for 'intermediate' mafic volcanic rocks. Rocks from the Glover's Harbour East, Seal Bay Bottom, Northern Arm and Nanny Bag Lake suites have negative Ta and Nb anomalies while those from the Badger Bay and Big Lewis Lake suites do not. Primitive mantle normalizing values are given in Appendix 7.
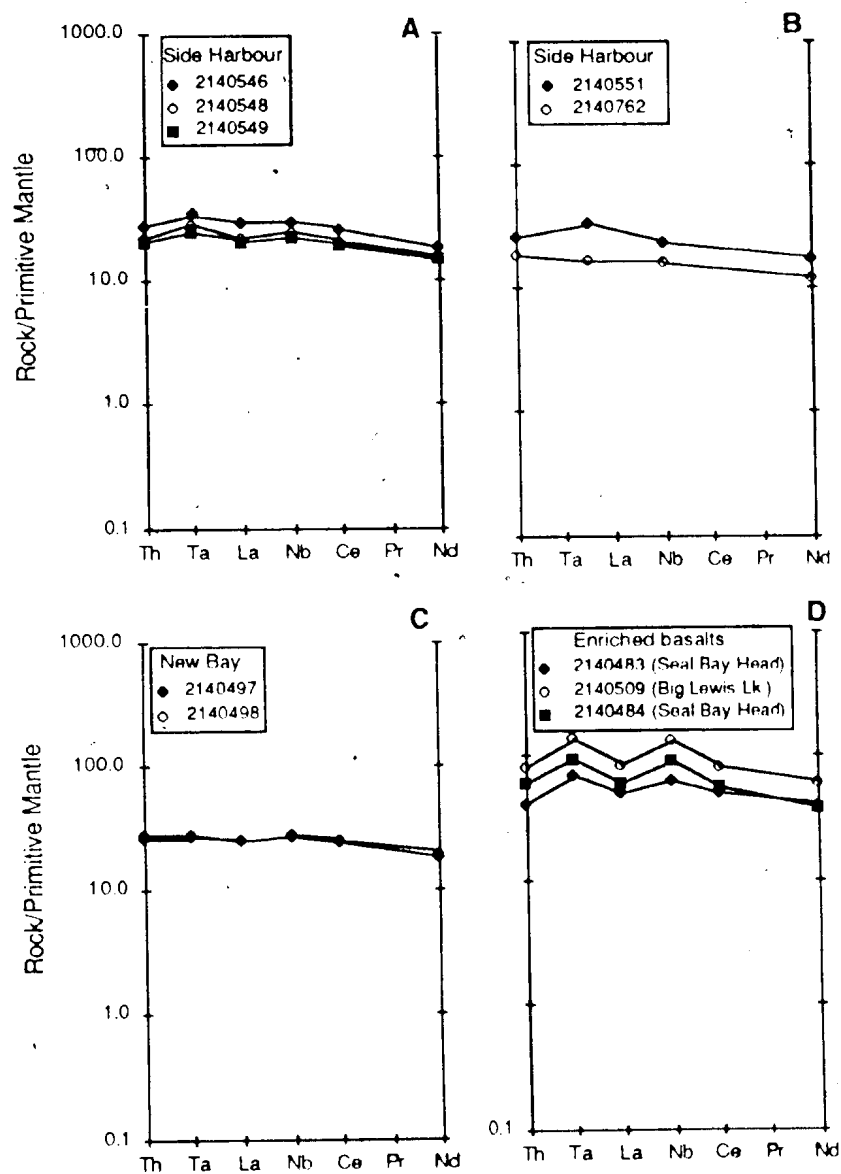
Figure 3.11: Partial extended REE plots for 'transitional' and 'enriched' mafic volcanic rocks. The former (A,B, and C) have smooth REE patterns while the latter (D) has slight positive Ta and Nb anomalies Primitive mantle normalizing values are given in Appendix 7.

the LFSE was characteristic of island arc lavas. This can be graphically expressed on a chondrite- or primitive mantle- normalized, extended rare earth plot where island arc lavas generally show distinctive negative Ta and Nb anomalies relative to La while the LFSE elements plot in an irregular pattern at normalized abundances generally greater than the LREE. Mid-ocean ridge basalts (MORB) and various within plate settings generally produce lavas in which the LFSE plot in a smooth curve, underabundant with respect to the LREE, and Ta and Nb are comparable to or slightly overabundant with respect to the LREE. Of course, in ancient rocks, the mobility of the LFSE elements severely limits their usefulness; in the present study, the only LFSE element which is used for this type of interpretation is Th (see Section 3.2).

Partial extended REE diagrams (Th to Nd) for 'depleted' samples are presented in Figure 3.9. In some samples, Ta was below the detection limits as was Nb in most samples. However, where abundances could be measured, the samples show a clear island arc signature with positive Th and negative Ta and Nb anomalies. Detection limits for Nb are approximately 0.77 X primitive mantle on this diagram so that all samples in which Nb is below the detection limit probably also have negative Nb anomalies.

Samples of 'intermediate' composition, plotted in Figure 3.10, comprise two types. Those from the Glover's Harbour East suite and the Seal Bay Bottom, Northern Arm and Nanny Bag Lake suites have distinct negative Ta and Nb and generally positive $(Th/La)_n$ (the subscript 'n' designates concentrations that have been chondrite-normalized) characteristic of island arc volcanic rocks. In contrast, samples from the Badger Bay and Big Lewis Lake suites have smooth patterns with a slight underabundance of Th with respect to La. $(La/Ta)_n$ and $(La/Nb)_n$ are near 1.

Samples of 'transitional' and 'enriched' compositions likewise lack the island arc signature (Figure 3.11) having smooth patterns and a slightly negative $(Th/La)_n$. Ta and Nb in the enriched group show slight but distinct positive anomalies. On the basis of HFSE, LFSE and REE abundances, therefore, two broad groups can be defined, one with apparent island arc affinities and the other without.

The Ti-Y-Zr diagram (Pearce and Cann, 1973) gives a similar result and has the added

·advantage that all samples in the Wild Bight Group have been analysed for these elements; for this reason, it provides a more universal test of the grouping. On Figure 3.12, 'depleted' rocks are more depleted in Zr than the reference field of island arc tholeiites and are displaced away from the Zr apex outside the fields of normal IAT. 'Intermediate' rocks from the Nanny Bag Lake, Seal Bay Bottom, Glover's Harbour East and Northern Arm suites plot in the plate marginal fields; the Nanny Bag Lake suite is most similar to normal island arc tholeiites while the others plot mainly within the indeterminate CAB-IAT-MORB field and spill across the boundary into the field of calc alkalic basalt. Two samples from the Glover's Harbour East suite plot just across the upper field boundary in the within plate basalt field. In contrast, all Badger Bay and Big Lewis Lake samples plot in the WPB field, emphasizing the dichotomy between them and other rocks of 'intermediate' composition. All of the 'transitional' and 'enriched' basalts plot as expected in the WPB field

From this evidence, the Wild Bight Group can be viewed as broadly bimodal, with geochemical affinities to two paleotectonic environments. The 'depleted' and some of the 'intermediate' rocks have characteristics of island arc magmatism in their HFSE and REE elements and plot in plate marginal fields on the Ti-Zr-Y diagram. The remainder of the 'intermediate' rocks as well as those of 'transitional' and 'enriched' compositions, exhibit no island arc affinities on the extended REE diagrams and plot in the WPB field on the Ti-Zr-Y diagram. Although it is recognized that interpretation of the paleotectonic environments at this point is premature, the subdivision is necessary in order for the geochemical data to be presented coherently. The justification must await detailed presentation of the geochemical and isotopic data.

The classification of Wild Bight Group mafic volcanic rocks arising from the above discussion is illustrated schematically in Figure 3.13. For convenience in description, the five groups that comprise it are designated

a) Island Arc depleted (IAD) group; Glover's Harbour West suite, Indian Cove suite, Side Harbour 'depleted' samples;

b) Island arc intermediate (IAI) group; Glover's Harbour East suite, Seal Bay Bottom, Northern Arm, Nanny Bag Lake suites;
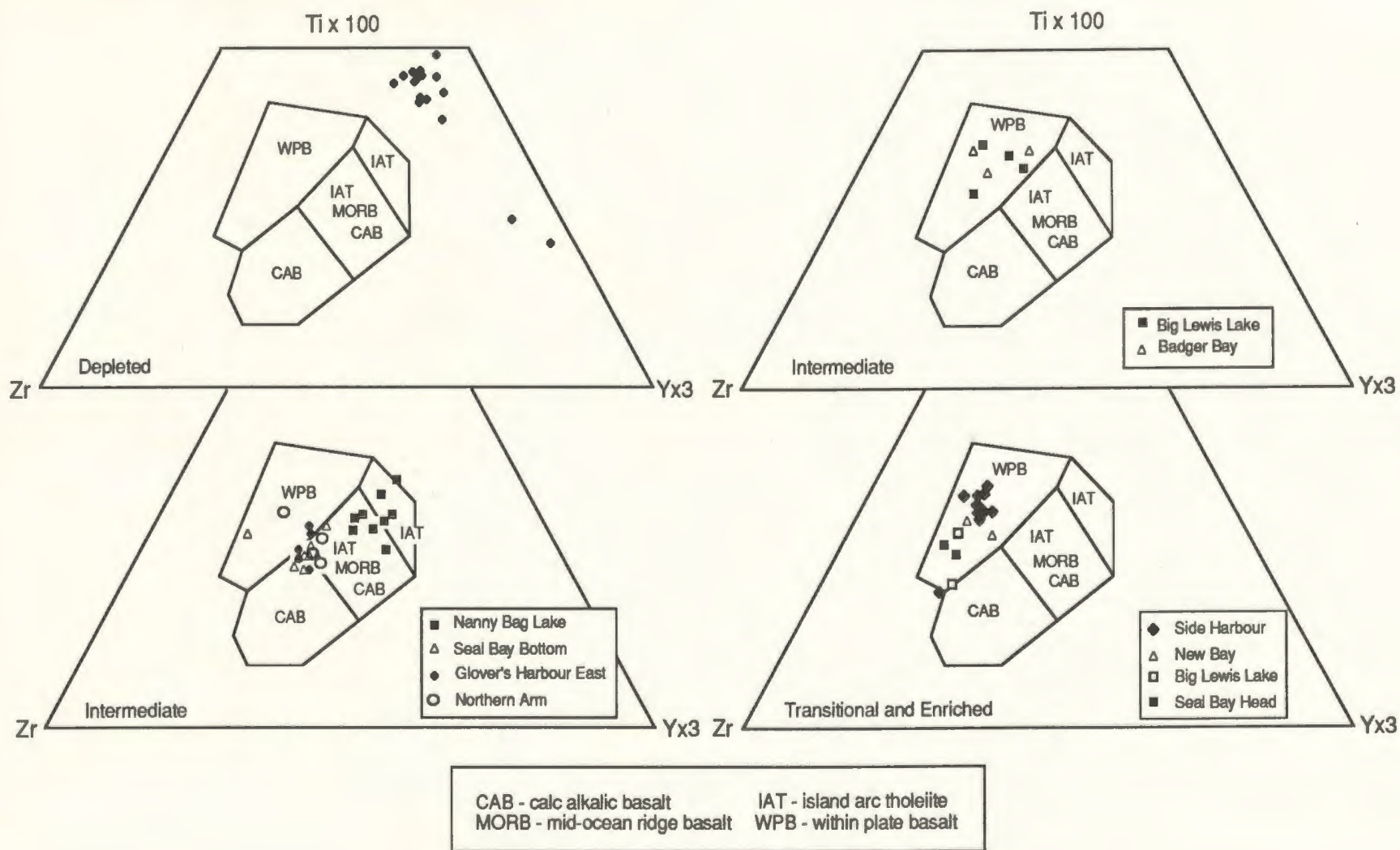
Figure 3.12: Ti-Y-Zr plot (Pearce and Cann, 1973) of mafic volcanic rocks of the Wild Bight Group. 'Intermediate' rocks form two groups; those with negative Ta and Nb anomalies (Figure 3.9) plot in the plate-marginal fields while those lacking negative Nb and Ta anomalies plot with the 'transitional' and 'enriched' rocks in the WPB field. 'Depleted' rocks plot outside the field of IAT indicating extreme Zr depletion.
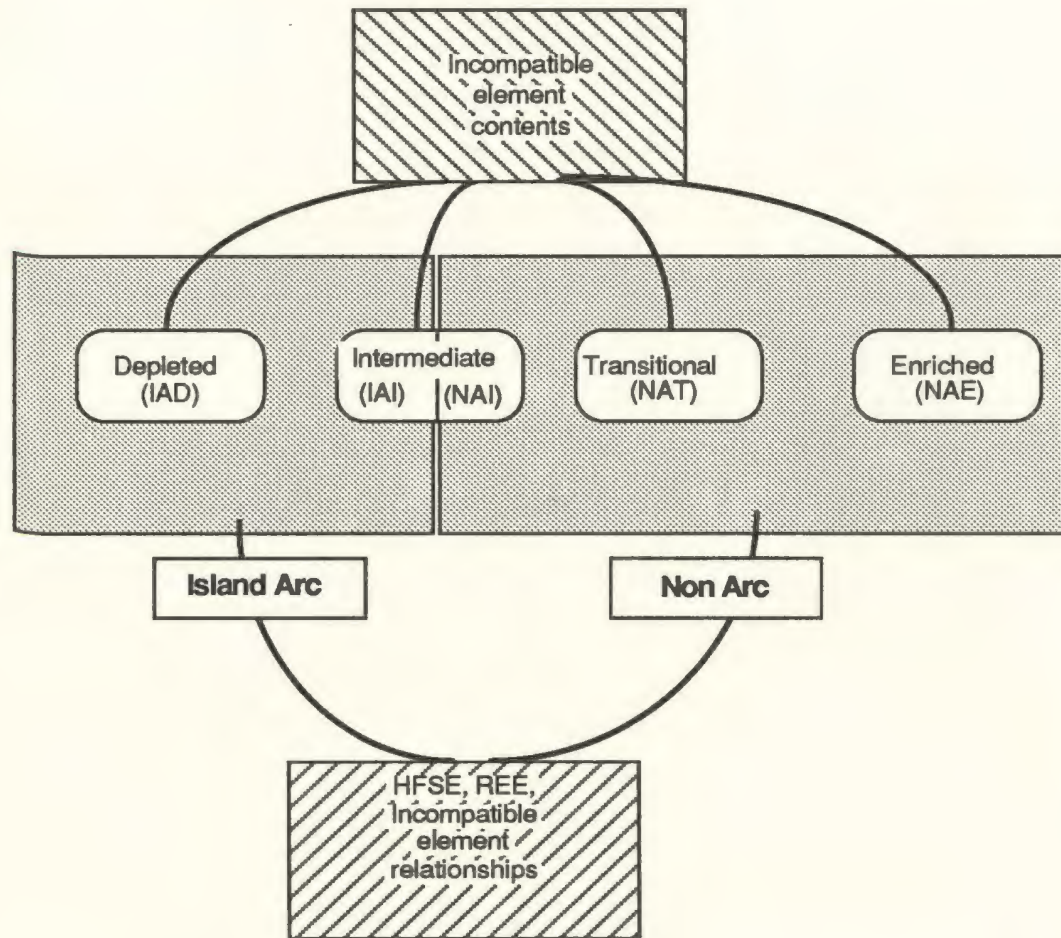
Figure 3.13: Schematic illustration of the geochemical subdivision of the Wild Bight Group mafic volcanic rocks. Four groups are defined on the basis of incompatible element abundances (white rectangles). These are assigned to two broad environments showing affinities to 1)island arc and 2) non-arc environments (stippled fields) based on HFSE, REE and Ti-Zr-Y relationships. The 'intermediate' samples are further subdivided on this basis leading to the final subdivision into five groups (IAD, IAI, NAI, NAT, NAE) defined in the text.

c) Non-arc intermediate (NAI) group (Badger Bay suite and 'intermediate' rocks from the

Big Lewis Lake suite)

d) Non-arc transitional (NAT) group; Side Harbour 'transitional' rocks and New Bay suite

e) Non-arc enriched (NAE) group; Seal Bay Head, 'enriched' samples from Side Harbour

and Big Lewis Lake suites

3.3.4 Statistical Test of the Subdivision; Discriminant Function Analysis

The validity of this empirically-derived geochemical subdivision can be tested by

discriminant function analysis. The variables on which the functions are based are TiO_2, P_2O_5,

Zr, Y, Nb and V, the incompatible elements which 1) are least likely to have been affected by

alteration, and 2) have been analysed in all rock samples. A description of the method,

parameters, possible limitations and a tabulation of the results including the discriminant scores

are included in Appendix 8.

Statistically, the five groups appear to be geochemically distinct with respect to the six

elements considered. Four functions define the separation of the five geochemical groups

(Table 3.1) successfully classifying 95.6% of the volcanic rock samples. Functions 1 and 2

together account for 98% of the variance and a territorial plot using these functions (Figure 3.14)

illustrates that a good separation of the five groups has been achieved. The misclassified cases

are all from the IAI and NAI groups reflecting the relative difficulty of distinguishing these rocks of

similar overall composition in the absence of HFSE and REE relationships. The considerable

success achieved by the two functions in separating these two groups is mainly attributable to Y,

which is slightly more abundant in the IAI group.

Two further comments regarding Figure 3.14 are in order. First, the assignment of each

sample to a group carries a statistical probability that it actually belongs to this or another group.

For samples near the field boundaries, the probability that the sample has been correctly

assigned is locally calculated to be less than 70%. particularly for small groups, this may still

Table 3.1: Unstandardized canonical discriminant functions calculated from incompatible element data for Wild Bight Group mafic volcanic rocks.

	Function	Eigenvalue	Percent Variance	Cumulative percentage
Fct. 1	$11.69TiO2 - 1.22P2O5 + .984Y + 4.69Zr - 7.86Nb - 5.86V + 3.42$	25.65	87.48	87.48
Fct. 2	$14.55TiO2 + 1.68P2O5 - 3.37Y - 9.67Zr + 2.74Nb - 3.00V + 27$	3.09	10.53	98.01
Fct.3	$-3.96TiO2 + 2.77P2O5 - 9.68Y + 4.15Zr + .02Nb + 8.87V - 13.91$	.48	1.64	99.65
Fct. 4	$-7.60TiO2 + 2.63P2O4 + 2.95Y - 2.06Zr + 2.47Nb + 5.9V - 12.91$	.10	.35	100
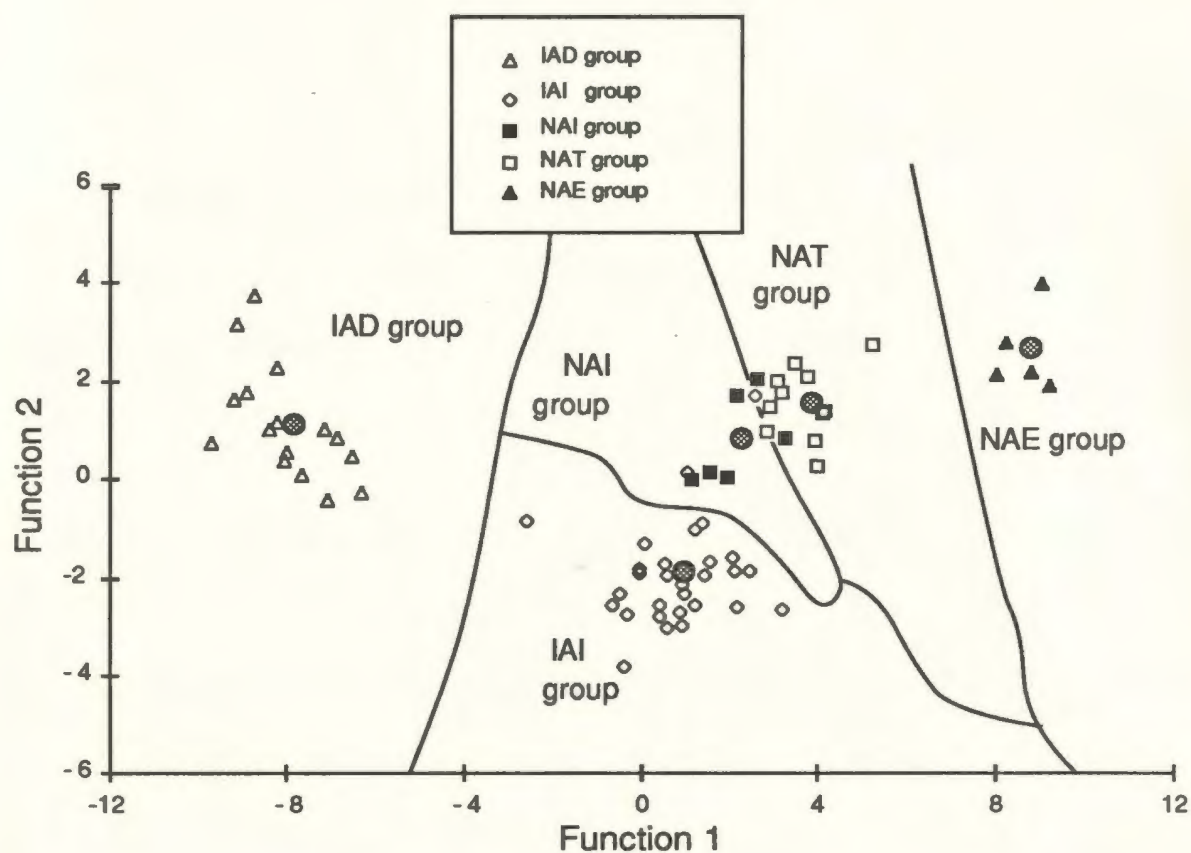
Figure 3.14: Territorial plot of discriminant functions 1 and 2
for all Wild Bight Group mafic volcanic rocks. Solid lines outline
the fields in two dimensional space of the geochemical groups
defined on four functions. Symbols indicate the groups to
which samples were previously assigned on geochemical
evidence. Stippled circles are group centroids.

underestimate the uncertainty of classification (see Appendix 8). Second, there is one sample

that the discriminant functions correctly classified as belonging to the NAI group but which plots in

the NAT field on this diagram. Any of three factors may be responsible for this: 1) the probability

that it belongs to the NAT group is 66%, compared to 34% for the NAE group; 2) 2% of the total

variance is accounted for by the two functions that do not appear on this diagram.

As a result of this analysis, it is concluded that the empirically defined groups probably

have a valid statistical base. They form the framework for discussions of the detailed geochemical

relationships, which constitute the rest of this Chapter.

3.4 Description of the Mafic Volcanic Rocks

3.4.1 Background for Classification and Description

The geochemical classification of Wild Bight Group mafic volcanic rocks outlined in Section

3.3 provides the framework for discussing their geochemistry. In the following Section, the nature

of the magma series represented in each group (and where necessary in individual suites within

the groups) is discussed and the rocks are compared to modern examples with similar

geochemical characteristics. The discussion includes interpretations of possible paleotectonic

environments and qualitative estimates of source region characteristics and fractionation

histories. Quantitative modelling is reserved until Chapter 4 so as to have the benefit of Nd

isotopic analyses.

A series of diagrams and discrimination plots have been chosen, from the large number of

such plots available in the literature, to illustrate the geochemical features of these rocks. The

descriptive approach and the diagrams used are briefly described below.

3.4.1.1 Magma Series

Gill (1981) has defined magma series as "magmas which are related to each other by some

differentiation process(es) or by being separate partial melts of a common source under similar

conditions". Assigning ancient rocks to a particular magma series, however, may be hindered by:

a) lack of agreement as to the criteria for separating the various magma series; and b) the variably altered nature of ancient rocks which render many of the classifications based on mobile major elements unreliable.

There is general agreement as to the geochemical separation of alkalic and non-alkalic series rocks; in fresh rocks, this is generally accomplished on the basis of relative alkali contents (MacDonald and Katsura, 1964) and/or alkali-lime indices (Peacock, 1931). Floyd and Winchester (1975) have provided a basis for separating these magma series in altered rocks using TiO_2, Zr, Y, Nb and P_2O_5 contents and their diagrams are used extensively for this purpose in the following Sections.

Conclusions in this regard can be checked with reference to the composition of primary minerals in the rock, if such minerals can be identified (e.g. clinopyroxene, see Section 3.6)

The separation of non-alkalic tholeiites from calc alkalic rocks is less straightforward. Most workers consider the "iron-enrichment trend" and the "iron depletion trend" to define, respectively, the tholeiitic and calc alkalic trends in non-alkalic rocks (Nockolds and Allen, 1953, 1954, 1956; Irvine and Baragar, 1971; Miyashiro, 1974) There is, however, considerable discussion as to whether, in orogenic environments, an iron enrichment trend is necessary to define a tholeiitic magma series (e.g. Osborn, 1962) or whether a high Fe/Mg ratio without substantial increase during subsequent differentiation is sufficient (e.g. Miyashiro, 1974).

Jakes and Gill (1970) suggested that low contents of large ion lithophile elements (LILE) are characteristic of tholeiitic rather than calc alkalic rocks in island arc environments and on this basis defined an "island arc tholeiite" series characterised by low LILE contents and chondrite-normalized REE patterns that are flat to slightly LREE depleted.

Gill (1981) reviewed these arguments and concluded that the initial Fe/Mg ratio and rate of change of Fe/Mg with increasing SiO_2 provide the best practical means of distinguishing tholeiitic from calc alkalic rocks in orogenic environments; he used Miyashiro's (1974) SiO_2 versus FeO/MgO diagram for this purpose. Following Jakes and Gill (1970), he further concluded that LILE contents (as reflected by K_2O) could be used to identify contrasting petrogeneses in

orogenic environments, and on this basis, defined low-K, medium-K and high-K suites, each encompassing representatives of tholeiitic and calc alkalic differentiation series.

For the purposes of classifying rocks in the Wild Bight Group, Gill's conceptual approach will be followed as much as possible. However, because the use of SiO_2, FeO and MgO is not always feasible in ancient rocks because of the effects of alteration, these elements are not used directly. TiO_2 and V vary sympathetically with FeO in the non-alkalic series (Miyashiro, 1974; Miyashiro and Shido, 1975; Shervais, 1982) and, following these authors, increasing or decreasing TiO_2 and V with differentiation (represented by atomic Mg/[Mg+Fe], the Mg#) is taken in this study as evidence for tholeiitic or calc alkalic magma series, respectively. In the absence of reliable K_2O data, the distinction between low-K, medium-K and high-K suites can be made on the basis of REE patterns (Gill, 1981). As a general rule, low-K suites have slightly negative to slightly positive REE patterns ($La_n/Yb_n < \sim 1.5$), medium-K suites moderately positive slopes ($La_n/Yb_n \sim 1$ to 5) and high-K suites steep positive slopes ($La_n/Yb_n > 5$). The distinction can also be made on the basis of the relative abundances of La and Th (Gill, 1981), as Th distribution in the magmas parallels that of K_2O. High Th/La ratios indicate high-K suites and low Th/La, low-K suites.

A relatively uncommon non-alkalic magma type, termed the boninite series by Meijer (1980), Hickey and Frey (1982), Cameron et al. (1983) among others, has been identified at some consuming plate margins. These magmas are characterised by high MgO and compatible trace element concentrations, andesitic SiO_2 contents, and severe depletion of incompatible elements (particularly Ti and the HREE but also the other HFSE). Chondrite-normalized Zr and Hf are generally enriched relative to the MREE, Ti/Zr ratios are characteristically very low (< 60, Hickey and Frey, 1982) and the REE patterns are commonly, although not in every case, concave-upward.

3.4.1.2 Paleotectonic environment

There are a number of approaches in the literature to discriminate between volcanic rocks

formed in different tectonic environments, most based on observations of modern rocks in known environments and extrapolation of these results to unknown ancient environments (e.g. Pearce and Cann, 1973; Miyashiro, 1974; Garcia, 1978; Wood et al., 1979; Pearce, 1980; Meschede, 1986). Of particular value in interpreting ancient volcanic rocks has been the recognition that the LFSE and some of the HFSE behave coherently in normal mantle environments but are decoupled in a subduction environment, the LFSE being anomalously enriched and the HFSE, particularly Ta and Nb, being depleted relative to the LREE. This characteristic has lead to a number of discrimination diagrams, the best known of which is the Ta-Hf-Th diagram of Wood et al. (1979).

Preliminary conclusions regarding the paleotectonic environment of the various groups have already been presented in Section 3.3.3. In the following discussion, these are supplemented by four additional diagrams. The Ti-V diagram (after Shervais, 1982) provides some separation of tholeiitic basalt types but is most useful in distinguishing within-plate groups of transitional and alkalic nature. The Zr/Y - Zr plot of Pearce and Norry (1979) provides some separation between plate marginal and within plate types and more importantly, a visual illustration of subdivisions within the groups distinguished by different incompatible element ratios. The Ta-Hf-Th plot provides a good separation of arc from non-arc types and related binary plots from Wood et al. (1979) further illustrate this separation. Finally, chondrite-normalized REE plots allow comparison with modern rocks of known tectonic affinity and lead into a discussion of possible source areas and fractionation histories.

3.4.1.3 Fractionation histories

The origin of geochemical trends developed in the various suites and subsuites (e.g. fractional crystallization, partial melting, mixing) is investigated in a preliminary way in this Chapter using combinations of trace and major elements. Detailed considerations await the presentation of isotopic data in Chapter 4.

Fractionation pathways for different element pairs can be calculated for any assumed

fractionation model and compared to the actual variation of these two elements, assuming that the observed variation is results from fractional crystallization. By choosing elements that have high distribution coefficients for only one of the minerals likely to be crystallizing in the magma, and in concert with petrographic observations of phenocryst abundances, this approach can yield a qualitative estimate of the minerals potentially involved in the fractionation.

The approach is illustrated, for suites that have a sufficient number of samples, by a series of binary plots. The Ti - Y plot provides an estimate of the total fractionation and the Cr - Ni plot, an illustration of olivine and pyroxene fractionation. Plagioclase fractionation is estimated from the Al_2O_3 - Ti plot of Pearce and Flower (1977).

Preliminary modelling of trace element concentrations has been used: 1) to test whether the trends can be reasonably interpreted as the result of fractional crystallization; 2) to provide an estimate of the amount of fractionation represented by the available sample set; and 3) to estimate the approximate proportions of the minerals involved. Rayleigh fractional crystallization was assumed. Distribution coefficients used in these calculations are detailed and referenced in Appendix 9. The modelling approach is as follows:

1) A selection of both incompatible and compatible elements were plotted against Mg#.

2) The endpoints of a least squares regression line through the data for the incompatible element data were taken as the maximum and minimum of the concentration range of the element and used to calculate the amount of fractional crystallization necessary to account for the variation. Where each incompatible element yielded a similar estimate of the amount of fractionation, the hypothesis that the observed variation results principally from fractional crystallization was accepted. Where different incompatible elements gave different estimates of total fractionation for the same sample set, the hypothesis was rejected.

3) In most suites in the Wild Bight Group, petrographic and/or geochemical evidence suggests that olivine, clinopyroxene and plagioclase were the most important minerals during fractional crystallization. The approximate proportions of olivine and clinopyroxene crystallization were estimated by adjusting the proportions of these minerals in the model to produce the

observed changes in Cr and Ni (the endpoints of regression lines through the data plotted against Mg#) after the appropriate total fractionation (estimated from incompatible element changes). If plagioclase was the only other mineral on the liquidus, its proportion in the model is, therefore, fixed; this was checked qualitatively against the estimate provided by the Pearce and Flower (1977) Al_2O_3/Ti versus Ti diagram.

3.4.2 The IAD Group

The IAD group is characterised by very low contents of incompatible elements and by SiO_2 contents that vary widely but are generally in the andesitic range (Table 3.2). In the Glover's Harbour West suite, TiO_2 and V increase regularly with decreasing Mg# (Figure 3.15). The least fractionated samples have Mg# of approximately 0.6 and low contents of both Ni and Cr, indicating that some fractionation has occurred prior to eruption. SiO_2 does not show such a consistent relationship with Mg# which is not surprising considering the abundant petrographic evidence for mobility of silica during alteration (e.g. free quartz in vesicles, veins and groundmass). The relationships between secondary quartz and silica content of the rocks is not straightforward. Some rocks with the most abundant amygdule-filling quartz actually have relatively low silica contents (e.g. 2140471, 2140476) while other samples with relatively high silica contents contain little optically resolvable free quartz (e.g. 2140462, 2140477). As previously noted, in the absence of abundant free quartz in amygdules and veins, the silica content of sub-seafloor, hydrothermally altered, basalt is likely to represent a minimum for the original silica content. It is tentatively concluded that at least some of these rocks may have been originally andesites, although their silica contents may have been redistributed somewhat during alteration.

Cr and Ni abundances are generally very low and decrease steadily with decreasing Mg#, consistent with continued fractionation involving olivine and pyroxene.

The sample from the Indian Cove suite has incompatible element contents and Mg# similar to the Glover's Harbour West suite and may be petrogenetically related. However, the elevated Cr

Table 3.2: Major (wt. %) and trace (ppm) element compositions of samples in the IAD group.

Suite	|-Indian Cove-	|-Side Harbour**--------|	|-------Glover's Harbour West-------------			
Sample	2140492	2140526	2140765	2140456	2140458	2140460	2140462	2140471
SiO2	59.07	58.91	62.57	54.81	54.86	49.42	66.23	50.39
Al2O3	14.29	14.32	12.89	15.29	15.63	17.12	12.02	16.52
Fe2O3	3.61	2.83	1.62	3.38	2.19	3.3	1.86	4.12
FeO	4.67	10.17	8.28	7.09	7.39	8.39	5.75	8.89
MgO	5.06	4.38	3.37	5.46	7.04	7.14	5.09	5.26
CaO	8.79	3.79	5.8	6.77	8.64	10.65	4.52	12.37
Na2O	3.77	4.65	4.58	6.01	3.38	2.51	1.38	1.53
K2O	0.17	0.16	0.13	0.12	0.26	0.79	2.24	0.11
TiO2	0.46	0.54	0.52	0.67	0.47	0.52	0.45	0.62
MnO	0.1	0.22	0.19	0.13	0.12	0.16	0.15	0.17
P2O5	0.03	0.04	0.05	0.28	0.03	0.01	0.31	0.03
LOI	5.95	2.75	3.86	5.68	5.68	4.10	4.83	4.86
Total*	100.42	99.84	99.43	100.18	99.74	100.21	99.65	99.92
Cu	51	160	141	178	117	26	108	138
Zn	58	117	91	92	77	58	69	87
Ni	75	4	5	6	12	12	12	7
Cr	461	50	28	48	62	64	45	50
V	245	403	364	361	310	355	235	375
Sc	41.7			41	45.6			
Co	30			32	45.6			
Rb	1.9	7	<0.5	1.6	2.5	12	24	1.3
Sr	83	50	55.0	40	116	88	75	82
Ba	<20	43	<20	38	33	50	87	35
Th	0.24			0.05	0.14			
Y	8	7	8	28	5	6	25	7
Zr	6	7	8	11	7	9	4	7
Nb	<0.5	<0.5	0.7	0.6	0.5	0.6	<0.5	<0.5
Hf	2.90			0.43	0.21			
Ta	0.01			0.01	0.01			
La	0.81	0.6		2.1	0.59	0.8		
Ce	2.1			5	1.5	0.8		
Nd	1.4	1.1		3.9	1	1.9		
Sm	0.71	0.7		1.6	0.58	0.8		
Eu	0.29			0.66	0.29	0.4		
Gd	0.01	0.9		2.6	0.01	1.1		
Tb	0.21			6.55	0.19			
Dy		1				1.7		
Er		0.8				1.2		
Yb	0.87			3.3	0.76	0.7		
Lu	0.14			0.5	0.15			
La/Ta	81.0			210.0	59.0			
Th/Ta	24.00			5.00	14.00			
(La/Sm)n	0.70			0.80	0.62	0.61		
Ti/Zr	451	460	405	380	425	353	636	507
Zr/Nb			11	19	13	14		
Ti/V	11	8	9	11	9	9	11	10
Zr/Y	0.7	1.0	1.0	0.4	1.2	1.5	0.2	1.0
Ti/Y	333	472	410	143	515	516	106	503
Mg#	0.56	0.41	0.41	0.52	0.60	0.55	0.58	0.45

* - analytical total; major element concentrations are recalculated to 100% anhydrous
** - Side Harbour suite samples from Point Leamington deposit footwall

Table 3.2 (continued)

	-----------Glover's Harbour West (continued)-----------						
Sample	2140472	2140473	2140474	2140475	2140476	2140477	2140478	2140480
SiO2	55.14	58.71	56.88	48.44	51.72	59.16	53.21	51.48
Al2O3	14.85	13.56	15.3	21.07	16.36	14.02	15.32	18.85
Fe2O3	4.57	3.02	3.04	1.57	5.18	3.68	2.3	1.84
FeO	6.45	7.51	5.88	8.06	6.5	6.81	6.79	8.85
MgO	4.5	5.49	3.87	6.1	4.65	4.5	5.41	7.82
CaO	13.04	8.22	13.67	9.36	10.96	6.08	10.12	4.05
Na2O	0.57	2.64	0.47	3.04	3.83	4.94	6.08	6.17
K2O	0.17	0.12	0.25	1.82	0.04	0.06	0.07	0.21
TiO2	0.52	0.53	0.47	0.35	0.57	0.66	0.49	0.48
MnO	0.16	0.16	0.14	0.16	0.17	0.06	0.2	0.22
P2O5	0.02	0.03	0.03	0.01	0.02	0.03	0.01	0.02
LOI	4.41	3.18	4.99	8.03	3.44	2.96	5.62	5.98
Total*	100.32	99.41	100.10	100.10	100.31	99.99	99.59	99.61
Cu	116	113	123	94	109	101	113	110
Zn	71	69	69	68	63	165	64	70
Ni	6	6	7	15	6	7	10	12
Cr	47	45	42	63	45	54	56	71
V	330	307	302	239	325	425	313	300
Sc		46.6			45.8			
Co		33.6			30.8			
Rb	1.3	1.0	2.0	14	<0.5	<0.5	<0.5	<0.5
Sr	36	19	12	38	19	30	64	53
Ba	32	22	25	52	20	50	21	44
Th		0.14			0.16			
Y	5	7	7	4	7	9	6	6
Zr	5	4	4	4	6	9	3	6
Nb	1.4	<0.5	<0.5	<0.5	<0.5	<0.5	<0.5	<0.5
Hf		0.24			0.27			
Ta		0.01			0.01			
La		0.4			0.55			
Ce		1.2			1.4			
Nd		0.9			1.3			
Sm		0.52			0.65			
Eu		0.25			0.29			
Gd		1.1			0			
Tb		0.18			0.19			
Dy								
Er								
Yb		0.87			0.87			
Lu		0.18			0.16			
La/Ta		40.0			55.0			
Th/Ta		14.00			16.00			
(La/Sm)n		0.47			0.52			
Ti/Zr	620	714	676	578	563	430	1053	503
Zr/Nb	4							
Ti/V	9	10	9	9	11	9	9	10
Zr/Y	1.0	0.6	0.6	0.8	0.8	1.0	0.5	0.9
Ti/Y	590	439	392	487	473	418	500	474
Mg#	0.46	0.52	0.47	0.56	0.45	0.47	0.55	0.60

* - analytical total; major element concentrations are recalculated to 100% anhydrous
** - Side Harbour suite samples from Point Leamington deposit footwall
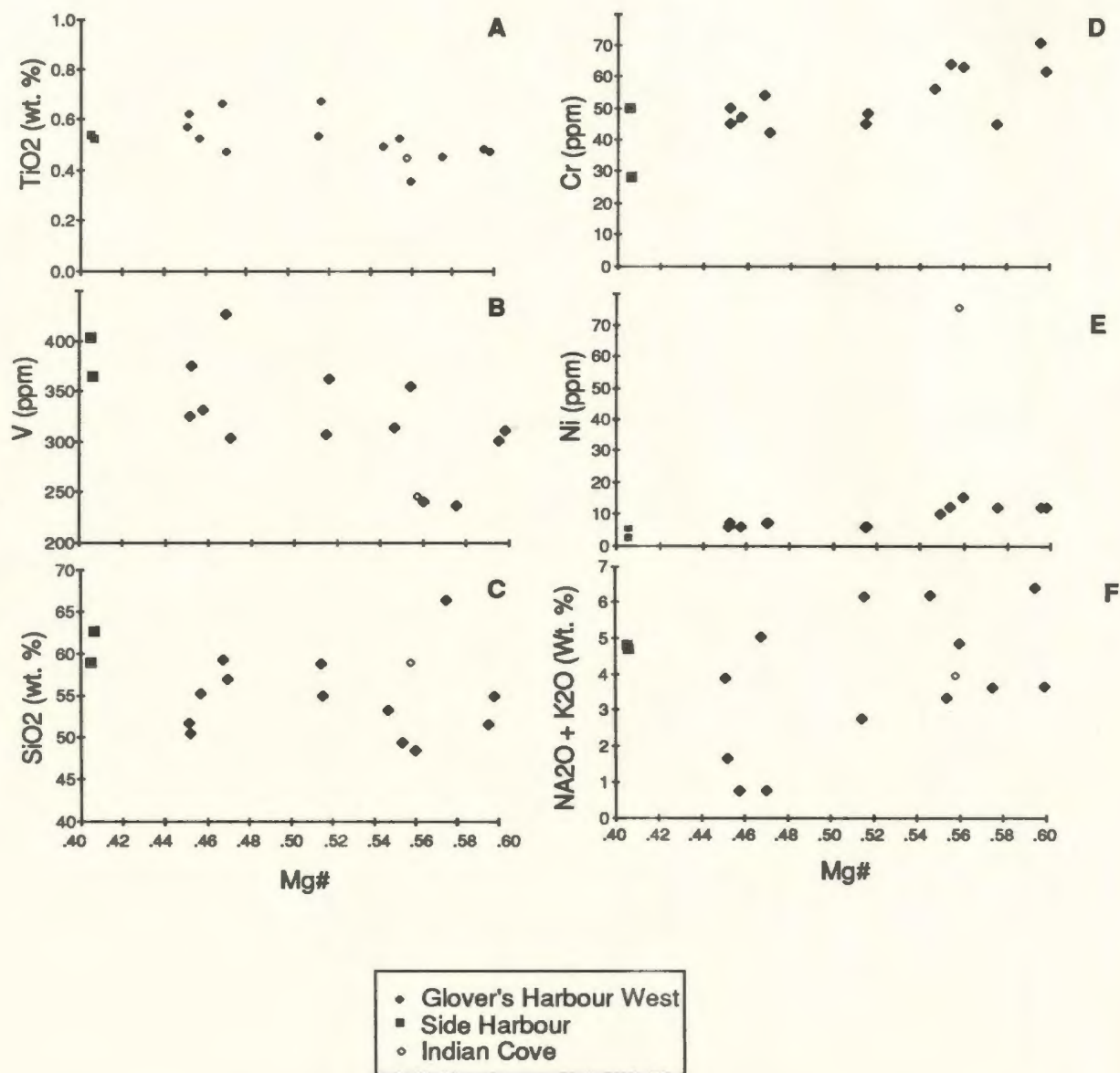
Figure 3.15: TiO2, V, SiO2, Cr, Ni and total alkalis, versus Mg# for the IAD group. The regular increase of TiO2 and V with decreasing Mg# and the corresponding decrease in Cr and Ni suggest fractional crystallization. Scatter in the SiO2 data probably results from silica remobilization during alteration. Total alkalis, used as an index of alteration, show no correlation with Mg# in the Glover's Harbour West suite suggesting that variation in Mg# is not closely linked to alteration.

and Ni contents probably reflect cumulate olivine and pyroxene and this analysis may not be a liquid composition. The two samples from the Side Harbour suite have considerably lower Mg#, reflecting lower MgO and marginally lower FeO^t (the superscript refers to total iron, in this case calculated as FeO) concentrations. Their incompatible element concentrations, however, are, similar to the other suites. These two samples were taken in the footwall of the Point Leamington massive sulphide deposit and their field and petrographic characteristics suggest a more intense hydrothermal alteration than is normal for regional greenschist metamorphism in the Wild Bight Group. In this situation, Mg and Fe have probably been mobile and the Mg# may not accurately reflect the degree of differentiation of the protolith.

Samples 2140456 and 2140462 in the Glover's Harbour West suite have anomalously high P_2O_5 and $\dot{Y}$ contents but are not otherwise remarkable. This may indicate the presence of some accumulated apatite.

The very low TiO_2 contents and Nb/Y ratio <1 dictate that these rocks are non-alkalic (Floyd and Winchester, 1975) (Figure 3.16). The increasing TiO_2 and V contents with differentiation (Figure 3.15A,B) suggest that they are tholeiites.

In Table 3.3, the depleted group is compared to representatives of similarly depleted magma series from modern oceanic volcanic environments. Specific points of comparison are illustrated in Figures 3.17 and 3.18. Four pairs of samples are chosen to illustrate the comparison, comprising two boninites from the Mariana-Bonin arc system (representing melting of refractory sources in a supra-subduction environment), two normal low-K tholeiitic, basaltic andesites from the intra-oceanic Tongan arc, two unusually depleted basaltic andesites from the Tonga-Kermadec arc, and two island arc tholeiitic basalts from the New Britain reference suite of the Basaltic Volcanism Study Project. In all cases, the sample pairs represent the extremes of a range of compositions.

The IAD group displays similarities with each of the reference pairs while being strictly. comparable to none of them. Like the Tongan arc tholeiites, it has undergone moderate to substantial fractional crystallization (in contrast to the New Britain arc tholeiites and the boninites)
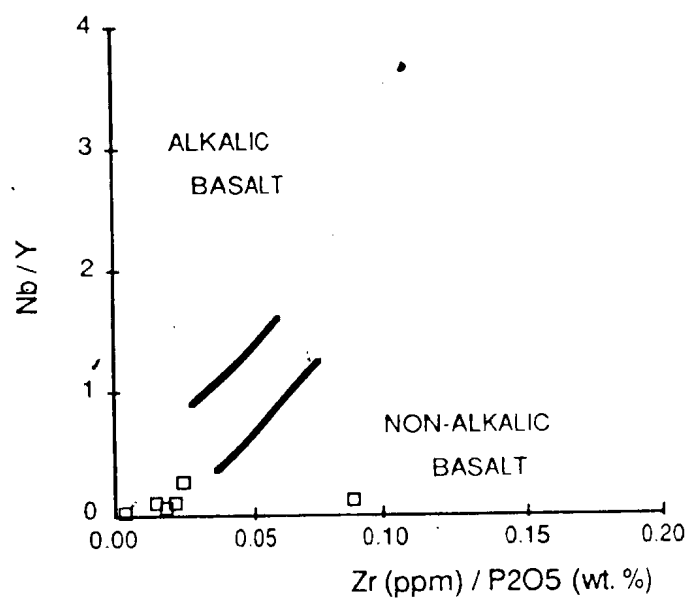
Figure 3.16: Discrimination of alkalic and non-alkalic basalts, after Floyd and Winchester (1975), for the IAD group. Stippled area is transitional. The very low Zr contents shift these rocks to the left of the field of normal basalts but the very low Nb / Y ratio confirms them as non-alkalic.

Table 3.3 Comparison of the IAD group with depleted basic volcanic rocks in modern plate marginal environments

	IAD group				Modern Examples							
	Mean	St Dev	Max	Min	A	B	C	D	E	F	G	H
SiO2	55.49	4.84	66.23	48.44	58.46	57.99	57.57	54.44	52.52	48.58	53.1	49.2
Al2O3	15.53	2.18	21.07	12.02	13.37	14.48	14.14	18.52	16.85	17.73	14.7	14.4
Fe2O3	3.04	1.05	5.18	1.57			3.6	2.08	5.34	2.24	1.91	1.4
FeO	7.7	1.98	13.34	4.67	8.27	8.03	8.62	6.73	4.87	8.07	6.9	8.1
MgO	5.35	1.18	7.82	3.37	9.39	6.71	3.29	4.16	6.04	6.77	9.2	10.8
CaO	8.28	3.26	13.67	3.79	8.11	10.47	8.49	11.31	11.95	12.84	10.9	11.4
Na2O	3.35	1.89	6.17	0.47	1.59	1.87	2.42	1.78	0.95	1.37	1.58	2.15
K2O	0.51	0.73	2.24	0.04	0.7	0.35	0.7	0.24	0.15	0.13	0.22	0.17
TiO2	0.54	0.12	0.87	0.35	0.1	0.23	0.8	0.49	0.36	0.69	0.3	1.15
MnO	0.16	0.04	0.22	0.06			0.21	0.16	0.18	0.18	0.16	0.18
P2O5**	0.03	0.01	0.01	0.06			0.12	0.06	0.04	0.02	0.03	0.11
Cu	117	40	189	26			215		67	94	97	86
Zn	85	32	165	58					72	76	2.6	1.9
Ni***	8	4	15	3	140		9	26	23	33	88	196
Cr***	15	13	64	22	538	197	6	54	62	54	283	535
V	324	54	425	235	174		410	260	315	350	188	230
Sc*	44.14	2.59	46.60	41.00	36.2	33.3	41	35			42	33
Co*	34.4	6.4	45.6	30.0			31	26	34	34		
Rb	5	7	24	<0.01	12.2	85	9	120	56	23	2.6	2.4
Sr	60	38	158	12.0	97.2	89.1	225	85	145	175	167	187
Ba	39	22	87	13	30	26.8	165	120	2	2.3	40	38
Th*	0.15	0.07	0.24	0.05			0.27	0.16	0.13	0.21	0.07	0.29
Y**	7	2	13	4.3	4.9	7	25	16	6	9.4	6	25
Zr	7	2	11	2.8	25.4	28	38	24	7.6	16	15.7	64
Nb	0.4	0.3	1.4	<0.5			0.63	0.52			1.4	3.89
Hf*	0.29		0.43	0.21	0.69	0.62	0.92	0.73			0.5	1.75
Ta*	0.01	0.01	0.01	<0.01								
La*	0.89	0.69	2.10	0.40	1.27	0.75	2.9	1.6	1	1.1	0.74	3.97
Ce*	2.24	1.58	5.00	1.20	2.57	2.1	7.1	3.6	2.3	3	2.05	12.1
Nd*	1.70	1.25	3.90	0.90	1.65	1.72	5.45	3	1.8	2.8	1.68	9.33
Sm*	0.81	0.45	1.60	0.52	0.43	0.57	1.9	1.2	0.59	0.96	0.6	2.7
Eu*	0.36	0.17	0.66	0.25	0.15	0.23	0.69	0.45	0.26	0.42	0.26	0.98
Gd*	0.74	1.14	2.60	0.00			2.4	1.5	0.94	1.5	0.86	3.23
Tb*	0.26	0.16	0.55	0.18	0.1	0.16	0.43	0.3	0.18	0.27	0.16	0.59
Dy*									1.1	12.8		
Er*									0.87	1.2		
Yb*	1.33	1.10	3.30	0.76	0.59	0.74	2.3	1.5	0.85	1.18	0.74	2.22
Lu*	0.23	0.15	0.50	0.14	0.1	0.12					0.11	0.34
La/Ta*	89.0	69.2	210.0	40.0								
Th/Ta*	14.6	6.8	24.0	5.0								
(La/Yb)n*	0.4	0.1	0.6	0.3	1.4	0.7	0.8	0.7	3.2	3.5	0.7	1.18
Tv/Zr	541.7	169.0	1053	352.6	23.4	49.2	126.2	122.4	283.9	258.5	114.5	107.7
Zr/Nb	18.8	8.1	36.8	3.6			60.3	46.2			11.2	16.4
Tv/V	10.1	1.9	16.6	8.0	3.4		11.7	11.3	6.9	11.8	9.6	30
Zr/Y**	0.9	0.3	1.5	0.2	5.2		1.5	1.5	1.3	1.7	2.6	2.56
Tv/Y**	465.9	63.8	590.3	106.5	122.3	4.0	1.8	183.6	359.6	440.0	299.7	275.7
Mg#	0.50	0.07	0.60	0.41	0.67	0.60	0.35	0.49	0.55	0.57	0.68	0.70

* - INAA data only
** - Excluding 2140456 and 2140462 due to probability of cumulate apatite
***- Excluding 2140492 because of the probability of cumulate olivine and/or pyroxene

A - Chichi Jima, Bonin Islands, bonninite, volatile free whole rock microprobe analysis by G. Jenner,
    quoted by Hickey and Frey (1982).
B - DSDP site 458, sample No. 28-1, Mariania forearc, bonninite, volatile free whole rock analysis from Meijer (1980)
C - Island arc tholeiite L 13 from Lale, Tonga Arc (Ewart et al., 1973)
D - Island arc tholeiite, basal flow from Hunga Ha'apai, Tonga Arc (Ewart et al., 1973)
E - Island arc depleted tholeiitic basalt Tahafi 116, northern Tonga (Ewart et al., 1977)
F - Island arc depleted tholeiitic basalt Raoul 7128, Kermadec arc (Ewart et al., 1977)
G- Island arc tholeiite IA-1 from the New Britain reference suite, Basaltic Volcanism Study Project (1981)
H - Island arc tholeiite IA-11 from the New Britain reference suite, Basaltic Volcanism Study Project (1981)
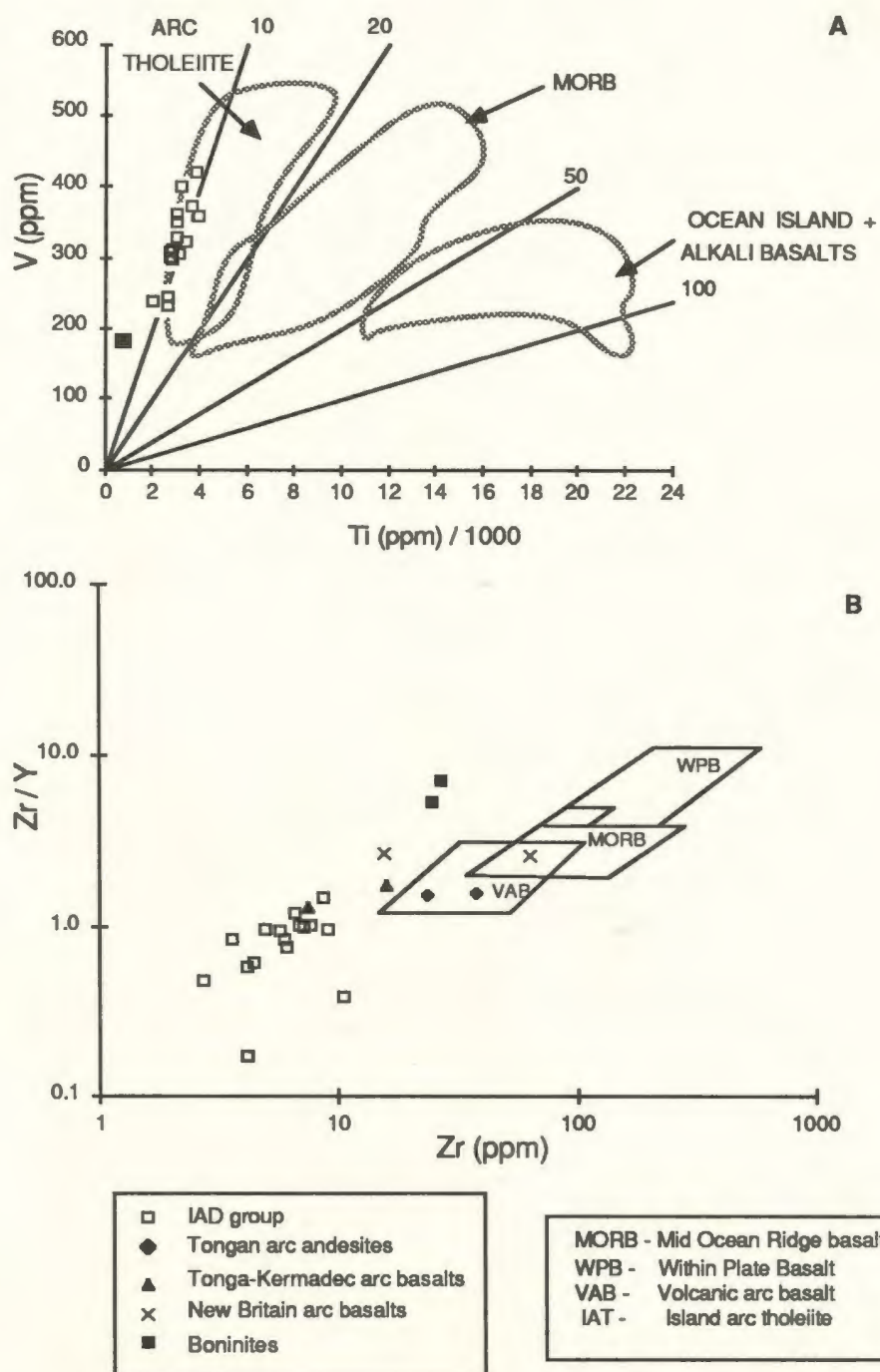
Figure 3.17: Ti-V (Shervais,1982) and Zr / Y - Zr (Pearce and Norry, 1979) plots for the IAD group. In A, the IAD group plots in the arc tholeiite field with approximately chondritic ratios. Tongan and New Britain arc tholeiites (not shown) plot in the same area but boninites (closed square) plot closer to the origin with less than chondritic ratios. Solid lines are equal Ti / V ratios. In B, all IAD group samples plot outside the field of normal arc basalts due to extreme Zr depletion.
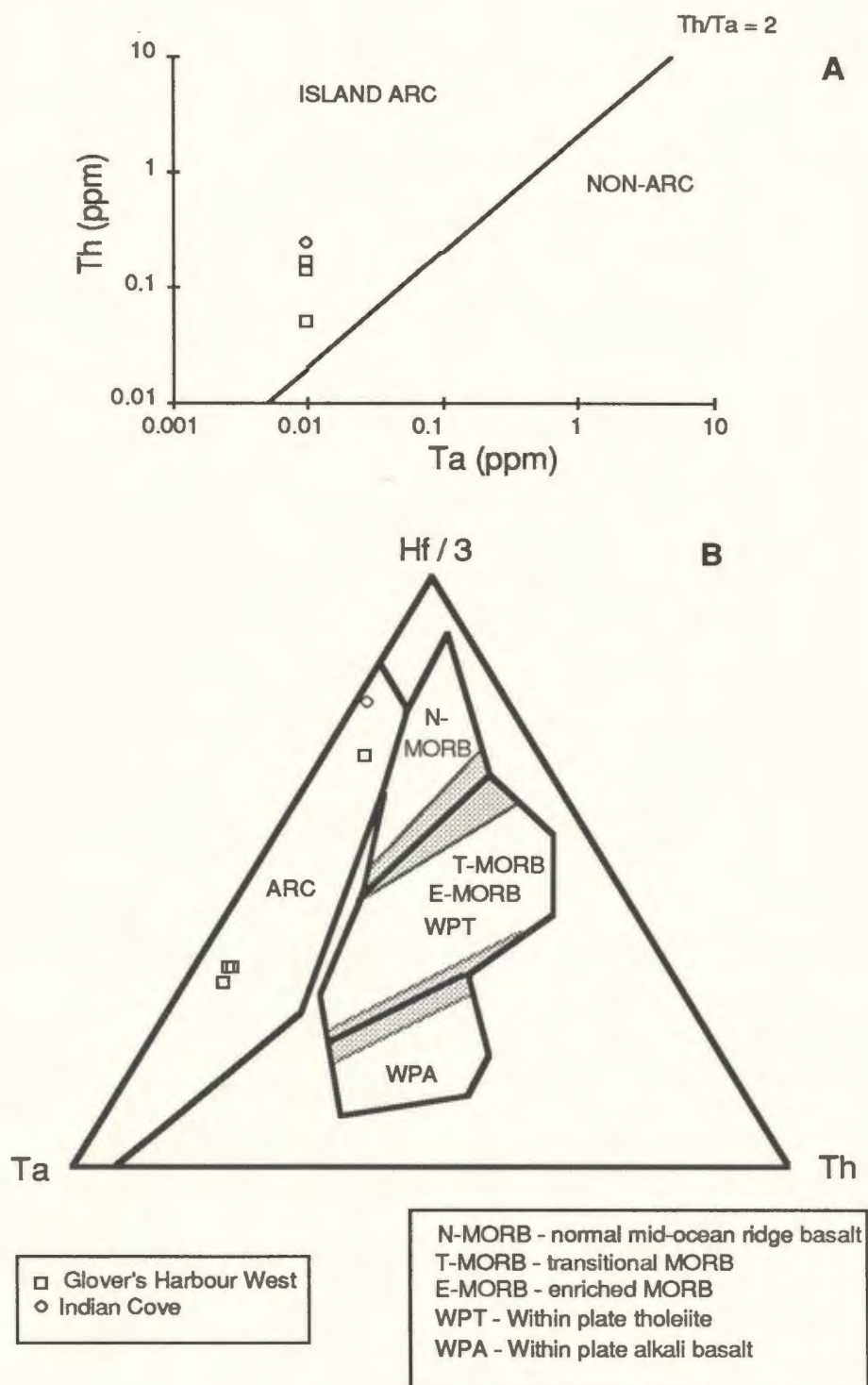
Figure 3.18: Th-Ta and Hf-Ta-Th diagrams for the IAD group. All samples plot in the arc fields. Stippled areas in B are fields of overlap.

and as a result has comparably low Ni, Cr and Mg# (although the depleted Tonga arc samples are generally less fractionated than the normal arc tholeiites).

Ti and V contents and the Ti/V ratio of both the IAD group and the two modern island arc suites are approximately chondritic and within the range of typical island arc tholeiites (Figure 3.17). Boninites generally have lower Ti contents and less than chondritic Ti/V, plotting closer to the origin of this diagram.

The IAD group is very strongly depleted in Zr, Nb and the LREE compared to all except the depleted Tonga-Kermadec tholeiites and has higher Ti/Zr ratios than all of the modern arc suites. However, absolute abundances of other incompatible elements are similar to those in the arc suites as are incompatible element ratios (e.g. Zr/Y and Ti/Y). Compared to boninites, the IAD group is strongly depleted in Zr, Nb and Hf and enriched in Sc, TiO_2 and V. It lacks the very low Ti/Zr ratios characteristic of boninites (Hickey and Frey, 1982).

On the Zr/Y-Zr diagram (Figure 3.17B), the IAD group plots outside the field of arc lavas because of its extreme Zr depletion (as previously seen on the Ti-Zr-Y diagram, Figure 3.12). In this respect, it is most similar to the depleted Tonga-Kermadec rocks. The wide variation in Zr/Y ratio probably results mainly from analytical imprecision at very low abundances. Normal Tongan arc tholeiites and all but the most depleted New Britain tholeiites plot within the VAB field. Boninites also plot outside the arc field but have considerably higher Zr/Y values.

The affinity with island arc environments, although with an abnormal HFSE depletion, is further supported by Ta-Hf-Th relationships (Figure 3.18). Th/Ta ratios are considerably greater than 2 and characteristic of island arc environments (Wood et al., 1979). All samples plot in the arc field on the ternary diagram.

Chondrite normalized rare earth patterns for the IAD group (Figure 3.19) show them to be severely depleted in the LREE (La_n/Yb_n=0.45), even relative to the Tongan and New Britain arc tholeiites (La_n/Yb_n=0.66 to 1.2). The intervals La to Nd and Eu to Tb have flat trends and there is a distinctive 'step' upward between Nd and Eu. A single sample, 2140456, has anomalously high REE abundances and a smoother pattern with slightly positive $(La/Ce)_n$ and $(Yb/Lu)_n$. This
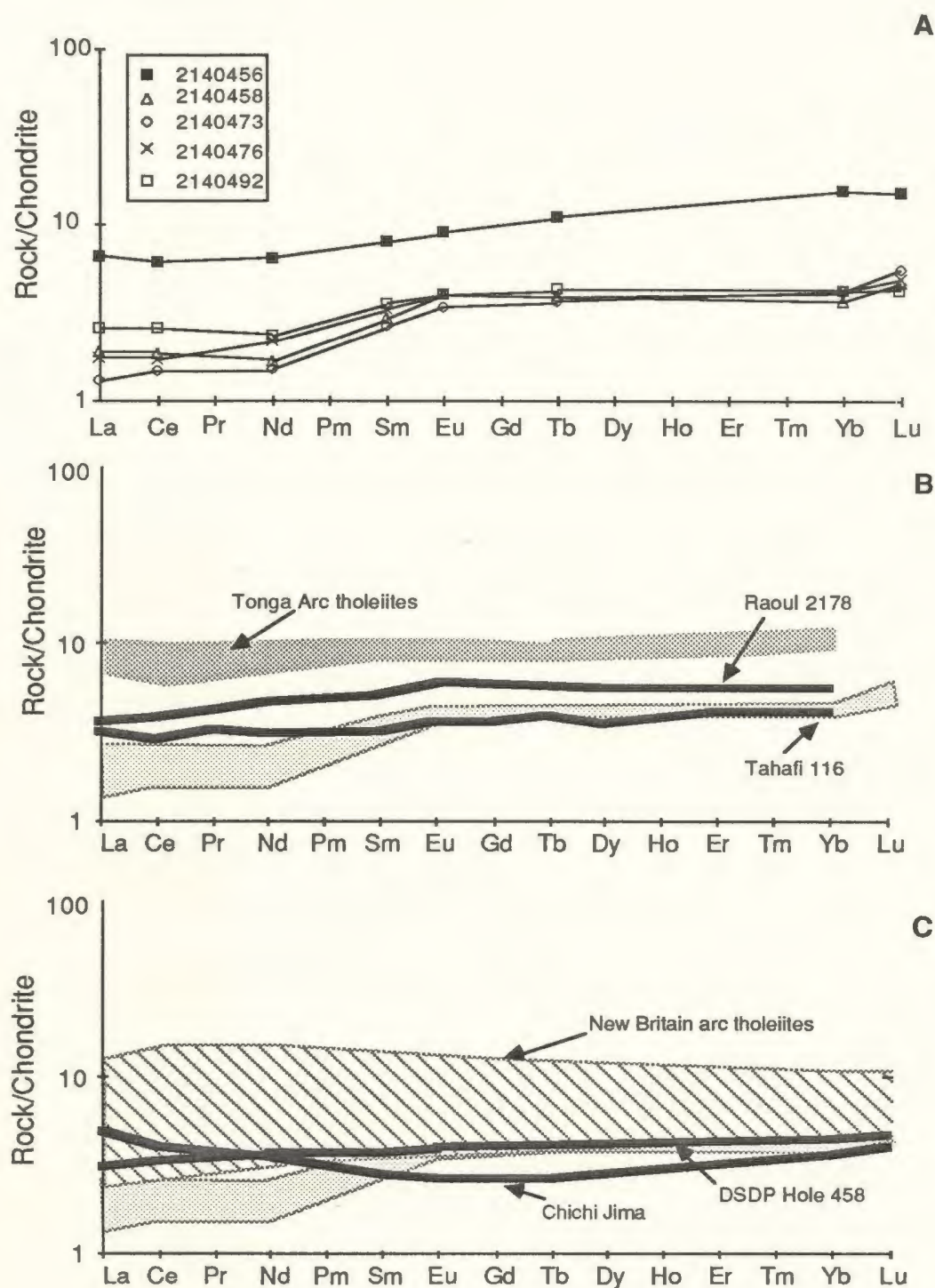
Figure 3.19: Chondrite-normalized REE plots for the IAD group (A) and selected samples from modern arcs (B and C). Chondrite normalization values after Taylor and Gorton (1977). Light stippled field in B and C is IAD group field excluding 2140456.

sample probably contains cumulate apatite (see above); the high crystal-liquid distribution coefficient for the rare earths in apatite may account for this anomalous pattern.

The middle rare earth elements (MREE) and HREE in the IAD group have similar distribution and abundances to the Mariana forearc boninite, the depleted Tonga-Kermadec andesites and the most primitive New Britain arc basalts but are considerably more depleted than the normal Tongan arc andesites. The Tonga and New Britain rocks have flat to slightly LREE-depleted patterns (La_n/Yb_n=0.66 to 1.2). The Bonin Islands boninite has MREE and HREE abundances approximately similar to the IAD group (although without the 'step' between Nd and Sm) but is LREE enriched, displaying a concave - upward REE pattern. This pattern, common in boninites (Hickey and Frey, 1982), is generally interpreted as resulting from a two stage melting history involving an early partial melting of a mantle source followed by remelting of the refractory source coupled with metasomatic introduction of LREE (e.g. Sun and Nesbit, 1978, 1980; Hickey and Frey, 1982). MREE and HREE abundances and patterns in DSDP Hole 458 boninites and the depleted Tonga-Kermadec andesites are similar to the IAD group but they are less depleted in the LREE (La_n/Yb_n=0.67).

Clearly, the IAD group must represent melting of a very refractory source. MREE and HREE abundances suggest that this source was at least as depleted as those postulated for boninites and more so than the sources of most island arc tholeiites. This question is considered in more detail in Chapter 4.

As previously noted, the Glover's Harbour West suite apparently records fractionation of a tholeiitic magma that has previously undergone substantial olivine and clinopyroxene crystallization. The TiO_2-Y diagram (Figure 3.20A) suggests that approximately 20 to 25 percent crystallization of a combination of clinopyroxene, olivine and plagioclase crystallization has occurred. Approximately 20-25 percent plagioclase fractionation is indicated by the Al_2O_3/TiO_2-Ti diagram (Figure 3.20B) and confirms that the single Al_2O_3-rich sample (2140475) is probably a plagioclase cumulate. The Cr-Ni and Cr/Ti-Ti diagrams suggest that both clinopyroxene and olivine were on the liquidus. The likelihood of orthopyroxene crystallization
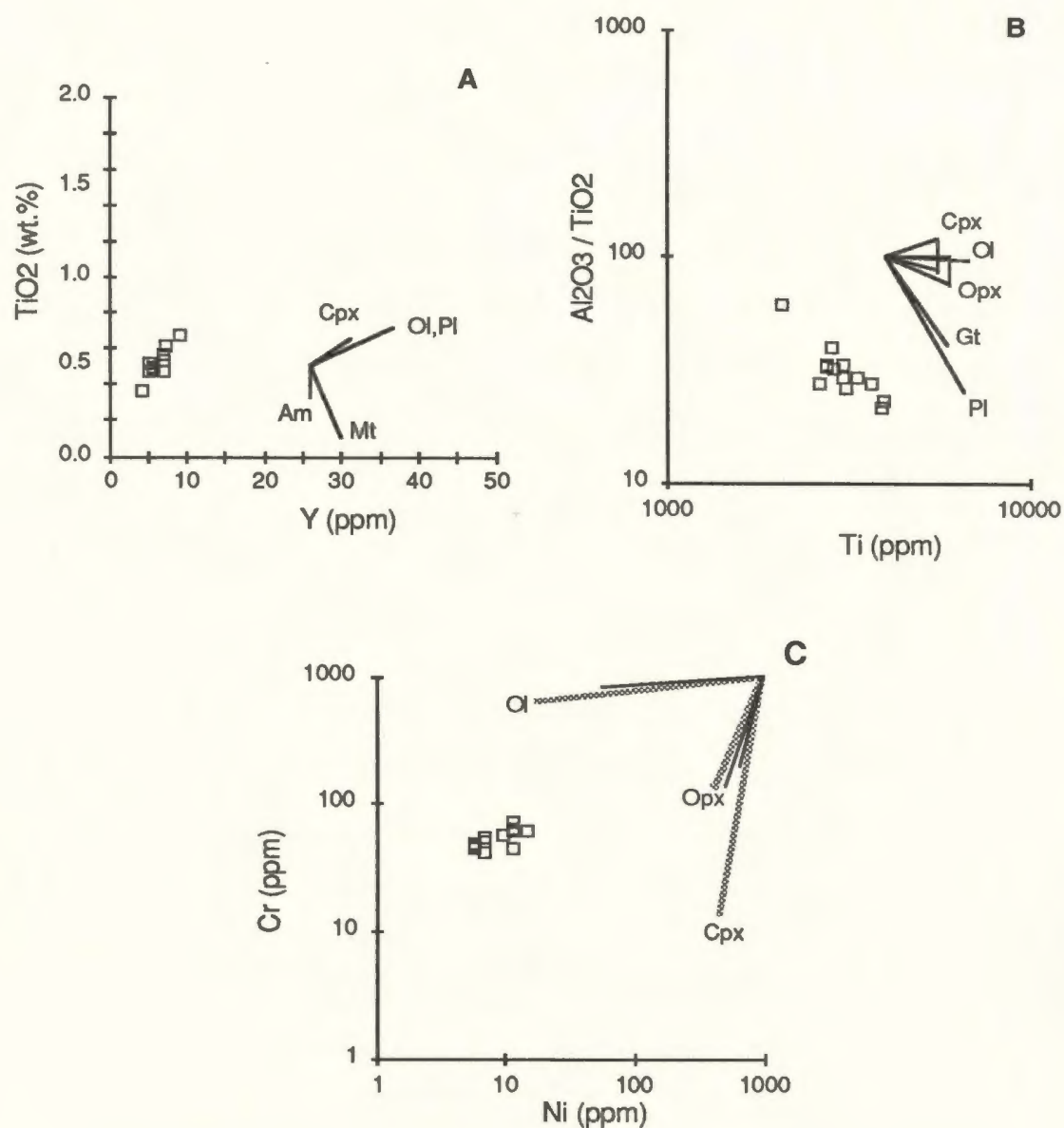
Figure 3.20: Binary plots with Rayleigh fractionation vectors as indicators of the fractionation history of the Glover's Harbour West suite. A-after Perfit et al. (1980) with 30% fractionation vectors; B - after Pearce and Flower (1977) with 50% fractionation vectors. D - 20% fractionation vectors (ol:cpx:pl = 0.2:0.2:0.6) calculated from distribution coefficients in Appendix 9 (solid lines - primitive basalt; stippled lines -fractionated basalt).

cannot be evaluated by the available data. However, its presence on the liquidus would not substantially change the conclusions of the preliminary modelling below.

Zr and Nb cannot be used in preliminary modelling of the Glover's Harbour West suite as their concentrations in the most primitive samples are either below detection limits or so low that they have very high analytical-uncertainties. Results of modelling using Ti and V are summarized in Table 3.4. Changes in both Ti and V are consistent with approximately 25-30 percent Rayleigh fractionation, indicating that the trends developed in Figures 3.4A and B indeed result from fractional crystallization. An ol:cpx:pl ratio of approximately 0.2:0.2:0.6 can account for the observed decrease in Cr and Ni over this fractionation interval and the 15 to 18 percent plagioclase fractionation that this indicates is in reasonable agreement with the 20 to 25 percent suggested by Figure 3.20B.

3.4.3 The IAI Group

The IAI group is the most geochemically heterogeneous in the Wild Bight Group. Intersuite variations within this group suggest that a number of contrasting petrogeneses are represented, and even within some suites, relatively subtle variations suggest additional complications in their genesis. Compositions of the IAI group samples are found in Table 3.5 and the mean compositions of the various suites are compared in Table 3.6. In broad terms, the IAI group is geochemically bipartite; the Glover's Harbour East, Seal Bay Bottom and Northern Arm suites have similar incompatible element abundances and ratios, (Table 3.6) and are distinctly different from the Nanny Bag Lake suite, which has relatively higher concentrations of FeO^t, TiO_2, V, P_2O_5 and Y and lower concentrations of Al_2O_3, Zr, Nb, Ta, Hf and Th. Consistent contrasts in incompatible element ratios between the Glover's Harbour East/ Seal Bay Bottom / Northern Arm suites and the Nanny Bag Lake suite further emphasize this dichotomy, and suggest contrasts in the source regions and melting histories of these rocks.

Plots of various elements versus Mg# (Figure 3.21) further emphasize the dichotomy and illustrate geochemical relationships within the group. In all suites, TiO_2 and Zr increase regularly

Table 3.4. Results of trace element modelling of fractionation in the Glover's Harbour West suite.

Model parameters: ol:cpx:pl=0.2:0.2:0.6
Distribution coefficients: primitive basalt (Appendix 9)

	Starting Composition	Ending Composition	% Total Fractionation
TiO$_2$ (wt. %)	0.45	0.59	22-30 (±5%)
V (ppm)	281	356	25-36 (±5%)
Cr (ppm)	62	45.5	20-27 (±5%)
Ni (ppm)	12.8	5.8	17-34 (±20%)

Table 3.5: Major (weight percent) and trace (ppm) element compositions of the IAI group

Suite	Glover's Harbour East					Seal Bay Bottom		
Sample	2140463	2140464	2140467	2140468	2140470	2140553	2140554	2140555
SiO2	53.17	52.52	55.96	55.65	56.34	53.98	53.18	55.88
Al2O3	18.49	19.75	16.93	15.94	18.06	16.92	18.33	16.65
Fe2O3	1.8	1.87	3.08	4.16	2.71	2.06	1.95	1.84
FeO	5	4.83	5.85	5.3	6.11	8.8	5.87	7.02
MgO	4.77	4	2.75	2.48	3	5.26	5.7	4.27
CaO	9.84	11.11	6.49	7.74	5.15	4.63	9.6	6.75
Na2O	5.06	4.69	6.57	6.51	6.46	6.18	3.78	5.46
K2O	0.67	0.13	0.53	0.55	0.74	0.24	0.26	0.32
TiO2	0.94	0.87	1.49	1.37	1.11	1.51	0.99	1.44
MnO	0.17	0.15	0.15	0.13	0.14	0.23	0.21	0.19
P2O5	0.09	0.08	0.21	0.17	0.18	0.2	0.14	0.18
LOI	4.11	5.12	2.49		2.26	2.56	4.07	2.31
Total*	99.84	100.33	99.35	98.77	99.71	99.81	100.35	99.30
Cu	32	33	20	26	138	21	41	29
Zn	63	54	84	81	75	88	72	83
Ni	22	20	<1	<1	10	2	48	3
Cr	90	100	34	34	34	41	178	42
V	189	171	287	282	375	330	198	247
Sc	30.1		29.6			37.1	21.1	
Co	30		23.2			30.4	28.2	-
Rb	14	1.5	4	7	16	2.7	7	6
Sr	104	79	79	86	137	141	139	118
Ba	158	80	184	138	171	193	107	130
Th	1.8		4.3			4.1	3.62	
Y	14	14	27	30	19	29	21	27
Zr	61	59	131	127	91	120	95	132
Nb	1.3	3.3	8	7	6	7	5	7
Hf	1.64		3.36			3.2	2.47	
Ta	0.25		0.59			0.51	0.39	
La	7.4		15.7			13.6	12.1	16.4
Ce	16.8		36.2			33.8	28.9	34.7
Nd	8.8		18.8			17.6	14.3	17.3
Sm	2.51		4.68			4.48	3.52	4.3
Eu	0.88		1.42			1.39	1.09	1.2
Gd	0.01		5.30				0.00	4
Tb	0.48		0.82			0.84	0.63	0.7
Dy								3.9
Er								2.4
Yb	1.70		2.74			2.84	2.16	
Lu	0.28		0.44			0.46	0.34	
La/Ta	29.6		26.6			26.7	31.0	
Th/Ta	7.20		7.29			8.04	9.28	
(La/Sm)n	1.8		2.0			1.9	2.1	
Ti/Zr	92	88	68	65	73	75	63	65
Zr/Nb	48	18	17	17	15	18	19	18
Ti/V	30	31	31	29	18	27	30	35
Zr/Y	4.5	4.3	4.8	4.2	4.8	4.2	4.5	4.9
Ti/Y	411	379	326	275	352	314	284	320
Mg#	0.59	0.55	0.39	0.35	0.41	0.49	0.60	0.49

* - analytical total; major element concentrations are recalculated to 100% anhydrous

Table 3.5 (continued)

	----------------Seal Bay Bottom (continued)----------------							
Sample	2140750	2140751	2140752	2140753	2140754	2140755	2140756	2140758
SiO2	54.23	54.04	51.46	55.15	55.7	51.19	55.46	51.94
Al2O3	18.79	18.41	17.47	17.93	17.65	21.78	17.17	18.31
Fe2O3	2.31	3.1	3.05	2.11	1.87	0.72	1.99	2.07
FeO	6.51	4.9	4.94	6.34	6.49	6.09	8.36	5.85
MgO	3.74	3	3.6	4.07	4.21	4.95	5.01	4.65
CaO	7.55	11.81	17.9	9.46	7.49	7.63	6.03	13.32
Na2O	4.73	3.06	0.24	3.32	5.09	5.24	4.16	2.25
K2O	0.61	0.26	0.02	0.04	0.12	1.34	0.02	0.13
TiO2	1.19	1.1	0.99	1.23	1.09	0.76	1.44	1.16
MnO	0.18	0.16	0.18	0.19	0.15	0.21	0.19	0.2
P2O5	0.17	0.16	0.15	0.16	0.13	0.09	0.18	0.13
LOI	3.57	4.10	5.86	4.26	3.17	6.46	4.01	4.43
Total*	99.92	99.77	100.88	99.91	100.11	99.83	99.48	99.63
Cu	69	75	27	21	66	38	21	36
Zn	77	72	64	64	70	51	78	65
Ni	15	14	46	10	17	40	6	19
Cr	39	41	154	69	44	149	56	82
V	230	223	167	224	238	158	284	199
Sc								
Co								
Rb	16	6	<0.5	<0.5	0.9	32	<0.5	3.6
Sr	114	306	56	152	171	200	103	249
Ba	150	84	28	33	80	173	47	49
Th								
Y	21	22	20	22	22	13	26	19
Zr	102	86	88	88	85	56	108	72
Nb	6	4	4	4	4	2.7	6	4
Hf								
Ta								
La								
Ce								
Nd								
Sm								
Eu								
Gd								
Tb								
Dy								
Er								
Yb								
Lu								
La/Ta								
Th/Ta								
(La/Sm)n								
Ti/Zr	70	77	67	84	77	82	80	97
Zr/Nb	17	22	20	21	24	21	18	18
Ti/V	31	30	36	33	27	29	30	35
Zr/Y	4.8	3.9	4.3	4.0	4.0	4.2	4.1	3.7
Ti/Y	335	300	291	337	304	345	328	359
Mg#	0.46	0.44	0.48	0.49	0.50	0.59	0.49	0.54

* - analytical total; major element concentrations are recalculated to 100% anhydrous

Table 3.5 (continued)

Sample	2140530	2140531	2140532	2140533	2140534	2140540	2140541
SiO_2	50.42	55	54.26	52.64	51.67	54.63	54.17
Al_2O_3	15.2	15.44	15.43	16.29	17.03	15.49	15.19
Fe_2O_3	3.33	3.5	5.2	3.12	3.57	3.65	4.3
FeO	11.93	9.12	7.87	11.12	10.21	9.42	8.92
MgO	6.82	5.42	3.53	7.89	7.46	4.79	4.74
CaO	6.87	5.53	4.65	1.39	2.15	4.37	4.56
Na_2O	3.96	3.94	6.88	4.84	5.73	5.54	5.5
K_2O	0.15	0.39	0.11	0.87	0.63	0.24	1
TiO_2	1.01	1.33	1.58	1.52	1.26	1.49	1.26
MnO	0.27	0.21	0.25	0.23	0.19	0.22	0.21
P_2O_5	0.05	0.12	0.25	0.09	0.1	0.15	0.14
LOI	2.93	2.52	1.04	2.67	2.36	1.43	1.75
Total*	99.32	99.98	98.90	99.36	99.52	99.91	100.14
Cu	88	33	38	53	42	50	36
Zn	113	110	108	140	94	104	102
Ni	15	2	2	11	4	4	<1
Cr	65	31	26	57	52	33	35
V	446	422	322	610	558	449	461
Sc	43.6		39.5				38.4
Co	42.5		29.3				38.3
Rb	<0.5	2.0	0.6	8	5	2.8	6
Sr	63	75	64	53	65	88	86
Ba	51	58	52	51	50	43	146
Th	0.29		0.44				0.65
Y	17	28	27	27	33	29	26
Zr	28	52	55	76	68	82	61
Nb	1.3	1.2	1.4	2.1	1.5	3.3	1.2
Hf	0.92		1.6				1.65
Ta	0.03		0.08				0.09
La	1.06		2.75				5.0
Ce	3.3		8.8				12.7
Nd	3.8		7.5				8.4
Sm	1.47		2.75				2.77
Eu	0.62		1.13				1.03
Gd							
Tb	0.40		0.69				0.64
Dy							
Er							
Yb	1.77		3.05				2.81
Lu	0.28		0.47				0.44
La/Ta	35.3		34.4				55.6
Tb/Ta	9.67		5.50				7.22
(La/Sm)I	0.4		0.6				1.1
Ti/Zr	216	154	171	120	110	108	124
Zr/Nb	22	45	39	36	45	25	51
Ti/V	14	19	29	15	14	20	16
Zr/Y	1.7	1.9	2.0	2.8	2.1	2.9	2.3
Ti/Y	358	289	351	335	229	310	288
Mg#	0.48	0.47	0.36	0.53	0.52	0.43	0.42

Header span: |----------Nanny Bag Lake----------|

* - analytical total; major element concentrations are recalculated to 100% anhydrous

Table 3.5 (continued)

Sample	|-Nanny Bag Lake (cont'd)-|	|--------Northern Arm--------|		
	2140543	2140544	2140771	2140772	2140773	2140774
SiO2	54.36	52.17	54	54.14	49.78	52.73
Al2O3	14.83	14.73	18.99	16.06	14.93	15.93
Fe2O3	3.79	4.44	1.15	1.69	2.64	1.16
FeO	9.68	9.48	7.31	6.39	7.81	6.92
MgO	5.13	5.36	3.91	5.14	9.05	7.02
CaO	4.82	6.53	7.09	10.15	9.78	11.32
Na2O	5.54	5.1	5.53	4.98	3.33	2.52
K2O	0.09	0.07	0.67	0.14	0.65	1.05
TiO2	1.3	1.73	1.07	0.96	1.61	1.02
MnO	0.22	0.2	0.16	0.19	0.19	0.18
P2O5	0.24	0.19	0.12	0.16	0.22	0.14
LOI	2.66	1.98	2.93	3.25	2.58	2.70
Total*	99.04	98.40	99.60	99.86	100.10	99.80
Cu	34	49	54	36	67	63
Zn	110	108	75	63	91	66
Ni	<1	3	24	15	176	127
Cr	21	30	59	65	531	347
V	346	471	227	194	221	185
Sc						
Co						
Rb	<0.5	<0.5	22.2	2.7	9.9	22.3
Sr	47	71	290	41	120	228
Ba	52	56	98	43	116	331
Th						
Y	27	31	19	21	17	19
Zr	56	80	72	80	105	79
Nb	1.4	2.9	4.0	2.8	19	3.6
Hf						
Ta						
La				10.3		10.4
Ce				24.4		21.7
Nd				15		11.8
Sm				4		3.1
Eu				1.1		0.7
Gd				4.2		3
Tb						1
Dy				4.4		3.4
Er				2.5		2.1
Yb						
Lu						
La/Ta						
Th/Ta						
(La/Sm)n				1.6		2.0
Ti/Zr	139	130	89	72	92	77
Zr/Nb	40	28	18	29	6	22
Ti/V	23	22	28	30	44	33
Zr/Y	2.0	2.6	3.8	3.9	6.1	4.2
Ti/Y	284	332	343	281	561	325
Mg#	0.44	0.44	0.48	0.56	0.64	0.64

* analytical total; major element concentrations are recalculated to 100% anhydrous

Table 3.6: Mean major and trace element concentrations by suites in
the IAI group

Suite	Glover's Harbour East	Seal Bay Bottom	Northern Arm	Nanny Bag Lake
SiO_2	54.73	53.80	52.66	53.26
Al_2O_3	17.83	18.15	16.48	15.51
Fe_2O_3	2.72	2.06	1.66	3.88
FeO	5.42	6.48	7.11	9.75
MgO	3.40	4.44	6.28	5.68
CaO	8.07	9.31	9.59	4.54
Na_2O	5.86	3.96	4.09	5.23
K_2O	0.52	0.29	0.63	0.39
TiO_2	1.16	1.17	1.17	1.39
MnO	0.15	0.19	0.18	0.22
P_2O_5	0.15	0.15	0.16	0.15
Cu	50	40	55	47
Zn	71	71	73.75	110
Ni	11.4	20.0	85.5	4.8
Cr	58	107	251	39
V	261	252	207	454
Rb	9	7	14	2.8
Sr	97	168	170	68
Ba	146	96	147	62
Y	21	21	19	27
Zr	94	95	84	62
Nb	5	6	7	1.8
Ti/Zr	77	75	83	142
Zr/Nb	23	18	19	37
Ti/V	28	30	34	19
Zr/Y	4.5	4.6	4.5	2.2
Ti/Y	348	345	377	308
Mg#	0.46	0.51	0.58	0.45
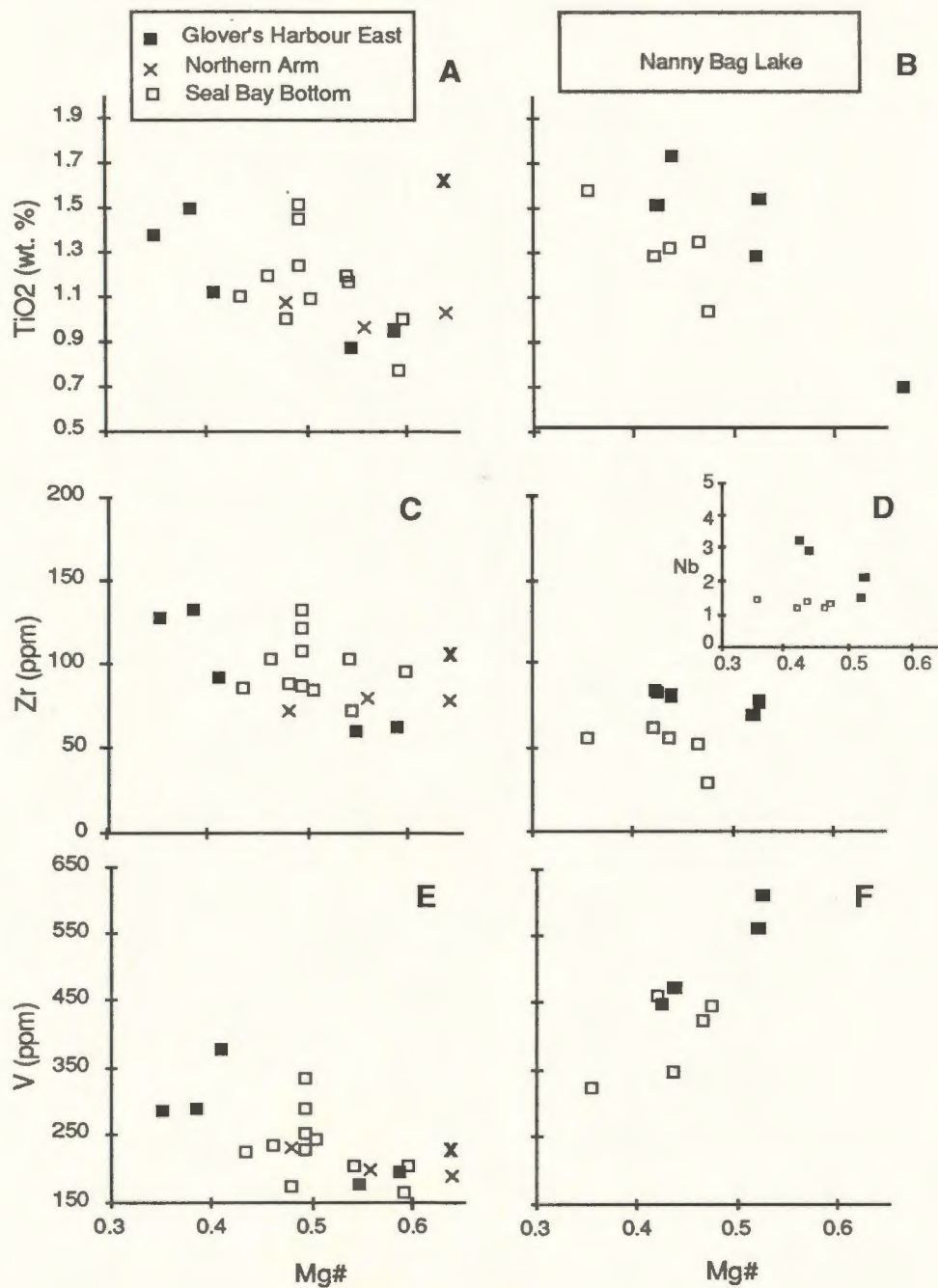
Figure 3.21: Binary plots of selected elements versus Mg# in the IAI group. Open and closed squares in the Nanny Bag Lake suite designate trends NBL-1 and NBL-2 respectively. Anomalous Northern Arm sample (2140773) indicated by bold "x".
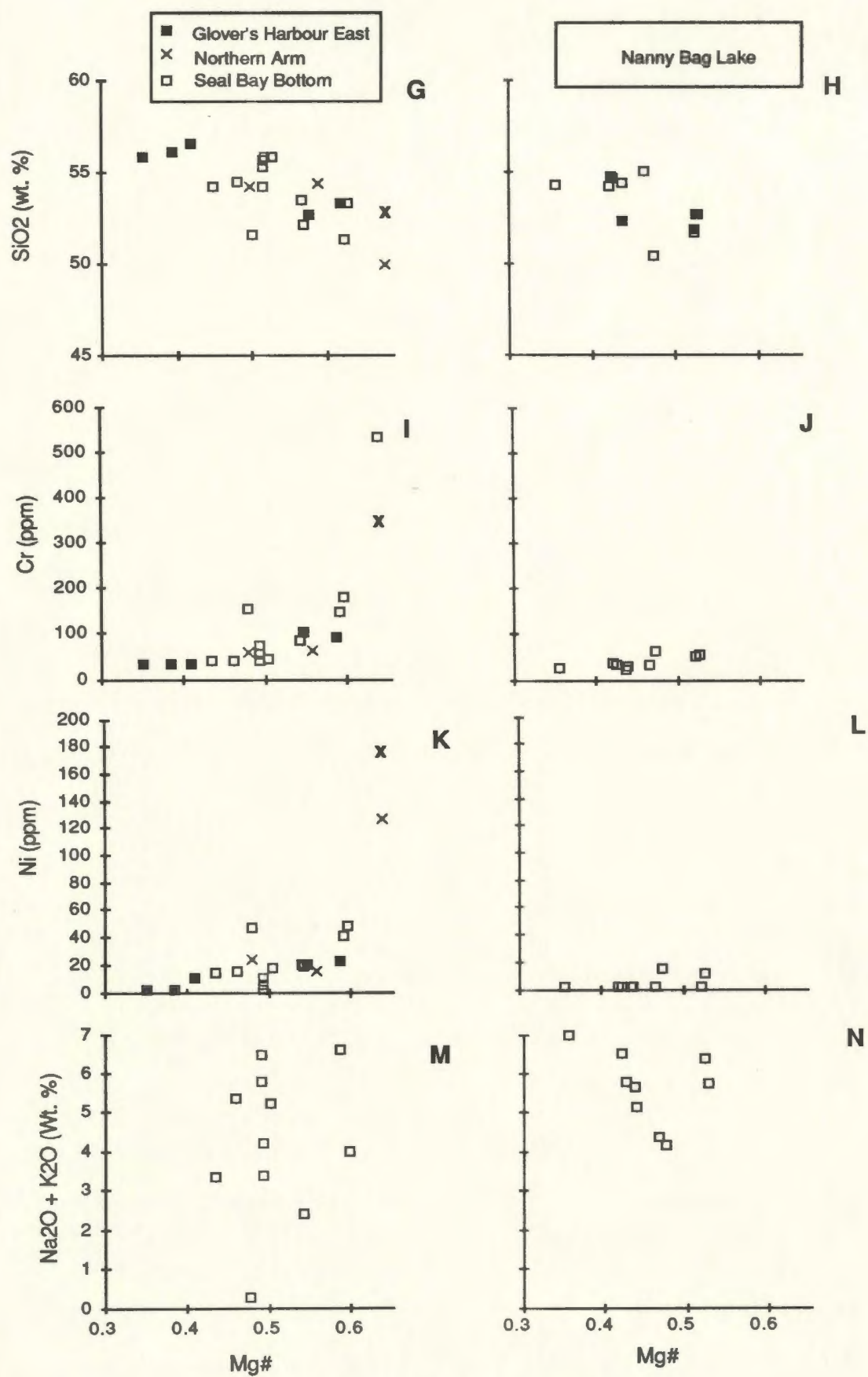
Figure 3.21 (continued)

with decreasing Mg# suggesting that these trends may result from fractional crystallization. There is considerable scatter, particularly in the Seal Bay Bottom suite, which may indicate further complexities resulting from partial melting, contamination, accumulation of minor phases, or other causes. In the Northern Arm suite, one sample (2140773) has anomalously high TiO_2. It is also very enriched in Nb and has very different incompatible element ratios from the other three samples in this suite. In these respects, it is very similar to samples in the NAI and NAT groups (Sections 3.4.4 and 3.4.5), a point that is returned to in the synthesis and conclusions at the end of this Chapter. A second sample in this suite has anomalously high Cr and Ni contents (2140774) suggesting it is a pyroxene and/or olivine cumulate.

The Nanny Bag Lake suite has generally higher TiO_2 and lower Zr contents than the other three suites at equivalent Mg#. There is a suggestion that this suite is actually bipartite, with parallel trends of incompatible element enrichment at contrasting incompatible element concentrations (see also Nb versus Mg#, inset in Figure 3.21D). The lower trend (open squares, termed for convenience NBL-1) is defined by five samples but the upper (closed squares, termed NBL-2) is essentially a two-point line defined by two pairs of samples and is not well constrained. Samples from NBL-1 have slightly lower Ti/Zr and higher Zr/Y ratios than NBL-2 and the two may represent separate magma batches. The petrogenetic relationship between these two trends is further investigated in Chapter 4.

Vanadium increases regularly with decreasing Mg# in the Glover's Harbour East, Seal Bay Bottom and Northern Arm suites and this coupled with the similar increase in TiO_2 indicates that these are part of a tholeiitic magma series. This is in striking contrast to the Nanny Bag Lake suite where V and FeO^t (Figure 3.22) decrease sharply with decreasing Mg#. There is no obvious process to account for these trends; crystallization of an iron oxide should also cause a parallel decrease in Ti.

SiO_2 contents are mostly in the basaltic andesite range, less commonly basaltic, and are negatively correlated with Mg# in all suites (Figure 3.21G,H). These trends have less scatter than in the Glover's Harbour West suite. Petrographic evidence of silica remobilization is less prevalent
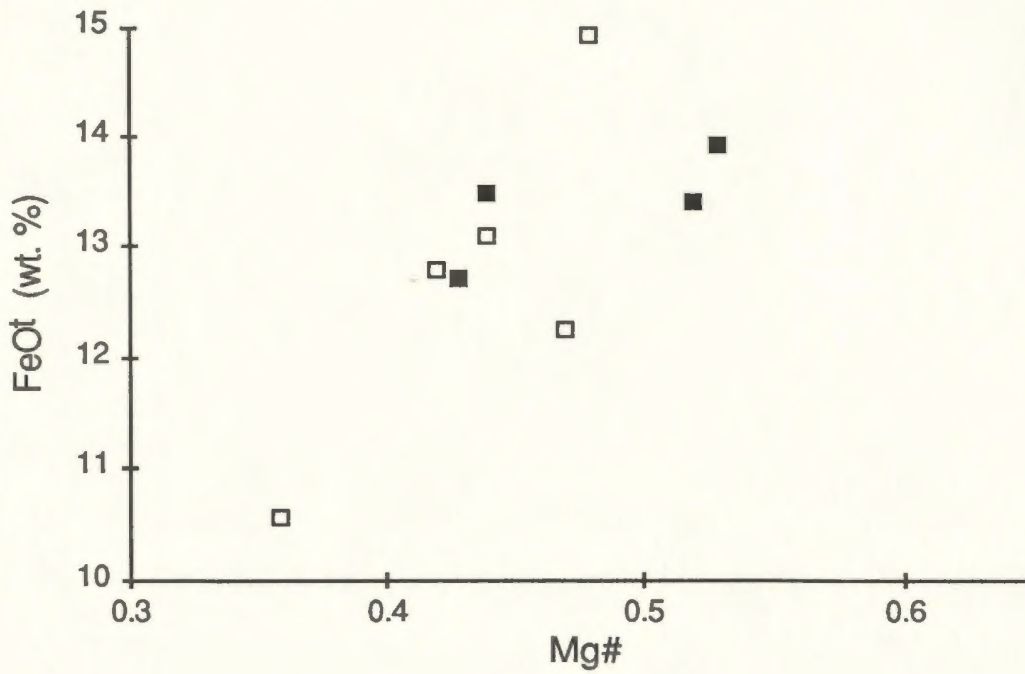
Figure 3.22: Total iron versus Mg# for the Nanny Bag Lake suite. Open squares are NBL-1 trend; closed squares are NBL-2 trend. In both trends, FeO(t) parallels vanadium and decreases with decreasing Mg#.

in these rocks as well and the andesitic compositions probably reflect andesitic protoliths.

The Seal Bay Bottom suite defines a continuous trend of decreasing Cr and Ni with decreasing Mg# suggesting clinopyroxene and olivine crystallization. The most primitive samples have the highest Cr and Ni concentrations and the highest Mg#'s of any liquid compositions in the IAD and IAI groups.

In the Nanny Bag Lake suite, Mg#'s of the least differentiated samples are approximately 0.53, suggesting that these rocks were the most evolved of all IAI group volcanic rocks prior to eruption. This is supported by very low initial Cr and Ni contents. Cr and Ni do decrease slightly over the range of Mg# represented by the sample set indicating additional pyroxene and olivine fractional crystallization.

The IAI group plots principally in the non-alkalic field on the Nb/Y-Zr/P_2O_5 diagram (Figure 3.23). Note that the single anomalous Northern Arm suite sample plots in the transitional field on this diagram and is clearly different from the remainder of the Northern Arm samples.

The Ti-V ratios of the Glover's Harbour East, Seal Bay Bottom and Northern Arm suites are somewhat higher than normal for island arc tholeiites and they plot in the field of MORB and back-arc basin basalts in Figure 3.24A. The most primitive Nanny Bag Lake suite samples have Ti-V ratios typical of arc tholeiites but because of their peculiar trend of increasing V with decreasing Ti, their Ti/V increases to MORB-like values in the most differentiated samples (Figure 3.24B).

The contrast between the Glover's Harbour East, Seal Bay Bottom and Northern Arm suites and the Nanny Bag Lake suite is further emphasized on the Zr/Y - Zr diagrams (Figure 3.24C, D, E). The latter plot in the field of overlap between MORB and VAB. The former, in keeping with their general enrichment in the more incompatible elements relative to normal arc tholeiites, have higher Zr/Y ratios and plot mainly in the WPB field.

Th and Ta values for the Glover's Harbour East, Seal Bay Bottom and Nanny Bag Lake suites (there are no Ta or Th data for the Northern Arm suite) are generally greater than 2 (Figure 3.25A) and all samples plot well within the arc field on the ternary Ta-Hf-Th discrimination plot of
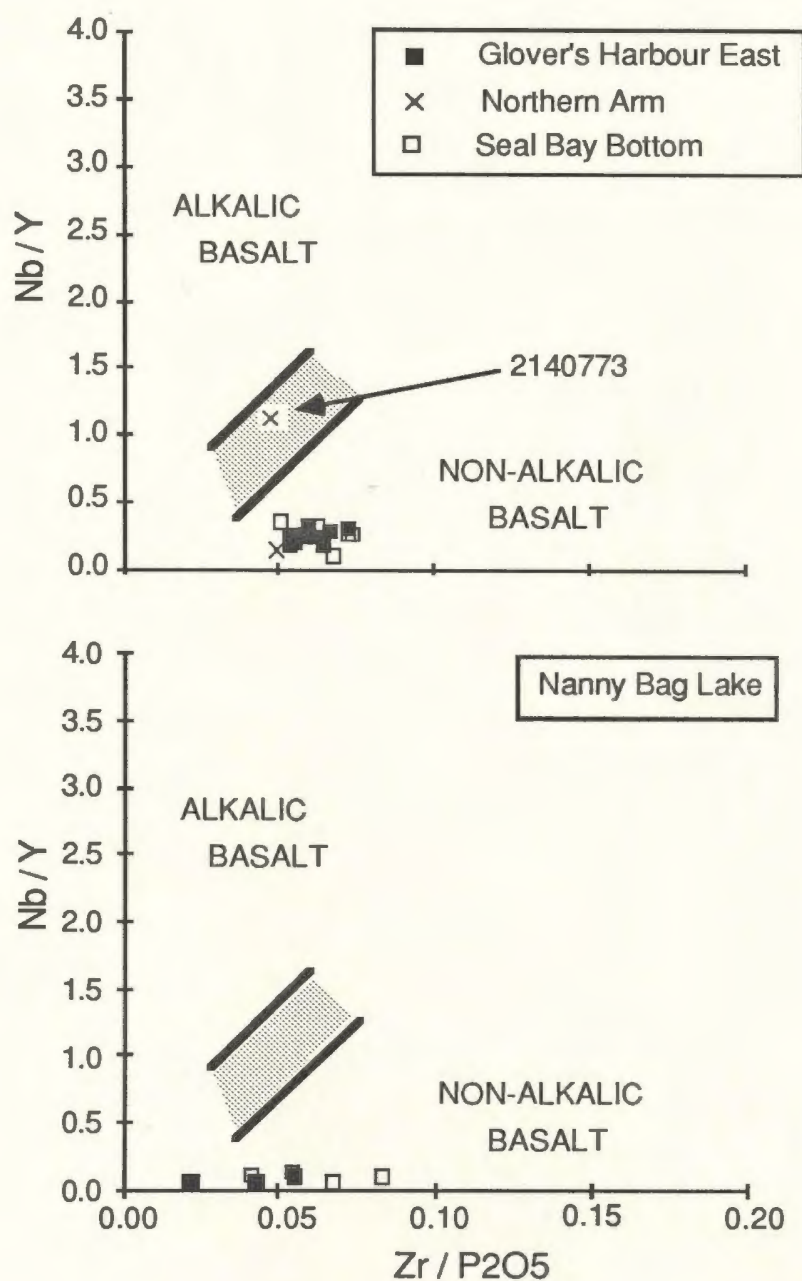
Figure 3.23: Discrimination of alkalic and non-alkalic basalts, after Floyd and Winchester (1975), for the IAI group. Stippled area is transitional. All except the anomalous Northern Arm sample, 2140773, plot in the non-alkalic field.
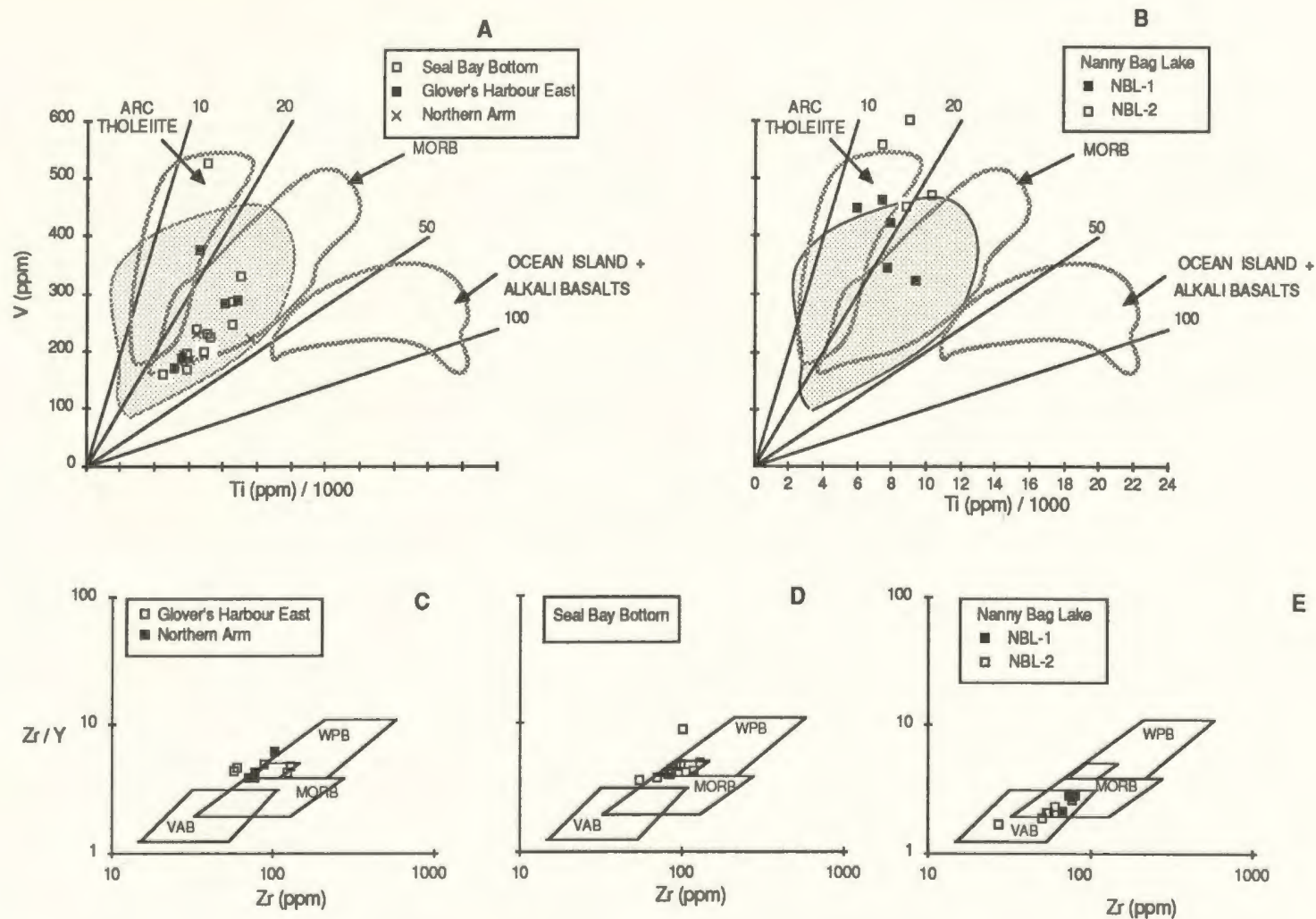
Figure 3.24: Ti-Y (Shervais, 1982) and Zr/Y-Zr (Pearce and Norry, 1979) plots for the IAI group. In A and B, the stippled field is back-arc basin volcanic rocks (BABV). The Glover's Harbour East, Seal Bay Bottom and Northern Arm suites have higher Ti/V ratios than normal arc tholeiites and plot in the MORB-BABV field. In C, D, and E, Glover's Harbour East, Seal Bay Bottom and Northern Arm suites are again enriched in the more incompatible elements relative to arc basalts and plot in the WPB field.
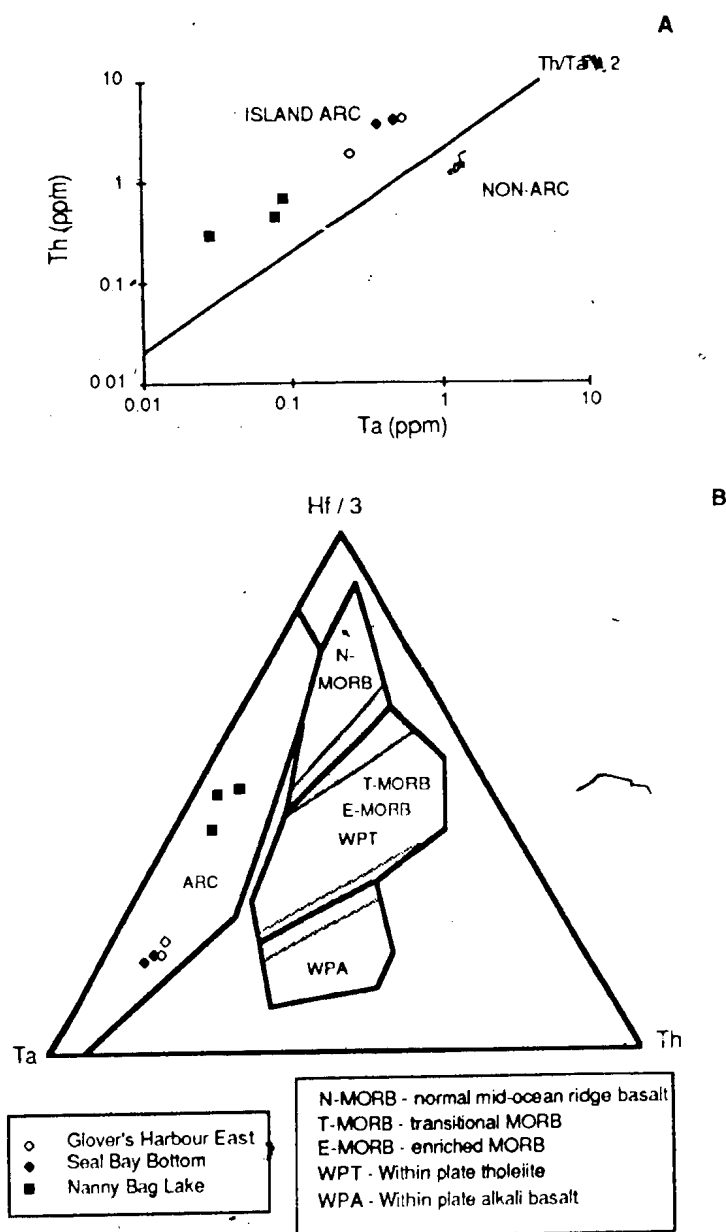
Figure 3.25: IAI group samples plotted on Th-Ta and Ta-Th-Hf diagrams. All samples plot within the arc fields on both diagrams.

Wood *et al.*, (1979)(Figure 3.25B), consistent with preliminary conclusions reached in Section 3.3.3. Notwithstanding the slightly abnormal enrichment in the incompatible elements noted above, these rocks are clearly of island arc affinity.

The geochemical contrast between Nanny Bag Lake suite and the Glover's Harbour East/ Seal Bay Bottom/ Northern Arm suites is also apparent in the REE (Figure 3.26). The Nanny Bag Lake basalts generally have LREE-depleted patterns with flat MREE and HREE at 10 to 20 times chondrite. Sample 2140541 is anomalously enriched in La and Ce but has MREE and HREE abundances similar to 2140532. This sample is also relatively enriched in K_2O and Ba (Table 3.5) but Ta and Nb contents of the two samples are virtually identical. This suggests that the anomalous LREE enrichment may be an artifact of alteration, although a LREE/LFSE enrichment resulting from metasomatism in the source regions above the subduction zone cannot be ruled out. The Nanny Bag Lake suite REE patterns and abundances are similar to those of island arc tholeiites from the Tonga and New Britain arcs (Figure 3.26A) and all samples plot in the field of low-K tholeiites on Gill's (1981) La-Th diagram (Figure 3.27). Despite its peculiar V and FeO relationships, this suite is probably best interpreted as part of a low-K island arc tholeiite series.

The Glover's Harbour East and Seal Bay Bottom volcanic rocks, in contrast, are LREE enriched with a gentle positive slope in the MREE and flat HREE. This is not unexpected, considering the consistent enrichment of these rocks in more incompatible (e.g. Ti, Zr) compared to less incompatible (e.g. V, Y; see Figure 3.24) elements. With reference to modern island arcs, the degree of LREE enrichment (La_n/Yb_n=2.87 to 3.78) suggests similarity with medium-K to high-K tholeiites (Gill, 1981) such as andesites from Okmok volcano in the Aleutians described by Kay (1977) (Figure 3.26B, C, D). This is further illustrated by La - Th relationships in Figure 3.27 where the samples span the boundary between medium- and high-K tholeiites (Figure 3.27).

Geochemically similar rocks have also been reported from back-arc basins in the early stages of opening. Weaver *et al.* (1979) described three suites of volcanic rocks from the Bransfield Strait, where magma genesis is complicated by the presence of several sources and the possible influence of a subducting slab. Rare earth patterns from two of these suites are
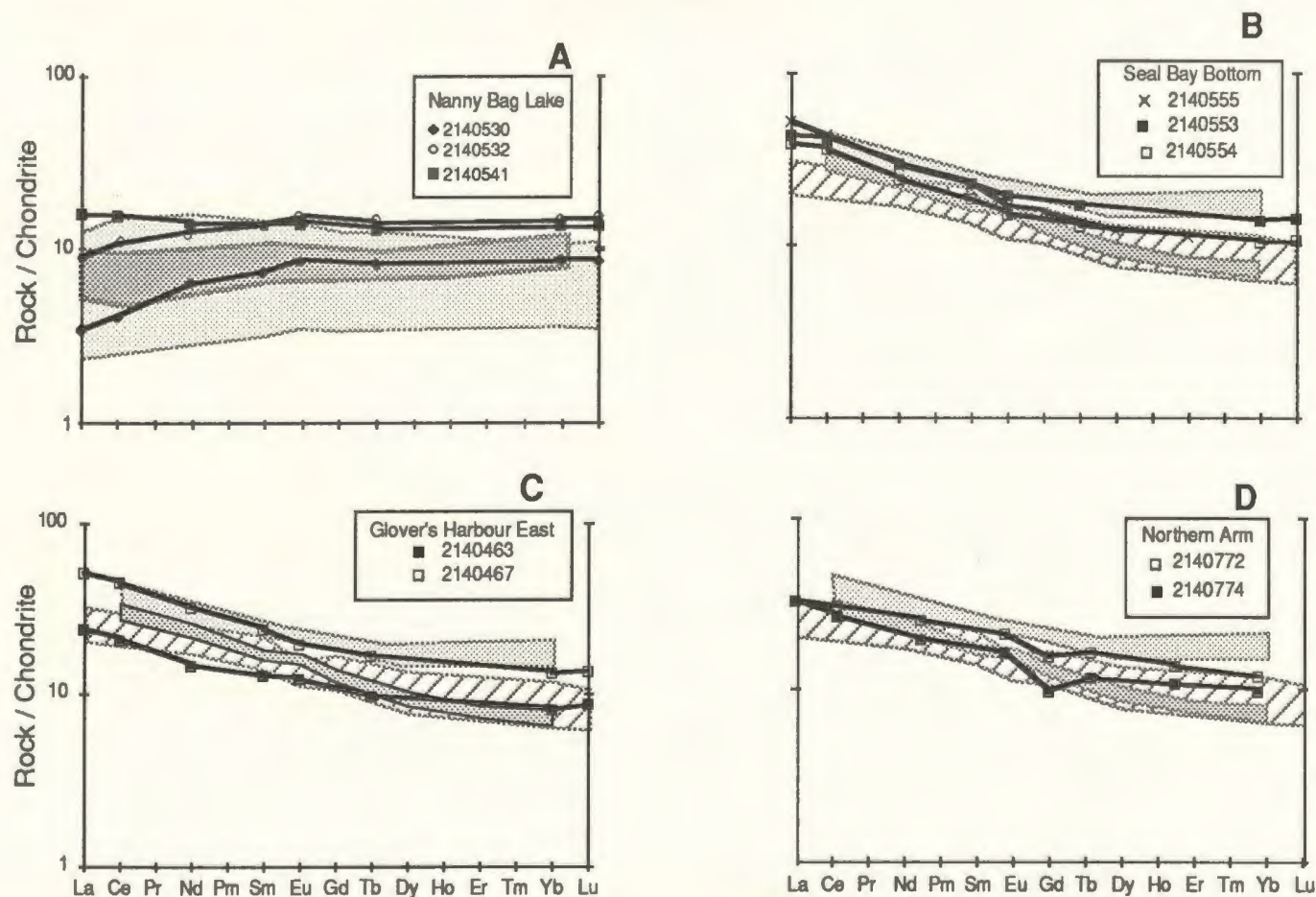
Figure 3.26: REE plots for the IAI group. In A, the Nanny Bag Lake suite has flat to LREE-depleted patterns typical of island arc tholeiites. Light stipple is field of New Britain arc tholeiites (Basaltic Volcanism Study Project, 1981) and heavy stipple is field of Tongan arc tholeiites (Ewart et al., 1973). In B, C, and D, the other three IAD group suites have LREE-enriched patterns similar to medium- to high-K tholeiites. Hatched area is field of medium-K tholeiites from Okmok volcano , Aleutian Islands (Kay, 1977). Stipple indicates fields of Bransfield Strait basic volcanic rocks (Weaver et al., 1979); light stipple is olivine basalt and basaltic andesite from Deception Island while dark stipple is basaltic andesite from Penguin Island.
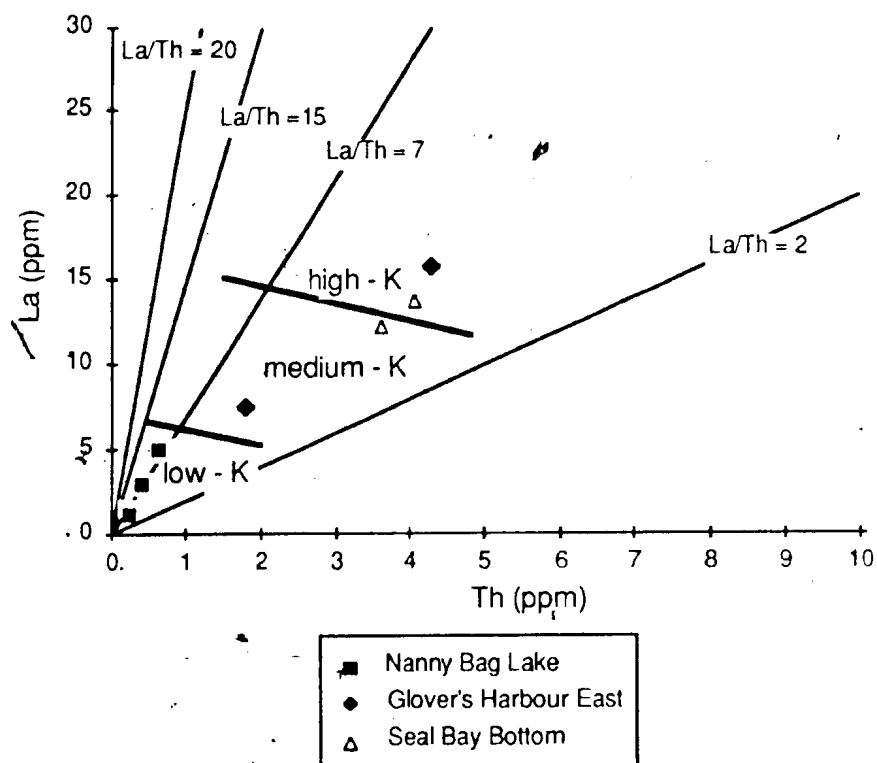
Figure 3.27: La-Th diagram after Gill (1981) further emphasizing the similarity between the Nanny Bag Lake suite and low-K tholeiites and between the Glover's Harbour East / Seal Bay Bottom / Northern Arm suites and medium- to high-K tholeiites.

illustrated on Figure 3.26B to D). These rocks also have marked negative (chondrite normalized) Nb anomalies compared to Ce.

Clinopyroxene and lesser plagioclase are the only identified phenocryst phases in the Seal Bay Bottom and Glover's Harbour volcanics. Plagioclase is dominant in the Nanny Bag Lake suite and rare clinopyroxene was seen in only one thin section. Diagrams illustrating the effects of fractional crystallization in the IAI group (Figure 3.28) show the influence of crystallization of these minerals and also reflect the presence of olivine. Comparison of TiO_2-Y trends with modelled fractionation pathways is consistent with fractionation involving some combination of pyroxene, plagioclase and olivine (Figure 3.28A). The Northern Arm suite is the only suite which does not appear to represent a significant fractionation interval on this diagram.

Plagioclase fractionation is indicated for all suites by the Al_2O_3/TiO_2 versus Ti diagram (Figure 3.28B). The two trends within the Nanny Bag Lake suite may record ~15 percent to 25 percent plagioclase fractionation. In the Seal Bay Bottom suite, the single Al_2O_3-rich sample is a plagioclase cumulate; the remaining samples record 20 to 30 percent plagioclase fractionation. The Glover's Harbour East samples plot on a trend that could indicate as much as 30 to 35 percent plagioclase fractionation. In all suites, the trends are flatter than the plagioclase fractionation vector indicating some influence from fractionating ferromagnesian minerals.

Trends on the Cr-Ni diagram (Figure 3.28C) are intermediate between the calculated pyroxene and olivine vectors suggesting that each has influenced the composition of the rocks during fractionation. There is no indication of iron-titanium oxides on the liquidus for any suite, and no explanation for the previously noted decrease of V and FeO^t with differentiation in the Nanny Bag Lake suite.

Preliminary modelling of trace element relationships (Table 3.7) shows that the trends in the Nanny Bag Lake and Seal Bay Bottom suites can be explained by crystal fractionation. Nb cannot be used in either suite because of the relatively large uncertainties at the measured abundance levels, but modelling of changes in both TiO_2 and Zr in all cases yield consistent total fractionation. In the Nanny Bag Lake suite, samples of the NBL-1 trend may represent between
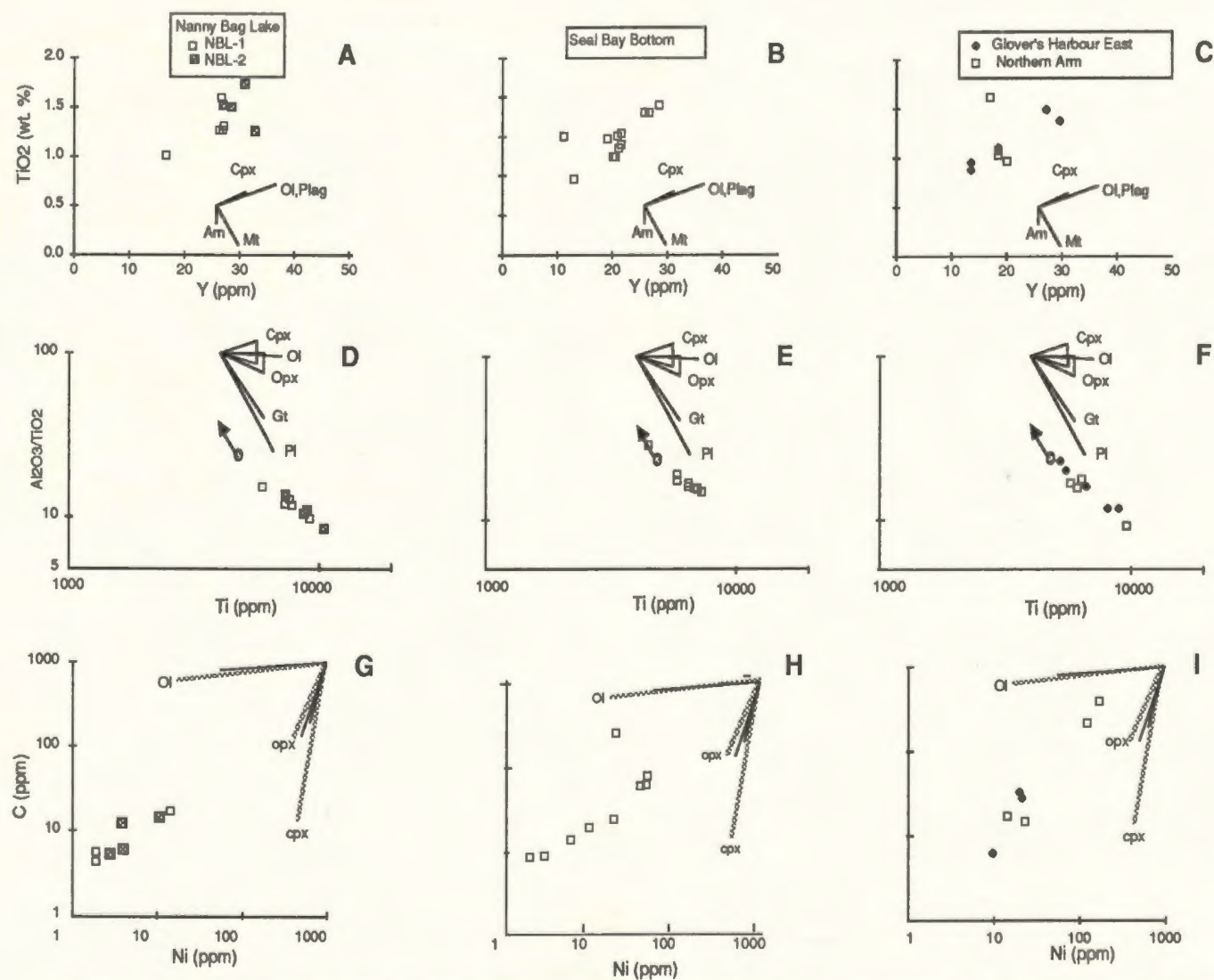
Figure 3.28: Binary plots with Rayleigh fractionation vectors as indicators of the fractionation history of the IAI group. A - after Perfit et al. (1980) with 30% fractionation vectors; B - after Pearce and Flower (1977) with 50% fractionation vectors. C - 20% fractionation vectors calculated from distribution coefficients in Appendix 9 (solid lines - primitive basalt; stippled lines - fractionated basalt). Arrows in D to F are plagioclase accumulation vectors.

Table 3.7: Results of Trace element modelling of fractionation in the IAI group
The range of fractionation is calculated based on ±5% of the ending composition
or 1/2 of the detection limit, whichever is greater.

Nanny Bag Lake Suite, Depleted trend (NBL-1)
Model Parameters: ol:cpx:pl = 0.x:0.1:0.x
Distribution coefficients: Fractionated basalt (Appendix 9)

	Starting Composition	Ending Composition	% Total Fractionation
TiO2 (wt. %)	1.26	1.73	25 - 34 (±5%)
Zr (ppm)	44	62	25 - 34 (±5%)
Cr (ppm)	44	21	21 - 37 (±5 ppm)

Nanny Bag Lake Suite, Enriched trend (NBL-2)
Model Parameters: ol:cpx:pl = 0.x:0.2:0.x
Distribution coefficients: Fractionated basalt (Appendix 9)

	Starting Composition	Ending Composition	% Total Fractionation
TiO2 (wt. %)	1.4	1.61	10 - 20 (±5%)
Zr (ppm)	72	82	8 - 18 (±5%)
Cr (ppm)	55	30	12 - 19 (±5 ppm)

Seal Bay Bottom Suite
Model Parameters: ol:cpx:pl = 0.3:0.3:0.4
Distribution coefficients: Fractionated basalt (Appendix 9)

	Starting Composition	Ending Composition	% Total Fractionation
TiO2 (wt. %)	1.00	1.33	24 - 34 (±5%)
Zr (ppm)	81	107	22 - 32 (±5%)
Cr (ppm)	199	25	27 - 32 (±5 ppm)
Ni (ppm)	36	6	22 - 33 ±2.5 ppm)

Glover's Harbour East Suite
Model Parameters: ol:cpx:pl = not calculated
Distribution coefficients: Fractionated basalt (Appendix 9)

	Starting Composition	Ending Composition	% Total Fractionation
TiO2 (wt. %)	0.86	1.39	42 - 49 (±5%)
Zr (ppm)	54	126	61 - 66 (±5%)
Nb (ppm)	1.80	8	79 - 82 (±5 %)

25 and 34 percent total fractionation and those in the NBL-2 trend slightly less, between 10 and 18 percent. Ni contents of the most fractionated samples of both trends are below detection limits and cannot be used to calculate the proportion of olivine fractionation. Cr contents suggest on the order of 2 to 3.5 percent clinopyroxene crystallization in both cases. The amount of plagioclase fractionation can be crudely estimated from Figure 3.28 as on the order of 20 percent in the NBL-1 trend and somewhat less in the NBL-2 trend (~15 percent). This may limit olivine crystallization to roughly the same proportion as clinopyroxene in both cases.

Total fractional crystallization in the Seal Bay Bottom suite is estimated at between 24 and 32 percent from TiO_2 and Zr. The observed decrease in Cr and Ni suggests that clinopyroxene and olivine each accounted for .3 of this, with plagioclase accounting for the remaining .4 (or 10 to 13 percent). This is in good agreement with the 10 to 12 percent plagioclase fractionation estimated from Figure 3.28B.

In the case of the Glover's Harbour East suite, different incompatible elements give inconsistent estimates of the amount of fractional crystallization. This is taken as evidence that geochemical trends in these rocks may not result from fractional crystallization, an inference that is further supported by a consistent although relatively small difference in incompatible element ratios between the more and less differentiated members of this suite (e.g. Ti/Zr and Ti/Y, Table 3.5). Alternative explanations are further explored in Chapter 4 following presentation of isotopic data.

3.4.4 The NAI Group

The NAI group is represented in only two suites and by only six samples. Table 3.8 and Figure 3.29 illustrate some of the features of this group and permit comparisons with the IAI group which it, in many respects, resembles.

Mg#'s range from 0.6 to 0.8, generally higher than in the IAI group. Likewise, Cr and Ni contents are very high (Figure 3.29E,F). Pyroxene phenocrysts (or altered psuedomorphs) are relatively rare in the Big Lewis Lake samples but common in the Badger Bay suite. In particular

Table 3.8: Major (weight percent) and trace (ppm) element contents of the NAI group

Suite	Badger Bay					Big Lewis Lake			
Sample	2140503	2140505	2140506	Mean		2140510	214051t	2140767	Mean
SiO2	50.09	49.85	44.81	48.25		50.65	49.40	54.85	51.63
Al2O3	14.00	6.66	15.06	11.91		11.08	14.85	14.70	13.54
Fe2O3	2.74	1.74	3.04	2.51		2.32	2.11	3.50	2.64
FeO	8.17	8.30	10.94	9.14		7.52	8.67	6.37	7.52
MgO	9.27	19.40	12.47	13.71		10.81	10.33	7.20	9.45
CaO	9.65	11.48	9.13	10.09		12.59	9.13	7.06	9.59
Na2O	2.88	0.70	1.99	1.86		2.95	2.82	4.50	3.42
K2O	1.60	0.04	0.38	0.67		0.19	1.02	0.08	0.43
TiO2	1.33	1.48	1.80	1.54		1.57	1.39	1.40	1.45
MnO	0.17	0.17	0.17	0.17		0.15	0.16	0.16	0.16
P2O5	0.10	0.19	0.21	0.17		0.17	0.11	0.06	0.11
LOI	3.99	3.92	5.88	4.60		5.38	3.10	2.83	3.77
Total*	100.42	100.01	98.50			100.15	100.07	100.01	
Cu	70	57	67	65		63	86	109	86
Zn	83	73	97	84		77	78	82	79
Ni	195	781	418	465		444	218	51	238
Cr	588	1074	819	827		646	487	244	459
Sc	29.2						32.5		
Co	51.9						60.1		
V	231	196	254	227		190	218	315	241
Rb	27	0.1	7	11		2.9	24	1.5	9
Sr	91	42	265	133		137	174	104	138
Ba	302	67	55	141		59	136	33	76
Th	0.46						0.61		
Y	17	12	19	16		13	19	16	16
Zr	60	86	115	87		84	72	72	76
Nb	3.0	9	10	7		10	5	7	7
Hf	1.71						1.95		
Ta	0.26						0.35		
La	3.7		9.10			9.2	4.8	10.5	
Ce	10.0		21.90			22.1	13.1	21.4	
Nd	7.4		13.20			14.4	9.2	13.2	
Sm	2.43		3.70			3.0	2.74	3.7	
Eu	0.89		1.20			1.3	0.97	1.3	
Gd			3.90			3.8		3.8	
Tb	0.51		0.90				0.57		
Dy			3.50			3.9		3.7	
Er			2.10			2.2		1.8	
Yb	1.56					1.1	1.98	1.3	
Lu	0.25						0.30		
La/Ta	14.2						13.7		
Th/Ta	1.77						1.74		
(La/Sm)n	0.9		1.5			1.9	1.1	1.7	
Ti/Zr	133	104	94	110		112	115	117	
Zr/Nb	20	9	12	14		9	15	10	11
Ti/V	35	45	42	41		50	38	27	38
Zr/Y	3.5	6.9	6.0	5.5		6.3	3.7	4.4	4.8
Ti/Y	463	713	564	580		700	430	518	549
Mg#	0.63	0.80	0.64	0.69		0.69	9.66	0.60	0.65

* --analytical total; major element concentrations are recalculated to 100% anhydrous
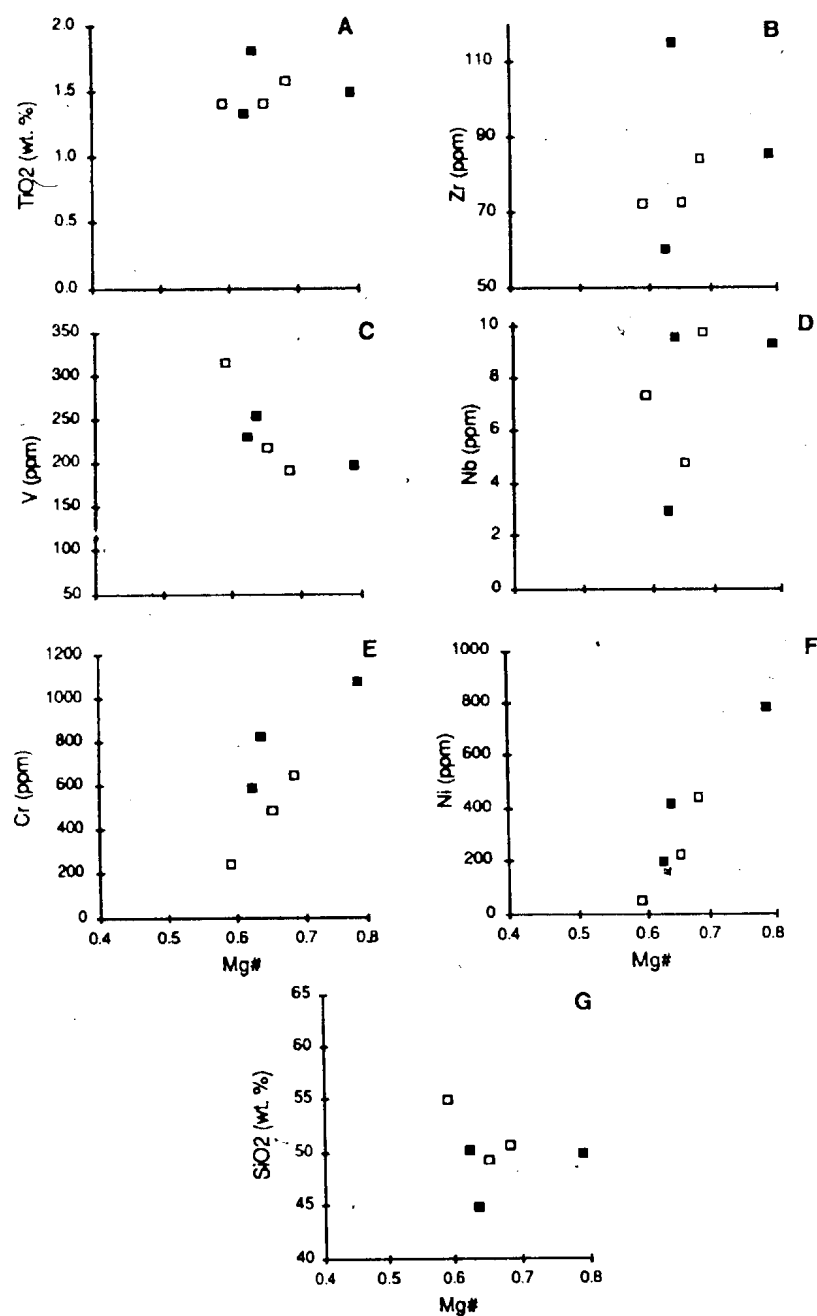
Figure 3.29: Selected elements plotted against Mg# for the NAI group. Closed squares are Badger Bay suite, open squares are Big Lewis Lake suite.

sample 2140505 contains 45-55 modal percent altered pyroxene (and perhaps olivine) phenocrysts; not coincidentally, it is the most Cr- and Ni-rich and has the highest Mg#. The high modal percentage of ferromagnesian cumulate phenocrysts also accounts for the low Al_2O_3 contents of this rock. The geochemical relationships may be somewhat obscured by alteration (the sample with the highest Mg# is also the most altered) but the systematic relationship between Ni and Cr (which are relatively immobile during alteration) and the Mg# suggests that the relationship cannot be explained by alteration alone. It seems likely that these rocks record the eruption of relatively primitive, unfractionated magmas whose composition is in some cases modified by ferromagnesian mineral accumulation.

TiO_2 and V contents are similar to or slightly higher than the IAI group at comparable Mg# while Zr is approximately the same. Nb has a bimodal distribution; two samples have relatively low concentrations (<5 ppm) while the remainder have higher (>7 ppm) amounts. This dichotomy also is found in some incompatible element ratios (the samples with lower Nb also have consistently higher Zr/Nb and lower Zr/Y and Ti/Y) and in REE patterns (the Nb-depleted rocks are relatively LREE-depleted, see below). This dichotomy, therefore, may not be random variation but a reflection of different magma batches with different source characteristics. There are too few samples to define this relationship further .

There is no consistent chemical difference between the two suites; in fact, the notable chemical differences (as detailed above) cross suite boundaries. Given the evidence for both crystal accumulation and different magmas, coupled with the paucity of samples in this group, their magma series affiliation remains indeterminate.

Application of the Nb/Y versus Zr/P_2O_5 diagram (Figure 3.30) suggests that most samples are non-alkalic although two samples plot in the transitional field between alkalic and non-alkalic types.

On the Ti-V diagram (Figure 3.31A) they plot generally within the MORB and BABV fields, and in this respect are similar to the IAI group.

The apparent dichotomy in sources within the suites is also apparent on the Ti/Y-Zr
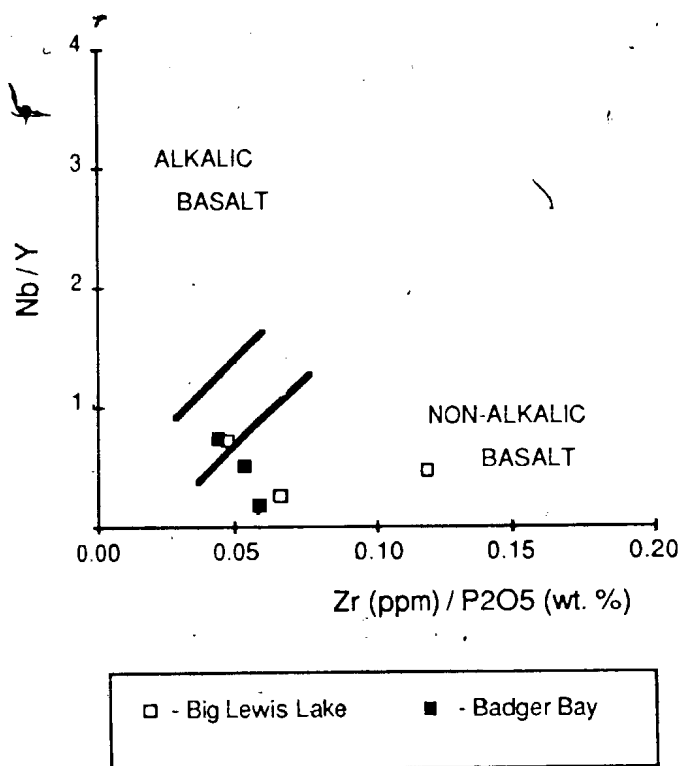
Figure 3.30: Discrimination of alkalic and non-alkalic basalts, after Floyd and Winchester (1975), for the NAI group. Stippled area is transitional.
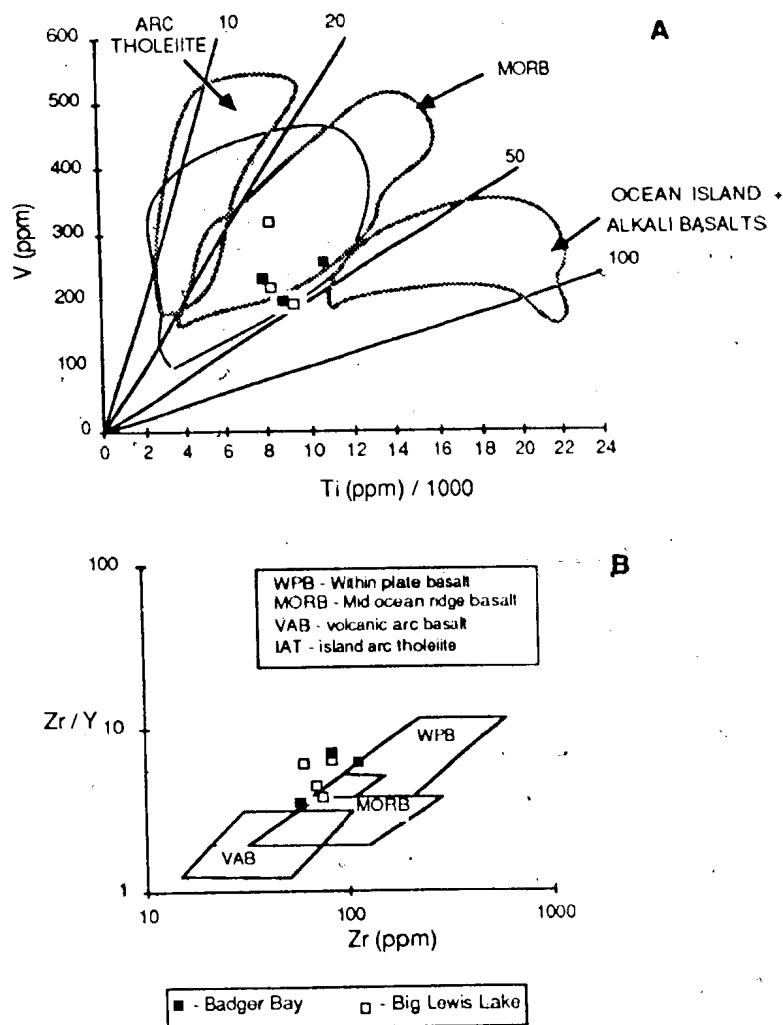
Figure 3.31: Ti - V (Shervais,1982) and Zr / Y - Zr (Pearce and Norry, 1979) plots for the NAI group. In A, stippled field is BABV.   Ti / V ratios are similar to those of the Glover's Harbour East / Seal Bay Bottom / Northern Arm suites (see Figure 3.24). In B, Zr / Y ratios are in the range of MORB and WPB.

diagram (Figure 3.31B). The Nb-depleted samples have Zr/Y ratios in the upper MORB range but the other samples have higher Zr/Y ratios typical of WPB (these are generally higher than the IAI subgroup, another manifestation of the difference between these groups).

REE data for five of the six samples (Figure 3.32) confirm the bipartite nature of the group. The Nb-depleted samples have flat to slightly depleted LREE's and mildly convex-upward patterns. The Nb-enriched samples are LREE-enriched but with HREE abundances similar to the Nb-depleted samples.

There are abundant analogues for LREE-enriched rocks in non-arc environments, both in oceanic spreading centers and in back-arc basins. LREE enriched tholeiitic magmas, termed "P" (plume, e.g. Sun *et al.*, 1979) or "E" (enriched, e.g. Wood *et al.*, 1979; Sun, 1980) MORB are similar to oceanic island enriched basalts and have been identified at many major accreting plate boundaries. Typically they are enriched in radiogenic isotopes as well as incompatible elements. Magmas intermediate between 'enriched' and 'normal' MORB have also been identified and termed transitional (T) MORB by Schilling *et al.* (1983). These are typically slightly LREE-depleted to LREE-enriched ($La_n/Sm_n = 0.7$-1.8; Schilling *et al.*, 1985) and in this respect are a good analogue for the NAI group which has $(La/Sm)_N = 0.9$ - 1.85 (see Figure 3.32 and Table 3.8).

Further similarities between the NAI group and T-MORB are found in Hf, Th and Ta relationships (Figure 3.33). Wood *et al.* (1979) have suggested that Hf-Th ratios are a particularly sensitive discriminant of the different types of MORB erupted along the Mid-Atlantic ridge and their Th-Hf diagram binary plot supports the comparison between the NAI group and T-MORB. Similarly, on the Ta-Th-Hf diagram, the NAI group plots in the E-MORB + T-MORB + WPT field but near the N-MORB boundary suggesting transitional affinities.

Similar rocks to the NAI group also occur in modern back-arc basins. For example, on the South Scotia Sea spreading center, Hawkesworth *et al.* (1977) and Saunders and Tarney (1979) have reported basalts with REE patterns parallel to but slightly less LREE-enriched than the NAI group. The Scotia Sea Rise samples have lower Ti/Zr ratios (62 to 75) and higher Ti/Y and Zr-Y
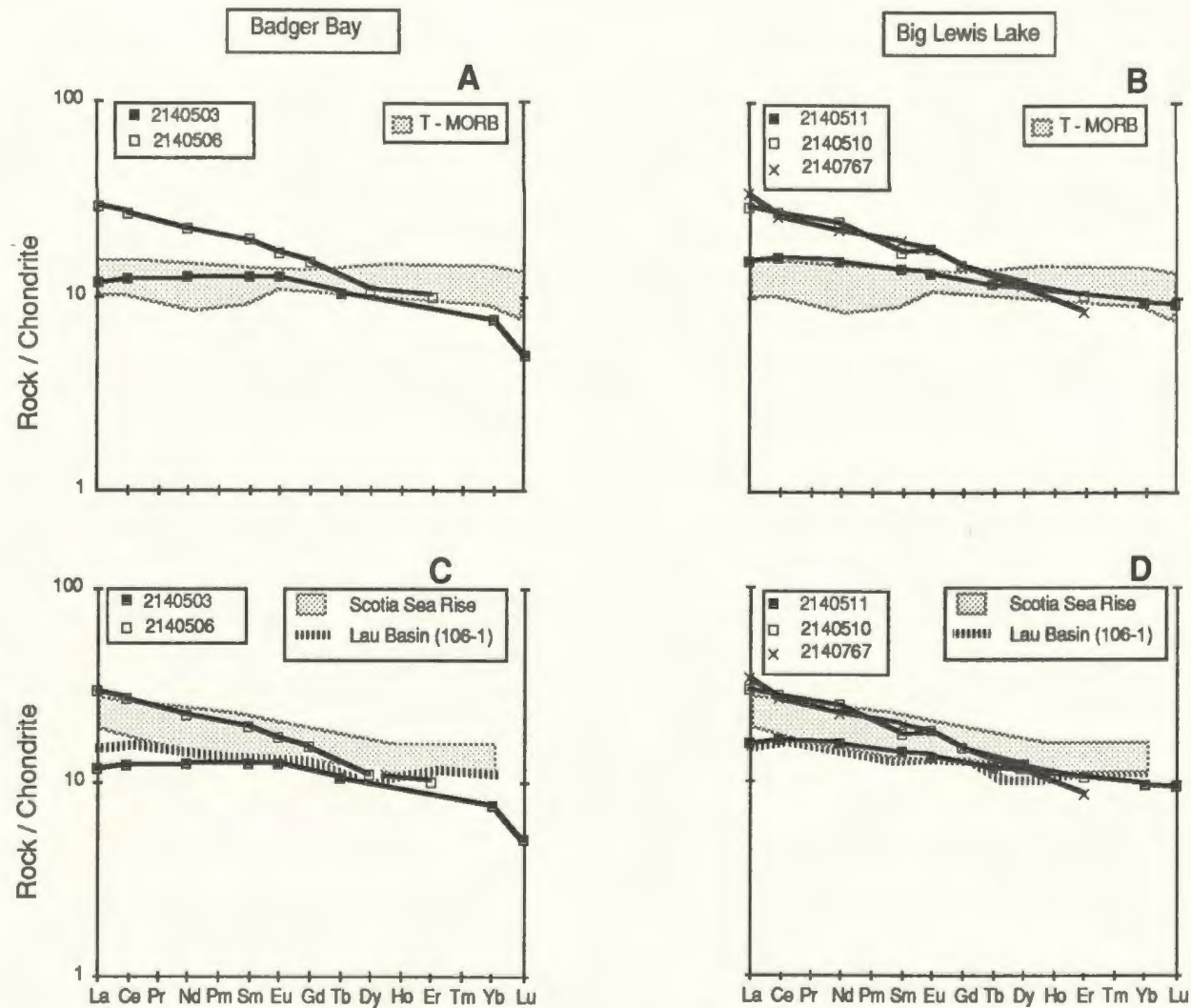
Figure 3.32: Chondrite - normalized REE patterns for the NAI group compared to T-MORB from the mid-Atlantic ridge (A, B) after Schilling et al. (1977) and back-arc basin basalts (C, D) from the Lau Basin (Gill, 1976) and Scotia Sea Rise (Hawkesworth et al., 1977).
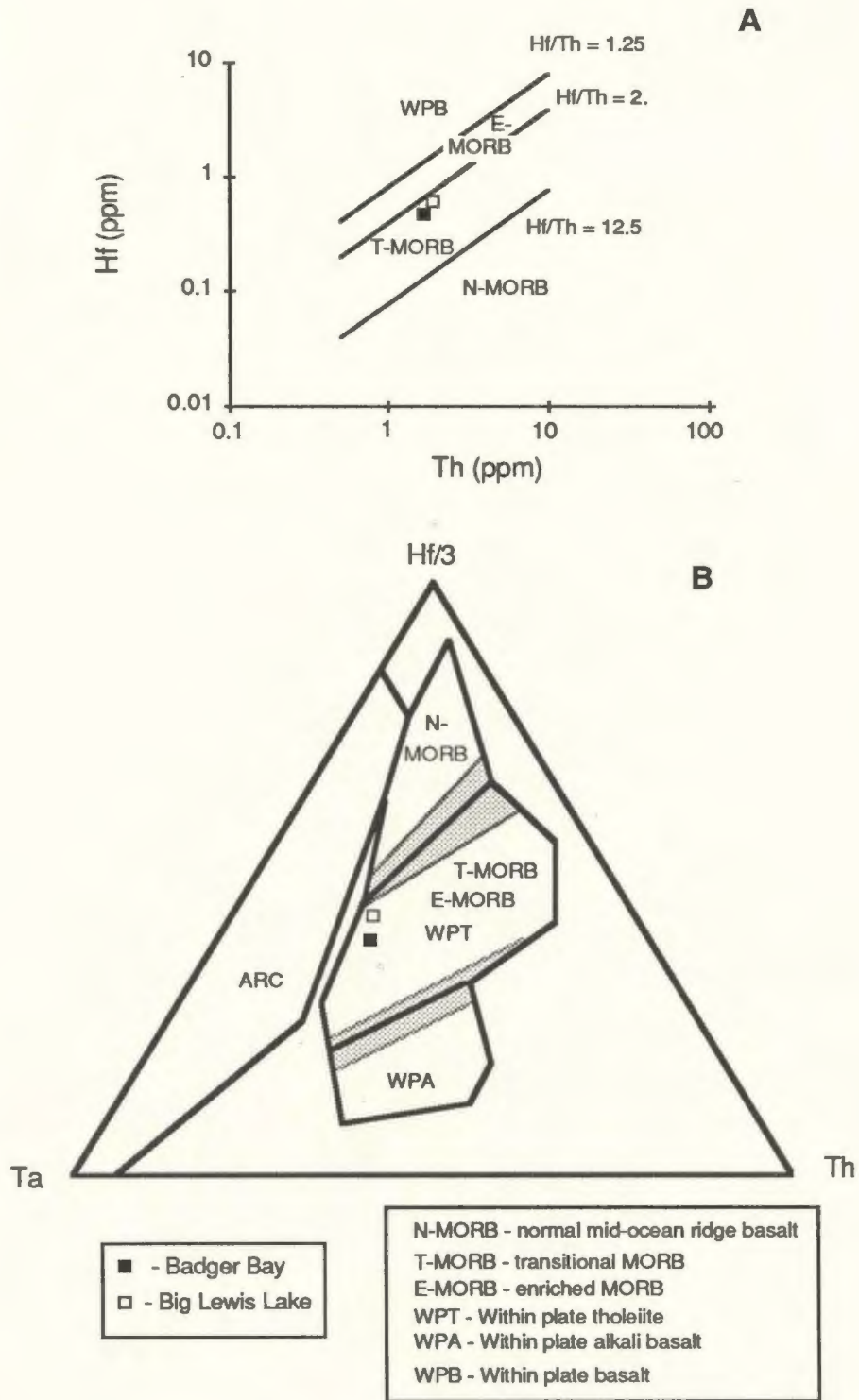
Figure 3.33: Ta-Hf-Th relationships in the NAI group. Hf-Th diagram after Wood et al. (1979).

ratios.

Gill (1976) reported an analysis from a dredge sample from the Lau Basin that appears to be a good analogue for the Nb-depleted samples of the NAI group. Although relatively enriched in TiO_2 (1.92 percent), this sample has similar REE contents (Figure 3.32C, D) and is similarly depleted in Zr and Y (78 and 17 ppm, respectively). Like the NAI group and unlike the Scotia Sea samples, it plots in the WPB field on the Ti-Zr-Y diagram. Gill (1976) did not suggest a source for this sample. It is atypical of most samples from the Lau Basin which are generally more akin to N-MORB (Hawkins, 1976; Jenner et al., 1987).

In summary, the geochemical relationships do not uniquely constrain the petrogenesis or tectonic environment of the NAI group. Good geochemical analogues can be found both at major spreading centers and within modern back-arc basins. The slightly incompatible element - enriched chemistry of the NAI group suggests volcanic activity at either a transitional (i.e. from N-MORB to E-MORB) spreading ridge segment or a within-plate oceanic island (either in a major ocean basin or a back-arc basin).

3.4.5 The NAT and NAE Groups

Compositions of samples in these groups are listed in Tables 3.9 and 3.10 and the mean major and trace element compositions are compiled in Table 3.11. Both suites are dominantly basaltic. There is little petrographic or chemical evidence for substantial SiO_2 mobility and silica contents are thought to reflect approximately original values. Some of the inter- and intra-suite variations are illustrated in Figure 3.34. Compared to the NAT group, the NAE group is consistently enriched in the more incompatible elements TiO_2, Zr and Nb (as well as Y and P_2O_5 and the LREE, see Table 3.9). The NAE group also has consistently lower Mg#'s and is relatively depleted in V, Cr and Ni (which are generally close to or below detection limits in the NAE group), Sc, MgO and CaO.

The Side Harbour suite is the largest in the NAT group and the only one with enough samples to define possible fractionation trends. Continuously increasing TiO_2 and V with

Table 3.9: Major (weight percent) and trace (ppm) element contents of the NAT group

Suite	New Bay		Side Harbour				
Sample	2140497	2140498	2140545	2140546	2140547	2140548	2140549
SiO_2	50.77	50.04	49.58	50.31	49.94	48.90	51.54
Al_2O_3	14.06	14.39	15.18	14.10	16.92	13.37	14.55
Fe_2O_3	3.22	4.18	6.44	3.35	4.34	2.72	3.89
FeO	10.67	10.14	4.88	8.11	7.15	8.03	5.87
MgO	5.29	5.44	7.38	7.07	4.79	11.96	5.50
CaO	7.61	7.42	9.23	9.37	9.89	8.46	9.80
Na_2O	4.53	4.88	3.30	4.50	2.84	2.94	4.64
K_2O	0.82	0.50	1.44	0.60	1.32	1.25	2.09
TiO_2	2.42	2.43	2.15	2.12	2.29	1.94	1.74
MnO	0.26	0.22	0.14	0.17	0.17	0.17	0.11
P_2O_5	0.35	0.37	0.28	0.30	0.35	0.25	0.26
LOI	2.02	1.45	2.61	2.85	2.10	4.22	3.80
Total*	99.13	98.38	100.43	100.04	99.02	99.93	99.65
Cu	70	74	49	85	39	93	46
Zn	109	109	97	96	100	85	75
Ni	14	15	65	62	45	212	124
Cr	50	54	146	104	92	579	228
V	455	439	288	288	325	280	212
Sc	40.3	40.8		30.8		33.3	27.8
Co	40.5	40.5		43.9		53.3	45.5
Rb	15	8	34	6	27	20	21
Sr	192	100	247	359	347	95	87
Ba	177	164	240	162	362	133	197
Th	2.26	2.45		2.4		1.91	1.77
Y	35	25	22	21	26	17	17
Zr	181	184	146	138	162	117	112
Nb	18	18	15	20	20	16	14
Hf	4.4	4.5		3.4		3.1	2.9
Ta	1.06	1.12		1.33		1.14	0.97
La	15.70	15.70		18.50		13.70	12.80
Ce	38.50	38.70		41.40		32.20	30.30
Nd	22.20	24.00		22.30		18.20	17.50
Sm	5.93	6.17		5.19		4.46	4.31
Eu	1.91	1.92		1.78		1.55	1.51
Gd	6.70						
Tb	1.12	1.13		0.82		0.72	0.71
Dy							
Er							
Yb	3.61	3.63		1.98		1.63	1.71
Lu	0.60	0.56		0.30		0.26	0.25
La/Ta	14.81	14.02		13.91		12.02	13.20
Th/Ta	2.13	2.19		1.80		1.68	1.82
(La/Sm)n	1.61	1.55		2.17		1.87	1.81
Ti/Zr	80	79	88	92	85	99	93
Zr/Nb	10	10	10	7	8	7	8
Ti/V	32	33	45	44	42	42	49
Zr/Y	5.1	7.2	6.5	6.7	6.2	6.8	6.4
Ti/Y	412	572	575	620	526	671	599
Mg#	0.44	0.44	0.58	0.56	0.46	0.69	0.54

* - analytical total; major element concentrations are recalculated to 100% anhydrous

Table 3.9 (continued)

Sample	Side Harbour (continued)				
	2140550	2140551	2140761	2140762	2140764
SiO2	47.94	46.76	48.23	49.13	49.68
Al2O3	13.38	15.35	15.14	15.18	14.83
Fe2O3	2.6	2.89	4.56	3.94	3.95
FeO	7.62	8.54	7.36	6.93	6.7
MgO	8.01	7.48	8.21	7.48	7.65
CaO	13.42	11.1	10.76	11.65	11.49
Na2O	4.11	3.53	3.34	2.62	2.67
K2O	0.62	0.95	0.03	0.92	0.81
TiO2	1.93	2.83	2.01	1.73	1.77
MnO	0.16	0.19	0.16	0.17	0.16
P2O5	0.21	0.39	0.22	0.24	0.29
LOI	6.03	7.85	3.64	2.18	2.23
Total*	99.48	98.74	100.15	100.19	100.46
Cu	69	85	118	175	99
Zn	84	110	96	85	82
Ni	168	32	90	72	95
Cr	339	21	226	187	241
V	230	329	246	253	248
Sc					
Co					
Rb	10	8	0	15	13
Sr	101	266	102	424	317
Ba	84	96	41	243	287
Thn					
Y	17	22	19	20	19
Zr	105	179	116	109	115
Nb	13	21	14	11	15
Hf					
Ta					
La		26.7		11.6	
Ce		60.7		25.2	
Nd		36.7		14.6	
Sm		8.9		3.9	
Eu		2.6		1	
Gd		7.6		3.7	
Tb					
Dy		1.8		3.4	
Er		3.2		2.1	
Yb		1.1		1.2	
Lu					
La/Ta					
Th/Ta					
(La/Sm)n		1.83		1.81	
Ti/Zr	110	95	104	95	92
Zr/Nb	8	8	8	10	8
Ti/V	50	52	49	41	43
Zr/Y	6.1	8.2	6.2	5.4	6.0
Ti/Y*	671	778	647	517	549
Mg#	0.61	0.57	0.59	0.59	0.60

Table 3.10: Major (weight percent) and trace (ppm) element contents of the NAE group

Suite	|--Big Lewis Lake--------|	|-----Seal Bay Head-----|	|-Side Hbr--|
Sample	2140509	2140768	2140483	2140484	2140763
SiO_2	48.91	51.9	49.59	47.95	49.45
Al_2O_3	16.75	14.32	14.25	15.62	17.13
Fe_2O_3	4.46	3.72	4.61	3.27	3.37
FeO	9.58	8.87	10.11	11.83	9.47
MgO	4.78	4.51	4.89	4.99	4.56
CaO	4.55	6.11	6.74	6.39	4.54
Na_2O	5.91	5.03	5.37	3.31	4.43
K_2O	0.09	0.41	0.16	2.17	2.8
TiO_2	3.26	3.87	3.15	3.51	2.76
MnO	0.34	0.28	0.29	0.25	0.18
P_2O_5	1.38	0.98	0.83	0.7	1.31
LOI	3.02	4.73	2.05	3.30	3.47
Total*	99.73	99.72	99.24	99.02	99.33
Cu	10	13	11	23	13
Zn	153	133	149	149	137
Ni	<1	6	<1	<1	3
Cr	<5	13	<5	<5	7
V	158	179	187	219	95
Sc	18.5		25	24	
Co	28.1		27.1	33.9	
Rb	1.0	4	2.4	32	30
Sr	252	327	138	312	476
Ba	128	226	156	276	697
Th	7.1		3.6	5.2	
Y	57	41	41	38	48
Zr	414	324	311	336	396
Nb	85	60	40	58	66
Hf	9.4		7.4	7.7	
Ta	5.40		2.73	3.70	
La	53.10		30.50	37.20	53
Ce	129.00		77.00	86.00	112.6
Nd	73.00		48.00	45.00	57.5
Sm	14.90		11.30	10.20	12.1
Eu	4.48		3.75	3.26	2.9
Gd	0.00		0.01	10.30	9.9
Tb	2.12		1.66	1.49	
Dy					7.4
Er					4.3
Yb	5.10		3.49	3.49	2.9
Lu	0.76		0.53	0.54	
La/Ta	9.83		11.17	10.05	
Th/Ta	1.31		1.32	1.41	
(La/Sm)n	2.17		1.65	2.22	2.67
Ti/Zr	47	72	61	63	42
Zr/Nb	5	5	8	6	6
Ti/V	124	130	101	96	174
Zr/Y	7.2	7.9	7.5	8.9	8.2
Ti/Y	341	563	458	559	343
Mg#	0.41	0.42	0.40	0.40	0.42

* - analytical total; major element concentrations are recalculated to 100% anhydrous

Table 3.11: Mean major and trace element concentrations of the NAT and NAE groups

Suite	New Bay	Side Harbour	Big Lewis Lake	Seal Bay Head	Side Harbour
SiO2	50.41	49.20	50.41	48.77	49.45
Al2O3	14.23	14.80	15.54	14.94	17.13
Fe2O3	3.70	3.87	4.09	3.94	3.37
FeO	10.41	7.12	9.23	10.97	9.47
MgO	5.37	7.55	4.65	4.94	4.56
CaO	7.52	10.52	5.33	6.57	4.54
Na2O	4.71	3.45	5.47	4.34	4.43
K2O	0.66	1.00	0.25	1.17	2.80
TiO2	2.43	2.05	3.57	3.33	2.76
MnO	0.24	0.16	0.31	0.27	0.18
P2O5	0.36	0.28	1.18	0.77	1.31
Cu	72	85.8	11.5	17	13
Zn	109	91	143	149	137
Ni	15	97	4	3	3
Cr	52	216	8	3	7
V					
Sc	40.6	30.6	18.5	24.5	
Co	40.5	47.6	28.1	30.5	
Rb	11	15	3	17	30
Sr	146	235	290	225	476
Ba	171	185	177	216	697
Th	2.36	2.03	7.10	4.40	
Y	30	20	49	39	48
Zr	183	130	369	323	396
Nb	18	16	72	49	66
Hf	4.45	3.13	9.40	7.55	
Ta	1.09	1.15	5.40	3.22	
La	15.70	17.93	53.10	33.85	53.0
Ce	38.60	41.15	129.00	81.50	112.6
Nd	23.10	23.68	73.00	46.50	57.5
Sm	6.05	5.72	14.90	10.75	12.1
Eu	1.92	1.86	4.48	3.51	2.9
Gd	3.36	1.90	0.00	5.16	9.9
Tb	1.13	0.75	2.12	1.58	
Dy					7.4
Er					4.3
Yb	3.62	1.77	5.10	3.49	2.9
Lu	0.58	0.27	0.76	0.54	
La/Ta	14.41	13.04	9.83	10.61	
Th/Ta	2.16	1.77	1.31	1.36	
(La/Sm)n	1.58	1.90	2.17	1.94	2.7
Ti/Zr	80	95	59	62	42
Zr/Nb	10	8	5	7	6
Ti/V	33	46	127	99	174
Zr/Y	6.2	6.5	7.6	8.2	8.2
Ti/Y	492	615	452	508	343
Mg#	0.44	0.58	0.42	0.40	0.42
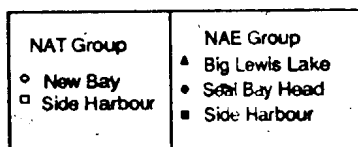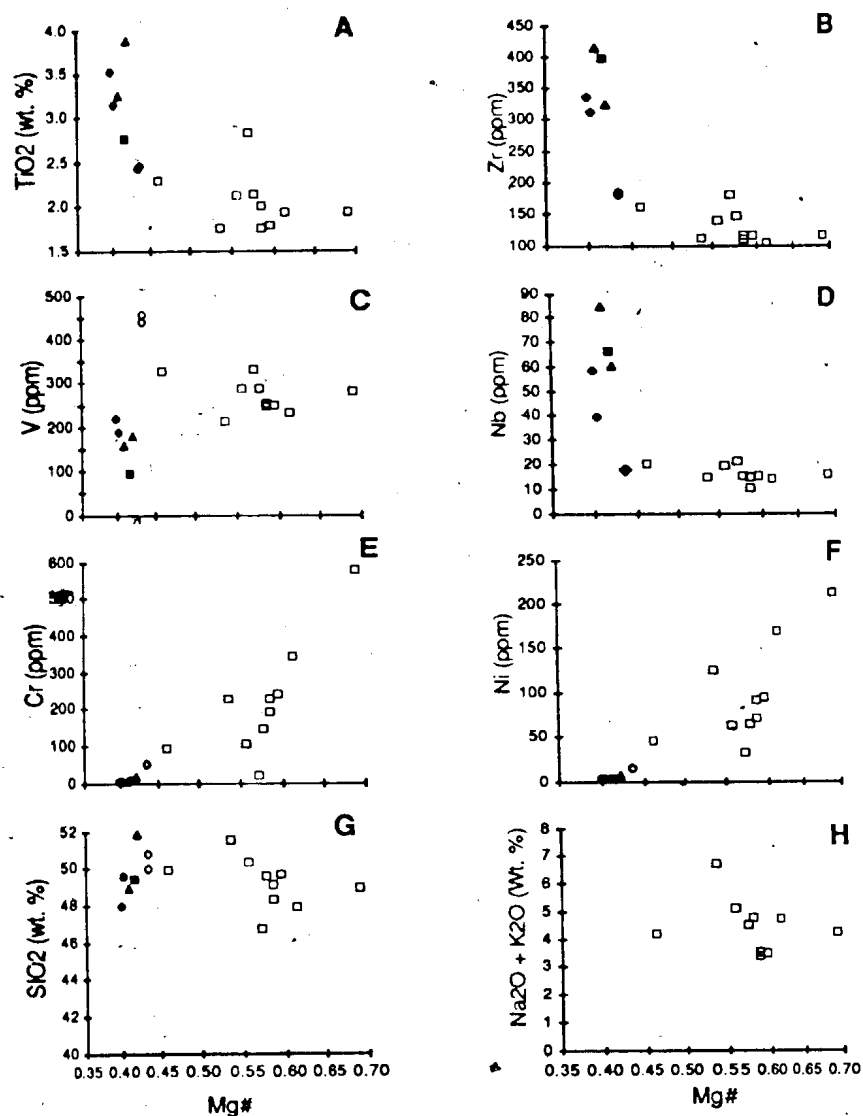
Figure 3.34: Selected elements plotted against Mg# for the NAT and NAI groups. Note lack of correlation between total alkalis and Mg# in the Side Harbour suite.

decreasing Mg# indicates that it comprises part of a tholeiitic fractionation trend. Sample 2140548 has the highest Mg# (0.69) in this suite but contains up to 20 modal percent clinopyroxene and psuedomorphed olivine phenocrysts (also evident in the very high Cr and Ni contents) and its analysis is not a liquid composition. Potentially, the interval between Mg# = 0.61 and 0.46 records fractional crystallization with consistently increasing TiO_2, Zr and V and decreasing Cr and Ni; this is further investigated below.

The New Bay basalt samples are somewhat different from the Side Harbour samples, with lower Mg#'s, higher incompatible element contents and slightly different incompatible element ratios suggesting both a slightly different melting history and a greater degree of fractionation.

The NAT and NAE groups are unlikely to be related by fractional crystallization. Although Mg#'s of the latter are lower, SiO_2 contents do not increase correspondingly from the NAT to the NAE suites and the NAE samples do not lie on the extension of Side Harbour suite trends on incompatible element - Mg# plots. Furthermore, incompatible element ratios in the NAE group are consistently enriched in the more incompatible elements (e.g. LREE over HREE, La and Th over Ta, Zr and Nb over Ti, Ti and Zr over Y and V).

The Nb/Y versus Zr/P_2O_5 diagram (Figure 3.35) indicates that the NAE group is alkalic. The NAT group overlaps the non-alkalic and transitional fields on this diagram. Evidence from clinopyroxene chemistry presented in Section 3.6 provides further evidence that the NAT group comprises enriched tholeiites rather than alkali basalt.

The TiO_2 versus V diagram (Figure 3.36A) further emphasizes the contrasts between the two groups. The NAT group has Ti/V ratios consistently around 40 to 50 and plots near the MORB-BABV field boundary. However, the NAE group has much higher ratios, and plots in and near the field of alkali and oceanic island basalts.

On the Zr/Y-Zr diagram (Figure 3.36B), all samples plot within the WPB field as expected. The NAE group has slightly higher Zr/Y ratios but the difference is barely resolvable.

Hf/Th ratios in both groups are greater than 1.25 (Figure 3.37A) indicating an affinity to E-MORB rather than WPB according to Wood et al. (1979). On the Ta-Th-Hf triangular diagram
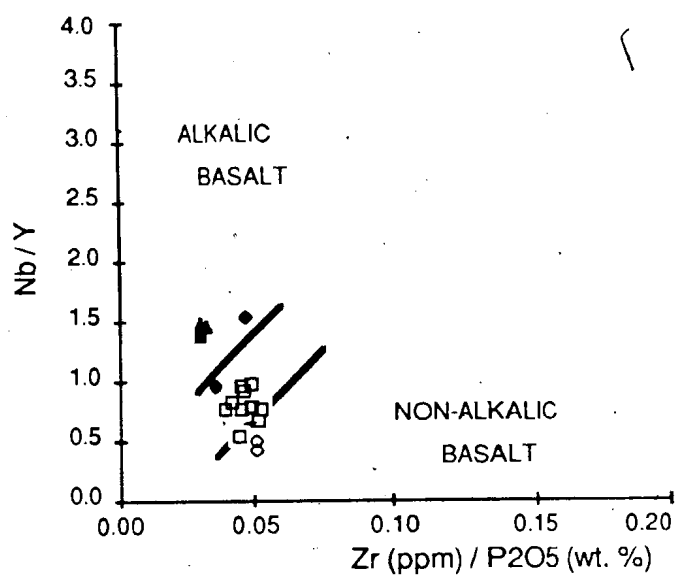
Figure 3.35: Discrimination of alkalic and non-alkalic basalts, after Floyd and Winchester (1975), for the NAT and NAE groups. Most NAT group samples plot in the transitional fields while NAE group samples plot mainly in the alkalic basalt field.
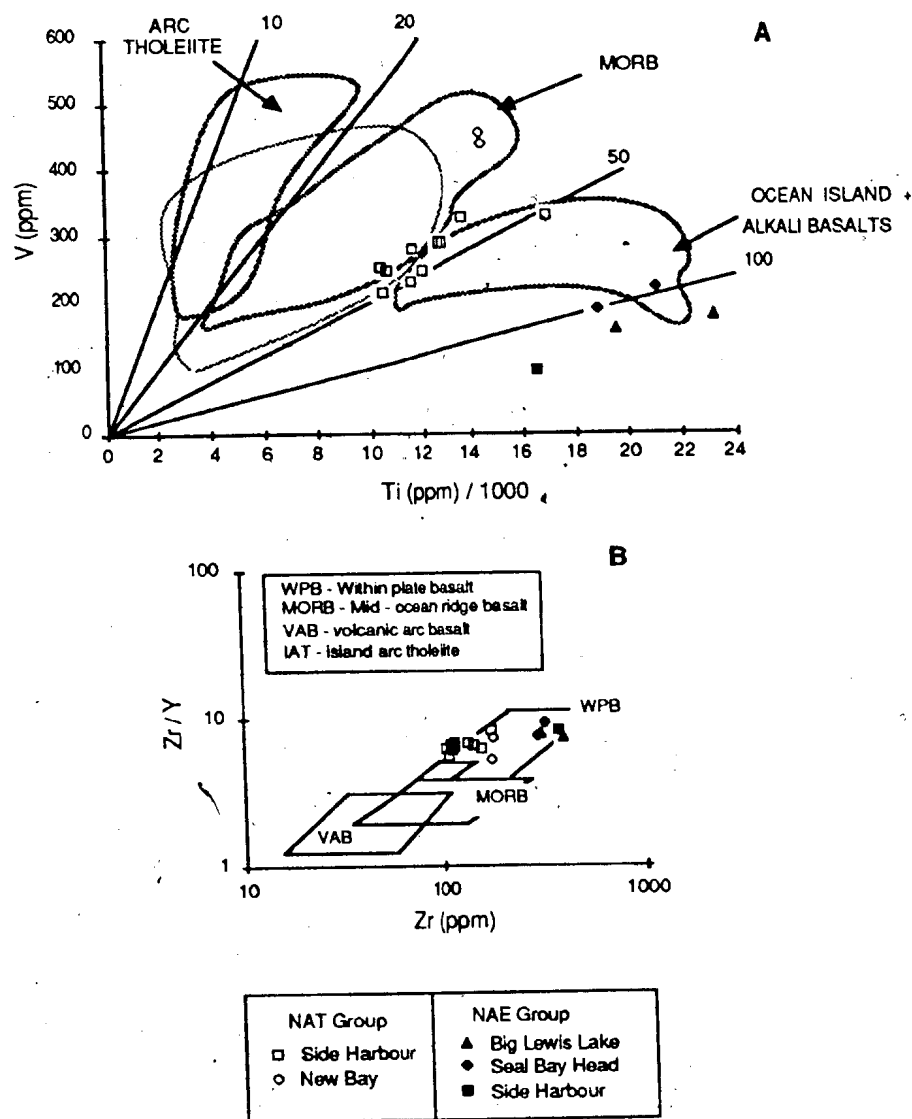
Figure 3.36: Ti - V (Shervais,1982) and Zr/Y-Zr (Pearce and Norry, 1979) for the NAT and NAE subgroups. In A, stippled field is BABV.There is a strong contrast in Ti / V ratios between the two groups. In B, both groups have similar high Zr / Y ratios typical of within plate environments.
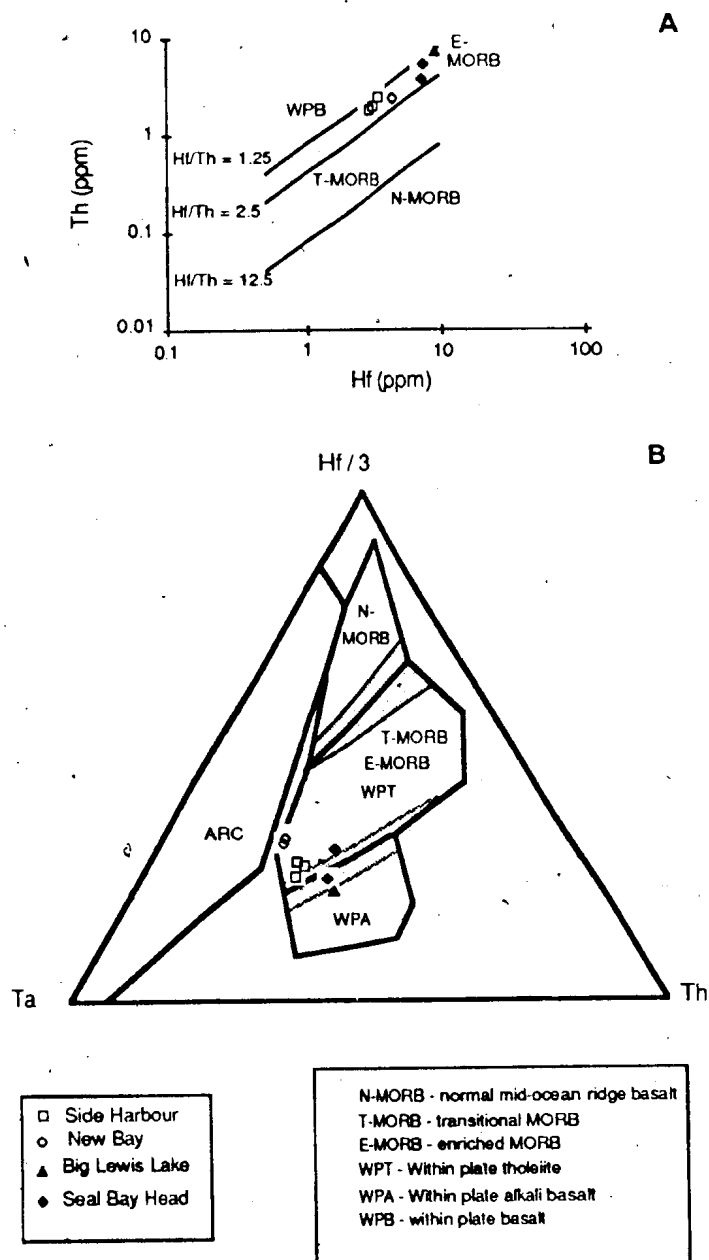
Figure 3.37: Th-Hf and Ta-Hf-Th diagrams for the NAT and NAE groups.

(Figure 3.38B), the NAT group plots in the combined field of E-MORB and WPT although close to the boundary with the WPA field. The NAE group plots in the boundary area between these two fields, perhaps suggesting a mildly alkalic affinity.

The NAT group is consistently LREE-enriched (Figure 3.38). The Side Harbour suite has higher $(La/Yb)_n$ ratios than the New Bay suite (average 3.55 as opposed to 2.86); the flatter trend of the New Bay samples relative to the Side Harbour samples is manifested as a relative enrichment of HREE at approximately equivalent LREE contents. Although the two suites are not obviously related to each other through fractional crystallization of the same parental liquid, they may be related to each other by virtue of different degrees of partial melting of the same source. The New Bay basalts are considerably more fractionated than the Side Harbour rocks; higher degrees of partial melting of a source with HREE contents in the range of the Side Harbour suite followed by extensive fractional crystallization could produce REE abundances showing the New Bay-Side Harbour relationships. This problem will be further addressed in Chapter 4.

Volcanic rocks with geochemical characteristics (including REE contents) similar to the NAT group have been documented in various oceanic environments. E-type MORB erupted at various locations on the Mid-Atlantic Ridge (MAR), represented in Figure 3.38 by samples from DSDP Leg 82 between $30°$ and $40°N$ (Schilling et al., 1983), are similarly LREE enriched but have generally lower abundances than the NAT group. The MAR E-MORB basalts also have lower Ti/Zr ratios and, in contrast to the NAT group, plot in the MORB rather than WPB field on diagrams such as Pearce and Cann's (1973) Ti-Zr-Y ternary plot.

A better analogue for the Side Harbour suite appears to be oceanic island tholeiites, represented on Figure 3.38 by Kilauean tholeiites. These basalts, like the MAR E-MORB, have REE abundances and slopes $(La_n/Yb_n > 4.5)$ similar to the Side Harbour suite but somewhat steeper than the New Bay suite. The oceanic island tholeiites have relatively more TiO_2 than E-MORB at equivalent Y producing Ti/Y ratios greater than 550, similar to the TiO_2-rich samples of the Side Harbour suite.

Basalts with similar REE contents have also been recognized in some back-arc basin
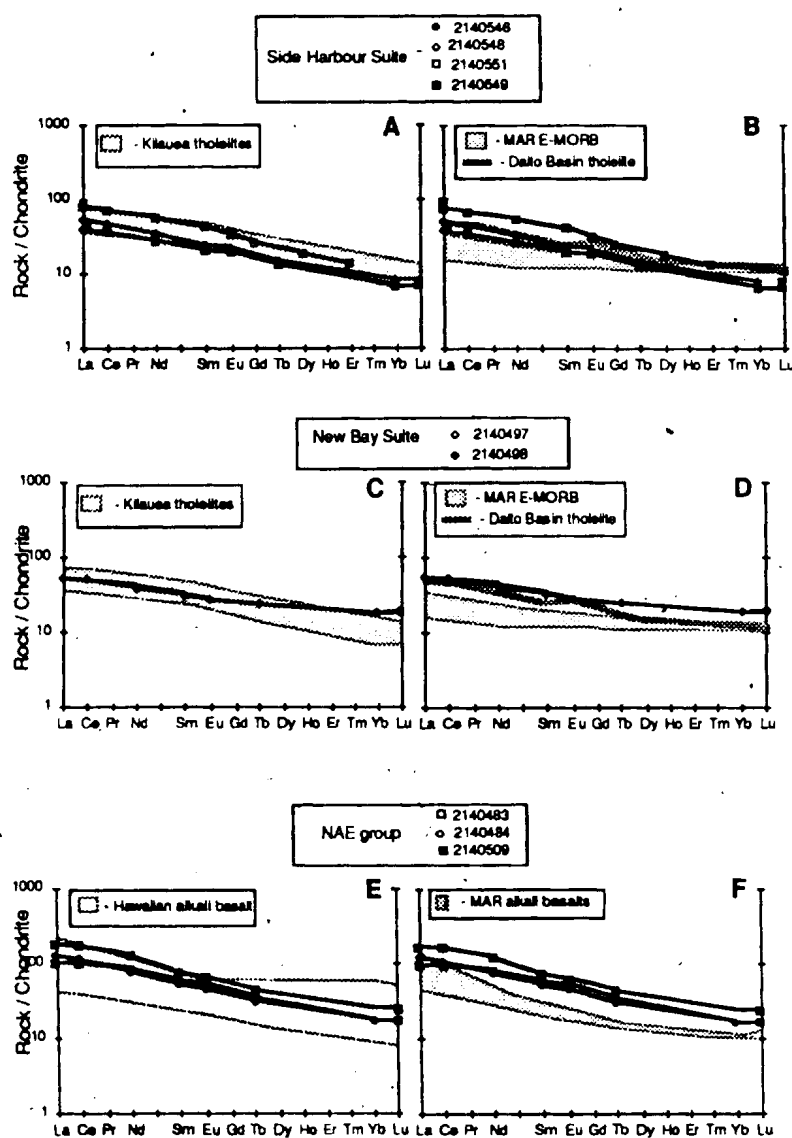
Figure 3.38: Chondrite-normalized REE patterns for samples from the NAT (A to D) and NAE (E and F) groups. The NAT group is compared to typical E-MORB from the Mid-Atlantic ridge (Schilling et al., 1977), and back - arc basin enriched tholeiites from the Daito Basin (Marsh et al., 1980). NAE group is compared to Hawaiian alkali basalts (Basaltic Volcanism Study Project, 1981) and to MAR alkali basalts (Schilling et al., 1977).

environments. A single sample from the Lau Basin reported by Gill (1976) is closely analogous to the NAT group. It has very similar LREE contents and $(La/Yb)_n = 4.43$, intermediate between the Side Harbour and New Bay suites. It is similar in most other trace element contents and ratios to the Wild Bight Group samples. Unfortunately, this was a dredged sample and the origin and setting of the volcanism that produced it is not certain. Another good analogue may be found in the Daito Basin in the northwestern part of the Philippine Sea. Samples recovered during Leg 58 of the Deep Sea Drilling Program included enriched tholeiites and alkali basalt sills which lie somewhat off the axis of the Daito Ridge. Marsh et al. (1980) and Wood et al. (1980) described the chemistry of these rocks but did not report full REE analyses; however, approximate REE patterns for the tholeiitic rocks, which they constructed using Y in place of Er, shows them to be very similar to the NAT group. Other incompatible element concentrations and ratios are likewise similar. Geophysical evidence and geochemical evidence from a few dredge hauls (Murauchi et al., 1968; Karig, 1975; Marsh et al., 1980) suggest that the Daito and Oki-Daito ridges represent an island arc-remnant arc pair separated during the opening of a small marginal-basin (the Daito Basin). The enriched tholeiitic and alkalic sills are interpreted as off axis magmatism related to the opening of this basin (Marsh et al.,1980).

REE patterns of the NAE group are slightly more LREE enriched ($(La/Yb)_n \sim 6$ to 7) than the Side Harbour suite at higher overall abundances. REE abundances in the NAE group are considerably higher than typical E-MORB or oceanic tholeiites but are similar to oceanic alkali basalts, represented on Figure 3.38 by MAR $45°N$ basalts and Kilauean alkali basalts. As with the NAT group, the analogy with the Hawaiian rocks is particularly good.

Some inferences regarding the fractionation history of the Side Harbour suite can be drawn from Figure 3.39 and from preliminary trace element modelling of the Side Harbour suite summarized in Table 3.12. Clinopyroxene and plagioclase both occur as phenocrysts in this suite. Up to 30 percent total fractional crystallization of some combination of olivine, clinopyroxene and plagioclase is indicated by the Ti-Y diagram (Figure 3.39A). Figures 3.39B and C indicate that all of these minerals were crystallizing in the observed differentiation interval. The
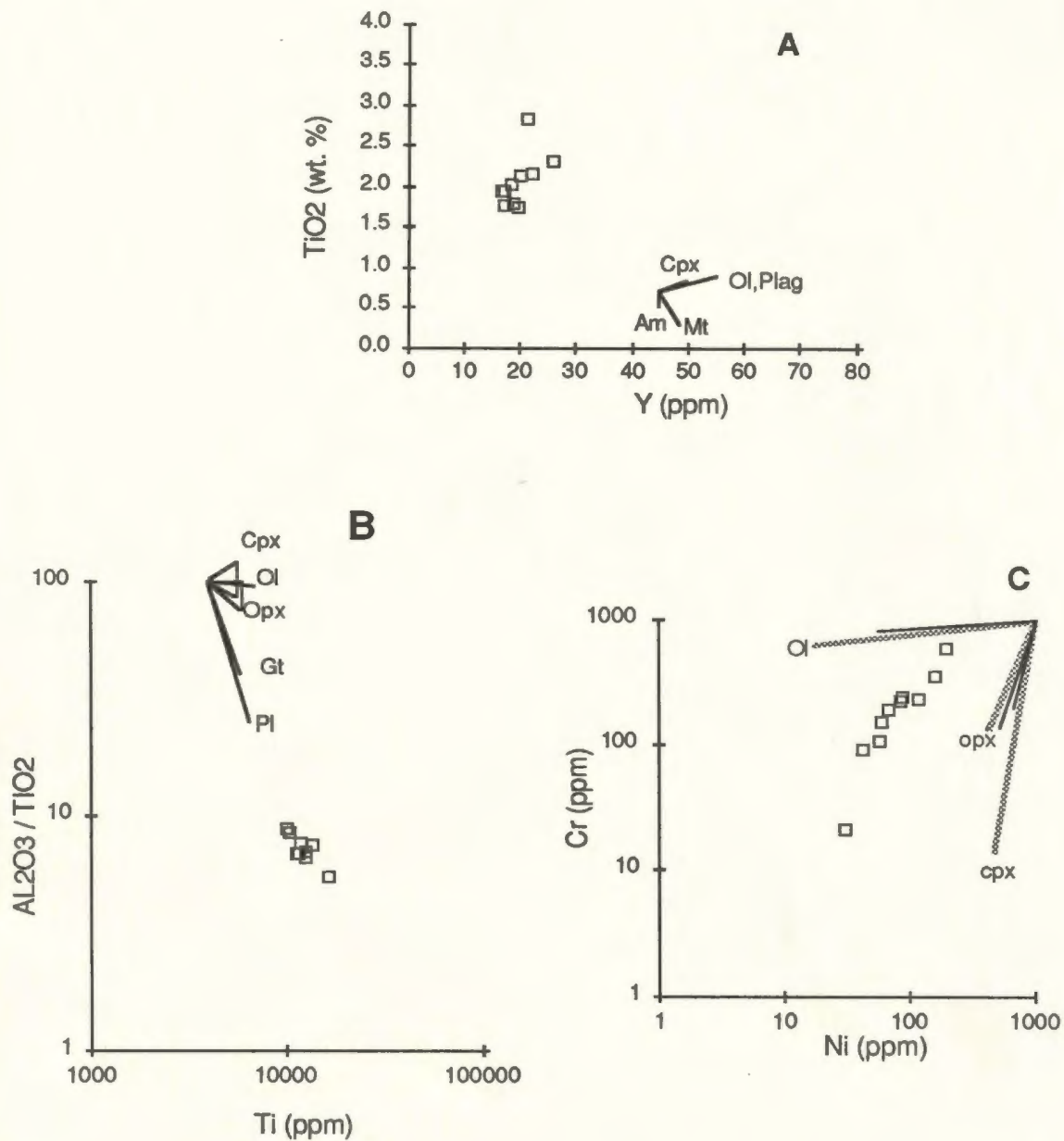
Figure 3.39: Fractionation diagrams for NAT group samples in the Side Harbour suite. A - after Perfit et al. (1980) with 30% fractionation vectors; B - after Pearce and Flower (1977) with 50% fractionation vectors; C - vectors calculated from distribution coefficients in Appendix 9 (primitive basalt - solid lines, fractionated basalt - stippled lines) assuming 20% fractionation of olivine:clinopyroxene:plagioclase = 0.2:0.2:0.6.

Table 3.12 : Results of trace element modelling of fractionation in 'transitional' rocks of the Side Harbour suite.

Model Parameters: ol:cpx:pl = 0.2:0.2:0.6
Distribution coefficients: Fractionated basalt (Appendix 9)

	Starting Composition	Ending Composition	% Total Fractionation
TiO_2 (wt.%)	1.70	2.23	22 - 30% (±5%)
Zr (ppm)	122.4	154	18 - 27% (±5%)
Nb (ppm)	13.8	20.2	29 - 36% (±5%)
Y (ppm)	18.2	25	26 - 36% (±5%)
V (ppm)	247	315	22 - 32% (±5%)
Cr (ppm)	230	60	27 - 35% (±5%)
Ni (ppm)	105	39	21 - 28% (±5%)

estimate of total fractional crystallization is supported by preliminary modelling summarized in Table 3.12. The only elements for which fractionation estimates at the quoted uncertainties do not overlap are Zr and Nb, and the discrepancy between them is small. Approximately 25 to 30 percent fractional crystallization can account for the observed change in incompatible element contents and for this amount of fractional crystallization, olivine:clinopyroxene: plagioclase ≈ 0.2:0.2:0.6 can account for the observed changes in Cr and Ni. This constrains plagioclase fractionation to the range of approximately 15 to 18 percent, in good agreement with the 12 to 20 percent range estimated from Figure 3.39B.

3.5 Geochemistry of the Mafic Subvolcanic Rocks

3.5.1 Introduction

Field relationships suggest that the mafic intrusives in the Wild Bight Group are genetically related to the associated volcanic rocks. In the following Section, the nature of this relationship is assessed geochemically. The geochemistry of the intrusive rocks is considered in terms of the volcanic geochemical groups and the individual samples are assigned to one or another of the geochemical groups using the procedures outlined in Section 3.4. Following this, possible petrogenetic relationships between the volcanic and mafic intrusive rocks are evaluated.

3.5.2 Classification vis a vis Volcanic Rock Groups

3.5.2.1 General statement

The mafic intrusive rocks of the Wild Bight Group, like the volcanic rocks, span a considerable compositional range (Table 3.13). Most have SiO_2 contents in the basalt range. Mg# ranges from 0.65 to 0.4 indicating, along with similarly variations in Cr and Ni contents, that relatively primitive as well as fractionated magmas are represented. TiO_2 contents span the complete range of the volcanic rocks and there is also a wide range of other incompatible element concentrations.

Table 3.13: Major (weight percent) and trace (ppm) element contents of mafic intrusive rocks

Sample	2140465	2140461	2140512	2140496	2140495	2140491	2140481
SiO2	52.61	53.94	52.34	53.99	48.41	48.79	49.21
Al2O3	17.52	16.07	17.29	18.30	18.59	19.91	15.22
Fe2O3	1.60	3.63	1.98	2.25	1.51	3.49	4.91
FeO	7.75	11.05	5.98	7.38	6.57	5.03	10.18
MgO	8.89	5.11	7.35	4.78	7.21	5.39	6.01
CaO	9.18	4.57	10.15	7.44	12.95	12.79	8.29
Na2O	1.34	4.05	2.31	4.08	2.47	2.67	3.53
K2O	0.48	0.35	1.34	0.27	0.67	0.24	0.09
TiO2	0.49	0.99	1.00	1.17	1.30	1.37	1.97
MnO	0.12	0.15	0.14	0.19	0.16	0.15	0.27
P2O5	0.02	0.09	0.12	0.15	0.15	0.17	0.31
LOI	5.31	5.48	2.91	4.16	3.10	2.65	2.82
Total*	100.35	99.11	100.92	98.99	100.19	99.60	99.75
Cu	80	15†	61	71	70	76	54
Zn	66	112	66	88	105	65	92
Ni	35	5	106	14	79	35	17
Cr	182	50	299	55	144	69	44
V	246	515	190	255	185	227	472
Sc				31.4	32.2	31.3	38.2
Co				29	39.3	36.5	46.5
Rb	5	6	33	5	15	4	<0.5
Sr	67	391	270	155	289	346	154
Ba	32	37	222	107	91	110	59
Th				3.2	1.09	1.15	2.1
Y	5	17	20	23	15	16	28
Zr	3	19	94	101	78	89	94
Nb	0.5	1.0	5	6	8	10	6.7
Hf				2.64	2.01	2.2	2.45
Ta				0.38	0.55	0.66	0.41
La				12.2	7.2	8.7	13.5
Ce				27.7	17.0	20.6	31.4
Nd				13.7	10.6	12.4	18.9
Sm				3.61	2.83	3.21	4.84
Eu				1.14	1.07	1.22	1.68
Gd					3.30	3.40	0.01
Tb				0.68	0.48	0.54	0.86
Dy							
Er							
Yb				2.44	1.42	1.58	2.74
Lu				0.39	0.22	0.25	0.44
La/Ta				32.1	13.1	13.2	32.9
Th/Ta				8.42	1.98	1.74	5.12
(La/Sm)n				2.1	1.6	1.7	1.7
Ti/Zr	901	320	64	69	100	92	125
Zr/Nb	6	18	17	16	9	9	14
Ti/V	12	12	32	28	42	36	25
Zr/Y	0.6	1.1	4.7	4.4	5.1	5.4	3.3
Ti/Y	561	348	300	307	511	500	417
Mg#	0.66	0.41	0.65	0.50	0.64	0.57	0.45

* - analytical total; major element concentrations are recalculated to 100% anhydrous

Table 3.13 (continued)

Sample	2140482	2140508	2140502	2140485	2140450	2140501	2140486
SiO2	46.07	50.16	45.35	46.33	49.32	48.62	50.90
Al2O3	19.61	17.76	21.95	15.67	17.74	17.15	14.96
Fe2O3	3.45	3.76	2.27	3.56	3.54	2.82	3.86
FeO	7.46	7.16	7.35	9.74	7.50	9.21	8.71
MgO	5.41	6.58	3.92	7.44	4.32	3.92	4.14
CaO	12.67	7.21	12.29	10.18	7.03	9.24	6.74
Na2O	2.45	3.73	3.26	3.29	3.90	4.25	5.33
K2O	0.52	0.80	0.59	0.59	2.77	1.19	1.10
TiO2	1.98	2.25	2.59	2.73	2.88	3.00	3.41
MnO	0.15	0.29	0.14	0.19	0.32	0.20	0.23
P2O5	0.25	0.31	0.29	0.29	0.68	0.38	0.63
LOI	3.08	2.94	4.16	3.19	3.96	5.70	1.93
Total*	100.75	100.62	100.08	99.88	100.07	99.28	99.18
Cu	85	35	19	70	12	21	17
Zn	81	89	64	95	100	98	120
Ni	36	49	8	48	4	6	<1
Cr	52	72	8	39	9	<5	<5
V	262	266	303	347	226	279	247
Sc		27.8	23.6		17.8		
Co		39.5	33.1		22.9		
Rb	8	22	13	10	43	22	16
Sr	541	413	406	471	234	530	230
Ba	130	350	165	123	497	269	380
Th		1.84	1.44		4		
Y	17	32	11	18	30	22	30
Zr	129	180	101	155	246	188	241
Nb	17	10	15	24	47	32	38
Hf		4.09	2.64		5.7		
Ta		0.76	1.12		3.1		
La		12.0	13.6		34.4		
Ce		30.9	31.1		76.0		
Nd		19.9	18.0		39.6		
Sm		5.18	8.92		8.61		
Eu		1.81	1.41		2.71		
Gd							
Tb		0.93	0.55		1.18		
Yb		3.04	1.21		2.62		
Lu		0.48	0.17		0.4		
La/Ta		15.8	12.1		11.1		
Th/Ta		2.42	1.29		1.29		
(La/Sm)n		1.4	2.1		2.4		
Ti/Zr	92	75	153	105	70	96	85
Zr/Nb	8	18	7	6	5	6	6
Ti/V	45	51	51	47	76	64	83
Zr/Y	7.4	5.7	9.1	8.5	8.3	8.5	8.1
Ti/Y	686	426	1395	899	580	814	688
Mg#	0.50	0.55	0.45	0.53	0.45	0.40	0.40

* - analytical total; major element concentrations are recalculated to 100% anhydrous

Table 3.13 (continued)

Sample	2140454	2140457	2140489
SiO2	49.20	45.12	46.06
Al2O3	14.45	14.85	15.09
Fe2O3	4.16	4.39	6.58
FeO	9.95	11.06	9.45
MgO	4.78	6.19	5.99
CaO	6.87	9.92	9.45
Na2O	4.62	3.40	2.13
K2O	1.30	0.46	0.51
TiO2	3.79	3.94	4.00
MnO	0.22	0.21	0.22
P2O5	0.66	0.46	0.53
LOI	2.48	2.44	3.52
Total	100.04	100.40	99.92
Cu	14	48	45
Zn	156	108	126
Ni	<1	28	24
Cr	<5	26	9
V	293	375	402
Sc	22.2	26.7	
Co	37.1	55.4	
Rb	18.1	10.3	4.5
Sr	167.0	383.3	494.5
Ba	443	157	174
Th	3.76	2.81	
Y	35.7	23.6	26.2
Zr	273.0	181.1	209.6
Nb	53.3	38.1	41.7
Hf	6.4	4.6	
Ta	3.7	2.76	
La	34.5	24.6	
Ce	80	56.4	
Nd	42.2	31.1	
Sm	9.07	6.69	
Eu	3.1	2.26	
Gd	9.2	7	
Tb	1.34	0.96	
Yb	3.17	2.3	
Lu	0.45	0.32	
La/Ta	9.3	8.9	
Th/Ta	1.02	1.02	
(La/Sm)n	2.3	2.2	
Ti/Zr	83	130	114
Zr/Nb	5	5	5
Ti/V	78	63	60
Zr/Y	7.6	7.7	8.0
Ti/Y	636	1002	914
Mg#	0.41	0.45	0.44

3.5.2.2 Discriminant functions and the Ti-Zr plot

As a first approximation, the discriminant functions and the TiO_2-Zr diagram derived in Section 3.4 can be used to classify the mafic intrusive rocks *vis a vis* the volcanic rock groups. Discriminant scores were calculated for the mafic intrusive rocks using the four discriminant functions derived for the volcanic rock groups (Appendix 8). On the basis of these scores, each sample was assigned a probability of belonging to one or another of the volcanic rock groups. Classification of the samples is summarized in Table 3.14 and illustrated on a territorial plot in Figure 3.40. Approximately 65% of the samples were classified with greater than 90% confidence and 88% with greater than 70% confidence. The discriminant function analysis suggests that the intrusive sample suite includes representatives of all geochemical groups defined by the volcanic rocks. Note that on the territorial plot, approximately 65% of the samples, although classified on the basis of the volcanic rock groups, plot outside the areas occupied by the volcanic rocks suggesting that, despite the successful classification, there may not be a one to one petrogenetic relationship between volcanic and intrusive rocks.

The TiO_2-Zr classification diagram (Figure 3.41) reveals further complications including:

1) one sample classified as IAD is more Ti-rich than normal and plots on the boundary of the intermediate field;

2) almost half of the samples classified as NAT plot outside any of the defined fields. Most of these are more TiO_2-rich than volcanic rocks that define the NAT group but less Zr-rich than volcanic rocks of the NAE group.

3) None of the intrusive rocks classified as NAE is as Zr-rich as the volcanic rocks that define this group.

This highlights some potential problems in using only the incompatible element contents to classify unknown samples in this way: 1) the fields on the element concentration diagrams and the discriminant functions are defined only for the range of fractional crystallization represented by the known samples (in this case, the volcanic rock groups). Unknowns which represent the same magma batch but are substantially more or less fractionated than the volcanic rock end

Table 3.14: Probability that intrusive rocks belong to one or the other of the various volcanic rock groups based on discriminant function analysis

Sample No.	Highest Probability Group (probability in brackets)	Second Highest Prob. Group (probability in brackets)
2140491	NAI (67%)	IAI (31%)
2140481	NAT (70%)	NAI (27%)
2140482	NAT (94%)	NAI (6%)
2140508	NAT (85%)	NAI (15%)
2140502	NAT (>99.9%)	NAI (<0.1%)
2140485	NAT (>99.9%)	NAI (<0.1%)
2140465	IAD (100%)	
2140461	IAD (100%)	IAI (<.1%)
2140512	IAI (>99.9%)	NAI (<.1%)
2140496	IAI (>99.9%)	NAI (<.1%)
2140495	NAI (95%)	NAT (3%)
2140450	NAE (61%)	NAT (40%)
2140501	NAT (98%)	NAE (2%)
2140486	NAE (96%)	NAT (4%)
2140454	NAE (99.8%)	NAT (.2%)
2140457	NAT (83%)	NAE (17%)
2140489	NAT (89%)	NAE (11%)
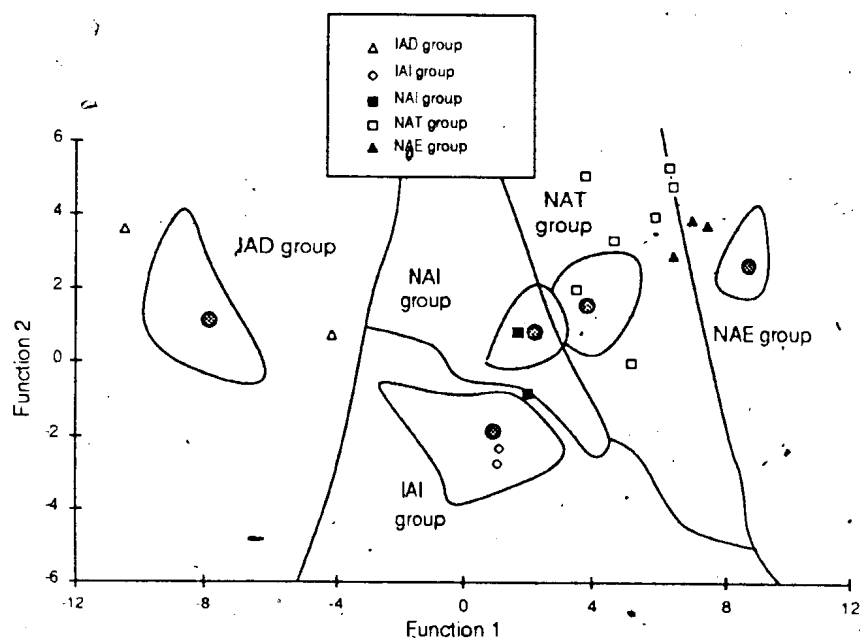
Figure 3.40: Territorial plot of discriminant functions 1 and 2
showing distribution of mafic intrusive rocks. Fields are the
same as Figure 3.14. Distribution of volcanic rock samples
indicated by stippled fields. Dark stippled circles are group
centroids. Symbols indicate classification of individual samples
based on four functions (Table 3.14).
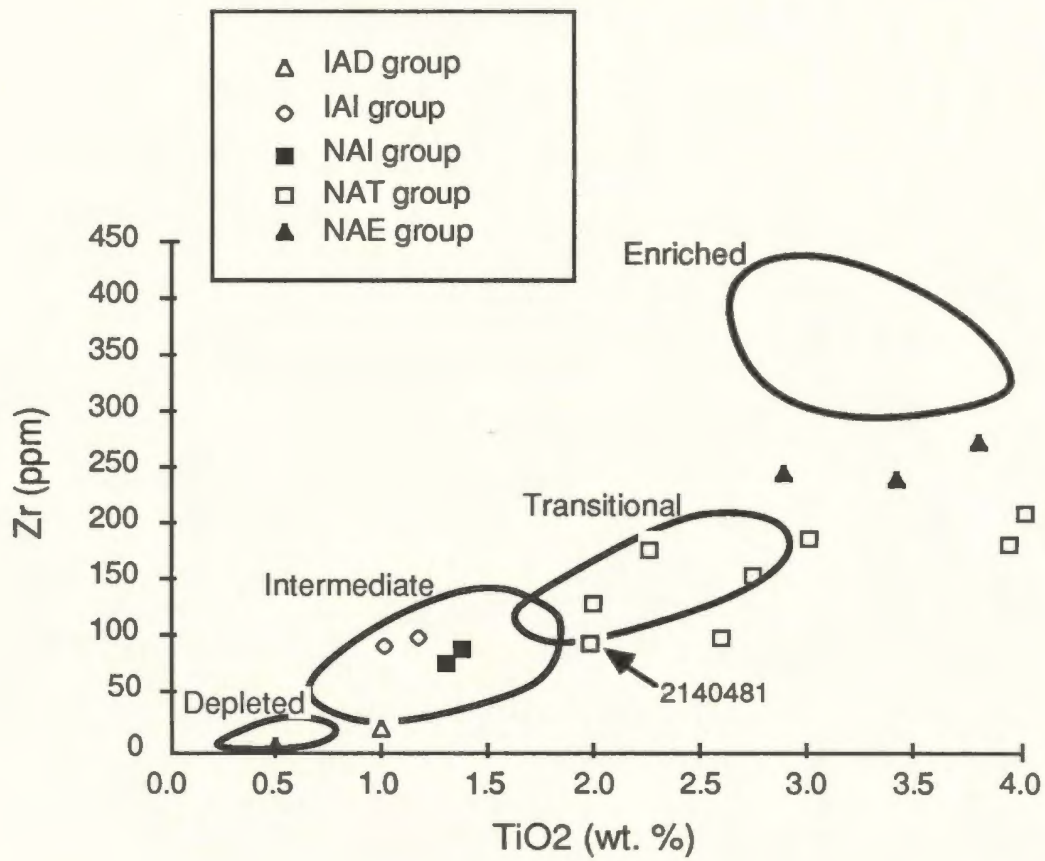
Figure 3.41: TiO2 - Zr diagram for the mafic intrusive rocks. Fields are from Figure 3.7. Symbols indicate classification based on discriminant function analysis.

members may be misclassified by this approach; 2) any accumulation of crystals with high crystal-liquid distribution coefficients for the elements being used (e.g., iron-titanium oxides or apatite in the present case) may likewise cause samples to be misclassified; 3) there may be intrusive rocks for which there are no sampled volcanic equivalents (i.e. magmas that did not erupt or volcanic rocks that do not outcrop at the present level of exposure); and 4) samples from different geographic or stratigraphic settings may have been affected by different degrees or styles of alteration. Therefore, it is necessary to confirm the above classification by other methods and to compare the intrusive rocks closely with the appropriate, possibly cogenetic, volcanic rocks before any final interpretations based on their similarity can be made.

3.5.2.3 Refinement of classification; extended REE and Ti-Zr-Y plots, incompatible element ratios

The preliminary classification achieved above can be checked with reference to the REE, HFSE relationships and by comparing incompatible element ratios of the intrusive rocks with ratios with those of volcanic rocks in each group.

The partial extended REE plots in Figure 3.42, in general, confirm the classification of samples predicted by the incompatible element contents. With one exception, samples classified in groups of island arc affinity (IAD, IAI) have the characteristic negative Ta and/or Nb anomalies, while those classified in groups of non-arc affinity do not. The one exception is sample 2140481, assigned to the NAT group by the discriminant functions and the Ti-Zr plot, but nevertheless having prominent negative Nb and Ta anomalies (Figure 3.42A) and similar abundances to sample 2140496 which clearly belongs to the IAI group. Detailed comparison of the composition of 2140481 with volcanic rocks of the IAI and NAT groups shows that it has incompatible element concentrations similar to the Glover's Harbour - Seal Bay Bottom - Northern Arm suites, the main divergence being somewhat higher concentrations of TiO_2 (1.97 versus <1.51) and V (472 versus <375). Incompatible element ratios not involving Ti and V (e.g. Zr/Nb, Zr/Y, Table 3.13) are also similar to the Glover's Harbour East/ Seal Bay Bottom/ Northern Arm suites and unlike those
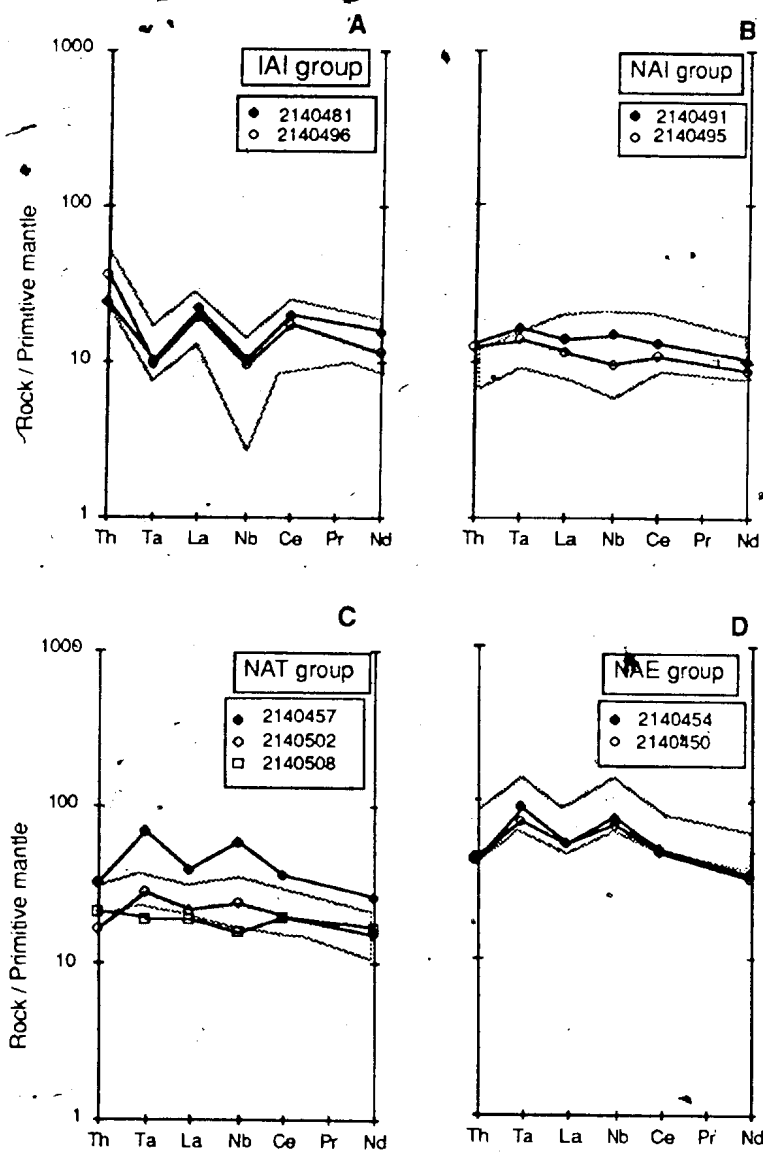
Figure 3.42: Partial extended REE plots for the mafic intrusive rocks.
Stippled fields indicate range of volcanic rock compositions in each group
(from Figures 3.9, 3.10 and 3.11).

in the NAT group. The rock clearly resembles the IAI subgroup in most respects and is reclassified as such on the basis of the above observations. The high Ti and V contents are interpreted to result from some iron oxide accumulation..

On the partial extended REE plots, there are two distinct types of samples assigned to the NAT group(Figure 3.42C). One, represented by samples 2140502 and 2140508, has flat, slightly LREE-enriched, patterns similar to the least fractionated samples from the Side Harbour suite. The other, represented by 2140457, has relatively higher abundances, is more LREE-enriched, and has prominent positive Nb and Ta anomalies similar to those in the NAE group.

The Ti-Y-Zr and Ta-Hf-Th ternary diagrams (Figure 3.43) further confirm the classification of the intrusive rocks samples. Almost all samples plot in the field appropriate to their classification (e.g. the same field as their volcanic group counterparts). Note that sample 2140481 (see above) plots in the WPB field of the Ti-Zr-Y diagram (but very close to the field boundary with plate-marginal basalt) and well within the arc field on the Ta-Hf-Th diagram further supporting its reassignment to the IAI group.

3.5.3 Relationship of Mafic Intrusive to Mafic Volcanic Rocks

The possibility that individual mafic intrusive rocks may be related to specific volcanic rock magmas in the Wild Bight Group can be further investigated by comparing them on compatible and incompatible element versus Mg# diagrams (Figure 3.44 to Figure 3.47). The two samples assigned to the IAD group are more and less fractionated, respectively, than their volcanic counterparts (Figure 3.44). The sample with the higher Mg# also has low TiO_2 and V contents and may plausibly be a primitive representative of the fractionation trend defined by the Glover's Harbour West suite. Such an interpretation is also suggested by its relative enrichment in Cr and Ni. This interpretation may have some regional importance as this sill intrudes the Indian Cove volcanics where the only mafic volcanic rocks are cumulate and difficult to correlate with the Glover's Harbour suite. If this sill is related to the Glover's Harbour magmas, it suggests that the
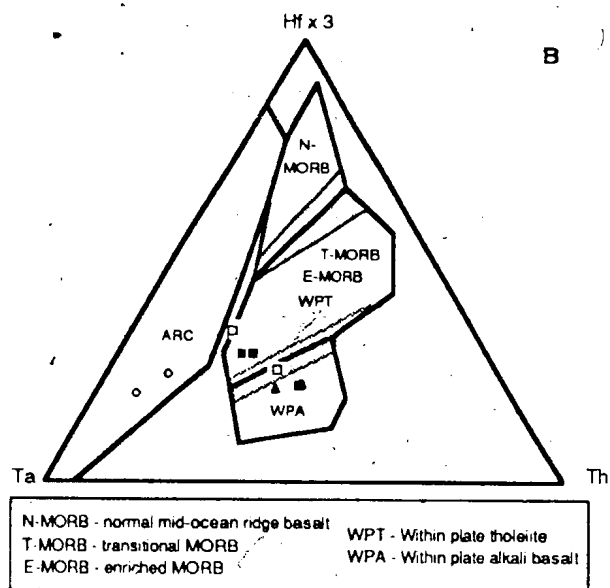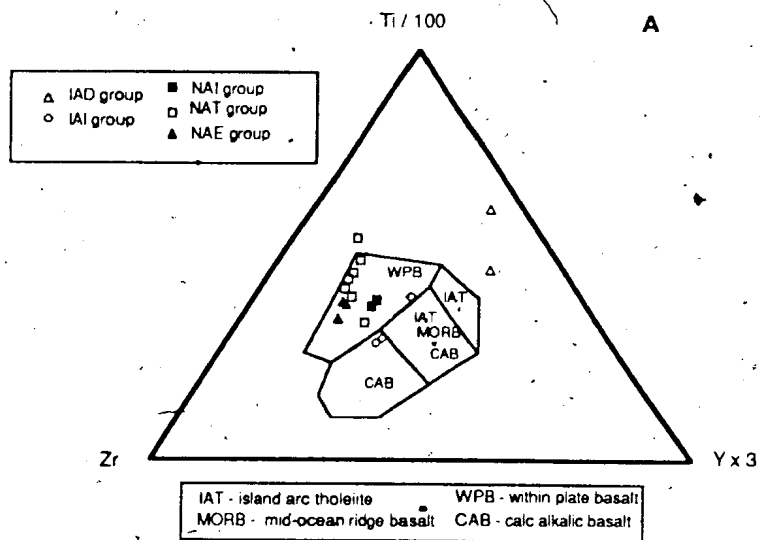
Figure 3.43: Ti-Zr-Y and Ta-Hf-Th diagrams for the mafic intrusive rocks. Symbols indicate classification based on discriminant function analysis and extended REE plots.
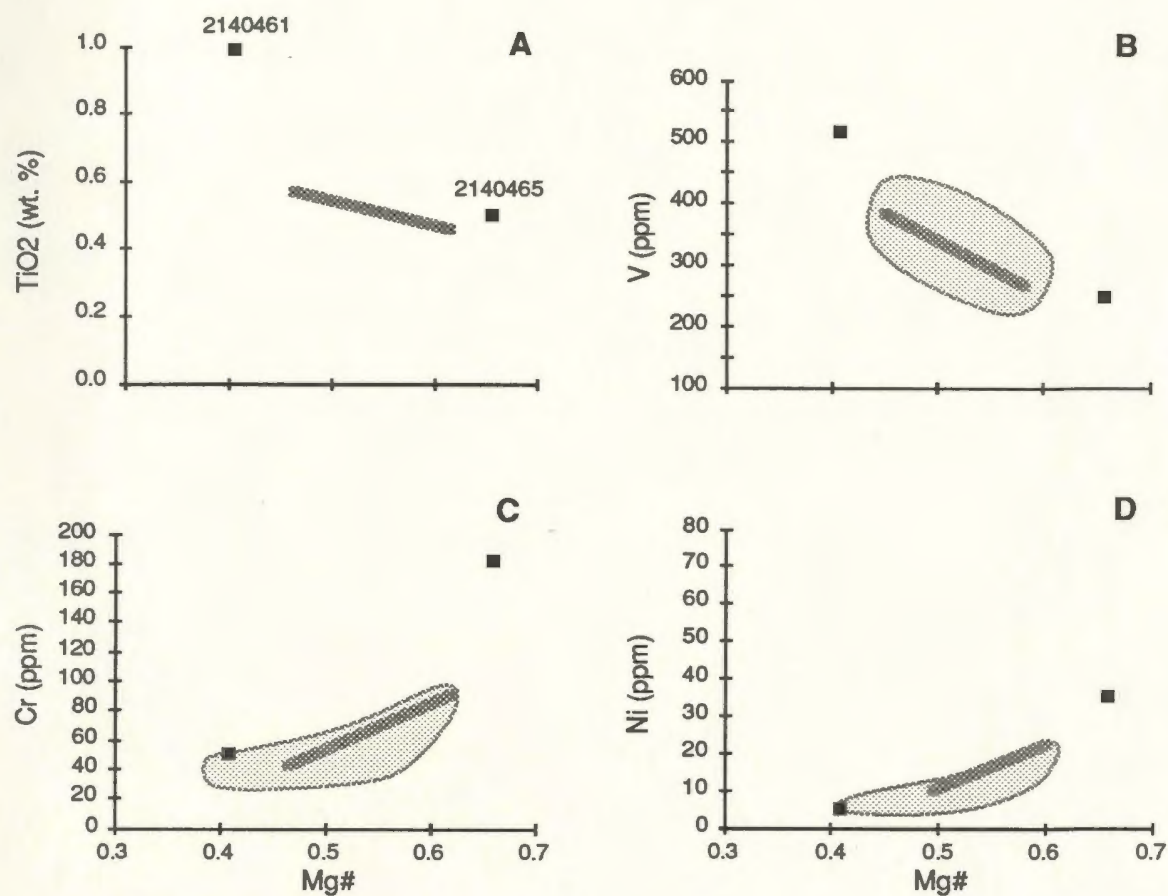
Figure 3.44: Comparison of mafic intrusive rocks assigned to the IAD group with their volcanic counterparts. Stippled area encompasses all IAD group mafic volcanic rocks; heavy stippled line is Glover's Harbour West trend. Intrusive sample numbers indicated in A.

Indian Cove and Glover's Harbour volcanic units may have been part of the same magmatic event.

The low-Mg# IAD group dyke, which intrudes the Glover's Harbour volcanics, is apparently more fractionated than any IAD group volcanic rocks (further suggested by very low Cr and Ni contents) but is enriched in TiO_2 and V to an extent that it plots well above the extension of the Glover's Harbour West fractionation trend. This composition is unlikely to have resulted from simple fractionation of the IAD magmas and is tentatively attributed to accumulation of an oxide phase (there is approximately 4% modal opaque oxides in thin section).

The two least fractionated intrusive rocks assigned to the IAI group are geochemically very similar to rocks in the Glover's Harbour/ Seal Bay Bottom/ Northern Arm suites and lie close to the fractionation trends defined by rocks of the Seal Bay Bottom suite (Figure 3.45). The third sample, 2140481, has considerably higher TiO_2 and V at equivalent Mg# than this trend (this is the sample that the discriminant function incorrectly assigned to the NAT group because of high TiO_2, see above). However, other incompatible elements as well as Cr and Ni plots close to the trend.

Intrusive rocks assigned to the NAI group have relatively primitive Mg#, similar to the most fractionated volcanic rocks of this group (Figure 3.46). Low Cr and Ni contents relative to the volcanic rocks also suggest that the intrusive rocks are generally more fractionated than in their volcanic counterparts.

Relationships between the volcanic and extrusive rocks assigned to the NAT group are more complex (Figure 3.47). For ease of discussion, they are broken into small groups and discussed separately as follows:

Group i)- samples 2140482, 2140485, 2140508, and 2140502 plot close to the Side Harbour fractionation trends on all diagrams (although 2140502 is somewhat depleted in Zr relative to this trend). On the basis of geochemical relationships, they can be interpreted as forming part of this trend.

Group ii) 2140489, 2140457, and 2140501 includes two very TiO_2-rich samples which also have anomalously high V and Nb relative to the Side Harbour trend. These samples are
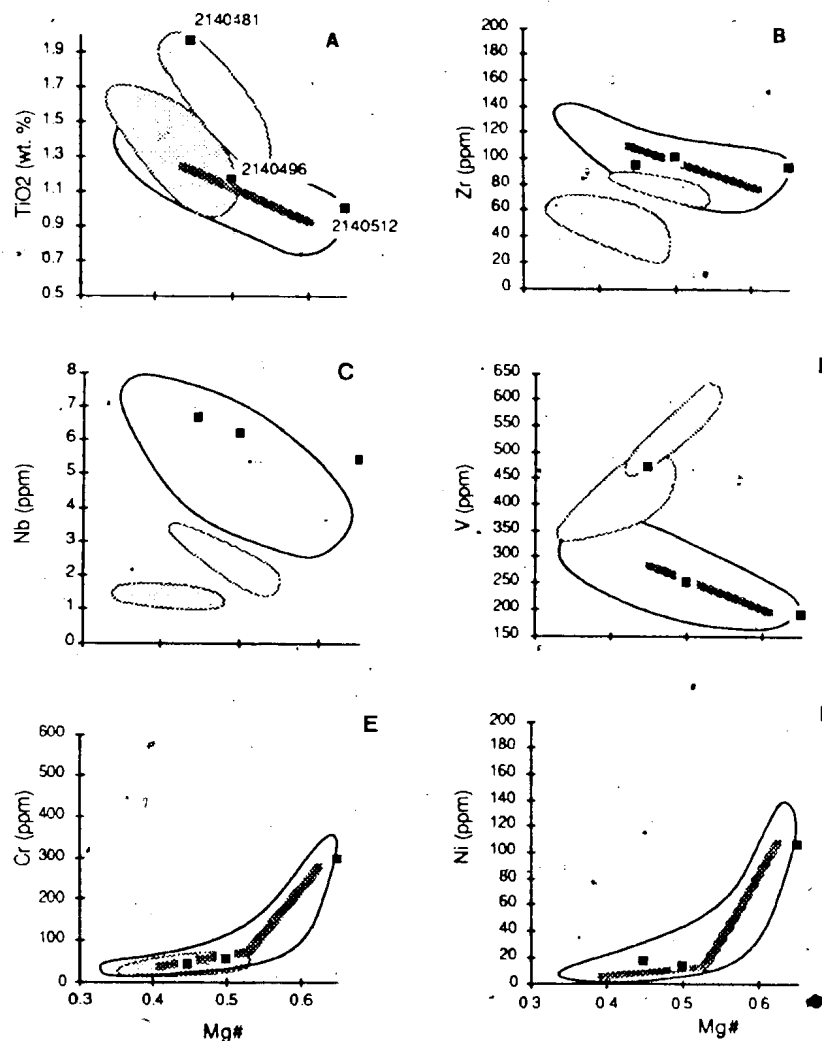
Figure 3.45: Comparison of intrusive rocks assigned to the IAI group with their volcanic counterparts. Solid curve outlines field of Glover's Harbour East, Seal Bay Bottom and Northern Arm suites; heavy stippled line is Seal Bay Bottom fractionation trend. Stippled fields (dark and light respectively) are NBL-1 and NBL-2 trends of the Nanny Bag Lake suite. Sample numbers given in A.
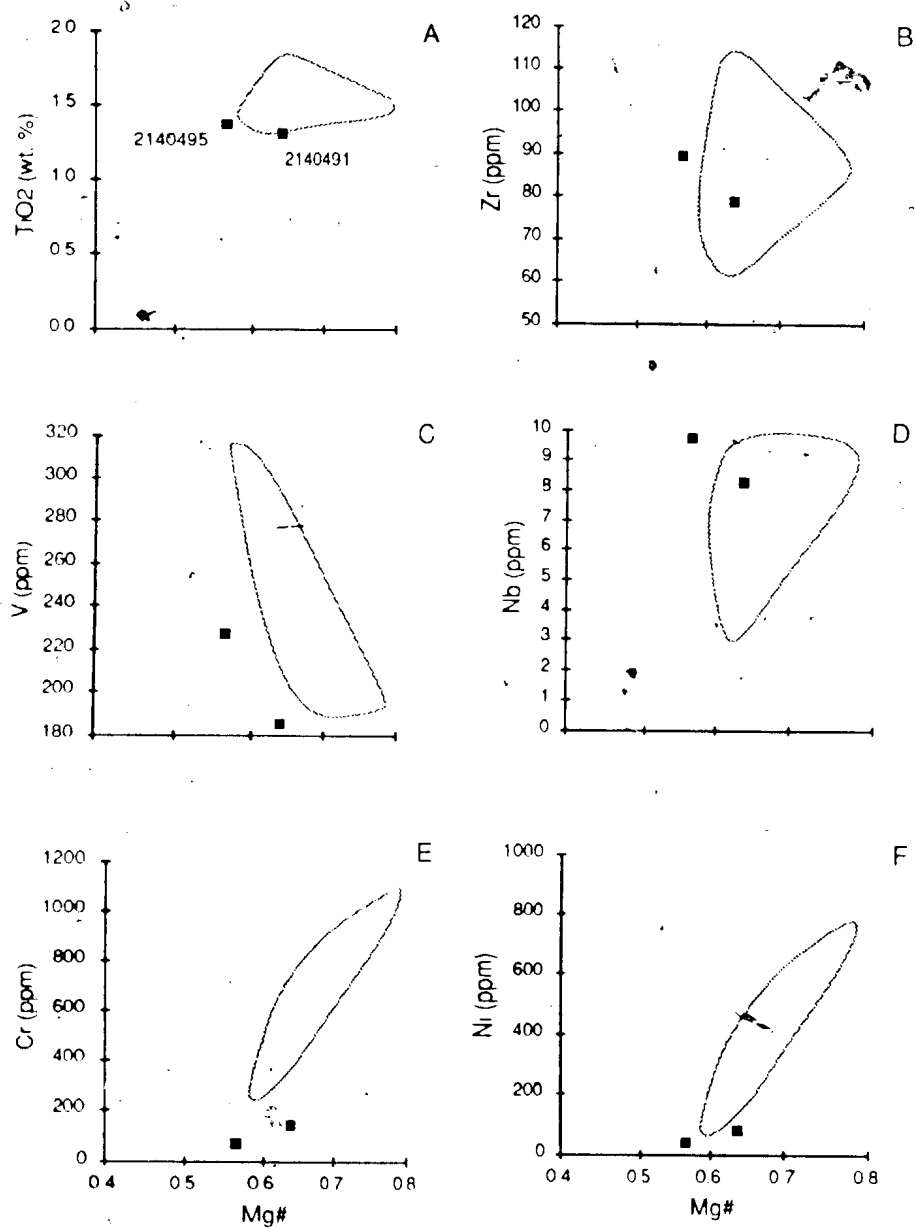
Figure 3.46: Comparison of intrusive rocks assigned to the NAI group and their volcanic counterparts. Stipp'ed area is field of volcanic rocks. Sample numbers are given in A.
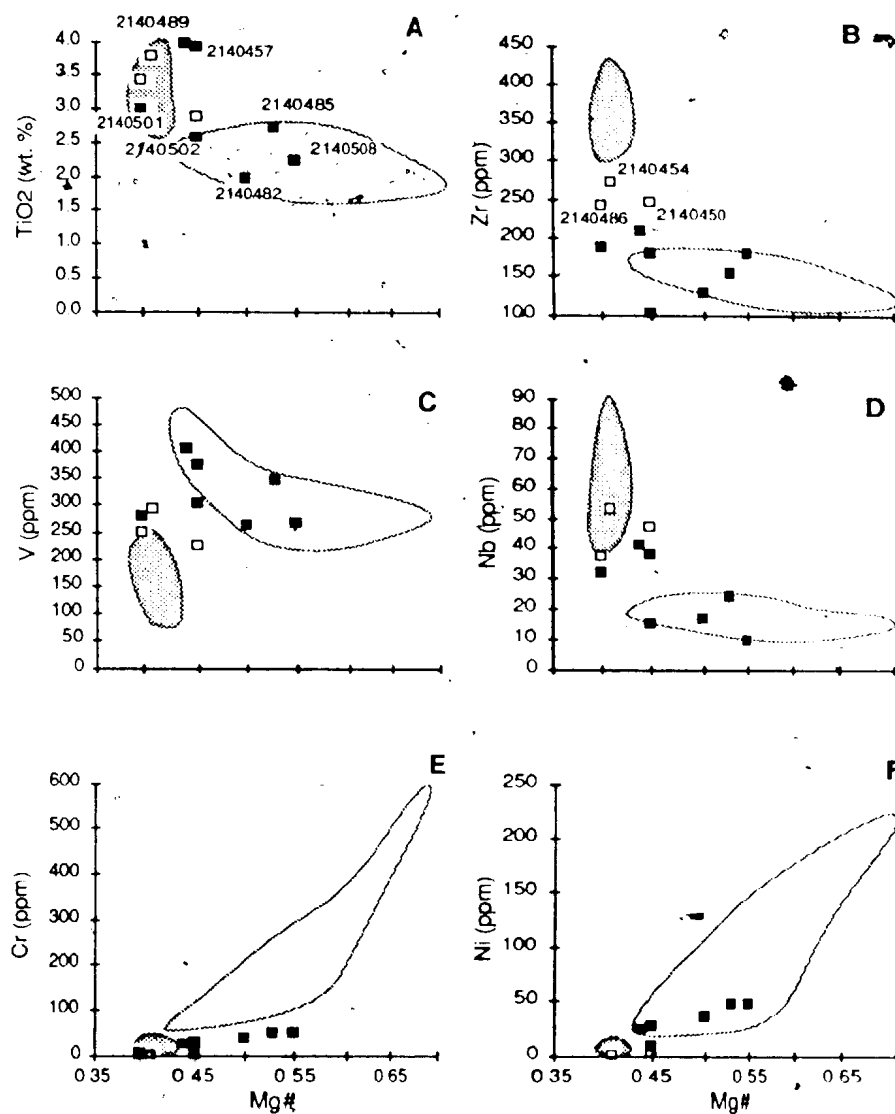
Figure 3.47: Comparison of intrusive rocks assigned to the NAT and NAE groups with their volcanic counterparts. Light stipple is field of NAT volcanic rocks, dark stipple is field of NAE volcanic rocks. Samples assigned to NAT group are numbered in A, and to the NAE group in B.

enriched in FeO^t relative to both the NAT intrusives and the Side Harbour volcanic rocks and in

thin section contain 5 to 7 percent modal magnetite. Despite their high Ti contents, the high Ti/V

ratios of these rocks suggest they are not related to the NAE group. They are better interpreted

as either fractionated representatives of the Side Harbour suite with Ti and V contents modified

by iron oxide accumulation or as an NAT-like magma that is not represented in the volcanic rocks

sampled. The third sample in Group ii, 2140501, is more similar to the NAE than the NAT group

on most diagrams (note particularly the depleted V contents relative to normal NAT rocks at

equivalent Mg#) although its Zr contents are abnormally low for NAE rocks. It is not easily related

by any simple fractionation mechanism to any volcanic rocks in either group.

3.5.4 Stratigraphic Relationships of Mafic Intrusive Rocks

Although mafic subvolcanic rocks intrude at virtually all stratigraphic levels of the Wild Bight

Group, there is a regularity to their distribution vis a vis their geochemical affinities which may have

some stratigraphic significance (Table 3.15). Intrusive rocks that are considered to belong to the

IAD or IAI groups occur in the lower and central parts of the stratigraphic succession, intruding

only volcanic and nearby epiclastic rocks that are also of island arc affinity. However, intrusive

rocks that are considered to belong to the NAI, NAT and NAE groups occur throughout the

stratigraphic sequence, intruding both rocks of arc and non-arc affinity.

This stratigraphic regularity in the subvolcanic rocks has two important consequences: 1)

It reinforces the earlier suggestion that rocks of non-arc affinity generally overlie rocks of island arc

affinity; and 2) it requires that the relationship between the two be stratigraphic rather than

purely structural; i.e. the rocks of arc affinity which are intruded by sills of non-arc affinity were

basement to the non-arc magmatic rocks.

3.6 Chemistry of Clinopyroxene in the Wild Bight Group Mafic Rocks

3.6.1 Occurrence

Clinopyroxene occurs in approximately 30% of the mafic volcanic rocks and 70% of the

		AFFINITY OF INTRUDED SEQUENCE							
		IAD			IAI	NAI		NAT	NAE
		Glover's Harbour West	Indian Cove	Long Pond	Seal Bay Bottom	Badger Bay	Big Lewis Lake	Side Harbour	Seal Bay Head
AFFINITY OF INTRUSIVE ROCKS	IAD	▓	▓						
	IAI		▓	▓	▓				
	NAI		▓		▓				
	NAT	▓	▓			▓	▓	▓	▓
	NAE	▓							

Table 3.15: Stratigraphic relationships of subvolcanic rocks. A filled square indicates that the sequence on the horizontal axis is intruded by rocks of affinity indicated by the vertical axis.

mafic subvolcanic rocks in the Wild Bight Group. In volcanic rocks, it occurs principally as subhedral to euhedral phenocrysts from 0.5 to 4 mm in long dimension and less commonly as subhedral microphenocrysts (less than 0.25 mm). In a few samples, clinopyroxene forms the lesser component of plagioclase-pyroxene glomerocrysts. Clinopyroxene phenocrysts are rarely zoned or twinned.

. Most show some evidence of alteration. In extreme cases the crystals are completely psuedomorphed by a greenschist assemblage and in most samples where alteration is advanced to this state, little or no original mineral remains in any crystal. More commonly, the crystals are slightly altered on the rims and along cracks with some discoloration and growth of chlorite ± sphene ± magnetite. These altered areas are easily avoided during microprobe analyses.

Groundmass pyroxene was seen in only a few thin sections; in most cases, the groundmass is completely altered to a greenschist assemblage.

In fine grained subvolcanic mafic rocks, pyroxene occurrence is similar to that in the volcanic rocks. In coarse grained rocks, euhedral to subhedral crystals are commonly intergrown with plagioclase and less commonly olivine.

3.6.2 Composition of Wild Bight Group Pyroxenes

Analytical results from microprobe analyses of clinopyroxenes are presented in Appendix 3 and plotted on the pyroxene quadrilateral in Figure 3.48. Clinopyroxene in the IAD, IAI and NAI groups is dominantly augitic but includes a minor component of endiopside. Clinopyroxene in the NAT and NAE groups is almost all augite. The latter plot above the Skaergaard trend and are the most calcic in the Wild Bight Group, consistent with their alkalic whole rock geochemical affinities.

A broad distinction between rocks of arc and non-arc affinity can be seen on this diagram. More than 80 percent of clinopyroxenes from the former plot on and below the Skaergaard trend while more than 80 percent from the latter plot above it.

In Table 3.16, mean compositions of clinopyroxene from the different groups are
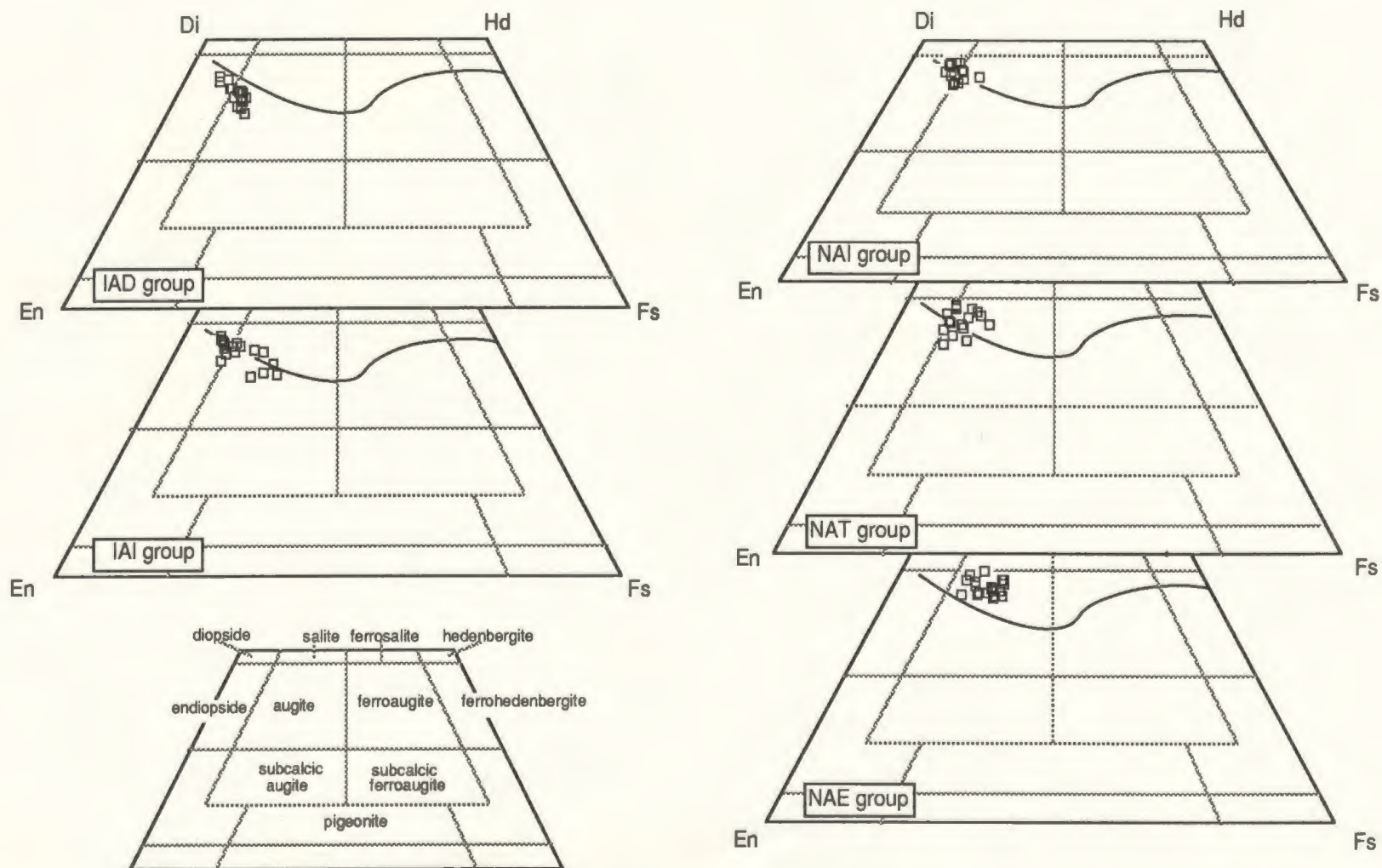
Figure 3.48: Wild Bight Group clinopyroxenes plotted on the pyroxene quadralateral. Nomenclature after Poldervaart and Hess (1951). Solid curve is Skaergaard trend. Samples from suites of island arc affinity generally plot below the Skaergaard trend while those of non-arc affinity are more calcic.

Table 3.16: Mean compositions of clinopyroxenes in the Wild Bight Group.

Host class'n	IAD group	IAI group	NAI group	NAT group	NAE group
SiO2	53.90	51.74	51.86	51.09	50.62
Al2O3	2.02	3.00	3.20	3.41	3.44
FeO(t)	6.88	7.89	6.35	7.48	10.89
MgO	17.44	15.91	16.09	15.64	13.30
CaO	19.34	19.61	20.47	20.14	19.94
Na2O	0.15	0.31	0.34	0.33	0.44
K2O	0.02	0.01	0.02	0.01	0.01
TiO2	0.11	0.66	0.86	0.96	1.64
MnO	0.20	0.24	0.14	0.18	0.30
Cr2O3	0.15	0.33	0.46	0.26	0.01
Si	1.965	1.915	1.909	1.897	1.889
Al	0.086	0.130	0.138	0.149	0.151
Fe	0.210	0.244	0.195	0.232	0.340
Mg	0.948	0.877	0.882	0.865	0.740
Ca	0.755	0.777	0.807	0.801	0.797
Na	0.010	0.022	0.023	0.024	0.031
K	0.001	0.000	0.001	0.000	0.000
Ti	0.002	0.018	0.023	0.026	0.046
Mn	0.005	0.008	0.004	0.005	0.009
Cr	0.004	0.008	0.013	0.007	0.000
Fe/Fe+Mg	0.165	0.216	0.16	0.195	0.293

compared. In many respects, clinopyroxene compositions mimic the whole rock variations between groups. The IAD group, consistent with its andesitic, incompatible element-depleted whole rock chemistry, has the most Si-rich and Ti- and Na-poor clinopyroxene. The NAE group pyroxenes, as in the whole rocks, are the most Ti- and Na-rich and Mg- and Cr-poor. The consistent increase in Ti from island arc to non-arc is consistent with whole rock compositions and is paralleled to a lesser extent by Na.

The NAE group has the highest Fe# (atomic Fe/[Fe+Mg]), consistent with its highly fractionated whole rock chemistry while the NAI group has the most primitive Fe#, also consistent with whole rock chemistry. However, generalizations about the relative fractionation in the various groups are hampered by the fact that clinopyroxene analyses do not represent all fractionation intervals in each group.

Ti and Cr, respectively, increase and decrease regularly with Fe# in all of the tholeiitic groups (Figure 3.49). In the case of Ti, this probably reflects increasing concentrations of Ti in the magmas with differentiation leading to its increased incorporation with Fe in the octahedral sites. The sharp decrease of Cr with differentiation in these suites reflects its early incorporation in pyroxene and subsequent depletion in the magmas with advancing fractional crystallization. The extreme depletion of Cr in the NAE group suggests that the magmas from which these rocks crystallized contained little Cr, in accord with the whole rock data.

Ti in the NAE group pyroxenes lacks the clear positive Ti-Fe# correlation seen in other suites. This is in agreement with the observations of Schweitzer et al. (1979) who found that pyroxene from deep sea alkali basalts, in contrast to that in tholeiites, generally contains little Cr and shows either no correlation or an inverse correlation between Ti and differentiation. They attributed the latter to a relative decrease in the importance of the coupled substitution Ti^{iv}-$2Al^{iv}$ relative to Fe^{2iv}-$2Al^{iv}$ in the later stages of alkali basalt fractional crystallization. This may also explain the relatively high Fe# in NAE group pyroxenes relative to those in tholeiitic rocks of similar whole rock Mg#.
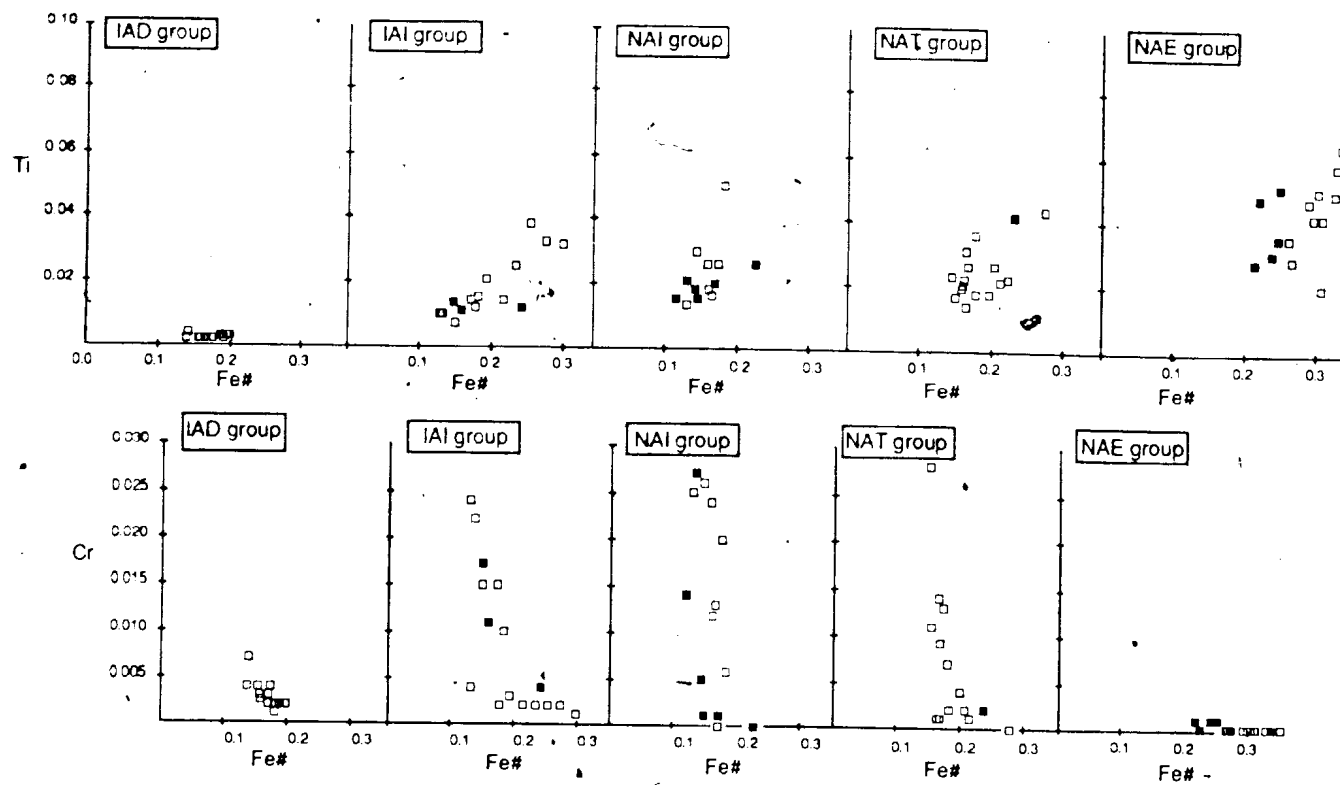
Figure 3.49: Ti and Cr versus Fe# (atomic Fe/[Fe+Mg] for the Wild Bight Group clinopyroxenes. Open symbols are from volcanic rocks, closed symbols from intrusive rocks.

3.6.3 Pyroxenes as Indicators of Magmatic Affinity

A number of workers have investigated the correlation between pyroxene composition and the nature of the liquids from which they crystallize and have shown that the composition can be interpreted both in terms of the magma type from which it crystallized (e.g. Kushiro, 1960; LeBas, 1962; Verhoogen, 1962; Schweitzer et al., 1979) and the tectonic environment in which the magma was generated (e.g. Nisbet and Pearce, 1977; LeTerrier et al., 1982). The geochemistry of clinopyroxene can provide a useful check on conclusions reached on the basis of whole rock geochemistry, particularly when the whole rocks are altered and the pyroxenes are not.

Kushiro (1960) demonstrated a correlation between magma type and the variation of Si, Al and Ti contents in pyroxenes. Reasoning that pyroxenes crystallizing from non-alkalic, alkalic and peralkalic magmas should, respectively, have higher Al and Ti and lower Si contents (because of the increased Al occupancy of the tetrahedral sites in SiO_2-undersaturated magmas), he constructed binary discrimination diagrams utilizing these elements to discriminate the magma types.

LeBas (1962) extended Kushiro's work by calculating the percentage of Al in the z position and using the correlation between this and Ti and Si do define the alkalinity of the parent magma. Working mainly with groundmass pyroxenes, he showed that atomic proportions of the major cations change regularly with differentiation and magma type and constructed fields in the pyroxene quadrilateral to discriminate non-alkalic, alkalic and peralkaline magma types. On this diagram (Figure 3.50), almost all Wild Bight Group pyroxenes from tholeiitic rocks plot in the non-alkalic field as do 85 percent of those from the NAT group. Over 80 percent of the NAE group pyroxenes plot in the alkalic field. LeBas (1962) noted that use of phenocrysts rather than groundmass on this diagram could result in slightly greater scatter, and perhaps a few samples being misclassified, on this plot.

In recent years, a number of authors have constructed plots using the cations Si, Al, Na, Ca, Mg, Ti and Cr to discriminate the tectonic environment of magmas from which clinopyroxenes
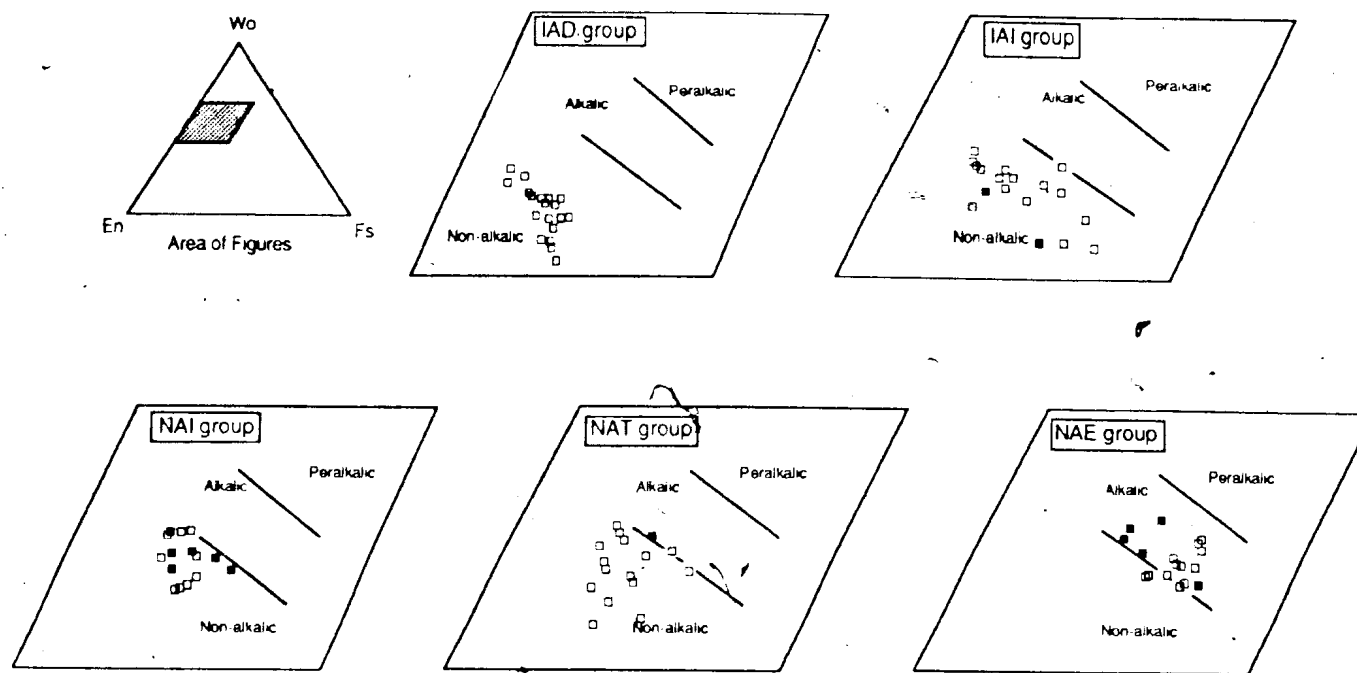
Figure 3.50: Detail of the pyroxene quadralateral with magma series discrimination fields after LeBas (1962). Open squares are from volcanic rocks, closed squares from intrusive rocks.

have crystallized. The discrimination is based on the observation that chemical differences in the magmas in these different environments is, to a certain extent, reflected in the pyroxene compositions, inasmuch as pyroxene accepts most of the major elements that provide the basis for such discrimination. Nisbet and Pearce (1977) made the first major effort in this direction; they calculated discriminant functions (based on published and unpublished analyses of pyroxenes from various tectonic environments) which they used on a territorial plot in conjunction with ternary and binary plots involving these elements to distinguish pyroxene from various plate marginal and within plate settings. They found the discrimination to be generally acceptable but less precise than trace element geochemistry of whole rocks. LeTerrier et al (1982) reviewed the use of such diagrams, noting that there were a number of factors which could obscure the correlation between magma type and pyroxene composition including: 1) coupled substitution (the entry of an element into the lattice being more strongly controlled by the presence of other element(s) than by its own availability; 2) crystallization order of minerals (early crystallization of phases may reduce the availability of some elements when clinopyroxene is finally on the liquidus); 3) cooling rate of the magma (partitioning of major elements tends to be rate independent while that of minor elements depends on cooling rate and bulk rock composition); 4) variations in temperature and pressure inducing variations in the crystal-liquid partition coefficients. In addition, they felt that problems with the Nesbit and Pearce (1977) diagrams, including the small number of analyses to define the fields, lack of precision in determining the most important variables in the discriminant functions (e g. TiO_2, MnO and Na_2O which are generally close to detection limits) and the difficulty of achieving a complete discrimination using only one diagram, limited the usefulness of this approach and introduced some ambiguity into the interpretations.

Working from a file of 1225 pyroxene analyses, LeTerrier et al. (1982) found that a better discrimination could be achieved using a series of diagrams in which elements that play the most important role in discriminating specific settings are used in sequence to define the magmatic affinity of the rocks. Thus, Ti, Ca and Na provide a separation between alkalic and non-alkalic

types, a further separation of non-alkalic types into those produced in orogenic and non-orogenic environments is achieved using Ti, Cr and Ca and a final separation of orogenic types into calc alkalic and tholeiitic types results from Ti and Al relationships.

Use of the LeTerrier *et al.* (1982) diagrams for the Wild Bight Group clinopyroxenes (Figures 3.51 to 3.53) generally supports interpretations based on the LeBas diagrams and the whole rock chemistry. The IAD and IAI group pyroxenes are clearly non-alkalic on the Ti versus Ca+Na diagram. However, more than 75 percent of samples from the NAI and NAT groups plot in the field of overlap between alkalic and non-alkalic basalts. Likewise, almost half of the NAE group samples plot in this field, with less than 35% plotting unequivocally in the alkali basalt field. The results are consistent with, but generally less discriminating than, interpretations based on the LeBas (1962) diagram and whole rock chemistry.

On the Ti+Cr versus Ca diagram for pyroxenes from non-alkalic basalts (Figure 3.52), the IAD group plots in the orogenic field in accord with whole rock geochemical results but the IAI group plots mainly in the field of overlap between the two settings. Five analyses that plot well within the non-orogenic field are from sample 2140468, which is extremely highly fractionated (Mg# = 0.35). This highlights a potential problem with using these diagrams; rocks that are highly fractionated, with a correspondingly high Ti content, may yield results which are inconsistent with interpretations based on considerations of the whole suite from which it comes. The NAI and NAT pyroxenes plot, as expected mainly in the non-orogenic field on this diagram.

The samples from orogenic environments are plotted on the calc alkalic-tholeiitic discriminant diagram in Figure 3.53. The IAD group plot in the tholeiitic field, although considering the highly depleted nature of these magmas which probably indicates a highly refractory source compared to normal mantle (see Chapter 4), the low Ti contents are inevitable and not very meaningful with respect to this diagram. The IAI group plots mainly in the area of overlap and does not conclusively indicate the affinity of the samples. As in Figure 3.52, pyroxene from the highly fractionated sample 2140468 are anomalously enriched in Ti and give results inconsistent with whole rock chemistry.
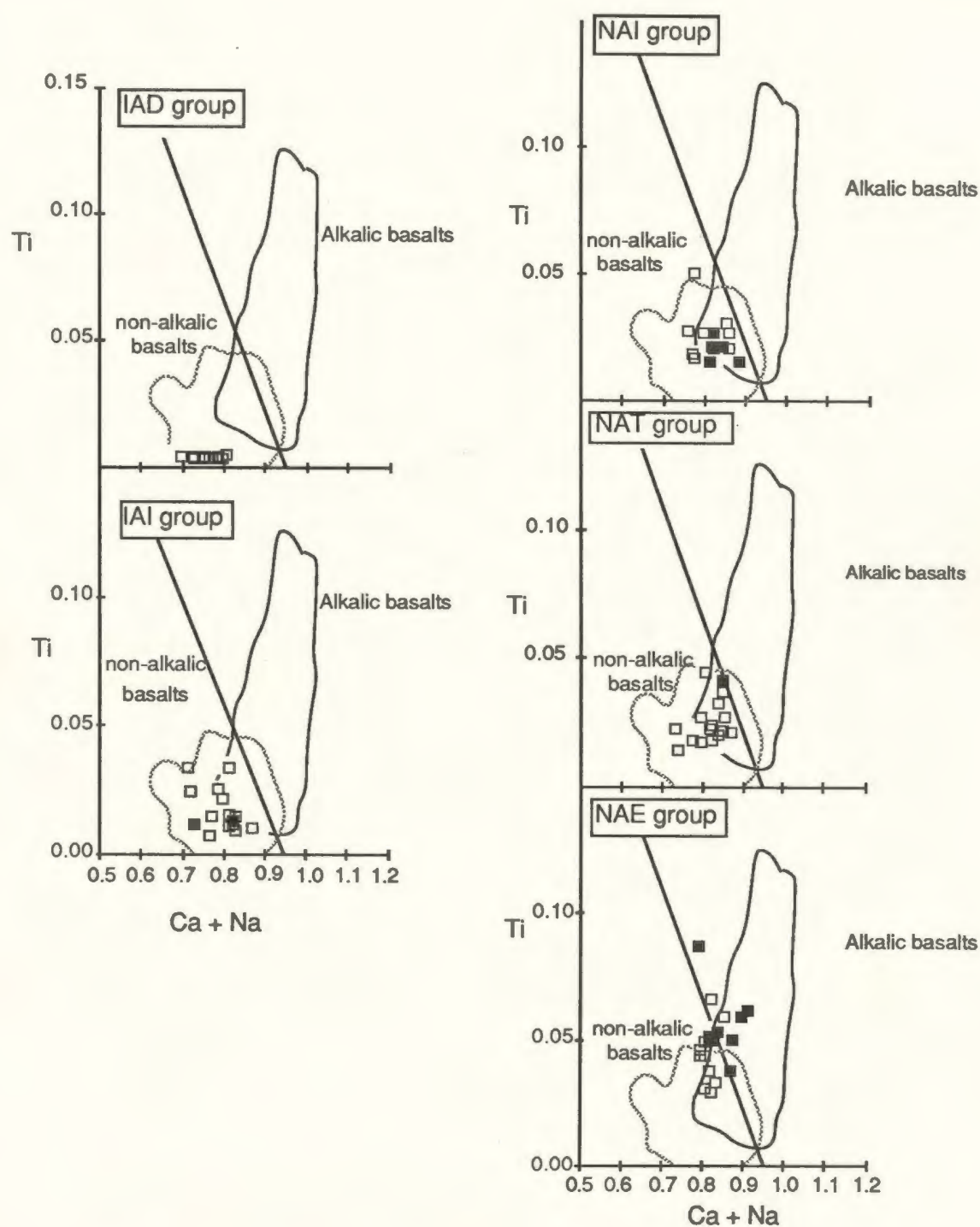
Figure 3.51: Discrimination of clinopyroxene from alkalic and non - alkalic basalts after LeTerrier et al. (1982). Fields of data used to construct the diagram are outlined.
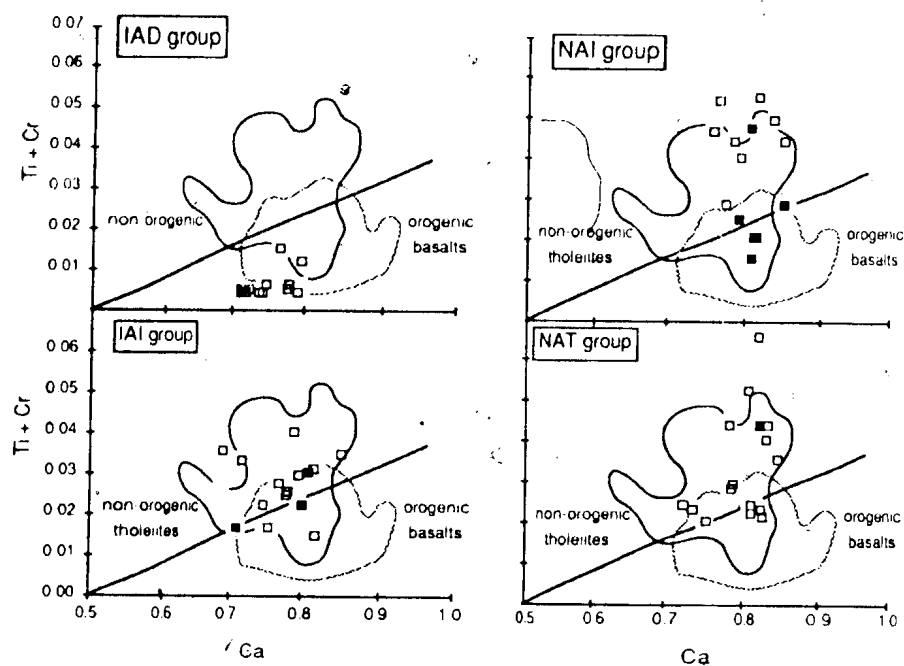
Figure 3.52: Discrimination of clinopyroxene from orogenic and non-orogenic environments after LeTerrier et al. (1982). Fields of data used in constructing the diagram are outlined.
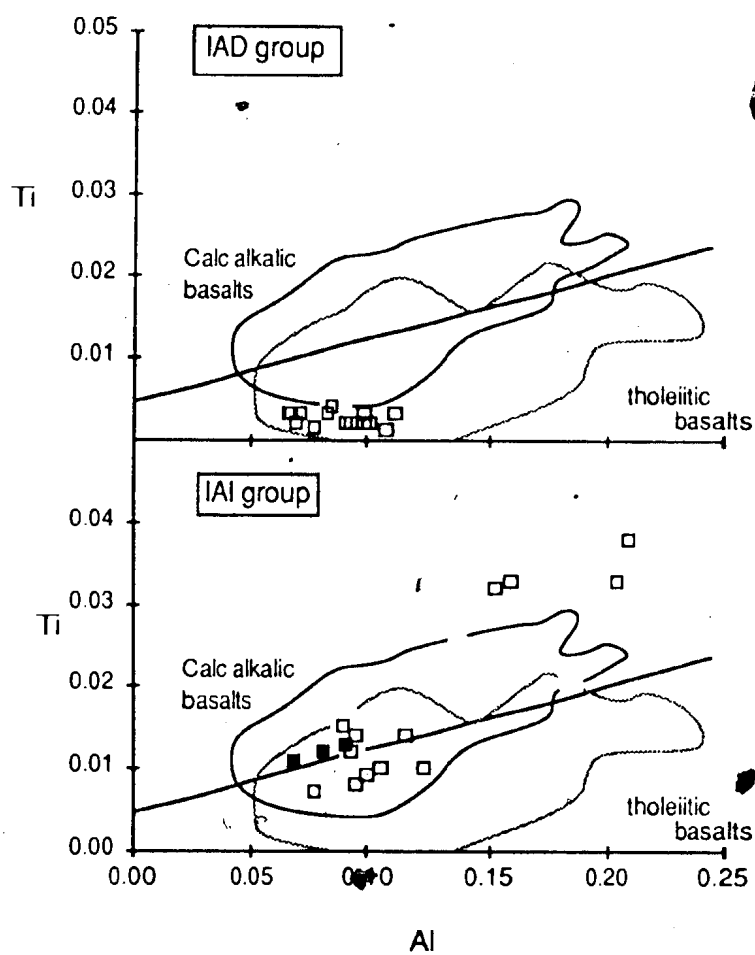
Figure 3.53: Discrimination of clinopyroxene from calc alkalic and tholeiitic basalts after LeTerrier et al. (1982) Fields of data used to construct the diagram are outlined.

3.6.4 Significance of the Wild Bight Group Clinopyroxene Analyses

Analysis of primary clinopyroxene in the Wild Bight Group mafic rocks leads to
interpretations of magma series and paleotectonic environments that are generally consistent
with those reached from consideration of the whole rock data. In accord with the previous
conclusions of Nesbit and Pearce (1977) and LeTerrier et al. (1982), the pyroxene data appear to
be less definitive and the interpretations more equivocal than those reached from whole rock
data. However, the interpretations reached on the basis of analyses of primary minerals, rather
than altered whole rocks, data do provide important confirmation of these interpretations from an
independent source.

In particular, the pyroxene data tend to confirm the non-alkalic, tholeiitic nature of the IAD,
IAI and NAI groups, the transitional (non-alkalic to alkalic) nature of the NAT group and the alkalic
nature of the NAE group. They further support the assignment of the IAD and IAI groups to an
island arc series and the NAI, NAT and NAE groups to a within plate setting. Apparently spurious
results from highly fractionated samples emphasize the necessity for caution in interpreting
pyroxene data in the absence of confirmatory data from other sources.

3.7 Geochemistry of the Felsic Volcanic Rocks

3.7.1 Felsic / Mafic Volcanic Associations

In most cases, felsic volcanic rocks in the Wild Bight Group are associated with mafic
volcanic rocks of island arc geochemical affinities, specifically the Glover's Harbour, Indian Cove
and Side Harbour mafic volcanic rocks assigned to the IAD group and the Nanny Bag Lake suite
of the IAI group. Evidence for this association in the case of the Long Pond rhyolite is more
equivocal as the only mafic volcanic rocks in this sequence comprise a thin pillow breccia unit
which is too altered to provide useful geochemical data. However, sedimentary rocks near and in
apparent stratigraphic continuity with the rhyolite are intruded by a sill of IAI affinity and elsewhere
in the Wild Bight Group, similar sills only intrude sequences with volcanic rocks of island arc

affinity.

Wood *et al.* (1979) have argued that Ta, Hf, Th and LREE relationships can be used to discriminate the tectonic environment of felsic as well as mafic volcanic rocks because, unlike Zr and Ti, they do not readily enter common liquidus phases in silicic magmas. Wild Bight Group felsic volcanics have prominent negative Ta and Nb anomalies and positive Th anomalies with respect to the LREE and plot well within the arc field on the Ta-Th-Hf diagram (Figure 3.54).

3.7.2 Classification of Wild Bight Group Felsic Volcanic Rocks

The Wild Bight Group felsic volcanic rocks all have silica contents greater than 75% (Table 3.17) and there are no rocks of intermediate composition between basaltic andesite and high-silica rhyolite. The rocks are very soda-rich and potash-poor (Na/K ratios are, with few exceptions, greater than 5), are generally mildly corundum normative (peraluminous) (Table 3.18) and plot in the field of trondhjemite and quartz keratophyre on the normative feldspar classification diagram of O'Connor (1965) (Figure 3.55).

The mobility of alkali elements, calcium and silica during alteration raises the question as to whether their concentrations in these rocks are liquid compositions or reflect secondary metasomatic alteration. Of particular interest is whether the high SiO_2 and the alkali element ratios (i.e. the very low K_2O contents) are an original feature or reflect metasomatism of rocks which originally had lower SiO_2 contents and Na/K ratios (e.g Amstutz, 1974). The fact that the rhyolitic rocks are generally very fine grained, and probably were originally more or less glassy (although no shards are preserved in thin section), as well as petrographic evidence for alteration (e.g. some saussuritization of feldspar phenocrysts, local epidote and quartz veining, recrystallization of groundmass) suggests that some metasomatic redistribution is to be expected. The SiO_2 contents are abnormally high for rhyolitic rocks in island arc environments (see below) indicating some silicification has probably occurred. Although some alkali redistribution is to be expected in this situation, three lines of petrographic evidence suggests that low K_2O contents (and high Na_2O/K_2O ratios) are an original feature of the rocks:
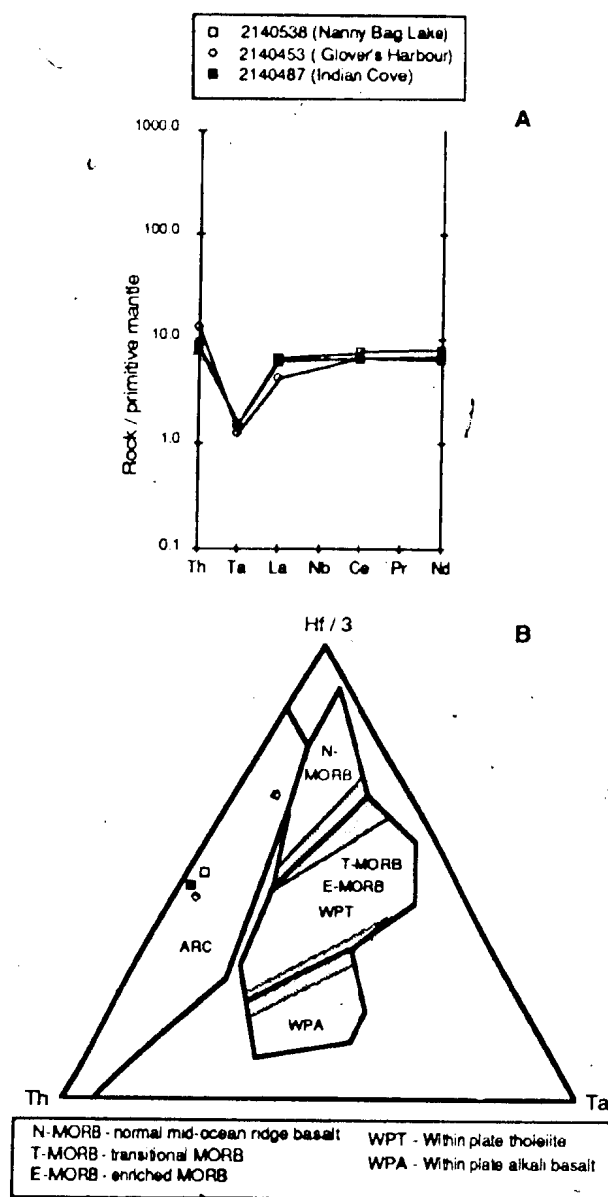
Figure 3.54: Partial Extended REE plot (A) and Ta-Hf-Th ternary diagram (B) for the felsic volcanic rocks. Negative Ta anomalies in the former suggest an island arc affinity and all samples plot in the arc field on the latter.

Table 3.17: Major (weight percent) and trace (ppm) element contents of felsic volcanic rocks

Sample	2140452	2140453	2140466	2140487	2140488	2140490	2140493
volcanic unit**	gh	gh	ic	ic	ic	ic	ic
SiO_2	77.02	76.86	79.06	78.98	76.82	75.85	76.60
Al_2O_3	12.17	12.36	11.24	12.03	13.16	13.28	12.36
Fe_2O_3	0.60	0.12	0.02	0.92	1.49	1.35	1.91
FeO	1.72	2.74	1.76	0.40	0.24	0.19	1.41
MgO	0.73	0.88	0.18	0.08	0.09	0.07	0.96
CaO	0.49	0.48	1.34	0.76	3.13	2.60	0.93
Na_2O	5.89	6.14	5.61	5.37	2.96	5.48	4.83
K_2O	0.98	0.07	0.02	0.97	1.69	0.69	0.68
TiO_2	0.32	0.28	0.46	0.40	0.33	0.40	0.27
MnO	0.04	0.03	0.02	0.03	0.03	0.04	0.02
P_2O_5	0.04	0.03	0.27	0.04	0.06	0.05	0.03
L.O.I.	1.08	1.10	0.58	0.81	1.47	0.70	1.08
Total*	99.24	100.24	99.74	99.69	99.10	100.11	98.99
Cu	3	5	5	36	3	3	2
Zn	46	43	66	60	90	49	70
Ni	<1	<1	<1	<1	<1	<1	<1
Cr	8	5	6	<5	5	<5	<5
V	22	<20	<20	24	26	26	<20
Sc		8.2		8.9			
Co		2.9		2.9			
Rb	6	2.8	0.7	6	10	2.3	4
Sr	37	38	44	46	93	81	86
Ba	130	26	26	115	215	85	71
Th		1.12		0.68			
Y	34	31	40	30	35	43	44
Zr	82	90	44	50	65	58	96
Nb	<0.5	<0.5	<0.5	0.6	<0.5	<0.5	<0.5
Hf		3.1		1.77			
Ta		0.05		0.06			
La		2.6		3.8			
Ce		10.4		10.4			
Nd		8.5		7.5			
Sm		2.94		2.63			
Eu		0.64		0.67			
Gd		3.70		3.70			
Tb		0.71		0.69			
Yb		3.80		3.56			
Lu		0.52		0.54			
Th/Ta		22.40		11.33			
(La/Sm)n		0.54		0.88			
K/Rb	1287.0	208.2	247.8	1355.4	1416.9	2522.9	1393.6
Na/K	5.4	78.2	250.1	4.9	1.6	7.1	6.3
Rb/Sr	0.2	0.1	0.0	0.1	0.1	0.0	0.0
Zr/Y	2.4	2.9	1.1	1.7	1.8	1.3	2.2

* - analytical total; major element concentrations are recalculated to 100% anhydrous
**gh - Glover's Harbour; ic - Indian Cove; nbl - Nanny Bag Lake; lp - Long Pond; sh - Side Harbour

(continued)

Sample	2140525	2140535	2140537	2140538	2140556	2140513	2140528
volcanic unit	nbl	nbl	nbl	nbl	lp	lp	sh
SiO2	75.79	76.28	76.20	77.44	81.19	79.07	76.33
Al2O3	11.23	12.49	12.94	11.86	10.78	11.17	12.26
Fe2O3	1.33	1.07	0.91	0.65	0.48	0.41	0.15
FeO	3.78	3.29	1.31	1.86	0.25	1.37	3.66
MgO	1.33	1.20	0.90	0.32	0.09	0.35	1.50
CaO	3.84	0.36	0.33	0.54	1.06	1.61	0.58
Na2O	1.52	4.36	7.07	3.71	5.15	5.14	4.69
K2O	0.73	0.48	0.11	3.32	0.70	0.57	0.44
TiO2	0.32	0.34	0.18	0.23	0.22	0.24	0.30
MnO.	0.06	0.06	0.02	0.02	0.01	0.02	0.04
P2O5	0.06	0.06	0.02	0.04	0.13	0.04	0.05
L.O.I.	2.24	1.50	0.48	0.68	1.44	1.80	1.54
Total*	99.74	98.77	99.43	99.34	100.22	99.81	98.62
Cu	24	29	5	93	57	30	6
Zn	100	117	45	45	24	50	71
Ni	<1	<1	<1	<1	<1	<1	<1
Cr	<5	7	5	11	5	8	10
V	<20	<20	<20	<20	<20	<20	<20
Sc				15.9			
Co				1.1			
Rb	8	0.0	<0.5	22	7	8	4
Sr	115	75	63	38	69	54	67
Ba	27	45	28	148	80	66	78
Th				0.75			
Y	38	44	54	43	25	33	31
Zr	56	70	114	73	36	41	41
Nb	<0.5	<0.5	<0.5	<0.5	<0.5	<0.5	<0.5
Hf				2.4			
Ta				0.06			
La				4.1			
Ce				12.0			
Nd				9.6			
Sm				3.91			
Eu				1.05			
Gd				0.00			
Tb				1.05			
Yb				5.30			
Lu				0.84			
Th/Ta				12.50			
(La/Sm)n				0.64			
K/Rb	723.9			1266.4	846.9	586.2	953.5
Na/K	1.9	8.1	57.3	1.0	6.6	8.0	9.5
Rb/Sr	0.1	0.0		0.6	0.1	0.1	0.1
Zr/Y	1.5	1.6	2.1	1.7	1.5	1.2	1.3

Table 3.18: CIPW norms for Wild Bight Group felsic volcanic rocks

Sample	2140452	2140453	2140466	2140487	2140488	2140490	2140493
Quartz	35.95	36.55	42.84	42.38	46.42	36.42	42.26
Corundum	0.61	1.38	0.19	0.85	0.89	0	2.04
Zircon	0.02	0.02	0.01	0.01	0.01	0.01	0.02
Orthoclase	5.79	0.41	0.12	5.73	9.98	4.08	4.02
Albite	49.83	51.95	47.47	45.44	25.04	46.36	40.86
Anorthite	2.21	2.2	4.9	3.55	15.2	9.6	4.46
Diopside	0	0	0	0	0	0.38	0
Wollastonite	0	0	0	0	0	0.85	0
Hypersthene	4.02	6.72	2.94	0.2	0.22	0	2.99
Magnetite	0.87	0.17	0.03	0.23	0	0	2.77
Ilmenite	0.61	0.53	0.87	0.76	0.57	0.49	0.51
Hematite	0	0	0	0.76	1.49	1.35	0
Sphene	0	0	0	0	0	0.35	0
Rutile	0	0	0	0	0.03	0	0
Apatite	0.09	0.07	0.64	0.09	0.14	0.12	0.07

Sample	2140525	2140535	2140537	2140538	2140556	2140513	2140528
Quartz	51.61	44.53	32.01	40.46	46.4	42.73	41.19
Corundum	1.09	4.27	0.63	1.26	0	0	3.12
Zircon	0.01	0.02	0.02	0.02	0.01	0.01	0.01
Orthoclase	4.31	2.84	0.65	19.62	4.2	3.37	2.6
Albite	12.86	36.89	59.81	31.39	43.57	43.49	39.68
Anorthite	18.7	1.43	1.53	2.46	4.2	5.72	2.59
Diopside	0	0	0	0	0.48	1.72	0
Wollastonite	0	0	0	0	0.06	0	0
Hypersthene	8.74	7.69	3.63	3.33	0	1.81	9.91
Magnetite	1.93	1.55	1.32	0.94	0.2	0.59	0.22
Ilmenite	0.61	0.65	0.34	0.44	0.42	0.46	0.57
Hematite	0	0	0	0	0.34	0	0
Sphene	0	0	0	0	0	0	0
Rutile	0	0	0	0	0	0	0
Apatite	0.14	0.14	0.05	0.09	0.12	0.09	0.12

An

Tonalite/
Dacite

Adamellite

Trondhjemite /
Quartz Keratophyre

Continental trondhjemite

Granite

Ab

Or.

- ◆ Glover's Harbour
- ○ Indian Cove
- ■ Long Pond
- □ Nanny Bag Lake
- ▲ Side Harbour
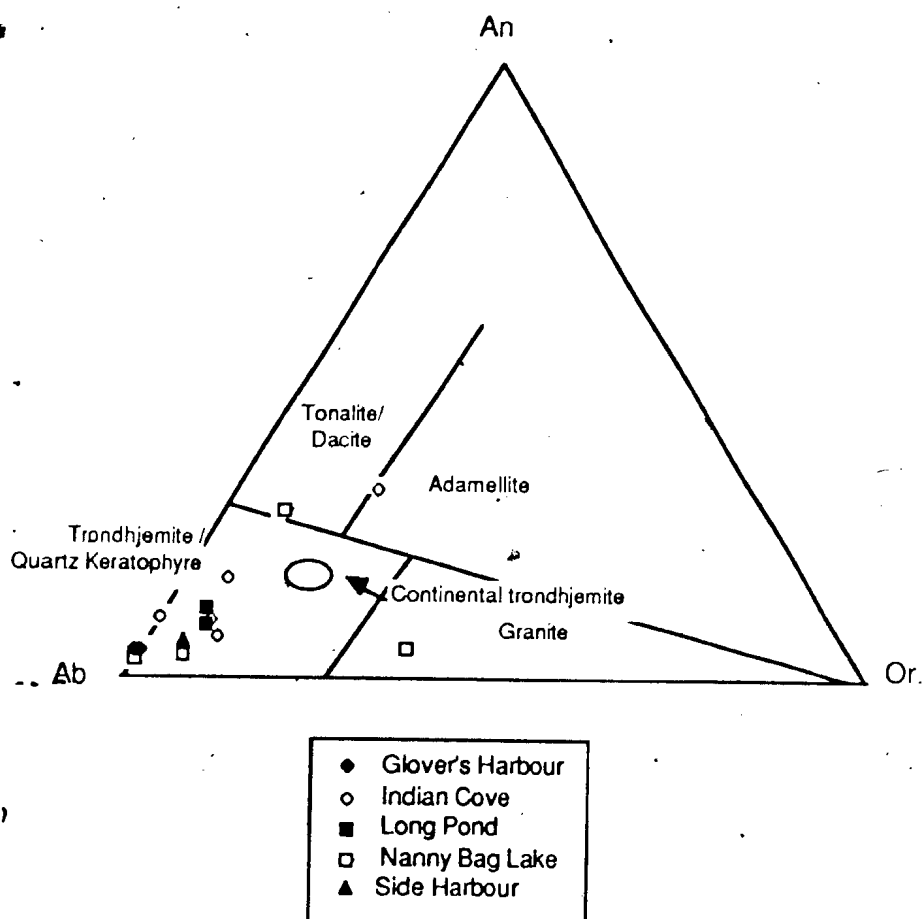
Figure 3.55: Classification of granitoid rocks based on normative feldspar compositions after O'Connor (1965). Wild Bight Group felsic volcanic rocks plot mainly in the field of trondhjemite and quartz keratophyre.

1) There is no potassium feldspar in the rocks, either as phenocrysts or in the groundmass suggesting that the crystallizing magma was K-poor.

2) Although the rocks have certainly been subjected to some secondary alteration, there is no petrographic evidence of extensive or pervasive hydrothermal alteration. Furthermore, the most K_2O-rich samples (2140488 and 2140538) show the most alteration in thin section and have abnormally high amounts of sericite in the groundmass. In the case of 2140538, the sericite is concentrated in microveinlets (Plate 2.13) suggesting that components such as K may have been added to the rock through secondary hydrothermal activity. The effect of the most severe alteration has, therefore, apparently been addition rather than removal of K_2O and the low K_2O contents are reasonably interpreted as an original igneous feature. A similar argument holds for Rb which has generally low abundances but is most enriched in the two samples showing evidence of potassium metasomatism.

3) Perhaps most persuasive are the very low abundances of incompatible elements Zr, Nb and Ba (Ba, again not coincidentally, is relatively enriched in the most altered samples), not indicative of sialic crustal sources from which granitic rocks are commonly interpreted to derive but rather of depleted sources such as mafic igneous rocks, commonly cited as potential sources of trondhjemitic liquids through partial melting in island arc environments (further referenced discussion of this point follows below).

Barker *et al.* (1976) classified trondhjemites into low- Al_2O_3 (<15 percent) and high- Al_2O_3 (>15 percent) varieties, based on their studies of Precambrian examples in the western United States. Their studies indicated that the former resulted from partial melting of amphibolite and hornblende-bearing gabbro, with plagioclase but not hornblende or garnet as a residual phase. The latter, they interpreted as the result of hornblende-controlled fractionation of basaltic liquid or partial melting of basaltic rocks with garnet and/or hornblende in the residua. The Wild Bight Group rhyolites, with Al_2O_3 contents in the 11 to 13 percent range, correspond to the low- Al_2O_3 trondhjemites of this classification.

3.7.3 Composition of Wild Bight Group Felsic Volcanic Rocks

The major and trace element composition of the Wild Bight Group rhyolites is illustrated by a series of Harker diagrams in Figure 3.56. All are 'high-silica' with SiO_2 contents greater than 75 percent. Most cluster in the silica range between 75 and 78 percent although four samples have approximately 79 to 81 percent silica. Aluminum, iron and magnesium all show a strong anticorrelation with silica. In the case of alumina, this may reflect the influence of plagioclase, either during fractional crystallization or residual after partial melting (see also negative Eu anomalies in REE patterns, Figure 3.57). Sodium, potassium and calcium all vary non-systematically with silica; all are very mobile in fluid phases and are likely to have been affected by fluid interaction during magmatism. Some secondary alteration is also likely although, as discussed previously, this has probably not effected a wholesale redistribution of these elements in most samples. TiO_2 is present in similar concentrations in all rocks, and, according to petrographic observations, is probably present mainly in fine grained groundmass oxide phases.

Incompatible trace elements, both LFSE and HFSE, have generally low abundances in these rocks. None varies systematically with silica. The consistently low abundances of Rb and Ba suggests that this is probably an original feature of the rocks, although the absolute concentrations may have been readjusted slightly by alteration. The abundances of the HFSE Zr, Y, Nb, Ta and Hf are likewise very low for felsic rocks and show little variation between suites. Ratios between more and less compatible elements (i.e. Zr/Y, Table 3.17) are generally chondritic or less.

REE patterns for the Wild Bight Group rhyolites (Figure 3.57) are distinctive for felsic rocks. Abundances are approximately 10 times chondritic (consistent with HFSE abundances) and there is a slight LREE depletion ($[La/Sm]_n$=.54 to .88), consistent with HFSE ratios. All samples have small negative Eu anomalies (Eu/Eu*=0.58-0.71).

The compositions of these rocks are further discussed in Section 3.7.5 where they are compared to modern examples of low-K, high-SiO_2 rhyolite and some Newfoundland oceanic plagiogranites.
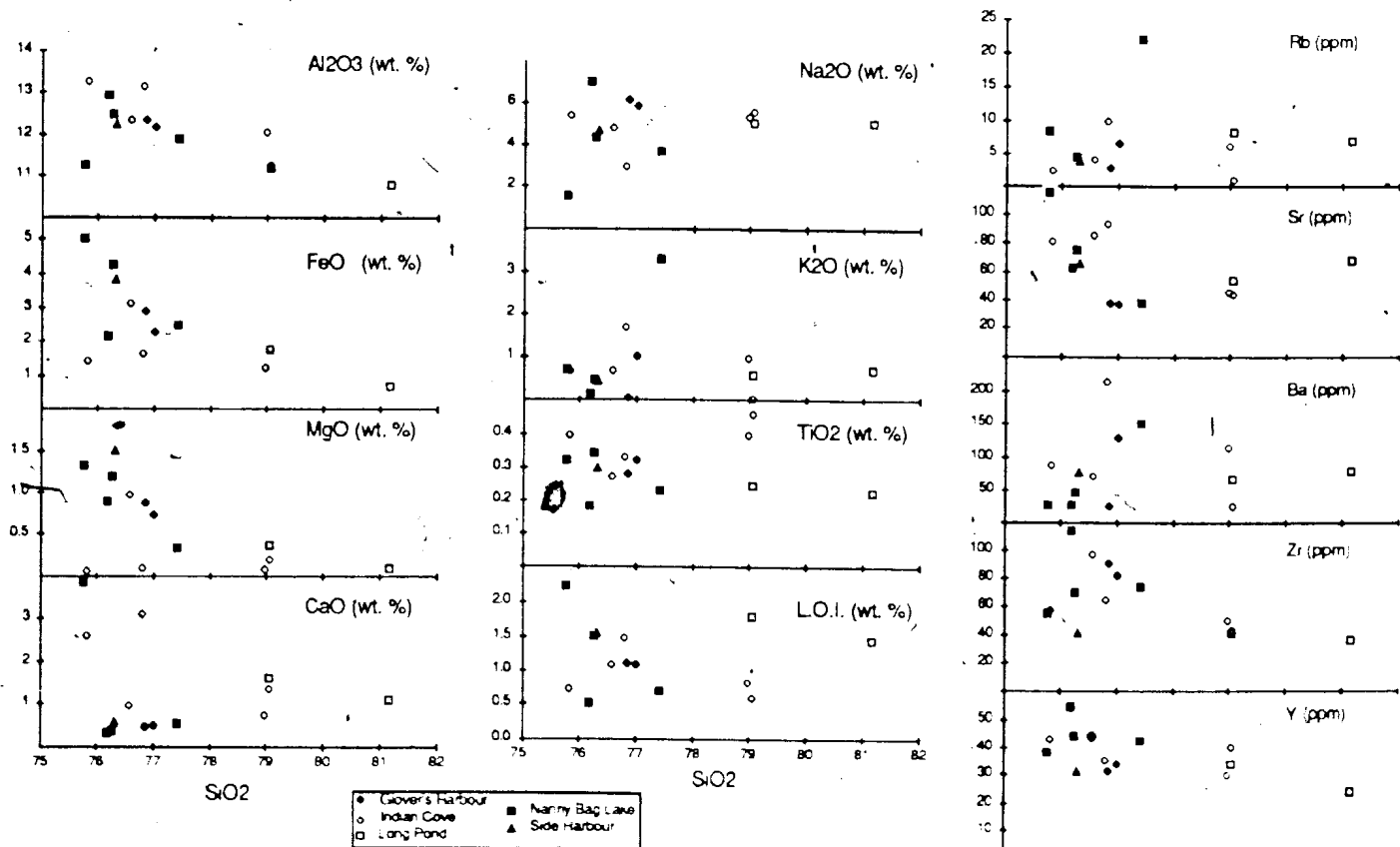
Figure 3.56: Harker diagrams for the felsic volcanic rocks. Variation is
discussed in text.
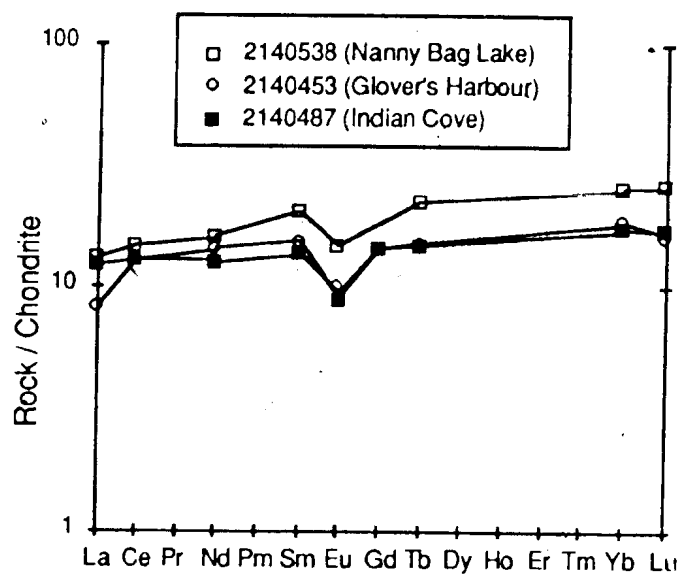
Figure 3.57: Chondrite-normalized REE patterns of the Wild Bight Group rhyolites.

3.7.4 Trondhjemite / Quartz Keratophyre in Orogenic Environments

3.7.4.1 High-SiO_2, low K rhyolites in modern island arcs

High-SiO_2, low-K, peraluminous rhyolites and dacites with trondhjemitic/tonalitic liquid compositions are a characteristic feature of modern island arcs. Ewart (1979) reviewed the occurrence of these rocks on a world wide scale, compiling available geochemical data and summarizing their tectonic settings. He noted that they are generally found in settings characterised by relatively young crust and/or in intra-oceanic island arcs.

It is beyond the scope of this review to summarize all known examples. However, brief consideration of four particularly well studied areas, the Tongan arc, the Miocene sequences of Fiji, the Cenozoic New Britain arc of Papua New Guinea, and Eocene rhyolites of the Mariana forearc will suffice to illustrate the principal features, the major evidence and lines of argument in the debate over their petrogenesis and possible analogies to the felsic rocks of the Wild Bight Group. In particular, the discussion is intended to emphasize the considerable geochemical diversity that characterizes these rocks in different areas and to highlight the different types of petrogenetic interpretations that have been advanced to explain their origin. Representative geochemical analyses are given in Table 3.19.

The first-studied representatives of dacitic rocks from the Tongan arc were drift pumice (Bryan, 1968,1971). Melson et al. (1970) first described the chemistry of high-SiO_2 dacitic pumice from the eruption of Metis Shoal and these data were used by Ewart et al. (1973) in the first major petrogenetic study of the Tongan arc as a whole. They noted that a complete range of compositions were present in this arc from basaltic andesite through dacite and showed that major element data for rocks and phenocrysts could be successfully modelled by least squares analysis in terms of fractional crystallization of observed island arc tholeiitic andesites. Although the felsic whole rocks generally contained less than 69 percent silica and cannot be considered 'high-silica', residual glass in the Metis Shoal dacite contained more than 73 percent silica and was interpreted by Ewart et al. (1973) as the extreme end product of this fractional crystallization. This

Table 3.19: Mean compositions of Wild Bight Group rhyolites compared to high-SiO2, low-K rhyolites in modern island arcs and early Palaeozoic island arc plagiogranites in Newfoundland

	Glover's Hbr.	Indian Cv.	Long Pond	Side Hbr.	Nanny Bag Lk.	1	2	3	4	5	6	7	8	9	10	11	12	13	14	15
SiO_2	76.94	77.46	80.13	78.33	75.14	71.01	73.15	73.60	66.79	75.01	74.19	77.40	71.40	72.40	71.40	78.20	80.23	79.20	71.42	74.45
Al_2O_3	12.27	12.41	10.98	12.26	12.04	15.39	14.85	12.29	13.75	12.99	12.89	11.80	14.90	13.40	14.30	10.58	10.61	11.10	13.56	13.02
Fe_2O_3	0.36	1.14	0.45	0.15	1.24				1.32	1.39	1.35	2.62*	3.18*	0.88	2.55			0.52	0.81	2.62*
FeO	2.23	0.80	0.81	3.66	2.91	3.33	3.25*	3.89*	6.28	1.47	2.15					10.58	10.61	11.10	13.56	13.02
MgO	0.81	0.28	0.22	1.50	1.20	0.94	0.72	1.07	1.54	0.54	0.68	0.48	0.69	1.48	0.61	1.3	.9	0.90	2.09	2.62*
CaO	0.49	1.75	1.34	0.58	1.89	4.28	3.30	3.61	5.43	2.57	3.13			0.81	0.50	0.22	0.12	0.38	0.95	0.28
Na_2O	8.02	4.85	5.15	4.89	4.08	3.65	2.85	3.17	3.17	4.37	3.13	4.27	6.05	2.75	2.75	1.28	1.07	2.08	2.22	1.65
K_2O	0.53	0.81	0.64	0.44	1.08	0.55	0.50	1.47	0.79	1.18	1.10	1.09	0.94	4.05	3.90	3.54	3.83	3.40	4.97	5.03
TiO_2	0.30	0.37	0.23	0.30	0.31	0.49	0.44	0.52	0.62	0.34	0.46	0.30	0.71	1.64	1.72	1.89	1.47	1.58	0.70	0.47
MnO	0.04	0.03	0.02	0.04	0.05	0.16	0.16	0.06	0.14	0.09	0.07	0.03	0.10	0.31	0.46	0.17	0.09	0.23	0.23	0.22
P_2O_5	0.04	0.09	0.09	0.05	0.05	0.07	0.06	0.07	0.17	0.22	0.08	0.13	0.18	0.07	0.08	0.04	0.03		0.12	0.07
Cu	4	10	44	8	49			2	18	2	32			8	8				0.10	0.01
Zn	45	67	37	71	74			12	124	82	49			35	56					17
Ni	3	9	3	3	3	2	4	173	3	37	2	<5	<5	<1	<1					39
Cr	7	4	7	10	11				3	20	2		3	6	4					
V	18	19	13	16	54	17	1.30		64	8	39		16	30	24			19	8.4	43.4
Rb	5	5	7	4	9	5	21	13	11	n.d.	13	9	9						19	43.4
Sr	38	70	81	67	85	170	130	125	218	117	145	100	148	23	28.5		20.1	15	11.7	10
Ba	78	102	73	78	58	254	610		243	403	289	117	218	200	278	230		74.7	92	128.9	97	74
Y	32	38	29	31	38	47	25		27	11	34	47	56	14	26		135	175	68.2	74
Zr	86	63	38	41	84	90	68	283	63						100			23	20.9	
Nb	<0.5	<0.5	<0.5	<0.5	<0.5	4		36	83	n.d.	95	156	188	84	100			125	60.5	88
Hf	3.10	1.77			2.40				2.2	3.7	3.4	2.7		1	1			0.54	5.8	5
La	2.8	3.8			4.1				3.90	6.70	4.00			3.40	6.80			5.50		2.6
Ce	10.4	10.4			12.0				11.90	22.00	9.80			9.10	18.00		9.96	15.00		
Nd	8.5	7.5			9.6									5.50	12.00		7.71	9.20		
Sm	2.94	2.63			3.91									1.40	3.30		2.48	2.00		
Eu	0.64	0.67			1.05									0.45	0.94		0.54	0.65		
Gd	3.70	3.70			0.00									1.70	4.10		3.31	3.00		
Tb	0.71	0.69			1.05									0.32	0.66			0.70		
Yb	3.80	3.56			5.30				3.90	4.90	n.d.			1.80	2.50		2.40	1.90		
Lu	0.52	0.54			0.84												0.43			
$(La/Sm)_n$	0.54	0.88			0.64													1.68		
Eu/Eu^*	0.60	0.66			0.69													0.69		
K/Rb	958.64	1472.40	708.03	953.52	974.45	913.00	197.62	938.54	596.09		702.31	1005.22	866.89	591.83	500.91	0.69	0.69	0.69	498.0	390.1
Na/K	10.21	5.34	7.22	9.50	3.37	5.92	5.08	1.92	3.58	3.15	3.16	3.49	5.74	2.20	2.02		607.01	874.27	6.31	9.54
Rb/Sr	0.12	0.07	0.12	0.06	0.11	0.03	0.16	0.10	0.05		0.09	0.09	0.06	0.12	0.10	1.87	2.32	1.92	6.31	9.54
Zr/Y	2.84	1.63	1.33	1.33	1.68	1.91	2.72		2.33		2.79	3.32	3.36	6.00	3.85		0.27	0.16	0.09	0.10
																		5.43	2.9	

1 - microprobe analysis of glass from Tonga Ridge pumice (Hawkins, 1985)
2 - microprobe analysis of glass from Tonga Ridge pumice (Hawkins, 1985)
3 - residual glass from Metis Shoal high-SiO2 dacite (Melson et al. 1970)
4 - average of 3 high-SiO2 dacites from the Tonga-Kermadec arc (Ewart, 1979)
5 - average 'high-SiO2 dacite' (>73%) from Japan-Kuriles-Saipan (compiled by Ewart, 1979)
6 - average 'high-SiO2 dacite' (>73%) from the S.W. Pacific (compiled by Ewart, 1979)
7 - average of 3 Undu Group (Fiji) 'high-silica dacites' (Gill and Stork, 1979)
8 - average of 4 Wainamala Group (Fiji) 'high-silica dacites' (Gill and Stork, 1979)
9 - high-silica, low-K rhyolite E2/10, Sulu Range, New Britain (Johnson and Chappell, 1979)
10 - high-SiO2, low-K rhyolite F6/3 from Cape Reinitz, New Britain (Johnson and Chappell, 1979)
11 - average Saipan rhyolite (Schmidt, 1957)
12 - Saipan rhyolite S-299 (Barker et al., 1976)
13 - Saipan rhyolite S-139 (Taylor et al., 1969)
14 - average of 11 Little Port Complex trondhjemites, western Newfoundland (Malpas, 1979)
15 - average of 33 Twillingate Trondhjemite analyses (Payne and Strong, 1979)
* - total iron

view of extreme differentiation of basaltic andesite liquids to form high-SiO_2 rhyolite in the Tongan arc has more recently been supported by Bryan (1979) and Hawkins (1985) who analysed whole rock and residual glass separated from pumice dredged from the Tonga Ridge. Noting its close chemical and mineralogical similarity with the Metis Shoal dacites and its apparent trace element relationship with arc tholeiite series magmas, Hawkins (1985) argued that the high-SiO_2 glass therein was best interpreted as the end product of fractional crystallization of the island arc tholeiitic series magmas.

High-SiO_2, low-K, dacites and trondhjemites are a major component of the Mid-Miocene sequences of Fiji, which comprise the voluminous products of island arc volcanism in the Tonga Arc preceding the opening of the Lau Basin (Gill, 1976). Analyses of these rocks have been published by Gill (1970), Colley and Rice (1975) and Gill and Stork (1979). According to Gill and Stork (1979), high-SiO_2 volcanic rocks constitute 30 to 40 percent of the basement Wainamala Group of Viti Levu and form domes, breccias and tuffs within the Undu Group of northern Vanua Levu. Related trondhjemite plutons intrude the Wainamala Group. The high-silica volcanic rocks plot in the trondhjemite field on the normative feldspar diagram and have REE patterns, LILE relationships and $^{87}Sr/^{86}Sr$ ratios which closely resemble those of the associated mafic volcanic rocks leading (Gill and Stork, 1979) to suggest that the petrogenesis of the silicic and mafic magmatic rocks was closely related. They noted that although there was no clear evidence as to whether the relationship was one of partial fusion or fractional crystallization, there were several lines of reasoning that indicated the former as a principal process including:

1) the bimodality of the volcanic suites (e.g. lack of intermediate compositions) suggesting separate sources;

2) normative compositions plotted on an Ab-An-Qz ternary diagram do not cluster near or spread along the quartz-plagioclase cotectic suggesting limited influence of fractional crystallization;

3) High Ab/Or ratios coupled with peraluminous character suggest equilibrium with hornblende which, because it is not a consistent fractionating mineral in the volcanic rocks, is

more easily ascribed to the residuum of partial fusion;

4) REE patterns of the plutonic trondhjemites appeared to be consistent with partial fusion of either the Wainamala Group mafic volcanic rocks or the underlying oceanic crust (although no such simple interpretation was universally applicable to the more variable dacites).

However, they noted that problems with this interpretation including abnormally high K/Rb ratios and the constancy of Ab/Or ratios which imply the absence of refractory plagioclase. They noted that considering the potential complexities introduced by fractional crystallization, their data base did not permit more detailed genetic modelling.

Late Cenozoic volcanic activity has, in several instances along the New Britain arc of Papua New Guinea, included the eruption of high-SiO_2, low-K, peraluminous rhyolite. The petrogenesis of these rocks in New Britain and nearby islands has been extensively studied by Lowder (1970), Lowder and Carmichael (1970), Heming (1974), Heming and Rankin (1979), Johnson and Chappell (1979) among others, most of whom ascribed them to crystal fractionation of basaltic parents on the basis of least squares calculations on whole rocks and phenocryst compositions. However, some difficulties with this interpretation have recently been outlined by Smith and Johnson (1981) including:

1) in some cases, the least squares fit is very poor;

2) the proportions of different volcanic rock types in some areas are considerably different from that predicted by the least squares calculations;

3) the stratigraphy based on field relationships locally shows the supposed basaltic parents to be stratigraphically above and presumably younger than the supposedly derivative silicic rocks;

4) local textural and mineralogical features suggest magma mixing and incorporation of components from other sources, raising difficulties with establishing a simple fractional crystallization sequence to account for the origin of the rhyolites;

5) in some areas, a slight enrichment of radiogenic [87]Sr in felsic rocks compared to basaltic varieties further complicates any model that depends mainly on fractional crystallization.

Smith and Johnson (1981) suggested that an equally acceptable alternative model is

rhyolite production through partial fusion of island arc crust, explaining isotopic differences in felsic and mafic rocks by aging of the sources or alteration of the crust and across-arc differences in chemistry by systematic differences in the composition of the sources. They cited clustering of samples near the low-pressure minimum in the Qz-Ab-Or system as supporting evidence.

Meijer (1983) considered the origin of low-K, high-SiO_2 rhyolites that occur in the Mariana frontal arc, building on the previous studies of Schmidt (1957), Taylor et al. (1969) and Barker et al. (1976). Using whole rock and mineral geochemical data from the previous studies supplemented by new mineral and glass analyses, he showed that the observed major element abundances as well as REE patterns could be successfully modelled, using partition coefficients derived for Saipan andesite, by approximately 78% crystal fractionation of a liquid of typical high-Mg andesite from a DSDP hole in the Mariana forearc. Such a mechanism was supported by similar $^{87}Sr/^{86}Sr$ and $^{143}Nd/^{144}Nd$ in the high-Mg andesite and rhyolite. Although the exact REE pattern of the rhyolite could not be reproduced, Meijer (1983) suggested that variable relative REE contents in the source rocks could explain the observed variation.

In summary, the petrogenetic history of high-SiO_2, low-K rhyolites in modern island arc environments is normally not well constrained. In some cases, modelling of fractional crystallization of mafic liquids observed in the island arc (either island arc tholeiites or high-Mg andesites) can successfully reproduce the observed felsic rock compositions. In other areas, however, there are strong arguments, in favour of partial fusion of basal island arc basaltic crust (perhaps with further modification resulting from fractional crystallization, magma mixing or contamination from other sources prior to eruption) as the dominant process.

3.7.4.2 Oceanic plagiogranites

Oceanic plagiogranites were first discussed in detail by Coleman and Peterman (1976). These rocks are common, although not generally voluminous, components of ophiolites, where they are commonly interpreted as differentiates of the tholeiitic liquids of the plutonic suites (e.g. Coleman and Peterman, 1976; Coleman and Donato, 1979). However, the role of fluid phases

has been stressed by some workers, particularly with respect to the abnormally low K contents of these rocks. For example, Sinton and Byerly (1980) ascribed the K depletion of granophyre in recent basalt from the Mid-Atlantic Ridge to metasomatic alteration by late vapour phases. However, it is not clear from these studies to what extent theories of plagiogranite petrogenesis in an oceanic spreading ridge environment can be applied to the island arc environment.

Malpas (1979) was the first to describe and contrast examples of ancient spreading ridge and island arc trondjemites. He found that trondhjemites in the Bay of Islands Ophiolite Complex, interpreted as oceanic crust formed at an oceanic or marginal basin spreading axis, have Na_2O > 6 percent, Rb/Sr~0.01, little K_2O and relatively high abundances of the incompatible trace elements. In contrast, those in the nearby Little Port Complex, interpreted as the basal part of an island arc complex, have Na_2O ~ 5 percent, Rb/Sr~0.1 and very low incompatible element abundances. He interpreted these geochemical features coupled with field relationships (the association of the Bay of Islands trondhjemites with the ophiolitic plutonic suite versus the intimate association of Little Port Complex trondhjemites with amphibolites) as indicating that the former resulted from partial melting of amphibolites near the base of an island arc and the latter through fractional crystallization of basaltic liquid in the ophiolite. He noted that these chemical differences might prove useful in defining the origin of trondhjemites elsewhere.

The Twillingate Trondhjemite in eastern Notre Dame Bay has low Al_2O_3, K_2O, Sr and Ba, high SiO_2 and Na_2O (Payne and Strong, 1979). It intrudes greenschist facies tholeiitic basalts of the Sleepy Cove Group. Various workers have remarked on the geological similarities between the Twillingate and Little Port trondhjemites (e.g. Williams and Payne, 1975). Geochemical data from the Twillingate Trondhjemite, particularly its depleted incompatible element contents, lack of evidence for extended plagioclase fractionation and geochemical links with nearby amphibolites, as well as the intimate spatial association of trondhjemite with the amphibolites led Payne and Strong (1979) to suggest that it could have formed from partial fusion of basaltic material at the base of a volcanic sequence about 12 km thick (i.e. near the base of an island arc in the presence of a high geothermal gradient).

3.7.5 Comparison of the Wild Bight Group Rhyolites with Modern Orogenic Rhyolites and Early Paleozoic Newfoundland Plagiogranites

All of the examples discussed above are low- Al_2O_3 trondhjemites according to the Barker *et al.* (1976) classification (Table 3.19). However, they are not a homogeneous suite and show varying similarities and also some significant differences with the Wild Bight Group rhyolites.

The Wild Bight Group rhyolites are generally more SiO_2-rich than either modern high-silica rhyolites or ancient trondhjemites, suggesting that they have undergone post-depositional silicification.

REE patterns in high-SiO_2, low-K rhyolites are highly variable reflecting their varied sources as well as melting and crystallization histories. As in the Wild Bight Group, these rocks have REE abundances of approximately 10 times chondrite and minor to pronounced negative europium anomalies (Figure 3.58). Unlike the Wild Bight Group, most are slightly LREE-enriched, although three (the Tonga dacites, rhyolites from the Undu Group, Fiji, and the Saipan rhyolite) are LREE-depleted and, in this respect, closely resemble the Wild Bight Group rocks.

Wild Bight Group REE patterns are very similar to those in the Twillingate Trondhjemite, which are variably slightly LREE-depleted to slightly LREE-enriched with abundances in the areas of 10 x chondrites (Figure 3.58). Although the two are not of same age (the Twillingate Trondhjemite is late Cambrian according to Williams *et al.* (1976) their similar REE patterns argue for a similar petrogenesis.

Figure 3.59 illustrates that the Wild Bight Group rhyolites have generally similar Zr contents to both the modern orogenic rhyolites and the Newfoundland plagiogranites. The Ba contents of the Wild Bight Group rocks, although similar to the Newfoundland plagiogranites (which are consistently less than 150 ppm), are distinctly lower than those in the modern oceanic rhyolites (which are generally greater than 200 ppm). As with the REE, the oceanic arc rhyolites that are most similar to the Wild Bight Group rocks are the Undu Group, Fiji, and Saipan rhyolites.

Rb/Sr ratios in the Wild Bight Group rocks, although showing some scatter which may

A

Field of Twillingate trondhjemites (D.F. Strong, unpub. data)

C

Representative analyses of high-SiO2, low-K rhyolites from New Britain (Smith and Johnson, 1981)

La Ce Pr Nd Pm Sm Eu Gd Tb Dy Ho Er Tm Yb Lu

La Ce Pr Nd Pm Sm Eu Gd Tb Dy Ho Er Tm Yb Lu

Rock / Chondrite

B

Representative high-SiO2, low-K rhyolites from the Undu and Wainamaia Groups, Fifi (Gill and Stork, 1979)

D

Low-K rhyolites from Saipan, Mariana frontal arc (Meijer, 1983).

La Ce Pr Nd Pm Sm Eu Gd Tb Dy Ho Er Tm Yb Lu

La Ce Pr Nd Pm Sm Eu Gd Tb Dy Ho Er Tm Yb Lu

Rock / Chondrite

Figure 3.58: REE patterns for the Wild Bight Group rhyolites compared with the Twillingate Trondhjemite and high-SiO2, low-K rhyolites from modern arcs: In A, symbols for Wild Bight Group rocks are same as in Figure 3.51. Field of Wild Bight Group rhyolites represented by stippled field in B, C and D.
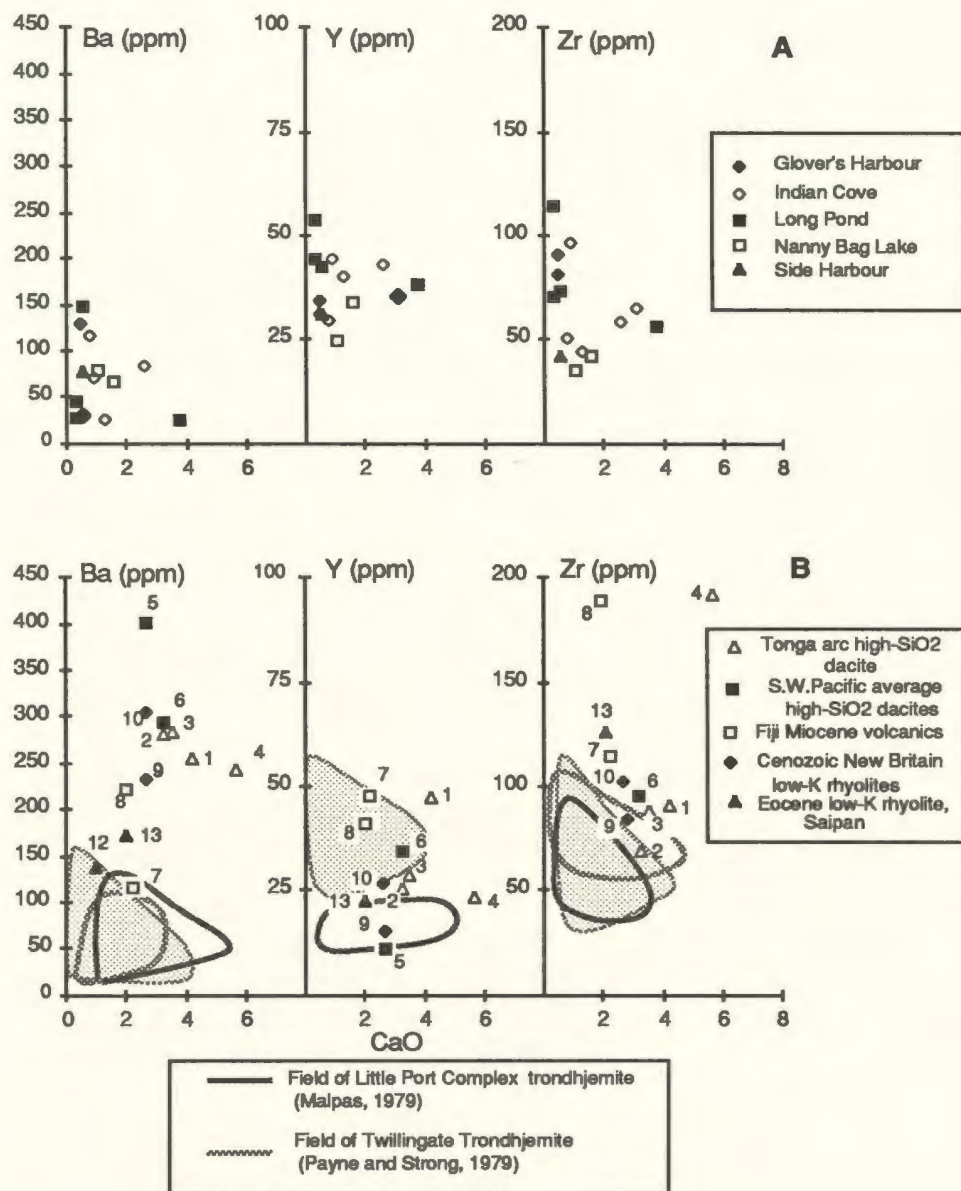
Figure 3.59: Ba, Y and Zr plotted against CaO (Malpas,1979) comparing the Wild Bight Group rhyolites (plotted in A and stippled field in B) to high-SiO2, low-K rhyolites from modern arcs and Newfoundland trondhjemites of probable arc origin. Numbers in B are keyed to Table 3.18.

result form alteration, are generally closer to 0.1 than 0.01 on the Rb/Sr diagram (Figure 3.60). In this regard, they more like continental trondhjemite than oceanic plagiogranite, according to Coleman and Peterman (1976), although Rb and Sr abundances are generally lower than in continental trondhjemite. High-SiO_2, low-K rhyolites of modern arcs have similar Rb/Sr ratios to the Wild Bight Group rhyolites although with somewhat higher Sr contents (the exceptions again being the Undu Group rhyolites of Fiji and the Saipan rhyolites, which plot within the field of Wild Bight Group rocks). The Little Port and Twillingate trondhjemites occupy identical fields to the Wild Bight Group rocks.

Figure 3.60 suggests that the Rb (and K_2O, with which it is positively correlated) enrichment of the Wild Bight Group rocks, relative to oceanic plagiogranites, is a consistent feature of island arc magmas. It parallels the well-documented potassium enrichment of island arc mafic magmas relative to those at spreading ridges, which is generally interpreted as resulting from LILE metasomatism resulting from dehydration of the subducting slab (e.g. Sun, 1980; Wood et al., 1979). However, whatever the reason, the data suggest that an additional field can be defined on this diagram for arc related felsic rocks, both plutonic and eruptive, which straddles the Rb/Sr = 0.1 line between the oceanic and continental plagiogranite (Figure 3.60).

In summary, although low-K, high SiO_2 rhyolites in modern arcs display a considerable geochemical diversity, they also show some broad similarities to the Wild Bight Group rhyolites. These similarities are best displayed in broadly similar REE abundances (although not always parallel patterns), Rb/Sr ratios and incompatible element abundances). Locally in this environment, very good geochemical analogues for the Wild Bight Group rhyolites can be identified (i.e. Undu Group, Fiji and Saipan rhyolites). Elsewhere in Newfoundland, plagiogranites interpreted as the results of partial melting in an island arc environments are also very similar geochemically to the Wild Bight Group rhyolites.

3.7.6 Fractional Crystallization or Partial Melting?

The close spatial association of rhyolite and mafic volcanic rocks of island arc affinity in the
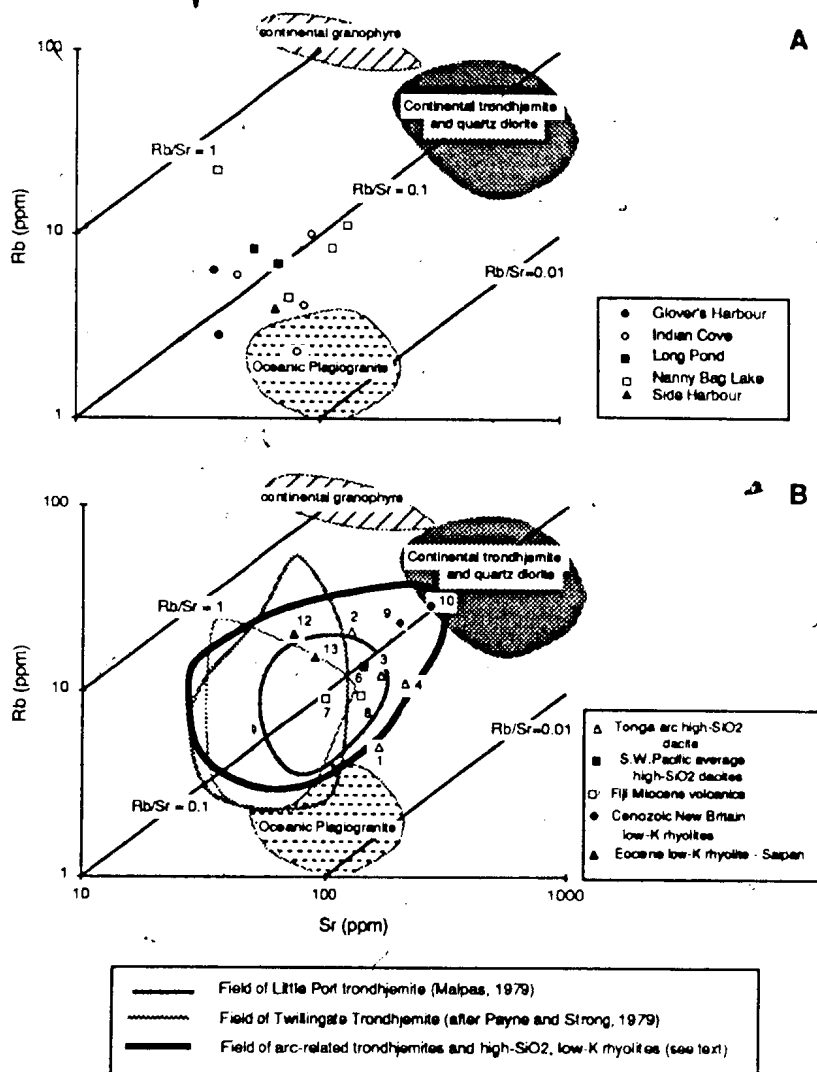
Figure 3.60: Rb-Sr diagram for plagiogranites after Coleman and Peterman (1976). In A, Wild Bight Group rhyolites have Rb/Sr ratio similar to continental trondhjemite but at lower Rb and Sr contents. In B, Wild Bight Group samples (light stipple) are similar to Twillingate and Little Port trondhjemites. Rb/Sr ratio is similar to high-SiO2, low-K rhyolites from modern arcs but Sr abundances are lower. Numbers are keyed to Table 3.18.

Wild Bight Group argues for some genetic relationship as well. Genetic models for the Tonga and Saipan rhyolites (discussed above) suggest that these types of rocks may be derived through extended fractional crystallization of island arc tholeiitic and/or high-Mg andesitic magmas. However, given the very low incompatible element contents of the Wild Bight Group rhyolites, it is difficult to imagine them as the products of extreme fractional crystallization of even very incompatible element-depleted mafic liquids. There are other arguments against advanced fractional crystallization and in favour of partial fusion of mafic rocks in the arc crust. Gill and Stork (1979) presented a number of them, including absence of intermediate compositions, peraluminous compositions, lack of consistent relationship between whole rock compositions and the low pressure quartz-plagioclase cotectic, with reference to the Fiji high-SiO_2, low-K rhyolites. Such arguments, particularly the lack of intermediate compositions, are also persuasive with respect to the Wild Bight Group rocks.

If these rocks do result from partial fusion of mafic arc crust, the slight positive slopes in HREE patterns require that garnet was not a residual phase during partial melting. Coupled with the slight LREE-depletion, they also argue against hornblende as a fractionating phase, unless the source was extremely LREE-depleted. The low Al_2O_3 and Sr contents and the marked negative Eu anomalies suggest that plagioclase was a fractionating phase, either during partial melting or fractional crystallization.

The close geochemical similarity between the Wild Bight Group rhyolites and the Twillingate trondhjemite suggests that their petrogeneses may be similar. Payne and Strong (1979) suggested that the Twillingate trondhjemitic liquids formed by *in situ* melting of basalts leaving an amphibolite residue. They were able to identify tentatively potential source rocks as well as amphibolite residua in outcrop. Using Hoffman's (1976) projections of quartz-plagioclase-(H_2O) relationships and comparing the results with the solidus for a 1921 Kilauea basalt from Holloway and Burnham (1972), they estimated that melting occurred at $P(H_2O) = P_T = 4$ kb and slightly over $700°C$. These are amphibolite grade metamorphic conditions at depths of approximately 12 km and a reasonable estimate for conditions at the base

of an island arc volcanic and sedimentary sequence (Payne and Strong, 1979).

The genetic models derived by Barker *et al.* (1976), although based mainly on Precambrian low-Al_2O_3 trondhjemites, also suggest a possible origin for the Wild Bight Group rhyolitic liquids. Noting that the generally flat HREE, low abundances of Rb and Sr and lack of marked LREE enrichment precluded hornblende and/or garnet as a fractionating phase during either partial melting or fractional crystallization, they proposed an origin via partial melting of hornblende-bearing gabbro with complete hornblende fusion and a plagioclase-clinopyroxene residue. Such a model is consistent with the low incompatible element contents, chondritic or lower ratios between more- and less-incompatible elements (e.g. Zr/Y), and REE patterns of the Wild Bight Group rhyolites.

The conditions of melting proposed by Payne and Strong (1979) would seem to be reasonable analogy for the origin of the Wild Bight Group rhyolites. Possible sources in the basalt arc crust would include basaltic and andesitic volcanic rocks and also gabbroic cumulates, relicts of the extensive magmatism, which would provide a very plausible source in view of their strong incompatible element (including LREE) depletion. The island arc signature in the HFSE and REE would, in such a scenario, be inherited from melting of these rocks, which would already carry this signature. The experimental data of Helz (1976) suggest that the liquids produced under these conditions would be somewhat less siliceous than the Wild Bight Group rhyolites; either superimposed secondary silicification or fractional crystallization would be necessary to account for their present silica contents. Further discussion of potential sources and the petrogenesis of these rocks follows presentation of Nd isotope data in Chapter 4.

3.8 Synthesis and Conclusions

Mafic volcanic and subvolcanic rocks of the Wild Bight Group are variably altered, mainly as a result of sub-seafloor processes. This alteration has redistributed the more mobile elements (e.g. Na, K, Rb, Sr, Ca) in most volcanic rocks and also, to a lesser extent, in the mafic subvolcanic rocks, but has generally not affected the less mobile and immobile elements. In particular,

AFFINITY	GEOCHEM GROUP	SUITE	MAFIC ROCK TYPE	MAGMA TYPE	MAGMA SERIES	MEAN INCOMPATIBLE ELEMENT ABUNDANCE TiO2 (wt %)	Zr (ppm)	INCOMPATIBLE ELEMENT RATIOS Ti/Y	Zr/Nb	Zr/Y	Th/La	TECTONIC SETTING DISCRIMINANTS Ti-Zr-Y	Ti-V	Zr/Y-Zr	Ta-Hf-Th	RARE EARTH ELEMENTS (La/Sm)$_n$	AFFINITY	CLINOPYROXENE MINERALOGY	MAGMA TYPE	MAGMA SERIES
ISLAND ARC	IAD	Glover's Harbour West	Andesite	Non-alkalic	Tholeiitic	0.52	6.0	427.5		0.80	0.25	depleted IAT	~10 Arc tholeiite	depleted VAB	Arc	0.58	depleted island arc	Augite-endiopside	Non-alkalic	Orogenic tholeiite
	IAD	Indian Cove*	Andesite	Non-alkalic	unknown	0.46	6.1	333		0.74	0.24	depleted IAT	~10 Arc tholeiite	depleted VAB	Arc	0.69	depleted island arc			
	IAD	Side Harbour	Andesite	Non-alkalic	unknown	0.50	7.4	441	10.8	1.01		depleted IAT	~10 Arc tholeiite	depleted VAB						
	IAT	Glover's Harbour East	Andesite / basalt	Non-alkalic	unknown	1.16	93.9	348.5	23	4.5	7.25	CAB/MORB/IAT	~28 MORB/BABV	WPB/MORB	Arc	1.92	medium K IAT	Augite-endiopside	Non-alkalic	Non-orogenic tholeiite
	IAT	Seal Bay Bottom	Andesite / basalt	Non-alkalic	Tholeiitic	1.17	94.6	344.9	18.2	4.6	8.66	CAB/MORB/IAT	~30 MORB/BABV	WPB/MORB	Arc	1.98	medium K IAT	Augite-endiopside	Non-alkalic	Orogenic tholeiite
	IAT	Northern Arm	Andesite / basalt	Non-alkalic	unknown	1.17	83.9	377.5	18.5	4.5		CAB/MORB/IAT	~30 MORB/BABV	WPB/MORB		0.53	medium K IAT			
	IAT	Nanny Bag Lake	Andesite / basalt	Non-alkalic	Tholeiitic	1.39	82.0	308.4	36.7	2.3	7.46	CAB/MORB/IAT	Indeterminate	VAB/MORB	Arc	1.81	low-K IAT			
	UNKNOWN	Long Pond																		
NON-ARC	NAI	Badger Bay	Basalt	Non-alkalic	unknown	1.54	86.8	580.2	13.8	5.5	1.74	WPB	~41 MORB/BABV	WPB-MORB	T-MORB/WPT	0.93-1.5	T-MORB/BABV			
	NAI	Big Lewis Lake	Basalt	Non-alkalic	unknown	1.45	76.2	532.3	14.1	5.2	1.77	WPB	~41 MORB/BABV	WPB-MORB	T-MORB/WPT	1.07-1.87	T-MORB/BABV	Augite-endiopside	Non-alkalic	Non-orogenic tholeiite
	NAT	New Bay	Basalt	Transitional	unknown	2.43	162.5	491.8	10.35	6.2	2.16	WPB	~32 MORB/BABV	WPB	E-MORB/WPT	1.58	E-MORB/BABV	Augite	Non-alkalic	Non-orogenic tholeiite
	NAT	Side Harbour	Basalt	Transitional	Tholeiitic	2.05	129.9	615.3	8.29	6.5	1.77	WPB	~46 MORB/WPA	WPB	E-MORB/WPT	1.90	E-MORB/BABV	Augite	Non-alkalic	Non-orogenic tholeiite
	NAE	Seal Bay Head	Basalt	Alkalic		3.57	369.2	452.1	5.14	7.6	1.31	WPB	~127 OIB/WPA	WPB	E-MORB/WPT/WPA	2.17	WPA	Augite	Alkalic	Non-orogenic tholeiite
	NAE	Big Lewis Lake	Basalt	Alkalic		3.33	323.3	508.5	6.80	8.2	1.36	WPB	~99 OIB/WPA	WPB	E-MORB/WPT/WPA	1.94	WPA			
	NAE	Side Harbour*	Basalt	Alkalic		2.75	396.4	343.3	5.99	8.2		WPB	~174 OIB/WPA	WPB	E-MORB/WPT/WPA	2.67	WPA			
IAT (Sun, 1980)			Basalt-andesite	Non-alkalic	Tholeiitic	8.50	22	250	31	1.8	10[2]									
N-MORB (Sun, 1980)			Basalt	Non-alkalic	Tholeiitic	1.6	85	321	27	2.9	13									
E-MORB (Sun, 1980)			Basalt	Non-alkalic	Tholeiitic	1.3	75	366	9	3.4	12									
Ocean Island tholeiite (Hawaii) (Basaltic Volcanism Study Project,1981)			Basalt	Non-alkalic	Tholeiitic	2.3	112	667	4	7.3	1.13[3]									
Ocean Island alkali basalt (Hawaii) (Basaltic Volcanism Study Project,1981)			Basalt	Alkalic		2.7	391	534	15	5.5										

* - Single sample   1 - excluding 2140773   2 - from Saunders et al., 1980   3 - from Sun (1980).

Table 3.20: Summary of the geochemical characteristics of the Wild Bight Group volcanic and subvolcanic rocks. Typical characteristics of mafic volcanic rocks from modern oceanic environments are also shown for comparison.

relationships between immobile elements and the Mg# have apparently been preserved.

Significant aspects of the geochemistry of the Wild Bight Group volcanic and subvolcanic rocks are summarized in Table 3.20. Some representative trace element ratios from typical oceanic volcanic settings are shown for comparison, although these numbers should be viewed critically; the absolute values of "typical" ratios for these settings vary considerably between different authors. Nonetheless, the relative abundances and ratios of these elements in various environments are distinctive and useful for comparison with the Wild Bight Group samples.

The Wild Bight Group mafic volcanic rocks are geochemically heterogeneous. Consideration of absolute abundances of incompatible elements and relationships between HFSE, LILE and LREE indicate that these rocks broadly constitute two groups: 1) incompatible element-poor, basaltic andesites and basalts which have pronounced negative Ta and Nb and positive Th anomalies with respect to normalized LREE and show affinities to island arc basalts on most trace element discrimination diagrams; and 2) incompatible element-rich basalts which have smooth normalized HFSE, LILE, LREE patterns and plots in WPB fields on HFSE discriminant diagrams. The rocks of island arc affinity have consistently lower Ti/Y, Zr/Y and Ti/V and higher Zr/Nb and Th/Ta with respect to the non-arc suites. Intersuite variations in clinopyroxene compositions are less discriminating than, but generally confirm interpretations based on, the whole rock studies.

Geochemical evidence, therefore, strongly indicates that these two broad groups represent volcanism in two distinct environments, the first an island arc setting in which magma generation was influenced by the subducting slab and the second a non-arc environment where few of the magmas show any geochemical evidence of a subducting slab.

Within each of these environments, there are well-defined geochemically distinctive groups in the mafic volcanic rocks, two in the island arc environment and three in the non-arc environment. Their characteristics can be briefly summarized as:

1: *The groups of island arc affinity*

i) the IAD (island arc depleted) group is very depleted in all incompatible elements and has

distinctive REE patterns with flat LREE at 1 to 5 times chondritic and a step up to flat MREE and HREE at 6 to 8 times chondritic. Samples plot outside the fields of island arc volcanics on all discriminant diagrams indicating abnormal relative depletion of the most incompatible elements. Low Cr and Ni contents and Mg# in some samples indicate that these rocks have undergone considerable fractional crystallization. Ti and V increase with decreasing Mg# suggesting that these are best characterised as very depleted island arc tholeiites.

ii) the IAI (island arc intermediate) group has higher incompatible element contents (0.8 > TiO_2>1.8 weight percent) and is itself divisible into two magma types: a) a LREE-enriched type defined by the Glover's Harbour East, Seal Bay Bottom and Northern Arm suites; and b) a LREE-depleted type defined by the Nanny Bag Lake suite. The former has higher Ti/Y and Zr/Y, lower Zr/Nb, plots in WPB fields on discrimination diagrams involving more-to-less incompatible element ratios (e.g. Zr/Y versus Zr). Apart from the HFSE, LILE, LREE characteristics which clearly label it as part of an island arc environment, it has geochemical enrichments that are more typical of enriched, non-arc magmatism (e.g. contrast the above mentioned ratios to E-MORB). In this respect, it is similar to medium-K tholeiites in some modern arcs.

2: *The groups of non-arc affinity*

i) the NAI (non-arc intermediate) group has absolute incompatible element concentrations similar to the IAI group. However, apart from the negative Nb and Ta anomalies (and the resulting lower Th/Ta ratio), its higher Ti/Y and Zr/Y and lower Zr/Nb show it to be geochemically distinct. It plots in the WPB field on most discrimination diagrams, has flat to slightly LREE-enriched patterns and is geochemically similar to T-MORB and to some basalts erupted in back-arc basins.

ii) the NAT (non-arc transitional) group has TiO_2 contents between 1.7 and 3.2 weight percent, slightly overlapping the IAI and NAI fields. Compared to the NAI group, it is more LREE enriched, has higher Zr/Y and lower Zr/Nb. It plots in the WPB field on most diagrams and shows geochemical affinities to both E-MORB and oceanic within plate tholeiites (particularly the latter; note the Ti/Y and Zr/Y ratios).

iii) the NAE (non-arc enriched) group has very high incompatible element contents (TiO_2>

2.75 weight percent), strong LREE enrichment, low Zr/Nb and high Zr/Y ratios and plots in the alkali basalt field on discrimination plots. On the Ta-Hf-Th plot, which purports to separate within plate tholeiites from alkalic basalts and also on most diagrams utilizing clinopyroxene compositions, the alkalic trend is not strongly developed, suggesting that these rocks may best be considered as marginally alkalic. They show geochemical affinities to within plate alkali basalts from oceanic island and back-arc settings and to the more enriched varieties of E-MORB.

Mafic intrusive rocks, which on field evidence are interpreted as subvolcanic, have geochemical trends similar to the volcanic rocks. All of the above geochemical groups are represented in the intrusive rocks, although individual dykes can seldom be directly correlated with observed flows on the basis of their geochemistry. Intrusions of island arc affinity are seen to intrude only stratified rocks of island arc affinity while intrusions of non-arc affinity intrude throughout the sequence. This suggests a sequence of events in which products of an early island arc magmatic episode (both volcanics, subvolcanics and associated sediments) were later intruded through and overlain by volcanic and subvolcanic rocks and associated sediments in a non-arc environment.

Felsic volcanic rocks in the Wild Bight Group are rich in silica and sodium and poor in K_2O and compositionally can be classified as high SiO_2 rhyolites or keratopyhres. They occur only in association with mafic volcanic rocks of island arc affinity and themselves have negative Nb and Ta anomalies. The rhyolites are characterised by very low incompatible element contents and are slightly LREE depleted with negative Eu anomalies. They are geochemically similar to low-K, high-SiO_2 rhyolites in modern island arc environments and to early Paleozoic oceanic plagiogranites elsewhere in Newfoundland which have been interpreted as resulting from partial melting of basal island arc crust.

The stratigraphic relationships of the various types of volcanic and subvolcanic rocks are partially constrained by the following (summarized in schematic form in Figure 3.61):

1) volcanic rocks at the lowest exposed stratigraphic levels of the Wild Bight Group (the Seal Bay Bottom basalt) are of island arc affinity. Most other arc-related sequences occur near the
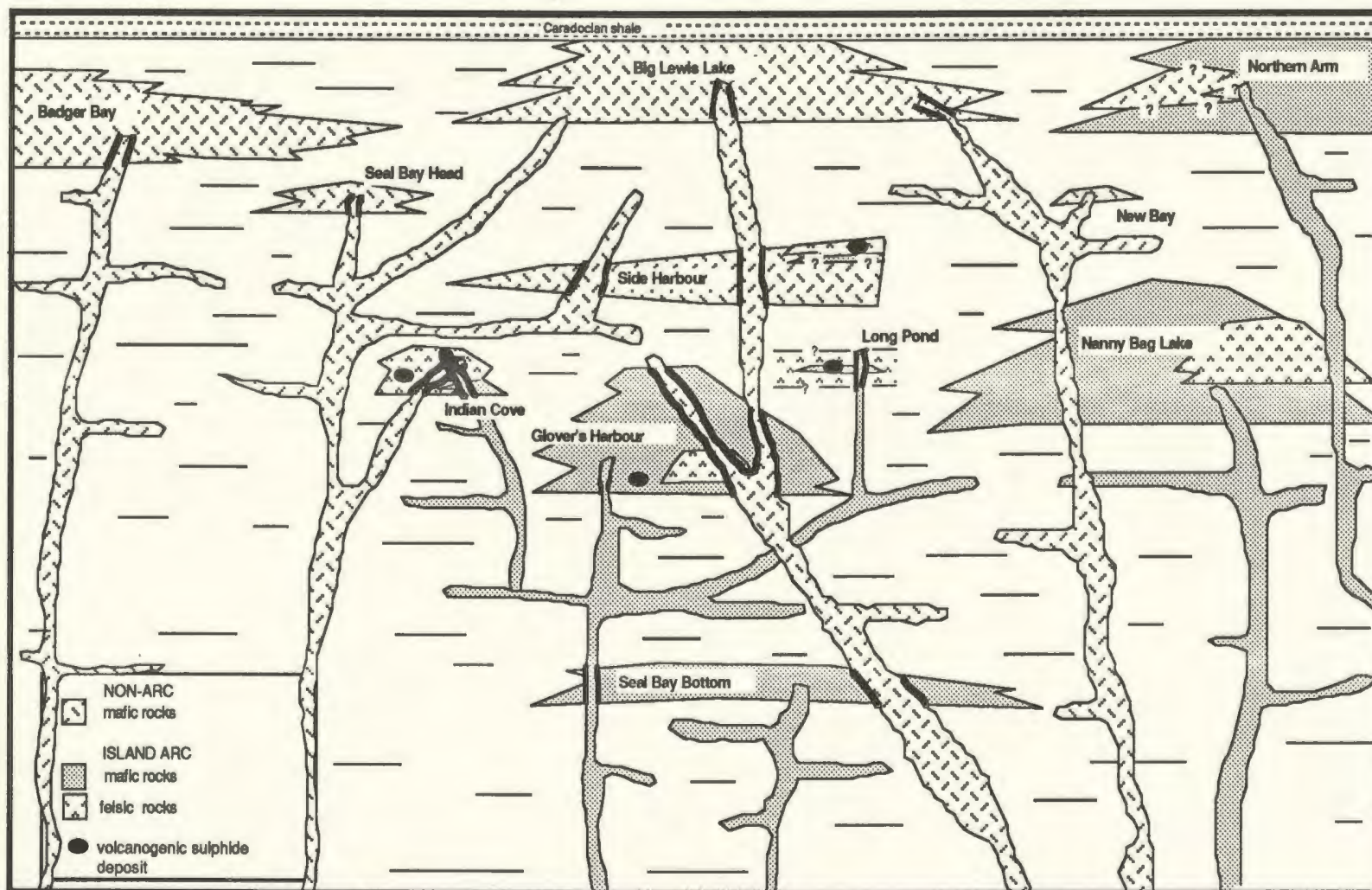
Figure 3.61: Schematic illustration of stratigraphic relationships in the Wild Bight Group. Mafic volcanic and subvolcanic rocks have the same pattern. Observed cross-cutting relationships indicated by heavy contacts.

middle of the stratigraphic section except the Northern Arm basalt which is at the top.

2) Except for the Northern Arm basalt, other volcanic units in the upper part of the Wild

Bight Group are of non-arc affinity and where stratigraphic relationships can be observed or

inferred, they are apparently above all arc sequences except the Northern Arm basalt.

3) mafic intrusions of non-arc affinity cut stratified rocks of the arc suites and non-arc

magmatism must be, at least in part, later than the arc-related activity;

4) the two types of island arc-related activity are closely related stratigraphically in the

Glover's Harbour area. Likewise, different non-arc groups are interbedded with each other (NAI

and NAE types in the Big Lewis Lake volcanic unit, NAT and NAE types in the Side Harbour

volcanic unit). Magmatism of different types within each environment is interpreted, on this basis,

to have been approximately contemporaneous.

5) In view of (1) to (4) above, the position of the arc-related Northern Arm basalt at the top

of the Wild Bight Group is anomalous and suggests either: a) that waning island arc volcanic

activity continued during the eruption of the non-arc products; or b) that the Northern Arm unit

was exposed as a topographic high during non-arc volcanism and was not covered by the

volcanic products of this episode. In this regard, the nature of the single anomalous sample in this

suite, 2140773, attains considerable importance. This sample, which is apparently interbedded

with rocks of arc affinity, plots in WPB fields on discrimination diagrams; has Ti/Y=561, Zr/Nb=5.6

and Zr/Y=6.1, all clearly indicating an affinity with non-arc products, specifically the NAI or NAT

groups. Although it is risky to base major conclusions on only one sample, it appears that, at least

locally, arc and non-arc volcanic products are interbedded in the latest stages of Wild Bight Group

volcanism. Nd isotope evidence which supports this interpretation is presented in Chapter 4.

The overall picture of volcanic activity in the Wild Bight Group suggests an early episode of

island arc volcanic activity followed and possibly in part overlapped by magmatic activity without

the geochemical signature of the subducting slab. Nd isotopic data in Chapter 4 further constrain

the models for magma genesis in these rocks.

CHAPTER 4

Nd ISOTOPES AND PETROGENESIS OF THE WILD BIGHT GROUP VOLCANIC AND SUBVOLCANIC ROCKS

4.1 Introduction

The development of techniques for precise analysis of the isotopic compositions of elements has led to the expanded use of isotopes as tracers in petrogenetic studies. This has provided an important constraint in modelling the origin of magmatic suites, as the isotopic composition of the magmas is a direct reflection of the isotopic composition(s) of their source(s). Because crustal growth results in the fractionation of some radioactive parent/radiogenic daughter pairs (notably, for petrogenetic purposes, Rb with respect to Sr, Sm with respect to Nd, U and Th with respect to Pb), different parts of the earth (e.g. crust and mantle) experience different isotopic growth histories over the long term. Magmas derived from these different source areas carry the isotopic signature that has developed in them.

The isotopic composition of any given element, unlike its geochemical composition, is not fractionated by either partial melting or fractional crystallization. The isotopic composition of an igneous rock is, therefore, directly related to the isotopic composition of its source(s) and provides an important tool for interpreting both the nature of its sources and the petrogenetic processes that lead to its formation.

The first use of isotopes in the interpretation of petrogenetic processes involved the Rb/Sr system (the decay of ^{87}Rb to ^{87}Sr). However, the Rb/Sr system has a major drawback for use in oceanic basalts and/or ancient altered rocks in that the elements involved are LFSE and are relatively mobile in hydrous phases. The isotopic composition of Sr can, therefore, be modified by alteration after the rocks have been formed and the present composition of the rocks may, in this case, not accurately reflect that of the magmatic sources.

Similar difficulties are encountered in the application of U- and Th-Pb systems. All of these elements may be mobile during alteration and these systems have the added complication of an

extended decay scheme with intermediate steps which may likewise be interrupted by alteration producing disequilibrium between parent and daughter elements.

The REE have two radioactive decay systems that are potentially useful in petrogenetic studies, the decay of ^{176}Lu to ^{176}Hf and the decay of ^{147}Sm to ^{143}Nd. Both radioactive parents have long half lives relative to ^{87}Rb and the present range of radiogenic isotope ratios is accordingly much smaller, demanding more sophisticated (i.e. precise) analytical procedures. Petrogenetic applications of the former system have been explored by, for example, White and Patchett (1984), but have not found broad acceptance, because of analytical difficulties. However, the development and dissemination of analytical procedures for the precise analysis of Nd and Sm isotopic compositions in the last decade has led to an ever expanding use of this system in petrogenesis (e.g. DePaolo and Wasserburg, 1976; O'Nions et al., 1979; Hawkesworth and van Calsteren, 1983). The Sm/Nd system has an important advantage over the Rb/Sr system in the study of old, altered whole rocks because Nd is not mobile in hydrous phases. It is present in sea water in very low concentrations and, therefore, sub-seafloor alteration does not result in a change in the Nd isotopic composition of the rock. Neither is it sufficiently mobile under greenschist metamorphic conditions to be altered by later low grade metamorphism.

During the course of the present study, the Nd isotopic composition was determined for thirty-four selected samples, representing the complete range of lithological and geochemical variation in the Wild Bight Group volcanic and subvolcanic rocks. The purpose of the isotopic study was: 1) to further test the geochemical groupings to see whether the geochemically based correlations were supported by isotopic compositions; 2) to identify possible sources for the volcanic magmas and, in doing this, provide a basis for modelling the petrogenetic history of the individual geochemical groups and the Wild Bight Group magmatism as a whole.

The Nd isotopic compositions (Nd IC) were determined by thermal ionization mass spectrometry at the Max-Planck Institut fuer Chemie, Memorial University and the Geological Survey of Canada. Separation and concentration of Nd from whole rock powders was accomplished by a three-stage, ion exchange chromatographic technique described in detail in

Appendix 10. On all except six samples, the $^{147}Sm/^{144}Nd$ ratio was determined by isotope dilution on spiked aliquots of the same samples dissolved for Nd IC analysis. For the remaining six samples, this ratio was determined by Inductively Coupled Plasma - Mass Spectrometry (ICP-MS) at Memorial University of Newfoundland. Details of sample preparation, laboratory and analytical techniques, calculations, standard and blank analyses and duplicate data are in Appendix 10.

4.2 Nd Isotope Data Presentation

4.2.1 Introduction

There are seven naturally occurring, stable isotopes of Nd, having mass numbers 142, 143, 144, 145, 146, 148 and 150. Although there are three naturally occurring nuclides decaying to isotopes of Nd (^{147}Sm, ^{148}Sm, ^{149}Sm to ^{143}Nd, ^{144}Nd, ^{145}Nd, respectively), only the first is sufficiently short-lived (^{147}Sm half life ~ 10^{11} yr.) to produce a measurable variation in the daughter isotope over geological time.

The decay of ^{147}Sm to ^{143}Nd provides the basis for Sm-Nd isotope chemistry. Because isotopic ratios are more readily measured than are absolute abundances of single isotopes, the analyses are commonly reported as a ratio of the daughter isotope to one of the non-radiogenic isotopes of that element. In the case of Nd, the isotopic composition is commonly measured as the ratio $^{143}Nd/^{144}Nd$.

For any isotopic analysis by mass spectrometry, the data must be corrected for instrumental mass fractionation. In this study, all $^{143}Nd/^{144}Nd$ analyses are normalized to $^{146}Nd/^{144}Nd = 0.7219$, after O'Nions et al. (1979).

4.2.2 Measured Versus Initial Ratios

The measured $^{143}Nd/^{144}Nd$ ratio of an ancient rock reflects not only the petrogenetic history of that rock at the time it was formed but also the radioactive growth history of the rock from that time to the present. This presents a major limitation in the direct use of such data for comparisons with other rocks or with presumed reservoirs in the earth's crust or mantle. Direct

comparisons for petrogenetic purposes can be profitably made only with rocks of the same age or with reservoirs extant at the time the rock was formed.

The initial isotopic ratio (i.e., the isotopic composition at the time the rock was formed) can be calculated from the radioactive decay equations. Calculation of the initial ratios for the rocks and the possible source reservoirs allows a direct comparison of their isotopic compositions that is petrogenetically meaningful. For Nd, the appropriate expression is:

$$[^{143}Nd/^{144}Nd]_0 = [^{143}Nd/^{144}Nd] - [^{147}Sm/^{144}Nd][e^{\lambda t} - 1]$$

where $[^{143}Nd/^{144}Nd]$ and $[^{147}Sm/^{144}Nd]$ are measured, $[^{143}Nd/^{144}Nd]_0$ is the initial ratio at time = t (in Ma) and λ is the decay constant $6.54 \times 10^{-12}a^{-1}$.

4.2.3 Epsilon$_{Nd}$ and CHUR

In order to facilitate interpretation of the data, a common technique in the current literature is calculate the initial isotopic composition of the rocks (i.e. at the time they were formed) and to report this ratio relative to the isotopic composition of the bulk earth at this time. DePaulo and Wasserburg (1976) have developed a notation, currently in wide use, which facilitates comparison of Nd isotopic ratios of rocks and reservoirs at different times. They devised a number, termed "epsilon$_{Nd(t)}$", which expresses the fractional deviation of the isotopic composition of the sample from the isotopic composition of a uniform reservoir at any time, "t" million years ago. The uniform reservoir for Nd is generally designated as CHUR (Chondritic Uniform Reservoir) and is based on the best estimate for the composition of the bulk earth. The expression "epsilon$_{Nd}$", therefore, is an expression of the amount by which the isotopic composition of a rock at time = t differs from the theoretical composition of CHUR. It is expressed as:

$$epsilon_{Nd(t)} = \left(\frac{[^{143}Nd/^{144}Nd_{sample(t)}]}{[^{143}Nd/^{144}Nd_{CHUR(t)}]} \right) - 1 \times 10^4$$

where $[^{143}Nd/^{144}Nd]_{CHUR}$ today is 0.512638 and $[^{147}Sm/^{144}Nd]_{CHUR}$ is 0.1967.

As can be seen from this expression, epsilon$_{Nd}$ of CHUR at any time is 0. A rock that has $^{143}Nd/^{144}Nd_{(t)}$ > CHUR will have positive epsilon$_{Nd}$ while one with $^{143}Nd/^{144}Nd_{(t)}$ < CHUR wil have negative epsilon$_{Nd}$. The implications of this with respect to the evolution of the crust and interpreting mantle and petrogenetic processes in oceanic volcanic environments are explored in the following Section.

4.2.4 Estimation of t

In order to calculate the initial ratios for the rocks, as well as for CHUR and for possible reservoirs that may have figured in their petrogenesis, it is necessary to know the rocks' age. Because there is no direct date for the Wild Bight Group (see Section 2.3), a brief discussion is necessary on the choice of an age and the possible errors in the calculation of the initial ratios that are inherent in this choice.

The age of the Wild Bight Group is constrained by the age of the overlying Shoal Arm Formation, which contains a *Nemagraptus Gracilis* zone (late Llandeilian - early Caradocian) fauna (Chapter 2). According to the time scale of van Eysinga (1975), this represents an age of about 450 Ma but perhaps ranging from 445 Ma to 460 Ma. Accordingly, the initial ratios for the Wild Bight Group samples have been calculated at 465 Ma. There are two potential errors in this choice: 1) given the uncertainty of the absolute age of the fossil suite as well as the possibility that there may be an unrecognized, albeit short, hiatus between the Wild Bight Group and the Caradocian shale, the estimated age may be in error by as much as 15 to 20 Ma, and 2) the bottom of the group is undoubtedly somewhat older than the top and there may, therefore, be an inconsistency in assuming that rocks from these extremes have the same age.

In the first case, the stratigraphic continuity between the fossiliferous strata and the underlying Wild Bight Group render it unlikely that there is a substantial age gap between them. However, assuming that there may be a gap of as much as 15 Ma between the Caradocian shale

and the volcanic rocks (or that the absolute age of the shale may be in error by this much), the resulting changes in the calculated epsilon$_{Nd}$ of the rock are shown in Table 4.1 for selected samples representing a range of $^{143}Nd/^{144}Nd$ and $^{147}Sm/^{144}Nd$. The age difference does cause a small change in the absolute value of epsilon$_{Nd}$, but the difference is less than the uncertainty resulting from analytical errors in all cases (see Figure 4.2). Little change in the relative epsilon$_{Nd}$ of different samples results and the conclusions of this study would not be substantially affected by such an error.

The possibility that the top and bottom of the group are not precisely the same age is potentially more serious. In this case, the calculated epsilon$_{Nd}$ of samples at the bottom and top of the sequence may not be consistent with each other, or with theoretical reservoirs at the chosen time . It seems unlikely that the age range of the Wild Bight Group spans more than 20 Ma, based on comparisons with modern environments such as Fiji (see Chapter 6). A comparison of epsilon$_{Nd}$ for one sample from the basal Seal Bay Bottom suite calculated at 465 and 485 Ma is presented in Table 4.1. The difference in epsilon$_{Nd}$ is considerably less than analytical uncertainty. In fact, even if the bottom of the Wild Bight Group is as much as 45 Ma older than the top, the change in epsilon$_{Nd}$ is still less than the analytical uncertainty.

It is concluded on the basis of the above discussion that possible errors in the estimation of the age of the Wild Bight Group do not substantially affect the calculation of epsilon$_{Nd}$, nor the interpretations that arise from using it in petrogenetic arguments that follow.

4.3 Nd Isotopes as Petrogenetic Tracers

4.3.1 Nd Isotopes and the REE

Radiogenic isotopes are a powerful tool in interpreting the petrogenesis of magmatic rocks. Studies in modern volcanic environments have provided a wealth of information concerning the Nd isotopic composition of volcanic rocks in various tectonic environments and these have in turn

Table 4.1: Representative errors as a result of uncertainties in estimating "t"

A - Errors arising from uncertainty in absolute age
Samples with a range of epsilon Nd and 147Sm/144Nd are recalculated at various ages.

sample No.	t (Ma)	147Sm/144Nd	epsilon Nd
2140467	450	0.151	0.7
	465	0.151	0.8
	480	0.151	0.9
2140492	450	0.307	-0.7
	465	0.307	-0.9
	480	0.307	-1.1
2140532	450	0.222	7.2
	465	0.222	7.1
	480	0.222	7.1
2140497	450	0.162	5.4
	465	0.162	5.5
	480	0.162	5.6

B - Errors arising from possible age difference between top and bottom of the sequence
One sample from the bottom of the sequence is recalculated to possible older ages

Sample No.	t (Ma)	epsilon Nd
2140553	465	1.19
	480	1.27
	500	1.38

led to speculations concerning the isotopic composition of various possible magmatic sources in the mantle and crust. The isotopic composition of Nd in any long-term reservoir is, of course, principally dependent on its LREE contents. Let us consider the fractionation of the REE through earth history and its impact on Nd isotopic compositions in various reservoirs.

The primeval earth is believed to have been approximately chondritic in REE composition. Processes that have tended to differentiate the earth into crust and mantle have also tended to fractionate the REE. The LREE, being larger and more incompatible than the HREE, have tended to be fractionated into the continental crust and the result has been generation of continental crust with a marked LREE-enrichment and a broadly complementary mantle with a marked LREE-depletion (on a chondrite-normalized basis). This is clearly an oversimplification of the actual case but will serve to illustrate the relationship between the REE and Nd isotopic compositions.

Rocks that have spent a considerable part of their history in a LREE-depleted environment (i.e. normal depleted mantle) will have experienced an isotopic growth in an environment where the Sm/Nd ratio is greater than that in CHUR. This means that in this environment, relatively more ^{147}Sm will decay to ^{143}Nd than will occur in CHUR and, given time, the LREE-depleted region will develop a $^{143}Nd/^{144}Nd$ ratio that is increasingly higher than that in CHUR. Expressed another way, epsilon$_{Nd}$ of a time-integrated, LREE-depleted, reservoir will be positive and become more so with time.

The reverse is true for reservoirs that have a time-integrated LREE-enrichment. The Sm/Nd ratio in this case is lower than that of CHUR leading to a relative underabundance of $^{143}Nd/^{144}Nd$ with time. Epsilon$_{Nd}$ in this situation will be negative and will become more so with time.

Petrogenetic relationships in modern volcanic rocks are generally consistent with these interpretations. The fact that most oceanic basalts have positive epsilon$_{Nd}$, the generally higher $^{143}Nd/^{144}Nd$ of mid-ocean ridge basalts compared to those in other environments and the

strong negative correlation between $^{143}Nd/^{144}Nd$ and $^{87}Sr/^{86}Sr$ all argue for widespread, LREE-depleted, sources in the mantle. Strongly negative epsilon$_{Nd}$ in old crustal rocks argues for LREE-enriched sources there. However, there are additional complexities. For example, the mantle apparently contains LREE-enriched as well as LREE-depleted sources, continuing crustal evolution has occurred in sources with varying degrees of LREE-enrichment and experiencing radioactive growth over various time periods, and the juxtaposition of multiple sources in subduction zone environments can provide complex possibilities for source melting and mixing.

In the following Sections, and before presenting the data for the Wild Bight Group, a brief review of possible sources for oceanic volcanic rocks is presented. The expected isotopic characteristics are reviewed and integrated with trace element characteristics where this can provide further constraints on interpreting the petrogenetic history of the rocks. The trace elements are discussed, as much as possible, with reference to Figure 4.1, where extended REE plots for some typical oceanic basalt types are presented.

4.3.2 The Heterogeneous Mantle

Geochemical and isotopic evidence have unequivocally established that the mantle is chemically and isotopically heterogeneous. However, there is no good agreement on the nature of the various mantle components, their size, physical structure or their chemical and isotopic compositions and histories.

The most voluminous basalt type erupted at oceanic constructional plate margins is a LREE-depleted tholeiite with strongly positive epsilon$_{Nd}$ (present day epsilon$_{Nd}$~+10) which is commonly termed typical mid-ocean ridge basalt or MORB. The ubiquitous eruption of this rock type in such a setting has been widely interpreted to mean that the upper mantle comprises mainly peridotite which has experienced a long-term depletion in the LREE and other incompatible elements (Sun et al., 1979; Morris and Hart, 1983; Davies, 1984; White and Patchett, 1984).

However, in this setting, and in intra-plate oceanic settings, basalts are commonly erupted
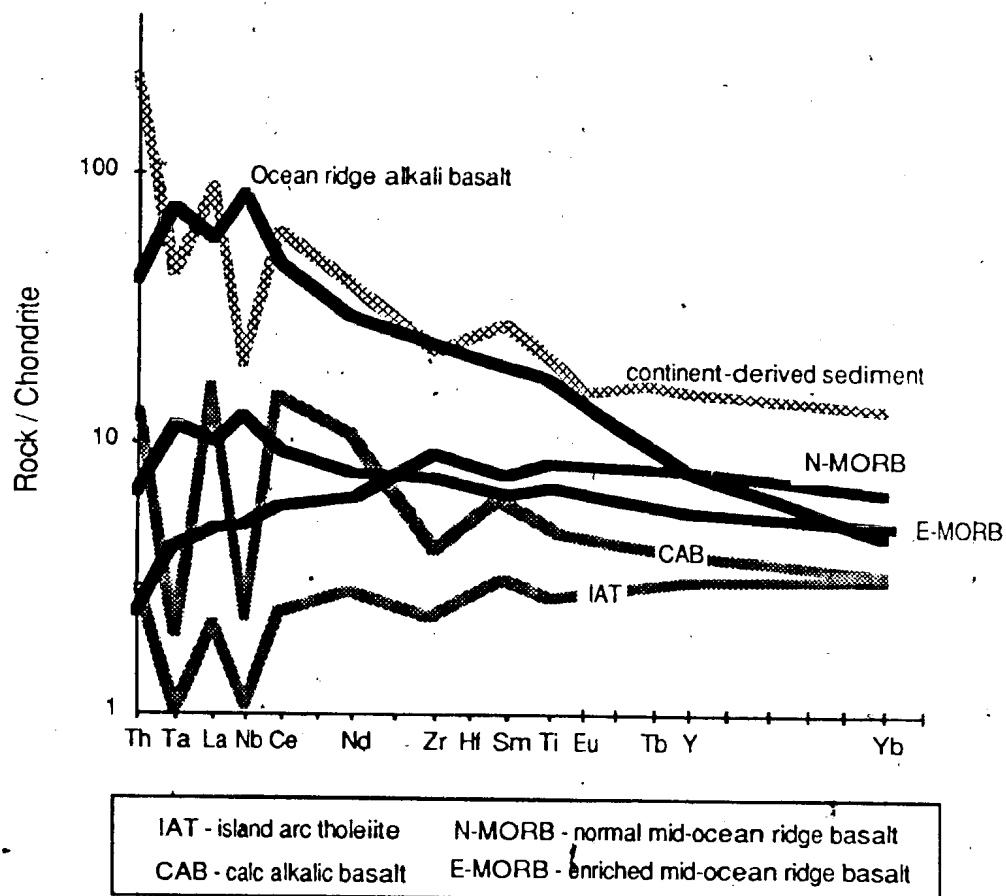
Figure 4.1: Typical extended REE patterns for oceanic basalts of different types after Sun (1980) and a typical continent-derived oceanic sediment from Hole et al. (1984). Island arc rocks are in stippled lines, non-arc rocks in black lines, and sediment is hatched line. Note prominent negative Ta and Nb anomalies and high Th in arc rocks and the continentally-derived sediment.

with relatively flat to LREE enriched patterns and epsilon$_{Nd}$ which is most commonly in the range +4 to +8 but locally somewhat lower and, in some cases, slightly negative. This appears to require that the mantle contains less voluminous heterogeneities, on both small and large scale, which have experienced time-integrated LREE enrichment (recently fully discussed by Zindler and Hart, 1986). Early conceptual models viewed the heterogeneous mantle as layered, with a depleted upper mantle underlain by a lower mantle of approximately primordial (undepleted) composition (e.g. Schilling, 1973; Wasserburg and DePaolo, 1979). The ascent of magmatic plumes from the latter provided relatively LREE-enriched magmatic sources which generated "enriched" or "plume"-type magmas (e.g. Schilling, 1973; Schilling et al., 1977; Sun et al., 1979) with LREE-enriched trace element characteristics and epsilon$_{Nd}$ considerably lower than MORB. The notion of a two-source mantle reservoir has been largely discredited by the recognition of mantle sources in oceanic islands which must have been significantly enriched in one or more isotopic systems relative to the theoretical primordial mantle (e.g. Hawkesworth et al., 1979; Zindler et al., 1979; Jenner et al., 1987). The recognition that oceanic islands appear to fall into four or five well defined isotopic groups has led some workers to suggest that these represent distinct types of mantles sources (e.g. White, 1985; Zindler and Hart, 1986).

These types of relatively enriched mantle sources have generally been termed ocean island basalt (OIB) sources, and yield LREE-enriched magmas that are typified by the E-MORB and oceanic island alkali basalt curves in Figure 4.1. In terms of trace element characteristics, they are characterised by smooth extended REE patterns with LREE-enrichment and a maximum between Ba and the LREE. In particular, the LREE, Ta and Nb have approximately equivalent normalized abundances in these rocks.

Relatively small scale heterogeneities in the upper mantle are generally viewed as veins or blobs of enriched material floating in depleted mantle. Wood (1979) envisaged a veined upper mantle cut on centimeter scale by partial melts of primordial mantle. Other workers have considered veining of the depleted mantle to be a result of interaction with mantle plumes (e.g. Schilling et al., 1985; LeRoex et al., 1987). Alternatively, the "plum-pudding" model (Davies,

1981, 1984; Morris and Hart 1983) views the mantle as riddled with "plums" of enriched material, either undepleted lower mantle material that has ascended into the depleted mantle region and frozen there (Davies, 1984; Alfegre and Turcotte, 1985), oceanic lithosphere and sediment recycled into the mantle by subduction (e.g. Chase, 1981; Hoffman and White, 1982; Cohen and O'Nions, 1982), the result of ubiquitous mantle heterogeneities (e.g. Sleep, 1984) or the result of mantle metasomatism (Bailey, 1970; Menzies and Murthy, 1980). Whether veins or plums, these sources would be enriched in the highly incompatible elements including the LREE and, therefore, have lower epsilon$_{Nd}$ than depleted mantle; mixing of these sources with depleted mantle could produce a spectrum of compositions (both geochemical and isotopic) depending on, among other things, the degree of partial melting, the variability of compositions of both depleted mantle and enriched heterogeneities in any given area, the proportions in which the various sources contribute to the melt and their subsequent crystallization history. These compositions are reflected in the wide variety of magmas erupted at oceanic island and enriched spreading ridge segments.

4.3.3 Sources of Island Arc Tholeiites

4.3.3.1 General Statement

The presence of the subducting slab in island arc environments presents an additional complication and introduces further possibilities for magma generation in arc environments. A wide variety of volcanic rocks has been documented in island arc environments although the most voluminous are calc alkalic andesites and island arc tholeiitic andesite and basalt. Likewise, there is a wide range of isotopic compositions, ranging from near +10 to strongly negative, suggesting that both time-integrated, LREE-enriched and LREE-depleted sources are variously involved in magma generation in this environment. Trace element signatures are also characteristic (Figure 4.1). In particular, there is commonly the strong underabundance of the highly incompatible HFSE and the overabundance of the LFSE with respect to the LREE. This leads to the characteristic extended REE pattern with pronounced negative Ta and Nb anomalies

illustrated in Figure 4.1.

The belief that calc alkalic andesite is the principal rock type in island arc environments led early workers to propose island arc petrogenetic models based mainly on melting of oceanic lithosphere in the subducted slab (e.g., Coats, 1962; Green and Ringwood, 1968). When subsequent studies showed that in fact island arc tholeiitic magmas dominate many active orogenic areas (e.g. Jakes and White, 1971; Ewart et al., 1973; Gill, 1974; Jakes and Gill, 1970) attention was focussed on models involving melting of peridotite in the mantle wedge above the subduction zone (e.g. Nicholls and Ringwood, 1973; Ringwood, 1974; Gill, 1981).

Although it is generally accepted by petrologists that depleted mantle with element ratios and isotopic characteristics of MORB is the principal source of island arc tholeiitic magmas (Ringwood, 1982, Kay, 1980; Green, 1980; Arculus and Johnson, 1981; White and Patchett, 1984; Arculus and Powell, 1986; Zindler and Hart, 1986), it is recognized that variations in geochemical and isotopic features of the magmas commonly require additional components. From these variations have sprung the current generation of complex, multi-stage petrogenetic models (e.g. Gill, 1970, 1974; Armstrong, 1971; Whitford et al., 1979; Sun, 1980; Kay, 1980; Gill, 1981; Arculus and Johnson, 1981; Arculus and Powell, 1986) involving partial melting of various source components in the mantle wedge, the subducting slab and the basal island arc crust. Within each of these potential source regions, there are complex possibilities for generation of melts of different characteristics through varying degrees and types of partial melting, mixing and fractional crystallization. Some of the pertinent points concerning source regions and their potential affect on melt characteristics are briefly considered below.

4.3.3.2 The Mantle wedge

The mantle wedge is inferred to consist mainly of depleted peridotite with geochemical and isotopic characteristics similar to the source for MORB, with both small and large scale heterogeneities as discussed above. Interaction between depleted mantle and melts and/or hydrous fluids from the slab allow for generation of additional heterogeneities, as envisaged, for

example, by Arculus and Powell (1986) who postulated veins in the depleted mantle formed by metasomatic enrichment from the subducting slab and multiple melting/freezing episodes during mass transport within the mantle wedge.

Mixing of enriched sources with partial melts of depleted peridotite has been suggested by some workers to be capable of producing the complete spectrum of compositions found in island arc magmas (e.g. Arculus, 1981; Stern, 1981; Morris and Hart, 1983).

4.3.3.3 The subducting slab

The effect of the slab in island arc tholeiitic magmas may be manifested in enrichment of alkali and alkaline earth elements, derived from altered oceanic crust or the overlying sedimentary layer and in the presence of continental crustally-derived material in subducted sediments. These components may be transported either magmatically or by hydrous fluids into the depleted mantle.

It is generally accepted that sediments overlying oceanic lithosphere may be carried into the subduction zone on the descending plate. (e.g. Karig and Kay, 1981; White and Hoffman, 1982). The subducted sediment would be expected to have the isotopic and trace element characteristics of the continental crust from which it is principally derived. These would include a strongly negative epsilon$_{Nd}$ (reflecting long-term residence in LREE-enriched crust) and negative normalized Ta and Nb anomalies with respect to the LREE. It is this trace element characteristic that distinguishes material with negative epsilon$_{Nd}$ derived from continental sources from those representing LREE-enriched mantle sources unrelated to the crust.

The influence of this sediment on the geochemical and isotopic characteristics of island arc magmas has been demonstrated in a number of modern island arcs where isotopic and geochemical variations in the magmas can be explained by the addition of a small amount (generally less than a few percent) of subducted sediment to modelled melts of depleted peridotite (e.g. the South Sandwich Islands, Cohen and O'Nions, 1982; Aleutian Islands, Kay *et al.*, 1978; von Drach *et al.*, 1986; Marianas, Meijer, 1976; Hole *et al.*, 1984; Lesser Antilles,

Davidson, 1983; Tonga, Kay, 1980). A major difficulty in modelling the effect of subducted sediments is the considerable variation in geochemical and isotopic compositions of sea-floor sediments in the modern oceans (Kay, 1980; White et al., 1985). On a broad scale, the detrital component of average oceanic sediment is expected to approach the average continental crust compositions and it has been shown by McLennan and Taylor (1981) that mixing of average Australian post-Archean shale with MORB or MORB-sources can successfully reproduce many of the geochemical features of island arc basalts. In particular, subducted sediment has been invoked by some workers to explain the prevalent high LFSE/HFSE ratios in most island arc lavas, either through direct mixing of this sediment in the magmas or through fluid transport of the more soluble LFSE elements into the mantle wedge, metasomatizing the magma sources with a fluid of even higher LFSE/HFSE ratios (e.g the "IRS fluid" of Gill, 1981). Precise interpretation of the structure of island arc magmas, however, requires a detailed knowledge of the subducted sediment, which may locally differ considerably from average crust because of local anomalous crustal sources, presence of a significant arc-derived component or an abundant authigenic component (e.g. White et al., 1985; Hole et al., 1984) This, of course, poses a particularly serious problem in the case of ancient island arcs, where close analogues of the subducted sediments can seldom be identified.

Mixing of subducted sediments and MORB sources cannot explain all of the features of island arc magmas. In particular, anomalous variations in $^{87}Sr/^{86}Sr$ with respect to $^{143}Nd/^{144}Nd$ (DePaolo and Wasserburg, 1977; O'Nions et al., 1977) and the high alkali and alkaline earth abundances with respect to the REE (Kay, 1980; White and Patchett, 1984) have led these and other authors to suggest the involvement of sea water. The most likely contributor is subducted oceanic crust that has been hydrothermally altered on the sea floor. The mass transfer may occur either through partial melting on the top of the slab and ascent of the resulting melt (e.g. Kay, 1980; Marsh, 1979; von Drach et al., 1986) or through the action of fluids evolved during dehydration of the slab as suggested by Ringwood (1974) (see also Anderson, et al., 1979; Hawkesworth et al., 1979; White and Patchett, 1984 and references therein).

4.3.3.4 The sub-arc crust

Although a contribution from sub-arc crust is not required for many island arc tholeiites, interaction with such crust could explain some geochemical features of these lavas. This is particularly true of lavas erupted through continental margins (e.g. Tilton and Barriero, 1980; Leeman, 1983) but less likely to be a factor in intra-oceanic arcs (Arculus and Powell, 1986). Davidson (1983, 1986) has suggested that some Lesser Antillean magmas interacted with sub-arc crust that included interbedded sediments with a continental detrital component during ascent. This provides a possible mechanism for contamination of intra-oceanic arc magmas.

4.4 Nd Isotope Data

4.4.1 Introduction

The Nd isotope data for the Wild Bight Group samples are given in Table 4.2 and plotted on Figures 4.2 and 4.3. For each sample, the measured and calculated initial ratios (at t = 465 Ma) are given together with epsilon$_{Nd}$. The estimated precision is displayed as error bars in epsilon$_{Nd}$ in Figures 4.2 and 4.3.

As was the case for geochemical characteristics, there is a wide range of Nd isotopic compositions in the Wild Bight Group. The isotopic data show some interesting variations, both between the previously identified geochemical groups and within them.

4.4.2 Variation in Nd Isotopes Between Groups

All of the geochemical groups defined in Chapter 3 show distinctive and, for the most part, mutually exclusive, Nd isotopic characteristics. Some of the features of the between-group variations on Figure 4.2 are summarized below:

1) Most rocks of island arc affinity, excluding the felsic volcanic rocks and the Nanny Bag Lake Suite, have lower epsilon$_{Nd}$ than most of the rocks of non-arc affinity. Those arc rocks with

Table 4.2 Nd and Sm isotope ratios for Wild Bight Group whole rock samples

Sample No.	Suite	143Nd/144Nd(m)	143Nd/144Nd(i)	147Sm/144Nd	epsilon Nd(t)
IAD GROUP					
2140476	Glover's Hbr. W.	0.513072 ±24	0.51226	0.266	4.3
2140456	Glover's Hbr. W.	0.512975 ±15	0.51229	0.226	4.8
2140458	Glover's Hbr. W.	0.512916 ±14	0.51213	0.257	1.9
2140473	Glover's Hbr. W.	0.512924 ±14	0.51219	0.242	2.9
2140492	Indian Cove	0.512927 ±26	0.51199	0.307	-0.9
2140526	Side Harbour	0.512938 ±14	0.51216	0.255	2.4
2140465	IAD intrusive	0.512742 ±13	0.51198	0.251	-1.2
IAI GROUP					
2140467	Glover's Hbr. E.	0.512539 ±17	0.51208	0.151	0.8
2140463	Glover's Hbr. E.	0.512594 ±8	0.51211	0.158	1.4
2140774	Northern Arm	0.512628 ±9	0.51216	0.153	2.4
2140532	Nanny Bag Lk.	0.513078 ±22	0.51240	0.222	7.1
2140544	Nanny Bag Lk.	0.512958 ±8	0.51234	0.204	5.8
2140553	Seal Bay Bottom	0.512569 ±11	0.51210	0.154	1.2
2140756	Seal Bay Bottom	0.512567 ±12	0.51212	0.146	1.6
2140496	IAI intrusive	0.512593 ±27	0.51216	0.143	2.3
2140512	IAI intrusive	0.512505 ±10	0.51205	0.151	0.1
FELSIC VOLCANIC ROCKS					
2140453	Glover's Hbr.	0.512941 ±12	0.51233	0.202	5.6
2140538	Nanny Bag Lk.	0.512958 ±11	0.51229	0.220	4.9
NAI GROUP					
2140503	Badger Bay	0.512992 ±28	0.51243	0.184	7.6
2140506	Badger Bay	0.512825 ±8	0.51235	0.156	6.0
2140511	Big Lewis Lake	0.512901 ±35	0.51235	0.180	6.1
2140491	NAI intrusive	0.512770 ±7	0.51231	0.151	5.3
NAT GROUP					
2140497	New Bay	0.512812 ±17	0.51232	0.162	5.5
2140546	Side Hbr.	0.512824 ±7	0.51240	0.141	7.0
2140549	Side Hbr.	0.512750 ±12	0.51230	0.149	5.0
2140762	Side Hbr.	0.512833 ±14	0.51237	0.152	6.5
2140773	Northern Arm	0.512713 ±9	0.51228	0.143	4.7
2140481	NAT intrusive	0.512820 ±24	0.51235	0.155	6.1
2140502	NAT intrusive	0.512734 ±9	0.51233	0.132	5.7
NAE GROUP					
2140509	Big Lewis Lake	0.512672 ±36	0.51228	0.127	4.8
2140483	Seal Bay Head	0.512759 ±7	0.51233	0.141	5.7
2140763	Side Harbour	0.512702 ±6	0.51231	0.127	5.4
2140454	NAE intrusive	0.512719 ±24	0.51230	0.139	5.0

143Nd/144Nd(m) - measured; quoted errors are twice the standard error of the mean,
based on in-run statistics
143Nd/144Nd(i) - initial
Data are fractionation corrected to 143Nd/144Nd = 0.7219.
λ =6.54x10(-12)a(-1)
143Nd/144Nd(CHUR) today is 0.512638, 147Sm/144Nd(CHUR) today is 0.1967
t = 465 Ma.
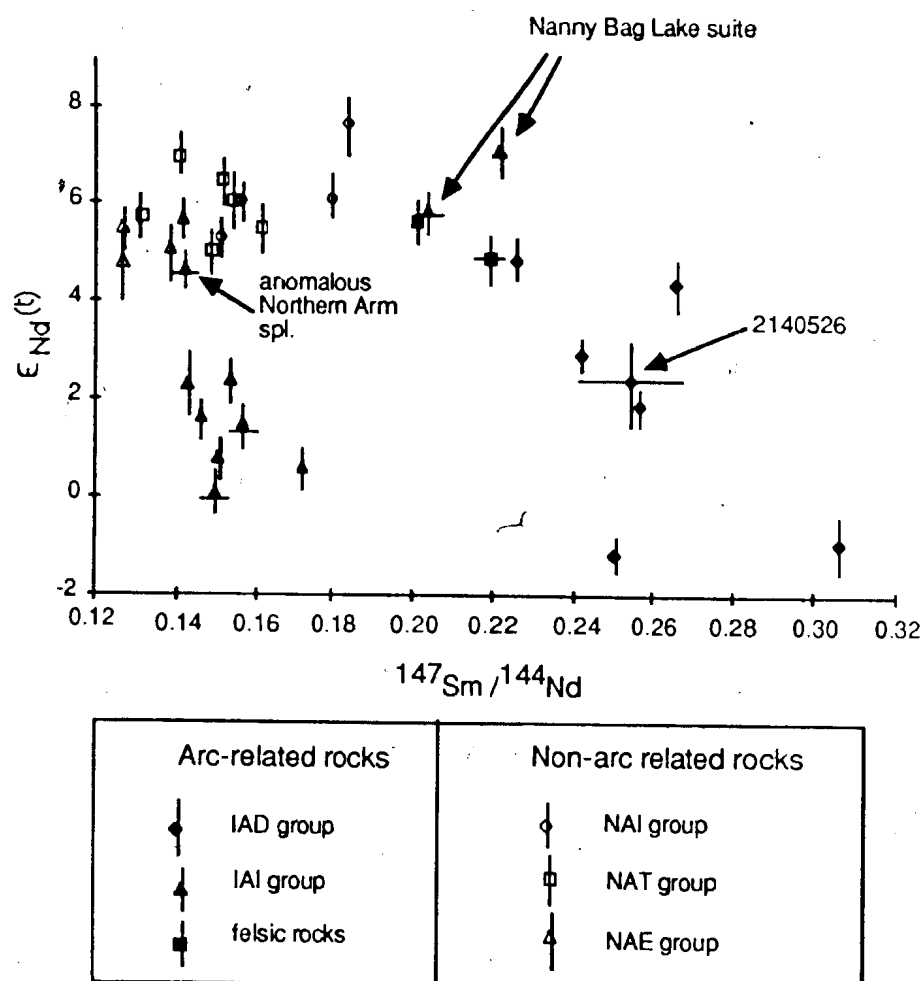
Figure 4.2: Nd isotopic composition of Wild Bight Group volcanic and subvolcanic rocks. Horizontal errors are negligible except for those analyses by ICP-MS where ±2% error bars are shown. Sample 2140526 has horizontal error bar of ±5% (see Appendix 10). Vertical error bars are twice the standard error of the mean, based on in-run statistics, or ±0.000015 on the measured 143Nd / 144Nd ratio, whichever is greater. Error in epsilon Nd due to imprecision in ICP-MS analyses is less than the analytical uncertainty for errors of ±2%. For sample 2140526, error in epsilon Nd due to uncertainty in 147Sm / 144Nd is greater than analytical uncertainty and constitutes the vertical error bar.
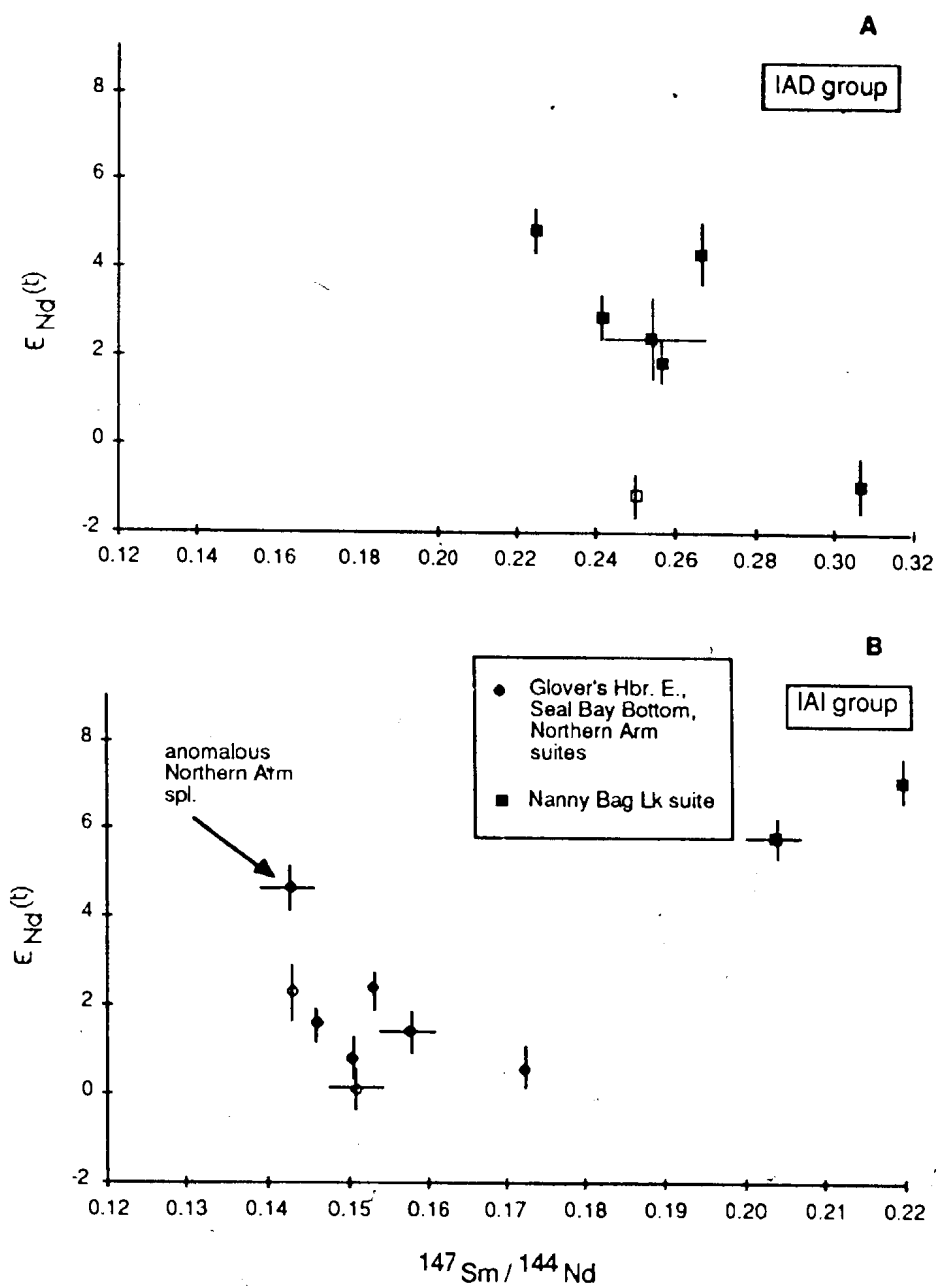
Figure 4.3: Detailed plots of isotopic compositions by groups. Closed symbols are volcanic, open symbols intrusive. Note expanded horizontal scale in B and C. Error bars as for Figure 4.2.
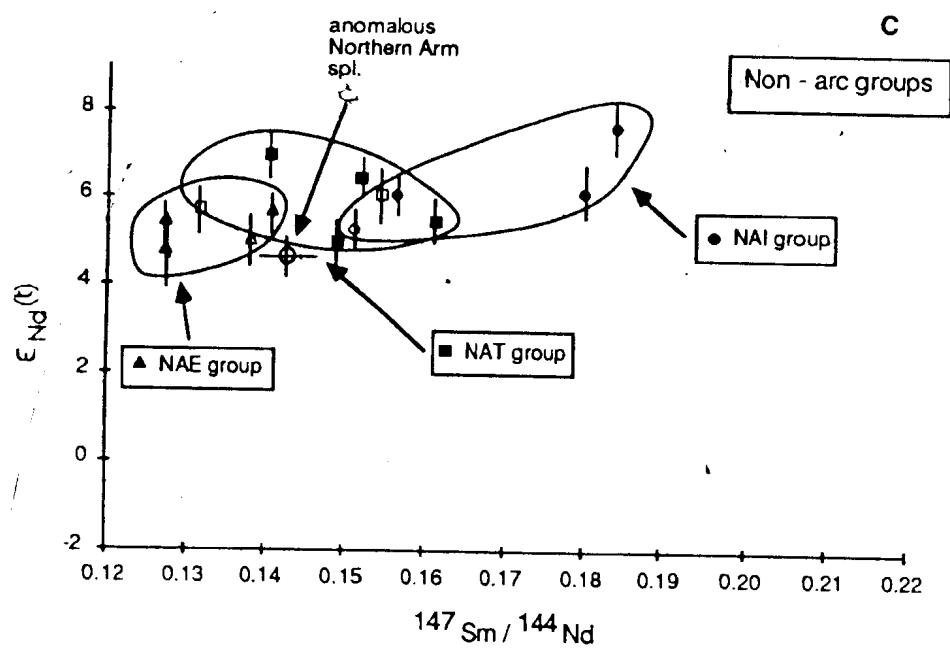
Figure 4.3 (continued)

epsilon$_{Nd}$ > +4 are more LREE depleted than the non arc rocks and rocks from the two settings

do not generally overlap on Figure 4.2.

2) The Nanny Bag Lake Suite, consistent with its geochemical characteristics, is isotopically

distinct from the other IAI group suites. It is characterised by higher epsilon$_{Nd}$ and lower

$^{147}Sm/^{144}Nd$ than the other IAI group suites.

3) Felsic volcanic rocks, although represented by only two samples, appear to be

characterised by relatively high epsilon$_{Nd}$, intermediate between those typical of the Nanny Bag

Lake Suites and the other island arc suites. Having a slight LREE-depletion, these rocks plot near

both the Nanny Bag Lake suite and part of the IAD group.

4) Within the non-arc suites, there is a tendency for maximum epsilon$_{Nd}$ to increase from the

alkalic NAE group through the transitional NAT group to the non-alkalic NAI group tholeiites.

4.4.3 Variation of Nd Isotopes Within Groups

In all geochemical groups, there are sufficient isotopic determinations to evaluate not only

the general compositions but also trends within them. Some of the significant within-suite

variations in isotopic composition are displayed on Figure 4.2, where some of the groups have

been plotted separately and with expanded scales:

i) *IAD group*: This group has the widest variation in epsilon$_{Nd}$ of any of the groups, ranging

from +4.9 to -0.9. A striking feature of this group is the good negative correlation between

epsilon$_{Nd}$ and $^{147}Sm/^{144}Nd$.

ii) *IAI group*: The dichotomy between the Nanny Bag Lake suite and the Glover's Harbour

East, Seal Bay Bottom, Northern Arm suites, identified geochemically in Chapter 3, is further

emphasized by the Nd isotopes. The former has epsilon$_{Nd}$ between approximately +6 and +7

while the latter plot together at relatively low epsilon$_{Nd}$ (+0.1 to +2.4). In the former, there is a

positive correlation between epsilon$_{Nd}$ and $^{147}Sm/^{144}Nd$ (although with only two samples!). In

the latter, there is a suggestion of a negative epsilon$_{Nd}$ - ^{147}Sm/^{144}Nd correlation; however, this is effectively a two-point line, strongly controlled by one point with relatively high ^{147}Sm/^{144}Nd, and, as in the case of the Nanny Bag Lake Suite, should be interpreted as a trend with caution.

The isotopic compositions provide further evidence for conclusions about the Northern Arm Suite, reached on the basis of geochemistry in Chapter 3. First, the isotopic similarity of sample No. 2140774 and the Glover's Harbour East and Seal Bay Bottom samples supports the correlation of most of the samples in this suite with the IAI group suites. Secondly, the distinctly higher epsilon$_{Nd}$ of sample 2140773 causes it to plot with the NAT group, further evidence for the interpreted dichotomy in this suite and for the coexistence of island arc and non-arc rocks within it.

iii) *Felsic volcanic rocks:* Although there are only two samples, their epsilon$_{Nd}$ is higher than most of the arc-related rocks. There may be a negative epsilon$_{Nd}$-^{147}Sm/^{144}Nd correlation, although this needs to be confirmed with more samples.

iv) *NAI group:* The LREE-depleted varieties in this group have higher epsilon$_{Nd}$ than the LREE-enriched types (Chapter 3) producing a positive correlation between epsilon$_{Nd}$ and ^{147}Sm/^{144}Nd within this group.

v) *NAT group:* Despite a variable ^{147}Sm/^{144}Nd, these rocks do not appear to show any consistent correlation between epsilon$_{Nd}$ and ^{147}Sm/^{144}Nd. They overlap the isotopic composition of both the NAI and NAE groups.

vi) *NAE group:* These samples have the most restricted ^{147}Sm/^{144}Nd range of the non-arc groups and their epsilon$_{Nd}$ range overlaps with most of the NAT group. There is no consistent variation of epsilon$_{Nd}$ with ^{147}Sm/^{144}Nd.

A final observation concerning Figure 4.3 is that the intrusive rocks generally plot with the

mafic rocks of the group to which they were assigned on geochemical grounds. This is further evidence that they are subvolcanic and petrogenetically related to the intrusive rocks.

4.5 Petrogenesis of Rocks of Island Arc Affinity

4.5.1 Introduction

In this and the following Sections (4.4, 4.5), an attempt is made to model the petrogenesis of the Wild Bight Group volcanic rocks in terms of the isotopic and geochemical compositions of the observed rocks and a minimum number of hypothetical sources.

The discussion generally follows a two-fold approach. The first is numerical; the REE and Nd isotopic composition of a minimum number of hypothetical sources are used to calculate partial melting-mixing models that correspond to the isotopic and REE compositions of the various observed groups and suites. Mixing calculations are carried out using the equations of Langmuir et al. (1978). The second is more schematic, in which the various sources and the observed rocks are plotted on a Nd-Sm isochron diagram and possible mixing and partial melting relationships are illustrated.

The source characteristics for the island arc suites are described in Section 4.5 2. Some of these are also used to model the non-arc suites in Section 4.6. Additional sources postulated for these suites are introduced in that Section.

4.5.2 Model Parameters

The choice of source parameters is problematic in modelling the genesis of ancient rocks. There is no unanimous agreement in the literature as to the composition of either depleted mantle or the various heterogeneities within it that are needed to account for the wide range of compositions of oceanic, within plate eruptives (e.g. Zindler et al., 1984; White, 1985; Zindler and Hart, 1986). In addition, there is considerable debate as to whether primitive mantle actually exists (e.g. Davies, 1984; Zindler and Hart, 1986). In the present case, actualistic modelling of the magmatism is further hindered by the fact that only one isotopic system is available and that

mineral phases that have, from geochemical evidence, played a part in the fractionation history of the rocks, are not preserved in the observed samples.

Although it is unlikely, given these problems, that precise models of Wild Bight Group magma genesis can be formulated, generalized models can be derived that illustrate possible mechanisms of magma genesis. In the following discussion, the approach has been to use reasonable approximations of assumed mantle sources in various partial melting/mixing models in an attempt to generate an approximation to the observed REE patterns and isotopic compositions. The models are further constrained by HFSE and compatible element characteristics as well as interpretations of tectonic environment and fractionation histories that have been presented earlier in this thesis. The aim of this modelling is to illustrate a reasonable scenario by which the observed compositions could be derived and to integrate these in a general model for magma genesis in the Wild Bight Group.

For the purposes of modelling the suites of island arc affinity, three mantle sources are used: 1) typical depleted mantle; 2) a refractory mantle source termed 'highly depleted mantle'; and 3) a highly enriched source (strong LREE-enrichment, negative $epsilon_{Nd}$). This may be either a crustal source, recycled crustal material or a time-integrated, LREE-enriched source of unknown origin in the mantle. Isotopic data alone might not be able to distinguish between enriched crustal and non-crustal sources. However, the former will also be characterised by negative Nb and Ta anomalies on the extended REE plots (Figure 4.1) while the latter will not.

Various workers have presented calculated or assumed compositions for various mantle components and used these for petrogenetic modelling. For the present purposes, the compilations of McLennan and Taylor (1981) are used. The derivation of these values, described in more detail in McLennan and Taylor (1981), can be summarized as follows:

i) A value for MORB was arbitrarily taken as 15 x chondrite for the HREE and 7 x chondrite for the LREE;

ii) Depleted mantle (DM) was taken as a factor of ten lower than MORB in the HREE and slightly more than this in the LREE;

iii) Values for highly depleted mantle (HDM) were taken as 0.2 x chondritic in the LREE and 0.15 x chondritic in the HREE. This is meant to represent a depleted mantle source that has been partially melted and an island arc tholeiitic basalt removed.

McLennan and Taylor (1981) used the average post-Archean Australian shale (PAAS, after Nance and Taylor, 1977) to represent the average composition of crustal sources.

The hypothetical REE compositions of these sources are tabulated in Table 4.3 and illustrated in Figure 4.4, with comparisons to representative analysed or calculated sources taken from the literature. Epsilon$_{Nd}$ is taken as +7.6 for MORB at 465 Ma (calculated using present day MORB composition epsilon$_{Nd}$ = +10 and $^{147}Sm/^{144}Nd$ = 0.24), 0 for primitive mantle and -8 for crustal sources, based on an average value of approximately -12 for continentally-derived sediments in modern oceans (e.g. White et al., 1985) recalculated to 465 Ma.

In the schematic modelling diagrams (Figures 4.6, 4.11, 4.17, 4.20, 4.24), DM has been assigned a field that encompasses most of the expected variation in this source. The limits of this field are calculated using an estimated peak range of epsilon$_{Nd}$ values for MORB (0.51305 to 0.51325) from the compilation of Morris and Hart (1983) recalculated to 465 Ma using $^{147}Sm/^{144}Nd$ = 0.23. The range of $^{147}Sm/^{144}Nd$ encompasses slight to moderate LREE-depletion and is within the field for oceanic tholeiites presented by Zindler and Hart (1986). The HDM field is the DM field, repositioned according to the Sm/Nd ratio in the HDM source (Table 4.2). The field of the enriched source is based on the composition discussed in the previous paragraph allowing for a variation of ±2 in epsilon$_{Nd}$. The variation in epsilon$_{Nd}$ in this field underestimates the actual range in oceanic sediments but is appropriate for illustrative purposes.

In the following discussion, the IAI group is treated first as it is more easily explained by straightforward melting and mixing processes. This allows the approach to be introduced in relatively simple models. The IAD group, which requires more complex arguments, is then discussed.

Table 4.3: Compositions of sources used in petrogenetic modelling (ppm)
Origin of source compositions referenced in text.

	DM	HDM	PAAS
La	0.184	0.0110	38.0
Ce	0.622	0.0479	80.0
Nd	0.676	0.0604	32.0
Sm	0.277	0.0277	5.6
Eu	0.113	0.0122	1.1
Tb	0.082	0.0104	0.8
Yb	0.372	0.0496	2.8

DM - depleted mantle
HDM - highly depleted mantle
PAAS - Post-Archean average Australian shale
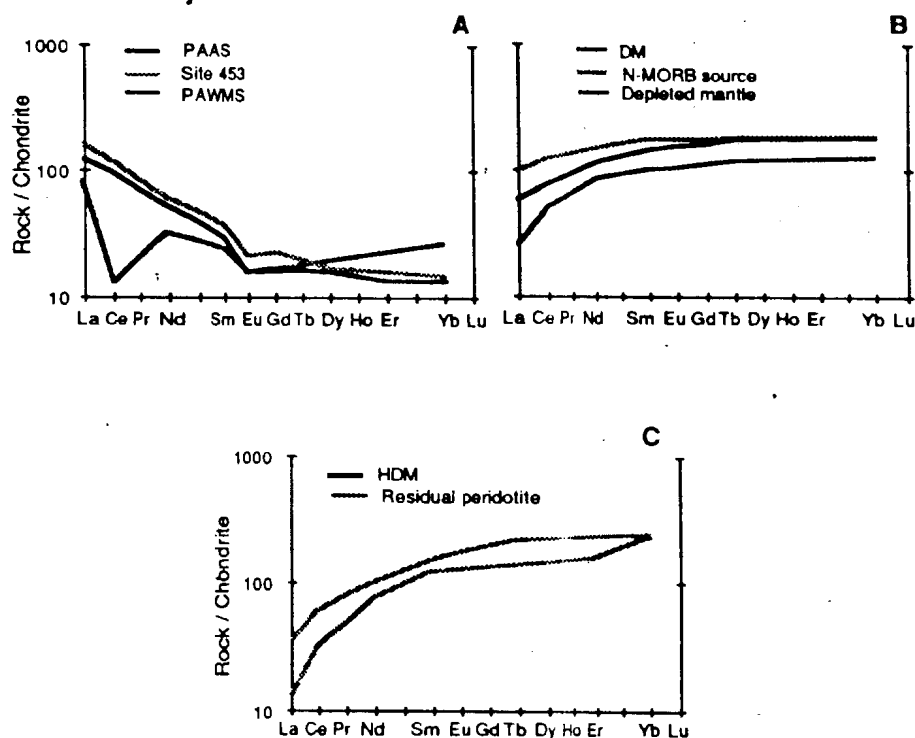
Figure 4.4: Source compositions used in modelling (black lines) and some comparisons with other estimates from the literature. See text for further explanation of McLennan and Taylor (1981) estimated values.

A - Average post - Archean Australian shale (PAAS) from Nance and Taylor (1977), compared with modern sediments on the ocean floor. "Site 456" is average of 6 continentally derived sediments from DSDP Site 453, southwest Atlantic from White et al. (1985); PAWMS is Pacific authigenic weighted mean sediment from Hole et al., 1984).

B - DM from McLennan and Taylor (1981), N-MORB source estimated by Wood (1979) and depleted mantle, calculated assuming 10% partial melting of observed N-MORB from the Costa Rica rift (Hole et al., 1984).

C - HDM from McLennan and Taylor (1981), residual peridotite from Kay (1980) calculated as residue in equilibrium with ocean floor basalt after 20% partial melting (ol:opx:cpx = 71:24.5:4.5).

4.5.3 The IAI group

4.5.3.1 General statement

The geochemical and isotopic characteristics of this suite clearly indicate a bipartite petrogenesis, the Nanny Bag Lake suite being different geochemically and isotopically from the Glover's Harbour East, Side Harbour and Northern Arm suites. Figure 4.5 contrasts the trace element relationships of these suites on extended rare earth plots. The principal features of these suites to be explained by any petrogenetic model include:

1) Epsilon$_{Nd}$ ranging between ~ +0.5 and +2.5 in the Glover's Harbour East, Seal Bay Bottom and Northern Arm Suites but greater than +5.8 in the Nanny Bag Lake Suite;

2) Mg# maximum of .64 but generally less than .6 indicating that there are probably no primary mantle liquids preserved;

3) Positive LREE slopes and pronounced negative Ta and Nb anomalies in the Glover's Harbour East, Seal Bay Bottom and Northern Arm Suites in which Nb* (normalized Nb value extrapolated from La and Ce)/Nb decreases with increasing REE abundances. Negative Ta and Nb anomalies are present but less prominent in the Nanny Bag Lake suite, which is LREE depleted. The highest concentrations of Ta and Nb in the Nanny Bag Lake Suite are similar to the lowest concentrations in the Glover's Harbour East, Seal Bay Bottom and Northern Arm Suites;

4) Slight negative Ti anomalies in the Glover's Harbour East, Seal Bay Bottom and Northern Arm Suites and slight positive anomalies in the Nanny Bag lake suite but similar Ti abundances in both suites;

5) Flat HREE patterns of similar abundances in all suites.

The correspondence in Ta, Nb, Ti and HREE abundances between the two magma types suggests that a unified model should be sought to explain the two. The fact that the LREE-depleted Nanny Bag Lake suite has epsilon$_{Nd}$ only slightly less than MORB while the Glover's Harbour East, Seal Bay Bottom and Northern Arm Suites have much lower values
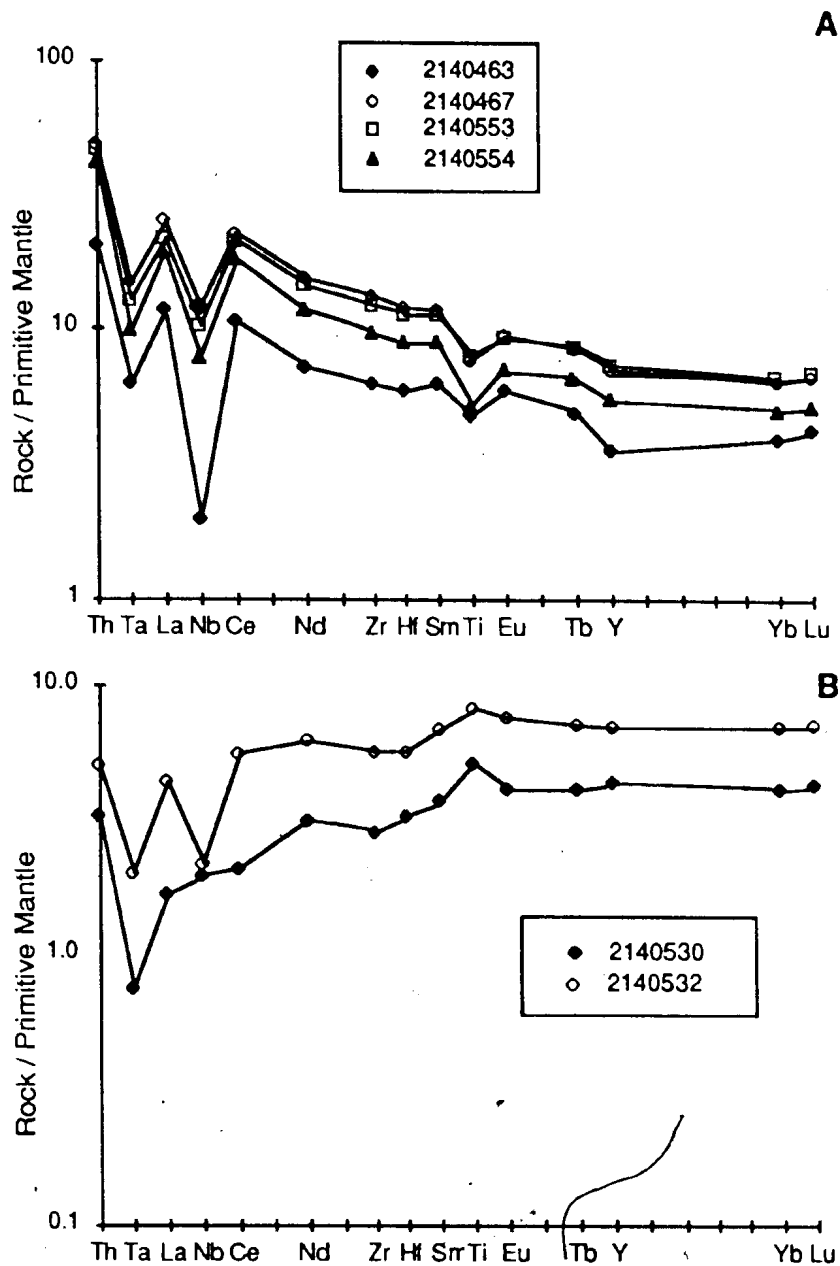
Figure 4.5:. Extended REE plots for the IAI group. A- Glover's Harbour East, Seal Bay Bottom and Northern Arm suites; B- Nanny Bag Lake suite. Note different vertical scales.

suggests that a model involving mixing of a depleted mantle source (LREE-depleted, epsilon_{Nd} > +7) and an enriched source (LREE-enriched, epsilon_{Nd}< 0), followed by partial melting and variable fractional crystallization, may be applicable. In the following Sections, an approximation to such a model is derived and some of the implications explored.

4.5.3.2 The Glover's Harbour East, Seal Bay Bottom and Northern Arm suites

The incompatible element abundances and isotopic compositions of these suites are generally compatible with two types of genetic models: 1) small amounts of partial melting of a mantle source or 2) mixing between depleted and enriched sources. In the first case, it might be considered that partial melting of a primordial mantle source (epsilon_{Nd}~0) might yield an appropriate melt. The relatively flat HREE patterns of these rocks preclude garnet as a refractory phase in such a melt; model calculations indicate that for degrees of melting required to produce the appropriate HREE abundances, the necessary LREE enrichment cannot be generated. In addition, such a model does not explain the pronounced negative Ta and Nb and positive Th anomalies unless one wishes to resort to special residual accessory phases during partial melting. Finally, this model does not unify Glover's Harbour East, Seal Bay Bottom, Northern Arm and Nanny Bag Lake magmatism.

Mixing of a depleted mantle source with an enriched component is, therefore, preferable and is illustrated schematically in Figure 4.6. In order to generate epsilon_{Nd} in the range +1 to +3, from depleted mantle, a time-integrated, LREE-enriched source is required and the strong negative Ta and Nb anomalies (Figure 4.5) indicate that this is best interpreted as crustal material. Figure 4.7 illustrates modelling of REE variation resulting from such a process using subducted sediment as the enriched source.

In Figure 4.7A, mixing of PAAS with DM followed by 5 and 10 percent partial melting is compared with Glover's Harbour East, Seal Bay Bottom and Northern Arm suite compositions.

Figure 4.6: Schematic illustration of the petrogenesis of the IAI group. The field of DM is the peak range of N-MORB from Morris and Hart (1983) recalculated to 465 Ma. Mixing between sources DM and ES produces a spectrum of compositions that include the Glover's Harbour East, Seal Bay Bottom and Northern Arm suites. The Nanny Bag Lake suite has higher epsilon Nd and plots within and close to the field of normal MORB.
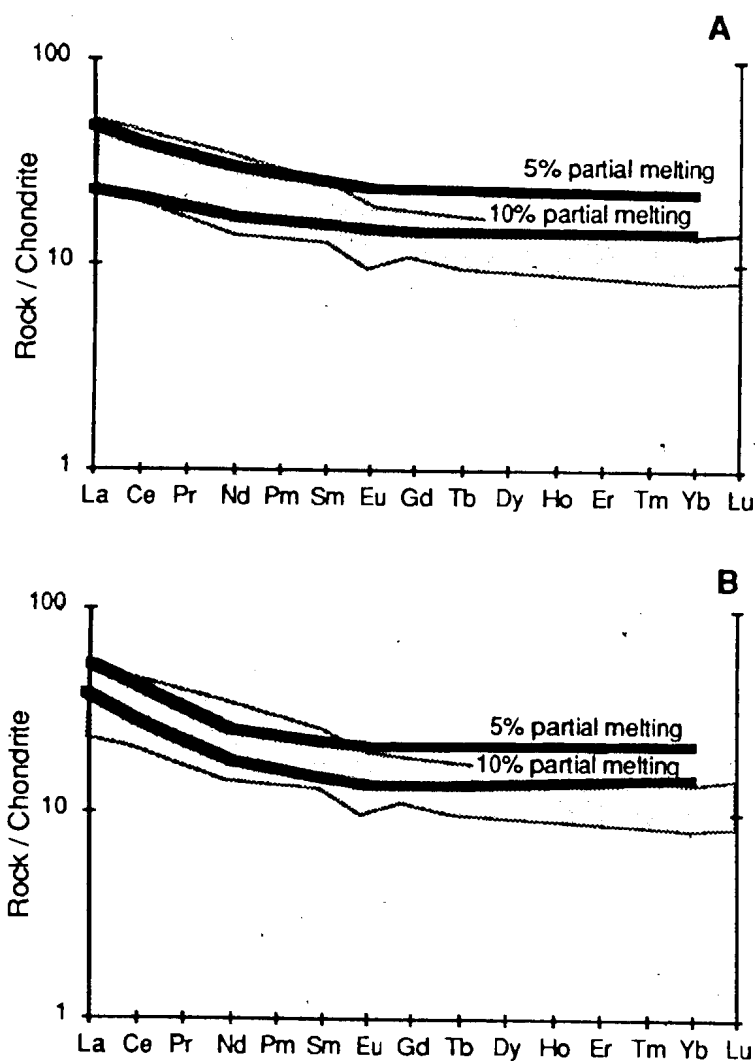
Figure 4.7: Comparison of mixing - partial melting models with observed compositions of Glover's Harbour East, Seal Bay Bottom, Northern Arm suites (stippled field). In A- modelled compositions calculated from mixing PAAS and depleted mantle in proportions 1.5:98.5 followed by 5 and 10 percent partial melting. Epsilon Nd for this mix is +1.06. In B - the enriched component of the mixture is a 10% partial melt of PAAS, mixed in the same proportions and followed by the same partial melting. Epsilon Nd is +1.19.

The mixing proportions are constrained by the amount of sediment necessary to generate the approximate isotopic composition of the suites. The resulting compositions are a good match in the LREE but less depleted in the HREE than the observed rocks. Use of a composition derived by 10 percent partial melting of the sediment followed by mixing in the manner described above produces the patterns in Figure 4.7B in which the LREE but not the HREE are more fractionated. Simply assuming a more LREE-enriched sediment does not produce a more satisfactory solution as mixing calculations suggest that within the bounds of reasonable compositions, such enrichment will not sufficiently increase the La/Yb ratio. However, assuming a less LREE-depleted mantle composition (e.g. similar to that of Wood, 1979) does improve the fit.

An alternative is that there is a third component in the mix. Approximately 30 to 35 percent increase in La/Yb would account for the discrepancy between the model and the observed rocks. Such an enrichment could have occurred, for example, by additional contamination with melt derived from a small degree of partial melting of depleted mantle (illustrated in Figure 4.6) or through action of a fluid phase bringing a LREE-enriched component from the oceanic lithosphere in the slab. Both would have $epsilon_{Nd}$ similar to depleted mantle and if added to the mantle before addition of the LREE-enriched component, would have little effect on the final $epsilon_{Nd}$ of the mixture. Lead and strontium isotopes as well as alkali and alkaline earth elements in many modern island arc tholeiites point to a component in arc magmas derived from layer 2 of the slab (e.g. Anderson *et al.*, 1979; Perfit *et al.*, 1980; Kay, 1980; White and Patchett, 1984; Arculus and Powell, 1986.

4.5.3.3 The Nanny Bag Lake suite

Moderately LREE-depleted patterns and $epsilon_{Nd}$ greater than +5.8 suggest that the Nanny Bag Lake suite is best modelled as dominantly a partial melt of normal depleted mantle. The negative Ta and Nb anomalies suggest a probable minor contribution from subducted sediment or a crustally-derived inhomogeneity in the mantle wedge. The generally low Mg#'s of

even the most primitive samples in the Nanny Bag Lake suite (0.52 - 0.53, see Table 3.5) require that considerable fractional crystallization be allowed for in any model.

Figure 4.8 illustrates that a very satisfactory match for Nanny Bag Lake compositions can be attained in such a model. A mixture of PAAS and depleted mantle in the proportions 0.1:99.9 produces a mixture with epsilon$_{Nd}$ = +6.9 and 25 percent partial melting of this mixture yields a melt of composition PAAS/DM on Figure 4.8. Following 20 percent Rayleigh fractional crystallization, a liquid is derived that very closely matches the composition of the most primitive Nanny Bag Lake suite sample. A further 35% fractional crystallization yields a composition with HREE abundances very similar to the most fractionated sample but somewhat more LREE depleted. This is consistent with degrees of fractional crystallization estimated for this suite on the basis of incompatible element variation in all samples (approximately 25 to 35 percent, Table 3.7).

The slight LREE enrichment in the most fractionated rock relative to the model may reflect an additional minor component in the melt. However, as shown in Figure 3.26, there has been metasomatism in the Nanny Bag Lake suite which has variably enriched the LREE in at least one sample and is, therefore, a possible explanation the slight LREE enrichment in this case.

4.5.3.4 Synthesis of IAI group petrogenesis

The above discussions suggest that despite geochemical and isotopic differences among the suites in this group, a unified petrogenetic model can explain most of the observed features. Both LREE-enriched and LREE-depleted varieties can be derived from mixing time-integrated, depleted mantle and a time-integrated, LREE-enriched, component best interpreted as slab-derived crustal material; the isotopic and geochemical differences between the two magma types can be accounted for by variations in the amount of contamination that occurred and the degree of partial melting. In the case of the Nanny Bag Lake suite, only 0.1% of the crustal source is required whereas up to 1.5% may be needed for the LREE-enriched suites. On the other hand, up to 20% partial melting of DM is indicated for the Nanny Bag Lake suite while models for the LREE-enriched suites require only 5 to 10% partial melting of this source.
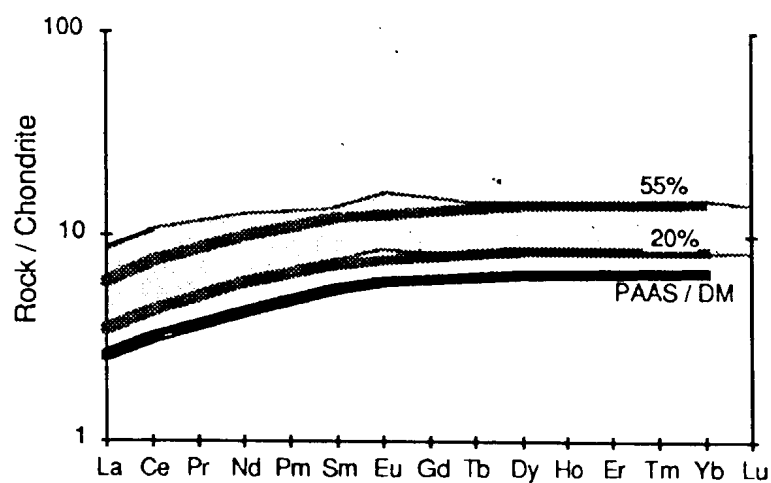
Figure 4.8: Mixing, partial melting and fractional crystallization model for the Nanny Bag Lake suite (stippled field). The heavy black curve (PAAS / DM) is generated by mixing PAAS and DM in the proportions 0.1:99.9 (producing a mixture of epsilon Nd = +6.9) followed by 25% partial melting. The two stippled curves marked 20% and 55% are generated by the respective amounts of Rayleigh fractional crystallization of PAAS / DM.

The observed LREE-enriched suites are always more LREE-enriched than the model predicts. This may signal a third component in the magma sources, for example a hydrous phase from subducted oceanic lithosphere.

It is interesting that the least contaminated rocks (the Nanny Bag Lake suite) have a slight positive Ti anomaly while the most contaminated (LREE-enriched) samples have a negative Ti anomaly. It is suggested that the positive Ti anomaly is best interpreted as a source characteristic that has been overwhelmed by addition of a LREE-rich, Ti-poor crustal component.

4.5.4 The IAD group

4.5.4.1 General statement

The principal geochemical and isotopic characteristics of the IAD group that must be explained by any petrogenetic model are listed below. Some of these are illustrated on the extended REE plot in Figure 4.9.

1) epsilon$_{Nd}$ ranging from approximately +4.4 to -1.2, an inverse correlation between this ratio and both Sm/Nd and Mg# (Figures 4.3 and 4.10),

2) Mg# ranging from 0.6 to 0.4 coupled with very low Cr and Ni and high Sc contents;

2) An extreme depletion in all incompatible elements;

3) flat normalized LREE (La to Nd) patterns; —— — ---

4) flat normaliжed HREE patterns;

5) the "step" in normalized REE abundances between Nd and Eu;

6) negative normalized Ta, Nb and Zr and positive Th and Ti anomalies with respect to REE of similar ionic character.

The most thoroughly documented rocks in modern orogenic settings that are similarly depleted in incompatible elements are boninites. Although it has been shown previously (Section 3.4) that the IAD group is significantly different from boninites *sensu stricto* (e.g. low Mg# and compatible element contents, extreme LREE depletion, chondritic Ti/V, enriched Ti and depleted Zr leading to very high Ti/Zr), the two rock types must have a similarly refractory mantle
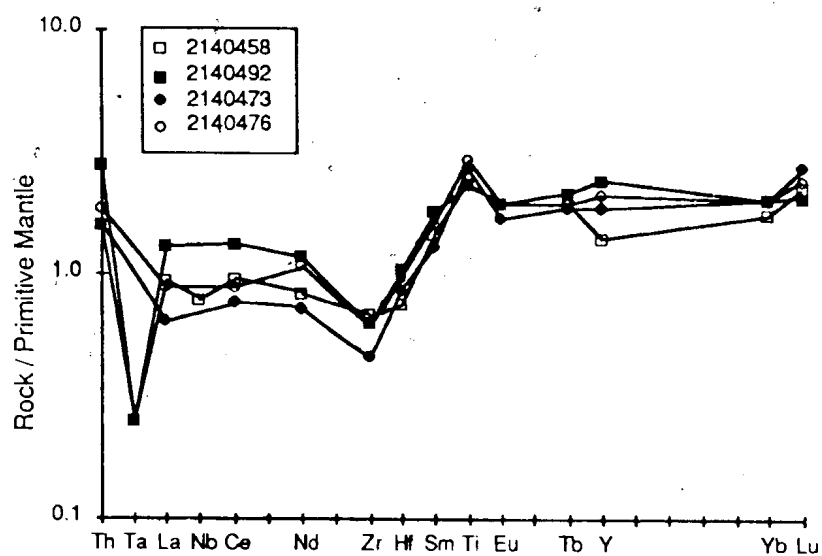
Figure 4.9: Extended REE plot for the IAD group normalized to primitive mantle. Note prominent negative Ta and Zr and positive Th and Ti anomalies.
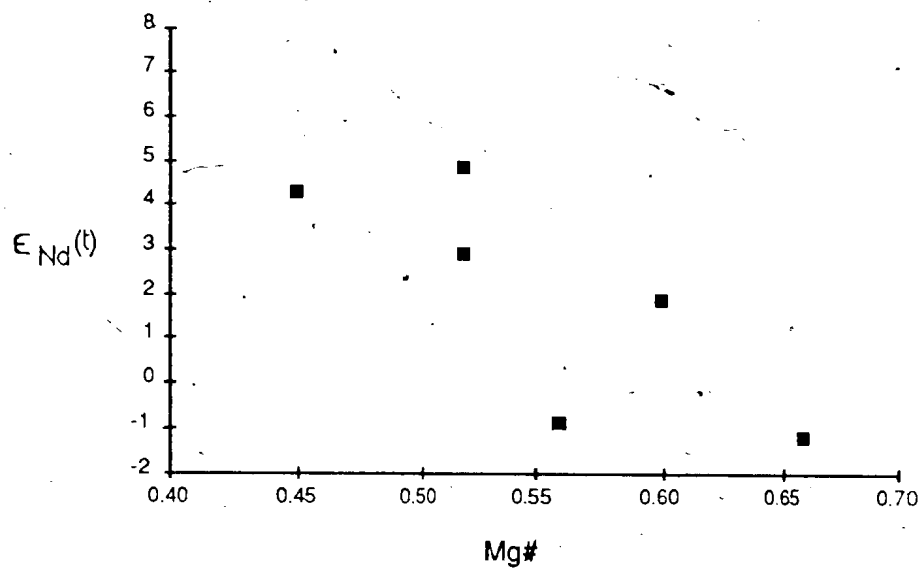
Figure 4.10: Epsilon Nd plotted against Mg# for the IAD group.

source as a component of their petrogenesis and it is, therefore, instructive to consider briefly models of boninite petrogenesis.

Sun and Nesbitt (1978) were the first to suggest that boninitic compositions resulted from mixing of a depleted MORB-like source and a component enriched in LREE (hence the concave-upward REE patterns). Meijer (1980) suggested that boninites in Western Pacific arcs generally are erupted after primitive arc tholeiites and inferred that they resulted from second stage hydrous melting of depleted mantle residua after the removal of the arc tholeiite magma. Hickey and Frey (1982) and Cameron *et al.* (1983) also advocated models involving hydrous melting of highly depleted peridotite that had previously been metasomatized by a LFSE-rich fluid. Hickey and Frey (1982) presented two possible scenarios: 1) first stage melting of a MORB source-like peridotite and removal of arc tholeiite basalt followed by LFSE metasomatism and hydrous partial melting of the refractory source (similar to Meijer's model); 2) derivation of arc tholeiites and boninites from fertile and refractory areas, respectively, in a variably depleted peridotite metasomatized by a small amount of LFSE-bearing fluid. The effect of this fluid would be more important in the boninites than in the arc tholeiites because of their lower incompatible element contents.

There are too few constraints to define unambiguously the source regions and melting history of the rocks in the IAD group. In particular, altered ancient rocks are unlikely to preserve original alkali, alkaline earth, Sr isotope, or Pb isotope compositions, so that there can be no definitive evidence for a component of altered oceanic crust in the magmas. Any petrogenetic model is, therefore, limited by the available data and likely to be simpler than the actual case.

The extreme depletion of incompatible elements in the IAD group argues for models that involve hydrous, second stage, melting of refractory peridotite as a major factor in their petrogenesis. A second major constraint on petrogenetic models for this group is epsilon$_{Nd}$ which range as low as -1.2, demanding a component derived from a time-integrated, LREE-enriched, source. The negative Ta and Nb anomalies in this group argue that this probably represents a crustal source. However, the strong negative correlation between epsilon$_{Nd}$ and

$^{147}Sm/^{144}Nd$ (Figure 4.3) is exactly the opposite of that expected from the simple addition of a little continental crust or sediment to mantle peridotite (and seen in boninites, see Hickey and Frey, 1982; Coish et al., 1982). This negative correlation demands a complex partial melting history as part of their petrogenesis and suggests either: 1) that the crustal source was strongly LREE-depleted when added to the depleted peridotite (i.e. underwent a dramatic LREE-depletion shortly before incorporation in the source region); or 2) that some process acted to produce LREE depletion in the contaminated peridotite (or its melt) in inverse proportion to the amount of contaminant in the rocks. The implications of these speculative models, respectively termed the "pre-mixing depletion model" and the "in situ depletion model", and illustrated schematically in Figure 4.11A and B, respectively, are explored below. It should be emphasized that these models do not uniquely constrain the origin of these enigmatic rocks. In fact, each model has indeterminate factors built into it that render the process arguable. Other models are possible as are variations on those presented below. However, these do illustrate the problems involved in explaining the features of the IAD group and provide alternative explanations.

4.5.4.2 The "pre-mixing depletion" model

The basis of this model is that the Nd isotopic composition and the Sm/Nd ratio of the IAD group rocks are controlled by a strongly LREE-depleted component with the Nd isotopic composition of continental crust. Because both this and the refractory peridotite component are LREE-depleted, a minimum third component is necessary to explain the flat LREE patterns in the rocks. Further complexities may be necessary to explain fine structure in the element relationships as detailed below.

The characteristics of the three components are:

1) Component 1: This is refractory peridotite in the mantle, most conveniently considered as depleted mantle that has undergone major partial melting. This is the HDM source (Table 4.2). Kay (1980) showed that basaltic liquid can be derived from this composition by partial melting. Liquid compositions of 20, 10 and 5 percent partial melts of HDM are shown in Figure 4.12. Five
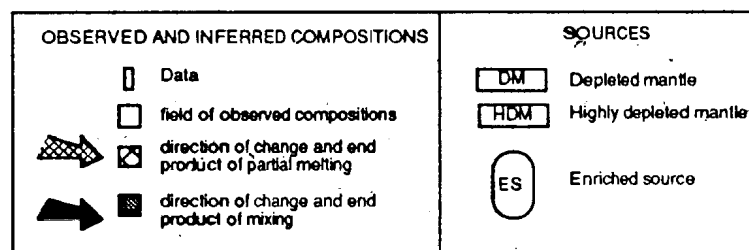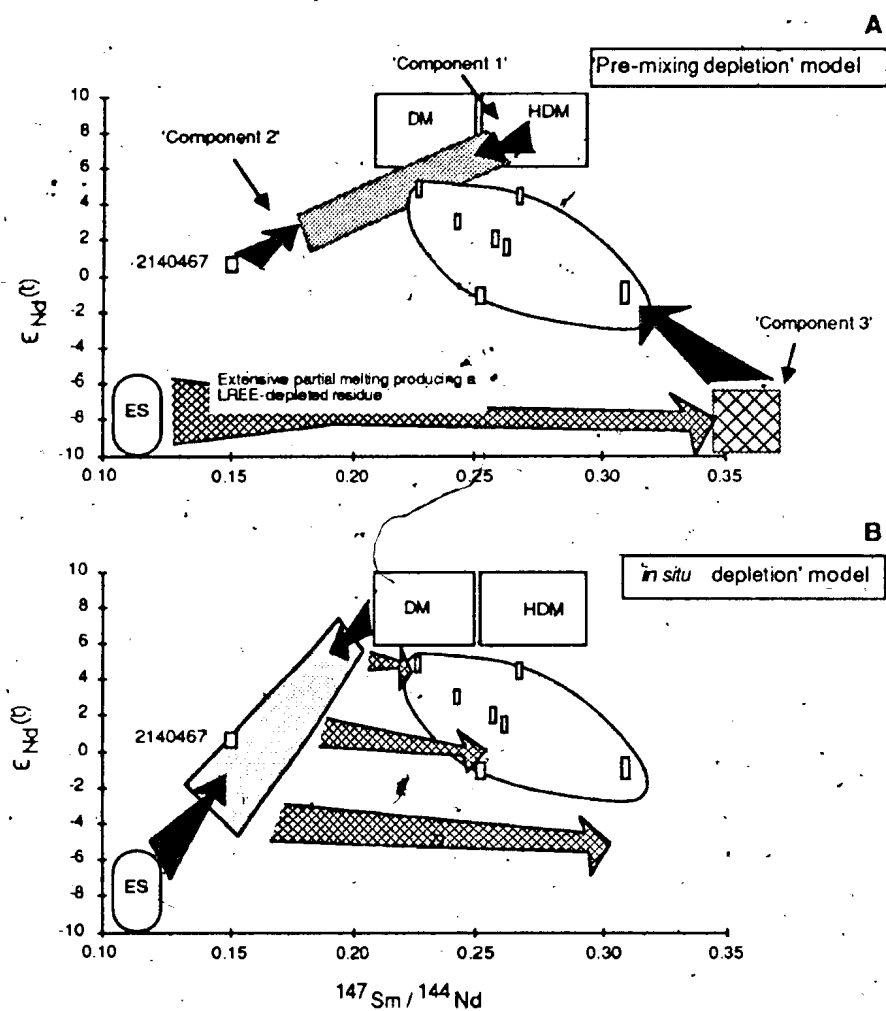
Figure 4.11: Schematic illustration of partial melting-mixing models for the IAD group.
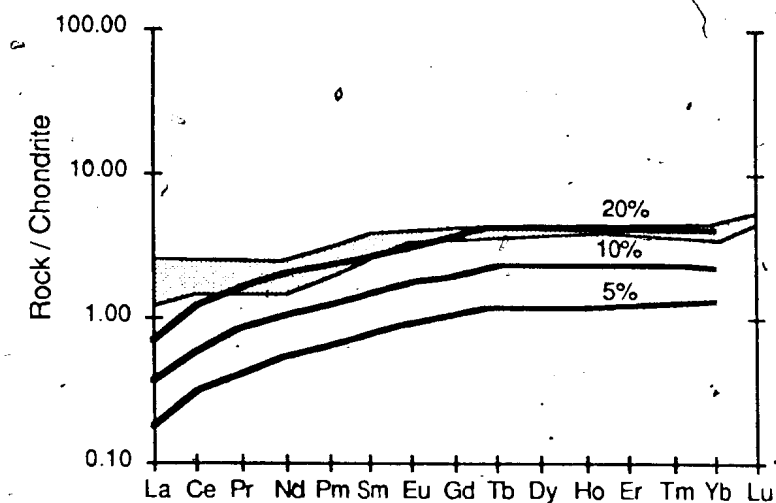
Figure 4.12: Composition of melts derived from refractory mantle peridotite. Compositions of 5, 10 and 20 percent equilibrium batch partial melts of HDM are shown (source mode ol:opx:cpx = 0.71: 0.245:0.045 after Kay, 1980, and phases entering the melt in proportions ol:opx:cpx=0.2:0.2:0.6). Percentage of partial melting shown on the curves. Stippled field is observed IAD group.

percent partial melting reproduces the HREE abundances of the IAD group while slightly greater

degrees of partial melting (10 to 20 percent) would produce relatively REE-depleted liquids which

would, however, allow some room for minor HREE enrichment by further mixing with

REE-enriched components or fractional crystallization.

This component would also be very depleted in all HFSE elements including Zr and Ti.

Therefore, it provides no explanation for the apparent decoupling of these elements seen in the

extended REE plot (Figure 4.9).

2) *Component 2*: This is the component that caused flattening of LREE and is, therefore,

LREE-enriched. Two possible contributors of this source are close at hand; 1) subducted

sediment or upper crustal material recycled in the mantle (or LREE-enriched fluids derived from

them); and 2) LREE-enriched tholeiitic melts similar to those erupted as the IAI group.

Either can be mixed with melts of HDM to provide an appropriately flat LREE pattern.

However the negative Zr anomaly in the extended REE plot argues against the presence of any

source that would deliver a lot of Zr to the mixture (ie. crustally-derived sediment). Hydrous fluids

may also be Zr-rich, according to studies of boninites which always have high Zr with respect to

the adjacent REE's. Hickey and Frey (1982), Nelson *et al.* (1984) and others ascribed this to

metasomatism by a Zr-rich hydrous fluid, although the process is not well understood. The IAI

group arc tholeiites, on the other hand, have normalized Zr abundances similar to the adjacent

REE (Figure 4.5). They are known from field evidence to occur both stratigraphically below and

above the IAD group and both magma types were, therefore, probably contemporaneous and

provided with opportunities for mixing.

To illustrate the effect of this, sample 2140467 (representing typical arc tholeiite

compositions) is mixed with 5, 10 and 20 percent melts of HDM in Figure 4.13. It is apparent that

this process can reproduce both the flat HREE patterns on the one hand and the flat LREE

patterns on the other by varying the amount of partial melting of HDM and admixed enriched

source. However, the relative abundances of LREE to HREE are not well modelled by this binary

mixture and the characteristic step up between Nd and Eu is not reproduced.
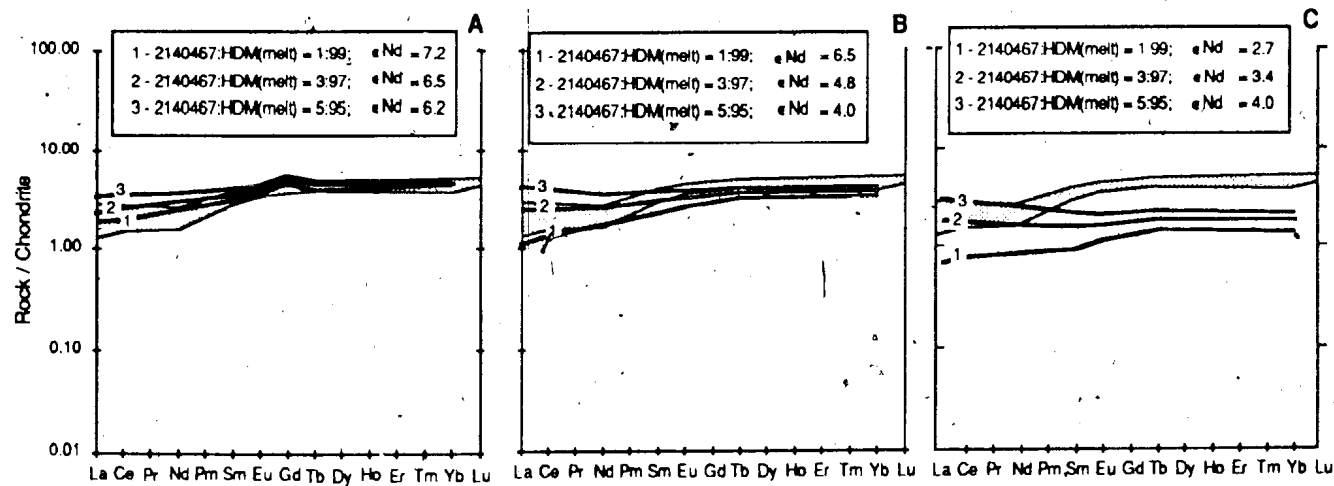
Figure 4.13: Effects of mixing varying amounts of sample 2140467 from the IAI group with various partial melts of HDM. A - 214-467 with 5%partial melt of HDM; B - 2140467 with 10% partial melt of HDM; C - 2140467 with 20% partial melt of HDM.In A and B, mixtures of 99 parts HDM melt to 1 part 2140467 closely reproduce REE abundances and patterns with relatively little change in epsilon Nd; mixtures with 20% melting(C) parallel the IAD group REE patterns but at lower abundances.

The total amount of Component 2 that can be added to the mixture is constrained by the highest epsilon_{Nd} value in the IAD group, +4.4 in sample 2140476. In fact, epsilon_{Nd} of the component 1-component 2 mixture needs to be somewhat higher than this to allow for addition of the LREE-depleted component 3 (see below).

3) *Component 3*: In this model, Component 3 provides most of the isotopic variability in the IAD group. It must have $\text{epsilon}_{Nd} < -1.2$ (the lowest epsilon_{Nd} value in the IAD group), $^{147}Sm/^{144}Nd > 0.31$ (the least radiogenic Sm/Nd ratio in the IAD group) and have reasonably abundant Nd (so that not a large amount of this source is needed to produce the observed changes in epsilon_{Nd})

How does such a source, with a time integrated LREE-enrichment recorded in its isotopic composition, come to deliver a *LREE-depleted* component to the IAD group melts? There appear to be at least two possibilities:

1). It may have been the product of very limited partial melting of a LREE-enriched material involving a refractory phase that retained the LREE at the expense of the HREE. Such a phase would certainly be accessory; currently accepted distribution coefficients allow no major phase to cause so dramatic a LREE depletion, even during very small amounts of partial melting (although admittedly, the Kd's for hydrous melting of sediments in these circumstances are poorly known). Based on published observation and experimental work, such a phase could perhaps be sphene. Dodge and Mays (1972) analysed sphene from the Sierra Nevada batholith and found it to be LREE-enriched with a distinctive step down between Sm and Eu (considering the roughly complementary step up in the IAD group samples, this may be significant). Green (1980) argued that sphene might be a stable phase in the mantle under high pressure, hydrous conditions based on its presence in some hydrous eclogites and in high pressure experimental runs on hydrous andesites. Experimental work by Hellman and Green (1979), aimed at studying the reactions and melt products in subducted ocean crust, identified primary sphene between 10 and 18 kb. and up to 1020°C in runs of olivine tholeiite composition. They concluded that

sphene may be a refractory phase under such conditions with up to 60 percent partial melting. Distribution coefficients for REE in sphene, calculated by Hellman and Green (1979) based on experimental data, range from Ce=245 to Lu=3.01 emphasizing the affinity for the REE overall and the LREE in particular and the ability of sphene to reduce markedly the total REE content of the melt. They cautioned that data for REE in sphene in the literature varies widely and more work is needed to define the effect of this phase on REE distribution in hydrous mafic melts at high pressure. A difficulty with sphene is that it should also retain Ti, and produce a negative rather than positive Ti anomaly on the extended REE plot. It is not known whether it could retain enough Zr to preserve the negative Zr anomaly.

2) The component may have been the refractory end product of partial melting of subducted sediment or a crustally-derived mantle heterogeneity. This model preserves the very low Zr contents of the refractory peridotite (the Zr would go in early melt fractions) but does not explain the positive Ti anomaly.

Note that the timing of mixing of the components is not critical. For example, if component 2 is IAI group tholeiite, then components 1 and 3 may have mixed and then undergone partial melting prior to mixing magmatically with component 2. Alternatively, if component 2 is a sediment melt or metasomatic component, all three components may have been mixed prior to final partial melting and magma production.

Two further features of the IAD group, the positive Ti anomaly and the low Mg#, bear further comment vis a vis the "pre-mixing depletion" model. The positive Ti may simply reflect an original Ti-enrichment in one of the sources or the activity of an otherwise obscure accessory phase at some stage; neither can be ruled out. Alternatively, it may reflect minor oxide accumulation during fractional crystallization and be unrelated to the melting history of the rocks. As opposed to boninite series rocks, there are no high Mg# compositions in the IAD group that would have been in equilibrium with mantle olivine. It was earlier suggested that the low Mg#'s in the IAD group indicated extensive fractional crystallization (Section 3.4.2); however, this fails to explain the inverse Mg#-epsilon$_{Nd}$ correlation (Figure 4.10). If this correlation is not purely fortuitous, then

this might also be a result of contamination of the mantle peridotite by component 3.

4.5.4.3 The "in situ depletion" model

In this model, the depleted mantle source is contaminated by material from the enriched source (either through ascent of sediment-derived melt or LFSE-rich hydrous fluids from the slab) prior to partial melting. The contaminated source region (heavy stippled field, Figure 4.11B) would then be variably LREE-enriched, have a wide range of epsilon$_{Nd}$ depending on the degree of contamination, and show a *positive* correlation between epsilon$_{Nd}$ and $^{147}Sm/^{144}Nd$.

To produce the observed IAD group relationships, a LREE-depleted refractory source must be produced from this contaminated source, with the most contaminated (e.g. lowest epsilon$_{Nd}$) samples being the most depleted. At least two ways can be imagined in which this may occur:

a) *stabilization of a LREE-depleted phase during melting leaving a LREE-depleted residue*: In this case, contamination of the depleted mantle source might result in stabilization during partial melting of a phase with a high ratio of HREE/LREE distribution coefficients. The amount of LREE-depletion resulting from this process would be related to the amount of crustal contaminant in the source, producing an indirect inverse correlation between epsilon$_{Nd}$ and LREE.

A crucial question in this model is whether there is a refractory phase under these conditions that is capable of producing such a dramatic LREE-depletion. Sphene is one possibility. However, uncertainty regarding the appropriate distribution coefficients and conditions under which it may be stable (e.g. Hellman and Green, 1979) make its possible contribution equivocal. As discussed above, the involvement of sphene also does not explain the positive Ti anomaly or the negative Zr anomaly in Figure 4.9.

b) *variable partial melting of the contaminated source*: In this case, complex melting of the contaminated source is invoked to produce an increasing depletion in the LREE with increased.

melting. The more siliceous (i.e. most contaminated) parts of this source might have lower solidus temperatures than the less contaminated areas (this is a major indeterminate factor in this model) and might, therefore, be the first to melt. In these early melting regions, more extensive partial melting might lead to more severe LREE depletion. In the resulting spectrum of refractory source compositions, LREE depletion (e.g. degree of melting) would be related to the amount of contamination and, therefore, indirectly to the $epsilon_{Nd}$ composition.

Although this model fails to provide a satisfactory explanation for the inverse $epsilon_{Nd}$-Mg# correlation, it does account for the negative Zr anomaly, as Zr would presumably depart in the earliest melt fractions. The Ti anomaly is less easily explained unless early stabilization of a Ti-bearing phase is postulated.

A further potential problem with this model is that a single episode of partial melting may not sufficiently deplete the source in LREE to produce the observed Sm/Nd ratios at low $epsilon_{Nd}$. Partial melting calculations on compositions within the contaminated field at $epsilon_{Nd} \sim -2$ indicate that even greater than 50 percent melting will not produce $^{147}Sm/^{144}Nd$ ratios much greater than 0.25. Two or more stages of melting could be invoked, but the connection between LREE-depletion and contamination then becomes tenuous.

4.5.4.4 Summary of IAD group petrogenesis

Clearly, although some aspects of the petrogenetic history of the IAD group can be inferred from isotopic and geochemical data, much remains enigmatic. Some important conclusions that can be reached are:

1) the highly depleted incompatible element concentrations indicate that hydrous melting of a highly refractory mantle source is an important part of their petrogenesis. The source can reasonably be interpreted as the residue from previous partial melting of either normal or variably contaminated depleted mantle;

2) negative Nb and Ta anomalies and generally low $epsilon_{Nd}$ together suggest that crustal

material is involved, either from the subducting slab or from recycled crustal material in the mantle;

3) the negative correlation between Sm/Nd and epsilon$_{Nd}$ and between Mg# and epsilon$_{Nd}$ require further complexities in the melting history which are not easily understood.

4.5.5 The Wild Bight Group Rhyolites

Rhyolites from the various felsic volcanic accumulations in the Wild Bight Group have a relatively homogeneous chemical composition (Figure 4.14) and a limited range in epsilon$_{Nd}$ (Figure 4.1). Some of the features of these rocks that must be explained by any petrogenetic model are:

1) Epsilon$_{Nd}$ in the range +4.9 to +5.6.

2) LREE-depleted extended REE patterns at relatively low abundances (~ 8 to 11 X primitive mantle).

3) Prominent negative Ta anomalies (and probably also Nb which is always below the detection limit of approximately 7 to 8 X primitive mantle).

3) Negative Eu and strong negative Ti anomalies as well as very low V contents.

The close association of rhyolite with rocks of island arc affinity has already been noted and geochemical arguments have been presented in favour of an origin by partial melting of basic rocks in the basal part of an island arc. The Nd isotopic analyses do not further constrain the melting relationships but are consistent with partial melting of rocks with similar isotopic compositions to the observed mafic rocks of island arc affinity. With only two analyses, it is not proposed to attempt any more detailed petrogenetic proposals than this. However, given that the isotopic data are consistent with the rhyolites having formed through partial melting at the base of an island arc, some comments are appropriate concerning the significance of some of the geochemical features noted above.

The LREE-depleted nature of these rocks indicates that the sources were likewise LREE-depleted. Field evidence suggests that the observed volcanic rocks are, at most, of the
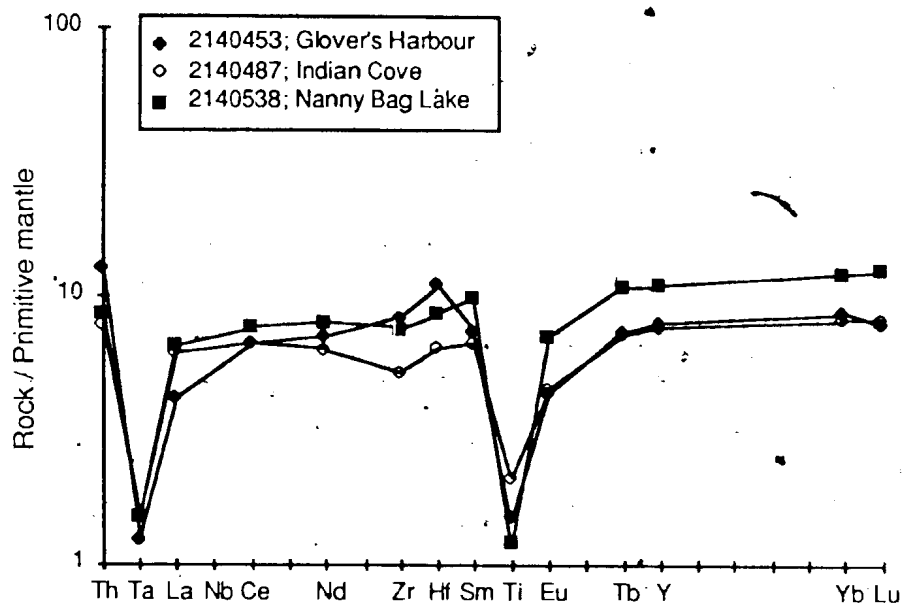
Figure 4.14: Extended REE plot for the Wild Bight Group rhyolites.

order of 3 to 5 km stratigraphically below the rhyolites. There is, therefore, little likelihood that the source rocks for the rhyolites can be found among the observed volcanic rocks. In any case, there are no mafic volcanic or subvolcanic rocks in the sequence that have appropriate compositions to be source rocks for the rhyolites. The LREE-depleted Nanny Nag Lake suite has too high epsilon$_{Nd}$ and REE abundances similar to the rhyolites; partial melting of these rocks would produce REE abundances considerably greater than those observed.

The low REE abundances and LREE depletion suggests that appropriate source rocks should be sought in cumulate rocks at the base of the arc rather than in the evolved liquid compositions. Such rocks would be LREE-depleted, and have very low REE abundances.

The negative Ta and Nb anomalies in this scenario are interpreted as inherited from the source rocks which, by virtue of their arc petrogenesis, would also have this characteristic. The negative Eu and Ti are interpreted to reflect the respective influence of plagioclase and iron oxide (the latter supported by the very low V contents), either as a residual phase during melting or as a fractionating phase during crystallization. Hornblende may also have been involved, contributing to the Ti anomaly.

4.6 Petrogenesis of the Non-arc Volcanic Rocks

4.6.1 Model Parameters

Epsilon$_{Nd}$ for all the non-arc groups is in the range +4.8 to +7.6, indicating that the petrogeneses of these rocks involve mainly mantle sources with time-integrated LREE-depletion. Minimum epsilon$_{Nd}$ in all groups is low enough that it is unlikely that all suites result from differing degrees of partial melting of a normal, depleted mantle source.

The variable LREE-enrichment and epsilon$_{Nd}$ in the range +4 to +8 support the comparisons of these rocks with basalts in enriched spreading ridges ("E-MORB") and oceanic islands ("OIB") and suggest that a mantle source similar to these can be invoked to model the

non-arc petrogenesis in the Wild Bight Group. Selection of such a source is, of necessity, a rather *ad hoc* process. It is clear from the recent literature that there are probably a multitude of such sources in the mantle (discussed in Section 4.3) The Nd isotopic composition of such sources, as indicated by the composition of oceanic island basalts, is most commonly in the range epsilon$_{Nd}$ ~ +4 to +8 but may range from strongly positive to strongly negative (e.g. see compilations of Morris and Hart, 1983 or von Drach *et al.*, 1986).

With respect to the Wild Bight Group non-arc groups, the simplest case for derivation of all rocks by melting-mixing variations between two sources would be the involvement of normal depleted mantle and an "OIB" source with slightly LREE-enriched to slightly LREE-depleted patterns (i.e. $^{147}Sm/^{144}Nd = 0.17$ to 0.22) and moderately positive epsilon$_{Nd}$ (i.e. in the +4 to +7 range). Such a source would be isotopically similar to a large number of modern oceanic island suites (see compilations previously cited) and is also broadly similar to the "prevalent mantle" or PREMA discussed by Zindler and Hart (1986) as a possible source for many modern oceanic island basalts.

For purposes of illustrative numerical modelling, the slightly LREE-enriched, typical E-MORB of Sun (1980) is taken as a starting point. The REE concentrations in the mantle source are taken as a factor of ten lower than this. For the numerical models, this source composition (in ppm) is: La = .63; Ce = 1.5; Nd = .9; Sm = .25; Yb = .22. It is very similar to the E-MORB source calculated by Wood (1979) and the "enriched source" for Hawaiian basalts used by Chen and Frey (1981).

4.6.2 The NAI group

As shown in Section 3.4, the NAI group comprises at least two magma types, one having flat LREE to slight LREE enrichment and the other being distinctly LREE-enriched. Some trace element features of the relatively LREE-depleted varieties (there are no INAA REE data for the LREE-enriched varieties) are displayed on the extended REE plot in Figure 4.15 and illustrate some of the characteristics that must be accounted for in any petrogenetic model including:
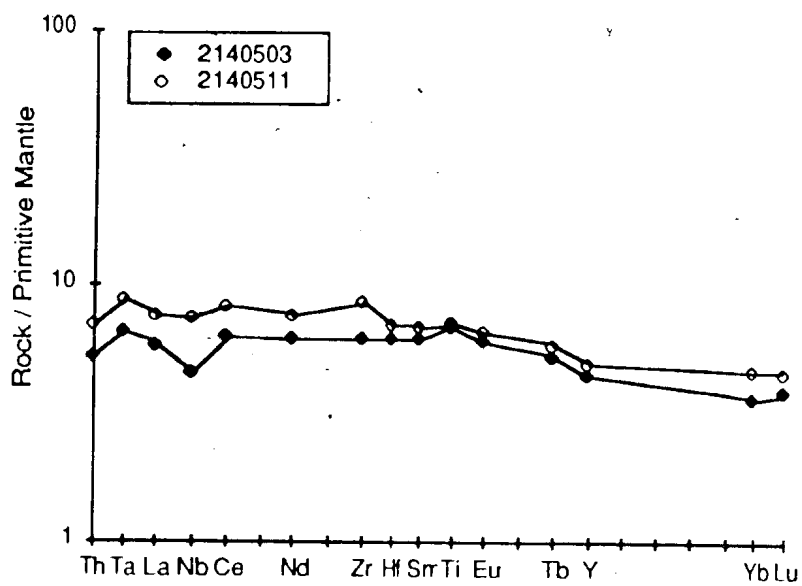
Figure 4.15: Extended REE plot for the NAI group

1) epsilon$_{Nd}$ values overlap in the range +5.3 to +7.6;

2) high Mg#'s indicating that little fractional crystallization has taken place;

3) smooth, flat to slightly convex upward REE patterns at approximately 10 times chondrite.

Generation of the LREE-enriched rocks in this group can be modelled as a simple advanced partial melting of the "OIB" source (illustrated by Curve 3, Figure 4.16). These rocks, with epsilon$_{Nd}$ ~ +5 to +6, have isotopic compositions within the range that might be expected in such a source and a moderate amount of partial melting of the postulated source material produces REE patterns that are broadly similar to the observed rocks. This process is illustrated schematically on Figure 4.17.

Such a process, however, does not easily explain the isotopic and geochemical compositions of the LREE-depleted varieties. The schematic relationships of Figure 4.17 suggest that a simple, two-component mixing between the "OIB" melts and melts of DM might be applicable. However, such simple models encounter difficulty in the numerical modelling. Because the rocks are slightly to strongly LREE-enriched, but have MORB-like Nd isotopic ratios, modelling by addition of sufficient LREE-enriched "OIB"-derived material to MORB to produce the observed flat LREE invariably results in epsilon$_{Nd}$ values that are unacceptably low. Alternatively, adjusting the mixture to produce an appropriate epsilon$_{Nd}$ invariably results in a LREE-depleted pattern (illustrated by Curve 1, Figure 4.16).

One possible solution is that the DM in the mixture had a much higher epsilon$_{Nd}$ than postulated in Section 4.4. This is illustrated by Curve 4, Figure 4.16, which shows that an approximately flat REE pattern at appropriate total REE abundances can be generated from the two sources if epsilon$_{Nd}$ is assumed to be +10. This is equivalent to using a source near the top of the DM partial melt field in Figure 4.17.

An alternative explanation is that there is another component in the mixture. In order to generate the high epsilon$_{Nd}$ and flat REE patterns, this source would have to have had a
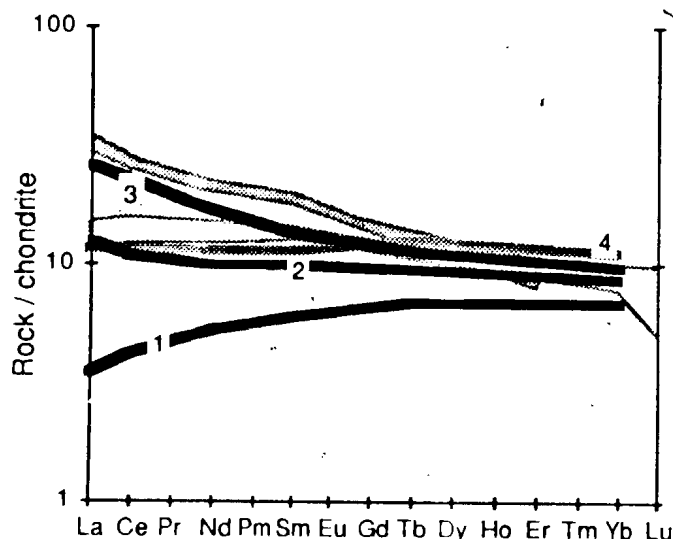
Figure 4.16: Melting-mixing models for the NAI group compared to observed compositions. Heavy-stipple is field of LREE-enriched samples and light stipple of LREE-depleted samples.

Curve 1 is generated through mixing of a 20% partial melt of DM (source mode ol:opx:cpx=0.6:0.2:0.2 and melt fractions ol:opx:cpx=0.2:0.2:0.6) and a 20% partial melt of "OIB" (same source mode and melt fractions) in proportions 85:15. Epsilon Nd is +6.9, assuming epsilon Nd = +4 for "OIB".

Curve 2 is a mixture of 10% partial melt of DM, 10% partial melt of "OIB" (both as for Curve 1) and 0.1% partial melt of DM in proportions 69:23:8.

Curve 3 is generated by 7% partial melting of "OIB". Epsilon Nd is same as this source.

Curve 4 is generated through mixing of same materials as Curve 1 but assuming DM to have epsilon Nd = +10. This substantially changes the mixing proportions. Epsilon Nd of the mixture is +7.2.

Figure 4.17: Schematic illustration of petrogenetic models for the NAI group. The derivation of the "OIB" source is discussed in the text. Seven percent partial melting of this source is illustrated and is equivalent to Curve 3, Figure 4.15. A 10 percent partial melt of this source would lie slightly to the left of the indicated composition and mixing with advanced and incipient partial melts of DM could produce Curve 2, Figure 4.15 and the range of compositions in the NAI group.

time-integrated LREE-depletion, but became LREE-enriched shortly before incorporation in the observed melts (i.e. it now has high-epsilon$_{Nd}$ and LREE-enrichment). Such a source might result from some form of mantle metasomatism (e.g. Bailey, 1970; Menzies and Murthy, 1980) but such processes are not well understood and it would be difficult to model.

An alternative, and less indeterminate, solution involves incorporation of the results of very small degrees of partial melting of depleted mantle. These would have the required LREE-enrichment but MORB-like isotopic characteristics. Mixing with melts formed by more complete melting of depleted mantle would effect flattening of the LREE in the mixture with no significant change in epsilon$_{Nd}$.

Curve 2, Figure 4.15, is constructed assuming that depleted mantle epsilon$_{Nd}$ is +7.6 and a small amount of "OIB" source is used to depress this value slightly in the melt. A more LREE-enriched source could be used instead, in which case less would be required in the mixture. The model curve is a good fit to the observed values in the HREE and has appropriate La abundance. Ce to Sm are lower than observed concentrations and there is a steep negative slope from La to Nd. This is also a feature of some calculated models for the NAT and NAE groups (see below). Considering the uncertainties in the composition and nature of the sources for these magmas, it is not surprising that the model is less than a perfect match. The problem of underabundant Ce-Sm in the model stems from the need for a major LREE-enriched component with depleted mantle isotopic characteristics (because of high epsilon$_{Nd}$). In terms of the simplified source regions assumed in this study, this is most easily modelled as liquid resulting from very small amounts of partial melting of depleted mantle. This process, calculated using the assumed depleted mantle compositions, produces a liquid with higher La/Ce, La/Nd and La/Sm than the observed magmas and REE patterns in the resulting mixtures that do not provide a good match in the Ce to Sm range. This is probably not a serious problem. Assuming slightly different source characteristics and/or additional components in the mixture could produce an even closer match between modelled and observed compositions.

4.6.3 The NAT group

There are two distinct basalt types within the NAT group, represented by the Side Harbour and New Bay suites, respectively. Both have approximately equivalent LREE abundances but the latter are relatively enriched in the HREE (Figure 4.18). Among the features of these rocks that must be explained by any petrogenetic model are:

1) Epsilon$_{Nd}$ ranging from +4.7 to +7 of which the lowest values are in the New Bay suite;

2) strong LREE enrichment and steep negative slopes to the REE patterns;

3) slight positive Ta and Nb and negative Th anomalies;

4) moderate Mg# in the Side Harbour and low Mg# in the New Bay suites indicating substantial fractional crystallization;

5) enriched HREE in the New Bay suite relative to the Side Harbour.

Epsilon$_{Nd}$ for this group is generally within the range to be expected of the "OIB" source, suggesting that it may be best modelled through partial melting of this source. Figure 4.19 shows that a reasonably good match can be obtained in this manner and the process is schematically illustrated in Figure 4.20. In order to model the observed compositions strictly as partial melts of the "OIB" source, it is assumed that epsilon$_{Nd}$ of this source may range from approximately +4.5 to +7 (the range of observed compositions, stippled in Figure 4.20). There is no positive trend between epsilon$_{Nd}$ and $^{147}Sm/^{144}Nd$ (Figure 4.3) and no evidence that DM is involved in the petrogenesis.

The observed compositions of the New Bay Suite can be modelled reasonably well assuming a moderate amount of partial melting of the "OIB" source involving only olivine and pyroxene fractionation. Five percent partial melting produces a pattern parallel to but at slightly lower total REE than the observed compositions (Curve 1, Figure 4.19A). These rocks have Mg# of 0.44 indicating substantial fractional crystallization and Curve 2, Figure 4.19A shows that 30% fractional crystallization of the liquid represented by Curve 1 produces a close approximation to
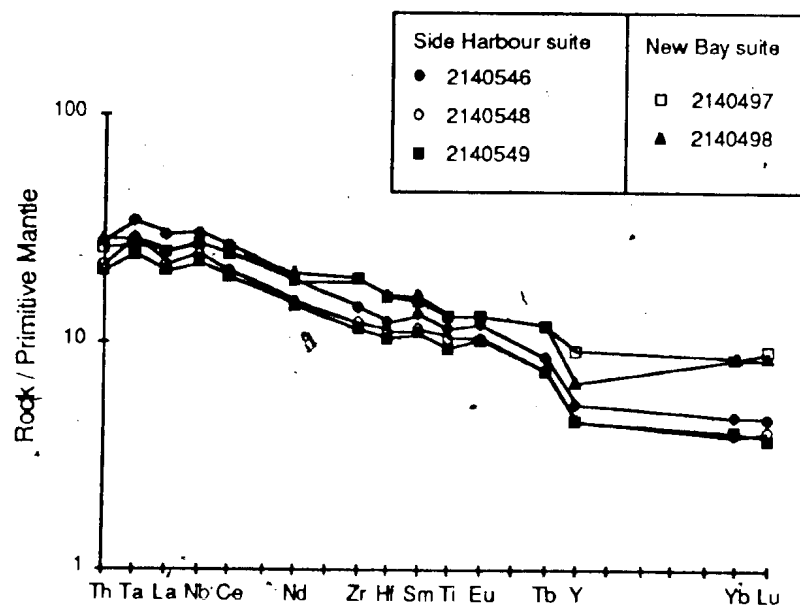
Figure 4.18: Extended REE plot for the NAT group.
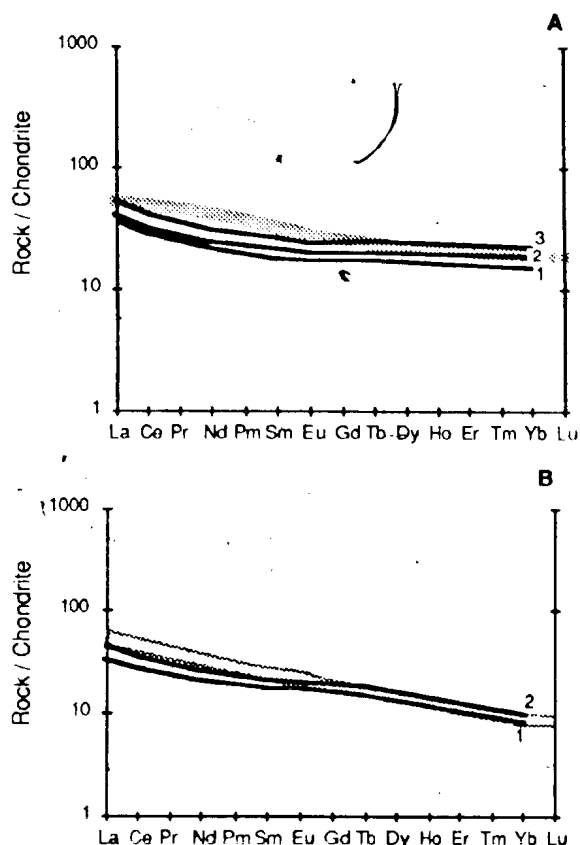
Figure 4.19: Melting-mixing models for the NAT group; A-New Bay suite; B-Side Harbour suite. Observed REE patterns are stippled.

In A, curve 1 is mixing of liquids generated by 0.2% partial melting of DM (source mode: ol:opx:cpx=0.6:0.2:0.2 and melt fractions ol:opx:cpx=0.2:0.2:0.6) and 30% partial melting of PM (same source and melt fractions) in proportions 30:70. Epsilon Nd is +6.2. Curves 2 and 3 represent respectively 10% and 30% fractional crystallization of A.

In B, curve 1 is a binary mix of 0.1% melt of DM (source mode ol:opx:cpx:ga=0.58:0.2:0.2:0.02; melt fractions ol:opx:cpx:ga = 0.15:0.15:0.4:0.3) and 30% partial melting of PM (as in Curve 1 of A) in proportions 30:70. Epsilon Nd is +5.9. Curve 2 is a ternary mixture of the two components in 1 plus PAAS in proportions 34.8:64.7:0.5. Epsilon Nd is +6.0.
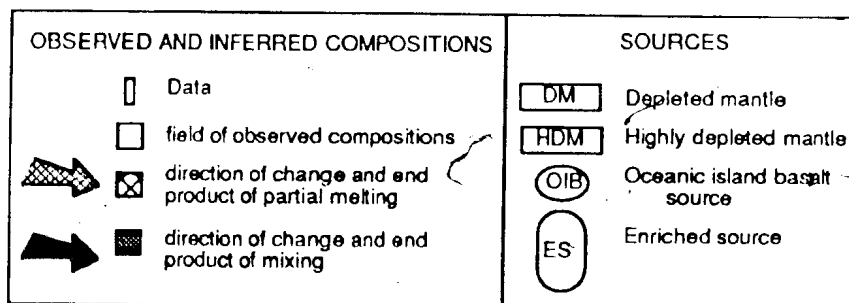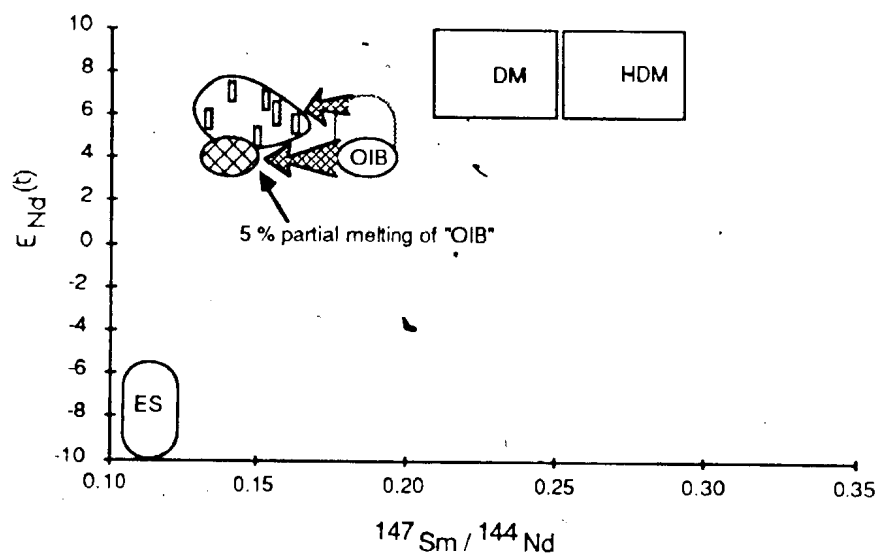
Figure 4.20: Schematic illustration of the petrogenetic model for the NAT group. Limited amounts of partial melting of the "OIB" source can account for the observed compositions, if it is assumed that this source may have epsilon Nd ranging from +4 to greater than +6 (i.e. the area inside the stippled curve above the "OIB" field). If epsilon Nd of this source is assumed to be +4 or lower, mixing with DM partial melts is needed to account for the observed variation.

the observed compositions.

Such a process cannot produce the somewhat greater HREE-depletion observed in the Side Harbour Suite (Figure 4.19B). However, by assuming a small amount of garnet in the residue, the REE patterns are steepened and a close approximation to the observed compositions can be achieved by approximately 4% partial melting of the "OIB" source.

Consideration of incompatible element ratios (Figure 4.21) suggests that the process is actually more complex than the model would suggest. In particular, there is a range of incompatible element ratios that suggests that the observed range of compositions does not come from a simple homogeneous source. The data may define a diffuse curve in Figure 4.21A that could be a relict of binary mixing, but they plot in a very diffuse straight line on the reciprocal plot (Figure 4.21B). In terms of the modelling, this is probably best interpreted as a feature of the "OIB" source which may itself be a mixture of two or more other distinct mantle sources (as suggested by Zindler and Hart, 1986, for their "prevalent mantle"). Alternatively, small amounts of other mantle sources (e.g. LREE-enriched sources which may or may not be derived from recycled crustal material, partial melts of normal depleted mantle) may be contributing to the final products. These could be accommodated in the models without difficulty by varying the amounts of partial melting and mixing.

The small positive Nb and Ta anomalies are not explained by the model. The fact that these are much better developed in the NAE group (see below) suggests a genetic link that will be explored following discussion of the NAE data in the following Section.

4.6.4 The NAE group

Some features of the NAE group that must be accounted for by petrogenetic models are illustrated on Figure 4.22 and summarized below:

1) Epsilon$_{Nd}$ of the samples overlap in the range +4.8 to +5.7,

2) very low Mg#, suggesting extensive fractional crystallization;

3) high LREE and MREE abundances and more LREE-enrichment than the NAT samples;
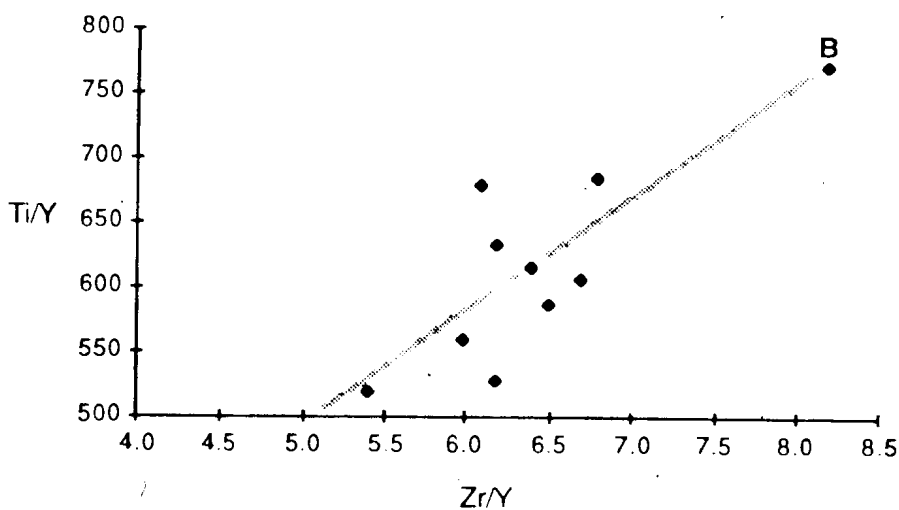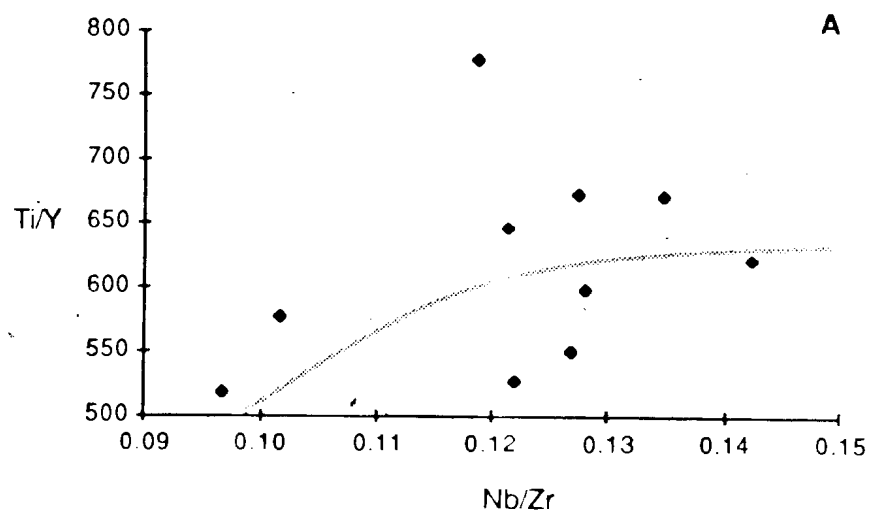
Figure 4.21: Ratio-ratio plots for the NAT group. Variations due to binary mixing should plot along a smooth curve in A and a straight line in the reciprocal plot B (Langmuir et al., 1980). There is considerable scatter about very diffuse trends suggesting that although some of the variation in the NAT group may reflect binary mixing, this process is not the principal control on geochemical variations.
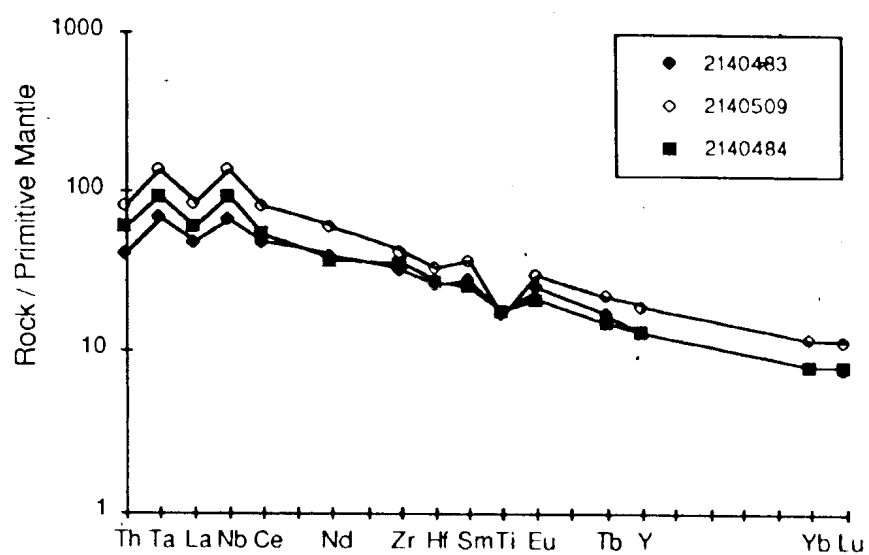
Figure 4.22: Extended REE plot for the NAE group.

4) HREE abundances similar to the New Bay suite;

5 pronounced positive Ta and Nb and negative Th anomalies;

6) negative Ti anomaly.

The NAE group is the most LREE-enriched in the non-arc suites. Epsilon$_{Nd}$ is similar to that in the New Bay Suite but lower than much of the Side Harbour suite suggesting that a major contribution from the "OIB" source can likewise be invoked to model the petrogenesis of these rocks.

Figure 4.23 illustrates that a small amount of partial melting of the "OIB" source involving pyroxene and olivine fractionation can produce a close approximation to the observed NAE group compositions (also illustrated schematically on Figure 4.24). The HREE are slightly higher than observed compositions, perhaps suggesting that a small amount of garnet should be included in the model residue.

Mixing models involving small amounts of partial melting of DM and "OIB" sources can also successfully account for the composition of the NAE group (Curves 2 and 3, Figure 4.23). This is also illustrated on Figure 4.24.

However, melting of a single homogeneous source or binary mixing between melts of two homogeneous sources does not satisfactorily account for other features of the NAE group magmas including their positive Ta and Nb and negative Ti anomalies. In addition, trace element ratio-ratio plots like that in Figure 4.25 indicate that simple binary mixing does not adequately account for the variation in magma characteristics. As in the case of the NAT group, it seems necessary to postulate either a complex "OIB" source or the incorporation of small amounts of additional sources to explain the trace element ratio characteristics.

The positive Ta and Nb anomalies (Figure 4.22) are the complement of the negative anomalies characteristic of the island arc suites and it is tempting to attribute them to a contribution from a source that was depleted in the LREE relative to HFSE in the convergent plate margin setting and subsequently recycled in the mantle where partial melting produced a Nb and Ta-rich liquid. Such a process, first suggested by Wood (1979) who noted that E-MORB lavas
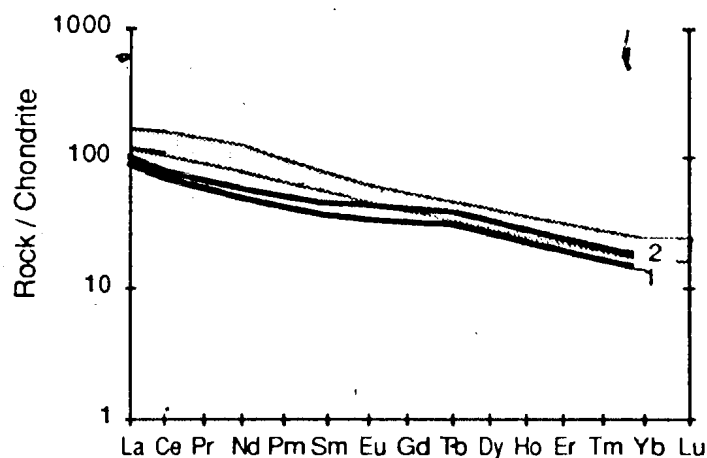
Figure 4.23: Melting-mixing models for the NAE group. Observed compositions are stippled field.

Curve 1 is generated by mixing of liquids derived by 0.1% partial melting of DM (source mode: ol:opx:cpx:ga=0.59:0.2:0.2:0.01; melt fractions ol:opx:cpx:ga = 0.15:0.15:0.4:0.3) and 2% partial melting of PM (source mode: ol:opx:cpx:ga = 0.55:0.2:0.2:0.05; melt fractions: ol:opx:cpx:ga = 0.15:0.15:0.4:0.3) in proportions 65:35. Epsilon Nd is +5.1.

Curve 2 is a ternary mixing model of 1% partial melt of DM (source mode: ol:opx:cpx:ga = 0.58:0.2:0.2:0.02; melt fractions: ol:opx:cpx:ga = 0.15:0.15:0.4:0.3), 10% partial melt of PM (source mode: ol:opx:cpx = 0.6:0.2:0.2; melt fractions: ol:opx:cpx = 0.2:0.2:0.6) and PAAS in proportions 72:18:10. Epsilon Nd is +5.4.
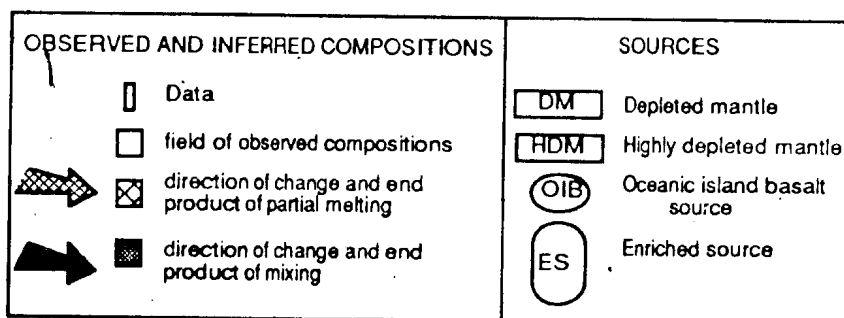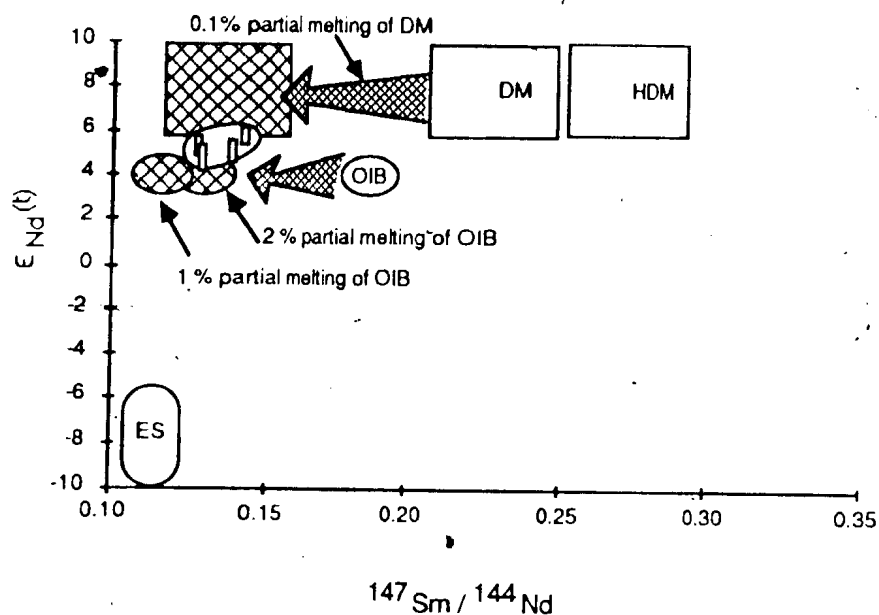
Figure 4.24: Schematic illustration of petrogenetic modes for the NAE group. 1% partial melting of the OIB-source is illustrated and produces Curve 1, Figure 4.23. Mixing between 2%partial melting of this source (also illustrated) and 0.1% partial melt of DM can also account for the observed range of compositions.
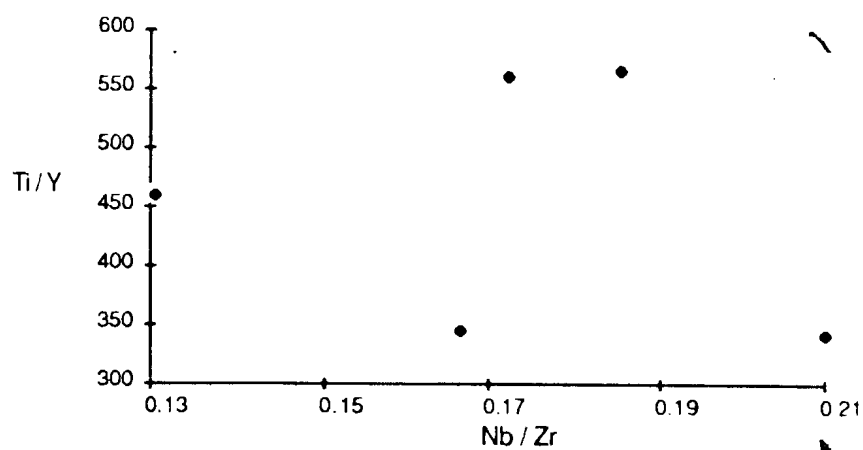
Figure 4.25: Ratio-ratio plot for the NAE group. Variation cannot be explained as binary mixing between two end members.

from the mid-Atlantic ridge have overabundant Ta and Nb with respect to the adjacent LREE, is a ·common feature of intraplate oceanic island volcanic rocks as well (e.g. Hawaii, see data in Basaltic Volcanism Study Project, 1981). The contribution of such a source cannot be modelled as the relative REE and HFSE concentrations of the potential source are not known. However, it may be noted that if such a source is a strongly LREE-enriched mantle source, it may be among the first to melt, explaining its prominence in the melts derived from the smallest degree of partial melting (the NAE group) and its declining importance in those formed through progressively higher degrees of partial melting.

4.7 Magmatic History of the Wild Bight Group; Summary and Synthesis

The Nd Isotopic data, in conjunction with the geochemical data, permit the petrogenetic history of the Wild Bight Group to be interpreted in more detail than has previously been attempted for any Ordovician volcanic sequence in Newfoundland. A summary of interpretations for the petrogenesis of the Wild Bight Group volcanic rocks is presented in Table 4.4 These interpretations are incorporated in the model for the geological development of the Wild Bight Group presented in Chapter 5 and many of the details appear in schematic form on Figure 5.3.

The earliest magmatic history of the Wild Bight Group is recorded in LREE-enriched island arc tholeiites of the Seal Bay Bottom volcanic unit. The base of the Wild Bight Group is not exposed and so it is possible, even likely, that there is an extensive prior history of island arc magmatic activity that has not been preserved (as is preserved in other volcanic sequences elsewhere in Central Newfoundland). The only record of this activity in the Wild Bight Group is in the volcanogenic detritus in turbiditic sandstones of the basal Omega Point Formation.

The Seal Bay Bottom magmatism probably reflects the interaction of slab-derived crustal material and normal depleted mantle above the subduction zone. The negative Ta and Nb and positive Th anomalies reflect the former but do not indicate whether this component reached the mantle wedge as a melt or in a metasomatic fluid. The possibility of additional contributions from subducted oceanic lithosphere cannot be tested with the present data. This style of magma

Table 4.4: Summary of petrogenetic models for Wild Bight Group volcanic and subvolcanic rocks

GROUP	SUITES	GEOCHEMICAL AND ISOTOPIC CHARACTERISTICS	SOURCE COMPONENTS (IN ORDER OF IMPORTANCE)	COMMENTS
NAI	Big Lewis Lake Badger Bay	- minimal fractional crystallization - flat to positive LREE; flat HREE - ε Nd ~ +5.3 to +7.6	- moderate to advanced partial melting of "OIB" source - advance partial melt of DM - ± incipient partial melt of DM	- LREE - enriched varieties reflect dominantly melting of "OIB" source. Mixing with melsi of DM produces increasingly less LREE - depletion and higher epsilonNd.
NAT	Side Harbour	- moderate fractional crystallization - LREE - rich (more than New Bay) - slight + Ta and Nb anomalies - ε Nd ~ +5 to +7	- moderate partial melt of "OIB" source, possibly with garnet in residue - ± partial melts of DM	- possibility of garnet in residue suggests deeper sources than for New Bay suite
NAT	New Bay	- advanced fractional crystallization - LREE - rich (less than Side Harbour) - HREE abundance >Side Harbour - slight + Ta and Nb anomalies - ε Nd ~ +5	- moderate partial melt of "OIB" source, no garnet in residue	- doesn't involve garnet so perhaps shallower melting than Side Harbour - similar petrogenesis to NAE but more advanced partial melting of "OIB" source
NAE	Big Lewis Lake Side Harbour Seal Bay Bottom	- advanced fractional crystallization - very LREE - enriched (more than NAT) - strong + Ta, Nb and - Ti anomalies - ε Nd ~ +4.8 to +5.7	- incipient partial melt of "OIB" source - ± incipient partial melt of DM	- perhaps first melts related to non-arc magmatism
Felsic volcanics	Glover's Harbour, Indian Cove, Side Harbour, Nanny Bag Lake	- LREE depleted; total REE ~ 10 X chondrite - strong negative Ta, Ti and Eu anomalies - ε Nd ~ +4.9 to +5.6	- basal island arc crust, perhaps mafic cumulates	- probably result from higher heat flow and deeper water circulation related to arc fragmentation and/or depression of lower arc crust by accumulation of later arc products
IAD	Glover's Hbr. West Side Hbr. Indian Cove Lond Pond(?)	- moderate to advanced fractional crystallization - strongly depleted in incompatible elements - flat LREE with step up between Sm and Eu to flat HREE - negative Ta, Nb,Zr, positive Th, Ti anomalies - ε Nd from -1.2 to + 4.8 negatively correlated with Sm / Nd and Mg#	- highly depleted mantle (residue from removal of island arc tholeiite from DM) - slab - derived crustal source (sediment?) - ± LREE - enriched source (LREE-rich IA melts?, PAAS?, incipient DM melt?)	- complex melting / mixing required to generate REE patterns and isotopic correlations - requires hydrous melting of refractory source
IAI	Nanny Bag Lake	- moderate fractional crystallization - LREE - depleted - negative Ta, Nb, positive Th, Ti anomalies - flat HREE - ε Nd ~ +5.8 to +7.1	- advanced partial melting of DM - slab-derived crustal source (minor)	- typical island arc tholeiite
IAI	Glover's Hbr. East Seal Bay Bottom Northern Arm	- minimal to moderate fractional crystallization - LREE - enriched with flat HREE - prominent negative Ta, Nb and small Ti anomaly - ε Nd ~ -1.2 to +4.8	- minimal to moderate partial melting of DM - slab - derived crustal source	- compared to Nanny Bag Lake, higher proportion of slab component and lower degrees of DM partial melting result in LREE enrichment

generation (i.e. low to moderate degrees of partial melting and a major contribution to depleted mantle from crustal sources) apparently persisted throughout the magmatic history of the Wild Bight Group, as similar lavas occur in the central part of the succession (Glover's Harbour suite) as well as at the top (Northern Arm suite).

A second style of tholeiitic magmatism, with pronounced LREE-depletion and MORB-like Nd isotopes, began somewhat later in the magmatic history of the Wild Bight Group (the Nanny Bag Lake suite). These lavas probably represent the same sources as the LREE-enriched suites but appear to record a much smaller relative crustal contribution and more complete partial melting of the contaminated depleted mantle.

Conceptually, the magmatism that produced the two types of island arc tholeiite can perhaps be most easily visualized as partial melting of regions in the mantle wedge that have variable concentrations of veins or plums of enriched material. The degree of LREE-enrichment and the Nd isotopic composition would depend on the relative concentration of veins or plums in the region of melt generation. Melting in these regions would initially involve principally the enriched material (Wood, 1979) but with advanced melting, the importance of the depleted mantle in the mixture would increase. It is not certain whether areas of relatively sparse veins or plums are necessary to produce the Nanny Bag Lake magmas. Perhaps they could be produced by partial melting of the depleted mantle source that continued past the amount typical of the LREE-enriched varieties and overwhelmed the early LREE-rich compositions with LREE-depleted liquid.

During the later stages of arc volcanism, an enigmatic suite of very incompatible element-depleted magmas (the IAD group) was erupted. The very depleted nature of these lavas requires hydrous melting of a very refractory source which, in terms of Wild Bight Group history, is perhaps best thought of as the residue from production of the early IAI group tholeiites. This part of the model is conceptually similar to those proposed by Meijer (1980), Hickey and Frey (1982) and others for generation of boninites. The IAD group, however, has not been modified by a Zr-rich and/or Ti-poor fluid and its REE patterns require more complex models than the simple

LREE-depleted or concave-upward patterns of boninites (particularly in view of the negative epsilon$_{Nd}$ - Sm/Nd correlation). These features can be accounted for by postulating a complex interaction of slab-derived fluids, refractory mantle and a LREE-enriched component that can be modelled as small amounts of the IAI group, LREE-enriched, liquids. The very low Mg#'s suggest that the magmas underwent considerable fractional crystallization before eruption. Because they did not equilibrate with each other chemically or isotopically, it seems likely that they did not pool in shallow magma chambers. The implication is that they were erupted directly from their source regions, suggesting conditions that permitted easy access from depth to the surface.

At the same time that these magmas were being erupted, silicic melts were also being generated, probably through hydrous partial fusion of pre-existing arc crust. These melts, which are LREE-depleted and have positive epsilon$_{Nd}$, cannot be successfully modelled as partial melts of observed mafic volcanic compositions using major phases but they may be partial melts of pyroxene-plagioclase-bearing cumulates at the base of the arc crust.

The common association of rhyolite with IAD group andesites suggests a genetic relationship. Although it is not likely that they are directly related through partial melting or fractional crystallization, it is very likely that both reflect a magmatic response to changing tectonic conditions within the arc, the andesites requiring higher temperatures and more water in the mantle wedge and the felsic magmas similarly requiring hotter, more hydrous conditions in the basal arc crust. This relationship is further explored in Chapter 5.

It is interesting that the only felsic volcanics not spatially related to IAD group andesites occur with the Nanny Bag Lake suite. This may suggest a temporal link between the Nanny Bag Lake suite and the IAD group and raises the possibility that the changing tectonic conditions that allowed generation of the IAD group and the rhyolites were also somehow responsible for the LREE-depleted arc tholeiites (perhaps higher temperatures promoting higher degrees of partial melting in less contaminated regions away from the slab?).

Magmatism following the eruption of the IAD group generally represents different sources and in particular shows no evidence of the subducting slab. The stratigraphic succession in the

upper Wild Bight Group suggests that NAT group lavas probably represent the first non-arc eruptions followed by NAE group lavas. NAI group lavas are generally at the top of the succession and are the last new magma type to appear during Wild Bight Group volcanic activity.

Most of the isotopic and geochemical features of the NAI, NAT and NAE groups can be accounted for in a unified model of magma genesis, by postulating the presence of a mantle source similar to that which produces "E-MORB" or oceanic island basalts in modern volcanic settings. Most of the rocks in the non-arc groups can be modelled as resulting from various degrees of partial melting of this source, locally with input from depleted mantle.

The NAT and NAE groups were the first non-arc magmas to be erupted. They can be successfully modelled as the products of moderate and low, respectively, degrees of partial melting of this source although the presence of minor amounts of melt derived from depleted mantle cannot be ruled out. The possibility that garnet was a residual phase during production of the Side Harbour Suite NAT group lavas suggests source regions deeper than approximately 30 km. However, all other suites were probably derived from shallower levels.

This style of magma generation apparently was prevalent throughout the volcanic phase that is recorded in the upper Wild Bight Group. However, in the latter stages, it was joined by lavas characterised by more complete partial melting of the "OIB" source (NAI group). LREE-depleted rocks also occur in this group and appear to require a substantial input from normal depleted mantle. Variation within the NAI group can be successfully modelled as a mixing between these two sources although incipient melts of depleted mantle may have also entered the melts and locally enhancing the LREE contents.

As noted above, magmas with characteristics of LREE-enriched island arc tholeiites continued to erupt sporadically through this time and, with the NAI group, mark the end of active volcanic activity recorded by the Wild Bight Group. Shortly after initiation of the NAI group activity, magmatism ceased and Caradocian sedimentation initiated the final phase of the oceanic geological history of the northern Dunnage Zone.

CHAPTER 5

GEOLOGICAL AND PALEOTECTONIC DEVELOPMENT OF THE WILD BIGHT GROUP,
MODERN ANALOGUES AND ANCIENT CORRELATIVES

5.1 Introduction

The geochemical and isotopic results presented in Chapters 3 and 4 allow a consistent interpretation of the nature of the source regions and melting history of the Wild Bight Group magmas. However, these data do not in themselves provide direct evidence for the geological and paleotectonic history recorded by the Wild Bight Group. Extrapolation of the petrogenetic interpretations of ancient rocks to include interpretations of paleotectonic history rely on comparisons between the relationships displayed by the ancient rocks and those in modern settings.

Such comparisons were made for the individual suites in Chapter 3 as part of the discussion of their geochemical relationships. In particular, parallels were drawn between the arc-related suites and various types of island arc tholeiites and between the non-arc suites and lavas erupted in modern oceanic islands and/or enriched segments of spreading ridges. Geological relationships provide a clear sequence of events in which an early episode of island arc-related activity was succeeded and partially overlapped by a later phase of magmatism which was not related to subduction.

In the following Chapter, comparisons are drawn between the geological and geochemical relationships in the Wild Bight Group and those in specific modern environments where similar relationships have been documented. These comparisons are used as the basis for presenting a model of the geological and paleotectonic history of the Wild Bight Group.

Finally, the interpretations with respect to the development of the Wild Bight Group are applied to coeval rocks elsewhere in central Newfoundland, as a contribution towards the understanding of the regional Llanvirnian to Caradocian history of the Newfoundland Central Mobile Belt.

5.2 Modern Analogues

5.2.1 General Statement

In order to present an acceptable analogue for the Wild Bight Group, a modern setting should have, as a minimum requirement: 1) an early stage of volcanic activity in which magmas carry a geochemical signature of subduction; 2) a transition to back-arc activity and magmatism which does not have the arc geochemical signature; and 3) a time period during which arc and non-arc volcanic activity overlapped, leading to the interbedding of volcanic rocks with disparate petrogeneses in the stratigraphic record. Such a stratigraphic succession is not common in the modern record, although it may be more common than has been observed to date, given the number of Cenozoic back-arc basins that have formed in the South Pacific alone. One problem with observing such a succesion in the modern record, of course, is that most back-arc basins (and remnant arcs in them) subside rapidly as the newly-formed crust cools and so most modern analogues are now in very deep water, beyond the reach of the geologist's hammer.

There is, however, at least one good analogue in the modern record, Fiji and the Lau Islands, where tectonic circumstance has kept parts of the remnant arc and subsequent volcanic products above the surface of the sea and more than 20 years of concentrated study has produced a remarkably good data base. In addition, interbedding of arc and non-arc related volcanic rocks has been reported from DSDP drill holes in the Mariana Trough. In the following Sections, these are briefly described. Comparisons with the Wild Bight Group are drawn in Section 5.3.6.

5.2.2 Fiji: A Cenozoic Arc to Back-arc Transition

The islands of Fiji and the Lau Islands to the east (Figure 5.1) offer a unique opportunity to observe the changing volcanic activity associated with a change in tectonic regime from island arc to back-arc basin. The geochemistry of the island arc volcanic rocks was described by Gill (1970) who showed that island arc volcanism as recorded on Viti Levu progressed from early island arc

Figure 5.1 - Principal tectonic elements of the Vanuatu - Fiji - Tonga region. Active island arcs are in dark stipple, remnant arcs in light stipple and trenches in dark shading.
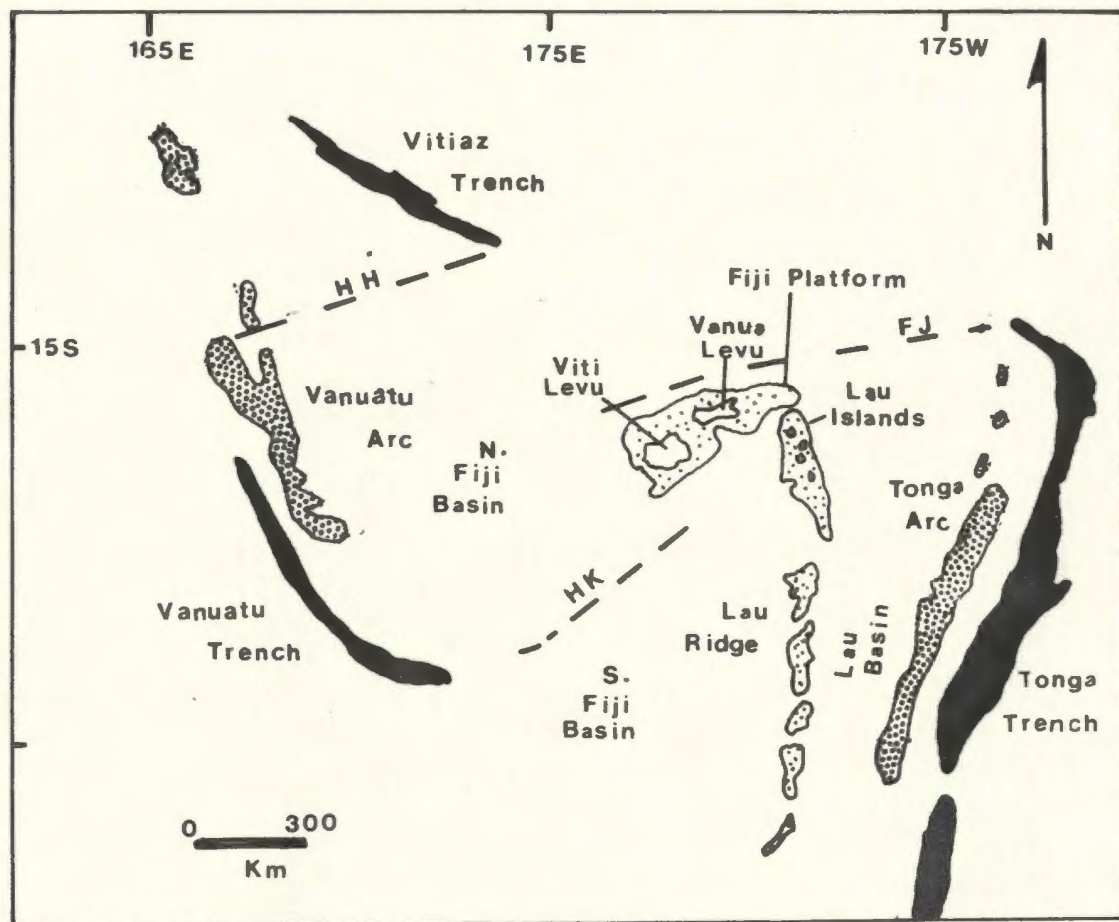
tholeiites through calc alkalic andesite to shoshonite. In several later papers, Gill and co-workers have provided an extensive geological, geochemical, geochronological and isotopic data base for magmatic rocks on the Fiji Platform, showing that following cessation of island arc volcanism, Fiji became a remnant arc between the Lau and North Fiji Basins (Gill, 1976). Recent volcanic activity, consisting dominantly of alkali olivine basalt lacking any arc-related geochemical signature, reflects back-arc magmatic processes.

Figure 5.2 is a summary of the tectonic and magmatic history of the Fiji platform, compiled from data in Gill (1970, 1976, 1984), Gill and Stork (1979), Gill et al. (1984), Whelan et al. (1985) and Colley and Hindle (1985). In particular, geochronological data of Whelan et al. (1985) and isotopic data of Gill (1984) are critical to understanding the magmatic history of Fiji.

Briefly the model states that from approximately 35 Ma to 8 Ma before present, Fiji was part of the Tonga -Kermadec - Vanuatu island arc formed above the Vitiaz Trench. During this time, the principal volcanic products in Fiji were low-K, island arc tholeiitic andesites, formed through extensive partial melting of sources that included components of MORB source, oceanic island basalt (OIB) source and recycled crust (both oceanic lithosphere and sediment). Twice during this period, trondhjemite and gabbro plutons were intruded into the sequence. At about 8 Ma, there was a change in the nature of the volcanic activity, probably in response to forces that would soon initiate fragmentation of the arc and opening of the North Fiji Basin, separating Fiji from Vanuatu. Calc alkalic andesites became the dominant magma type, representing lower degrees of partial melting of sources similar to the IAT sources (producing magmas with more prominent OIB and slab-crust components). At this time, there was also a voluminous outpouring of low-K trondhjemitic rhyolites on Vanua Levu, interpreted to represent partial melting of early-formed island arc crust (Gill and Stork, 1979; Stork and Gill, 1982).

In the last stages of fragmentation of the Fiji arc, calc alkalic andesites were succeeded by dominantly basaltic volcanism, ranging from shoshonite through transitional varieties to non-alkalic basalts (geographically, this is a west to east progression with increasingly non-alkalic magmas forming farther from the zone of active rifting). The shoshonites represent the smallest

AGE (Ma)	Epoch		Tectonic Configuration	Felsic Magmatism	Mafic Magmatism	Chemical Characteristics	Nd isotopes	Magma generation
	PLEISTOCENE		opening of Lau back arc basin with Fiji as a remnant arc		Alkali olivine basalt	High TiO2, OIB element ratios, no arc signature	∈ Nd= + 4 to + 5	OIB / MORB sources (high ratio); no slab-derived component, little differentiated
1.8								
	PLIOCENE							OIB, MORB & slab-derived sources. Low partial melting, enriched sources imp. in shoshonites
5	MIOCENE		Arc fragmentation and opening of North Fiji Basin (~ 6.5 - 5.5 Ma) followed by anticlockwise rotation of Fiji and opening of Lau Basin (~ 3.5 Ma)		Shoshonite, transitional and subalkalic basalt	Arc signature in trace element ratios	∈ Nd = +7 (shoshonites)	
		LATE		Low-K rhyolite (ms)	Calc - alkaline andesite	Medium to high K, LREE enriched arc signature in trace element ratios	∈ Nd ~ 7.6	OIB / MORB / slab-derived sources; low partial melting means enriched sources imp. relative to IAT
10.5				trondhjemite ± gabbro			∈ Nd = +8 to +10	
		MIDDLE			Low-K island arc tholeiite			High degrees of partial melting of MORB / OIB and minor slab-derive d sources. Advanced partial melting and MORB source dominates
30			Island arc - subduction of the Pacific Plate under the Indian Plate along the Vitiaz Arc			MORB - like with arc signature in trace element ratios		
34	OLIGOCENE			trondhjemite ± gabbro				

Figure 5.2: Summary of Oligocene to Recent magmatic and tectonic history of Fiji and the Lau Islands. "ms" indicates deposition of volcanogenic sulphide deposits. Stippled area is time of overlap of arc- and non arc-related magmatism.

degree of partial melting in the Fiji arc sequences, with a concomitant increase in the relative importance of OIB and slab-derived crustal sources. Gill (1984) suggested that this reflected quick access to the surface of the incipient melts as a result of rifting accompanying the final arc fragmentation. Coeval transitional and non-alkalic basalts have, respectively, higher degrees of partial melting and relatively less influence of the enriched sources.

With the opening of the Lau Basin, Fiji was carried beyond the influence of the Tonga subduction zone and the last volcanic activity represents melting of mantle sources with no slab component. Isotopic and geochemical data suggest that the sources are dominantly OIB with a lesser MORB-like component, and the magmas are the product of advanced partial melting.

It is important to note that the magmatic episodes described here are more complex than the model. Volcanic rocks with boninitic and calc alkalic characteristics were erupted in minor quantities during the main phase of arc volcanism (Gill, 1984) and medium-K tholeiites are common in this interval in the Lau Islands to the east (Cole *et al.*, 1985). Boundaries between the magmatic types are not clear cut and on a regional scale, there is temporal overlap at all transitions. In particular, there was a period of approximately 500,000 years when lavas with arc and non-arc geochemical signatures were erupted together in Fiji (Whelan *et al.*, 1985), represented by the stippled field on Figure 5.2.

5.2.3 The Mariana Trough: Coeval Back-arc and Slab-related Volcanism

Deep Sea Drill Project (DSDP) Leg 60 investigated the relationships between back-arc, arc and fore-arc volcanic rocks in a series of holes in a transect across the Mariana trough, ridge, fore-arc and trench. Two of these holes, numbers 454 and 456A drilled in the respective center and the east side of the Mariana Trough, penetrated an interbedded sequence of aphyric to olivine and feldspar-phyric massive and pillowed basalts. Geochemical study of these basalts, particularly using REE and HFSE, led Wood *et al.* (1981) to conclude that they represented a sequence of calc alkalic basalts with an island arc signature interbedded with N-MORB basalts related to back-arc processes.

The stratigraphic relationships are summarized in Figure 5.3. Wood *et al.* (1981) noted that the interbedding of the two basalt types occurred during an early stage of back-arc basin opening and has important implications for the nature of magmatic processes during initial opening of marginal basins. They suggested that early stages of basin formation would provide opportunities for arc influence in the magmas by processes such as magma mixing and/or arc-derived sediment assimilation while more mature basins would not show this influence.

There are too few data to attempt a detailed comparison of the Mariana Trough magmatism with the Wild Bight Group. In particular, it is unlikely that two holes penetrating a total of less than 200 m of section are representative of all the magmatic types that may have reached the surface during opening of the Mariana Trough. The significance of these results is that they demonstrate, as does the Fiji example, that arc and non-arc magmas can coexist at this stage of the tectonic development of a back-arc basin. They provide an actualistic model for relationships in the upper Wild Bight Group where such a process appears to be recorded.

5.2.4 Other Evidence of Slab Influence in Back-arc Magmas

In most back-arc basins, the approximately simultaneous eruption of different magmas with clear arc and non-arc signatures has not been recorded. More widely documented, however, are arc-like trace element characteristics in some back-arc basin magmas which are otherwise similar to MORB (e.g. the Lau Basin, Gill, 1976; Jenner *et al.*, 1987; the East Scotia Sea, Saunders and Tarney, 1979; the Mariana Trough, Hart *et al.*, 1972; Hawkins and Melchior, 1985). Many authors have suggested that back-arc basin basalts can in many cases be distinguished from MORB formed at a major ocean spreading center by subtle alkali, alkaline earth and Sr isotope relationships (e.g. Saunders and Tarney, 1979; Tarney *et al.*, 1981). However, given the mobility of the critical elements, such distinctions are less likely to be preserved in ancient rocks.

HOLE 454

DEPTH (m)	LITHOLOGY	GEOCHEMICAL AFFINITY
	Vitric mud	
3900	Massive, olivine, plagioclase basalt	
	Graded breccia	Calc alkalic basalt
	M. gr., aphyric bslt.	
3920	Olivine, plagioclase pillow lavas and interbedded vitric mud	
3940		
3960	Sparsely olivine, plagioclase - phyric massive basalt flows	
	Vitric mud	
3980	olivine - microphyric pillow basalts	N - MORB
4000		

Hole 456A

DEPTH (m)	LITHOLOGY	GEOCHEMICAL AFFINITY
3720	Vitric tuff, mud	
	Plag.-phyric bslt.	N - MORB
3740	Vesicular pillow lava	Calc alkalic basalt
	sparsely phyric vesicular pillow lava	N-MORB
3760	Vesicular apyric pillow lava	Calc alkalic basalt

Figure 5.3: Summary of basalt types penetrated by DSDP Holes 454 and 456A in the Mariana Trough. Lavas of arc and non arc affinity are interbedded in Hole 456A.

5.3 Geological and Paleotectonic History of the Wild Bight Group

5.3.1 General Statement

Geological, geochemical and isotopic studies reported in this thesis together with comparisons with modern settings where similar relationships have been documented indicates that the Wild Bight Group stratigraphic succession records a transition from island arc to back-arc environments. The developmental model for the Wild Bight Group, illustrated in Figure 5.4, suggests a geological and paleotectonic history for the Wild Bight Group which is consistent with the data previously presented and with the sequence of events in such modern settings. Four developmental stages are recognized: *Stage 1*: the island arc; *Stage 2*: arc fragmentation; *Stage 3*: early back-arc basin development, and *Stage 4*: late back-arc basin development.

In the following Section, the essential features of each model stage are described. Additional details are provided by the caption to Figure 5.4.

5.3.2 Stage 1: The Island Arc

The lower part of the Wild Bight Group apparently preserves the final stages of the history of an island arc. The base is not exposed and the extent of arc activity that occurred prior to deposition of the exposed Wild Bight Group is not known. A sparse record of volcanic activity that predated the exposed section is found in mafic and felsic volcanic detritus in basal argillites and distal turbidites.

Volcanic rocks form less than 20 percent of this part of the sequence suggesting that the Wild Bight Group actually preserves a part of the arc that was somewhat removed from the main volcanic centers, perhaps on the distal flank of or between volcanoes. The illustration in Figure 5.4 is, therefore, very schematic rather than actualistic and the reader should not be mislead by the large, dominantly volcanic, arc depicted there.

The earliest volcanic activity, the LREE-enriched island arc tholeiites of the Seal Bay Bottom and Glover's Harbour East suites, probably formed through limited to moderate partial melting of a depleted mantle region contaminated by a slab-derived crustal component.

LEGEND

Rocks		Group		Magmas
Oceanic lithosphere		IAD		highly depleted tholeiite
island arc volcanic products		IAI		LREE - enriched island arc tholeiite
volcanogenic sediments				LREE depleted island arc tholeiite
debris flows, proximal turbidites				rhyolite
oceanic sediments		NAE		alkalic basalt
		NAT		enriched non-arc tholeiite
		NAI		intermediate non-arc tholeiite

Figure 5.4: Schematic illustration of the geologic history of the Wild Bight Group.

Stage 1: The Island Arc
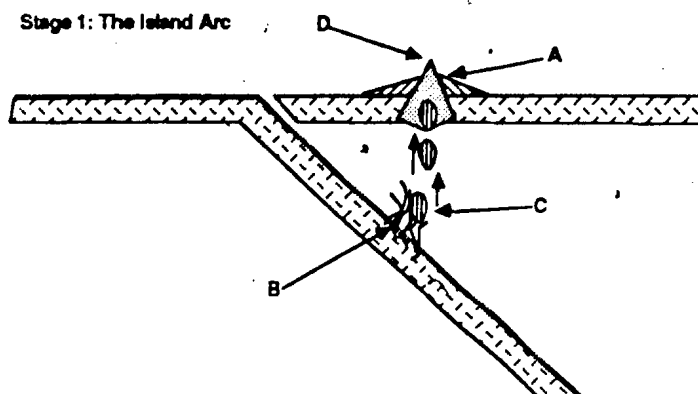
Stage 1: An island arc is already in place as the base of the Wild Bight Group is encountered. The lower part of the group may record the last phase of a more extensive period of island arc volcanic activity. A - volcaniclastic sedimentation around the arc. The fine grained nature of basal sediments and the relative sparsity of volcanic rocks suggests that the Wild Bight Group represents a distal-volcano or inter-volcano position in the arc. B - mass transfer of LFSE elements from the subducting slab to the overlying depleted mantle wedge. C - generation of LREE-enriched tholeiitic magmas through limited to moderate partial melting of depleted mantle contaminated with slab-derived material. D - eruption of LREE-enriched tholeiitic magma.

Stage 2: Arc Fragmentation
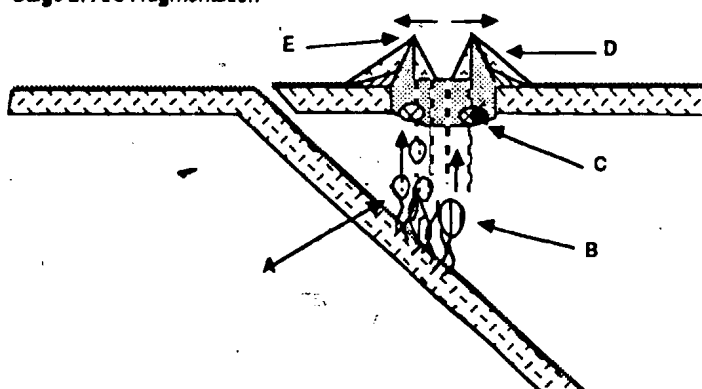
Stage 2: Rifting and the concomitant breakup of the arc is accompanied by a greater variety of magma types. A - Rising geotherms permit hydrous melting of previously melted refractory peridotite (light stipple) producing highly depleted tholeiitic magmas. Melts formed here undergo some fractional crystallization before being tapped by deep fractures and erupt without substantial equilibration with each other. B - Advanced partial melting of contaminated, depleted mantle peridotite (perhaps similar to that which melted in Stage 1) produces LREE-depleted tholeiites. C - hydrous melting of amphibolite at the base of the arc, perhaps promoted by deep circulation of hydrous fluids as a result of rifting, produces trondhjemitic liquids. D - sedimentation accompanying block faulting, and the considerable topographic relief that it creates, consist mainly of debris flows and proximal turbidites. E -eruption of magmas generated in A to D in close proximity to each other, both in time and space.

Stage 3: Early Back Arc Basin
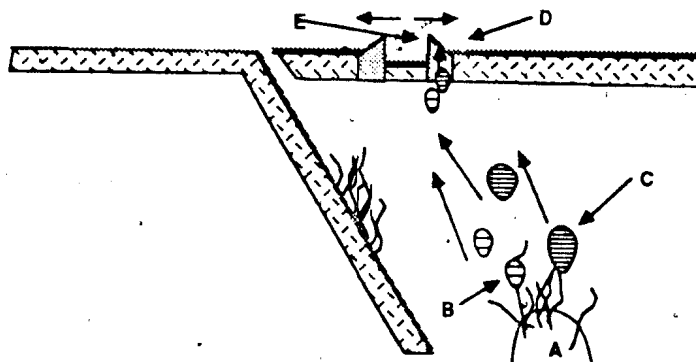
Stage 3: Arc rifting is followed by development of a back arc basin and the arc products are carried into this basin, perhaps as a remnant arc. "Enriched" or "plume" -type magmatism commences in the back arc shortly after the waning of volcanism related to arc breakup, perhaps due to the presence of a deep mantle plume (A) or fusion related to deep rifting. B -incipient melting of ocean island-like mantle sources produces alkali basalt which undergoes considerable fractional crystallization before eruption. Moderate amounts of partial melting yield enriched tholeiitic melts (C) which undergo less fractional crystallization and appear to have erupted first in this environment. D - subsidence related to back arc formation produces deep water, quiet environments which are reflected in fine grained turbidites and pelagic facies sediments. E - Magmas formed in B and C ascend and erupt through the previous arc products, perhaps following pre-existing conduits.

Stage 4: Late Back arc basin
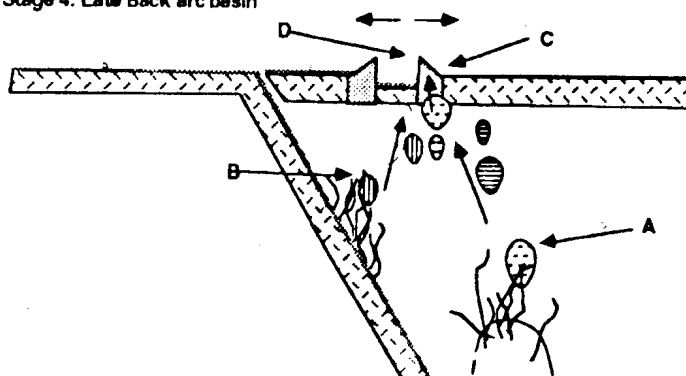
Stage 4: Further development of the back arc basin includes initiation of magmatism (A) which is depleted in incompatible elements relative to the previously erupted magmas, probably reflecting more advanced partial melting. Minor amounts of alkali and enriched tholeiite continue to erupt (B) as does a minor amount of LREE-enriched island arc tholeiite, the last vestiges of the arc magmatism (C), suggesting that the back arc basin is still quite small. Sedimentation is dominated by deep water and pelagic facies. The cessation of volcanic activity occurs in the early Caradoc, perhaps as the Wild Bight Group drifts away from the mantle plume and the volcanic products are covered by black shale, chert and associated pelagic sediments.

Sedimentary rocks become progressively coarser with increasing stratigraphic height. Minor conglomeratic debris flows, which are first in evidence immediately above the Seal Bay Bottom volcanics, increase gradually in size and importance upward, perhaps reflecting increased volcanic relief attendant with the early stages of arc breakup (cf. Carey and Sigurdsson, 1984).

5.3.3 Stage 2: Arc Fragmentation

This stage is the transitional period between normal island arc magmatism and the back-arc regime which follows. It is characterized by a proliferation in the varieties of magmatic rocks and by a culmination of the trend towards coarse-grained debris flow and proximal turbidite sedimentation.

The tectonic environment is envisaged as being dominantly extensional, with deep, throughgoing, fractures that reach mantle depths. Rising geotherms in the mantle wedge accompanying the onset of rifting are interpreted to have promoted hydrous partial melting of refractory, highly depleted mantle. This depleted source may be the residue from partial melting that formed the earlier arc tholeiites although this is not a necessary part of the model. These melts did not pool in shallow magma chambers but apparently fractionated in isolation from each other as they did not equilibrate isotopically. Their eruption, under these circumstances, may have been the result of tapping by deep fractures related to the initiation of arc rifting.

At the same time, trondhjemitic magmas were produced by hydrous partial melting of mafic rocks, probably in the basal arc crust. The production of high-SiO_2, low K rhyolitic magmas during this stage of Wild Bight Group development may have resulted from various factors including: 1) the arc may have attained sufficient thickness that temperature and pressure at the base allowed melting for the first time; 2) fractures related to the arc rifting may have allowed penetration of hydrous fluids and this, coupled with rising geotherms resulting from deep fracturing would produce a local environment in which basal arc crust could begin to melt.

The association of rhyolites with the Nanny Bag Lake LREE-depleted tholeiites suggests that these tholeiites also formed at this time. They apparently reflect more complete partial melting

of depleted mantle sources than was the case for the LREE-enriched tholeiites, perhaps reflecting a hotter sub-arc thermal regime.

The thick and abundant volcaniclastic debris flows at this stage of Wild Bight Group development also reflect the tectonic processes. As Carey and Sigurdsson (1984) have pointed out, the enhanced relief which results from block faulting accompanying arc rifting promotes the deposition of proximal turbidites and thick debris flows.

5.3.4 Stage 3: Early Back-arc

Magmatic activity that immediately followed the waning of magmatism related to arc rifting produced volcanic and subvolcanic rocks that both overlie and intrude the arc-related volcanic products. This is interpreted to indicate that, at the initiation of back-arc volcanic activity, the arc products were in the back-arc basin, perhaps forming a remnant arc.

The first volcanic rocks in the post-arc environment, enriched tholeiites of the Side Harbour suite, signal a major change in both magma sources and melting characteristics. Volcanic rocks resulting from deep melting of oceanic island basalt-type sources are encountered for the first time. One might expect the earliest-formed melts to have been the results of incipient partial melting (the alkali basalts of the NAE group). However, not these melts, but the enriched tholeiites resulting from more advanced partial melting, appear to have erupted first. The low Mg#'s in the alkali basalts suggest that they underwent considerably more fractional crystallization before erupting than did the Side Harbour suite; for some reason they were apparently not tapped during the earliest volcanic activity.

Partial melting may have simply resulted from rising geotherms related to deep fracturing during rifting. Alternatively, and by analogy with modern oceanic environments, the remnant arc may have passed over a mantle "plume" or "hot-spot" soon after arc rifting which initiated the activity. This is the scenario illustrated in Figure 5.4C.

Sedimentation in the back-arc environment consisted of deeper water facies characterised

by volcanically-derived distal turbidites, chert and very minor limestone and shale, also signalling a removal from the environment of active rifting and tectonic activity.

5.3.5 Stage 4: Late Back-arc

Volcanic activity in the upper part of the Wild Bight Group included continued, although waning, enriched tholeiite and alkali basalt volcanism, but is characterised by the onset of less enriched tholeiitic volcanism which appears to have resulted from higher degrees of partial melting of the OIB sources, perhaps including incorporation of normal depleted mantle material. These are the most MORB-like volcanic rocks preserved in the back-arc sequences may signal a more mature phase of back-arc development in which lessening intensity of rifting allowed more complete partial melting, reducing the influence of enriched mantle sources in the magmas.

The apparent interbedding of LREE-enriched back-arc tholeiites and enriched island arc tholeiites in the Northern Arm suite suggest that the influence of the subducting slab, although waning, was still evident and the marginal basin still in a relatively early stage of development.

5.3.6 Comments on the Comparison with Fiji

The changes in tectonic environments and the resultant changes in magmatism that are interpreted for the Wild Bight Group show some parallels and some contrasts with those recorded in Fiji. Because Fiji appears to be a particularly close modern analogue for the Wild Bight Group, some more detailed comments of the comparisons and contrasts between them are warranted.

The thick and long-lived successions of low-K island arc tholeiites that characterize the early history of Fiji are not present in the Wild Bight Group although the basal LREE-enriched tholeiites may be analogous to medium-K tholeiites which are common in the main stage of island arc volcanism in the Lau Islands (Cole et al., 1985). These rocks in the Wild Bight Group may also be analogous to the calc alkalic andesites that form the second stage of Fiji volcanism, from the standpoint that both apparently represent relatively low degrees of partial melting of similar sources. If the transition to this style of magmatism is characteristic of the initial stages of arc

fragmentation, then it may be that, in terms of the Fiji model, the Wild Bight Group preserves events which have already reached this second stage, the main stage arc volcanism not having been preserved.

The formation of low-K rhyolites at 7 Ma has been attributed by Stork and Gill (1982) to partial melting of basal arc crust promoted by rising geotherms accompanying incipient arc rifting. This is a similar interpretation to that proposed here for the Wild Bight Group rhyolites (and the correspondence is further heightened by the presence of volcanogenic mineralization in both cases, see Chapter 6). In Fiji, rhyolite eruption was apparently not accompanied in time by eruption of depleted tholeiitic magmas, as in the Wild Bight Group. However, Cole et al. (1985) noted that volcanic rocks in the Lau Ridge that record incipient fragmentation of the Fiji arc have regionally low Zr and La concentrations and Ti/V ratios as well as high Cr/Al ratios in their chrome spinels, perhaps indicating "magma generation from a very refractory mantle source, perhaps made possible by rising geothermal gradients that accompanied initial arc rifting".

In the Wild Bight Group, as in Fiji, the phase of magmatism following the LREE-enriched arc andesites and rhyolites is dominantly basaltic, resulting from very low degrees of partial melting. In Fiji, this magmatism is shoshonitic and carries an arc geochemical signature. In the Wild Bight Group, it is within-plate alkalic and transitional tholeiitic. Do these represent a response to similar tectonic conditions but different sources? This question is, of course, indeterminate, but it seems reasonable that in the Wild Bight Group, these melts may represent melting and easy access to the surface resulting from continued rifting accompanying the opening of the Caradocian back-arc basin. The deep fractures could well have had a similar influence to those that promoted incipient partial melting and rapid eruption of enriched, arc-related magmas in Fiji during late arc rifting. In this respect, the NAE and NAT group lavas may be genetically analogous to the Fiji shoshonites.

The apparent interbedded relationship of arc tholeiites and back-arc basalts in the Wild Bight Group suggests that the Wild Bight Group only records magmatism in the early stages of back-arc basin formation. The Fiji case demonstrates that there may be a period of time during arc

fragmentation when arc and non-arc magmas erupt simultaneously, although in the Fiji case, this
time period was very small.

5.4 The Wild Bight Group in the Context of the Geology of the Newfoundland Central Mobile Belt

5.4.1 General Statement

As outlined in Chapter 1, the Wild Bight Group is part of the youngest and most
widespread oceanic volcanic episode recorded in Central Newfoundland. Coeval sequences
include: 1) most of the pre-Caradocian rocks in central Notre Dame Bay south of the Lukes Arm
fault; 2) the Victoria Mine sequence, the Diversion Lake volcanics and most of the central
volcaniclastic sequences in the Victoria Lake Group in south-central Newfoundland; and 3) at
least parts of the Bay du Nord and Baie d'Espoir Groups in the Hermitage Flexure of southern
Newfoundland (Figure 5.5). The geochemical and isotopic studies of the Wild Bight Group
reported in this thesis are the most detailed to date from any volcanic rocks in Newfoundland
representing this period in the history of Iapetus. They have the potential to further our
understanding of the regional development of the Dunnage Zone by allowing reinterpretation of
available data for coeval sequences elsewhere in Central Newfoundland.

In the following Section, the other Central Newfoundland Llanvirnian to Caradocian
volcanic and sedimentary sequences are briefly described, compared and contrasted to the Wild
Bight Group, and integrated in a model for the Llanvirnian - Caradocian development of the
Dunnage Zone.

5.4.2 Central and Eastern Notre Dame Bay

5.4.2.1 The Exploits Group

The stratigraphy of the Exploits Group is very similar to that of the Wild Bight Group and
early workers in Notre Dame Bay (e.g. Heyl, 1938) considered them to be the same unit (even
though they are not in contact). Helwig (1967, 1969) outlined the stratigraphy of the Exploits
Group, identifying three volcanic members (in ascending order the Tea Arm, Saunders Cove and

Figure 5.5 - Distribution of Cambrian and Ordovician oceanic volcanic and sedimentary rocks in Central Newfoundland.

Dark stipple indicates Llanvirnian to Caradocian volcanic rocks: BdeE - Baie d'Espoir Group; BdeN - Bay du Nord Group; DL - Diversion Lake volcanics; E - Exploits Group; LH - Loon Harbour volcanics; SF - Summerford Group; VM - Victoria Mine sequence; WB - Wild Bight Group

Double broken pattern is Arenigian rocks of the Buchans - Robert's Arm belt (including the Cutwell Group): B - Buchans Group; CW - Cutwell Group; RA - Robert's Arm Group;

Single broken pattern is Cambrian to Arenigian volcanic sequences (including ophiolites): A - Annieopsquotch Complex and related ophiolitic fragments (e.g. Star Lake, King George IV Lake); BVRL - Baie Verte - Brompton Line; CP_1 - Catchers Pond Group; CP_2 - Coy Pond Complex; G - Glover Formation; GRUB - Gander River Ultrabasic Belt; LB - Lushs Bight and Western Arm Groups; MH - Moreton's Harbour Group; PF - Pine Falls Formation; PH - Pacquet Harbour Group; PP - Pipestone Pond Complex and Coldspring Pond Formation; S - Skidder basalt; SC - Sleepy Cove Group; SB - Snooks Arm Group and Betts Cove Complex; TH - Tulks Hill volcanics; TP - Tally Pond volcanics; TT - Twillingate Trondhjemite

Light stipple is Cambrian to Middle Ordovician sedimentary rocks, mainlly volcanically-derived turbidites and related rocks. Heavy dark lines are Caradocian shale: DM - Dunnage Melange; D - Davidsville Group.

Notre Dame Bay

PH

SB

BVBL

CW

SC   TT

SF

CF

MH

LAF

LB

CP₁   LCF

DM

RR

WB

E

LH

D

Grand Lk

B

G

Bad Indian

VM

DL

Gander Lk

GRUB

A

TH

TP

PF

PP

CP₂

Meelpaeg Lk

BdE

BdN

Hermitage

Flexure

Bay d'Espoir

0   40
km
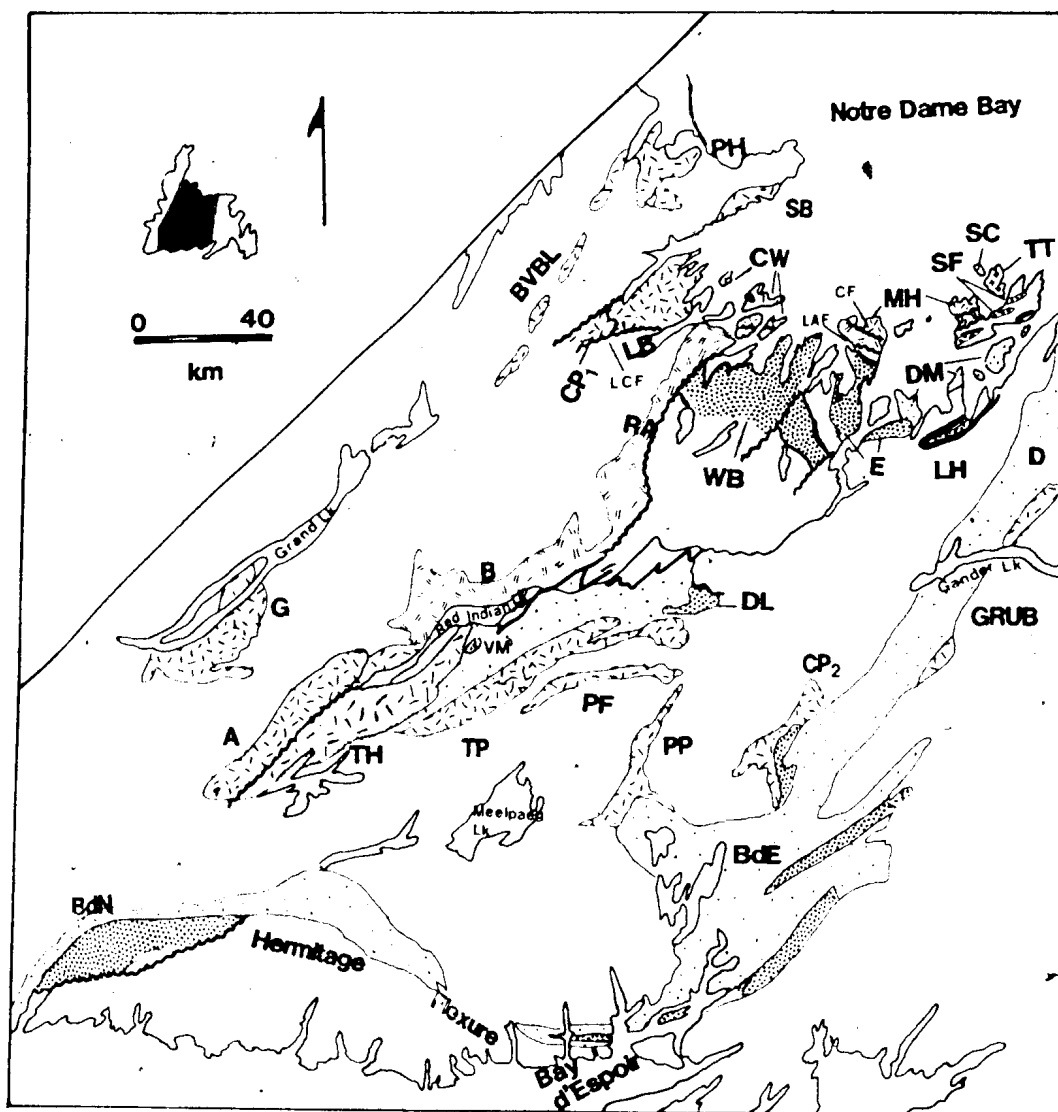
Lawrence Cove volcanics), the last being overlain by the Caradocian Lawrence Harbour shale (Heyl, 1936). The stratigraphic similarity. between the Wild Bight and Exploits Groups was recognized by Horne and Helwig (1969) and Helwig (1969) who correlated the two in regional stratigraphic reconstructions of Notre Dame Bay.

Recently published geochemical studies have identified two types of volcanic rocks in the Exploits Group: 1) Wasowski (1985) described the Tea Arm volcanics near the base of the group as comprising dominantly a lower unit of very fractionated lavas with $TiO_2>0.89\%$ and an upper unit of less fractionated lavas with $TiO_2<0.57\%$. He compared these to boninites and suggested that their presence was indicative of a forearc setting: 2) Wasowski and Jacobi (1984) described the geochemistry of the Lawrence Head volcanics at the top of the Exploits Group overlain by the Caradocian shale, as comprising basalts with average $TiO_2=1.76\%$ and with a trace element signature indicative of E-MORB or oceanic tholeiites. They emphasized the similarity between these rocks and oceanic seamounts.

These chemical relationships are similar to those in the Wild Bight Group. The Tea Arm volcanics appear to compare closely with the Glover's Harbour volcanic unit where intermediate-TiO_2 tholeiites (Glover's Harbour East suite) are overlain by depleted tholeiites (the Glover's Harbour West suite). The Lawrence Head volcanics appear to be geochemically similar to the intermediate and/or enriched tholeiites of the NAI and NAT groups; in the absence of detailed published information from Wasowski's study, more detailed comparisons are not possible.

In any event, volcanic rocks in the Exploits Group appear to record the same arc to back-arc transition as that in the Wild Bight Group. The more detailed information available for the Wild Bight Group suggests that the interpretations of the Tea Arm volcanics as a fore arc suite and the Lawrence Head volcanics as oceanic seamounts does not necessarily follow from the data. It is here suggested that the Tea Arm rocks are actually, like the IAD group, related to initial rifting of the island arc and the Lawrence Head volcanics to the establishment of the back-arc basin.

5.4.2.2 The Summerford Group

The Summerford Group (Horne and Helwig, 1969; Horne, 1970; Dean 1978) comprises dominantly pillow lavas and volcaniclastic sediments which outcrop in several linear, fault bounded slices on New World Island. Structural relationships in this part of Notre Dame Bay are very complex and have defied the best efforts of numerous workers over the years to produce a widely accepted stratigraphic and structural model. Abundant fossil evidence shows that three ages of volcanic rocks are represented, these being Tremadocian (Kay, 1967), late Arenigian to early Llanvirnian (Neuman, 1976) and late Llandeilian (Dean, 1970; Bergstrom et al., 1974; Fåhraeus and Hunter, 1981). The latter are overlain by the richly fossiliferous Cobbs Arm limestone, interpreted by Stouge (1981) and Fåhraeus and Hunter (1981) as a carbonate buildup on volcanic islands, and thence by Caradocian shale. Geochemical data for the northern part of the Summerford Group were first presented by Reusch (1983) (who termed these rocks the Squid Cove volcanics) and later by Jacobi and Wasowski (1985). Only samples representing the Arenigian/Llanvirnian and Llandeilian volcanic suites were analysed in these studies. Reusch's (1983) samples were drawn from a wider area than were Jacobi and Wasowski's and are, therefore, probably more representative of the Summerford Group as a whole. His samples have a very wide range of TiO_2 contents (0.86 to 3.37 percent) and his interpretation that they are all oceanic, non-orogenic tholeiites notwithstanding, representatives from more than one tectonic setting do not appear to be precluded. Jacobi and Wasowski (1985) presented only averages of their data (TiO_2 averages 1.78 with standard deviation of 0.32 for 11 samples) which they interpreted as indicative of E-MORB or oceanic island basalts. They interpreted the Summerford Group to represent a chain of seamounts of various ages structurally emplaced in an accretionary prism.

The chemistry of the younger (Llandeilian) Summerford Group volcanics, according to Reusch's data, suggest a correlation with the upper part of the Wild Bight Group. They may, therefore, represent the same back-arc volcanic activity as the upper Wild Bight and Exploits

Groups. However, most of Reusch's samples with relatively low TiO_2 contents (e.g.<1.80 %) come from the older (Arenig-Llanvirn) sequence and it is possible that these, in part, correlate with the lower, arc-related parts of the Wild Bight Group. The geochemical data are not sufficiently precise to pursue this comparison at present. More detailed chemistry from the Summerford Group is needed, including high precision trace element and REE data.

5.4.2.3 The Dunnage Melange

The Dunnage Melange (Kay and Eldridge, 1968) is a chaotic unit which outcrops extensively in eastern Notre Dame Bay comprising blocks of sedimentary, volcanic and intrusive rocks in a black shale matrix. Detailed mapping led Hibbard and Williams (1979) to interpret it as an olistostrome, the formation of which probably immediately predated deposition of the Caradocian shale. They speculated that it formed on the flanks of an island arc but were unwilling to specify whether forearc or back-arc. An historical bias in favour of the forearc origin (e.g. Horne, 1970; Jacobi and Schweickert, 1976; Kidd et al., 1977) has been predicated on the supposition that the melange might be a trench-fill deposit and this has been a major factor in locating the paleosubduction zone in many plate tectonic models (e.g. Dewey, 1969; Bird and Dewey, 1970). The arguments in favour of a back-arc environment generally point out that if an east-dipping subduction zone is accepted for this time period, the location of most island arc rocks to the west of the Dunnage Melange require it to be formed in a back-arc environment. Lorenz (1984) recently studied intrusions in the Dunnage Melange, including unique, ultramafic-bearing felsic intrusions, which she interpreted to have formed in a crustally-thinned, back-arc, setting. These remain, to this writer, the most convincing arguments, based on direct evidence, in favour of a back-arc setting.

The geochemistry of volcanic blocks in the Dunnage Melange has recently been reported by Wasowski and Jacobi (1985) who noted their geochemical similarity to both the Lawrence Head volcanics and the Summerford Group. This confirms Hibbard and Williams' (1979) impression that volcanic rocks in the melange could be correlated lithologically with the adjacent

intact formations. Wasowski and Jacobi (1985) were unwilling to specify the tectonic setting on the basis of this geochemistry. They noted that, on the one hand, a back-arc setting was consistent with the relative positions of the arc-related rocks in an east-dipping subduction system but that on the other, their earlier interpretations of the adjacent pillow lava units as seamounts (see discussion of Exploits and Summerford Groups above) could support an origin in an accretionary complex in the arc-trench gap.

The present correlation of the Lawrence Head and (albeit more tenuously) the younger Summerford Group volcanics with the upper Wild Bight Group suggest a back-arc origin rather than seamounts accreted in the fore arc. This would appear to lend further support to those who advocate a back-arc origin for the Dunnage Melange.

5.4/2.4 The Loon Harbour volcanics

The Loon Harbour volcanics (Kay, 1975) comprise mainly mafic pyroclastic and volcaniclastic rocks with lesser pillow lava and are overlain by Caradocian shale. Dean (1978) correlated them with the top of the Wild Bight Group on the basis of lithological similarity and stratigraphic position with respect to the Caradocian shale.

Fargo (1983) reported on a geochemical study of the mafic volcanic rocks which he interpreted to indicate a within plate oceanic setting. He suggested they may represent an oceanic seamount but did not publish the data.

The presence of within plate volcanic rocks in volcanics immediately beneath the Caradocian shale is consistent with relationships in the Wild Bight, Exploits and Summerford Groups. They may also represent back-arc volcanic activity following fragmentation of the Wild Bight arc.

5.4.3 South - Central Newfoundland

5.4.3.1 The Victoria Mine sequence

An aerially restricted sequence of mafic and felsic volcanic rocks outcrops on the Victoria River south of Red Indian Lake. This unit, which hosts the old Victoria Mine (Kean and Evans, 1986), contains fossiliferous limestone which has yielded a Llanvirnian - Llandeilian fauna (Stouge, 1981). Subvolcanic rhyolite near the fossiliferous horizon has yielded a radiometric age (U/Pb in zircon) of 462(+4/-2) Ma. (Dunning et al., 1986). The age and the presence of felsic volcanic rocks and volcanogenic sulphides are consistent with a correlation between these rocks and the arc fragmentation stage of the Wild Bight Group. There are no published geochemical data from the volcanic rocks and further comparisons with the Wild Bight Group are not possible.

5.4.3.2 The Diversion Lake volcanics

The Diversion Lake volcanics occupy the northeastern part of the Victoria Lake Group. They are overlain by the Caradocian shale and, therefore, are potentially time equivalents of the upper Wild Bight Group. Preliminary unpublished geochemical data (my own and that of B. F. Kean, personal communication, 1986) show these volcanics to be of non-arc character ($TiO_2 > 2$ %; no negative Ta or Nb anomalies) consistent with their correlation with back-arc related volcanic rocks of the Wild Bight Group.

5.4.4 The Hermitage Flexure

Ordovician volcanic sequences of southern Newfoundland, assigned to the Bay du Nord and Baie d'Espoir Groups (Figure 5.5) are dominantly felsic and have been interpreted by recent workers to have been deposited at or near an ancient continental margin (Colman-Sadd, 1980; Swinden and Thorpe, 1984). Recent radiometric dating of felsic volcanic rocks in the western Hermitage Flexure has yielded ages of 466(+3/-2) (Dunning et al., 1986) for the Baie du Nord Group and a preliminary date for the Baie d'Espoir Group is also Early or Middle Ordovician (Arenigian to Llandeilian) although not precisely known at the time of writing. (G.R. Dunning,

personal communication, 1986). These suggest that at least some of this volcanic activity was approximately coeval with the Wild Bight Group.

A direct relationship between volcanic rocks in the north and central Dunnage Zone and the Hermitage Flexure is difficult to establish. Swinden and Thorpe (1984) suggested, on the basis of lead isotopes in the contained sulphide deposits, that the continental margin with which the Hermitage Flexure sequences were associated also contributed lesser amounts of lead to the Wild Bight and Victoria Lake Group magmatic rocks. If this argument is accepted (and new lead isotope data presented in Chapter 6 do not contradict it) then it is possible that these rocks are from different parts of the same Llanvirnian to Llandeilian island arc which traversed both oceanic and continental margin settings. However, the data do not demand this and it is also possible that these volcanic rocks were not spatially related in the Ordovician and were brought together in Central Newfoundland during later orogenesis.

5.4.5 Summary of Llanvirnian-Caradocian Geological Events in the Dunnage Zone

In a regional sense, the Wild Bight Group and its correlatives record the last oceanic volcanic events in the part of Iapetus that is preserved in Central Newfoundland. This volcanic event is widely represented in the Dunnage Zone east of the Buchans - Robert's Arm Groups and south of the Lukes Arm Fault (Figure 5.5). During Llanvirnian time, an island arc was active throughout this region producing volcanic sequences now preserved in the northern and central Dunnage Zone (lower Wild Bight and Exploits Groups, perhaps some rocks now assigned the Summerford Group, the Victoria Mine sequence). Felsic volcanic rocks of the Bay du Nord and Baie d'Espoir Groups may also have been part of this island arc, erupting at or near a continental margin to the south.

Fragmentation of the arc, recorded in the Dunnage Zone sequences, probably did not begin before the late Llanvirn - early Llandeilo (the age of fossils associated with the Victoria Mine sequence). Once arc rifting had begun, new magma sources were soon established in all areas,

Back-arc basin volcanism similar to that in the upper part of the Wild Bight Group is probably recorded by the upper parts of the Exploits and Summerford Groups and the Loon Harbour volcanics in the northeast as well as in the Diversion Lake volcanics in the southwest. This volcanic activity was apparently short-lived as, by the beginning of the Caradocian, black shales containing a *Nemagraptus gracilus* fauna (latest Llandeilo - earliest Caradoc) were being deposited on the products of back-arc volcanism in western and central Notre Dame Bay. The beginning of Caradocian pelagic sedimentation started a little later in eastern Notre Dame Bay as a *Diplograptus multidens* fauna (early Caradoc) is the first fauna over the Summerford Group (Dean, 1978). This, of course, does not necessarily mean that volcanic activity continued longer in this area. The hiatus between the end of volcanic activity and the beginning of Caradocian sedimentation is filled by deposition of the Cobbs Arm limestone.

5.4.6 Relationship of the Wild Bight Group to older volcanic rocks in the Central Mobile Belt

The available geological and geochemical data support the hypothesis that Llanvirnian-Caradocian volcanic sequences east of the Buchans-Robert's Arm groups and south of the Lukes Arm Fault can be interpreted as parts of a single subduction complex. The question then arises as to their relationship to older magmatic and sedimentary rocks in this area such as the Tally Pond and Tulks Hill volcanics. Lead isotope data presented in Chapter 6 have a bearing on this question and further discussion is deferred until this evidence is presented.

At present there are no compelling geological links between sequences east and south of the Buchans - Robert's Arm belt and those to the northwest. In fact, the absence of the post-Caradocian flysch has long been pointed to as evidence for tectonostratigraphic contrasts between these two areas in post-Middle Ordovician time (Dean, 1978; Nelson and Casey, 1981). Evidence from lead isotopes in volcanogenic mineralization (Chapter 6) suggest further contrasts in volcanic environments in the two areas and the question is again addressed following presentation of these data in Chapter 6.

5.5 Summary and Conclusions

The Wild Bight Group is interpreted to record a Llanvirnian to Caradocian transition from island arc to back-arc basin environments. The paleotectonic history can be described in terms of four stages : 1) late island arc; 2) arc fragmentation; 3) early back-arc basin; and 4) late back-arc basin. Each stage has a distinctive magmatic history which can be modelled in terms of changing tectonic conditions. During Stage 1, only island arc tholeiites erupted (LREE-enriched members of the IAI group) but during Stage 2, a greater diversity of magmatism resulted from the initiation of rifting. Very depleted tholeiites (the IAD group), LREE-depleted island arc tholeiites of the IAI group and low-K, high-SiO$_2$ rhyolites were erupted during this time. Stage 3 records the initiation of back-arc volcanic activity, without the geochemical signature of the subduction slab. Magmatism resulted from relatively low degrees of partial melting, producing alkali basalts (the NAE group) and transitional enriched tholeiites (the NAT group). Maturing of the back-arc basin (Stage 4) was accompanied by magma production resulting from higher degrees of partial melting (the NAI group; perhaps a precursor to the eruption of N-MORB, which is not preserved in these sequences) as well as waning volcanism of early back-arc basin type. Local continued eruption of island arc tholeiites at this time suggest that the basin was still relatively narrow.

A good modern analogue for the Wild Bight Group is found in Oligocene to Recent sequences of the Fiji platform, a remnant arc between the Lau and North Fiji basins, where island arc, arc fragmentation and back-arc formation are recorded in a volcanic history that has many similarities with that of the Wild Bight Group. In particular, the narrow interval in which back-arc and arc lavas were erupted simultaneously provides a time framework in which to interpret the interval represented by Stages 3 and 4 of the Wild Bight Group. Alternating eruption of arc and back-arc magmas is also recorded in the Mariana Trough, suggesting that this may be characteristic of the early history of many back-arc basins.

Parts of the Llanvirnian to Caradocian, arc to back-arc transition recorded by the Wild Bight Group are preserved throughout central and eastern Notre Dame Bay and south-central

Newfoundland. Felsic volcanic sequences of the Hermitage Flexure are also, at least in part,
coeval with the Wild Bight Group volcanism, although their specific tectonostratigraphic
relationship to the Wild Bight Group is equivocal.

CHAPTER 6

VOLCANOGENIC SULPHIDE MINERALIZATION: FIELD RELATIONSHIPS,

PALEOTECTONIC SETTING AND LEAD ISOTOPES

6.1 Introduction

There are four documented volcanogenic sulphide occurrences in the Wild Bight Group (Figure 2.1), in decreasing order of size the Point Leamington deposit hosted by the Side Harbour volcanic unit, the Lockport deposit, hosted by the Glover's Harbour West suite, the Indian Cove deposit hosted by the Indian Cove volcanic unit and the Long Pond prospect hosted by the Long Pond volcanic unit. It is not the purpose of this Chapter to present detailed descriptions of the deposits, although brief descriptions are presented to provide necessary information concerning their field relationships, nature, and geological setting. Rather, the emphasis is on interpreting the setting of the deposits in terms of the paleotectonic models derived in previous Chapters and to compare this with deposits in similar sequences elsewhere in Newfoundland and the Appalachian-Caledonian orogen. The mineralized environments are compared to some recent deposits, where the settings are well known.

Lead isotopic studies have been conducted on the Point Leamington and Indian Cove deposits. These are compared with lead isotopic data from other deposits in various Iapetan oceanic sequences in an attempt to recognize different lead sources and identify sequences with different basement terranes. The results provide additional constraints as to correlation of events within the Newfoundland portion of Iapetus.

6.2 Descriptions of the Deposits

6.2.1 The Point Leamington Deposit

The Point Leamington deposit was discovered in the early 1970's by Noranda Exploration Ltd. A brief description of the deposit, based mainly on the results of diamond drilling, was published by Noranda Mines Staff (1974). Swinden (1984) later described the setting of the

deposit based on field studies and reexamination of core from eleven drill holes. Grade and tonnage figures have not been released but published dimensions indicate more than 20 million tonnes of massive sulphide grading approximately 0.5% Cu, 2% Zn and sporadic gold values.

Figure 6.1 is a representative section of the deposit, constructed from surface mapping and relogging of drill core. The deposit is a large, stratabound, massive sulphide (mainly pyrite with lesser chalcopyrite and sphalerite) body underlain by an extensive quartz-sericite and quartz-chlorite-pyrite alteration zone. The deposit occurs near the southwestern edge of the Side Harbour volcanic unit at the contact between a footwall rhyolitic quartz and quartz-feldspar crystal tuff and hanging wall mafic hyaloclastic and pyroclastic rocks.

i) *The Footwall sequence*: The immediate footwall to the deposit comprises dominantly rhyolitic crystal tuff and breccia and lesser quartz-feldspar porphyry interpreted as flows. Beneath the deposit, the normally pale buff to grey rhyolite is pervasively altered to a pale green quartz-sericite assemblage. Locally, intense silicification has destroyed primary textures in zones up to 1 m wide and 1 to 5 percent disseminated pyrite is present. A later, more localized, alteration consists mainly of black chlorite in veins ranging from several mm to 2 m wide, locally accompanied by up to 50 percent pyrite and chalcopyrite. This alteration is generally concentrated in relatively restricted zones immediately beneath the massive sulphides and is interpreted as feeders for the hydrothermal fluids that carried metals to the sea floor.

Beneath the massive sulphide deposit, the felsic volcanic unit is over 130 m thick and is underlain by pillowed mafic volcanic rocks, comprising incompatible element-depleted tholeiites the IAD group (Chapter 3). Outcrops of pillow lava in the immediate vicinity of the deposit are highly altered with extensive chlorite and epidote veining.

ii) *The Massive Sulphide*: The massive sulphide is up to 65 m thick, comprising a remarkably uniform body of generally fine grained pyrite, lesser chalcopyrite and sphalerite and erratic gold which is associated with zinc and locally attains economically interesting grades over mining widths. Hangingwall and footwall contacts are generally sharp and there are at least two separate ore lenses in the deposit (Figure 6.1) separated by a unit of altered felsic volcanic breccia. The

Figure 6.1 - Representative cross-section of the Point Leamington volcanogenic sulphide

deposit, constructed from relogging of diamond drill holes. Line of section is approximately

northeast (right) - southwest. No vertical exaggeration.

Legend: 1 - mafic intrusive rocks; 2 - epiclastic turbiditic greywacke, argillite; 3 - jasper and

jasper-bearing breccia; 4 - mafic pyroclastic and hyaloclastic rocks; 5 - grey chert, pyritic argillite; 6

- massive sulphide; 7 - rhyolite, rhyolite breccia; 8 - mafic volcanic rocks. Stratigraphic top is to the

left. Stippled area beneath the deposit is area of intense chlorite - quartz - sulphide footwall

alteration.

0   100
metres
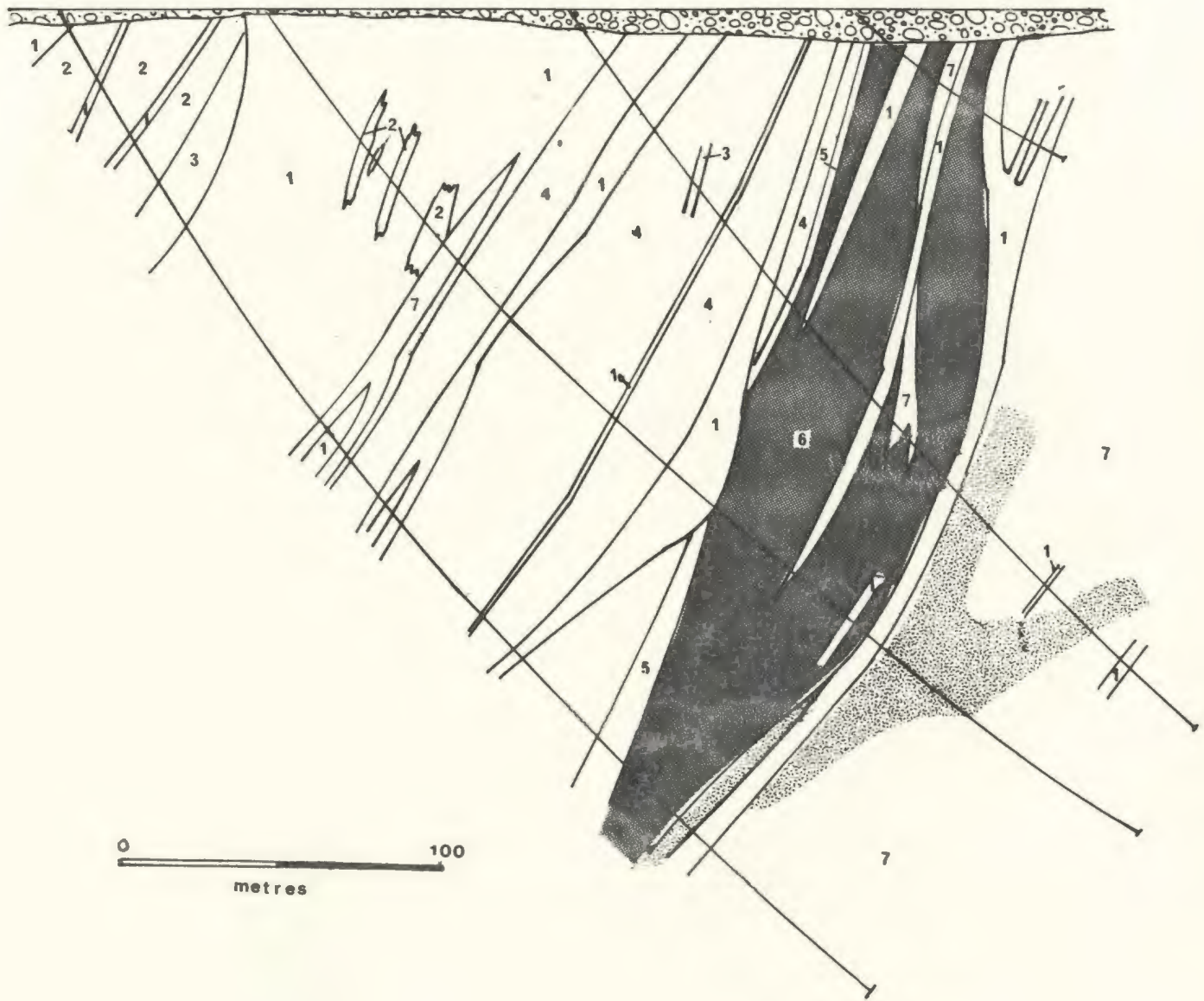
deposit strikes approximately northwest, dips to the west at about 50° and plunges shallowly to the southeast. Near surface sections are relatively low grade but down dip and down plunge, both zinc and gold grades increase gradually. At the time of writing, a mineable deposit has not been outlined but the deposit is open down dip and down plunge to continuing exploration.

The massive sulphide is capped by a thin unit of sulphidic argillite ranging from less than 3 m to more than 20 m thick, comprising grey chert interbedded with black argillite which locally has laminae up to 1 cm thick of massive pyrite.

iii) *The Hangingwall sequence*: The massive sulphide is immediately overlain by 75 to 100 m of mafic hyaloclastite (pillow breccia) and pyroclastic rocks comprising mafic volcanic and sedimentary rock fragments in a black, fine grained tuffaceous matrix. Thin beds of red to orange jasper are locally present. Above this, the succession is dominantly volcaniclastic rocks, green turbiditic sandstone, siltstone and lesser conglomerate. All hangingwall rocks are intruded by mafic sills up to 30 m thick, comprising diabase to gabbro.

The Point Leamington deposit is clearly a volcanogenic massive sulphide deposit. The underlying felsic volcanic rocks are interpreted as a rhyolite dome following a period of mafic volcanic activity. Hydrothermal circulation, possibly related to the felsic magmas, altered both the felsic rocks and the basement mafic volcanic rocks and these fluids carried metals to the sea floor where they were deposited near the vents. The deposition of massive sulphides marked a change in magmatic activity in the area and heralded an extended period of mafic pyroclastic and volcaniclastic deposition.

.6.2.2 The Lockport Deposit

The Lockport deposit was apparently discovered in the late 1870's or 1880's (although the discoverer's identity is not known) and received sporadic attention from exploration companies through the first half of the century. It was visited and reported upon by Heyl (1938), but it was not until the early 1950's that detailed exploration outlined a deposit of approximately 220,000 tonnes of material grading 1.21% Zn underlain to the northwest by approximately 392,000

tonnes grading 0.75% Cu (Fogwill, 1965). DeZoysa (1969) studied the old workings and the surrounding rocks and concluded that the deposit was probably volcanogenic in origin.

The deposit (Figure 6.2) is hosted by incompatible element- depleted pillow lava of the Glover's Harbour West suite (IAD group, Chapter 3). It occurs near the center of the exposed area of this suite, slightly east of the axis of a northeast-trending anticline and near the exposed base of the sequence (Figure 2.5). There is a small (400 m x 200 m) rhyolite dome approximately 400 m to the southwest along strike. Several other minor hydrothermal alteration zones are found in the immediate vicinity.

Mineralization is best exposed in a series of open cuts on the northwest side of the deposit and is well represented in dumps from the open cuts and several old shafts. The open cuts expose a pyrite- and chalcopyrite - bearing stockwork in which mafic pillow lavas of the host Glover's Harbour volcanic unit have been intensely altered to quartz-sericite ± chlorite assemblage. This stockwork apparently represents the copper-rich deposit described by (Fogwill, 1965). The overlying Zn-rich zone does not outcrop, nor is it well represented in dump material. Based on descriptions in old drill logs, which record greater than 75% sulphides in this section, the zinc-rich zone is tentatively interpreted as a small (less than 8 m thick and with a strike extent of less than 130 m) massive sulphide body.

The Lockport deposit, like the Point Leamington deposit, is a volcanogenic massive sulphide deposit with footwall stockwork zone. Although small and without present economic potential, the deposit demonstrates the operation of processes similar to those that formed the larger deposit to the south. In contrast to the Point Leamington, this deposit is hosted by mafic volcanic rocks and massive sulphide deposition did not mark a major change in volcanic and volcaniclastic activity. Rhyolitic rocks occur nearby along strike and may be genetically related to the deposit, although this relationship cannot be unequivocally demonstrated.

6.2.3 The Indian Cove Deposit

The Indian Cove deposit was discovered in the late 1800's, and received sporadic

Figure 6.2 - Cross section of the Lockport deposit compiled from diamond drill logs and redrawn after Howse and Collins (1979). Northwest is to the left.

Legend: 1 - silicified, sericitized pillow lava and volcanic breccia; 2 - mafic volcanic rocks; 3 - epiclastic rocks; 4 - mafic intrusive rocks; black shading is intensely altered stockwork and heavy stipple is probable massive sulphide.

opencut

3

4

1

2

4

1

4

2

1

2

1

0   25   50

metres

N ←——→ S
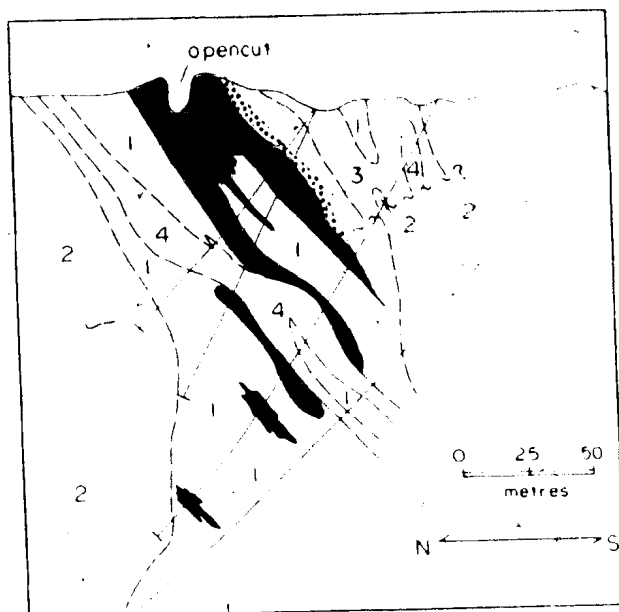
exploration through the early and mid 1900's. Hydrothermal alteration and mineralization is present throughout the felsic volcanic rocks of the host Indian Cove volcanic unit and several distinct showings, consisting mainly of disseminated pyrite and minor chalcopyrite, have been identified. The stratigraphy of the Indian Cove volcanic unit was previously described in Section 2.5.1.2.

The Indian Cove prospect is located approximately 300 m southwest of Indian Cove (Figure 2.1, 2.4) where disseminated and stringer pyrite, chalcopyrite, lesser sphalerite and rare galena occur in gossan-covered outcrops, several small trenches and a 2 m long adit. In addition, there is drill core on file at the Newfoundland Department of Mines core Library in Pasadena, recovered from eight drill holes that tested this showing in 1975. A schematic representation of the stratigraphy and mineralization in the Indian Cove unit is shown in Figure 6.3. The sulphides occur mainly in felsic pyroclastic rocks, near their contact with the basal rhyolite dome. The host rocks are strongly silicified, sericitized and locally chloritized. Sulphide minerals exceed 5 volume percent only in the most intensely altered zones, where they are associated with black chlorite and quartz. A single mafic volcanic flow in the volcanic unit consists of incompatible element-depleted tholeiites of the IAD group, but is not spatially related to the mineralization.

The Indian Cove deposit is interpreted as a particularly intense alteration facies of a hydrothermal system related to the Indian Cove felsic volcanic activity. There do not appear to be any exhalative sulphides associated with this mineralizing system. However, the abundant red chert that overlies the volcanic rocks (see Section 3.5.1.2) probably signals an abundant supply of iron in the sub-seafloor environment at this time and may record the exhalation of predominantly iron-bearing fluids related to the underlying alteration.

6.2.4 The Long Pond Prospect

The Long Pond prospect is a relatively minor showing hosted by altered felsic and minor mafic volcanic rocks of the Long Pond rhyolite 2.

The deposit consists of disseminated (1 to 5 percent) pyrite and minor chalcopyrite associated

SSW ← → NNE

Indian Cove prospect

Legend:
- ∿ hydrothermally altered rhyolite dome
- volcanic breccia, associated pyroclastic rocks
- pillow lava
- red argillite and chert, lesser green and black sulphidic argillite
- very coarse slump breccias;
- epiclastic rocks; mainly turbiditic greywacke, lesser conglomerate
- Locally intense alteration with base metal-bearing sulphides

Figure 6.3: Schematic representation of the Indian Cove volcanic complex and the associated volcanogenic mineralization. Hydrothermal activity related to the felsic magmatism results in alteration of the rhyolite dome and the overlying pyroclastic apron. Locally, particularly intense alteration produces disseminated sulphide concentrations with elevated base metal values. Red ferruginous argillite at the top of the complex may reflect exhalation related to this hydrothermal activity.

with pervasive chlorite - sericite - silica alteration. Base and precious metal values are very low and, to the writer's knowledge, this prospect has never been drilled.

There is a prominent band of red chert and argillite outcropping on the shores of Long Pond approximately 150 m to the west of the deposit. This may have formed from exhalations related to the hydrothermal system, similar to the situation at Indian Cove.

6.2.5 Summary of Deposit Characteristics

The principal characteristics of the four volcanogenic sulphide deposits in the Wild Bight Group are summarized in Table 6.1. The deposits are not identical; each is distinctive and exhibits physical and stratigraphic features that reflect the local setting of the hydrothermal alteration system within the respective volcanic sequence. There are, however, unifying characteristics of all deposits that indicate similarities in the processes of mineralization.

Two of the four deposits have exhalative sulphide bodies overlying footwall stockwork; the remaining two comprise mainly stockwork but have ferruginous sediments nearby which may record a hydrothermal exhalative component. This is not a fundamentally important difference but one of local environment, possibly reflecting the relative vigour of the hydrothermal systems, the presence or absence of reduced sulphur at the rock-water interface, and/or water depth. All of the stockwork alteration zones are physically and mineralogically, similar emphasizing the continuity of the processes irrespective of whether exhalative sulphides actually formed.

The deposits occur in settings characterized by a distinctive volcanic rock association. Three of the four deposits are hosted by and/or directly overlie a felsic volcanic accumulation while the fourth (Lockport) is stratigraphically associated with a small rhyolite dome. Furthermore, two of the four deposits are intimately associated with incompatible element-depleted tholeiites of the IAD group and a third (Indian Cove) has IAD group rocks in the immediate stratigraphic succession (the fourth, Long Pond, has no analysed mafic volcanics). The association of the two rock types (incompatible element-depleted tholeiite and rhyolite) seems to be an important prerequisite for volcanogenic mineralization. It may be noted that the only major felsic volcanic

Table 6.1: Summary of characteristics of volcanogenic sulphide deposits in the Wild Bight Group.

DEPOSIT NAME AND HOST VOLCANIC UNIT	DEPOSIT TYPE		STRATIGRAPHY	ASSOCIATED MAFIC VOLCANICS
	MASSIVE SULPHIDE	STOCKWORK		
Point Leamington (Side Harbour volcanic unit)	two ore lenses, fine grained py., cp, lesser sph., erratic gold. >20 million tonnes.	immediately underlies massive sulphide. Pervasive ser-qz alteration, local intense black chl-qz-sulphide	Deposit lies at top of west-facing volcanic rocks. Immediate footwall is rhyolite dome which overlies pillow basalts. Hangingwall is mafic hyaloclastite, pyroclastic and volcaniclastic rocks	IAD group depleted tholeiites
Lockport (Glover's Harbour West volcanic unit)	very small, zinc-rich, massive sulphide interpreted but not observed	immediately underlies massive sulphide, intense pervasive qz-ser-chl with dissem. and stringer py, cp.	Deposit hosted by pillowed andesite. No marked change in statigraphy above. Small rhyolitic dome 250 m along strike but genetic relationship uncertain	IAD group depleted tholeiites
Indian Cove (Indian Cove volcanic unit)	None. Possibly represented by ferruginous red argillite and chert	Extensive alteration (qz-ser-chl) associated with rhyolite dome and pyroclastics, dissem. and stringer py,cp. lesser sp, minor ga.	Alteration widespread in rhyolite flow and overlying pyroclastic rocks. Most intense and metal-rich facies is near contact between flows and overlying pyroclastics. Mafic volcanics present but not intimately assoc. with mineralization	IAD group depleted tholeiites
Long Pond (Long Pond volcanic unit)	As for Indian Cove	dissem py, minor cp in qz-ser-chl stockwork	mineralization hosted by rhyolite and a very narrow pillow breccia unit	unknown

accumulation in the Wild Bight Group that does not have prominent hydrothermal alteration and mineralization is the Nanny Bag Lake rhyolite, where the associated mafic volcanic rocks are normal, rather than highly depleted, arc tholeiites.

6.3 Paleotectonic Setting of Volcanogenic Sulphide Deposits

6.3.1 Setting of the Wild Bight Group Deposits, Modern and Ancient Analogues.

All volcanogenic sulphide deposits in the Wild Bight Group occur in the same geological setting, characterised by the association of IAD group depleted tholeiites and rhyolite. This strongly indicates that the mineralizing event(s) were localized in Stage 2 of the development of the Wild Bight Group, interpreted as a period of rifting associated with fragmentation of the Wild Bight arc. The association of mineralization with depleted tholeiite and rhyolite, and the lack of mineralization in other rocks associated with Stage 2 magmatism, further suggests a specific control on the mineralization within this environment.

The formation of volcanogenic massive sulphides during periods of tensional stresses in island arcs has been a fashionable notion in recent years. It has been proposed for many ancient deposits previously thought to be associated with island arc calc alkaline volcanic activity (e.g. Mitchell and Bell, 1973; Mitchell and Garson, 1976), including the Iberian pyrite belt (Munha, 1979), the East Australian Paleozoic belt (Scheibner and Markham, 1976; Sangster, 1979) and deposits in the upper allochthons of Scandanavia (Vokes, 1976; Vokes and Gale, 1976; Stephens, 1986).

A particularly cogent case for the generation of massive sulphides during island arc rifting has been made for the Kuroko deposits by Cathles et al. (1983). They listed a number of features of the mineralization that they considered as unusual including: 1) restriction of mineralization to the Green Tuff belt, simultaneous generation of deposits throughout this belt between 15.6 and 11 Ma and uneven intensity of mineralization on a regional scale; 2) change in volcanism from voluminous arc tholeiites to bimodal basalt-dacite quiescent volcanism; 3)

rapid pre-mineralization subsidence and post-mineralization uplift; 4) apparent control of mineralization by basement fractures. These, and other features considered by these authors, were interpreted in terms of a model which views the Kuroko deposits as products of a failed rift. In this model, pre-mineralization subsidence is a consequence of the onset of rifting. Hydrothermal activity is most intense at spreading centres which are also areas of anomalously high heat flow and permeability. Bimodal volcanism is a consequence of tapping of asthenospheric magma chambers by fractures related to the rifting. The principal differences between this model and the present model for the Wild Bight Group are that, in the Kuroko case, the rift failed to open into a marginal basin and, after rifting ceased, rapid uplift allowed the deposits to be exposed in their present position. Cathles *et al.* (1983) were sufficiently impressed by the evidence for the rifting/volcanogenic sulphide association that they suggested it may be a universal feature of massive sulphides in island arc environments (see also Sillitoe, 1982).

Volcanogenic massive sulphide deposits in the Miocene-Pliocene Undu Group felsic volcanics in Vanua Levu, Fiji (Colley and Greenbaum, 1980) probably provide a good tectonic analogue for the setting of the Wild Bight Group deposits. As previously noted, this period of felsic volcanic activity marked the early stages of fragmentation of the Fiji arc (see Figure 5.3) and is interpreted to be a good analogy for Stage 2 of the Wild Bight Group development. Felsic volcanic rocks in the Undu Group are a very close geochemical analogue for the Wild Bight Group rhyolites (Section 3.7, Figures 3.52, 3.53, 3.54). The tectonic analogy between the Fiji mineralization and that in the Kuroko district was emphasized by Colley and Greenbaum (1980).

The notion that massive sulphides in the Appalachian-Caledonian orogen are related to rifting events within the lapetan island arcs is, likewise, not new. Stephens (1982), in a detailed petrogenetic study of the Stekenjokk volcanites in western Sweden, was able to show that massive sulphides represented by the Stekenjokk-Levi deposits formed during a period of transition from arc tholeiitic to MORB-type volcanism. He interpreted this as a period of arc rifting. Reinsbakken (1986) has documented a similar setting for the Gjersvik deposit in nearby eastern

Norway. Stephens *et al.* (1984) suggested that volcanogenic mineralization related to arc rifting was probably a common feature of Caledonian-Appalachian metallogenesis. They noted that, for example, massive sulphide deposits in the Bathurst District, New Brunswick, and the Bald Mountain area, Maine, are associated with voluminous felsic volcanics which are overlain by alkalic basalts of probable non-arc origin, perhaps recording a rifted arc sequence.

Elsewhere in Newfoundland, evidence for the association of massive sulphide mineralization with arc rifting is less well documented. However, Coish *et al.* (1982) interpreted geochemical and Nd isotopic results from the Betts Cove ophiolite to indicate arc rifting (recorded in lower komatiitic basalts) followed by back-arc, MORB-like volcanic activity. The Betts Cove and Tilt Cove massive sulphide deposits (Upadhyay and Strong, 1973; Strong, 1984; Strong and Saunders, in press) are hosted by the lower basalts suggesting that they may represent a supra-subduction zone rifting environment (which is, however, considerably older than the Wild Bight Group). In view of the possible correlation of the Pacquet Harbour Group with the volcanic part of the Betts Cove ophiolite (Hibbard, 1983; however, for an alternative viewpoint, see Tuach, 1984), the Consolidated Rambler Mines deposits (Tuach and Kennedy, 1975; Tuach, 1984) may also have formed in such an environment.

6.3.2 Genetic Aspects of the Relationships between Mineralization and Tectonic Setting

Rifting events, whether intra-oceanic, intra-continental or intra-arc, provide a good opportunity for volcanogenic mineralization. The rifting provides deep, open fractures which enhance the permeability of the substrate and promote deep access of sea water. The rifting taps deep magma chambers and the increased magmatism is accompanied by increased heat flow which, in rifted arc regimes, may be an order of magnitude greater than in the normal arc (Cathles *et al.* 1983). The combination of high heat flow and enhanced permeability provides an ideal opportunity for enhanced hydrothermal circulation, metal transport and sulphide deposition (Cathles, 1983). The presence of volcanogenic mineralization in this setting in the

Wild Bight Group is, therefore, entirely consistent with current concepts of island arc metallogenesis.

However, the precise relationship between mineralization and the depleted tholeiite/rhyolite association (and the lack of mineralization in the normal island arc tholeiite/rhyolite association at Nanny Bag Lake) is less clear. The relationship between the small dacite domes and the associated sulphide deposits in the Kuroko district has been addressed by Cathles (1978), Urabe and Sato (1978), Ohmoto (1978) and Cathles et al. (1983). The consensus is that the domes themselves are probably not large enough to have had a cause and effect relationship with the associated sulphides. Cathles et al. (1983) postulated that the sulphide/dacite association is indirect, indicating that hydrothermal fluids and magmas utilized the same zones of crustal weakness created by the rifting.

If this is the case for the Wild Bight Group, then there would appear to be at least one other factor that particularly favoured the localization of mineralization in areas where depleted tholeiite was being erupted. This factor may be anomalously high heat flow associated with the depleted tholeiite magmas. These liquids would certainly have melted at higher temperatures than either normal arc tholeiites or felsic magmas. Lack of isotopic equilibration between these magmas (see Chapter 4) suggests that they did not pool in shallow magma chambers; the implication is that they were tapped at depth and brought to the surface rapidly and with most of their heat intact. It will be recalled that secondary amphibole is common only in the Glover's Harbour and Nanny Bag Lake suites , perhaps also a manifestation of higher ambient heat flow during this phase of Wild Bight Group history (Section 2.8, Figure 2.10). The rise of such hot magma would be an additional factor in promoting vigorous hydrothermal circulation. The ability of the fracture systems to bring these magmas to the surface as liquids may indicate that the fracturing in these areas was more intense (and, therefore, permeability more enhanced) further promoting hydrothermal circulation and metal leaching.

6.3.2 Coeval Mineralization Elsewhere in Central Newfoundland

By considering the correlations proposed in Chapter 5 for Llanvirnian to Caradocian volcanic sequences in Central Newfoundland, it is possible to suggest some volcanogenic deposits that may be temporal and paleotectonic equivalents of deposits in the Wild Bight Group.

The most obvious correlations are with the Exploits Group, where well developed volcanogenic alteration occurs in the Tea Arm volcanics (Helwig, 1967, Dean and Strong, 1976). The alteration is associated with felsic volcanic rocks (Helwig, 1967), and Wasowski and Jacobi (1984) have shown that the host mafic volcanics are similar to the IAD group depleted tholeiites in the Wild Bight Group.

No other coeval volcanogenic mineralization is known in eastern Notre Dame Bay. The upper Exploits and Summerford Groups, as well as the Loon Harbour volcanics, are interpreted as unlikely to be prospective as they appear to consist mainly of non-arc rocks which, according to the present model, post-date the period of arc fragmentation and volcanogenic mineralization. However, if further data show that the middle or lower Summerford Group volcanics have island arc characteristics, further exploration in this area may be warranted.

The only well - dated correlative deposit in south-central Newfoundland is the Victoria deposit, associated with late Llanvirn to early Llandeilo mafic and felsic volcanic rocks. The affinity of these rocks is not known as there are no published geochemical data but the presence of felsic volcanic rocks suggests a probable arc setting, by analogy with the Wild Bight Group. Although this deposit is more Zn, Pb and Ag-rich than those in the Wild Bight Group, this probably is a function of the greater relative volume of felsic volcanics in the underlying sequence and not an indicator of a fundamental difference in tectonic conditions.

Volcanogenic sulphide deposits in the Bay du Nord and Baie d'Espoir Groups in the Hermitage Flexure are probably coeval with the Wild Bight Group deposits. Two principal deposits, the Strickland (Stackhouse, 1976; Wynne and Strong, 1984) and the Barasway de Cerf (Swinden, 1982), are dominantly Zn-Pb-Ag deposits reflecting the dominance of felsic volcanic rocks (and perhaps continental crust) in the substrate. It is not clear whether the

transition to back-arc conditions is recorded in these sequences as there are no mafic volcanic rocks in the overlying stratigraphy.

Volcanogenic sulphide deposits elsewhere in Central Newfoundland, including those in the Tulks Hill (Tulks Hill, Tulks East) and Tally Pond (Boundary, Duck Pond) volcanic sequences, the Buchans-Robert's Arm Belt (Buchans, Gullbridge, Pilleys Island), the Baie Verte Peninsula (Consolidated Rambler Mines, Betts Cove, Tilt Cove), the Springdale Peninsula (Little Bay, Whalesback, numerous smaller deposits) and the Bay of Islands Complex in western Newfoundland (York Harbour deposit) are older than the Wild Bight Group deposits.

6.4 Lead Isotopes in Volcanogenic Sulphide deposits

6.4.1 Introduction

The isotopic composition of lead in 25 volcanogenic sulphide deposits and occurrences in Central Newfoundland has been determined and compiled from the literature, in order to allow comparison with the Wild Bight Group and to provide further evidence for regional correlations and paleotectonic interpretations within the Central Mobile Belt. In most cases, lead in galena was analysed. However, when galena was not available, trace amounts of lead in pyrite, sphalerite or stibnite were analysed.

Lead isotope data from volcanogenic mineral deposits complement whole rock radiogenic isotope data. As Gill (1984) has pointed out, the lead in any volcanogenic sulphide deposit is a composite of all the lead sources that are present within the volume leached by the hydrothermal convection cells. It, therefore, presents an integrated lead isotopic composition for the underlying rocks which, of course, is weighted towards those sources with abundant lead (e.g. sialic crustal sources) as opposed to depleted or primitive mantle sources. It should be pointed out that isotopic studies of volcanic rocks in modern oceanic islands suggest that some mantle sources are enriched in radiogenic lead with respect to primitive mantle (e.g. White, 1985; Zindler and Hart, 1986) and the presence of evolved lead in volcanogenic sulphide deposit may, therefore, not necessarily reflect a direct arc-related, sialic input. Interpretation of

observed relationships compared to, for example, the Zartman and Doe (1981) model growth curves should, therefore, be undertaken with caution.

Any observed lead isotopic composition measured in a volcanogenic sulphide deposit will probably be the result of at least two stages of mixing of lead from various sources, the first stage occurring during magma generation and the second during hydrothermal activity that produces the mineral deposits. As an illustration, consider the geological history of the Wild Bight Group as interpreted by this study. The arc related magmas are interpreted, on whole rock geochemical and isotopic evidence, to have formed through mixing and partial melting of two or more isotopically distinct source areas (Chapter 4). Lead is an incompatible element in these circumstances and will be concentrated in the melts. Each magma will have a lead isotopic composition which reflects the proportions and degree of partial melting of the different sources that contribute to the melt. Ascent and eruption of these magmas will produce a volcanic stratigraphy, with rocks of various isotopic compositions which have not equilibrated with each other isotopically and whose isotopic compositions reflect source area mixing processes. In some island arcs, this substrate may also include sialic crust, presenting an additional complication. During hydrothermal leaching and transport, lead is acquired, from the various, isotopically different, stratigraphic units and mixed in proportions that depend on a number of factors including: 1) *the ability of the fluid in any particular part of the hydrothermal cell to extract lead and transport it*; for example, the lead that prevails in areas where the fluids are hottest and most acidic might have a correspondingly greater influence in the mix than those from other areas. 2) *the presence of second stage partial melts in the sequence*; partial melting of mafic rocks in the sub-arc crust will concentrate lead further in the felsic products. The relatively high lead concentration in these rocks will allow it to exert a disproportionate influence on a mixture subsequently produced in hydrothermal fluids. 3) *Presence of sediments in the stratigraphy*; sediments are relatively porous with respect to most volcanic rocks and the effective surface area of the feldspars with respect to fluid circulation will be correspondingly higher. This lead will, therefore, be more readily acquired by the hydrothermal fluids.

This discussion is meant to highlight three pertinent points with respect to interpreting lead isotopic data in volcanogenic ore deposits: 1) all lead isotope compositions in volcanogenic sulphide deposits result from mixing (a corollary of this is that, in the absence of detailed knowledge of source areas and magmatic processes, the geochronological applications of the data are not straightforward); 2) each volcanic sequence (or perhaps, widespread volcanic rocks related to each subduction complex at any given time) will have a range field of lead isotopic compositions that are related to the magma sources and magmatic history of the complex; 3) stratigraphic variations and or variations in hydrothermal convection cell characteristics will produce a spectrum of lead isotopic compositions throughout the volcanic belt. This spectrum will define a field of compositions which, if distinctive, may provide a useful fingerprint for classifying sequences of unknown affinity.

In ancient terranes, the integrated lead isotope composition of a volcanic pile, as reflected in the ore lead, permits comparison and correlation of volcanic sequences which are lithologically similar but have different paleotectonic histories. Such an approach was successfully used, for example, by Sundblad and Stephens (1983) to test correlations of deposits in different nappe slices in northern Sweden; correlation on this basis of deposits in different geologic units has been proposed in the southern Appalachians by Kish and Feiss (1982) and LeHuray (1982).

In the following Section, lead isotopes in deposits from various volcanic sequences across the Central Mobile Belt are compared and correlated to support geologically and geochemically based correlations of the host volcanic sequences. These data are then used to test conclusions about the paleotectonic history of the Central Mobile Belt reached in Chapter 5 and to tentatively evaluate the significance of major structural discontinuities within the belt.

6.4.2 Analytical Methods

The data used in this study are a combination of previously published analyses and new data. Data from 14 deposits and a preliminary interpretation of their relationships were previously published by Swinden and Thorpe (1984) and data for the Buchans deposits, the Connell

Option and the Skidder basalt by Cumming and Krstic (in press).

The new data presented in this thesis was produced by Geospec Consultants, Edmonton, Alberta, under contract to the Geological Survey of Canada. Analytical methods have been described by Thorpe *et al.* (1984).

Analyses were performed on a Micromass MM-30 mass spectrometer and all measured isotope ratios have been normalized to approximately absolute values on the basis of numerous measurements of the U.S. National Bureau of Standards reference lead NBS-981.

Analytical uncertainty limits, estimated by the Geological Survey of Canada based on duplicate measurements of a large number of specimens over the period 1982 to 1986, are: $^{206}Pb/^{204}Pb \pm 0.064\%$, $^{207}Pb/^{204}Pb \pm 0.068\%$ and $^{208}Pb/^{204}Pb \pm 0.075\%$ (R.I. Thorpe, pers. comm., 1986). Duplicates reported in Table 6.2 for the Tulks Hill, Victoria and York Harbour deposits are within these uncertainty limits.

6.4.3 Results

6.4.3.1 Introduction

Analytical results are presented in Table 6.2 and the location of the sampled deposits is shown in Figure 6.4 . The data are plotted on standard lead isotopic diagrams on Figure 6.5. The data have been subdivided, for descriptive purposes, on the basis of the geological and/or interpreted paleotectonic environments of the host rocks and each deposit class is plotted separately. Model lead evolution curves from Zartman and Doe (1981) are shown and, for ease of reference, three fields representing: 1) deposits in the Buchans-Robert's Arm Belt, the Lushs Bight Group and the Bay of Islands ophiolite; 2) deposits in late Cambrian island arc sequences; and 3) deposits in Llanvirn-Llandeilo island arc sequences south and east of the Buchans-Robert's Arm Belt.

Table 6.2: Isotopic composition of lead in volcanogenic sulpide deposits in Central Newfoundland
* - new data acquired for this study. Other data sources are referenced in text.

NO.	SPL. NO.	DEPOSIT NAME	HOST	MINERAL	206/204	207/204	208/204
1 *	TQ 83-146	Luscomb Point	Shoal Arm Fm	galena	18.180	15.607	38.172
2 *	TQ 86-22	Taylors Room	Moreton's Harbour Gp.	galena	18.163	15.574	37.944
3 *	TQ 86-29	Stuckless (Moreton's Hbr.)	Moreton's Harbour Gp.	stibnite	18.156	15.580	37.957
4	TQ 83-30	Seal Bay	Wild Bight Group	galena	18.212	15.608	38.042
5 *	TQ 83-151	Point Leamington	Wild Bight Group	sphalerite	18.223	15.621	38.077
6 *	TQ 83-151	Point Leamington	Wild Bight Group	pyrite	18.214	15.607	38.032
7 *	TQ 83-152	Point Leamington	Wild Bight Group	pyrite	18.211	15.613	38.008
8 *	TQ 83-150	Point Leamington	Wild Bight Group	pyrite	18.883	15.664	37.870
9 *	TQ 83-153	Point Leamington	Wild Bight Group	pyrite	18.342	15.618	18.043
10	TQ 80-85	Victoria	Tulks Hill volcanics	galena	18.161	15.619	38.112
11	TQ 80-85a	Victoria	Tulks Hill volcanics	galena	18.159	15.624	38.102
12	TQ 82-1	Tulks Hill	Tulks Hill volcanics	galena	18.144	15.571	37.957
13	TQ 81-50	Tulks Hill	Tulks Hill volcanics	galena	18.142	15.575	37.955
14	TQ 81-54	Burnt Pond	Tally Pond volcanics	galena	18.138	15.576	37.862
15	TQ 83-29	Tally Pond	Tally Pond volcanics	galena	18.156	15.583	37.902
16 *	TQ 86-19	Duck Pond	Tally Pond volcanics	galena	18.153	15.568	37.855
17 *	TQ 86-29	Hayden Steady	Tally Pond volcanics	galena	18.156	15.580	37.957
18	TQ 80-83	Barasway de Cerf	Hermitage Flexure	galena	18.235	15.660	38.142
19	TQ 80-84	Strickland	Hermitage Flexure	galena	18.333	15.663	38.209
20	TQ 83-1	Facheux Bay	Hermitage Flexure	galena	18.217	15.630	38.096
21 *	TQ 86-84	Great Burnt Lake	Cold Spring Pond Fm.	pyrite	17.745	15.484	37.265
22 *	TQ 86-85	Great Burnt Lake	Cold Spring Pond Fm.	pyrite	17.846	15.485	37.261
23 *	TQ 86-86	Great Burnt Lake	Cold Spring Pond Fm.	pyrite	17.768	15.475	37.272
24 *	TQ 86-87	Great Burnt Lake	Cold Spring Pond Fm.	pyrite	17.797	15.488	37.313
25	TQ 81-52	Shamrock	Cutwell Group	galena	17.844	15.488	37.599
26	TQ 81-51	Oil Islands	Cutwell Group	galena	17.894	15.499	37.816
27	TQ 81-53	Catchers Pond	Catchers Pond Gp.	galena	17.544	15.428	37.495
28	TQ 72-63	Pilleys Island	Roberts Arm Gp.	galena	17.922	15.522	37.591
29	TQ 72-62	Pilleys Island	Roberts Arm Gp.	galena	17.937	15.529	37.613
30	SP 2999	Ming	Pacquet Hbr. Gp.	galena	18.175	15.613	38.066
31	SP 3033	Ming	Pacquet Hbr. Gp.	galena	18.169	15.598	38.025
32 *	TQ 86-88	Whalesback	Lushs Bight Group	pyrite	17.943	15.543	37.873
33 *	TQ 86-89	Whalesback	Lushs Bight Group	pyrite	17.903	15.513	37.569
34 *	TQ 83-58	Betts Cove	Betts Cove Complex	galena	17.997	15.571	37.806
35	TQ 72-78	York Harbour	Bay of Islands Complex	galena	17.851	15.489	37.485
36 *	TQ 72-78	York Harbour	Bay of Islands Complex	galena	17.857	15.498	37.487
37 *	TQ 72-78	York Harbour	Bay of Islands Complex	galena	17.864	15.508	37.523
38	SP 689	MacLean	Buchans Gp	galena	17.829	15.492	37.620
39	TQ 72-67	MacLean	Buchans Gp	galena	17.823	15.490	37.612
40	TQ 72-69	MacLean	Buchans Gp	galena	17.823	15.488	37.612
41	KQ 81-55	MacLean Extension	Buchans Gp	galena	17.621	15.488	37.606
42	KQB 82-4	MacLean Extension	Buchans Gp	galena	17.820	15.490	37.621
43	KQB 82-12	MacLean Extension	Buchans Gp	galena	17.832	15.496	37.628
44	KQ 74-18	Old Buchans	Buchans Gp	galena	17.818	15.496	37.654
45	KQ 81-58	Oriental #1 East Pit	Buchans Gp	galena	17.823	15.491	37.610
46	KQ 83-33	Oriental Extension	Buchans Gp	galena	17.825	15.497	37.632
47	KQ 83-21	Lucky Strike	Buchans Gp	galena	17.832	15.496	37.634
48	KQ 83-22	Lucky Strike	Buchans Gp	galena	17.829	15.493	37.619
49	KQ 83-17	Lucky Strike North	Buchans Gp	galena	17.826	15.492	37.617
50	KQ 83-19A	Lucky Strike North	Buchans Gp	galena	17.815	15.489	37.606
51	KQ 74-28	Engineer	Buchans Gp	galena	17.883	15.495	37.824
52	1884-1097	Clementine	Buchans Gp	galena	17.828	15.491	37.613
53		Connel Option	Buchans Gp.	sphalerite	17.735	15.488	37.560
54		Connel Option	Buchans Gp.	sphalerite	17.731	15.486	37.543
55		Connel Option	Buchans Gp.	sphalerite	17.732	15.486	37.543
56	KQ 83-72	Skidder	Skidder basalt	galena	17.639	15.457	37.458
57	KQ 82-73	Skidder	Skidder basalt	galena	17.586	15.445	37.498
58	KQ 83-78	Skidder	Skidder basalt	sphalerite	17.629	15.442	37.463
59	KQ 83-78	Skidder	Skidder basalt	sphalerite	17.634	15.445	37.461
60	KQ 83-77	Skidder	Skidder basalt	sphalerite	17.644	15.445	37.464
61	KQ 83-77	Skidder	Skidder basalt	sphalerite	17.638	15.452	37.491
62	KQ 83-08	Skidder	Skidder basalt	sphalerite	17.684	15.455	37.492
63	KQ 83-08	Skidder	Skidder basalt	sphalerite	17.685	15.455	37.481

Figure 6.4 - Location of deposits represented by lead isotope data. Base map and legend same as Figure 5.5. Deposit numbers are keyed to Table 6.2.
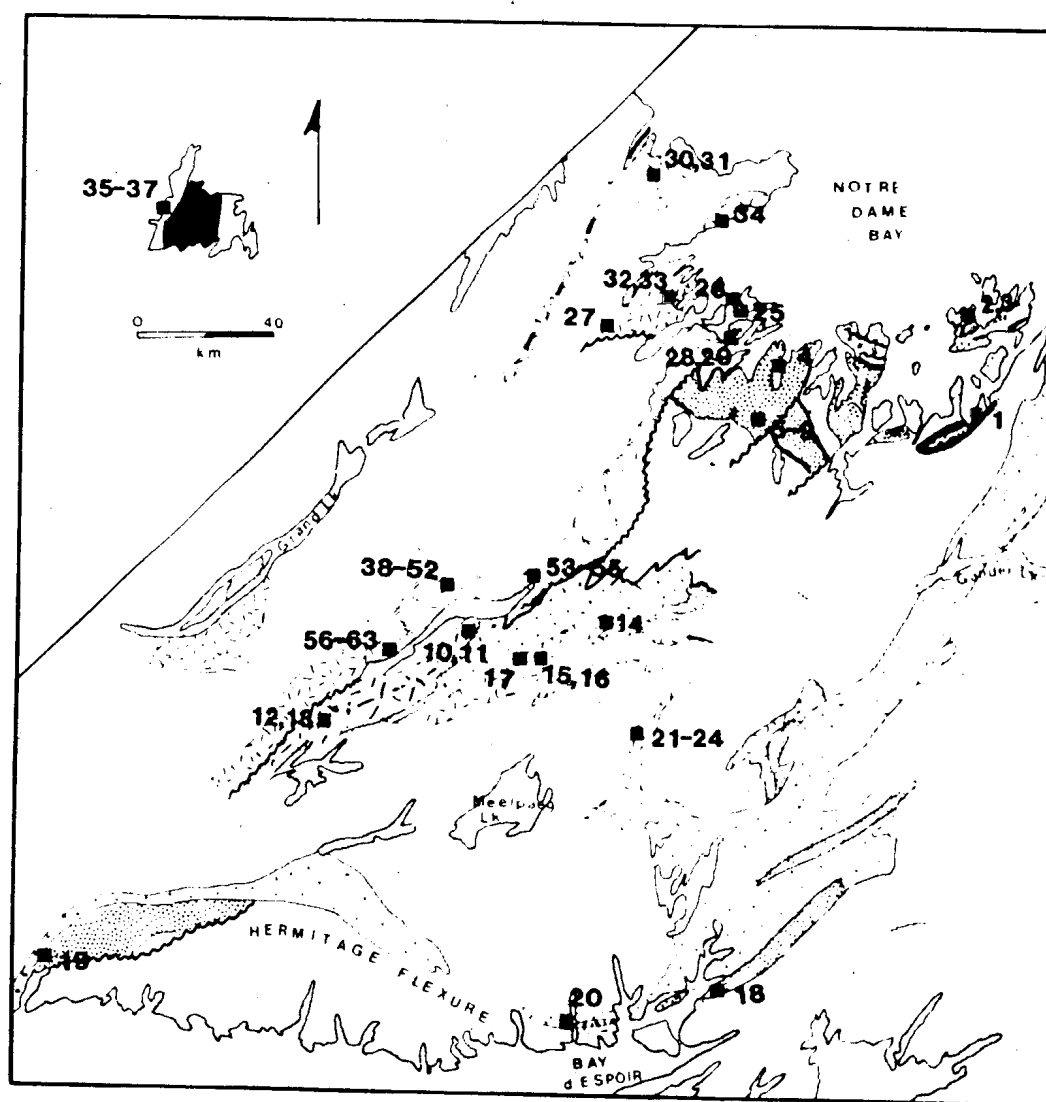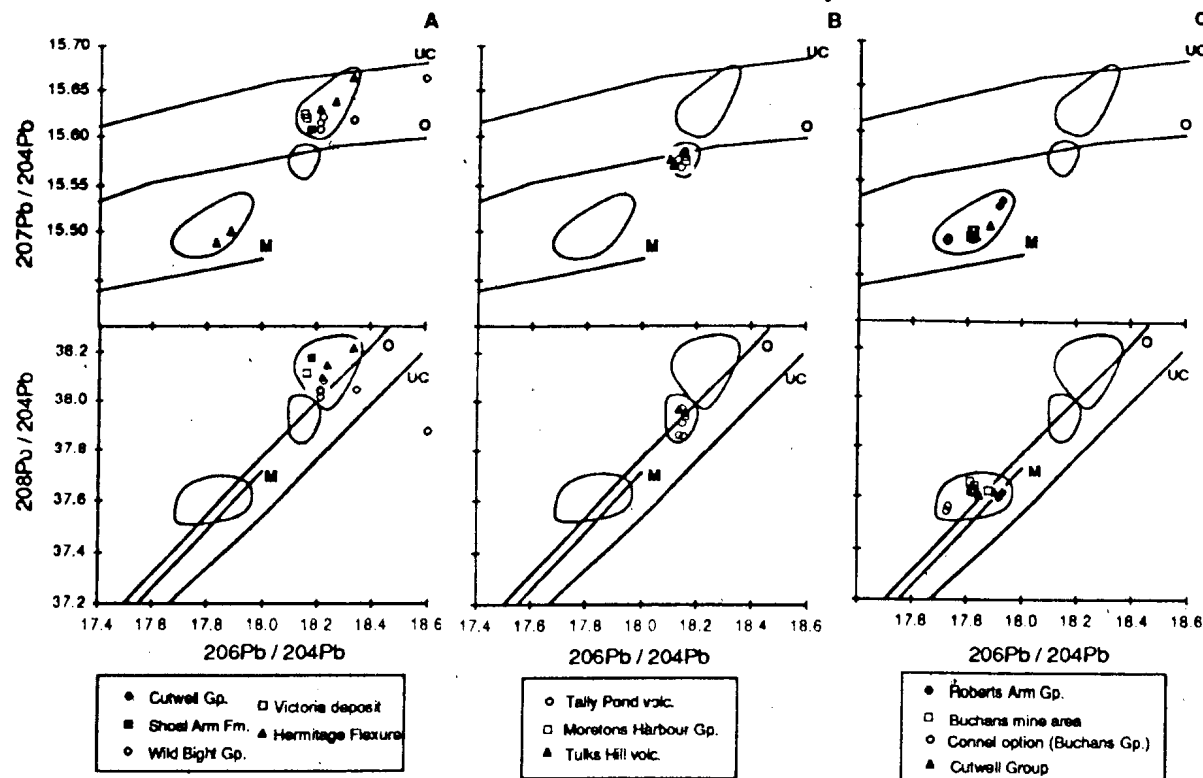
Figure 6.5: Isotopic composition of lead in Central Newfoundland volcanogenic sulphide deposits, subdivided for ease of reference into different geological and/or interpreted paleotectonic settings. Solid curves are model lead growth curves after Zartman and Doe (1981). UC - upper crust; O - Orogene; M - mantle. A - deposits in Llanvimian to Caradocian sequences; B - deposits in late Cambrian, arc-related rocks; C - deposits in the Buchans, Robert's Arm and Cutwell Groups; D- deposits in ophiolitic rocks in the western Dunnage and Humber Zones; E - deposits of uncertain affinity. On each diagram, fields arc-related deposits from Llanvimian-Caradocian deposits (from A), Cambrian deposits (from B) and Arenigian (from C) deposits are shown for reference.
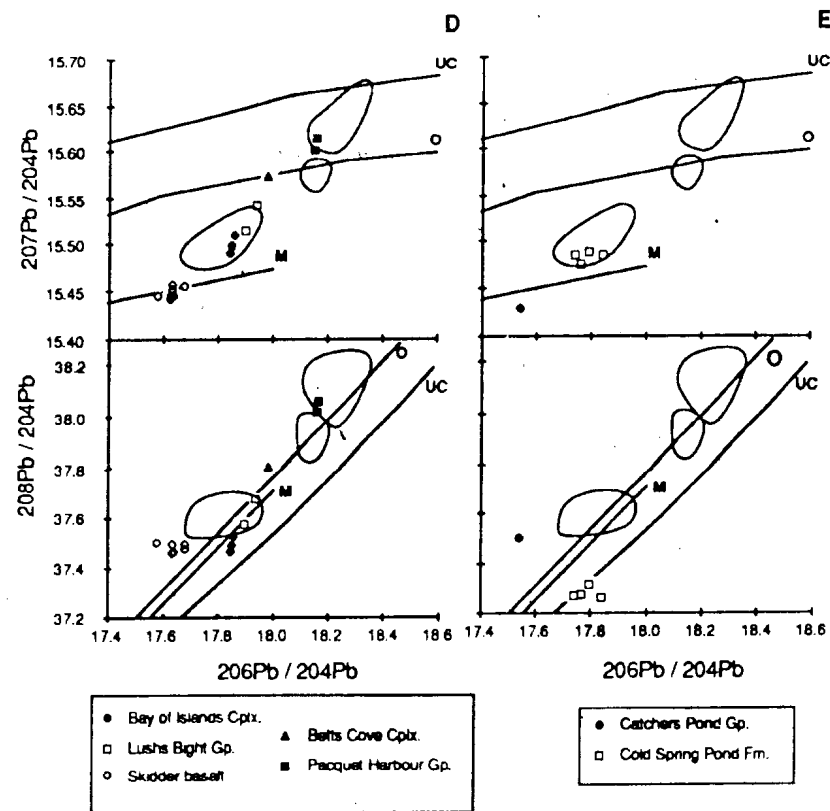
Figure 6.5 (continued)

6.4.3.2 Deposits in the Llanvirnian - Llandeilian arc sequences (including one in the Caradocian shale)(Figure 6.5A)

These deposits have the most radiogenic lead of any volcanogenic sulphide deposits in the Central Mobile Belt and plot mainly along a diffuse, steep trend between the Orogene and Upper Crustal growth curves on the $^{207}Pb/^{204}Pb$ plot.

Two deposits in the Wild Bight Group are represented, the Indian Cove and Point Leamington deposits. Because there is no galena in the latter, pyrite and sphalerite were analysed, and the data illustrate some problems in interpreting lead data from these minerals.

The isotopic composition of lead in any sulphide mineral can be modified by diffusion of lead into the crystal structure at any time after deposition. In the case of galena, this is not generally a serious problem, as lead in the mineral is sufficiently abundant that the addition of small amounts of a different composition will not effect much change in the bulk composition. However, in the case of lead-poor sulphide minerals, a significant change can be effected by secondary processes. Later addition of lead that has evolved through time in the region of the deposit, will produce a more pronounced change in the $^{206}Pb/^{204}Pb$ ratio than the $^{207}Pb/^{204}Pb$ because of the relative scarcity of ^{238}U in the Phanerozoic environment.

Lead data from pyrite and sphalerite must, therefore, be interpreted with caution. The approach here has been to analyse two or more specimens from each deposit. If the data cluster (particularly near compositions of similar or related deposits), it is assumed that they are relatively unaffected by secondary processes. Any samples that deviate significantly from the mean are rejected as probably contaminated.

In the case of the Point Leamington deposit, three of five samples cluster tightly at a composition similar to galena in the Indian Cove deposit. This composition is interpreted to lie within an integrated lead isotope composition field that is characteristic of the Wild Bight Group. Two samples that are anomalously enriched in radiogenic lead are interpreted to be contaminated and are not included in the discussion that follows.

Lead isotopes in approximately coeval deposits elsewhere in the Central Mobile Belt are

generally similar to those in the Wild Bight Group. The Victoria deposit and one analysis from a stratiform occurrence in the Caradocian Shoal Arm Formation plot with the Wild Bight Group samples suggesting similar lead sources. Deposits in the Hermitage Flexure area contain lead which has $^{207}Pb/^{204}Pb$ ratios consistently more radiogenic than in the other Llanvirnian - Caradocian deposits but $^{208}Pb/^{204}Pb$ ratios which overlap them.

6.4.3.3 Deposits in Cambrian volcanic-volcaniclastic sequences (Figure 6.5B)

These deposits represent the oldest arc-related volcanic sequences in Central Newfoundland and include the Tally Pond volcanics which have yielded a U/Pb (zircon) age of approximately 517 Ma (Dunning et al., 1986), at least part of the Tulks Hill volcanics which have a preliminary late Cambrian U/Pb (zircon) age (G. R. Dunning, pers. comm., 1987), and the Moreton's Harbour Group in Notre Dame Bay, which is intruded by the 507 Ma Twillingate Trondhjemite (Strong and Payne, 1973). Despite their geographical separation and contrasts in their stratigraphic succession (compare Strong and Payne, 1973, and Kean and Jayasinghe, 1980; 1982), the measured lead isotopic compositions in the three sequences are very similar, clustering near the Orogene model curve on the $^{207}Pb/^{204}Pb$ diagram. The compositions do not overlap with the deposits in the Llanvirnian-Caradocian deposits, being slightly but consistently less radiogenic.

6.4.3.4 Deposits in the Buchans - Robert's Arm Belt (including the Cutwell Group)(Figure 6.5C)

The isotopic composition of lead in deposits in Arenigian volcanic rocks of the Buchans - Robert's Arm Belt and the Cutwell Group is consistently less radiogenic than in both late Cambrian and Llanvirnian-Caradocian deposits to the south and east. The various deposits plot in a relatively shallow, linear, trend which generally lies between the Mantle and Orogene model curves on the $^{207}Pb/^{204}Pb$ diagram. There are significant variations between deposits in different parts of the belt but deposits in each specific area have distinctive and, in the case of

multiple deposits in the Buchans area, uniform, lead isotope compositions. The Pilleys Island deposits are significantly richer in $^{207}Pb/^{204}Pb$ but not in $^{208}Pb/^{204}Pb$ relative to the Buchans deposits.

6.4.3.5 Deposits in western Dunnage Zone ophiolitic rocks (Figure 6.5D)

Lead isotopes in deposits hosted by ophiolitic sequences north and west of the Buchans - Robert's Arm Belt appear to fall in three groups: 1) deposits in the Lushs Bight Group and the Bay of Islands Complex which are similar to the Pilleys Island deposit; 2) the Skidder deposit, which is less radiogenic than the Buchans deposits, particular in $^{206}Pb/^{204}Pb$, and 3) deposits associated with ophiolitic rocks on the Burlington Peninsula, (the Ming deposit in the Pacquet Harbour Group and the Betts Cove deposit) the former having relatively radiogenic lead and plotting with the Llanvirn - Llandeilo eastern arc deposits and the latter having less radiogenic lead, plotting closer to the field of Buchans - Robert's Arm Belt deposits.

6.4.3.6 Deposits of uncertain affinity (Figure 6.5E)

Two deposits are included under this heading. Both are in fault bounded sequences of uncertain relationship to adjacent units. The Catchers Pond deposit contains the least radiogenic lead of all deposits analysed. In this respect, it may represent the least radiogenic end of a western Dunnage Zone mixing line that includes the Buchans - Robert's Arm Belt.

The Great Burnt Lake deposit is hosted by basalt of the Cold Spring Pond Formation (Swinden, in press). This is the only analysed deposit south and east of the Buchans - Robert's Arm Belt which has non - radiogenic lead compositions. Lead isotopes in this deposit are distinctive; $^{207}Pb/^{204}Pb$ is similar to the Buchans deposits but $^{208}Pb/^{204}Pb$ is much lower and plots outside the Buchans - Robert's Arm field on the $^{208}Pb/^{204}Pb$ versus $^{206}Pb/^{204}Pb$ diagram.

6.4.4 Correlation of Geological Units and their Tectonostratigraphic Relationships

The lead isotope data generally support correlations previously suggested by geological and geochemical data, particularly with respect to the place of the Wild Bight Group in Central Mobile Belt development. The consistency of lead isotopic compositions in deposits from geographically separate but geologically correlative units in Central Newfoundland (e.g. the Wild Bight Group and the Victoria deposit) suggests that these deposits indeed record the integrated lead isotope composition of their volcanic hosts and probably represent a single tectonostratigraphic environment. A corollary to this is that consistent contrasts in lead isotopic compositions between geologic units (which may or may not be distinguished on geological grounds) serve to identify tectonostratigraphic terranes with contrasting lead sources and possibly different paleotectonic histories.

The data are consistent with the interpretation that the Llanvirn-Llandeilo, arc-related volcanic sequences are part of a single tectonostratigraphic terrane (Chapter 5). Taken as a whole, the integrated lead isotope composition of this terrane is the most radiogenic in the mobile belt (Figure 6.5). It is significant that the most radiogenic deposits are always those in the Hermitage Flexure, where geologically-based interpretations suggest an underlying continental crust (e.g. Colman-Sadd, 1980). These deposits, therefore, may closely approach the isotopic composition of this continental crust (also suggested by the fact that their compositions approach the Upper Crustal growth curve of Zartman and Doe, 1981; see Figure 6.5A).

The steep, diffuse, linear trend that the deposits, as a whole, define, is best interpreted as a mixing line. Continental crustal material, with lead isotopic composition similar to the Hermitage Flexure deposits, is probably the most radiogenic end member. Lead from the Hermitage Flexure subarc crust is most likely to have been introduced to the intra-oceanic arcs of the Victoria Lake and Notre Dame Bay area through subduction of continentally-derived sediments. Such a process is consistent with the postulated influence of subducted sediments on the Wild Bight Group magmas interpreted from geochemical and isotopic data (Chapter 3).

The less radiogenic end member may be a mantle source (cf. the Mantle model curve of

Zartman and Doe 1981). However, a more plausible suggestion is that it is the lead in the late Cambrian arc sequences. Older and younger rocks are structurally juxtaposed in most areas (e.g. the Tally Pond volcanics with the younger parts of the Victoria Lake Group and the Moreton's Harbour Group with the Exploits and Summerford Groups), the older sequences may record the early history of a long-lived, intermittently active, subduction complex, the end of which is recorded by the Wild Bight Group and equivalents. During the Llanvirn - Llandeilo, the Cambrian sequences may have been basement to younger arc, providing a mechanism for the incorporation of lead from them in the younger deposits.

Volcanogenic sulphide deposits in the Buchans - Robert's Arm Belt, and in island-arc related rocks of the Catchers Pond Group (Jenner and Szybinski, 1987) have much less radiogenic lead and in this respect are similar to deposits in adjacent ophiolitic rocks (the Lushs Bight Group and the Skidder basalt) and to the Bay of Islands ophiolite. The data spread out along a diffuse trend which, as for the deposits previously discussed, can be interpreted as a mixing line. Bell and Blenkinsop (1981) previously commented on the relatively non-radiogenic nature of the Buchans lead, suggesting that the lead must have evolved in a low-μ environment. They noted that similarly non-radiogenic lead had been shown to be characteristic of the Grenville Province in Ontario by Fletcher and Farquhar (1977) (subsequently expanded upon by Fletcher and Farquhar, 1982). Swinden et al. (in press) have recently shown that very non-radiogenic lead is also characteristic of epigenetic deposits in Cambrian carbonate rocks which overlie the Grenvillian basement in western Newfoundland and interpreted it to reflect a very low-μ basement source. The implication is that sedimentary lead sources in the island arcs of the Buchans - Robert's Arm belt may have been derived from crust with a considerably less radiogenic bulk radiogenic lead composition than those in the arcs to the east. The results of Fletcher and Farquhar (1982) and Swinden et al. (in press) indicate that such a source was probably present in the Grenvillian metamorphic terranes of the ancient North American continental margin.

Similarly non-radiogenic lead in the Lushs Bight Group may also include a contribution from

these non-radiogenic crustal sources. Preliminary geochemical data (G. A. Jenner and B. F. Kean, personal communication, 1987) indicate that at least some rocks in the Lushs Bight Group probably evolved in a supra-subduction zone environment. It is reasonable to suggest, on this basis, that lead from subducted sediments may have found its way into the magmas and the non-radiogenic compositions of the deposits suggests that this led was similar to that which contributed to the Buchans deposits. The Skidder basalt has the least radiogenic uranogenic lead of all the ophiolitic sequences although thorogenic lead is anomalously high (at constant $206Pb/204Pb$). The contributing sources were radiogenic lead-depleted but appear to have had somewhat different lead parent ratios. There are no independent data to suggest whether crustal lead may be a component in the Skidder magmas. However, the fact that it lies on an apparent mixing line between the Catchers Pond and Buchans deposits suggests a component of the same non-radiogenic lead (e.g. Grenvillian crust?) as these sequences.

Lead in the York Harbour deposit in the Bay of Islands Complex has isotopically similar lead to the Lushs Bight and Robert's Arm Group deposits. Although recent workers are agreed that this ophiolite probably formed in a back-arc basin (e.g. Upadhyay and Neale, 1979; Dunning and Krogh, 1985), geochemical data (Malpas, 1976, 1978) and Nd isotopic data (Jacobsen and Wasserburg, 1979) suggest that the magmas are N-MORB type and unlikely to have received much input from either crustal or enriched mantle sources. This being the case, the deposit may record an approximate composition for Early Ordovician depleted mantle

The position of the deposits on the Burlington Peninsula in this framework is equivocal. The very radiogenic lead in the Ming deposit suggests a correlation with the Llanvirn-Llandeilo arc sequences. However, stratigraphic relationships, particularly the correlation of the Betts Cove Complex-Snooks Arm Group transition with the Lushs Bight Group-Western Arm Group transition (Marten, 1971), suggest that a correlation between these rocks and the Lushs Bight Group is more geologically acceptable. Furthermore, lead in the Betts Cove deposit is rather less radiogenic than the Llanvirnian-Caradocian deposits, closer in composition to the Buchans-Robert's Arm belt. If the Betts Cove and Ming deposits are stratigraphically equivalent

(e.g. Hibbard, 1983), the range of lead isotope compositions in this area must be considerably different than (albeit overlapping) the field of younger deposits. It is possible that Ordovician volcanic sequences on the Burlington Peninsula are not tectonostratigraphically related to either the Buchans-Robert's Arm or younger sequences, but are part of a separate subduction complex with independent lead isotopic characteristics. For the time being, this question remains unresolved.

The affinity of the Cold Spring Pond Formation is likewise unresolved. Basalts that host the Great Burnt Lake deposit have a geochemistry suggestive of an oceanic island or E-MORB affinity (Swinden, in press) and, therefore, may not contain a contribution of slab-derived crustal lead from any continental area. Its distinctive lead isotopic composition, particularly with regard to the low $^{208}Pb/^{204}Pb$ at constant $^{206}Pb/^{204}Pb$, does not suggest a correlation with any other deposits in Central Newfoundland but probably reflects an integration of mantle sources in a back-arc basin. The age of the Cold Spring Pond Formation is unconstrained and there is no geological or isotopic reason to suggest whether this might have been a back-arc basin related to any (or none) of the identified island arcs in Central Newfoundland.

6.5 Implications for the Paleotectonic History of Central Newfoundland

The tectonostratigraphic history of the Dunnage Zone is apparently complex, and considerable data are still needed to clarify most of its aspects. However, the available data allow interpretation as to some of the Ordovician relationships of the various elements and encourage speculation as to some others.

There is a clear bipartite subdivision of geological units in the Central Mobile Belt based on the isotopic composition of lead in their volcanogenic sulphide deposits (Figure 6.6). The more radiogenic group comprises island arc sequences south and east of the Buchans - Robert's Arm belt (irrespective of age) and the less radiogenic, the island arc and ophiolitic sequences in and northwest of the Buchans- Robert's Arm Belt (also irrespective of age). Within this framework, there are two anomalies; deposits in ophiolitic rocks of the Burlington Peninsula have isotopic
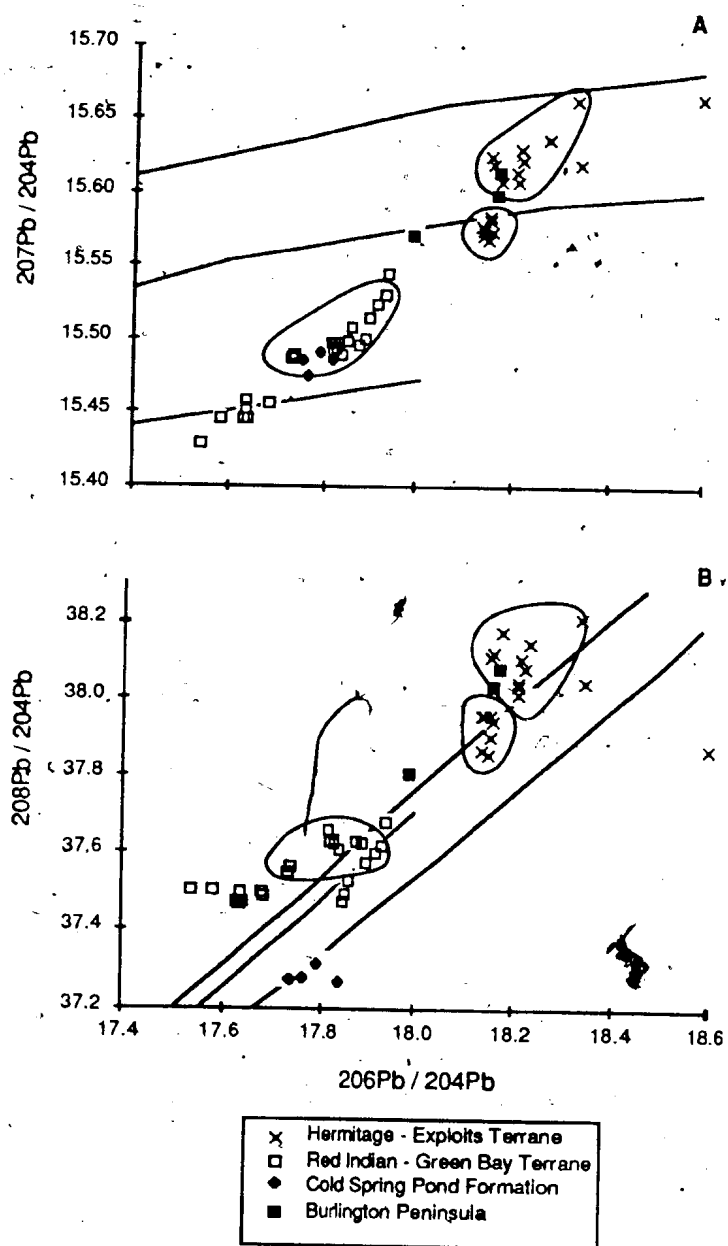
Figure 6.6: Compilation of lead isotope data for all deposits, keyed according to terranes on Figure. Model growth curves and fields as for Figure 6.5.

characteristics which appear to be intermediate between the two major subdivision while those in the Cold Spring Pond Formation in the southeastern Dunnage Zone have a thorogenic lead signature that is distinctly lower than any other in the Central Mobile Belt at equivalent $^{208}Pb/^{204}Pb$.

This bipartite distribution of lead isotopic compositions is best interpreted as reflecting the presence of at least two major tectonostratigraphic terranes in the Central Mobile Belt, here termed for convenience the Hermitage-Exploits Terrane to the southeast and the Red Indian-Green Bay Terrane to the northwest (Figure 6.7). The contact between these terranes is a major structural discontinuity which has several names along its strike extent. In the southwest it is termed the Lloyds River - Red Indian Lake Fault. Further north, this fault can be recognized east of Great Gull Pond as a zone of extensive ductile shear and mylonitization (Swinden and Sacks, 1986) and close to Notre Dame Bay, it is correlated with the Tommy's Arm Fault which forms the base of the Robert's Arm Group in this area. In Eastern Notre Dame Bay, this boundary is represented by the Luke Arm Fault, which can be traced from the Fortune Harbour Peninsula eastwards to New World Island.

The Hermitage - Exploits Terrane is interpreted to record a subduction complex that was active from the late Cambrian to latest Llandeilian or earliest Caradocian time. By analogy with modern plate margins, it is unlikely that this was a continuously active island arc for approximately 60 Ma. Rather, it is envisaged as a long-lived plate margin which probably saw intermittent subduction and back-arc activity. Two ages of island arcs have been identified to date; more may be identified as geochemical and isotopic studies are expanded in this area. The latest island arc activity may have spanned (or at least approached) a continental margin which lay under or directly south and east of the Hermitage Flexure. The polarity of this subduction system is not known. If the interpretation of the source of lead in the intra-oceanic deposits is correct, it implies that detritus from the Hermitage Flexure was being subducted, perhaps indicating subduction towards the north and west. If this is correct, the subduction zone must have been sited behind (i.e. south and east of) the present Hermitage Flexure in order for arc volcanism to have occurred

Figure 6.7 - Tectonostratigraphic subdivision of the Dunnage Zone based on lead isotope data. Base and legend as for Figure 5.5.
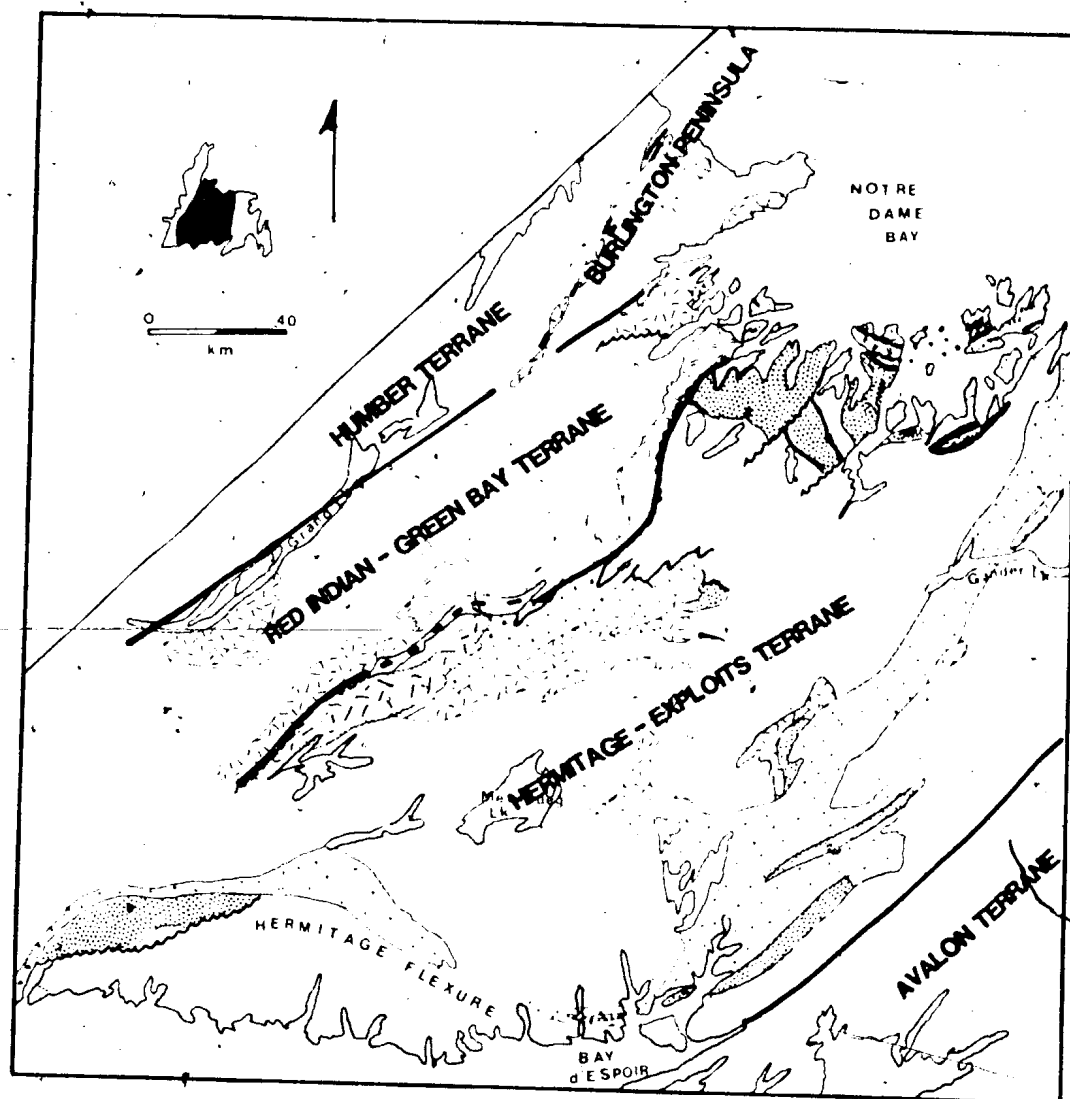
simultaneously in this area and in the ocean to the north and west. Alternatively, subduction may have been towards the south and east and sediment may have been carried across the forearc into the trench.

The only identified rocks of back-arc affinity associated with this subduction complex are those immediately beneath the Caradocian shale. It is possible that ophiolitic rocks of the GRUB and the Pipestone Pond-Coy Pond Complexes formed in a back-arc basin related to this subduction complex. Their age (approximately 494 Ma, Dunning and Krogh, 1986) is consistent with such an interpretation (i.e. they could have formed in a back-arc basin related to the late Cambrian arc sequences).

The Red Indian - Green Bay Terrane is interpreted to represent a different subduction complex in which lead from the ancient North American continental margin was a major contributor to the magmas and hence the associated ores. This is consistent with the long-held view of eastward subduction in Central Newfoundland (Church and Stevens, 1971; Strong et al., 1974b; Searle and Stevens, 1985), followed by collision of the island arc and obduction of oceanic sedimentary and ophiolitic rocks (the Taconian Orogeny). The apparent presence of lead in the arcs derived from a low-μ environment, tentatively identified as Grenvillian metamorphic terranes of the ancient North American Margin, is consistent with this interpretation. The Buchans - Robert's Arm Belt, the Lushs Bight Group, the Skidder basalt and the Bay of Islands Complex in this view could represent a complex series of arc and back-arc sequences of various ages related to this subduction complex. Other sequences which may be part of this system but for which there are no lead isotope data include the Annieopsquotch Complex and related rocks (Dunning and Chorlton, 1985; Dunning, 1987) and the Mansfield Cove/ Hall Hill Complexes immediately west of the Robert's Arm Group (Dunning et al., 1987).

It seems likely that these two subduction complexes were not closely related in space in the early Ordovician. The timing of their juxtaposition is somewhat equivocal. However, Nelson and Casey (1979) and Nelson (1981) interpreted the post - Caradocian flysch in central and eastern Notre Dame Bay (i.e. the Sansom and Point Leamington greywackes, the Goldson Formation

and related rocks) to be have been derived from uplifted Robert's Arm island arc and related

rocks which were advancing southwestwards as thrust sheets during the late Ordovician - early

Silurian. If this interpretation is correct, the Robert's Arm Group and rocks to the west were

shedding detritus eastwards into a back-arc basin that was partly floored by the upper Wild Bight

Group (because there is a conformable sequence from the Wild Bight Group upward into the

Caradocian shale and, thence, into the Point Leamington greywacke). The structural boundary

between the Robert's Arm Group and the sequences to the southeast, then, may be more

significant than merely another back-arc thrust (e.g. Kusky and Kidd, 1985). It may, in fact, record

the tectonic juxtaposition of two separate paleotectonic terranes during continued telescoping

of the remains of Iapetus following the Taconian event.

The place of the Burlington peninsula ophiolites in this framework is equivocal. The lead

isotopic evidence does not clearly relate them to either terrane. Their boundary with the Red

Indian-Green Bay Terrane is the Green Bay fault, a major structure whose latest movement

appears to be strike slip (Coyle and Strong, 1987; A. Z. Szybinski, pers. comm., 1987), but the

amount of displacement is uncertain. Latest movement on this fault is at least as young as

Silurian because it affects Springdale Group rocks of this age. Any earlier movement history is, to

date, unresolved. The lead isotopic evidence does not suggest a clear correlation with any

deposits in the Burlington Peninsula with the Red Indian - Green Bay Terrane and, in fact, is

more supportive of a correlation with the Hermitage-Exploits Terrane. Further structural studies

of the Green Bay Fault and isotopic studies on deposits on the Burlington Peninsula are

necessary to assess their relationship with the sequences in the Red Indian-Green Bay Terrane.

The correlation of the Moreton's Harbour Group in eastern Notre Dame Bay with the arcs of

the Hermitage - Exploits Terrane (suggested by the lead isotope data), as well as correlation of

the Chanceport and Cottrells Cove Groups in this area with the Robert's Arm Group, raise a

question of structural style in this area. If the correlations are correct, it suggests that

representatives of the two terranes are structurally interleaved. This correlation also raises a

serious question as to the wisdom of correlating the Lobster Cove and Chanceport Faults

between Triton Island and the Fortune Harbour Peninsula (Dean and Strong, 1976, 1977). While these faults define the structural top of the Buchans - Robert's Arm Belt in their respective areas, it now appears that the hangingwall rocks are of quite different affinity in eastern and western areas. In western Notre Dame Bay, the Lobster Cove Fault is only one of many strike slip faults (A. Z. Szybinski, pers. comm., 1987) within the Red Indian - Green Bay Terrane and juxtaposes rocks (the Robert's Arm and Cutwell Groups) which may not be greatly different in age. In eastern Notre Dame Bay, however, the Chanceport Fault brings in much older rocks, which are apparently tectonostratigraphically unrelated to hangingwall rocks in the Green Bay area. This would appear to obviate the major rationale for correlating these faults to begin with (i.e. the inference that correlative rocks were present to the north and south in both areas). The current view of this fault as a single, sinuous, structure which traverses virtually all of Notre Dame Bay needs to be reexamined. The Lobster Cove Fault may equally well trend northeastwards out to sea from Triton Island, the Chanceport Fault being an altogether separate structure.

A final possibility that might be entertained is that the Burlington Peninsula and the Moreton's Harbour-Twillingate area are part of a single large structural terrane, isotopically related to the Hermitage-Exploits Terrane but separated from it structurally. This is consistent with the lead isotopic data and would require that the Green Bay Fault swings around to the southeast under Notre Dame Bay, joining up with the Chanceport Fault on the Fortune Harbour Peninsula. There are too few data to further test this idea at the present time.

It is clear from the above discussion that there are still major problems to be addressed in reconstructing the Ordovician geological history of the Newfoundland Central Mobile Belt. It is equally clear that detailed geochemical and isotopic studies have the capability of both pointing out some of the problems and also suggesting some of the solutions. In particular, lead isotopes in volcanogenic sulphide deposits appear to provide good fingerprints of broad tectonostratigraphic environments in this area and lead to a broad, and undoubtedly still oversimplified, subdivision of the Mobile Belt into three contrasting regimes. If this subdivision is correct, the boundaries of these tectonostratigraphic terranes can be well defined on the

, ground. This provides a good opportunity for detailed structural studies along these boundaries aimed at determining whether the sense and timing of movements a) are compatible with the proposals presented in this thesis and b) further constrain the timing of major structural events in the Central Mobile Belt.

6.6 Summary and Conclusions

There are four volcanogenic mineral deposits in the Wild Bight Group. They occur exclusively in rocks associated with Stage 2 (arc rifting) of Wild Bight Group development and within this environment, are commonly associated with depleted tholeiites and rhyolites. The mineralizing event is interpreted to have been promoted by open fractures and rising geotherms related to the onset of arc rifting and, in this respect, is similar to well documented modern and ancient deposits elsewhere.

The volcanogenic sulphide deposits in the Wild Bight Group can be correlated on the basis of their paleotectonic setting with deposits in the Exploits Group and the Victoria Mine sequence, strengthening correlations previously suggested by geochemical data (Chapter 5).

Lead isotopic studies of volcanogenic sulphide deposits in the Wild Bight Group and 23 other volcanogenic sulphide deposits in Central Newfoundland, show that deposits in the Hermitage Flexure and those in Cambrian arc sequences in the Victoria River and eastern Notre Dame Bay areas can also be correlated with the Wild Bight Group deposits (as tentatively suggested in Chapter 5). The relatively radiogenic isotopic composition of lead in these deposits contrasts sharply with less radiogenic lead in the Buchans - Robert's Arm Belt and adjacent ophiolitic rocks and this is interpreted to reflect the presence of two distinct tectonostratigraphic terranes in the Mobile Belt, termed the Hermitage - Exploits and Red Indian - Green Bay Terranes. These terranes are interpreted to have formed over separate subduction complexes and to have been juxtaposed during the late Ordovician and/or early Silurian during telescoping of the remnants of Iapetus following the Taconian Orogeny.

CHAPTER 7

SUMMARY AND PRINCIPAL CONCLUSIONS OF THE THESIS

7.1 Introduction

This thesis presents the results of a detailed geological, petrological, geochemical and isotopic study of Ordovician volcanic rocks and their associated mineral deposits in the Wild Bight Group, Central Newfoundland. It is the first detailed study of the geological relationships in the Wild Bight Group as a whole but, perhaps more significantly, it is the most detailed geochemical and isotopic study to date of any Ordovician volcanic sequence in the Newfoundland Dunnage Zone. The 34 Nd isotope analyses presented in Chapter 4 probably are the largest data set of this kind for similar rocks in the whole Appalachian Orogen.

The thesis presents a body of precise, internally consistent, geochemical and isotopic data for a comprehensive, carefully chosen and prepared, sample suite. These data provide an opportunity to examine relationships between whole rock geochemistry and both whole rock Nd and ore lead isotopes, and present a detailed picture of the changing magmatic and paleotectonic conditions that accompanied continued volcanic activity recorded by the Wild Bight Group.

. The Insights into the geological evolution of the Wild Bight Group provided by these data have important wider implications with respect to the paleotectonic development of the Newfoundland Central Mobile Belt. Correlations with coeval volcanic rocks, for which there are fewer geochemical data, permit a tentative interpretation of their significance with respect to paleotectonic events recorded by the Wild Bight Group.

The study has important implications for economic geology, particularly regional metallogeny. It has identified a specific rock association with which volcanogenic mineral deposits are associated in the Wild Bight Group and an interpretation of the tectonic conditions which may have favoured mineralization. It provides a basis for focussing further exploration for this deposit type both in the Wild Bight Group and in nearby stratigraphically equivalent volcanic rock units.

7.2 Principal Results and Conclusions

1) The Wild Bight Group is a thick (probably >8 km) sequence of dominantly epiclastic (~75%) and volcanic (~25%) rocks. The base of the Group is not exposed. The top is overlain conformably by fossiliferous Caradocian (Middle Ordovician) shale.

Epiclastic rocks show a broad facies change through the stratigraphic sequence. Basal units are dominantly fine grained greywacke, siltstone and argillite. These pass upwards into a thick central succession of interbedded turbiditic greywacke and coarse, polylithic, chaotic conglomerates interpreted as debris flows. The top of the succession is characterized by a finer-grained facies, with argillite and fine epiclastic greywacke, but generally lacking conglomerates.

Volcanic rocks, dominantly pillow lava with lesser massive basalt and minor rhyolite, occur at all stratigraphic levels in the succession. All rocks are cut by fine to coarse grained mafic sills and dykes. Field, geochemical and isotopic data are all consistent with these intrusions being cogenetic with the Wild Bight Group mafic volcanic rocks.

2) Eleven separate volcanic accumulations have been identified within the Wild Bight Group. Pillow lava dominates the mafic succession in ten of these, massive basalt the other. Felsic volcanic rocks occur in five of these successions, generally forming small rhyolite domes within the sequence. Volcanogenic sulphide mineralization is present in four of the volcanic sequences.

3) Mafic volcanic rocks now consist of a spilitic assemblage including some or all of chlorite - albite - quartz - epidote - sphene - amphibole - magnetite - calcite, indicating metamorphism in the greenschist facies. The only preserved primary mineral is clinopyroxene, occurring most commonly as phenocrysts and less commonly in the groundmass. The metamorphism is interpreted as resulting from sub-seafloor, hydrothermal activity, generally involving low (probably

less than 3) water/rock ratios and temperatures in the range 200° to 300° C. It has caused considerable redistribution of the alkali and alkaline earth elements in the mafic volcanic and subvolcanic rocks but has not significantly affected the less mobile transition metals, HFSE, REE, or the Mg#, which can be used in most cases as an index of differentiation.

4) The Wild Bight Group mafic volcanic rocks are geochemically heterogeneous. They have undergone variable fractional crystallization and none are believed to represent primary liquids in equilibrium with mantle phases. Two broad paleotectonic environments, respectively of island arc and non-arc affinity, have been identified using HFSE and REE relationships. Further subdivision can be accomplished, using incompatible element relationships, and five groups are recognized, two of island arc affinity and three of non-arc affinity.

The five geochemical groups show internally consistent Nd isotopic compositions and relationships, supporting the validity of the subdivision.

The principal geochemical and isotopic characteristics of the geochemical groups, and the petrogenetic interpretations resulting from these characteristics, can be summarized as follows:

1) *Island Arc Affinity*

i) IAD group: These rocks have severe depletion in all incompatible elements, low Cr and Ni contents, distinctive REE patterns with flat LREE at 1 to 5 times chondritic and flat HREE at 6 to 8 times chondritic with a 'step' up between Nd and Eu.

Epsilon$_{Nd}$ ranges from -1.2 to +4.8 and there is a good *negative* correlation between epsilon$_{Nd}$ and both $^{147}Sm/^{144}Nd$ and Mg#.

These rocks are interpreted to result from a complex, multi-stage partial melting history that involved hydrous partial melting of a very refractory source. The source may have been the residue from partial melting of depleted mantle to form the IAI group magmas (see below). The sources contain components of both depleted mantle and crustally-derived material from the subducted slab.

ii) IAI group: These rocks have incompatible element concentrations and relationships typical of island arc tholeiites. They include both LREE-depleted (low-K tholeiites) and LREE-enriched (medium- to high-K tholeiites) varieties.

For the LREE-enriched varieties, low epsilon$_{Nd}$ (slightly negative to slightly positive) indicates mixing between depleted mantle and slab-derived crustal sources. Petrogenetic modelling indicates moderate degrees of partial melting. For the LREE-depleted varieties, epsilon$_{Nd}$ in the range +6 to +7 indicates relatively lower proportions of crustal source, perhaps as a result of more complete partial melting of the depleted mantle sources. These are typical low-K island arc tholeiites;

2) *Non-arc Affinity*

iii) NAI group: These rocks are non-alkalic basalts with incompatible element concentrations similar to the IAI group but lacking the island arc geochemical signature. REE patterns are flat to moderately LREE-enriched.

LREE-enriched varieties have epsilon$_{Nd}$ in the range +6 to +7.5 indicating mixing between sources typical of some oceanic island basalts and normal depleted mantle. The most LREE-enriched varieties have the lowest epsilon$_{Nd}$ and may represent moderate amounts of partial melting of only the OIB source;

iv) NAT group: These rocks are LREE-enriched tholeiites which are transitional between tholeiitic and alkalic basalts. They have epsilon$_{Nd}$ in the range +4.7 to +7.0 and can be modelled as limited partial melts of an oceanic island basalt source

v) NAE group: These rocks are alkalic basalts with epsilon$_{Nd}$ in the range +4.8 to +5.7. They can be modelled as the products of very small amounts of partial melting of an oceanic island basalt source.

5) Felsic volcanic rocks are similar in composition to low-Al_2O_3 trondhjemites. They have

slightly LREE-depleted patterns at approximately 10 times chondritic, and may result from partial melting of plagioclase - pyroxene cumulate rocks near the base of the arc crust. Felsic volcanic rocks are only associated with mafic volcanic rocks of island arc affinity. Volcanogenic mineralization is confined to sequences with an IAD group/rhyolite association.

6) As a general rule, volcanic rocks of island arc affinity are interpreted to occur stratigraphically below rocks of non-arc affinity (although arc-related rocks do occur locally at the top of the sequence). Subvolcanic intrusives of arc affinity cut only arc-related stratified rocks while those of non-arc affinity cut all stratified rocks, indicating that the two paleotectonic environments are stratigraphically linked and not merely structurally juxtaposed.

7) Geochemical and isotopic data can be integrated in a developmental model for the Wild Bight Group through comparisons with modern oceanic environments. The geological history of the Fiji platform provides a particularly good modern analogue. Medium- to high-K arc tholeiites at the base of the group probably record the final phase of island arc magmatic activity, which may have originally been more extensive. Fragmentation of the arc is recorded in continued eruption of LREE-enriched arc tholeiites, joined by depleted tholeiites of the IAD group, LREE-depleted arc tholeiites and rhyolites. Following the fragmentation of the arc, volcanic activity in a back-arc region was established with the initiation of magmatic activity without the slab-related geochemical signature. The broad environment was probably still in the supra-subduction zone setting, however, as arc tholeiites, interbedded with non-arc basalts, continued to erupt until the cessation of Wild Bight Group volcanic activity.

8) The association of volcanogenic mineralization with IAD-group pillow lavas and rhyolites indicates that it occurred during, and was a result of, arc fragmentation. This is consistent with recent interpretations of similar mineralization in younger settings such as Japan and Fiji. The localization of mineralization to this setting is probably related to anomalously high heat flow

associated with eruption of the IAD group magmas.

9) Lead isotope data for sulphide minerals in the Wild Bight Group and throughout the Newfoundland Central Mobile Belt provide a good complement to the whole rock geochemical data and suggest some correlations and patterns of tectonostratigraphic development across central Newfoundland. Lead isotope data suggest deposits in late Cambrian and Llanvimian to Caradocian deposits south and east of the base of the Buchans-Robert's Arm belt represent a broad tectonostratigraphic terrane which is different from that to the north and west. Within the former terrane, lead isotope distribution in the younger deposits can be interpreted as resulting from mixing between lead from the Cambrian sequences and a continental source that probably lay south and east of the Hermitage Flexure. The lead in the latter terrane contains a substantial component of non-radiogenic, lead which may have originated in the mantle or in the Grenvillian rocks of the North American continental margin.

The two tectonostratigraphic terranes, identified on the basis of lead isotope data, may reflect processes at two different subduction complexes, juxtaposed during the late Ordovician or early Silurian.

REFERENCES

Abbey, S. 1983: Studies in "standard samples" of silicate rocks and minerals. Geological Survey of Canada, Paper 83-15, 114 pages.

Allegre, C.J. and Turcotte, D.L. 1985: Geodynamic mixing in the mesosphere boundary layer and the origin of oceanic islands. Geophysical Research Letters, volume 12, pages 207-210.

Alt, J.C. and Emmermann, R. 1985: Geochemistry of hydrothermally altered basalts: Deep Sea Drilling Project Hole 504B, Leg 83. *In* Initial Reports of the Deep Sea Drilling Project, volume 83. U.S. Government Printing Office, Washington, pages 249-262.

Alt, J.C., Laverne, C. and Muehlenbachs, K. 1985: Alteration of the upper oceanic crust: mineralogy and processes in Deep Sea Drilling Project Hole 504B. Leg 83. *In* Initial Reports of the Deep Sea Drilling Project, volume 83. U.S. Government Printing Office, Washington, pages 217-247.

Amstutz, G.G. 1974: Spilites and spilitic rocks. Springer-Verlag, Berlin, Heidelberg and New York, 482 pages.

Anderson, R., DeLong, S and Schwartz, W. 1979: Thermal model for subduction with dehydration in the downgoing slab. Journal of Geology, volume 86, pages 731-739.

Arculus, R.J. 1981: Island arc magmatism in relation to the evolution of the crust and mantle. Tectonophysics, volume 75, pages 113-133.

Arculus, R.J. and Johnson, R.W. 1981: Island arc magma sources: a geochemical assessment of the roles of slab-derived components and crustal contamination. Geochemical Journal, volume 15, pages 109-133.

Arculus, R.J. and Powell, R. 1986: Source component mixing in the regions of arc magma generation. Journal of Geophysical Research, volume 91, pages 5913-5926.

Armstrong, R. 1971: Isotopic and chemical constraints on models of magma genesis in volcanic arcs. Earth and Planetary Science Letters, volume 12, pages 137-142.

Arnorsson, S., Gronvøld, K. and Sigurdsson, S. 1978: Aquifer chemistry of four high-temperature geothermal systems of Iceland. Geochimica et Cosmochimica Acta, volume 42, pages 523-536.

Bailey, D.K. 1970: Volatile flux, heat focusing and generation of magma. Geological Journal, Special Issue 2, pages 177-186.

Barker, F., Arth, F.G., Peterman, Z.E. and Friedman, I. 1976: The 1.7-to 1.8-b.y. old trondhjemites of southwestern Colorado and Northern New Mexico: geochemistry and depths of genesis. Geological Society of America Bulletin, volume 87, pages 189-198.

Basaltic Volcanism Study Project 1981: Basaltic Volcanism on the Terrestrial Planets. Pergamon Press, New York, 1286 pages.

Bell, K. and Blenkinsop, J. 1981: A geochronological study of the Buchans area, Newfoundland. *In* The Buchans Orebodies: Fifty Years of Geology and Mining. *Edited by* E.A. Swanson, D.F. Strong and J.G. Thurlow. Geological Association of Canada, Special Paper 22, pages 91-112.

Bell, K., Blenkinsop, J., Berger, A.R. and Jayasinghe, N.R. 1979: The Newport granite: its age, geological setting and implications for the geology of northeastern Newfoundland. Canadian Journal of Earth Sciences, volume 16, pages 264-269.

Bell, K., Blenkinsop, J. and Strong, D.F. 1977: The geochronology of some granitic bodies from eastern Newfoundland and its bearing on Appalachian evolution. Canadian Journal of Earth Sciences, volume 14, pages 456-476.

Belt, E.S. 1969: Newfoundland Carboniferous stratigraphy and its relation to the Maritimes and Ireland. *In* North Atlantic - Geology and Continental Drift. *Edited by* M. Kay. American Association of Petroleum Geologists, Memoir 12, pages 734-753.

Bence, A.E. and Albee, A.L. 1968: Empirical correction factors for the electron microanalysis of silicates and oxides. Journal of Geology, volume 76, pages 382-403.

Bergstrom, S.M., Riva, J. and Kay, K. 1974: Significance of conodonts, graptolites and shelly faunas from the Ordovician of western and north-central Newfoundland. Canadian Journal of Earth Sciences, volume 11, pages 1625-1660.

Bird, D.K. and Norton, D.L. 1981: Theoretical prediction of phase relations among aqueous solutions and minerals: Salton Sea geothermal system. Geochimica et Cosmochimica Acta, volume 45, pages 1479-1493.

Bird, J.M. and Dewey, J.F. 1970: Lithosphere plate - continental marginal tectonics and the evolution of the Appalachian Orogen. Geological Society of America Bulletin, volume 81, pages 1031-1060.

Bischoff, J.L. and Dickson, F.W. 1975: Seawater-basalt interaction at 25°C and 500 bars: implications for origin of sea-floor heavy-metal deposits and regulation of seawater chemistry. Earth and Planetary Science Letters, volume 25, pages 385-397.

Bonatti, E., Honnorez, J., Kirst, J. and Radicati, F. 1975: Metagabbros from the Mid-Atlantic Ridge at 60 N: Contact hydrothermal - dynamic metamorphism beneath the axial valley. Journal of Geology, volume 83, pages 61-78.

Bostock, H.H. 1978: The Roberts Arm Group, Newfoundland; geological notes on a Middle or Upper Ordovician island arc environment. Geological Survey of Canada, Paper 78-15, 21 pages.

Bouma, A.H. 1962: Sedimentology of some flysch deposits. A graphic approach to facies interpretation. Elsevier, Amsterdam, 168 pages.

Bradley, D.C. 1982: Subsidence in late Paleozoic basins in the northern Appalachians. Tectonics, volume 1, pages 107-123.

Briqueu, L., Bougault, H., and Joron, J.-L. 1984: Quantification of Nb, Ta, Ti, and V anomalies in magmas associated with subduction zones: petrogenetic implications. Earth and Planetary Science Letters, volume 68, pages 297-308.

Bryan, W.B. 1968: Low-potash dacite drift pumice from the Coral Sea. Geological Magazine, volume 105, pages 431-439.

Bryan, W.B. 1971: Coral Sea drift pumice stranded on Eua Island. Geological Society of America Bulletin, volume 82, pages 2799-2812.

Bryan, W.B. 1979: Low-K_2O dacite from the Tonga-Kermadec island arc: petrography, chemistry and petrogenesis. In Trondhjemites, Dacites and Related Rocks. Edited by F. Barker. Elsevier, New York, pages 581-600.

Cameron, W.E., McCulloch, M.T. and Walker, D.A. 1983: Boninite petrogenesis: chemical and Nd-Sr isotopic constraints. Earth and Planetary Science Letters, volume 65, pages 75-89.

Cann, J.R. 1971: Major element variations in ocean-floor basalts. Philosophical Transactions of the Royal Society of London, volume A268, pages 495-505.

Carey, S. and Sigurdsson, H. 1984: A model of volcanogenic sedimentation in marginal basins. In Marginal Basin Geology. Edited by B.P. Kokelaar and M.F. Howells. Geological Society Special Publication No.16, pages 37-58.

Cathles, L.M. 1978: Hydrodynamic constraints on the formation of Kuroko deposits. Mining Geology, volume 4, pages 257-265.

Cathles, L.M. 1983: An analysis of the hydrothermal system responsible for massive sulfide deposition in the Hokuroku basin of Japan. In The Kuroko and Related Volcanogenic Massive Sulfide Deposits. Edited by H. Ohmoto and B.J. Skinner. Economic Geology Monograph 5, pages 439-487.

Cathles, L.M., Guber, A.L., Lenagh, T.C. and Dudas, F.O. 1983: Kuroko - type massive sulphide deposits of Japan: products of an aborted island-arc rift. In The Kuroko and Related Volcanogenic Massive Sulfide Deposits. Edited by H. Ohmoto and B.J. Skinner. Economic Geology Monograph 5, pages 96-114.

Chase, C.G. 1981: Oceanic island lead: two stage histories and mantle evolution. Earth and Planetary Science Letters, volume 52, pages 277-284.

Chorlton, L. 1980: Geology of the La Poile River area (11O/16), Newfoundland. Newfoundland Department of Mines and Energy, Mineral Development Division, Report 80-3, 86 pages.

Church, W.R. and Stevens, R.K. 1971: Early Paleozoic ophiolite complexes of the Newfoundland Appalachians as mantle - oceanic crust sequences. Journal of Geophysical Research, volume 76, pages 1460-1466.

Coats, R. 1962: Magma type and crustal structure in the Aleutian arc: the crust of the Pacific Basin. American Geophysical Union Monograph 6, pages 92-102.

Cohen, R.S. and O'Nions, R.K. 1982: Identification of recycled continental material in the mantle from Sr, Nd and Pb isotope investigations. Earth and Planetary Science Letters, volume 61, pages 73-84.

Coish, R.A. 1977: Ocean floor metamorphism in the Betts Cove ophiolite, Newfoundland. Contributions to Mineralogy and Petrology, volume 60, pages 255-270.

Coish, R.A., Hickey, R. and Frey, F.A. 1982: Rare earth element geochemistry of the Betts Cove ophiolite, Newfoundland: complexities in ophiolite formation. Geochimica et Cosmochimica Acta, volume 46, pages 2117-2134.

Cole, J.W., Gill, J.B. and Woodhall, D. 1985: Petrologic history of the Lau Ridge, Fiji. In Geology and Offshore Resources of Pacific Island Arcs - Tonga Region. Edited by D.W. Scholl and T.L. Vallier. Circum-Pacific Council for Energy and Mineral Resources, Earth Science Series, Volume 2, pages 351-378.

Coleman, R.G. and Donato, M.M. 1979: Oceanic plagiogranite revisited. In Trondhjemites, Dacites and Related Rocks. Edited by F. Barker. Elsevier, New York. pages 149-168.

Coleman, R.G. and Peterman, Z.E. 1976: Oceanic plagiogranite. Journal of Geophysical Research, volume 80, pages 1099-1108.

Colley, H. and Greenbaum, D. 1980: The mineral deposits and metallogenesis of the Fiji Platform. Economic Geology, volume 75, pages 807-829.

Colley, H. and Hindle, W.H. 1984: Volcano-tectonic evolution of Fiji and adjoining marginal basins. In Marginal Basin Geology. Edited by B.P. Kokelaar and M.F. Howells. Geological Society Special Publication No. 16, pages 151-162.

Colley, H. and Rice, C.M. 1975: A Kuroko-type deposit in Fiji. Economic Geology, volume 75, pages 1373-1386.

Colman-Sadd, S.P. 1980: Geology of south-central Newfoundland and evolution of the eastern margin of Iapetus. American Journal of Science, volume 280, pages 991-1017.

Colman-Sadd, S.P. 1985: Geology of the Burnt Hill map area (2D/5), Newfoundland. Newfoundland Department of Mines and Energy, Mineral Development Division, Report 85-3, 94 pages.

Colman-Sadd, S.P. and Swinden, H.S. 1984: A tectonic window in Central Newfoundland? Geological evidence that the Appalachian Dunnage Zone may be allochthonous. Canadian Journal of Earth Sciences, volume 21, pages 1349-1367.

Coyle, M.L. and Strong, D.F. 1987: Geology of the Springdale Group: a newly recognized Silurian epicontinental-type caldera in Newfoundland. Canadian Journal of Earth Sciences, volume 24, pages 1135-1148.

Craig, H., Welhan, J.A., Kim, K., Poreda, R. and Lupton, J.E. 1980: Geochemical studies of the 21°N EPR hydrothermal fluids (abstract). EOS, Transactions of the American Geophysical Union, volume 61, page 992.

Cumming, G.L. and Krstic, D. in press: Detailed lead isotopic study of Buchans and related ores. In Buchans Geology, Newfoundland. Edited by R.A. Kirkham. Geological Survey of Canada, Paper 86-24, Report 13.

Davidson, J. 1983: Lesser Antilles isotope evidence of the role of subducted sediments in island arc magma genesis. Nature, volume 306, pages 253-256.

Davidson, J. 1986: Isotope and trace element constraints on the petrogenesis of subduction-related lavas from Martinique, Lesser Antilles. Journal of Geophysical Research, volume 91, pages 5943-5962.

Davies, G.F. 1981: Earth's neodymium budget and structure and evolution of the mantle. Nature, volume 290, pages 208-213.

Davies, G.F. 1984: Geophysical and isotopic constraints on mantle convection: An interim synthesis. Journal of Geophysical Research, volume 89, Number B7, pages 6017-6040.

Dean, P.L. 1978: The Volcanic Stratigraphy and Metallogeny of Notre Dame Bay. Memorial University of Newfoundland, St. John's, Newfoundland, Geological Report 7, 204 pages.

Dean, P.L. and Meyer, J.R. 1982: Metallogenic study of Mid-Ordovician cherts and shales of central Newfoundland. In Current Research. Newfoundland Department of Mines and Energy, Mineral Development Division, Report 82-1. pages 175-187.

Dean, P.L. and Strong, D.F. 1976: Compilation geological maps for north-central Newfoundland. Geological Survey of Canada, Open File Maps.

Dean, P.L. and Strong, D.F. 1977: Folded thrust faults in Notre Dame Bay, central Newfoundland. American Journal of Science, volume 277, pages 97-108.

Dean, W.T. 1970: Lower Ordovician trilobites from the Summerford Group at Virgin Arm. New World Island, northeastern Newfoundland. Geological Survey of Canada, Bulletin 240.

DeGrace, J.R., Kean, B.F., Hsu, E. and Green, T. 1976: Geology of the Nippers Harbour map area (2E/13), Newfoundland. Newfoundland Department of Mines and Energy, Mineral Development Division, Report 76-3, 73 pages.

DePaolo, D.J. and Wasserburg, G.J. 1977: The sources of island arcs as indicated by Nd and Sr isotopic patterns. Geophysical Research Letters, volume 4, pages 465-468.

DePaolo, D.J. and Wasserburg, G.J. 1976: Inferences about magma sources and mantle structure from 143Nd/144Nd variations. Geophysical Research Letters, volume 3, pages 743-746.

Dewey, J.F. 1969: Evolution of the Appalachian - Caledonian Orogen. Nature, volume 222, pages 124-129.

Dewey, J.F., Kennedy, M.J. and Kidd, W.F.S. 1983: A geotraverse through the Appalachians of northern Newfoundland. In Profiles of Orogenic Belts. Edited by N. Delaney and F.M. Rast. American Geophysical Union/Geological Society of America, Geodynamic Series, volume 10, 318 pages.

DeZoysa, T.H. 1969: Geology and base metal mineralization of Lockport area, Notre Dame Bay, Newfoundland. Unpublished M.Sc. thesis, Memorial University of Newfoundland, St. John's, 99 pages.

Dodge, F.C.W. and Mays, R.E. 1972: Rare earth fractionation in accessory minerals, central Sierra Nevada Batholith. U.S. Geological Survey, Professional Paper 800-D, pages 165-168.

Dunning, G.R. 1987: Geology of the Annieopsquotch Complex, southwest Newfoundland. Canadian Journal of Earth Sciences, volume 24, pages 1162-1174.

Dunning, G.R. and Chorlton, L. B. 1985: The Annieopsquotch ophiolite belt of southwest Newfoundland: geology and tectonic significance. Geological Society of America Bulletin, volume 96, pages 1466-1476.

Dunning, G.R., Kean, B.F., Thurlow, J.G. and Swinden, H.S. 1987: Geochronology of the Buchans, Roberts Arm and Victoria Lake Groups and the Mansfield Cove Complex, Newfoundland. Canadian Journal of Earth Sciences, volume 24, pages 1175-1184.

Dunning, G. R. and Krogh, T.E. 1985: Geochronology of ophiolites of the Newfoundland Appalachians. Canadian Journal of Earth Sciences, volume 22, pages 1659-1670.

Dunning, G.R., Krogh, T.E., Kean, B.F., O'Brien, S.J. and Swinden, H.S. 1986: U/Pb zircon ages of volcanic groups from the Central Mobile Belt, Newfoundland (Abstract). Geological Association of Canada, Programs with Abstracts, volume 11, page 66.

Edmond, J.M., Measures, C., McDuff, R.E., Chan, L.H., Collier, R., Grant, B., Gordon, L.I. and Corliss, J.B. 1979: Ridge crest hydrothermal activity and the balances of major and minor elements in the ocean: the Galapagos data. Earth and Planetary Science Letters, Volume 46, pages 1-18.

Edmond, J.M., von Damm, K.L., McDuff, R.E. and Measures, C. 1982: Chemistry of hot springs on the East Pacific Rise and their effluent dispersal. Nature, volume 297, pages 187-191.

Elias, P. and Strong, D.F. 1982: Paleozoic granitoid plutonism of southern Newfoundland: contrasts in timing, tectonic setting and level of emplacement. Transactions of the Royal Society of Edinbourgh: Earth Sciences, volume 73, pages 43-57.

Ellis, A.J. 1968: Natural hydrothermal systems and experimental hot water-rock interaction: reactions with NaCl solutions and trace metal extraction. Geochimica et Cosmochimica Acta, volume 12, pages 1356-1363

Espenshade, G.H. 1937: Geology and mineral deposits of the Pilleys Island area. Newfoundland. Newfoundland, Department of Natural Resources, Geological Section, Bulletin 6, 56 pages.

Evarts, R.C. and Schiffman, P. 1983: Submarine hydrothermal metamorphism of the Del Puerto Ophiolite. California. American Journal of Science. volume 283, pages 289-340.

Ewart, A. 1979: A review of the mineralogy and chemistry of Tertiary-Recent dacitic, latitic, rhyolitic and related sialic volcanic rocks. In Trondhjemites, Dacites and Related Rocks. Edited by F. Barker. Elsevier, New York, pages 13-121.

Ewart, A., Brothers, R.N. and Mateen, A. 1977: An outline of the geology and geochemistry of the younger volcanic islands of Tonga, Southwest Pacific. Journal of Volcanology and Geothermal Research, volume 2, pages 205-250.

Ewart, A., Bryan, W.B. and Gill, J. 1973: Mineralogy and geochemistry of the younger volcanic islands of Tonga. Journal of Petrology, volume 14, pages 429-465.

Fargo, T.R. 1983: A re-evaluation of the Loon Harbour volcanics of the Campbellton sequence, north-central Newfoundland (abstract). Geological Society of America, Programs with Abstracts, volume 14, page 189.

Flanagan, F.J. 1976: Description and analyses of eight new USGS rock standards. United States Geological Survey, Professional Paper-840.

Fletcher, I.R. and Farquhar, R.M. 1977: Lead isotopes in the Grenville and adjacent Paleozoic formations. Canadian Journal of Earth Sciences, volume 14, pages 56-66.

Fletcher, I.R. and Farquhar, R.M. 1982: The protocontinental nature and regional variability of the Central Metasedimentary Belt of the Grenville Province: lead isotopic evidence. Canadian Journal of Earth Sciences, volume 19, pages 239-253.

Floyd, P.A. and Winchester, J.A. 1975: Magma type and tectonic setting discrimination using immobile elements. Earth and Planetary Science Letters, volume 27, pages 211-218.

Fogwill, W.D. 1965: Interim report on Lockport copper-pyrite mine. Unpublished report for Newfoundland and Labrador Corporation, 7 pages.

Fåhraeus, L. and Hunter, D.R. 1981: Paleoecology of selected conodontophorid species from the Cobbs Arm Formation (middle Ordovician), New World Island, north-central Newfoundland. Canadian Journal of Earth Sciences, volume 18, pages 1653-1665.

Gale, G.H. 1971: An Investigation of some sulphide deposits in the Rambler area, Newfoundland. Unpublished Ph.D. thesis, University of Durham, Durham, England. 197 pages.

Gale, G.H. 1973: Paleozoic basaltic komatiites and ocean floor type basalts from northeastern Newfoundland. Earth Planetary Science Letters, volume 18, pages 22-28.

Garcia, M.O. 1978: Criteria for the identification of ancient volcanic arcs. Earth Science Reviews, volume 14, pages 147-165.

Giggenbach, W.F. 1981: Geothermal mineral equilibria. Geochimica et Cosmochimica Acta, volume 45, pages 393-410.

Gill, J.B. 1970: Geochemistry of Viti Levu, Fiji, and its evolution as an island arc. Contributions to Mineralogy and Petrology, volume 27, pages 179-203.

Gill, J.B. 1974: Role of underthrust continental crust in the genesis of a Fijian calc alkaline suite. Contributions to Mineralogy and Petrology, volume 43, pages 29-35.

Gill, J.B. 1976: Composition and age of Lau Basin and Ridge volcanic rocks: implications for evolution of an interarc basin and remnant arc. Geology, volume 87, pages 1387-1395.

Gill. J.B. 1981: Orogenic andesites and plate tectonics. Springer-Verlag, Heidelberg, 390 pages.

Gill, J.B. 1984: Sr-Pb-Nd Isotopic evidence that both MORB and OIB sources contribute to oceanic island arc magmas in Fiji. Earth and Planetary Science Letters, volume 68, pages 443-458.

Gill, J.B. and Stork, A.L. 1979: Miocene low-K dacites and trondhjemites of Fiji. In Trondhjemites, Dacites and Related Rocks. Edited by F. Barker. Elsevier, Amsterdam and New York. pages 629-649.

Gill, J.B., Stork, A.L. and Whelan, P.M. 1984: Volcanism accompanying back-arc basin development in the southwest Pacific. Tectonophysics, volume 102, pages 207-224.

Gilluly, J. 1935: Keratophyres of east Oregon and the spilite problem. American Journal of Science, volume 29, pages 225-252.

Goff, S.P. 1984: The magmatic and metamorphic history of the East Arm, Great Slave Lake, N.W.T. Unpublished Ph.D. thesis, University of Alberta, Edmonton.

Green, T.H. 1980: Island arc and continent-building magmatism - review of petrogenic models based on experimental petrology and geochemistry. Tectonophysics, volume 63, pages 367-385.

Green, T.H. and Ringwood, A.E. 1968: Genesis of the calc alkaline igneous rock suite. Contributions to Mineralogy and Petrology, volume 18, pages 105-162.

Hajash, A. 1975: Hydrothermal processes along mid-ocean ridges: an experimental investigation. Contributions to Mineralogy and Petrology, volume 53, pages 205-226.

Hajash, A. and Archer, P.L. 1980: Experimental seawater/basalt interactions: effects of cooling Contributions to Mineralogy and Petrology, volume 75, pages 1-3.

Harland, W.B. and Gayer, R. A. 1972: The Arctic Caledonides and earlier oceans. Geological Magazine, volume 109, pages 289-314.

Hart, S.R., Glassley, W.A. and Karig, D.E. 1972: Basalts and seafloor spreading behind the Mariana island arc. Earth and Planetary Science Letters, volume 125, pages 12-18.

Hawkesworth, C., Norry, M., Roddick, J., Baker, P., Francis, P. and Thorpe, R. 1979: 143Nd/144Nd, 87Sr/86Sr and incompatible element variations in calc alkaline andesites and plateau lavas from South America. Earth and Planetary Science Letters, volume 42, pages 45-57.

Hawkesworth, C.J., O'Nions, R.K., Pankhurst, R.J., Hamilton, P.J. and Evenson, N.M. 1977: A geochemical study of island arc and back arc tholeiites from the Scotia Sea. Earth and Planetary Science Letters, volume 36, pages 253-262.

Hawkesworth, C.J. and van Calsteren, P.W.C. 1983: Radiogenic isotopes - some geological applications. In Rare Earth Element Geochemistry. Developments in Geochemistry, volume 2, Edited by P. Henderson. Elsevier, Amsterdam, pages 375-421.

Hawkins, J.W. 1976: Petrology and geochemistry of basaltic rocks of the Lau Basin. Earth and Planetary Science Letters, volume 28, pages 283-297.

Hawkins, J.W. 1985: Low-K rhyolitic pumice of the Lau Basin. In Geology and Offshore Resources of Pacific Island Arcs - Tonga Region. Edited by D.W. Scholl and T.L. Vallier. Circum - Pacific Council for Energy and Mineral Resources, Earth Science Series, volume 2, pages 171-178.

Hawkins, J.W. and Melchior, J.T. 1985: Petrology of Mariana Trough and Lau Basin basalts. Journal of Geophysical Research, volume 90, No. B13, pages 11,431-11,468

Hayes, J. J. 1951: Preliminary Map, Marks Lake. Geological Survey of Canada, Paper 51-52.

Hellman, P.L. and Green, T.H. 1979: The role of sphene as an accessory phase in the high-pressure partial melting of hydrous mafic compositions. Earth and Planetary Science Letters, volume 42, pages 191-201.

Helwig, J.A. 1967: Stratigraphy and structural history of the New Bay area, north-central Newfoundland. Unpublished Ph.D. thesis, Columbia University, New York. 211 pages.

Helwig, J.A. 1969: Redefinition of Exploits Group, Lower Paleozoic, northeast Newfoundland. In North Atlantic-Geology and Continental Drift. Edited by M. Kay. American Association of Petroleum Geologists, Memoir 12, pages 408-413.

Helwig, J.A. and Sarpi, E. 1969: Plutonic - pebble conglomerates, New World Island, Newfoundland, and the history of eugeosynclines. In North Atlantic-Geology and Continental Drift Edited by M. Kay. American Association of Petroleum Geologists, Memoir 12, pages 443-446.

Helz, R.T. 1976: Phase relations of basalts in their melting ranges at $P_{H2O}=5$ kb. Part II. Melt Compositions. Journal of Petrology, volume 17, pages 139-193.

Heming, R.F. 1974: Geology and petrology of Rabaul caldera, Papua New Guinea. Geological Society of America Bulletin, volume 85, pages 1253-1264.

Heming, R.F. and Rankin, P.C. 1979: Ce-anomalous lavas from Rabaul caldera, Papua New Guinea. Geochimica et Cosmochimica Acta, volume 43, pages 1351-1355.

Hertogen, J. and Gijbels, R. 1971: Instrumental neutron activation analysis of rocks with a Low-energy photon detector. Analytica Chimica Acta, volume 56, pages 61-82.

Hertogen, J., Sachtleben, Th., Schimnke, H.-U., and Jenner, G.A. 1985: Trace element geochemistry and petrogenesis of basalts from Deep Sea Drilling Project Sites 556 - 559 and 561 - 564. In Initial Reports of the Deep Sea Drill Project, Leg 82. U.S. Government Printing Office, Washington, D.C. pages 449-457.

Hey, M.H. 1954: A new review of the chlorites. Mineralogical Magazine, volume 30, pages 277-292.

Heyl, G.R. 1936: Geology and mineral deposits of the Bay of Exploits area. Geological Survey of Newfoundland., Bulletin 3, 66 pages.

Heyl, G.R. 1938: Geology and mineral deposits of the New Bay area, Notre Dame Bay, Newfoundland. Geological Survey of Newfoundland., Unpublished report, 51 pages.

Hibbard, J.P. 1976: The southwest portion of the Dunnage Melange and its relationships to nearby groups. Unpublished M.Sc. thesis, Memorial University of Newfoundland, St. John's, 131 pages.

Hibbard, J.P. 1983: Geology of the Baie Verte Peninsula, Newfoundland. Newfoundland · Department of Mines and Energy, Mineral Development Division, Memoir 2, 279 pages.

Hibbard, J.P. and Williams, H. 1979: Regional setting of the Dunnage Melange in the Newfoundland Appalachians. American Journal of Science, volume 279, pages 993-1021.

Hickey, R.L. and Frey, A.F. 1982: Geochemical characteristics of boninite series volcanics: implications for their source. Geochimica et Cosmochimica Acta, volume 46, pages 2099-2115.

Hoffman, C. 1976: Natural granitic rocks and the granite systems Qz-Or-Ab-An(H2O) and Qz-Ab-An(H2O). Nues Jahrbuch fur Mineralogie, Monatshefte, pages 289-306.

Hoffman, A.W. and White, W.M. 1982: Mantle plumes from ancient oceanic crust. Earth and Planetary Science Letters, volume 57, pages 421-436.

Hole, M.J., Saunders, A.D., Marriner, G.F. and Tarney, J. 1984: Subduction of pelagic sediments: implications for the origin of Ce-anomalous basalts from the Mariana Islands. Journal of the Geological Society of London, volume 141, pages 453-472.

Holloway, J.R. and Burnham, C.W. 1972: Melting relations of basalt with equilibrium water pressures less than total pressure. Journal of Petrology, volume 13, pages 1-29.

Horne, G. S. and Helwig, J.A. 1969: Ordovician stratigraphy of Notre Dame Bay, Newfoundland. In North Atlantic-Geology and Continental Drift. Edited by M. Kay. American Association of Petroleum Geologists, Memoir 12, pages 308-407.

Horne, G.S. 1970: Complex volcanic-sedimentary patterns on the Magog Belt of northeastern Newfoundland. Geological Society of America Bulletin, volume 261, pages 1-9.

Howse, A.F. and Collins, C.J. 1979: An evaluation of the Lockport porperty. Newfoundland Department of Mines and Energy, Mineral Development Division, Open File Report 2E/6(376), 15 pages.

Hughes, C.J. 1973: Spilites, keratophyres and the igneous spectrum. Geological Magazine, volume 109, pages 513-527.

Humphris, S.E. and Thompson, G. 1978a: Hydrothermal alteration of oceanic basalts by seawater. Geochimica et Cosmochimica Acta, volume 42, pages 107-125.

Humphris, S.E. and Thompson, G. 1978b: Trace element mobility during hydrothermal alteration of oceanic basalts. Geochimica et Cosmochimica Acta, volume 42, pages 127-136.

Irvine, T.N. and Baragar, W.R.A. 1971: A guide to the classification of the common volcanic rocks. Canadian Journal of Earth Sciences, volume 8, pages 523-549.

Jacobi, R.D. and Schweickert, R.A. 1976: Implications of new data on stratigraphic and structural relations of Ordovician rocks on New World Island., north-central Newfoundland (abstract). Geological Society of America, Abstracts with Programs, volume 8, No. 2, page 206.

Jacobi, R. D. and Wasowski, J. J. 1985: Geochemistry and plate tectonic significance of the volcanic rocks of the Summerford Group, north-central Newfoundland, Geology, volume 13, pages 126-130.

Jacobsen, S.B. and Wasserburg, G.J. 1979: Nd and Sr isotopic study of the Bay of Islands ophiolite complex basalts. Journal of Geophysical Research, volume 84, pages 7429-7445.

Jakes, P. and Gill, J. 1970: Rare earth elements and the island arc tholeiite series. Earth and Planetary Science Letters, volume 9, pages 17-28.

Jakes, P. and White, A.J.R. 1971: Composition of island arcs and continental growth. Earth and Planetary Science Letters, volume 12, pages 224-230.

Jenner, G.A., Cawood, P.A., Rautenschlein, M. and White, W.M. 1987: Composition of back-arc basin volcanics, Valu Fa Ridge, Lau Basin: evidence for a slab-derived component in their mantle source. Journal of Volcanology and Geothermal Research, volume 32, pages 209-222.

Jenner, G. A. and Fryer, B. J. 1980: Geochemistry of the upper Snooks Arm Group basalts, Burlington Peninsula, Newfoundland: evidence against formation in an island arc. Canadian Journal of Earth Sciences, volume 17, pages 888-900.

Jenner, G.J. and Szybinski, Z.A. 1987: Geology, geochemistry and metallogeny of the Catchers Pond Group and Geochemistry of the Western Arm Group, Newfoundland. Unpublished report for the Geological Survey of Canada, 116 pages.

Johnston, R.W. and Chappell, B.W. 1979: Chemical analyses of rocks from the late Cainozoic volcanoes of north-central New Britain and the Witu Islands, Papua New Guinea. Report of the Bureau of Mineral Resources, Geology and Geophysics, Australia. page 209.

Karig, D.E. 1975: Basalt genesis in the Philippine Sea. In Initial Reports of the Deep Sea Drilling Project, volume 31. Edited by Karig, D.E., Ingle, J.C. Jr. et al. U.S. Government Printing Office, Washington, D.C., pages 857-879.

Karig, D.E. and Kay, R.W. 1981: Fate of sediments on the descending plate at convergent margins. Philosophical Transactions of the Royal Society of London, Series A301, pages 233-253.

Karlstrom, K.E., van der Pluijm, B. A. and Williams, P. F. 1982: Structural interpretation of the eastern Notre Dame Bay area, Newfoundland: thrusting and asymmetrical folding. Canadian Journal of Earth Sciences, volume 19, pages 2325-2341.

Kay, M. 1951: North American Geosynclines. Geological Society of America, Memoir 48, 143 pages.

Kay, M. 1967: Stratigraphy and structure of northeastern Newfoundland and bearing on drift in the North Atlantic. American Association of Petroleum Geologists Bulletin, volume 51, pages 579-600.

Kay, M. 1973: Tectonics of Newfoundland. In Gravity and Tectonics. Edited by K.A. DeJong and R. Scholten. Wiley - Interscience, pages 313-326.

Kay, M. 1975: Campbellton Sequence: manganiferous beds adjoining the Dunnage Melange, northeastern Newfoundland. Geological Society of America Bulletin, volume 86, pages 105-108.

Kay, M. and Eldridge, N. 1968: Cambrian trilobites in the central Newfoundland volcanic belt. Geological Magazine, volume 105, pages 372-377.

Kay, R.W. 1977: Geochemical constraints on the origin of Aleutian magmas. In Island Arcs, Deep Sea Trenches and Back-Arc Basins. Edited by M. Talwani and W.C. Pitman III. American Geophysical Union, Ewing Series, volume 1, pages 229-242.

Kay, R.W. 1980: Volcanic arc magmas: implications of a melting-mixing model for element recycling in the crust-upper mantle system. Journal of Geology, volume 88, pages 497-522.

Kay, R.W., Sun, S.-S. and Lee-Ha C.-N. 1978: Pb and Sr isotopes in volcanic rocks from the Aleutian Islands and Pribilof Islands, Alaska. Geochemica et Cosmochimica Acta, volume 42, pages 263-273.

Kean, B. F. 1973: Stratigraphy, petrology and geochemistry of volcanic rocks of Long Island, Newfoundland. Unpublished M. Sc. thesis, Memorial University of Newfoundland, St. John's, 155 pages.

Kean, B. F. 1977: Geology of the Victoria Lake map area (12A/6), Newfoundland. Newfoundland Department of Mines and Energy, Mineral Development Division, Report 77-4, 11 pages.

Kean, B. F. , Dean, P. L. and Strong, D. F. 1981: Regional geology of the Central Volcanic Belt of Newfoundland. In The Buchans Orebodies: Fifty Years of Geology and Mining. Edited by E.A. Swanson, D.F. Strong, and J.G. Thurlow. Geological Association of Canada, Special Paper 22, pages 65-78.

Kean, B. F. and Evans, D. T. W. 1986: Metallogeny of the Tulks Hill volcanics. Victoria Lake Group, central Newfoundland. In Current Research. Newfoundland Department of Mines and Energy, Mineral Development Division,' Report 86-1, pages 51-57.

Kean, B. F. and Jayasinghe, N. R. 1980: Geology of the Lake Ambrose (12A/10) - Noel Paul's Brook (12A/9) map areas, Central Newfoundland. Newfoundland Department of Mines and Energy, Mineral Development Division, Report 80-2, 29 pages.

Kean, B. F. and Jayasinghe, N. R. 1982: Geology of the Badger map area (12A/16), Newfoundland. Newfoundland Department of Mines and Energy, Mineral Development Division, Report 81-2, 37 pages.

Kean, B. F. and Strong, D. F. 1975: Geochemical evolution of an Ordovician island arc of the Central Newfoundland Appalachians. American Journal of Science, volume 275, pages 97-118.

Kennedy, M. J. 1975: Repetitive orogeny in the north-eastern Appalachians - new plate models based upon Newfoundland examples. Tectonophysics, volume 28, pages 39-87.

Kidd, W.S.F., Dewey, J.F. and Nelson, K.D. 1977: Middle Ordovician ridge subduction in central Newfoundland (abstract). Geological Society of America, Programs with Abstracts, volume 9, pages 283-284.

Kish, S.A. and Feiss, P.G. 1982: Application of lead isotope studies to massive sulfide and vein deposits of the Carolina Slate Belt. Economic Geology, volume 77, pages 352-363.

Kontak, D.J. and Strong, D.F. 1986: The volcano-plutonic Kings Point Complex, Newfoundland. In Current Research. Geological Survey of Canada, Paper 86-1, pages 465-470.

Kristmannsdottir, H. 1976: Hydrothermal alteration of basaltic rocks in Icelandic geothermal areas In Proceedings, Second United Nations Symposium on the Development and Use of Geothermal Resources, San Francisco, Volume 1. U.S. Government Printing Office, Washington, D. C., pages 441-445.

Kushiro, I. 1960: Si-Al relations in clinopyroxenes from igneous rocks. American Journal of Science, volume 258, pages 548-554.

Kusky, T.M. and Kidd, W.S.F. 1985: Middle Ordovician conodonts from the Buchans Group, central Newfoundland, their significance for regional stratigraphy of the Central Volcanic Belt: discussion. Canadian Journal of Earth Sciences, volume 22, page 484.

Langmuir, C.H., Bender, J.F., Bence, A.E., Hanson, G.N. and Taylor, S.R. 1977: Petrogenesis of basalts from the FAMOUS area: Mid Atlantic ridge. Earth and Planetary Science Letters, volume 36, pages 133-156.

Langmuir, G.H., Vocke, R.D. Jr., Hanson, G.H. and Hart, S.R. 1978: A general mixing equation with applications ti Icelandic basalts. Earth and Planetary Science Letters, volume 37, pages 380-392.

LeBas. M.J. 1962: The role of aluminum in igneous clinopyroxenes with relation to their, parentage. American Journal of Science, volume 260, pages 267-288.

LeHuray, A.P. 1982: Lead isotopic patterns of galena in the Piedmont and Blue Ridge ore deposits, southern Appalachians. Economic Geology, volume 77, pages 335-351.

LeRoex, A.P., Dick, H.J.B., Gulen, L., Reid, A.M., and Erlank, A.J. 1987: Local and regional heterogeneity in MORB from the Mid-Atlantic Ridge between 54.5° S and 51° S: Evidence for geochemical enrichment. Geochimica et Cosmochimica Acta, Volume 51, pages 541-555.

LeTerrier, J., Maury, R.C., Thonon, P., Girard, D. and Marchal, M. 1982: Clinopyroxene composition as a method of identification of the magmatic affinities of paleo-volcanic series. Earth and Planetary Science Letters, volume 59, pages 139-154.

Leake, B.E. 1978: Nomenclature of amphiboles. American Mineralogist, volume 63, pages 1023-1052.

Leeman, W.P. 1983: The influence of crustal structure on compositions of subduction-related magmas. Journal of Volcanology and Geothermal Research, volume 18, pages 561-588.

Liou, J.G. and Ernst, W.G. 1979: Oceanic ridge metamorphism of the East Taiwan Ophiolite. Contributions to Mineralogy and Petrology, volume 68, pages 335-348.

Lorenz, B.E. 1984: Mud-magma interactions in the Dunnage Melange, Newfoundland. In Marginal Basin Geology. Edited by B.P. Kokelaar and M.F. Howells. Geological Society Special Publication No. 16, pages 271-278.

Lorenz, B.E. and Fountain, J.C. 1982: The South Lake Igneous Complex, Newfoundland: a marginal basin - island arc succession. Canadian Journal of Earth Sciences, volume 19, pages 490-503.

Lowder, G.G. 1970: The volcanoes and caldera of Talasea, New Britain: mineralogy. Contributions to Mineralogy and Petrology, volume 26, pages 324-340.

Lowder, G.G. and Carmichael, I.S.E. 1970: The volcanoes and caldera of Talasea, New Britain: geology and petrology. Geological Society of America Bulletin, volume 81, pages 17-38.

Ludden, J.N. and Thompson,G. 1979: An evaluation of the behaviour of the rare earth elements during the weathering of sea-floor basalt. Earth and Planetary Science Letters, volume 43, pages 85-92.

MacDonald, G.A. and Katsura, T. 1964: Chemical composition of Hawaiian lavas. Journal of Petrology, volume 5, pages 82-133.

Malpas, J. 1976: The geology and petrogenesis of the Bay of Islands ophiolite suite, W. Newfoundland. Unpublished Ph.D. thesis, Memorial University of Newfoundland, St. John's, 435 pages.

Malpas, J. 1978: Magma generation in the upper mantle; field evidence from ophiolite suites and application to the generation of oceanic lithosphere. Philosophical Transactions of the Royal Society of London, Series A, volume 288, pages 527-546.

Malpas, J. 1979: Two trondhjemite associations from transported ophiolites in western Newfoundland: initial report. In Trondhjemites, Dacites and Related Rocks. Edited by F. Barker. Elsevier, Amsterdam, pages 465-487.

Marsh, B.D. 1979: Island arc development: some observations, experiments and speculations. Journal of Geology, volume 87, pages 687-713.

Marsh, N.G., Saunders, A.D. and Tarney, J. and Dick, H.J.B. 1980: Geochemistry of basalts from the Shikoku and Daito Basins, Deep Sea Drilling Project Leg 58. In Initial Reports of the Deep Sea Drilling Project, volume 58. U.S. Government Printing Office, Washington, D.C., pages 805-842.

Marten, B. E. 1971: Stratigraphy of volcanic rocks in the Western Arm area of the central Newfoundland Appalachians. Geological Association of Canada, Proceedings, volume 24, pages 73-84.

McLennan, S.M. and Taylor, S.R. 1981: Role of subducted sediments in island-arc magmatism: constraints from REE patterns. Earth and Planetary Science Letters, volume 54, pages 423-430.

Meijer, A. 1976: Pb and Cr isotopic data bearing on the origin of volcanic rocks from the Mariana island arc system. Geological Society of America Bulletin, volume 87, pages 1358-1369.

Meijer, A. 1980: Primitive arc volcanism and a boninite series: examples from western Pacific island arcs. In The Tectonic Evolution of southeast Asian seas and islands. Edited by D.E. Hayes. American Geophysical Union Monograph 23, pages 209-221.

Meijer, A. 1983: The origin of Low-K rhyolites from the Mariana frontal arc. Contributions to Mineralogy and Petrology, volume 83, pages 45-51.

Melson, W., Bowen, T., van Andel, T.H. and Siever, R. 1966: Greenstones from the central valley of the Mid-Atlantic Ridge. Nature, volume 209, pages 604-605.

Melson, W.G. and van Andel, T.H. 1966: Metamorphism in the Mid-Atlantic Ridge, 22° N latitude. Marine Geology, volume 4, pages 165-186.

Melson, W.G., Jarosewich, E., and Lundquist, C.A. 1970: Volcanic eruption at Metis Shoal, Tonga, 1967-1968: description and petrology. Smithsonian Contributions to Earth Sciences, volume 4, pages 1-18.

Menzies, M. and Murthy, V. R. 1980: Nd and Sr isotope geochemistry of hydrous mantle nodules and their host alkali basalts: implications for local heterogeneities in metasomatically veined mantle. Earth and Planetary Science Letters, volume 46, pages 323-334.

Merriman, R.J., Bevins, R.E. and Ball, T.K. 1986: Petrological and geological variations within the Tal y Fan intrusion: a study of element mobility during low grade metamorphism with implications for petrogenetic modelling. Journal of Petrology, volume 27, pages 1409-1436.

Meschede, M, 1986: A method of discriminating between different types of mid-ocean ridge basalts and continental tholeiites with the Nb-Zr-Y diagram. Chemical Geology, volume 56, pages 207-218.

Mitchell, A.H.G. and Bell, J.D. 1973: Island arc evolution and related mineral deposits. Journal of Geology, volume 81, pages 381-405.

Mitchell, A.H.G. and Garson, M.S. 1976: Mineralization at plate boundaries. Minerals Science and Engineering, volume 8, pages 129-169.

Mitchell, A.H.G. and Reading, H.G. 1971: Evolution of island arcs. Journal of Geology, volume 79, pages 253-284.

Miyashiro, A. 1974: Volcanic rock series in island arcs and active continental margins. American Journal of Science, Volume 274, pages 321-355.

Miyashiro, A. and Shido, F. 1975: Tholeiitic and calc alkali series in relation to the behaviour of titanium, vanadium, chromium and nickel. American Journal of Science, Volume 275, pages 265-277.

Miyashiro, A., Shido, F. and Ewing, M. 1971: Metamorphism in the Mid-Atlantic Ridge near 24° and 30° N. Philosophical Transactions of the Royal Society of London, volume A268, pages 589-603.

Morris, J.D. and Hart, S.R. 1983: Isotopic and incompatible element constraints on the genesis of island arc volcanics from Cold Bay and Amak Island, Aleutians, and implications for mantle structure. Geochimica et Cosmochimica Acta, volume 47, pages 2015-2030.

Mottl, M. J. 1983 Metabasalts, axial hot springs, and the structure of hydrothermal systems at mid-ocean ridges. Geological Society of America Bulletin, volume 94, pages 161-180.

Mottl, M.J. and Holland, H.D. 1978: Chemical exchange during hydrothermal alteration of basalt by seawater-I. Experimental results for major and minor components of seawater. Geochimica et Cosmochimica Acta, volume 42, pages 1103-1115.

Mottl, M. J. and Seyfried, W. E. 1980: Sub-seafloor hydrothermal systems: Rock- vs. seawater-dominated, In Seafloor Spreading Centers: Hydrothermal Systems. Edited by P.A. Rona and R.P. Lowell. Dowden, Hutchinson and Ross Inc., Stroudsburg, Pennsylvania, pages 869-884.

Munha, J. 1979: Blue amphiboles, metamorphic regime and plate tectonic modelling in the Iberian pyrite belt. Contributions to Mineralogy and Petrology, volume 69, pages 279-289.

Murauchi, S., Den, N., Asano, S., Hotta, H., Yoshii, T., Asanuma, T., Hagiwara, K., Ichikawa, H., Sato, T., Ludwig, W.J., Ewing, J., Edgar, N.T. and Houtz, R.E. 1968: Crustal structure of the Philippine Sea. Journal of Geophysical Research, volume 73, pages 3134-3171.

Murray, A. and Howley, J. P. 1881: Geologic Survey of Newfoundland. Edward Stanford, London, 536 pages.

Nance, W.B. and Taylor, S.R. 1977: Rare earth element patterns and crustal evolution, II. Archean sedimentary rocks from Kalgoorlie, Australia. Geochimica et Cosmochimica Acta, volume 41, pages 225-231.

Neale, E. R. W., Kean, B. F. and Upadhyay, H. D. 1975: Post-ophiolite unconformity, Tilt Cove - Betts Cove area, Newfoundland. Canadian Journal of Earth Sciences, volume 12, pages 880-886.

Nelson, D.R., Crawford, A.J. and McCulloch, M.T. 1984: Nd-Sr isotopic and geochemical systematics in Cambrian boninites and tholeiites from Victoria, Australia. Contributions to Mineralogy and Petrology, volume 99, pages 164-172.

Nelson, K.D. 1981: Melange development of the Boones Point Complex, north-central Newfoundland. Canadian Journal of Earth Sciences, volume 18, pages 433-442.

Nelson, K.D. and Casey, J.D. 1979: Ophiolitic detritus in the Upper Ordovician flysch of Notre Dame Bay and its bearing on the tectonic evolution of western Newfoundland. Geology, volume 7, pages 27-31.

Nesbitt, R.W. and Sun, S.-S. 1980: Geochemical features of some Archean and post-Archean high-magnesian, low-alkali liquids. Philosophical Transactions of the Royal Society of London, Series A297, pages 365-

Neuman, R.B. 1976: Early Ordovician (late Arenig) brachiopods from Virgin Arm, New World Island, Newfoundland. Geological Society of America Bulletin, volume 261, pages 11-61.

Nicholls, I.A. and Ringwood, A.E. 1973: Effect of olivine stability in tholeiites and the production of silica-saturated magmas in the island arc environment. Journal of Geology, volume 81, pages 285-300.

Nisbet, E.G. and Pearce, J.A. 1977: Clinopyroxene composition in mafic lavas from different tectonic settings. Contributions to Mineralogy and Petrology, volume 63, pages 149-160.

Nockolds, S.R. and Allen, R. 1953: The geochemistry of some igneous rock series, part 1. Geochimica et Cosmochimica Acta, volume 4, pages 105-142.

Nockolds, S.R. and Allen, R. 1954: The geochemistry of some igneous rock series, part 2. Geochimica et Cosmochimica Acta, volume 5, pages 245-285.

Nockolds, S.R. and Allen, R. 1956: The geochemistry of some igneous rock series, part 3. Geochimica et Cosmochimica Acta, volume 9, pages 34-77.

Noranda Mines Staff 1974: The Point Leamington sulphide deposit. In A Guidebook to Newfoundland Mineral Deposits. Edited by D.F. Strong,. NATO Advanced Studies Institute, pages 60-61.

O'Connor, J.T. 1965: A classification of quartz-rich igneous rocks based on feldspar ratios. U.S. Geological Survey Professional Paper 525B, pages B79-B84.

O'Nions, R.K., Carter, S.R., Evensen, N.M. and Hamilton, P.L. 1979: Geochemical and cosmochemical applications of Nd isotope analysis. Annual Reviews in the Earth Sciences, volume 7, pages 11-38.

O'Nions, R.K., Hamilton, P.J. and Evenson, N.M. 1977: Variations in $143Nd/144Nd$ and $87Sr/86Sr$ ratios in oceanic basalts. Earth and Planetary Science Letters, volume 34, pages 13-22.

Ohmoto, H. 1978: Submarine calderas: a key to the formation of volcanogenic massive sulfide deposits? Mining Geology, volume 28, pages 219-232.

Osborn, E.F. 1962: Reaction series for subalkaline igneous rocks based on different oxygen pressure conditions. American Mineralogist, volume 47, pages 211-226.

Payne, J.G. and Strong, D.F. 1979: Origin of the Twillingate trondhjemite, north-central Newfoundland: partial melting in the roots of an island arc. In Trondhjemites, Dacites and Related Rocks. Edited by F. Barker. Elsevier, Amsterdam, pages 489-516.

Peacock, M.A. 1931: Classification of igneous rock series. Journal of Geology, volume 39, pages 54-67.

Pearce, J.A. 1975: Basalt geochemistry used to investigate past tectonic environments on Cyprus. Tectonophysics, volume 25, pages 41-67.

Pearce, J.A. 1980: Geochemical evidence for the genesis and eruptive setting of lavas from Tethyan ophiolites. In Ophiolites, Proceedings of the International Ophiolite Symposium, Cyprus. Edited by A. Panayioutou. pages 261-272.

Pearce, J.A. and Cann, J.R. 1971: Ophiolite origin investigated by a discriminant analysis using Ti, Zr, and Y. Earth and Planetary Science Letters, volume 15, pages 271-285.

Pearce, J.A. and Cann, J. R. 1973: Tectonic setting of basic volcanic rocks determined using trace element analysis. Earth and Planetary Science Letters, volume 19, pages 290-300.

Pearce, J.A. and Flower, M.J.F. 1977: The relative importance of petrogenetic variables in magma genesis at accreting plate margins: a preliminary investigation. Journal of the Geological Society, volume 134, pages 103-127.

Pearce, J.A. and Norry, M.J. 1979: Petrogenetic implications of Ti, Zr, Y and Nb variations in volcanic rocks. Contributions to Mineralogy and Petrology, volume 69, pages 33-47.

Perfit, M.R., Gust, D.A., Bence, A.E., Arculus, R.J. and Taylor, S.R. 1980: Chemical characteristics of island-arc basalts: implications for mantle sources. Chemical Geology, volume 30, 227-256.

Poldervaart, A. and Hess, H.H. 1951: Pyroxenes in the crystallization of basaltic magma. Journal of Geology, volume 59, pages 472-

Reinsbakken, A. 1986: The Gjersvik Cu-Zn massive sulphide deposit in a bimodal metavolcanic sequence. In Stratabound Sulphide Deposits in the Central Scandinavian Caledonides. 7th IAGOD Symposium, Excursion Guide No. 2, pages 50-54.

Reusch, D. 1983   The Cobbs Arm volcanic belt and its relationship to nearby groups, New World Island, Newfoundland. Unpublished M.Sc. thesis, Memorial University of Newfoundland, St. John's.

Ringwood, A.E. 1974: Petrological evolution of island arc systems. Journal of the Geological Society of London, volume 130, pages 183-204.

Ringwood, A.E. 1982: Phase transformations and differentiation in subducted lithosphere: implications for mantle dynamics, basalt petrogenesis and crustal evolution. Journal of Geology, volume 90 pages 611-643.

Robinson, P., Higgins, N.C. and Jenner, G.A. 1986: Determination of rare -earth elements, Yttrium and Scandium in rocks by an ion-exchange - X-ray fluorescence technique. Chemical Geology, volume 55, pages 121-157.

Rosenbauer, R. J. and Bischoff, J. L. 1984: Uptake and transport of heavy metals by heated seawater: a summary of the experimental results. In Hydrothermal Processes at Seafloor Spreading Centers. Edited by P.A. Rona, K. Bostrom, L. Laubier, and K.L. Smith Jr. Plenum Publishing Company, pages 177-197.

Sampson, E. 1923: The ferruginous chert formations of Notre Dame Bay. Journal of Geology, volume 31, pages 571-598.

Sangster, D.F. 1979: Evidence of an exhalative origin for deposits in the Cobar District, New South Wales. Australian Bureau of Mines and Mineral Resources Journal, volume 4, pages 15-24.

Saunders, A.D. and Tarney, J. 1979   The geochemistry of basalts from a back-arc spreading centre In the East Scotia Sea. Geochemica et Cosmochimica Acta, volume 43, pages 555-572.

Saunders, A.D., Tarney, J., Marsh, N.G. and Wood, D.A. 1980: Ophiolites as ocean crust of marginal basin crust: a geochemical approach. In Ophiolites, Proceedings of the International Ophiolite Symposium, Cyprus. Edited by A. Panayioutou. pages 261-272.

Schiebner, E. and Markham, N.L. 1976: Tectonic setting of some strata-bound massive sulphide deposits in New South Wales, Australia. In Handbook of Strata-bound and Stratiform Ore Deposits, volume 6. Edited by K.H. Wolf. Elsevier, Amsterdam, pages 55-77.

Schilling J.-G. 1973: Icelandic mantle plume: geochemical evidence along the Reykjanes Ridge. Nature, volume 242, pages 565-571.

Schilling, J.-G., Kingsley, R. and Bergeron, M. 1977: Rare earth abundances in DSDP sites 332, 334 and 335, and inferences on the Azores Mantle Blob activity with time. In Initial Reports of the Deep Sea Drilling Project, volume 37. U.S. Government Printing Office, Washington, D.C., pages 591-597.

Schilling, J.-G., Thompson, G., Kingsley, R. and Humphris, S. 1985: Hotspot- migrating ridge interaction in the South Atlantic. Nature, volume 313, pages 187-191.

Schilling, J.-G., Zajac, M., Evans, R., Johnston, T., White, W., Devine, J.D. and Kingsley, R. 1983: Petrologic and geochemical variations along the mid-Atlantic ridge from 29 N to 73 N. American Journal of Science, volume 283, pages 510-586.

Schmidt, R.G. 1957: Petrology of the volcanic rocks. In Geology of Saipan, Mariana Islands, Part 2. U.S. Geological Survey Professional Paper B 280, pages 127-172.

Schrader, E.J. and Stow, S.H. 1983: Geochemistry and mineralogy of fresh and altered basalts from the Galapagos Rift. In Initial Reports of the Deep Sea Drilling Project, volume 70. U.S. Government Printing Office, Washington, D.C. pages 391-401.

Schweitzer, E.L., Papike, J.A. and Bence, A.E. 1979: Statistical analysis of clinopyroxenes from deep-sea basalts. American Mineralogist, volume 64, pages 510-513.

Searle, M.P. and Stevens, R.K. 1985: Emplacement of ophiolites - past, present and future. In Ophiolites and Oceanic Lithosphere. Edited by I.G. Glass et al.. Geological Society of London, Special Publication 13, pages 303-319.

Seyfried, W.E. and Bischoff, J.L. 1981: Experimental seawater-basalt interation at 300º and 500 bars: chemical exchange, secondary mineral formation and implications for the transport of heavy metals. Geochimica et Cosmochimica Acta, volume 45, pages 135-147.

Seyfried, W. E., Mottl, M. J. and Bischoff, J. L. 1978: Seawater/basalt ratio effects on the chemistry and mineralogy of spilites from the ocean floor. Nature, volume 275, no. 5677, p. 211-213.

Shervais, J.W. 1982: Ti-V plots and the petrogenesis of modern and ophiolitic lavas. Earth and Planetary Science Letters, volume 59, pages 101-118.

Sillitoe, R.H. 1982: Extensional habitats of rhyolite-hosted massive sulfide deposits. Geology, volume 109, pages 403-407.

Sinton, M.J. and Byerly, G.R. 1980: Silicic differentiates of abyssal oceanic magmas: evidence for late-magmatic vapor transport of potassium. Earth and Planetary Science Letters, volume 47, pages 423-430.

Sleep, N.H. 1984: Tapping of magmas from ubiquitous mantle heterogeneities: an alternative to mantle plumes? Journal of Geophysical Research, volume 89, pages 10029-10041.

Smith I.E.M. and Johnston, R.W. 1981: Contrasting rhyolite suites in the Late Cenozoic of Papua New Guinea. Journal of Geophysical Research, volume 86, pages B10257-B10272.

Smith, R.E. 1968: Redistribution of major elements in the alteration of some basic lavas during burial metamorphism. Journal of Petrology, volume 9, pages 191-219.

Snelgrove, A. K. 1928: The geology of the central mineral belt of Newfoundland, Canadian Institute of Mining and Metallurgy Bulletin, no. 197, pages 1057-1127.

Spooner, E.T.C., Beckinsdale, R.D., England, P.C. and Senior A. 1977: Hydration, 18O enrichment and oxidation during ocean floor hydrothermal metamorphism of ophiolitic metabasic rocks from E. Liguria, Italy. Geochemica et Cosmochimica Acta, volume 41, pages 857-871.

Spooner, E. T. C. and Fyfe, W. S. 1973: Sub-seafloor metamorphism, heat and mass transfer, Contributions to Mineralogy and Petrology, volume 42, pages 287-304.

Stackhouse, J.C. 1975: Economic geology of the southwestern Bay du Nord Group, North Bay, Newfoundland. Unpublished B.Sc. thesis, Memorial University of Newfoundland, St. John's, 59 pages.

Stauffer, M.R., Mukherjee, A.C. and Koo, J. 1975: The Amisk Group: an Aphebian (?) island arc deposit. Canadian Journal of Earth Sciences, volume 12, pages 2021-2035.

Stephens, M.B. 1982: Field relationships, petrochemistry and petrogenesis of the Stekenjokk Volçanites, central Swedish Caledonides. Sveriges Geologiska Undersokning, Series C, 111 pages.

Stephens, M.B. 1986: Metallogeny of stratabound sulphide deposits in the central Scandinavian Caledonides. In Stratabound Sulphide Deposits in the Central Scandinavian Caledonides, 7th IAGOD Symposium Excursion Guide No. 2, pages 5-16.

Stephens, M.B., Swinden, H.S. and Slack, J.F. 1984: Correlation of massive sulphide deposits in the Appalachian - Caledonian Orogen on the basis of Paleotectonic setting. Economic Geology, volume 79, pages 1442-1478.

Stern, C. and Elthon, D. 1979: Vertical variations in the effects of hydrothermal metamorphism in Chilean ophiolites: their implications for ocean floor metamorphism. Tectonophysics, volume 55, pages 179-213.

Stern, R.J. 1981: A common mantle source for western Pacific island arc and "hot spot" magmas - implications for layering in the upper mantle. Year Book, Carnegie Institute, Washington, volume 18, pages 455-462.

Stork, A.L. and Gill, J.B. 1982: Low-K Fijian dacites represent crustal fusion during arc fragmentation. EOS, Transactions of the American Geophysical Union, volume 63, page 1148.

Stouge, S. 1981: Lower and Middle Ordovician conodonts from central Newfoundland and their correlatives in western Newfoundland. In Current Research, Newfoundland Department of Mines and Energy, Mineral Development Division, Report 81-1, pages 134-142.

Strong, D.F. 1973: Lushs Bight and Robert's Arm Groups, central Newfoundland: possible juxtaposed oceanic and island arc volcanic suites. Geological Society of America Bulletin, volume 84, pages 3917-3928.

Strong, D.F. 1977: Volcanic regimes of the Newfoundland Appalachians. In Volcanic Regimes in Canada. Edited by W.R.A. Baragar, L.C. Coleman and J.M. Hall. Geological Association of Canada, Special Paper 16, pages 61-90.

Strong, D.F. 1980: Granitoid rocks and associated mineral deposits of Eastern Canada and Western Europe. In The Continental Crust and its mineral Deposits. Edited by D.W. Strangway. Geological Association of Canada, Special Paper 20, pages 741-770.

Strong, D.F. 1984: Geological relationships of alteration and mineralization at Tilt Cove, Newfoundland. In Mineral Deposits of Newfoundland - A 1984 Perspective. Edited by H.S. Swinden. Newfoundland Department of Mines and Energy, Mineral Development Division, Report 84-3, pages 81-90.

Strong, D.F. and Dickson, W.L. 1978: Geochemistry of Paleozoic granitoid plutons from contrasting tectonic zones of northeast Newfoundland. Canadian Journal of Earth Sciences, volume 15, pages 145-156.

Strong, D.F., Dickson, W.L., O'Driscoll, C.F. and Kean, B.F. 1974a: Geochemistry of eastern Newfoundland granitoid rocks. Newfoundland Department of Mines and Energy, Mineral Development Division, Report 74-3, 140 pages.

Strong, D.F., Dickson, W.L., O'Driscoll, C.F., Kean, B.F. and Stevens, R-K. 1974b: Geochemical evidence for an east-dipping Appalachian subduction zone in Newfoundland. Nature, volume 248, pages 37-39.

Strong, D.F. and Payne, J.G. 1973: Early Paleozoic volcanism and metamorphism of the Moretons Harbour-Twillingate area, Newfoundland. Canadian Journal of Earth Sciences, volume 10, pages 1363-1379.

Strong, D.F. and Saunders, C.M. in press: Ophiolitic sulphide mineralization at Tilt Cove, Newfoundland: controls by upper mantle and crustal processes. Economic Geology.

Sun, S.-S. 1980: Lead isotope study of young volcanic rocks from mid ocean ridges, ocean islands and island arcs. Philosophical Transactions of the Royal Society of London, volume 297, pages 409-445.

Sun, S.-S. and Nesbitt, R.W. 1978: Geochemical regularities and genetic significance of ophiolitic basalts. Geology, volume 6, pages 689-693.

Sun, S.-S., Nesbitt, R.W. and Sharaskin, A.Y. 1979: Geochemical characteristics of mid-ocean ridge basalts. Earth and Planetary Science Letters, volume 44, pages 119-138.

Sundblad, K. and Stephens, M.B. 1983: Lead isotope systematics of strata-bound sulfide deposits in the higher nappe complexes of the Swedish Caledonides. Economic Geology, volume 78, pages 1019-1107.

Swinden, H.S. 1982: Metallogenesis in the Bay d'Espoir area, southern Newfoundland: summary and implications for regional metallogeny in the Newfoundland Central Mobile Belt. Canadian Mining and Metallurgical Bulletin, volume 75, No. 839, pages 172-183.

Swinden, H.S. 1984: Geological setting and volcanogenic mineralization of the eastern Wild Bight Group, north-central Newfoundland. In Current Research, Geological Survey of Canada, Paper 84-1A, pages 513-520.

Swinden, H.S. in press: Geology and economic potential of the Pipestone Pond area (12A/1E; 12A/1NE), Newfoundland. Newfoundland Department of Mines, Mineral Development Division, Report.

Swinden, H.S., Lane, T.E. and Thorpe, R.I. in press: Lead isotope compositions of galena in carbonate-hosted deposits of western Newfoundland: evidence for diverse lead sources. Canadian Journal of Earth Sciences, volume 24.

Swinden, H.S. and Sacks, P.E. 1986: Stratigraphy and economic geology of the southern part of the Roberts Arm Group, central Newfoundland. In Current Research, Geological Survey of Canada, Paper 86-1A, pages 213-220.

Swinden, H.S. and Thorpe, R.I. 1984: Variations in style of volcanism and massive sulfide deposition in island arc sequences of the Newfoundland Central Mobile Belt. Economic Geology, volume 79, pages 1596-1619.

Tarney, J., Saunders, A.D., Mattey, D.P., Wood, D.A. and Marsh, N.G. 1981: Geochemical aspects of back-arc spreading in the Scotia Sea and western Pacific. Philosophical Transactions of the Royal Society of London, Series A, volume 300, pages 263-285.

Taylor, S.R. and Gorton, M.P. 1977: Geochemical application of spark source mass spectrography, III. Element sensitivity, precision and accuracy. Geochemica et Cosmochimica Acta, volume 41, pages 1375-1380.

Taylor, S.R., Capp, A.C., Graham, A.L. and Blake, D.H. 1969: Trace elements in andesites; part II, Saipan, Bougainville and Fiji. Contributions to Mineralogy and Petrology, volume 23, pages 1-26.

Thorpe, R.I., Guha, J., Franklin, J.M. and Loveridge, W.D. 1984: Use of the Superior Province lead isotope framework in interpreting mineralization stages in the Chibougamou District. In Chibougamou - Stratigraphy and Mineralization. Edited by J. Guha and E.H. Chown. Canadian Institute of Mining and Metallurgy, Special Volume 34, pages 496-516.

Thurlow, J.G. 1973: Lithogeochemical studies in the vicinity of the Buchans massive sulphide deposits, central Newfoundland. Unpublished M.Sc. thesis. Memorial University of Newfoundland, St. John's, 171 pages.

Thurlow, J.G. 1981: Geology, Ore Deposits and Applied Rock Geochemistry of the Buchans Group. Unpublished Ph.D thesis, Memorial University of Newfoundland, St. John's.

Thurlow, J.G., Swanson, E.A. and Strong, D.F. 1975: Geology and lithogeochemistry of the Buchans polymetallic sulphide deposits, Newfoundland. Economic Geology, volume 70, pages 130-144.

Tilton, G.R. and Barriero, B.A. 1980: Origin of lead in Andean calc alkaline lavas, southern Peru. Science, volume 210, pages 1245-1247.

Tomasson, J. and Kristmannsdottir, 1972: High temperature alteration minerals and thermal brines, Reykjanes, Iceland. Contributions to Mineralogy and Petrology, volume 36, pages 123-134.

Tuach, J. 1984: Geology and sulphide mineralization in the Rambler area, Newfoundland. In Mineral Deposits of Newfoundland - A 1984 Perspective. Edited by H.S. Swinden. Newfoundland Department of Mines and Energy, Mineral Development Division, Report 84-3, pages 91-97.

Tuach, J. and Kennedy, M.J. 1978: The geologic setting of the Ming and other sulfide deposits, Consolidated Rambler Mines, northwest Newfoundland. Economic Geology, volume 73, pages 192-206.

Upadhyay, H.D. 1973: The Betts Cove Ophiolite and Related Rocks of the Snooks Arm Group, Newfoundland. Unpublished Ph.D. Thesis, Memorial University of Newfoundland, St. John's, 224 pages.

Upadhyay, H.D. and Neale, E.R.W. 1979: On the tectonic regimes of ophiolite genesis. Earth and Planetary Science Letters, volume 43, pages 93-102.

Upadhyay, H.D. and Strong, D.F. 1973: Geological setting of the Betts Cove copper deposits, Newfoundland, Economic Geology, volume 68, pages 27-34.

Urabe, T. and Sato, T. 1978: Kuroko deposits of the Kosaka mine, northeast Honshu, Japan - products of submarine hot springs on Miocene sea floor. Economic Geology, volume 73, pages 161-179.

Vallance, T.G. 1965: On the chemistry of pillow lavas and the origin of spilites. Mineralogical Magazine, volume 34, pages 471-481.

van Eysinga, F.W.B. 1975: Geological Time Table, 3rd Edition. Elsevier Publishing Company, Amsterdam.

Verhoogen, J. 1962: Distribution of titanium between silicates and oxides in igneous rocks. American Journal of Science, volume 260, pages 211-220.

Vokes, F.M. 1976: Caledonian massive sulphide deposits in Scandinavia: a comparative review. In Handbook of Strata-bound and Stratiform Ore Deposits volume 6. Edited by K.H. Wolf. Elsevier, Amsterdam, pages 79-128.

Vokes, F.M. and Gale, G.H. 1976: Metallogeny relatable to global tectonics in southern Scandinavia. In Metallogeny and Plate Tectonics. Edited by D.F. Strong. Geological Association of Canada, Special Paper 14, pages 413-441.

von Drach, V., Marsh, B.D. and Wasserburg, G.J. 1986: Nd and Sr isotopes in the Aleutians: multicomponent parenthood of island arc magmas. Contributions to Mineralogy and Petrology, volume 92, pages 13-34.

Wadsworth, M.E. 1884: Notes on the rocks and ore deposits in the vicinity of Notre Dame Bay, Newfoundland. American Journal of Science, volume 28, pages 94-104.

Wagenbauer, H.A., Riley, C.A. and Dawe, G. 1983: Geochemical laboratory. In Current Research, Newfoundland Department of Mines and Energy, Mineral Development Division, Report 83-1, pages 133-137.

Wasowski, J.J. 1985: Trace element geochemistry of the Tea Arm volcanics, north-central Newfoundland: evidence for a forearc origin (abstract). Geological Society of America, Abstracts with Programs, volume 127, No. 1, page 68.

Wasowski, J.J. and Jacobi, R.D. 1984: Geochemistry and tectonic setting of the Lawrence Head volcanics, north central Newfoundland (abstract). Geological Society of America, Abstracts with Programs, volume 16, number 1, page 69.

Wasowski, J.J. and Jacobi, R.D. 1985: Geochemistry and tectonic significance of the mafic volcanic blocks in the Dunnage melange, north central Newfoundland. Canadian Journal of Earth Sciences, volume 22, pages 1248-1256.

Wasserburg, G.J. and DePaolo, D.J. 1979: Models of earth structure inferred from neodymium and strontium isotopic abundances. Proceedings of the National Academy of Science, U.S.A. volume 76, pages 3594-3598.

Weaver, S.D., Saunders, A.D., Pankhurst, R.J. and Tarney, J. 1979: A geochemical study of magmatism associated with the initial stages of back-arc spreading. Contributions to Mineralogy and Petrology, volume 68, pages 151-169.

Whelan, P.M., Gill, J.B., Kollman, E., Duncan, R.A. and Drake, R.E. 1985: Radiometric dating of magmatic stages in Fiji. In Geology and Offshore Resources of Pacific Island Arcs - Tonga Region. Edited by D.W. Scholl and T.L. Vallier. Circum-Pacific Council for Energy and Mineral Resources, Earth Science Series, volume 2, pages 379-414.

White, W.M. 1985: Sources of oceanic basalts: radiogenic isotope evidence. Geology, volume 13, pages 115-118.

White, W.M., Dupre, B., and Vidal, P. 1985: Isotope and trace element geochemistry of sediments from the Barbados Ridge-Demarara Plain region, Atlantic Ocean. Geochimica et Cosmochimica Acta, volume 49, pages 1875-1886.

White, W.M. and Hoffman, A.W. 1982: Sr and Nd isotope geochemistry of oceanic basalts and mantle evolution. Nature, volume 296, pages 821-855.

White, W.M. and Patchett, J. 1984: Hf-Nd-Sr isotopes and incompatible element abundances in island arcs: implications of magma origins and crust-mantle evolution. Earth and Planetary Science Letters, volume 67, pages 167-184.

Whitford, D.J., Nicholls, I.A. and Taylor, S.R. 1979: Spatial variations in the geochemistry of Quaternary lavas across the Sunda Arc in Java and Bali. Contributions to Mineralogy and Petrology, volume 70, pages 341-356.

Williams, H. 1963: Botwood map area. Geological Survey of Canada, Map 60-1963.

Williams, H. 1964: The Appalachians in Newfoundland - a two-sided symmetrical system. American Journal of Science, volume 262, pages 1137-1158.

Williams, H. 1978: Tectonic lithofacies map of the Appalachian Orogen. Memorial University of Newfoundland, Map 1.

Williams, H. 1979: Appalachian Orogen in Canada. Canadian Journal of Earth Sciences, volume 16, pages 792-807.

Williams, H., Dallmeyer, R.D. and Wanless, R.K. 1976: Geochronology of the Twillingate Granite and Herring Neck Group, Notre Dame Bay, Newfoundland. Canadian Journal of Earth Sciences, volume 13, pages 1591-1601.

Williams, H. and Hatcher, R.D. Jr. 1983: Appalachian suspect terranes. In Contributions to the Tectonics and Geophysics of Mountain Chains. Edited by R.D. Hatcher, H. Williams, and I. Zeitz. Geological Society of America, Memoir 158, pages 33-53.

Williams, H., Kennedy, M.J. and Neale, E.R.W. 1972: The Appalachian Structural Province. In Variations in Tectonic Styles in Canada. Edited by R.A. Price and R.J.W. Douglas. Geological Association of Canada, Special Paper 11, pages 181-261.

Williams, H., Kennedy, M.J. and Neale, E.R.W. 1974: The northeastern termination of the Appalachian Orogen. In The Ocean Basins and Margins, the North Atlantic, volume 2. Edited by A.E. Nairn and F.G. Stehli. Plenum Press, New York. pages 79-123.

Williams, H. and Payne, J.G. 1976: The Twillingate Granite and nearby volcanic groups: an island arc complex in Northeast Newfoundland. Canadian Journal of Earth Sciences, volume 12, pages 982-995.

Wilson, J.T. 1966: Did the Atlantic close and then re-open? Nature, volume 211, pages 676-681.

Winchester, J.A. and Floyd, P.A. 1975: Geochemical magma type discrimination: application to altered and metamorphosed basic igneous rocks. Earth and Planetary Science Letters, volume 28, pages, 459-469.

Wood, D.A. 1979: A variably veined suboceanic upper mantle- genetic significance for mid-ocean ridge basalts from geochemical evidence. Geology, volume 7, pages 499-503.

Wood, D.A. 1980: The application of a Th-Hf-Ta diagram to problems of tectonomagmatic classification and to establishing the nature of crustal contamination of basaltic lavas of the British Tertiary Volcanic Province. Earth and Planetary Science Letters, volume 50, pages 11-30.

Wood, D.A., Joron, J.-L., Marsh, N.G., Tarney, J. and Treuil, M. 1980: Major and trace element variations in basalts from the North Philippine Sea drilled during Deep Sea Drilling Project Leg 58: a comparative study of back-arc basin basalts with lava series from Japan and mid-ocean basins. In Initial Reports of the Deep Sea Drilling Project, volume 58. U.S. Government Printing Office, pages 873-895.

Wood, D.A., Joron, J.-L. and Treuil, M. 1979: A re-appraisal of the use of trace elements to classify and discriminate between magma series erupted in different tectonic settings. Earth and Planetary Science Letters, volume 50, pages 326-336.

Wood, D.A., Marsh, N.G., Tarney, J., Joron, J.-L., Fryer, P. and Treuil, M. 1981: Geochemistry of igneous rocks recovered from a transect across the Mariana trough, arc, fore-arc and trench, Sites 453 through 461, Deep Sea Drilling Project Leg 60. In Initial Reports of the Deep Sea Drilling Project, volume 60. U.S. Government Printing Office, pages 611-644.

Wynne, P.J. and Strong, D.F. 1984: The Strickland prospect of southwestern Newfoundland: a lithogeochemical study of metamorphosed and deformed volcanogenic massive sulfides. Economic Geology, volume 79, pages

Zartman, R.E. and Doe, B.R. 1981: Plumbotectonics - the model. Tectonophysics, volume 75, pages 135-162.

Zindler, A. and Hart, S.R. 1986: Chemical geodynamics. Annual Reviews of the Earth Sciences, volume 14, pages 493-571.

Zindler, A., Hart, S.R., Frey, F.A. and Jacobsen, S.P. 1979: Nd and Sr isotope ratios and rare earth element abundances in Reykjanes Peninsula basalts: evidence for mantle heterogeneity beneath Iceland. Earth and Planetary Science Letters, volume 45, pages 249-262.

Zindler, A., Staudigel, H. and Batiza, R. 1984: Isotope and trace element geochemistry of young Pacific seamounts: implications for the scale of upper mantle heterogeneity. Earth and Planetary Science Letters, volume 70, pages 175-195.

APPENDIX 1

PETROGRAPHIC TABLES FOR WILD BIGHT GROUP VOLCANIC AND SUBVOLCANIC ROCKS

Explanation of tables: Volcanic rocks are ordered by suite, subvolcanic rocks by fine grained and coarse grained rocks respectively. Numbers refer to visually estimated modal percentage; no point counting was undertaken.

Abbreviations: Ab - albite; Am - secondary amphibole; Bi - biotite; Ca - calcite; Ch - chlorite; crptx - cryptocrystalline material; Cpx - clinopyroxene; Ep - epidote; glx - glomerocryst; Hm - hematite; Il - ilmenite; Mag - magnetite; Ol - olivine; Opq - opaque minerals; Opx - orthopyroxene; Pl - plagioclase; Ser - sericite; Sp - sphene; Qz - quartz.

Petrographic tables for the mafic volcanic rocks

Sample No.	Ab	Cpx	Am	Ep	Sp	Opq	Ch	Ser	Qz	Ca	crptx	%	Ab	Cpx	Opx	gbz	%	Ch	Ep	Qz	Ser	Ca	%	Ch	Ep	Qz	Ser	Ca
Seal Bay Bottom																												
2140553	25			2			20				53	7	X	X			2	20	30			50						
2140554		4					10				90	4	X	X			1	20	30			50						
2140555							10				90	4	X	X			1	20	30			50						
Indian Cove																												
2140492			15			<1			15		70												10	2	1	2		95
Glovers Harbour (West)																												
2140456	40			3	1	3	30	1	1		25	2	X															
2140458	5		15	9	1		10				60	2	X				5					100	20	45	5			20
2140460	15		7	5		<1	5				68	1.5	X	X			<1					100	20	70				40
2140482	60			1-2		<1	20		1-2		15	<0.5	X	x			<1	50		50			20	70		10		20
2140471	<1					<1	25				75	<1	X	X									15	20		5		75
2140472	5					<1					95	5	x	X									10	60		10	30	
2140473	40		<1			<1	<2				40	2	X			X(?)							15			40	60	
2140474	7					<1	15		<1		78	1	x										15	30		60	5	5
2140475				2		<1	15				80	5	X										25	30				70
2140476	40		3	1		<1	?				20	15	X	X									35	15				85
2140477	35					<1	30		1?		35	<1	X										20	15				85
2140478	35		<2	5		<1	30		1-2		15	1	X	X									20	20		70		10
2140480	40			3		<1	15		1-2?		40	4	X	X									<5	65		35		
																							25	60	5			35
Glovers Harbour East																												
2140463	10	3		3		2	10				72	20	X	X			1		10			90	<0.5	95		5		
2140464	<1			<1			10		<1		90	20	X				4			20		80	6	80		10		
2140467	20			1-2		<1	10			1	82-86	2	X	X			<1		20	10		70						10
2140468	25					<1	10		2		65	2	x	X														
2140470	10			5		1	10				75	15	x	X			<1					100						
Nanny Bag Lake																												
2140529	5?			10		3	10		25	30-40	10	1																
2140530	35		25		3	<1	15		<1		20	3	X										7	60	7	3		30
2140531	25		1			1	10		1		63	<2	X										15	95		5		
2140532	45		35				6	10			4		X										10	20	30	50		
2140533	15			3				20			62		?										3	83	8	7		
2140534	30							10			60																	
2140539									30		70	2																
2140540	50		30					5			5		X															
2140541	40	5	20			5		10			7	<1		x	?								3	75	25			
2140543	40		10			2		5	35		20			x	x								5	60	5		35	
2140544	35	3	2			5		20			35			X														

402

Petrographic tables for the mafic volcanic rocks (continued)

Sample No.	Ab	Cpx	Am	Groundmass mineralogy								Phenocryst mineralogy					Veinlet mineralogy						Vesicle mineralogy					
				Ep	Sp	Opq	*Ch	Ser	Qz	Ca	crptx	%	Ab	Cpx	Opx	glx	%	Ch	Ep	Qz	Ser	Ca	%	Ch	Ep	Qz	Ser	Ca
Side Harbour																												
2140545	10	6		20		7-py					57						4		<0.5	80	40		<1			100		
2140546	45	25				8	15				7	2											10	25	3	2		70
2140547	30	10									60	8	x	x			2			30		70						
2140548	15	10	10?	7	3	<1	15				40	8	x	x									7	80				20
2140549	40	10									50	4	x	x									10		5	15		80
2140550	7	8		20	5	<1	15				45	5	x	x									7			5		95
2140551	5			10	1		20			1	65	4	x	x									10	30				70
Seal Bay Head																												
2140483	8			9	3	5-py	20				55	4	x	x			1	50	10	30		10	3	70	20			10
2140484	35	2	3	8	2		15				35	<1	x	x									7	100				
New Bay																												
2140497	25	30				<1	20				25	2	x	x		x	<1	100										
2140498	7		5	1		3-ilm	10					4	x	x			<1	90		10			<1	90		10		
Badger Bay																												
2140503	25			3		<5			2		70	15	x															
2140505	10		25			<5			2		65	30	x															
2140506	3										97	20	x															
Big Lewis Lake																												
2140509	55			13	2	3-py	20				7	5	x										7	100				
2140510	3	5					3				90	10	x	x														
2140511	40	6					25				30																	
Northern Arm																												
2140773	45			2		3	20				30												3	75	5	10		10
2140774	40			5		2	25				28												2	70				30

Petrographic tables for mafic intrusive rocks

Sample No.	Pl	Cpx	Opx	Ol	Am	Ep	Sp	Il/Mag	Ch	Ser	Qz	Bi	Ca	crptx
Diabase														
2140450	45	5		2(?)		5	<2	6	30	3	5			
2140454	30	10		2(?)		4	<2	6	20					28
2140461	30					7	2	4	55		2			
2140481	35	3			10	4	3	5	35		5			
2140486	55	10		1-2(?)		1-2	4	10	20					
2140489	10	5				25	2	5	25		3			25
2140496	25					5	3	1-2	2					65
Gabbro														
2140457	60	15		5				4	10			6		
2140482	75	10	2	5				<1	5					
2140485	35	30						5	30	5				3
2140495	55	20		3(?)				3	15	5				
2140499	30	5				2	2	5	10					
2140500	45	40		4		3		6	5		2			45
2140501	65	15				2		5	15		3			
2140502	60					10		5	20		5			
2140508	60	10		3(?)				5	20				2	
2140512	45	15		5				<1	25	5				

Petrographic tables for felsic volcanic rocks

Suite	Sample No.	Groundmass mineralogy									Phenocryst mineralogy				Veinlet mineralogy					
		Ab	Ch	Ep	Qz	Ser	Ca	Opq	crptx	%	Pl	Qz	%	Ch	Ep	Qz	Ser	Ca	Hm
Glover's Hbr.	2140452		10	1	40	1	1	1	46	<1	X	X	<1	10		90			
Glover's Hbr.	2140453	10	10	<1	60				20	35	X	X	3	8		90		2	
Indian Cove	2140466	5	10	8	35		1	<1	41	15	X	X							
Indian Cove	2140487		10	4	15	10		<1	60				4		60				40
Indian Cove	2140488		5	10	10	3		1	71				10	2	75	20		3	
Indian Cove	2140490		3	15	5				77				5		90				10
Indian Cove	2140493				5	10			85	17	X	X	5		3	10		3	84
Long Pond	2140513			5	40				55	10	X	X	7			60		40	
Nanny Bag Lk.	2140525			10	20	3	2		75	30	X	X	2			85		15	
Nanny Bag Lk.	2140535	10			55	2		<1	33	10	X	X	2			85		15	
Nanny Bag Lk.	2140537				55	5		3	37	7	X	X							
Nanny Bag Lk.	2140538		5		25	7		3	60	7	X	X	5				100		

APPENDIX 2

ELECTRON MICROPROBE OPERATING CONDITIONS AND ANALYSES OF STANDARDS

Clinopyroxene, plagioclase, chlorite and secondary amphibole were analysed at Memorial University of Newfoundland using a JEOL JX-5A electron microprobe microanalyser with three automated wavelength dispersive spectrometers run by the Krisel control system.

All analyses were performed using a beam current of 0.220 mA and an operating voltage of 15 kv. Data reduction was carried out by the Alpha program provided by Krisel using the Bence and Albee (1968) correction method. Pyroxene standards ACPX (Kakanui augite) and FCPX (Frisch pyroxene) were used for calibration.

Table A2.1 shows the results of replicate analyses of the standards, including standard deviation of the oxides and the homogeneity index. The latter index is a measure of the homogeneity of element distribution in the grain. Values less than 3 are generally considered to indicate a homogeneous distribution. Minor elements may show an inhomogeneous distribution because the calculation does not consider background counts.

Table A2.1 Replicate analyses of pyroxene standards

	ACPX			ACPX			FCPX		
	Averge 3 spots	Standard Deviation	Homogeneity Index	Averge 4 spots	Standard Deviation	Homogeneity Index	Averge 4 spots	Standard Deviation	Homogeneity Index
SiO_2	50.88	0.08	0.84	50.08	0.21	2.30	51.53	0.27	1.43
Al_2O_3	8.18	0.07	0.98	8.10	0.07	1.11	7.79	0.05	0.84
FeO	6.07	0.14	1.90	6.17	0.05	0.75	5.82	0.04	0.57
MgO	16.02	0.17	1.51	16.15	0.11	0.92	15.31	0.19	1.73
CaO	15.58	0.30	3.51	16.21	0.27	3.01	17.51	0.25	2.59
Na_2O	1.36	0.02	0.39	1.38	0.04	0.61	1.25	0.08	1.35
K_2O	0.01	0.00	3.71	0.01	0.00	3.55	0.00	0.01	25.60
TiO_2	0.82	0.02	1.40	0.85	0.03	2.71	0.79	0.02	1.82
MnO	0.14	0.05	7.11	0.15	0.02	2.60	0.13	0.02	2.51
Cr_2O_3	0.16	0.03	8.00	0.18	0.09	6.40	0.02	0.01	14.22
Total	99.22			99.28			100.15		
Si	1.853			1.831			1.864		
Al	0.350			0.349			0.331		
Fe	0.184			0.188			0.175		
Mg	0.870			0.879			0.825		
Ca	0.608			0.635			0.678		
Na	0.096			0.097			0.087		
K	0.000			0.000			0.000		
Ti	0.022			0.022			0.021		
Mn	0.004			0.004			0.003		
Cr	0.004			0.004			0.000		
Total	3.991			4.009			3.984		

APPENDIX 3

ELECTRON MICROPROBE MINERAL ANALYSES

Table A3.1: Electron microprobe analyses of plagioclase in Wild Bight Group mafic volcanic rocks

Sample No.	2140553	2140553	2140483	2140473	2140473	2140473	2140477	2140477	2140477
Volcanic unit*	sbb	sbb	sbh	gh	gh	gh	gh	gh	gh
Analysis No.	P177-1	P177-2	P78-1	P66-1	P66-2	P66-3	P70-1	P70-2	P70 3
SiO2	71.98	71.79	71.71	73.81	71.55	72.68	73.06	68.71	72.59
Al2O3	20.13	20.19	19.77	19.50	19.14	19.32	19.67	20.25	19.78
FeO(tot)	0.04	0.12	0.83	0.12	0.27	0.19	1.78	0.22	0.16
MgO	0.02	0.01	0.16	0.03	0.06	0.04	0.71	0.00	0.00
CaO	0.30	0.54	0.70	0.09	0.09	0.09	0.14	0.23	0.12
Na2O	11.03	9.95	7.59	11.16	11.44	11.30	8.85	11.92	11.03
K2O	0.05	0.09	0.13	0.03	0.07	0.05	0.10	0.12	0.05
TiO2	0.00	0.02	0.00	0.02	0.00	0.00	0.00	0.03	0.00
MnO	0.01	0.00	0.20	0.00	0.00	0.00	0.07	0.03	0.00
Cr2O3	0.00	0.04	0.01	0.01	0.00	0.00	0.00	0.01	0.03
Total	103.56	102.75	101.10	104.77	102.62	103.67	104.38	101.39	103.76
Si	3.019	3.027	3.056	3.054	3.035	3.045	3.040	2.968	3.039
Al	0.995	1.003	0.993	0.951	0.957	0.954	0.964	1.030	0.975
Fe	0	0.003	0.029	0.003	0.008	0.006	0.061	0.007	0.005
Mg	0	0	0.01	0.001	0.002	0.002	0.044	0.000	0.000
Ca	0.012	0.024	0.031	0.003	0.003	0.003	0.005	0.010	0.005
Na	0.897	0.812	0.626	0.895	0.941	0.917	0.714	0.989	0.894
K	0.001	0.003	0.006	0.001	0.003	0.002	0.005	0.006	0.002
Ti	0	0	0	0.000	0.000	0.000	0.000	0.000	0.000
Mn	0	0	0.006	0.000	0.000	0.000	0.001	0.000	0.000
Cr	0	0	0	0.000	0.000	0.000	0.000	0.000	0.000
Total (8 Ox.)	4.924	4.872	4.76	4.91	4.95	4.929	4.834	5.010	4.920

Sample No.	2140554	2140554	2140554	2140554
Volcanic unit*	gh	gh	gh	gh
Analysis No.	P177-1	P177-2	P177-3	P177-4
SiO2	71.19	70.76	70.50	70.68
Al2O3	19.65	20.01	19.68	19.27
FeO(tot)	0.18	0.07	0.07	0.27
MgO	0.00	0.02	0.01	0.11
CaO	0.36	0.31	0.16	0.28
Na2O	10.74	9.45	9.04	7.21
K2O	0.07	0.16	0.08	1.30
TiO2	0.00	0.05	0.04	0.03
MnO	0.01	0.01	0.01	0.03
Cr2O3	0.00	0.00	0.01	0.00
Total	102.20	100.84	99.60	99.18
Si	3.025	3.030	3.048	3.073
Al	0.984	1.009	1.002	0.986
Fe	0.006	0.002	0.002	0.009
Mg	0.000	0.001	0.000	0.006
Ca	0.016	0.014	0.006	0.013
Na	0.884	0.784	0.757	0.607
K	0.003	0.007	0.003	0.071
Ti	0.000	0.001	0.001	0.000
Mn	0.000	0.000	0.000	0.000
Cr	0.000	0.000	0.000	0.000
Total (8 Ox.)	4.918	4.85	4.819	4.765

* gh - Glover's Harbour; sbb - Seal Bay Bottom; sbh - Seal Bay Head

Table A3.2: Electron microprobe analyses of secondary amphibole from Wild Bight Group mafic volcanic rocks

Sample No.	2140473	2140473	2140477	2140477	2140477	2140532	2140532	2140532	2140532	2140532
Volcanic unit*	gh	gh	gh	gh	gh	nbl	nbl	nbl	nbl	nbl
Analysis No.	A66-1	A66-2	A70-1	A70-2	A70-3	A152-1	A152-2	A152-3	A152-4	A152-5
SiO2	52.30	50.09	53.88	53.12	54.26	49.49	49.46	47.15	48.74	50.20
Al2O3	2.99	4.37	1.62	2.08	2.36	5.72	7.65	7.52	4.59	5.58
FeO(tot)	14.30	15.86	16.71	18.07	16.29	16.33	19.99	19.66	18.14	18.70
MgO	13.15	12.26	12.81	13.08	11.69	10.96	11.15	9.63	11.27	10.13
CaO	12.29	11.35	11.75	10.99	10.65	11.14	8.46	11.11	11.27	10.13
Na2O	0.44	0.05	0.50	0.26	1.32	0.83	3.21	0.85	0.63	0.76
K2O	0.04	0.01	0.07	0.08	0.05	0.13	0.15	0.25	0.17	0.15
TiO2	0.01	0.66	0.03	0.02	0.00	0.18	0.27	0.52	0.17	0.15
MnO	0.39	0.35	0.20	0.08	0.14	0.56	0.54	0.52	0.16	0.12
Cr2O3	0.02	-0.00	0.00	0.02	0.02	0.05	0.03	0.54	0.64	0.61
Total	95.93	95.00	97.57	97.80	96.78	95.39	98.91	97.27	95.78	97.61
Si	7.739	7.527	7.893	7.794	7.968	7.454	7.250	7.107	7.408	7.458
Al	0.521	0.771	0.279	0.357	0.405	1.012	1.320	1.331	0.820	0.976
Fe	1.767	1.993	2.046	2.217	2.000	2.056	2.446	2.477	2.306	2.323
Mg	2.901	2.743	2.794	2.859	2.555	2.458	2.434	2.158	2.551	2.240
Ca	1.945	1.825	1.844	1.727	1.676	1.795	1.324	1.791	1.855	1.805
Na	0.125	0.013	0.137	0.073	0.371	0.238	0.339	0.248	0.183	0.218
K	0.004	0.000	0.008	0.013	0.008	0.022	0.025	0.044	0.031	0.026
Ti	0.000	0.075	0.000	0.000	0.000	0.018	0.025	0.057	0.018	0.013
Mn	0.047	0.044	0.021	0.008	0.013	0.070	0.064	0.066	0.080	0.074
Cr	0.000	0.000	0.000	0.000	0.000	0.004	0.000	0.006	0.000	0.000
Total (23 Ox.)	15.049	14.991	15.02	15.05	15.00	15.127	15.227	15.279	15.252	15.133
Mg/Mg+Fe	0.621	0.579	0.577	0.563	0.561	0.545	0.499	0.466	0.525	0.491

Sample No.	2140540	2140540	2140540	2140532	2140532	2140540	2140540	2140540
Volcanic unit*	nbl	nbl	nbl	nbl	nbl	nbl	nbl	nbl
Analysis No.	A162-1	A162-2	A162-3	A152-4	A152-5	A162-1	A162-2	A162-3
SiO2	48.50	46.73	50.58	48.74	50.20	48.50	46.73	50.58
Al2O3	9.13	7.77	6.34	4.59	5.58	9.13	7.77	6.34
FeO(tot)	19.22	19.22	19.98	18.14	18.70	19.22	19.22	19.98
MgO	8.70	9.17	9.35	11.27	10.13	8.70	9.17	9.35
CaO	12.05	10.80	11.25	11.42	11.34	12.05	10.80	11.25
Na2O	0.73	0.95	0.72	0.63	0.78	0.73	0.95	0.72
K2O	0.48	0.11	0.18	0.17	0.15	0.48	0.11	0.18
TiO2	0.12	0.27	0.16	0.16	0.12	0.12	0.27	0.16
MnO	0.43	0.58	0.58	0.64	0.61	0.43	0.58	0.58
Cr2O3	0.04	0.02	0.02	0.02	0.02	0.04	0.02	0.02
Total	99.40	95.62	99.16	95.78	97.61	99.40	95.62	99.16
Si	7.118	7.150	7.432	7.408	7.458	7.118	7.150	7.432
Al	1.576	1.396	1.095	0.820	0.976	1.576	1.396	1.095
Fe	2.355	2.457	2.453	2.306	2.323	2.355	2.457	2.453
Mg	1.899	2.088	2.043	2.551	2.240	1.899	2.088	2.043
Ca	1.890	1.770	1.767	1.855	1.805	1.890	1.770	1.767
Na	0.207	0.278	0.202	0.183	0.218	0.207	0.278	0.202
K	0.088	0.018	0.030	0.031	0.026	0.086	0.018	0.030
Ti	0.013	0.027	0.017	0.018	0.013	0.013	0.027	0.017
Mn	0.051	0.072	0.069	0.080	0.074	0.051	0.072	0.069
Cr	0.000	0.000	0.000	0.000	0.000	0.000	0.000	0.000
Total (23 Ox.)	15.20	15.256	15.108	15.252	15.133	15.20	15.256	15.108
Mg/Mg+Fe	0.446	0.459	0.454	0.525	0.491	0.446	0.459	0.454

* gh - Glover's Harbour; nbl - Nanny Bag Lake

Table A3.3: Electron microprobe analyses of chlorite from Wild Bight Group mafic volcanic rocks

Sample No.	2140553	2140553	2140553	2140477	2140477	2140477	2140477	2140477	2140477	2140477
Volcanic unit*	nbl	nbl	nbl	gh	gh	gh	gh	gh	gh	gh
Analysis No.	C152-1	C152-2	C152-3	C70-1	C70-2	C70-3	C70-4	C70-5	C70-6	C70-7
Grain type**	gm	gm	gm	am	am	am	am	am	gm	gm
SiO2	26.06	26.34	25.89	29.77	27.85	31.30	29.64	28.43	29.49	30.39
Al2O3	19.33	18.65	18.29	15.68	15.75	14.99	15.02	15.59	15.19	15.93
FeO(tot)	26.75	27.95	27.32	27.09	26.61	27.42	27.65	27.65	26.57	27.83
MgO	14.14	13.09	13.72	16.34	15.18	14.79	14.69	13.87	14.52	14.41
CaO	0.09	0.08	0.08	0.37	0.07	0.26	0.27	0.20	0.24	0.30
Na2O	0.09	0.00	0.00	0.05	0.04	0.07	0.02	0.11	0.00	0.06
K2O	0.14	0.07	0.03	0.03	0.01	0.03	0.01	0.03	0.04	0.01
TiO2	0.04	0.06	0.09	0.00	0.00	0.00	0.01	0.00	0.00	0.02
MnO	0.32	0.40	0.41	0.18	0.13	0.02	0.18	0.20	0.18	0.18
Cr2O3	0.00	0.02	0.02	0.03	0.00	0.17	0.04	0.01	0.02	0.00
Total	86.96	86.66	85.85	89.54	85.64	89.05	87.53	86.09	86.25	89.13
Si	5.595	5.704	5.664	6.175	6.060	6.508	6.316	6.182	6.340	6.333
Al	4.889	4.763	4.713	3.836	4.035	3.675	3.771	3.993	3.848	3.916
Fe	4.801	5.062	4.996	4.701	4.840	4.768	4.928	5.027	4.776	4.852
Mg	4.523	4.229	4.476	5.054	4.923	4.585	4.666	4.491	4.649	4.479
Ca	0.019	0.013	0.013	0.079	0.013	0.055	0.056	0.044	0.050	0.061
Na	0.031	0.000	0.000	0.018	0.013	0.024	0.006	0.038	0.000	0.018
K	0.038	0.019	0.006	0.006	0.000	0.006	0.000	0.006	0.006	0.000
Ti	0.006	0.006	0.013	0.000	0.000	0.000	0.000	0.000	0.000	0.000
Mn	0.057	0.070	0.070	0.030	0.019	0.024	0.031	0.032	0.031	0.030
Cr	0.000	0.000	0.000	0.000	0.000	0.000	0.000	0.000	0.000	0.000
Total (28 Ox.)	19.959	19.866	19.95	19.90	19.90	19.645	19.774	19.813	19.700	19.689
Fe/Fe+Mg	0.515	0.545	0.527	0.482	0.496	0.510	0.514	0.528	0.507	0.520

Sample No.	2140477	2140553	2140553	2140553	2140553	2140553	2140553	2140553	2140553	2140458
Volcanic unit*	gh	sbb	sbb	sbb	sbb	sbb	sbb	sbb	sbb	gh
Analysis No.	C70-8	C177-1	C177-2	C177-3	C177-4	C177-5	C177-6	C177-7	C177-8	C52-1
Grain type**	gm	gm	gm	gm	gm	gm	gm	gm	gm	gm
SiO2	28.60	26.54	28.29	28.38	28.23	28.18	27.85	27.69	28.7	29.44
Al2O3	15.96	16.39	16.23	16.92	17.55	16.99	16.84	17.17	16.93	15.64
FeO(tot)	28.41	27.48	28.24	27.52	28.65	28.55	27.73	28.13	27	19.51
MgO	15.09	13.40	13.39	13.48	14.40	13.54	13.79	14.46	13.82	18.7
CaO	0.24	0.13	0.09	0.04	0.06	0.05	0.09	0.07	0.1	0.05
Na2O	0.00	0.10	0.11	0.09	0.03	0.07	0.11	0.15	0.12	0.15
K2O	0.03	0.01	0.01	0.00	0.01	0.01	0.01	0.03	0.03	0
TiO2	0.00	0.04	0.02	0.00	0.02	0.01	0.02	0.01	0.02	0
MnO	0.14	0.61	0.60	0.65	0.61	0.65	0.6	0.66	0.64	0.17
Cr2O3	0.02	0.01	0.00	0.02	0.02	0	0.03	0	0.03	0.02
Total	88.49	84.71	86.98	87.10	89.58	88.05	87.07	88.37	87.39	83.68
Si	6.060	5.908	6.109	6.085	5.917	6.017	5.998	5.884	6.119	6.287
Al	3.988	4.300	4.125	4.273	4.336	4.275	4.272	4.299	4.254	3.936
Fe	5.034	5.117	5.102	4.934	5.019	5.096	4.993	4.998	4.812	3.485
Mg	4.766	4.444	4.310	4.311	4.496	4.306	4.424	4.58	4.392	5.955
Ca	0.049	0.026	0.019	0.006	0.012	0.006	0.019	0.012	0.019	0.006
Na	0.000	0.039	0.044	0.031	0.012	0.025	0.044	0.056	0.043	0.056
K	0.006	0.000	0.000	0.000	0.000	0	0	0.006	0.006	0
Ti	0.000	0.000	0.000	0.000	0.000	0	0	0	0	0
Mn	0.019	0.111	0.107	0.113	0.104	0.113	0.107	0.118	0.112	0.025
Cr	0.000	0.000	0.000	0.000	0.000	0	0	0	0	0
Total (28 Ox.)	19.92	19.945	19.816	19.753	19.896	19.838	19.857	19.953	19.757	19.750
Fe/Fe+Mg	0.514	0.535	0.542	0.534	0.527	0.542	0.530	0.522	0.523	0.369

* gh - Glover's Harbour; nbl - Nanny Bag Lake
** gm - groundmass; am - amygdule

(continued)

Sample No.	2140458	2140458	2140458	2140510	2140510	2140510	2140510	2140510	2140510	2140478
Volcanic unit[*]	gh	gh	gh	bll	bll	bll	bll	bll	bll	gh
Analysis No.	C52-2	C52-3	C52-4	C113-1	C113-2	C113-3	C113-4	C113-5	C113-6	C71-1
Grain type[**]	gm	gm	gm	am	am	am	gm	gm	gm	gm
SiO2	28.58	28.63	29.65	29.17	30.31	31.07	28.91	30.69	31.84	29.29
Al2O3	15.21	16.38	15.59	14.86	14.42	19.04	20.43	17.93	16.48	17.7
FeO(tot)	19.94	19.9	20.13	16.85	15.64	16.97	16.48	14.92	15.38	26.32
MgO	17.73	19.19	17.62	18.44	20.07	19.98	19.59	20.79	22.66	16.37
CaO	0.05	0.07	0.09	0.02	0.07	0.45	0.08	0.08	0.05	0.09
Na2O	0.18	0.15	0.21	0.19	0.98	0.13	0.23	0.17	0.17	0.03
K2O	0.01	0.01	0.01	0.03	0.01	0	0.01	0.01	0.17	0.03
TiO2	0	0	0	0	0.01	0.64	0.02	0.01	0.02	0.01
MnO	0.22	0.14	0.18	0.16	0.19	0.2	0.2	0.11	0	0.41
Cr2O3	0	0.02	0	0.08	0.02	0.01	0.01	0.01	0.14	0.02
Total	81.92	84.49	83.48	79.80	81.72	88.49	85.06	84.72	86.91	90.26
Si	6.272	6.075	6.36	6.454	6.508	6.149	5.782	6.277	6.363	5.992
Al	3.935	4.093	3.942	3.87	3.648	4.436	4.969	4.32	3.882	4.27
Fe	3.658	3.532	3.608	3.117	2.804	2.804	2.842	2.55	2.569	4.503
Mg	5.795	6.075	5.636	6.078	6.42	5.888	6.03	6.331	6.75	4.989
Ca	0.006	0.012	0.019	0	0.012	0.093	0.012	0.012	0.006	0.014
Na	0.071	0.056	0.082	0.078	0.403	0.046	0.091	0.066	0.064	0.019
K	0	0	0	0.006	0	0	0	0	0.006	0
Ti	0	0	0	0	0	0.093	0	0	0.006	0
Mn	0.039	0.025	0.031	0.026	0.031	0.029	0.03	0.018	0	0.005
Cr	0	0	0	0.013	0	0	0	0.018	0.023	0.051
Total (28 Ox.)	19.776	19.868	19.678	19.642	19.826	19.538	19.756	19.574	19.681	19.843
Fe/Fe+Mg	0.387	0.368	0.390	0.339	0.304	0.323	0.320	0.287	0.276	0.474

[*] gh - Glover's Harbour; nbl - Nanny Bag Lake
[**] gm - groundmass; am - amygdule

Table A3.4: Electron microprobe analyses of clinopyroxenes from the IAD group

Sample No.	2140458	2140458	2140458	2140458	2140458	2140458	2140473	2140473
Volcanic unit*	ghw	ghw	ghw	ghw	ghw	ghw	ghw	ghw
Analysis No.	P52-1	P52-2	P52-3	P52-4	P52-5	P52-6	P66-1	P66-2
Analysis type**	pc	pc	pc	pc	pc	pc	pc	pr
Rock Type	volcanic	volcanic	volcanic	volcanic	volcanic	volcanic	volcanic	volcanic
SiO_2	53.07	53.21	52.39	54.05	54.77	53.27	53 63	52 68
Al_2O_3	2.02	1.96	1.80	2.41	1.69	1.80	1 56	1 65
FeO(tot)	6.66	5.99	6.88	7.42	6.73	6 95	7 82	8.53
MgO	17.79	18.07	17.46	17.49	17.66	17 26	16 71	17 54
CaO	19.04	20.57	20.03	19.27	20.30	20.19	18 21	15 91
Na_2O	0.26	0.10	0.12	0.11	0.12	0.10	0 42	0 36
K_2O	0.03	0.01	0.01	0 00	0.01	0 00	0 11	0 13
TiO_2	0 08	0.13	0.11	0.11	0.11	0 09	0 10	0 11
MnO	0.14	0.16	0.18	0.23	0.11	0 19	0 24	0 26
Cr_2O_3	0.15	0.24	0.10	0.10	0.14	0 09	0 06	0 06
Total	99.24	100.04	99.08	101.19	101.64	99 94	98.86	98 23
Si	1.955	1.940	1.942	1.956	1.969	1.956	1 988	1 969
Al	0.083	0.087	0.078	0 102	0 070	0 077	0 067	0 072
Fe	0.205	0.183	0.213	0.224	0 201	0 213	0 242	0 267
Mg	0.977	0.982	0.965	0.943	0.946	0 944	0 923	0 977
Ca	0.752	0.804	0.795	0.747	0.781	0 794	0.723	0 677
Na	0.019	0.007	0.007	0.007	0 008	0 006	0.030	0.026
K	0.001	0.000	0.000	0.000	0.000	0.000	0.005	0.006
Ti	0 002	0.004	0.002	0.002	0.002	0 002	0 003	0 003
Mn	0.004	0.005	0.005	0.006	0 003	0.005	0.008	0 008
Cr	0.004	0.007	0.002	0.002	0 003	0 002	0.002	0 002
Total (6 Ox.)	4.002	4.019	4.009	3 989	3.983	3.999	3 991	4 007
Fe/Fe+Mg	0.159	0.144	0.166	0 176	0.161	0.169	0.191	0.197

Sample No.	2140473	2140473	2140473	2140473	2140478	2140478	2140478
Volcanic unit*	ghw	ghw	ghw	ghw	ghw	ghw	ghw
Analysis No.	P66-3	P66-4	P66-5	P66-6	P71-2	P71-3	P71-4
Analysis type**	pr	pr	pr	pc	pc	pc	pc
Rock Type	volcanic	volcanic	volcanic	volcanic	volcanic	volcanic	volcanic
SiO_2	53.34	54.21	54.11	53.54	53 69	52.26	54 00
Al_2O_3	1.98	1.53	1.62	1.98	2 24	2.57	1 99
FeO(tot)	8.31	8.03	8.25	8.31	5.67	7.38	7 54
MgO	16.62	17.75	17.95	16.62	17.52	17.14	17 94
CaO	18.49	18.58	18.46	18.49	20.01	19.91	18.53
Na_2O	0.39	0.09	0.13	0.39	0.12	0.07	0.16
K_2O	0.07	0.02	0.00	0.07	0.00	0 00	0 00
TiO_2	0.11	0.12	0.15	0.11	0.09	0.13	0 09
MnO	0.25	0.21	0.30	0.25	0.14	0.28	0 20
Cr_2O_3	0.08	0.05	0.08	0.08	0.16	0.16	0 14
Total	99.64	100.59	101.05	99.83	99.64	99.90	100 59
Si	1.971	1.973	1.965	1.971	1.960	1.924	1 962
Al	0.086	0.065	0.068	0.085	0.095	0 111	0.084
Fe	0.256	0.243	0.250	0.256	0.172	0.227	0 228
Mg	0.918	0.962	0.971	0.912	0.954	0.940	0 972
Ca	0.729	0.724	0.718	0.729	0.782	0.786	0.721
Na	0.028	0.005	0.008	0.028	0.008	0.004	0.010
K	0.003	0.000	0.000	0.003	0.000	0 000	0 000
Ti	0.003	0.003	0.003	0.003	0.002	0.003	0 002
Mn	0.008	0.005	0.008	0.008	0.003	0.008	0 005
Cr	0.002	0.001	0.002	0.002	0.004	0.004	0.003
Total (6 Ox.)	4.004	3.981	3.993	3.997	3.980	4.007	3 987
Fe/Fe+Mg	0.201	0.185	0.188	0.202	0.140	0.179	0 174

* ghw - Glover's Harbour West
** pc - phenocryst rim; pr - phenocryst core; gm - groundmass

2

Table A3 5: Electron microprobe analyses of clinopyroxenes from the IAl group

Sample No.	2140468	2140468	2140468	2140554	2140554	2140554	2140554	2140554
volcanic unit*	ghe	ghe	ghe	sbb	sbb	sbb	sbb	sbb
Analysis No.	P61-1	P61-2	P61-5	P178-1	P178-2	P178-3	P178-4	P178-5
Analysis type**	pc	pc	pc	pc	pr	gm	pc	pr
Rock type	volcanic	volcanic	volcanic	volcanic	volcanic	volcanic	volcanic	volcanic
SiO2	50.08	50.67	51.32	51.11	52.56	53.26	52.77	51.57
Al2O3	4.89	3.50	3.70	2.82	2.34	1.84	2.17	2.26
FeO(tot)	9.56	11.55	11.31	4.95	5.20	6.05	7.39	6.71
MgO	14.24	13.76	15.21	16.89	16.79	17.36	16.76	16.42
CaO	19.96	17.84	17.56	21.38	20.69	19.02	19.96	19.88
Na2O	0.62	0.32	0.38	0.33	0.25	0.27	0.47	0.48
K2O	0.01	0.00	0.01	0.02	0.01	0.01	0.01	0.03
TiO2	1.38	1.15	1.23	0.36	0.39	0.30	0.53	0.51
MnO	0.24	0.34	0.46	0.13	0.18	0.15	0.30	0.26
Cr2O3	0.07	0.05	0.08	0.83	0.80	0.54	0.35	0.51
Total	101.04	99.18	101.26	98.80	99.23	98.79	100.71	98.63
Si	1.850	1.908	1.890	1.898	1.936	1.965	1.932	1.927
Al	0.212	0.154	0.160	0.123	0.102	0.079	0.093	0.098
Fe	0.295	0.363	0.348	0.153	0.160	0.186	0.226	0.210
Mg	0.784	0.771	0.834	0.934	0.922	0.954	0.915	0.914
Ca	0.790	0.719	0.692	0.850	0.816	0.751	0.783	0.796
Na	0.044	0.022	0.027	0.022	0.017	0.018	0.033	0.035
K	0.000	0.000	0.000	0.000	0.000	0.000	0.000	0.001
Ti	0.038	0.032	0.033	0.010	0.009	0.007	0.015	0.014
Mn	0.008	0.010	0.014	0.003	0.005	0.004	0.009	0.008
Cr	0.002	0.001	0.002	0.024	0.022	0.015	0.010	0.015
Total (6 Ox.)	4.023	3.980	4.000	4.017	3.989	3.979	4.016	4.018
Fe/Fe+Mg	0.253	0.298	0.273	0.128	0.135	0.149	0.182	0.171

Sample No.	2140555	2140555	2140555	2140555	2150512	2140512	2140512
volcanic unit*	sbb	sbb	sbb	sbb			
Analysis No.	P179-2	P179-3	P179-4	P179-6	P117-1	P117-2	P117-3
Analysis type**	pc	pc	pc	pc	pr	pr	gm
Rock type	volcanic	volcanic	volcanic	volcanic	intrusive	intrusive	intrusive
SiO2	53.01	52.63	50.64	52.89	51.88	52.51	53.07
Al2O3	2.51	2.68	4.19	2.23	1.93	1.64	2.20
FeO(tot)	5.08	8.51	7.26	6.84	10.05	6.39	5.85
MgO	16.86	15.65	15.41	15.95	15.87	17.23	17.13
CaO	20.91	19.17	19.52	20.72	17.67	20.21	20.68
Na2O	0.15	0.27	0.27	0.14	0.30	0.21	0.24
K2O	0.00	0.01	0.00	0.01	0.00	0.01	0.01
TiO2	0.40	0.51	0.80	0.44	0.43	0.40	0.46
MnO	0.16	0.29	0.21	0.20	0.33	0.25	0.22
Cr2O3	0.80	0.08	0.13	0.10	0.14	0.38	0.58
Total	99.88	99.80	98.43	99.52	98.61	99.24	100.46
Si	1.939	1.943	1.895	1.952	1.949	1.944	1.937
Al	0.107	0.116	0.184	0.096	0.084	0.070	0.094
Fe	0.154	0.262	0.226	0.210	0.315	0.198	0.179
Mg	0.919	0.861	0.858	0.877	0.889	0.951	0.932
Ca	0.819	0.758	0.781	0.819	0.711	0.802	0.809
Na	0.010	0.018	0.019	0.009	0.021	0.015	0.017
K	0.000	0.000	0.000	0.000	0.000	0.000	0.000
Ti	0.010	0.014	0.021	0.012	0.012	0.011	0.013
Mn	0.022	0.008	0.005	0.005	0.011	0.008	0.007
Cr	0.004	0.002	0.003	0.002	0.003	0.011	0.017
Total (6 Ox.)	3.984	3.982	3.992	3.982	3.995	4.010	4.005
Fe/Fe+Mg	0.131	0.215	0.192	0.177	0.242	0.158	0.147

* ghe - Glover's Harbour East; sbb - Seal Bay Bottom
** pc - phenocryst core; pr - phenocryst rim; gm groundmass

Table A3.6: Electron microprobe analyses of clinopyroxene from the NAI group

Sample No.	2140510	2140510	2140510	2140510	2140510	2140510	2140510	2140510
volcanic unit*	bll	bll	bll	bll	bll	bll	bll	bll
Analysis No.	P113-1	P113-2	P113-3	P113-4	P113-5	P113-7	P113-8	P113-9
Analysis type**	pc	pc	pc	pc	pc	pc	pc	pc
Rock Type	volcanic	volcanic	volcanic	volcanic	volcanic	volcanic	volcanic	volcanic
SiO_2	51.21	52.18	50.89	48.68	52.56	53.68	53.28	50.55
Al_2O_3	3.72	3.11	3.59	5.66	4.20	2.32	2.00	3.30
FeO(tot)	5.41	5.09	5.85	6.97	6.68	6.73	6.50	4.78
MgO	16.05	16.97	15.59	15.60	15.75	17.11	17.10	16.45
CaO	20.84	20.21	21.20	19.09	20.32	19.98	19.48	21.46
Na_2O	0.61	0.42	0.36	0.27	0.27	0.17	0.26	0.18
K_2O	0.05	0.03	0.02	0.00	0.02	0.02	0.02	0.01
TiO_2	1.09	0.46	0.96	1.82	1.01	0.59	0.67	0.72
MnO	0.14	0.06	0.09	0.17	0.22	0.17	0.15	0.11
Cr_2O_3	0.88	0.96	0.82	0.19	0.68	0.46	0.43	0.88
Total	100.01	99.50	99.37	98.45	101.71	101.23	99.89	98.44
Si	1.883	1.916	1.888	1.821	1.897	1.940	1.951	1.884
Al	0.161	0.134	0.157	0.249	0.178	0.099	0.086	0.144
Fe	0.166	0.156	0.181	0.217	0.201	0.203	0.199	0.148
Mg	0.879	0.929	0.862	0.869	0.847	0.922	0.932	0.913
Ca	0.821	0.795	0.842	0.765	0.786	0.773	0.764	0.856
Na	0.043	0.030	0.025	0.019	0.018	0.011	0.018	0.013
K	0.002	0.001	0.000	0.000	0.001	0.000	0.000	0.000
Ti	0.030	0.013	0.026	0.050	0.026	0.016	0.018	0.020
Mn	0.004	0.002	0.002	0.004	0.006	0.004	0.004	0.003
Cr	0.026	0.028	0.024	0.005	0.019	0.013	0.012	0.025
Total (6 Ox.)	4.015	4.004	4.007	3.999	3.979	3.981	3.984	4.006
Fe/Fe+Mg	0.145	0.131	0.159	0.184	0.176	0.165	0.161	0.127

Sample No.	2140495	2140495	2140495	2140495	2140495	2140495
volcanic unit*						
Analysis No.	P91-1	P91-3	P91-4	P91-5	P91-6	P91-7
Analysis type**	pc	pc	pc	pc	pc	pc
Rock Type	intrusive	intrusive	intrusive	intrusive	intrusive	intrusive
SiO_2	51.10	52.37	53.45	53.52	51.76	51.30
Al_2O_3	2.02	2.81	3.03	1.98	3.34	2.87
FeO(tot)	8.78	4.20	6.57	5.94	5.58	9.31
MgO	15.09	15.86	16.16	17.23	16.89	14.02
CaO	19.61	21.58	21.02	20.78	21.01	20.91
Na_2O	0.53	0.57	0.25	0.19	0.29	0.39
K_2O	0.04	0.08	0.00	0.00	0.01	0.01
TiO_2	0.94	0.53	0.78	0.56	0.68	1.30
MnO	0.25	0.11	0.17	0.14	0.12	0.15
Cr_2O_3	0.02	0.48	0.07	0.05	0.21	0.00
Total	98.38	98.59	101.50	100.39	99.89	100.26
Si	1.931	1.939	1.930	1.949	1.898	1.907
Al	0.088	0.122	0.128	0.084	0.144	0.125
Fe	0.277	0.130	0.198	0.180	0.171	0.289
Mg	0.849	0.875	0.870	0.935	0.923	0.777
Ca	0.793	0.856	0.813	0.810	0.825	0.832
Na	0.038	0.041	0.017	0.013	0.019	0.028
K	0.001	0.004	0.000	0.000	0.000	0.000
Ti	0.026	0.015	0.020	0.015	0.018	0.036
Mn	0.007	0.003	0.004	0.004	0.003	0.004
Cr	0.000	0.014	0.001	0.001	0.005	0.000
Total (6 Ox.)	4.010	3.999	3.981	3.991	4.006	3.998
Fe/Fe+Mg	0.227	0.118	0.170	0.148	0.143	0.251

* bll - Big Lewis Lake
** pc - phenocryst core; pr - phenocryst rim; gm - groundmass

Table A3.7. Electron microprobe analyses of clinopyroxenes from the NAT subgroup

Sample No.	2140497	2140546	2140546	2140546	2140549	2140549	2140549	2140549
Volcanic unit*	nb	sh	sh	sh	sh	sh	sh	sh
Analysis No.	P93-1	P168-1	P168-2	P168-3	P171-1	P171-2	P171-3	P171-4
Analysis type**	pc	pc	pr	gm	gm	pc	pr	gm
Rock type	volcanic	volcanic	volcanic	volcanic	volcanic	volcanic	volcanic	volcanic
SiO2	48.82	52.14	52.03	51.02	52.64	51.43	50.42	52.70
Al2O3	4.72	2.20	2.34	4.51	1.93	3.52	4.16	2.08
FeO(tot)	10.49	7.37	6.37	6.33	6.22	6.02	6.70	7.03
MgO	13.65	16.79	16.64	15.41	17.28	15.44	15.34	17.55
CaO	19.29	18.82	20.86	21.12	19.83	21.42	21.00	18.52
Na2O	0.42	0.37	0.20	0.38	0.25	0.34	0.25	0.13
K2O	0.01	0.03	0.02	0.01	0.00	0.00	0.00	0.01
TiO2	1.57	0.66	0.71	0.98	0.62	0.75	1.31	0.51
MnO	0.28	0.18	0.14	0.10	0.18	0.13	0.16	0.21
Cr2O3	0.02	0.06	0.04	0.44	0.39	0.47	0.23	0.31
Total	99.27	98.62	99.35	100.30	99.34	99.52	99.57	99.05
Si	1.845	1.942	1.928	1.874	1.941	1.902	1.870	1.947
Al	0.209	0.096	0.101	0.195	0.083	0.153	0.182	0.090
Fe	0.330	0.230	0.197	0.194	0.192	0.186	0.208	0.217
Mg	0.768	0.932	0.918	0.844	0.950	0.851	0.848	0.966
Ca	0.780	0.751	0.827	0.831	0.784	0.849	0.835	0.733
Na	0.030	0.027	0.014	0.027	0.018	0.024	0.018	0.009
K	0.000	0.001	0.001	0.000	0.000	0.000	0.000	0.000
Ti	0.044	0.018	0.020	0.027	0.017	0.021	0.037	0.014
Mn	0.009	0.006	0.004	0.003	0.006	0.004	0.005	0.007
Cr	0.000	0.002	0.001	0.013	0.011	0.014	0.007	0.009
Total (6 Ox)	4.015	4.005	4.009	4.008	4.002	4.004	4.010	3.992
Fe/Fe+Mg	0.279	0.182	0.162	0.171	0.154	0.164	0.181	0.168

Sample No.	2140550	2140550	2140550	2140553	2140553	2140553	2140553	2140482
Volcanic unit*	sh	sh	sh	sh	sh	sh	sh	
Analysis No.	P172-1	P172-2	P172-3	P177-1	P177-2	P177-3	P177-4	1007511
Analysis type**	pc	pr	gm	gm	gm	gm	gm	pc
Rock type	volcanic	volcanic	volcanic	volcanic	volcanic	volcanic	volcanic	intrusive
SiO2	52.89	51.21	49.50	51.29	51.70	49.66	52.07	50.21
Al2O3	2.15	4.24	4.71	2.80	2.70	4.31	3.38	4.23
FeO(tot)	6.57	5.57	6.07	7.99	8.37	8.07	9.20	8.69
MgO	16.64	15.91	15.01	16.11	15.37	15.54	15.75	14.26
CaO	20.62	20.43	20.45	20.39	20.85	19.54	18.28	20.65
Na2O	0.15	0.29	0.31	0.27	0.35	0.19	0.21	0.46
K2O	0.00	0.00	0.01	0.00	0.00	0.00	0.00	0.03
TiO2	0.85	0.87	1.12	0.70	0.83	1.01	0.87	1.52
MnO	0.12	0.10	0.13	0.28	0.27	0.21	0.24	0.06
Cr2O3	0.05	0.96	1.11	0.17	0.05	0.08	0.04	0.08
Total	100.04	99.58	98.42	100.00	100.49	98.61	100.04	100.19
Si	1.940	1.885	1.855	1.902	1.911	1.864	1.920	1.866
Aliv	0.092	0.184	0.208	0.122	0.117	0.190	0.146	0.184
Fe	0.202	0.171	0.190	0.247	0.258	0.253	0.283	0.270
Mg	0.910	0.873	0.838	0.890	0.846	0.869	0.865	0.790
Ca	0.811	0.806	0.821	0.810	0.825	0.786	0.722	0.822
Na	0.011	0.021	0.023	0.018	0.025	0.013	0.014	0.033
K	0.000	0.000	0.000	0.000	0.000	0.000	0.000	0.001
Ti	0.023	0.024	0.032	0.018	0.022	0.027	0.023	0.042
Mn	0.004	0.003	0.004	0.008	0.007	0.006	0.006	0.002
Cr	0.001	0.028	0.033	0.004	0.001	0.002	0.001	0.002
Total (6 Ox)	3.994	3.995	4.004	4.019	4.012	4.010	3.980	4.012
Fe/Fe+Mg	0.167	0.150	0.169	0.200	0.215	0.208	0.227	0.235

* sh - Side Harbour; nb - New Bay
** pc - phenocryst core pr - phenocryst rim gm - groundmass

Table A3.8: Electron microprobe analyses of clinopyroxenes in the NAE group

Sample No.	2140483	2140483	2140483	2140483	2140483	2140483	2140483	2140483
Volcanic unit*	sbh	sbh	sbh	sbh	sbh	sbh	sbh	sbh
Analysis No.	P78-1	P78-2	P78-3	P78-4	P78-5	P78-6	P78-7	P78-8
Analysis type**	pc	pc	pc	pc	pc	pc	pc	pc
Rock Type	volcanic	volcanic	volcanic	volcanic	volcanic	volcanic	volcanic	volcanic
SiO_2	49.43	51.98	52.16	50.22	50.85	50.43	51.80	51.49
Al_2O_3	3.74	2.08	1.41	4.11	3.26	3.71	2.79	2.45
FeO(tot)	12.11	10.10	11.57	11.86	10.96	11.95	10.36	15.71
MgO	12.43	13.86	13.03	12.08	13.38	13.29	14.46	10.23
CaO	19.45	19.69	20.08	20.48	19.41	19.19	20.14	19.73
Na_2O	0.41	0.19	0.30	0.57	0.41	0.38	0.33	0.32
K_2O	0.00	0.00	0.00	0.02	0.00	0.00	0.01	0.00
TiO_2	1.74	1.05	0.75	2.12	1.73	1.58	1.36	1.03
MnO	0.34	0.23	0.31	0.38	0.34	0.36	0.21	0.52
Cr_2O_3	0.00	0.00	0.00	0.02	0.00	0.00	0.02	0.01
Total	99.65	99.18	99.61	101.86	100.34	100.69	101.48	101.49
Si	1.874	1.952	1.973	1.863	1.898	1.881	1.908	1.940
Al	0.167	0.091	0.062	0.178	0.143	0.163	0.120	0.108
Fe	0.384	0.317	0.366	0.368	0.341	0.372	0.319	0.494
Mg	0.702	0.776	0.735	0.667	0.744	0.739	0.793	0.574
Ca	0.790	0.792	0.814	0.813	0.775	0.766	0.794	0.796
Na	0.030	0.014	0.022	0.040	0.028	0.027	0.022	0.023
K	0.000	0.000	0.000	0.000	0.000	0.000	0.000	0.000
Ti	0.050	0.030	0.021	0.059	0.048	0.043	0.037	0.028
Mn	0.011	0.007	0.010	0.011	0.010	0.011	0.006	0.016
Cr	0.000	0.000	0.000	0.000	0.000	0.000	0.000	0.000
Total (6 Ox.)	4.008	3.979	4.003	3.999	3.987	4.002	3.999	3.979
Fe/Fe+Mg	0.330	0.269	0.309	0.332	0.292	0.312	0.266	0.436

Sample No.	2140484	2140484	2140484	2140450	2140450	2140450	2140486	2140486
Volcanic unit*	sbh	sbh	sbh					
Analysis No.	P79-2	P79-3	P79-4	P1-2	P1-3	P1-4	1008121	1008131
Analysis type**	pc	pc	pc	pc	pc	pc	pc	pc
Rock Type	volcanic	volcanic	volcanic	intrusive	intrusive	intrusive	intrusive	intrusive
SiO_2	50.21	50.45	49.85	50.16	51.68	50.55	52.14	51.16
Al_2O_3	3.18	3.61	4.54	3.84	2.05	3.61	2.24	3.21
FeO(tot)	11.80	11.30	12.03	8.34	8.63	9.32	9.89	9.37
MgO	12.88	13.00	11.91	14.59	15.69	13.93	15.64	14.22
CaO	18.92	19.87	19.69	21.16	20.05	20.19	18.66	21.18
Na_2O	0.38	0.34	0.54	0.44	0.41	0.47	0.45	0.42
K_2O	0.02	0.01	0.00	0.00	0.02	0.00	0.02	0.02
TiO_2	1.62	1.86	2.34	1.74	1.04	1.84	1.14	1.34
MnO	0.35	0.28	0.21	0.18	0.32	0.31	0.34	0.27
Cr_2O_3	0.04	0.02	0.00	0.00	0.04	0.04	0.05	0.03
Total	99.40	100.74	101.11	100.45	99.93	100.26	100.57	101.22
Si	1.900	1.882	1.857	1.861	1.922	1.881	1.927	1.890
Al	0.141	0.157	0.199	0.167	0.089	0.157	0.096	0.139
Fe	0.373	0.353	0.374	0.259	0.268	0.290	0.306	0.290
Mg	0.726	0.723	0.661	0.807	0.870	0.773	0.862	0.783
Ca	0.766	0.793	0.781	0.841	0.799	0.805	0.739	0.838
Na	0.027	0.024	0.038	0.032	0.030	0.034	0.032	0.030
K	0.000	0.000	0.000	0.000	0.001	0.000	0.001	0.001
Ti	0.045	0.051	0.065	0.049	0.029	0.052	0.032	0.037
Mn	0.011	0.008	0.006	0.006	0.010	0.010	0.011	0.008
Cr	0.000	0.000	0.000	0.000	0.001	0.001	0.001	0.001
Total (6 Ox.)	3.989	3.991	3.981	4.022	4.019	4.003	4.007	4.017
Fe/Fe+Mg	0.316	0.305	0.337	0.224	0.217	0.252	0.242	0.250

* sbh - Seal Bay Head
** pc - phenocryst core; pr - phenocryst rim; gm - groundmass

APPENDIX 4

DESCRIPTION OF SAMPLING AND SAMPLE PREPARATION METHODS

Three to five kg. samples were collected in the field with an 8 kg. sledge hammer and chisel. When sampling pillow lavas, samples were taken from as near the center of the interior of the pillow as possible. Pillow lava samples in all cases are taken from a single pillow. When sampling intrusive rocks, samples were taken from the interiors of the intrusion, avoiding chilled margins. Samples were selected in the field so as to minimize veining and secondary alteration.

In the laboratory, samples were cut into 5 to 10 mm thick slabs with a diamond saw and thoroughly washed. The slabs were then broken into chips less than 2 mm in diameter with a rock hammer, discarding all weathered surfaces, veins, vesicles (as much as possible), areas showing abnormal or unusual effects of secondary alteration and sawed surfaces. Approximately 200 grams of material was hand picked from these chips for crushing and analysis.

Before crushing, the chips were washed in distilled water and dried in an oven. The samples were then pulverized in a fused aluminosilicate disk grinder and the powders stored in clean medicine vials. The grinder was cleaned with spec.- pure silica sand between samples.

APPENDIX 5

UNIVERSAL TRANSVERSE MERCATOR GRID CO-ORDINATES OF

GEOCHEMICAL SAMPLES

Sample No.	Zone	N.T.S.	Easting	Northing		Sample No.	Zone	N.T.S.	Easting	Northing
2140450	21	2E/5	607900	5478390		2140511	21	2E/5	605420	5457950
2140452	21	2E/6	608770	5478020		2140512	21	2E/5	607120	5459280
2140453	21	2E/5	608710	5477720		2140513	21	2E/5	607960	5464430
2140454	21	2E/5	607610	5479700		2140525	21	2E/3	611750	5454460
2140456	21	2E/6	608850	5479640		2140526	21	2E/5	599700	5458940
2140457	21	2E/6	609050	5479820		2140528	21	2E/5	599200	5459040
2140458	21	2E/6	609140	5479830		2140530	21	2E/6	609530	5456450
2140460	21	2E/6	609520	5479920		2140531	21	2E/6	609800	5456730
2140461	21	2E/6	521430	5374010		2140532.	21	2E/6	610180	5456950
2140462	21	2E/6	609350	5479860		2140533	21	2E/6	610320	5456960
2140463	21	2E/6	610970	5480870		2140534	21	2E/6	610980	5456980
2140464	21	2E/6	610700	5480710		2140535	21	2E/6	611310	5457070
2140465	21	2E/5	518300	5375390		2140537	21	2E/6	612110	5457740
2140466	21	2E/5	602240	5471770		2140538	21	2E/6	612000	5458240
2140467	21	2E/6	610930	5481030		2140540	21	2E/6	609770	5457790
2140468	21	2E/6	610940	5480960		2140541	21	2E/6	609390	5457680
2140470	21	2E/6	610940	5481390		2140543	21	2E/5	608770	5457590
2140471	21	2E/6	608910	5479580		2140544	21	2E/5	608580	5457530
2140472	21	2E/6	608990	5479590		2140545	21	2E/5	601370	5459920
2140473	21	2E/6	609130	5479650		2140546	21	2E/5	599010	5461780
2140474	21	2E/6	609260	5479680		2140547	21	2E/5	599850	5462520
2140475	21	2E/6	609400	5479750		2140548	21	2E/5	599120	5464500
2140476	21	2E/6	609540	5479750		2140549	21	2E/5	599400	5464600
2140477	21	2E/6	609690	5479710		2140550	21	2E/5	598940	5466920
2140478	21	2E/6	609800	5479690		2140551	21	2E/5	599950	5470740
2140480	21	2E/6	609590	5479830		2140553	21	2E/5	603010	5468170
2140481	21	2E/5	601200	5473220		2140554	21	2E/5	604730	5469000.
2140482	21	2E/5	602370	5475820		2140555	21	2E/5	604930	5468970
2140483	21	2E/5	604520	5481290		2140556	21	2E/5	603270	5463370
2140484	21	2E/5	605010	5482190		2140750	21	2E/5	604990	5468860
2140485	21	2E/5	605710	5482100		2140751	21	2E/5	604990	5468860
2140486	21	2E/5	607690	5480890		2140752	21	2E/5	604870	5468890
2140487	21	2E/5	602700	5473900		2140753	21	2E/5	604850	5467920
2140488	21	2E/5	602840	5473570		2140754	21	2E/5	604940	5467960
2140489	21	2E/5	602880	5473290		2140755	21	2E/5	603590	5463970
2440490	21	2E/5	602970	5473320		2140756	21	2E/5	603670	5463970
2140491	21	2E/5	602900	5471410		2140758	21	2E/5	603320	5463390
2140492	21	2E/5	602820	5470770		2140761	21	2E/5	601710	5459270
2140493	21	2E/5.	602460	5469290		2140762	21	2E/5	601810	5459250
2140496	21	2E/5	604930	5474390		2140763	21	2E/5	599650	5460900
2140497	21	2E/6	616350	5482650		2140764	21	2E/5	601670	5459700
2140498	21	2E/6	616560	5482490		2140765	21	2E/5	599640	5458900
2140501	21	2E/6	599680	5478200		2140767	21	2E/5	602280	5458900
2140502	21	2E/6	597120	5473680		2140768	21	2E/5	603190	5457100
2140503	21	2E/5	597020	5471310		2140771	21	2E/3	616560	5452160
2140505	21	2E/5	595960	5470750		2140772	21	2E/3	616290	5451800
2140506	21	2E/5	544770	5471410		2140773	21	2E/3	615955	5451220
2140508	21	2E/5	602699	5456720		2140774	21	2E/3	616810	5451310
2140509	21	2E/5	603170	5457070						
2140510	21	2E/5	603810	5457180						

APPENDIX 6

GEOCHEMICAL ANALYTICAL METHODS WITH ESTIMATES OF ACCURACY AND PRECISION

Table A6.1 summarizes the methods and laboratories used for the analysis of major and trace elements during this study. Analytical procedures are described in detail below.

Table A6.1: Summary of analytical methods and laboratories for major and trace element geochemistry

ELEMENTS	METHOD	LABORATORY
Major element oxides; Cu, Zn, Ni	Atomic absorption spectrometry	Nfld. Department of Mines and Energy
Rb, Sr, Y, Zr, Nb, Ba, V, Cr, REE*	X-Ray fluorescence	Memorial University of Newfoundland
Hf, Sc, Ta, Th, Co, REE**	Instrumental neutron activation (INAA)	Universiteit Leuven, Leuven, Belgium

REE* - sample nos. 2140460, 2140506, 2140510, 21405262140551, 2140555, 2140762, 2140763, 2140767, 2140774.

REE** - other samples for which REE were determined

i) *Major element oxides:*

Major elements were determined in the laboratory of the Newfoundland Department of Mines and Energy (N.D.M.E.). The analytical procedures summarized below have been described in detail by Wagenbauer *et al.* (1983).

Approximately 0.1 g of sample powder was fused with lithium metaborate in a graphite crucible and digested in HCl and HF. During digestion, boric acid was added to complex excess HF. Following digestion, the solution was made up to volume and the oxides SiO_2, Al_2O_3, total iron as Fe_2O_3, MgO, CaO, Na_2O, K_2O, TiO_2, and MnO were determined by atomic absorption

spectrometry.

P_2O_5 was determined spectrophotometrically by reduction of the phospho- molybdate complex with hydrazine sulphate. Ferrous iron was determined by addition of vanadium and ferrous ammonium sulphate followed by titration with standard potassium dichromate using barium diphenylamine sulphonate as an indicator.

Loss on ignition was determined weighing a sample portion before and after heating to 1000° C.

Detection limits quoted by the analyst are 0.01 wt. %. Replicate analysis of standard materials (Table A6.2) blind duplicates of rock samples (Table A6.3) show good agreement with each other and, in the former case, with published recommended values for the material. Replicate analysis of standards MRG-1 and SY-2 for FeO gave, respectively, 8.59 (St. Dev.=0.39) and 3.63 (St. Dev. = .07).

ii) *Cu, Zn, Ni.*

These trace elements were determined in the N.D.M.E. laboratory. Analytical procedures have been described in detail by Wagenbauer *et al.* (1983).

Approximately 1 g of sample was dissolved in HF, HCl and $HClO_4$. Following dissolution, the sample was evaporated and taken up in HCl and Cu, Zn and Ni determined directly by atomic absorption spectrometry.

Detection limits are quoted as 1 ppm for each element. Analytical uncertainties are quoted as better than ±5% although these may be markedly greater near the detection limits. Replicate analysis of standard materials and blind duplicates, listed in Table A6.4, are within these quoted error limits.

Table A6.2: Analyses of standard rock materials for major element oxides in the N.D.M.E laboratory compared to recommended values

	Standard	No. of Determinations	Mean	St. Dev.	Abbey (1983)
SiO2	RGM-1	5	73.26	0.58	73.47
Al2O3	RGM-1	5	13.87	0.16	13.8
Fe2O3	RGM-1	5	1.78	0.03	1.89
MgO	RGM-1	5	0.29	0.01	0.28
CaO	RGM-1	5	1.19	0.01	1.15
Na2O	RGM-1	5	4.15	0.03	4.12
K2O	RGM-1	5	4.42	0.05	4.35
TiO2	RGM-1	5	0.29	0.03	0.27
MnO	RGM-1	5	0.04	0.01	0.04
P2O5	RGM-1	5	0.05	0.01	0.05

Standard	No. of Determinations	Mean	St. Dev.	Abbey (1983)
BCR-1	5	54.12	0.29	54.53
BCR-1	5	13.66	0.25	13.72
BCR-1	5	13.56	0.15	13.41
BCR-1	5	3.52	0.02	3.48
BCR-1	5	7.00	0.09	6.97
BCR-1	5	3.25	0.04	3.30
BCR-1	5	1.72	0.04	1.70
BCR-1	5	2.27	0.03	2.26
BCR-1	5	0.18	0.00	0.17
BCR-1	5	0.06	0.01	0.06

	Standard	No. of Determinations	Mean	St. Dev.	Abbey (1983)
SiO2	BHVO-1	6	49.63	0.29	49.9
Al2O3	BHVO-1	6	13.93	0.16	13.85
Fe2O3	BHVO-1	6	12.35	0.02	12.24
MgO	BHVO-1	6	7.41	0.12	7.31
CaO	BHVO-1	6	11.6	0.07	11.33
Na2O	BHVO-1	6	2.22	0.02	2.29
K2O	BHVO-1	6	0.51	0.02	0.54
TiO2	BHVO-1	6	2.76	0.04	2.69
MnO	BHVO-1	6	0.18	0.01	0.17
P2O5	BHVO-1	6	0.27	0.01	0.28

Standard	No. of Determinations	Mean	St. Dev.	Abbey (1983)
MGR-1	6	39	0.24	39.32
MGR-1	6	8.72	0.06	8.5
MGR-1	6	17.71	0.26	17.82
MGR-1	6	13.73	0.23	13.49
MGR-1	6	14.79	0.17	14.77
MGR-1	6	0.71	0.01	0.71
MGR-1	6	0.16	0.01	0.18
MGR-1	6	3.76	0.09	3.69
MGR-1	6	0.18	0	0.17
MGR-1	6	0.06	0.01	0.06

Table A6.3: Comparison of blind duplicate analyses of major element oxides,
recalculated to 100% anhydrous

Sample	2140468	2140468	2140512	2140512	2140546	2140546
SiO2	55.79	55.71	52.34	52.72	50.31	50.10
Al2O3	15.90	15.57	17.29	17.00	14.10	14.12
Fe2O3	4.14	4.28	1.98	2.04	3.35	3.54
FeO	5.28	5.21	5.98	6.01	8.11	8.16
MgO	2.47	2.50	7.35	7.35	7.07	7.03
CaO	7.71	7.92	10.15	10.00	9.37	9.32
Na2O	6.49	6.47	2.31	2.30	4.50	4.52
K2O	0.54	0.54	1.34	1.33	0.60	0.61
TiO2	1.36	1.51	1.00	0.99	2.12	2.11
MnO	0.13	0.12	0.14	0.14	0.17	0.18
P2O5	0.17	0.17	0.12	0.12	0.30	0.31
LOI	1.60	1.60	2.97	2.90	2.93	2.82

Sample	2140463	2140463	2140585	2140585	2140607	2140607
SiO2	41.06	41.35	51.95	52.99	54.82	54.93
Al2O3	19.15	19.06	15.52	16.05	16.55	16.72
Fe2O3	1.84	1.73	0.79	0.35	3.61	3.48
FeO	12.00	12.05	7.61	7.80	4.77	4.76
MgO	4.76	4.77	7.82	7.99	6.18	6.09
CaO	14.98	14.77	10.85	9.17	8.79	8.79
Na2O	4.29	4.31	4.39	4.51	3.03	3.00
K2O	0.15	0.15	<.01	<.01	0.98	0.97
TiO2	1.29	1.33	0.81	0.87	0.93	0.94
MnO	0.29	0.29	0.21	0.22	0.18	0.17
P2O5	0.20	0.18	0.06	0.06	0.15	0.15
LOI	15.26	15.35	12.45	13.02	1.73	1.63

Sample	2140619	2140619
SiO2	76.10	75.87
Al2O3	13.71	14.00
Fe2O3	0.56	0.55
FeO	0.29	0.30
MgO	0.33	0.34
CaO	0.73	0.69
Na2O	3.82	3.85
K2O	4.18	4.13
TiO2	0.19	0.17
MnO	0.07	0.07
P2O5	0.02	0.02
LOI	1.40	1.43

Table A6.4: Replicate analyses of standard materials and blind duplicates for Cu, Zn and Ni.
Recommended values after Abbey (1983)

STANDARDS

	MRG-1	Number	St. Dev.	Recommended Value		SY-2	Number	St. Dev.	Recommended Value
Cu	114	6	3.7	135		4.8	5	1.9	5
Zn	194	6	7.6	190		255	5	7	250
Ni	154	6	2.9	195		4.7	5	0.06	10

BLIND DUPLICATES

	2140468	2140468		2140491	2140491		2140512	2140512
Cu	26	27		76	80		61	60
Zn	81	80		65	69		66	65
Ni	1	3		35	37		106	106

	2140530	2140530		2140546	2140546		2140563	2140563
Cu	88	90		85	81		13	11
Zn	113	113		96	97		111	109
Ni	15	17		62	62		5	6

	2140585	2140585		2140607	2140607
Cu	32	33		27	27
Zn	61	60		87	87
Ni	52	53		60	61

iii) *Rb, Sr, Y, Zr, Nb, Ba, V, Cr.*

These trace elements were analysed with a Phillips 1450 X-Ray fluorescence spectrometer. Samples of approximately 10 grams were thoroughly mixed with approximately 1.5 grams of bakelite binder and then pressed into a pellet. The pellets were baked in an oven at 200°C for twenty minutes.

A Rh tube was used for all analyses. Ba, V and Cr were analysed using the LiF 200 crystal and 40 second counting times A monitor spiked with trace elements was calibrated against standards and the elements ratioed to it to correct for instrument drift. The Compton peak was used for matrix corrections. The detection limit of Ba is 35 ppm, of V, 20 ppm and of Cr, 5 ppm. Analyses are quoted by the laboratory as accurate to ±5%. Blind duplicate analyses tabulated in Table A6.5 are all within this limit except for one Ba duplicate (2140491). Comparison of analysis of standard materials with recommended values (Table A6.5) confirm similar limits for accuracy.

Rb, Sr, Y, Zr and Nb were analysed by a modified X-Ray fluorescence technique designed to provided lower detection limits and improved precision at low concentrations. This was necessary because of the very low concentrations of these elements in many samples and their importance in the petrogenetic interpretations. Analysis was carried out using a Rh tube and the LiF 200 crystal. The pellets were cycled 5 to 10 times during the run and the abundances calculated from the total counts (200 to 400 seconds of counting per element). The use of the LiF 200 crystal provides better discrimination of the peaks against background and the extended count times provided much improved counting statistics. In each run, the standards PCC-1 and BCR-1 were included. PCC-1 has negligible concentrations of these elements (Table A6.6) and was used to provide a zero baseline for abundance calculations. The data were zeroed and then calibrated to the most recent estimates of the composition of BCR-1 (Table A6.6). Note that the calibration value for BCR-1 of 34 ppm is probably low and should be in the range 36-38 ppm (B.J. Fryer, pers. comm. 1987). However, in the present study, this value has not been adjusted from Taylor's value.

Table A6.5: Replicate analyses of standard materials and blind duplicates for Ba, V and Cr.
Recommended values after Abbey (1983)

STANDARDS

	MRG-1	Number	St. Dev.	Recommended Value		SY-2	Number	St. Dev.	Recommended Value
Ba	78.5	15	49.6	50?		449	17	29.1	470
V	554	15	22.4	520		44.5	17	2.6	59
Cr	384:1	15	6.9	450		4.7	17	2.8	7.1

BLIND DUPLICATES

	2140468	2140468		2140491	2140491		2140512?	2140512
Ba	138	161		110	69		222	225
V	282	284		227	215		190	185
Cr	34	35		69	59		299	299

	2140530	2140530		2140546	2140546		2140568	2140563
Ba	51	56		162	166		53	50
V	446	442		288	285		390	394
Cr	65	57		104	106		29	28

	2140585	2140585		2140607	2140607		2140619	2140619
Ba	42	26		175	161		945	955
V	313	311		202	205		15	12
Cr	267	268		184	182		n.d	n.d.

Table A.6.6: Compositions of international standards BCR-1 and PCC-1 used to calculate element abundances from data for Rb, Sr, Y, Zr, and Nb. Abundances compiled by Dr. B.J. Fryer from Flanagan (1976) and recent data from spark source mass spectrometry at Australian National University by Drs. S.R. Taylor and S.M. McLennan (written communication, 1985).

ELEMENT	BCR-1	PCC-1
Rb	46.6	0.063
Sr	330	0.41
Y	34	0.05
Zr	195	7
Nb	13.5	0.09

Detection limits for this technique are quoted as 0.5 ppm for all elements. Because this is a new technique in the M.U.N. laboratory, a large number of duplicate analyses were carried out to provide estimates of the precision and confirmation of the detection limits for the elements. These duplicate analyses are tabulated in Table A6.7. For each determination, the error is expressed both as a percentage of the mean concentration and in ppm. Examination of the duplicates shows that Rb, Sr and Nb are generally repeatable at a precision of ±5% or 0.75 ppm (whichever is greater). This is true for Rb in more than 90% of duplicates and of Sr and Nb in more than 94% of the duplicates. Zr and Y show slightly less precision at low and intermediate concentrations and are precise to ±5% or 1.3 ppm in more than 92% of the analyses.

Analysis of international standards reported in Table 6.8 confirm the accuracy of the technique although slightly lower Y values than recommended reflect the slightly low values for BCR-1 used in the calibration..

iv) REE (INAA)

These analyses were carried out by J. Hertogen at Universiteit Leuven, Fysico-chemische geologie, Leuven, Belgium. Approximately 800 grams of whole rock powder were irradiated for 7 hours in the Thetis reactor, Ghent University, Belgium, in a thermal neutron flux of approximately 2×10^{12} neutrons $cm^{-1}sec^{-1}$. The gamma-ray intensities were measured in a large volume

Table A6.7: Duplicate analyses of Rb, Sr, Y, Zr and Nb by X-Ray fluorescence.

±(%) - difference in analyses expressed as a percentage of their mean
±(ppm) - 1/2 the difference in the analyses

2140452	Anal. 1	Anal. 2	±(%)	±(ppm)
Rb	6.3	6.5	1.56	0.1
Sr	37	37.4	0.54	0.2
Y	33.9	33.2	1.04	0.35
Zr	81.6	82.5	0.61	0.5
Nb	n.d.	n.d.		

2140473	Anal. 1	Anal. 2	±(%)	±(ppm)
Rb	2.6	0.99	44.85	0.805
Sr	22.4	19	8.21	1.7
Y	8.2	7.23	6.29	0.485
Zr	6.7	4.45	20.18	1.125
Nb	n.d.	n.d.		

2140480	Anal. 1	Anal. 2	±(%)	±(ppm)
Rb	1.6	n.d.		
Sr	55.8	52.7	2.86	1.55
Y	5.5	6.1	5.17	0.3
Zr	6.2	5.7	4.20	0.25
Nb	n.d.	n.d.		

2140539	Anal. 1	Anal. 2	±(%)	±(ppm)
Rb	43	43.5	0.58	0.25
Sr	68.9	69.7	0.58	0.4
Y	71.2	68.7	1.79	1.25
Zr	243	239.2	0.79	1.9
Nb	4.55	5.32	7.80	0.385

2140562	Anal. 1	Anal. 2	±(%)	±(ppm)
Rb	22	20.8	2.80	0.6
Sr	147.8	145.9	0.65	0.95
Y	20.9	23.1	5.00	1.1
Zr	52.8	53.1	0.28	0.15
Nb	0.85	1.71	33.59	0.43

2140571	Anal. 1	Anal. 2	±(%)	±(ppm)
Rb	18.9	18.9	0.00	0
Sr	135.6	133.1	0.93	1.25
Y	26.9	26.6	0.56	0.15
Zr	92.7	90	1.42	1.3
Nb	1.75	2.44	16.47	0.345

2140453	Anal. 1	Anal. 2	±(%)	±(ppm)
Rb	2.8	0.17	88.55	1.315
Sr	38.4	38.4	0.00	0
Y	31.1	31.5	0.64	0.2
Zr	90.3	85.4	2.79	2.45
Nb	n.d.	n.d.		

2140474	Anal. 1	Anal. 2	±(%)	±(ppm)
Rb	2.4	2	9.09	0.2
Sr	13.3	12	5.14	0.65
Y	8.7	7.2	9.43	0.75
Zr	5.6	4.2	14.29	0.7
Nb	n.d.	n.d.		

2140481	Anal. 1	Anal. 2	±(%)	±(ppm)
Rb	n.d.	3.24		
Sr	153.5	152.2	0.43	0.65
Y	28.3	26.8	2.72	0.75
Zr	94.5	94.2	0.16	0.15
Nb	6.71	6.7	0.07	0.005

2140544	Anal. 1	Anal. 2	±(%)	±(ppm)
Rb	n.d.	n.d.		
Sr	71.8	70.9	0.63	0.45
Y	29.8	31.2	2.30	0.7
Zr	79.3	79.7	0.25	0.2
Nb	1.45	2.9	33.33	0.725

2140563	Anal. 1	Anal. 2	±(%)	±(ppm)
Rb	4.8	0.34	86.77	2.23
Sr	144.1	135.1	3.22	4.5
Y	24.2	25.3	2.22	0.55
Zr	60.1	59.2	0.75	0.45
Nb	0.77	-2.67	55.23	0.95

2140574	Anal. 1	Anal. 2	±(%)	±(ppm)
Rb	43.4	43.2	0.23	0.1
Sr	36.4	36.1	0.41	0.15
Y	17.4	17.2	0.58	0.1
Zr	93.8	88.3	3.02	2.75
Nb	2.12	2.25	2.97	0.065

2140463	Anal. 1	Anal. 2	±(%)	±(ppm)
Rb	14.8	14	2.78	0.4
Sr	111.9	103.9	3.71	4
Y	16.6	13.7	9.57	1.45
Zr	63.2	61.5	1.36	0.85
Nb	2.18	2.8	12.45	0.31

2140475	Anal. 1	Anal. 2	±(%)	±(ppm)
Rb	14.6	14.4	0.69	0.1
Sr	40.1	37.6	3.22	1.25
Y	6.9	4.3	23.21	1.3
Zr	5.3	3.6	19.10	0.85
Nb	1.67	n.d.		

2140495	Anal. 1	Anal. 2	±(%)	±(ppm)
Rb	14.8	15.7	2.95	0.45
Sr	288.5	287.3	0.21	0.6
Y	15.2	14	4.11	0.6
Zr	78.1	79.1	0.64	0.5
Nb	8.2	7.9	1.86	0.15

2140558	Anal. 1	Anal. 2	±(%)	±(ppm)
Rb	8.2	6.7	10.07	0.75
Sr	165.8	163.7	0.64	1.05
Y	8.9	10.8	9.64	0.95
Zr	11.7	13.1	5.65	0.7
Nb	n.d.	n.d.		

Table A6.7 (continued)

2140567	Anal. 1	Anal. 2	±(%)	±(ppm)
Rb	12.4	11.5	3.77	0.45
Sr	264	262.8	0.23	0.6
Y	23.8	22.1	3.70	0.85
Zr	60.8	62	0.98	0.6
Nb	0.66	2.04	51.11	0.69

2140472	Anal. 1	Anal. 2	±(%)	±(ppm)
	1.4	1.28	4.48	0.06
	38.8	36.3	3.33	1.25
	6.7	5.3	11.67	0.7
	6.1	5	9.91	0.55
	0.93	1.41	20.51	0.24

2140579	Anal. 1	Anal. 2	±(%)	±(ppm)
Rb	50.4	52.9	2.42	1.25
Sr	53.9	52.8	1.03	0.55
Y	16.5	16	1.54	0.25
Zr	51.8	52.5	1.16	0.6
Nb	1.4	2.33	24.93	0.465

2140478	Anal. 1	Anal. 2	±(%)	±(ppm)
	1.4	n.d.		
	65.1	63.6	1.17	0.75
	4.5	5.9	13.46	0.7
	2.25	2.8	10.89	0.275
	n.d.	n.d.		

2140466	Anal. 1	Anal. 2	±(%)	±(ppm)
Rb	0.67	1.28	62.56	0.305
Sr	44.3	43	2.98	0.65
Y	39.9	37.1	7.27	1.4
Zr	43.8	41.3	5.88	1.25
Nb	n.d.	n.d.		

2140538	Anal. 1	Anal. 2	±(%)	±(ppm)
	21.7	21.8	0.23	0.05
	37.9	38.1	0.26	0.1
	44.8	42.6	2.52	1.1
	74.6	73.2	0.95	0.7
	n.d.	n.d.		

2140477	Anal. 1	Anal. 2	±(%)	±(ppm)
Rb	n.d.	n.d.		
Sr	31	29.9	3.61	0.55
Y	9.2	9.5	3.21	0.15
Zr	8.9	9.2	3.31	0.15
Nb	n.d.	n.d.		

2140561	Anal. 1	Anal. 2	±(%)	±(ppm)
	30.7	31.8	1.76	0.55
	123.3	127.1	1.52	1.9
	19.1	20.4	3.29	0.65
	51.9	53.6	1.61	0.85
	n.d.	1.71		

2140512	Anal. 1	Anal. 2	±(%)	±(ppm)
Rb	32.9	33.1	0.61	0.1
Sr	269.7	273.7	1.47	2
Y	20	19.3	3.56	0.35
Zr	93.6	94.5	0.96	0.45
Nb	5.44	5.42	0.37	0.01

2140570	Anal. 1	Anal. 2	±(%)	±(ppm)
	n.d.	1.24		
	171.8	166.5	1.57	2.65
	21.9	21.8	0.23	0.05
	62.7	60.3	1.95	1.2
	2.54	1.28	32.98	0.63

2140560	Anal. 1	Anal. 2	±(%)	±(ppm)
Rb	16.5	16.7	1.20	0.1
Sr	108.6	108.8	0.18	0.1
Y	31.5	29.7	5.88	0.9
Zr	83.3	82.7	0.72	0.3
Nb	1.14	1.59	32.97	0.225

2140584	Anal. 1	Anal. 2	±(%)	±(ppm)
	22.6	23.8	2.59	0.6
	93	92.8	0.11	0.1
	23.8	23.4	0.85	0.2
	58.8	58	0.68	0.4
	2.76	2.14	12.65	0.31

2140569	Anal. 1	Anal. 2	±(%)	±(ppm)
Rb	27.7	28.4	2.50	0.35
Sr	118.3	120.8	2.09	1.25
Y	17.3	17.3	0.00	0
Zr	43.7	46.1	5.35	1.2
Nb	n.d.	1.22		

2140587	Anal. 1	Anal. 2	±(%)	±(ppm)
	10.7	10.7	0.00	0
	141.5	142.9	0.49	0.7
	12.1	12.8	2.81	0.35
	26.1	27.7	2.97	0.8
	0.87	1.48	25.96	0.305

2140580	Anal. 1	Anal. 2	±(%)	±(ppm)
Rb	0.61	0.77	23.19	0.08
Sr	115.4	112.1	2.90	1.65
Y	22.8	21.4	6.33	0.7
Zr	50.6	49.7	1.79	0.45
Nb	1.33	1.01	27.35	0.16

2140592	Anal. 1	Anal. 2	±(%)	±(ppm)
	39.8	38.2	2.05	0.8
	40.8	40.8	0.00	0
	8.4	10.9	12.95	1.25
	27.8	28.5	1.24	0.35
	0.94	1.14	9.62	0.1

Table A6.7 (continued)

	2140503 Anal.1	Anal.2	±(%)	±(ppm)		2140503 Anal.1	Anal.2	±(%)	±(ppm)
Rb	28.8	27.3	2.67	0.75		28.8	27	3.23	0.9
Sr	94.4	91.9	1.34	1.25		94.4	91	1.83	1.7
Y	19	15.7	9.51	1.65		19	17.2	4.97	0.9
Zr	66.4	61	4.24	2.7		66.4	59.9	5.15	3.25
Nb	3.98	3.47	6.85	0.255		3.98	2.98	14.37	0.5

	2140503 Anal.1	Anal.2	±(%)	±(ppm)		2140566			
Rb	27.3	27	0.55	0.15		24	23.2	1.69	0.4
Sr	91.9	91	0.49	0.45		202.4	201.6	0.20	0.4
Y	15.7	17.2	4.56	0.75		20.1	20.7	1.47	0.3
Zr	61	59.9	0.91	0.55		52.4	53.4	0.95	0.5
Nb	3.47	2.98	7.60	0.245		n.d.	2.18		

Table A6.8: Analyses of standard materials for Rb, Sr, Y, Zr and Nb compared to with recommended values. Recommended values from B.J. Fryer (pers. comm. 1987) from literature and recent results of spark source spectrometry at Australian National University. DTS -1 is included as an indicator of zero.

	SY - 2 Measured	Accepted		G - 2 Measured	Accepted
Rb (ppm)	208	220	Rb (ppm)	158	170
Sr (ppm)	256	275	Sr (ppm)	455	480
Y (ppm)	118	130	Y (ppm)	5	?
Zr (ppm)	257	280	Zr (ppm)	289	300
Nb (ppm)	29	23	Nb (ppm)	11	13

	W - 1 Measured	Accepted		AGV - 1 Measured	Accepted
Rb (ppm)	22	21	Rb (ppm)	68	67
Sr (ppm)	180	190	Sr (ppm)	658	660
Y (ppm)	19	26	Y (ppm)	14	20
Zr (ppm)	86	95	Zr (ppm)	224	230
Nb (ppm)	7.5	9	Nb (ppm)	12.5	14.5

	BHVO - 1 Measured	Accepted		DTS - 1 Measured	Accepted
Rb (ppm)	10	10	Rb (ppm)	0.7	-
Sr (ppm)	378	396	Sr (ppm)	1	-
Y (ppm)	23	28	Y (ppm)	n.d.	-
Zr (ppm)	160	170	Zr (ppm)	0.5	-
Nb (ppm)	18	19.5	Nb (ppm)	n.d.	-

Ge(Li)-detector and a hyperpure Ge Low energy photon detector at Leuven University at intervals of 7 and 20-30 days after irradiation. Element concentrations are calculated relative to a secondary basalt standard which has been repeatedly calibrated against BCR-1. Details of the analytical procedure can be found in Hertogen and Gijbels (1971).

Analytical precision was monitored continuously by the analyst from counting statistics and the observed dispersion of results from different countings and/or different gamma rays. Errors were reported by Hertogen *et al.* (1985) and Rautenschlein *et al.* (1985) for samples run at about the same time as the present samples. They quoted the analyses as precise to better than 2% for Sc, Co, Sm and Eu; 6% for Hf, Tb and Yb and 12% for Ce and Lu. The errors for Nd, Ta and Th are quite large at low concentrations and may be greater than 20% for the most LREE-depleted samples.

Good agreement of an analysis of the international standard MRG-1 and recommended values of Abbey (1983) is illustrated in Figure A6.1. Likewise, good correspondance between INAA analyses of rock powders at Leuven and at Universite de Montreal are illustrated on this figure (from the unpublished data of Dr. D.F. Strong).

v) REE (X-Ray fluorescence)

An additional group of samples were analysed for REE using techniques modified after Robinson *et al.* (1986). These analyses were all done after the INAA analyses were in hand and were used to check conclusions based on the INAA data and to provide additional information in areas not adequately represented by the INAA data.

2.5 ml of Tm spike is weighed into a Ni crucible and evaporated to dryness, approximately 1 gram of sample powder is weighed into the crucible and 4 times the sample weight of sodium peroxide is added. This mixture is stirred and a thin layer of Na_2O_2 is sprinkled over the top.

The sample mixture is heated in a muffle furnace at 480°C. for 1 hour, the sinter cake placed in a beaker of 15 to 20 ml H_2O, the solution centrifuged and the liquid discarded. The
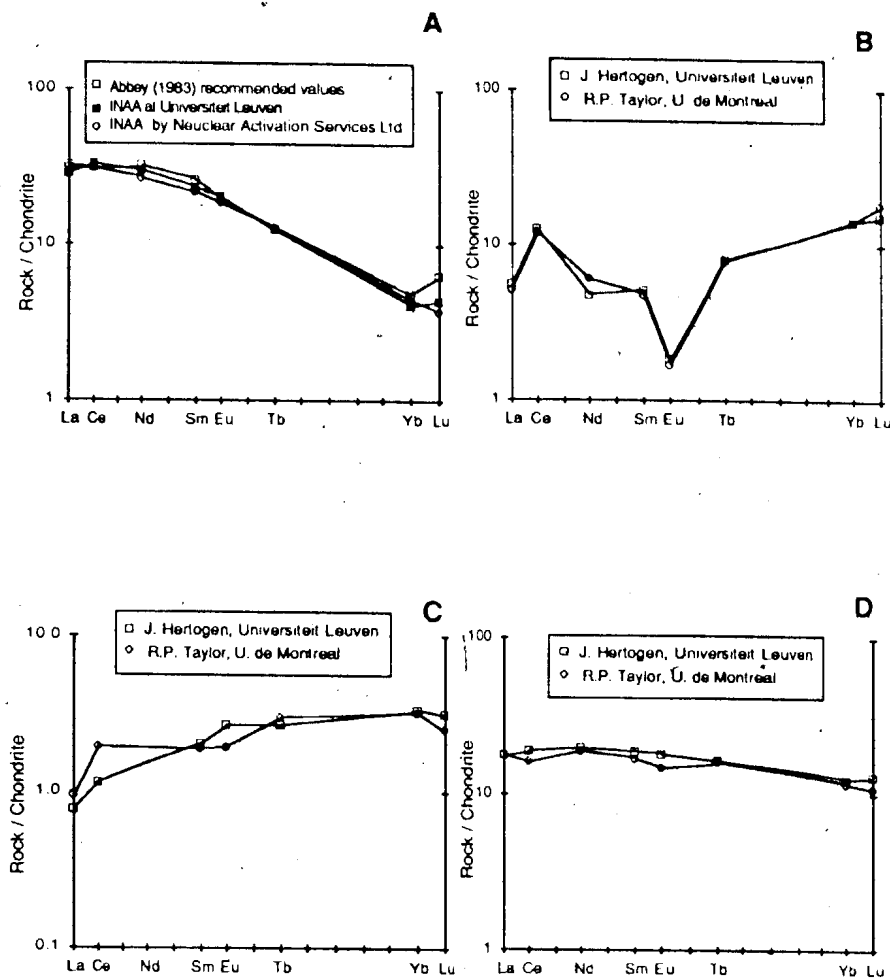
Figure A6.1: Comparison of INAA REE analyses with international standards and with results from other laboratories. In A, analyses from this study on international standard MRG-1, compared to Abbey's (1983) recommended values and 1983 INAA analyses at Nuclear Activation Services Ltd. (MacMaster, University). In B, C, D, replicate analyses of rock powders by INAA at Leuven and at University de Montreal (R.P. Taylor, analyst, 1983) show good agreement. Nuclear Activation Services and U.de Montreal data from Dr. D.F. Strong (unpublished).

Table A6.9: INAA analyses of rock samples and international standard MRG-1 from Universiteit Leuven, compared with other INAA analytical laboratories and recommended values of Abbey (1983).
Data courtesy of Dr. D.F. Strong (unpublished)

	Sample JP-28			Sample TC 362			Sample TC-351	
	HTGN	RPT		HTGN	RPT		HTGN	RPT
La	1.7	1.6	La	5.6	5.5	La	0.24	0.29
Ce	10.2	9.7	Ce	15.3	12.96	Ce	0.92	1.58
Nd	2.8	3.5	Nd	11.9	11.2	Nd	nd	2.44
Sm	0.97	0.9	Sm	3.61	3.23	Sm	0.39	0.36
Eu	0.13	0.12	Eu	1.31	1.06	Eu	0.19	0.14
Tb	0.38	0.37	Tb	0.77	0.75	Tb	0.13	0.14
Yb	2.96	2.99	Yb	2.64	2.44	Yb	0.6	0.67
Lu	0.49	0.58	Lu	0.42	0.35	Lu	0.1	0.09
Th	2.3	2.5	Th	0.47	0.4	Th	nd	nd
Ta	1.4	1.1	Ta	0.3	0.4	Ta	nd	nd

	Sample MUN-1			Sample MRG-1		
	HTGN	RPT		HTGN	NAS	Abbey (1983)
La	42.2	37.5	La	8.9	9.7	10?
Ce	82	70	Ce	26.5	25	25?
Nd	32.8	29.1	Nd	17.7	16	19?
Sm	6.4	5.6	Sm	4.45	4.14	5?
Eu	0.69	0.74	Eu	1.45	1.32	1.4?
Tb	0.89	0.67	Tb	0.58	0.6	1?
Yb	3.2	2.5	Yb	0.84	0.92	1?
Lu	0.48	0.49	Lu	0.14	0.12	0.2?
Th	34.9	29.4	Th	0.91	0.7	0.1?
Ta	11.7	3.1	Ta	0.26		

HTGN - INAA analysis at Universiteit Leuven, J. Hertogen, analyst
RTP - INAA analysis at Universite de Montreal, R.P. Taylor, analyst
NAS - INAA analysis by Nuclear Activation Services Ltd., MacMaster University

residue is rinsed with H_2O, centrifuged twice and dissolved in 40 to 60 ml of 1N HCl.

The REE are then concentrated by standard ion exchange techniques in two stages. In the first stage, the samples are loaded on 30 cm quartz columns with 15 cm of Amberlite CG-120 chromatographic grade ion exchange resin and the major elements eluted with 40 ml of 2.5N HCl. The REE and Ba are then collected with 120 ml of 6N HCl, the solution evaporated to dryness, and the residue converted to nitrate. Ba is then removed in 12 cm pyrex columns using 3 cm of ion exchange resin. The Ba is eluted with 26 ml of 1.5N HNO_3 and the REE collected with 15 ml of 8N HNO_3.

After evaporation, the REE are transferred to ion exchange paper for analysis by thin film X-Ray fluorescence.

Figure A6.2 shows replicate analyses of four samples, representing the full range of REE concentrations in the Wild Bight Group, by XRF and INAA. In samples 2140532, 2140498 and 2140484, the duplicates are mostly within ±10% although there is a tendency for the HREE (particularly Yb) to fall off in samples 2140532 and 2140484. Because of this problem in the HREE, values for Yb by XRF were not used in the thesis. Plotting La to Er in all cases produces a pattern which closely parallels the INAA pattern and is generally within ±10% in absolute abundances.

The correspondence for sample 2140476 is not as good, hardly surprising considering the low abundances. Although the precision is not good at these levels, and Ce, Eu and Yb are not useable because of interferences, the data do suggest that an approximation to the true pattern can be achieved by plotting La, Nd, Sm, Dy and Er. This pattern cannot be used quantitatively but should provide an approximation to the shape of the true pattern and a rough idea of the true abundances.
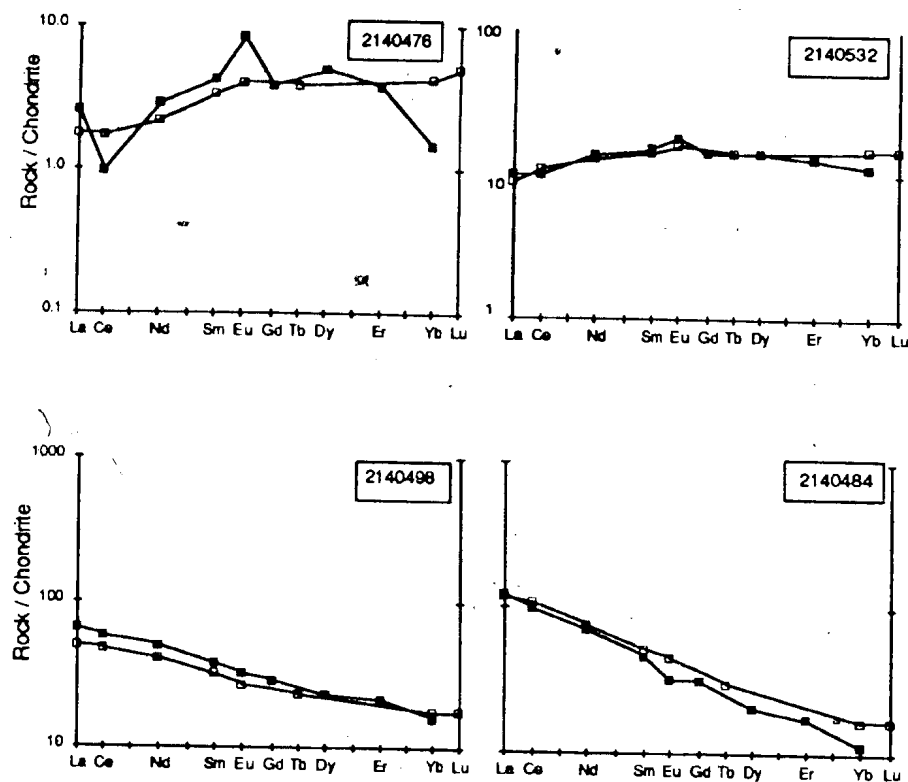
Figure A6.2: Comparison of samples analysed by INAA at
Universiteit Leuven, Leuven, Belgium (open squares) and by
X-Ray fluorescence at M.U.N. (closed squares).

APPENDIX 7

PRIMITIVE MANTLE NORMALIZING VALUES USED IN EXTENDED REE PLOTS

Normalizing values to primitive mantle were provided to the writer by Dr. G.A. Jenner. These are values that are in use at Max Planck Institutt fuer Chemie. They represent the current best estimate for primitive mantle composition at that institute but have not been published to date. They are generally in the range of 2 x chondritic but have been adjusted for some elements to bring them all into agreement. Normalizing to these values gives extended REE patterns that are essentially parallel to those resulting from chondrite normalization.

ELEMENT	PRIMITIVE MANTLE
La	0.63
Ce	1.59
Nd	1.21
Sm	0.399
Eu	0.15
Tb	0.0974
Yb	0.432
Lu	0.066
Ti	1134
Y	3.9
Nb	0.65
Zr	9.8
Hf	0.28
Ta	0.04
Th	0.088

APPENDIX 8

DISCRIMINANT FUNCTION ANALYSIS: DESCRIPTION AND RESULTS

Discriminant function analysis is the technique most commonly used to identify variables that are important in distinguishing among known groups, the cases of which have a number of known independent variables. It is also useful in predicting group membership for other cases, of unknown group membership. The procedure involves calculating linear combinations of the independent variables to serve as the basis for classifying cases into one of the known groups.

In the present study, functions were computed for the mafic volcanic rocks, which were grouped according to the geochemical criteria set out in Chapter 3. Using log-transformed data for the variables TiO_2, P_2O_5, Y, Zr, Nb and V, and sample groups IAØ, IAI, NAI, NAT and NAE defined in Chapter 3, four functions were calculated using the Statistical Package for the Social Sciences modified for personal computer use (SPSS-PC) which together explain 100% of the variance between groups. For statistical rigour, there should be a large number of cases in each group compared to the number of variables. Because this criterion does not hold for the Wild Bight Group samples, calculated probabilities may overestimate the actual probabilites associated with classifying the samples. However, two factors lend confidence in the results for the Wild Bight Group samples. Firstly, carrying out the calculation using only three variables (TiO_2, Zr and Y) produces a similar separation of the groups at similar probabilities. Secondly, the calculated functions successfully classify more than 95% of the known samples (Table A8.1, see also discussion in Section 3.3.4) suggesting a high degree of reliability in the results.

Discriminant scores were calculated for each function for each sample (Table A8.1) and each sample was assigned a statistical probability of belonging to any particular group. The highest and second highest probabilities for each sample are listed in Table A8.1.

The results have been used in two ways in this thesis. First, they provide a test of the statistical validity of the empirically-derived grouping by assessing the quality of separation of the groups and the success rate of sample classification using the derived functions. Secondly, they have been used to assign the mafic subvolcanic rocks to the appropriate geochemical groups.

Table A8.1: Discriminant scores for mafic volcanic and subvolcanic rocks

SAMPLE NO.	ACTUAL GROUP	HIGHEST PROBABILITY GROUP	PROBABILITY	SECOND HIGHEST PROBABILITY GROUP	PROBABILITY	DISCRIMINANT SCORES			
						FUNCTION 1	FUNCTION 2	FUNCTION 3	FUNCTION 4
Mafic Volcanic Rocks									
2140432	2	3	0.7591	2	0.2341	1.2363	0.1715	-0.7320	0.1830
2140456	1	1	1.0000	2	0.0000	-6.0538	0.4686	-1.8318	3.5827
2140458	1	1	1.0000	2	0.0000	-8.3497	1.0633	1.5347	0.0502
2140460	1	1	1.0000	2	0.0000	-7.0368	-0.4019	0.6662	-1.1116
2140462	1	1	1.0000	2	0.0000	-9.1234	1.6490	-3.9043	3.7528
2140463	2	2	0.9967	3	0.0033	0.4605	-2.7349	-0.0869	-2.0750
2140464	2	2	0.9935	3	0.0065	-0.0166	-1.8915	-1.8915	-1.1557
2140467	2	2	0.9577	3	0.0382	2.5089	-1.8065	0.2254	0.5949
2140468	2	2	0.9966	3	0.0033	2.2274	-2.5304	-0.3777	0.6468
2140470	2	2	0.9999	3	0.0001	-0.4110	-2.3235	2.4721	1.6617
2140471	1	1	1.0000	2	0.0000	-6.8529	0.8551	0.7011	-0.8446
2140472	1	1	1.0000	2	0.0000	-8.7058	3.7478	0.7747	0.7059
2140473	1	1	1.0000	2	0.0000	-8.1663	2.2578	-0.6075	-0.4217
2140474	1	1	1.0000	2	0.0000	-8.8691	1.8016	-0.5579	-0.0162
2140475	1	1	1.0000	2	0.0000	-9.6862	0.7728	-0.3720	-1.4304
2140476	1	1	1.0000	2	0.0000	1.0000	1.0419	-0.4351	-1.2584
2140477	1	1	1.0000	2	0.0000	-6.2837	-0.2371	0.4450	0.6161
2140478	1	1	1.0000	2	0.0000	-9.0707	3.2035	-1.6845	-1.2180
2140480	1	1	1.0000	2	0.0000	-7.9576	0.5640	0.1743	-1.0657
2140483	5	5	1.0000	4	0.0000	8.0438	2.1968	-1.2042	0.0885
2140484	5	5	1.0000	4	0.0000	8.2718	2.8055	-0.4587	0.1579
2140492	1	1	1.0000	2	0.0000	-7.6034	0.1150	-1.2333	-0.6419
2140497	4	4	0.9835	3	-0.1600	4.0110	0.2761	1.3202	1.6605
2140498	4	4	0.9949	3	0.0051	3.9853	0.8050	2.6278	1.1942
2140503	3	3	0.9504	2	0.0474	1.6159	0.1638	-1.0822	-1.5752
2140505	3	3	0.6898	4	0.3100	2.2316	1.7388	1.2004	-0.9262
2140506	3	4	0.5668	3	0.4323	3.2851	0.8742	0.7047	-0.4759
2140509	5	5	1.0000	4	0.0000	8.8418	2.2190	-2.1558	1.1004
2140510	3	3	0.7061	4	0.2938	2.6915	2.0833	0.4868	-1.1636
2140511	3	3	0.9314	2	0.0620	2.0074	0.0678	-1.1103	-1.0620
2140526	1	1	1.0000	2	0.0000	-8.0068	0.3833	1.7994	0.0666
2140530	2	2	0.9987	3	0.0013	-2.5584	-0.8395	0.0962	0.1793
2140531	2	2	0.9975	3	0.0025	-0.0012	-1.7850	-0.5001	0.1154
2140533	2	2	0.9995	3	0.0005	0.4595	-2.5014	1.1141	0.5769
2140534	2	2	1.0000	3	0.0000	-0.3294	-3.7590	0.2151	1.0600
2140540	2	2	0.9983	3	0.0017	0.6501	-1.9276	0.8941	1.1691

Table A8.1: (Continued)

SAMPLE NO.	ACTUAL GROUP	HIGHEST PROBABILITY GROUP	PROBABILITY	SECOND HIGHEST PROBABILITY GROUP	PROBABILITY	DISCRIMINANT SCORES			
						FUNCTION 1	FUNCTION 2	FUNCTION 3	FUNCTION 4
Mafic Volcanic Rocks									
2140541	2	2	0.9999	3	0.0001	-0.2761	-2.7150	0.6381	0.5171
2140543	2	2	0.9925	3	0.0074	0.1191	-1.2755	-0.2190	0.5876
2140544	2	2	0.8941	3	0.1005	1.4352	-0.8515	0.3047	0.8005
2140545	4	4	0.9464	3	0.0536	4.1160	1.3357	0.9936	0.0553
2140546	4	4	0.8480	3	0.1529	4.2001	1.3942	0.3698	-0.5369
2140547	4	4	0.9841	3	-0.1590	4.1867	1.4246	1.1725	0.8205
2140548	4	4	0.9271	3	-0.7290	3.1530	2.0070	1.617~	0.1272
2140549	4	4	0.7492	3	0.2507	3.2237	1.7927	0.6709	-0.2396
2140550	4	4	0.8007	3	0.1993	3.5489	2.3800	0.4849	-0.6473
2140551	4	4	0.9988	3	0.0012	5.2837	2.7412	1.9372	0.0366
2140553	2	2	0.9800	3	0.0184	2.1434	-1.8306	0.3179	0.8249
2140554	2	2	0.9996	3	0.0004	0.9576	-2.9345	-0.4443	0.0189
2140555	2	2	0.9597	3	0.0400	3.2467	-2.5803	-1.3741	-0.8589
2140750	2	2	0.9885	3	0.0114	1.5021	-1.9427	0.1106	0.1707
2140751	2	2	0.9975	3	0.0025	1.0360	-2.3098	-0.3893	-0.0013
2140752	2	2	0.9971	3	0.0029	1.2449	-2.4875	-1.0397	-0.4558
2140753	2	2	0.9544	3	0.0453	1.6101	-1.6179	-0.5093	-0.3213
2140754	2	2	0.9989	3	0.0011	0.9313	-2.6285	-0.2978	-0.1571
2140755	2	2	0.9995	3	0.0005	-0.6224	-2.5174	-0.4100	-1.0136
2140756	2	2	0.9411	3	0.0568	2.1127	-1.5444	-0.1262	0.3343
2140758	2	2	0.8228	3	0.1769	0.1281	-1.0207	-0.9647	-0.6927
2140761	4	4	0.8640	3	0.1360	3.7829	2.1005	0.5868	-0.4903
2140762	4	4	0.5585	3	0.4398	2.9024	0.9984	0.6292	0.0160
2140763	5	5	1.0000	4	0.0000	9.2412	1.9367	-3.2482	-0.1579
2140764	4	4	0.8161	3	0.1837	2.9558	1.5144	1.0008	0.3589
2140765	1	1	1.0000	2	0.0000	-8.1852	1.1487	1.4842	1.3548
2140767	3	3	0.7657	2	0.2239	1.1917	-0.0061	0.3149	-0.5951
2140768	5	5	1.0000	4	0.0000	9.0554	3.9948	-1.4435	-0.1049
2140771	2	2	0.9908	3	0.0092	0.5607	-1.7078	-0.2656	-0.2355
2140772	2	2	0.9997	3	0.0003	0.6273	-2.9675	-0.5420	-0.3052
2140773	2	4	0.6555	3	0.3441	2.5905	1.7231	0.7105	0.2623
2140774	2	2	0.9934	3	0.0066	0.9827	-2.1410	-0.6370	-0.5954

SAMPLE NO.	ACTUAL GROUP	HIGHEST PROBABILITY GROUP	PROBABILITY	SECOND HIGHEST PROBABILITY GROUP	PROBABILITY	DISCRIMINANT SCORES			
Mafic Volcanic Rocks						FUNCTION 1	FUNCTION 2	FUNCTION 3	FUNCTION 4
2140450		5	0.6057	4	0.3941	6.5360	2.9098	0.3899	0.6174
2140454		5	0.9984	4	0.0016	7.5345	3.7209	0.3043	0.6159
2140457		4	0.8253	5	0.1747	6.3975	5.3157	1.7586	0.1908
2140461		1	0.9997	2	0.0003	-4.0968	0.7275	0.6112	1.4191
2140465		1	1.0000	2	0.0000	-10.4446	3.5929	1.4550	1.1208
2140481		4	0.6977	3	0.2702	1.8463	0.7549	1.4035	1.5625
2140482		4	0.9420	3	0.0580	3.5979	1.1962	1.5020	-0.1125
2140485		4	0.9966	3	0.0014	4.7046	3.2627	2.3399	-0.0028
2140486		5	0.9620	4	0.0380	7.0784	3.8542	0.6965	0.3348
2140489		4	0.8909	5	0.1091	6.5343	4.7597	1.9837	0.5748
2140491		3	0.6748	2	0.3110	2.0847	-0.8470	0.6643	-1.2232
2140495		3	0.9505	4	0.0344	1.7868	0.7677	-0.1010	-0.6999
2140496		2	0.9979	3	0.0021	1.2279	-2.3296	0.0789	0.4539
2140501		4	0.9798	5	0.0197	5.9762	3.5721	1.1982	-0.1949
2140502		4	0.9983	3	0.0017	3.8595	5.0799	3.2375	-0.9417
2140508		4	0.8519	3	0.1470	5.1990	-0.0422	-0.3434	-0.3405
2140512		2	0.9989	3	0.0011	1.1299	-2.7386	-0.6367	-0.2782

APPENDIX 9

DISTRIBUTION COEFFICIENTS USED IN PETROGENETIC CALCULATIONS

Two sets of distribution coefficients were used for fractional crystallization and partial melting calculations in Chapters 3 and 4. Both have been compiled from the literature by Dr. G.A. Jenner. The coefficients used for fractional crystallization calculations are identified on the tables in which the calculations are reported. All partial melting calculations are done using the 'primitive basalt' coefficients. Mineral abbreviations as for Appendix 1.

PRIMITIVE BASALT

Element	Distribution Coefficients				
	Ol	Opx	Cpx	Pl	Ga
La	0.0005	0.0005	0.0200	0.1800	0.0010
Ce	0.0008	0.0009	0.0400	0.1200	0.0033
Nd	0.0013	0.0019	0.0900	0.0810	0.0184
Sm	0.0019	0.0028	0.1400	0.0670	0.0823
Eu	0.0019	0.0036	0.1600	0.3400	0.1333
Er	0.0022	0.1300	0.2000	0.0630	1.6000
Yb	0.0040	0.0286	0.2000	0.0670	4.0000
Ti	0.0020	0.0040	0.2000	0.0450	0.2000
Y	0.0050	0.0300	0.2000	0.0250	2.0000
Nb	0.0004	0.0004	0.0150	0.0100	0.0150
Zr	0.0020	0.0030	0.1200	0.0100	0.0450
V	0.0300	0.5000	1.5000	0.0800	0.2700
Cr	2.1000	10.0000	8.4000	0.400	0.1000
Ni	14.0000	4.0000	3.0000	0.0400	0.8000

FRACTIONATED BASALT

Element	Distribution Coefficients				
	Ol	Opx	Cpx	Pl	Ga
La	0.0089	0.0260	0.2880	0.1800	0.1210
Ce	0.0090	0.0325	0.3030	0.1200	0.1440
Nd	0.0100	0.0508	0.3790	0.0810	0.2320
Sm	0.0105	0.0790	0.4760	0.0670	0.5410
Eu	0.0110	0.0990	0.3540	0.3400	0.6230
Er	0.0190	0.3550	0.7060	0.0630	4.2400
Yb	0.0230	0.4700	0.7190	0.0670	5.7300
Ti	0.0100	0.1000	0.5000	0.0450	0.6900
Y	0.0200	0.4000	0.8000	0.0250	5.0000
Nb	0.0080	0.0150	0.2160	0.0100	0.1000
Zr	0.0100	0.0200	0.4200	0.0100	0.6000
V	0.0300	0.5000	1.0000	0.0800	0.2700
Cr	3.1000	10.0000	20.0000	0.0400	0.8000
Ni	19.0000	5.0000	4.4000	0.0400	0.8000

APPENDIX 10

Nd ISOTOPIC ANALYTICAL PROCEDURES AND DATA RELATING TO ACCURACY AND PRECISION OF Nd ISOTOPE ANALYSES

Chemical Procedures

Chemical separation of the REE was carried out under controlled, clean lab, conditions, at Max Planck Institutt fuer Chemie on samples analysed there (see Table A10.1) and at Memorial University of Newfoundland for all remaining samples. Chemical procedures at the former have recently been described by White and Patchett (1984). Procedures at the latter are described below.

Reagents were doubly distilled in quartz in a two-bottle teflon still. Approximately 0.15 to 0.35 g of sample (depending on Nd abundance) was dissolved in 2 ml HF and 2 ml 8N HNO_3 in closed teflon bombs. Following dissolution, samples were evaporated to dryness, taken up in 6N HCl, and split for NdIC and Nd and Sm ID analyses. Approximately 1/3 was taken off for ID analysis. Twenty μl of a mixed ^{150}Nd, ^{147}Sm spike (M.U.N. spike #1) was added to samples to be analysed by ID. The isotopic composition of the spike has been determined by Dr. B.J. Fryer at M.U.N.

The REE were then separated using standard ion exchange procedures in three stages as follows:

i) Stage 1: To separate the major elements from Ba and the REE, samples were passed in HCl through 18 cm of Amberlite CG-120 chromatographic grade ion exchange resin in 30 cm quartz columns. Major elements were eluted using approximately 40 ml of 2.5N HCl. Following this, the REE and Ba were collected in approximately 60 ml of 6N HCl in teflon beakers. Columns were cleaned with 6N HCl, backwashed in H_2O and re-equilibrated with 2.5N HCl.

ii) Stage 2: To separate Ba from the REE, samples were passed in HNO_3 through 7.5 cm of resin as above in 12 cm pyrex columns. Samples were loaded and Ba eluted in approximately 28

Table A10.1 Analytical history for Nd IC and Sm/Nd analyses.

Sample No.	ND IC analysis	Sm/Nd analysis
2140453	G.S.C.	G.S.C. (ID)
2140454	M.U.N.	G.S.C. (ID)
2140456	G.S.C.	G.S.C. (ID)
2140457	G.S.C.	G.S.C. (ID)
2140458	G.S.C.	G.S.C. (ID)
2140463	G.S.C.	M.U.N. (ICP-MS)
2140465	G.S.C.	G.S.C. (ID)
2140467	Max Planck	Max Planck (ID)
2140473	G.S.C.	G.S.C. (ID)
2140476	Max Planck	Max Planck (ID)
2140481	M.U.N.	G.S.C. (ID)
2140483	G.S.C.	G.S.C. (ID)
2140491	G.S.C.	G.S.C. (ID)
2140492	Max Planck	Max Planck (ID)
2140496	M.U.N.	G.S.C. (ID)
2140497	Max Planck	Max Planck (ID)
2140502	G.S.C.	G.S.C. (ID)
2140503	G.S.C.	G.S.C. (ID)
2140506	G.S.C.	G.S.C. (ID)
2140509	M.U.N.	G.S.C. (ID)
2140511	Max Planck	Max Planck (ID)
2140512	G.S.C.	G.S.C. (ID)
2140526	G.S.C.	M.U.N. (ICP-MS)
2140532	Max Planck	Max Planck (ID)
2140538	G.S.C.	M.U.N. (ICP-MS)
2140544	G.S.C.	M.U.N. (ICP-MS)
2140546	Max Planck	Max Planck (ID)
2140549	G.S.C.	G.S.C. (ID)
2140553	Max Planck	Max Planck (ID)
2140756	G.S.C.	G.S.C. (ID)
2140762	G.S.C.	G.S.C. (ID)
2140763	G.S.C.	G.S.C. (ID)
2140773	G.S.C.	M.U.N. (ICP-MS)
2140774	G.S.C.	G.S.C. (ID)

Max-Planck - samples run on a Finnigan-MAT, multi-collector mass spectrometer analyst, G.A. Jenner.
G.S.C. - samples run on a Finnigan-MAT, multi-collector mass spectrometer analyst, H.S. Swinden
M.U.N. - samples run on a VG MM-30 single collector mass spectrometer. analyst, H.S. Swinden
ID - Isotope dilution
ICP-MS - inductively coupled plasma mass spectrometry

ml of 1.5N HNO_3. The REE were then collected with 12 ml of 8N HNO_3 in teflon beakers.

Columns were cleaned in 8N HNO_3, backwashed in H_2O and re-equilibrated in 1.5N HNO_3.

Stage 3: Rare earth fractions were further separated using 10 cm of teflon powder, coated with di-2-ethylhexyl orthophosphoric acid in 12 cm quartz columns. Following collection after stage 2, samples were dried, dissolved in 4 ml 8N HNO_3 and 2 drops of $HClO_4$ to destroy organic material, and converted to chlorides.

For Nd IC samples, the samples were loaded and the REE lighter than Nd eluted in 5.5 ml 0.15 ml and 2 to 3 ml 0.18N HCl. Nd was then collected in 2 to 4 ml of 0.18N HCl and 3 to 5 ml of 0.30N HCl in teflon beakers, dried and stored in dilute HCl.

For Nd ID samples, the samples were loaded in 0.15N HCl, and the REE's lighter than Nd eluted in 3 ml of 0.18N HCl. Nd was then collected with 6 ml of 0.25N HCl and Sm with 5 ml of 0.50N HCl.

Mass Spectrometry

Samples were analysed on three mass spectrometers as detailed in Table A10.1.

At Max Planck Institutt fuer Chemie and the Geological Survey of Canada (G.S.C.), measurements were made on a Finnigan-MAT 261 mass spectrometer. The analyses at the former were done first, before the chemical procedures were developed in the M.U.N. laboratory. A range of samples was analysed based on preliminary geochemical interpretations so as to get an idea of the range of values present and allow a more informed decision as to which samples to analyse subsequently.

After Nd and Sm separations were begun at M.U.N., several of these samples were run on the MM 30 mass spectrometer at M.U.N. It quickly became apparent that this instrument could provide sufficiently precise determinations of the NdIC only on the most Nd-rich samples (e.g. those from the NAT and NAE groups). Running times for these samples were on the order of 12 to 14 hours per sample. Sample loads of less than approximately 500 ng of Nd would generally

not run long enough to provide a precise determination. Because more than half of the samples from the Wild Bight Group would have been at or below this limit on the MM-30, work was discontinued on this instrument and the remaining analyses (as well as all Nd and Sm separates for isotope dilution) were carried out on the MAT 261 multi-collector machine at the G.S.C. The opportunity to do this and much assistance in carrying out the analyses was kindly provided by O. van Breeman, C. Roddick and D. Loveridge of the G.S.C. Isotope Laboratory.

Analytical procedures at Max Planck are detailed by White and Patchett (1985) and were carried out by Dr. G.A. Jenner.

At the Geological Survey of Canada, Nd and Sm were loaded with H_3PO_4 on double Re filaments and measured as metal in multi-collector static mode. Backgrounds and interfering species were measured between blocks of 12 scans and baseline values after every third block. Typically, 80 to 120 ratios of Nd were collected for Nd IC and 70 to 100 ratios for Nd and Sm ID to achieve adequate precision. During Nd IC analyses, $^{150}Nd/^{144}Nd$ was also measured as a monitor of data quality. For Nd ID measurements, the $^{150}Nd/^{144}Nd$ ratio was measured and normalized to $^{146}Nd/^{144}Nd = 0.7219$. For Sm ID measurements, $^{152}Sm/^{149}Sm$ was measured and normalized to the first $^{147}Sm/^{149}Sm$ in the run.

At Memorial University of Newfoundland, Nd isotopic ratios were measured on a VG Micromass-30, single collector mass spectrometer. Samples were loaded in dilute HCl and H_3PO_4 on Re triple filaments. Backgrounds and interfering species were measured between blocks of 10 scans. Typically, 1200 to 1800 ratios of Nd were collected to achieve the desired precision. During Nd IC analyses, $^{150}Nd/^{144}Nd$ was also measured as a monitor of data quality.

Analytical accuracy was monitored with the La Jolla standard and data corrected to $^{143}Nd/^{144}Nd$(La Jolla) = 0.51185. A further check was made by analysing the BCR-1 international standard, for which accepted $^{143}Nd/^{144}Nd$ ratio is 0.51265.

White and Patchett (1984) gave analytical data for multiple analyses of La Jolla during 1982-83, shortly before the present analyses were done there. Little change was recorded in

later analyses done during the time of the present analyses (G.A. Jenner, pers. comm., 1987).
The values cluster at 0.51185 within analytical error (0.511847±21) and analyses of BCR-1 at this
laboratory reported by White and Patchett (1984) and Rautenschlein *et al.* (1985) are
$^{143}Nd/^{144}Nd = 0.512647±22$ and 0.512653±16 respectively. These demand no further
correction to the present data.

Repeated measurement of the $^{143}Nd/^{144}Nd$ ratio of the La Jolla standard at M.U.N.
during the time that these measurements were done are shown in Figure A10.1A. They cluster in
the range of 0.51185 within analytical error (0.511859±29 where the uncertainty is twice the
standard deviation of the mean) and demand no further correction of the present data.

Repeated measurements of the $^{143}Nd/^{144}Nd$ ratio on the La Jolla standard at the
Geological Survey of Canada during the time of the present measurements are plotted on Figure
A10.1B. At 0.511828±14, they are generally lower than the accepted value for La Jolla. A similar
result was obtained from measurements of BCR-1 (two measurements, $^{143}Nd/^{144}Nd =$
0.512613±11 and 0.512610±13 respectively). Accordingly, $^{143}Nd/^{144}Nd$ ratios measured on
this instrument were standardized by addition of +0.00003.

Analytical precision is reported in the above descriptions and in Table 4.1 as twice the
standard error on the mean, calculated on in-run statistics. This accurately estimates the
instrumental precision of each analysis but may overestimate the overall precision considering
imprecisions introduced during laboratory procedures and instrumental variation with time.
Duplicate analyses of 8 samples are reported in Table A10.2. Two of these are samples prepared
from separate splits of powder from the same sample. The others are replicate analyses of
different splits of the same Nd concentrate. It is clear that for very clean runs, where the standard
error is very low, this statistic may underestimate the true precision of the analysis. In all duplicates
analysed, the worst analytical precision is ±11 and most are better than this. In the use of analytical
data in the text, therefore, analytical precision is conservatively reported to be, at best, ±15 and
this is considered to more than account for imprecision above and beyond that introduced by the
instrumental analysis.
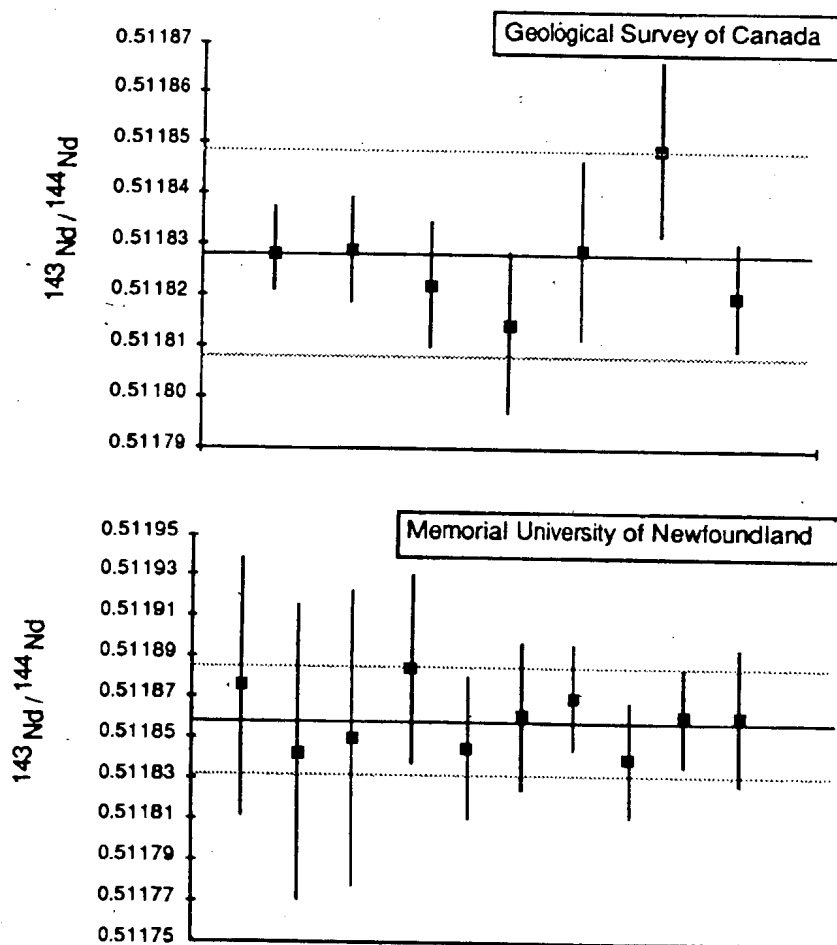
Figure A10.1: Results for the La Jolla Nd standard run at the Geological Survey of Canada and Memorial University of Newfoundland during the periods that analyses for this study were carried out. The former are multi-collector data, the latter single collector data, fractionation corrected to 146Nd / 144Nd = 0.7219. Error bars are twice the standard error on the mean for individual runs. Mean indicated by solid line and 2 sigma for the population by dotted lines.

Table A10.2: Duplicate Nd isotopic analyses. Asterisk indicates samples prepared separately from powder. Others are duplicate analyses of separate aliquots of the same Nd concentrate. Quoted analytical uncertainties are twice the standard error on the mean based on in-run statistics

Sample No.	Analysis 1	Analysis 2	Difference
2140456*	0.512942 ±13	0.512925 ±15	0.000017
2140544*	0.512907 ±11	0.512928 ±11	0.000021
2140491	0.512718 ±7	0.512740 ±7	0.000022
2140483	0.512737 ±3	0.512728 ±7	0.000009
2140571	0.512425 ±9	0.512419 ±10	0.000006
2140506	0.512813 ±6	0.512795 ±8	0.000018
2140512	0.512477 ±9	0.512475 ±10	0.000002
2140756	0.512520 ±8	0.512537 ±12	0.000017

Nd and Sm blanks processed in the M.U.N. clean lab at the same time as the present samples are reported in Table A10.3. All are negligible with respect to the amounts in the samples during analysis.

Sm/Nd ratios for most samples were measured by isotope dilution. Nd and Sm separates were prepared from spiked aliquots of the samples dissolved for Nd IC analysis and concentrations of Nd and Sm were calculated from measured $^{150}Nd/^{144}Nd$ and $^{152}Sm/^{149}Sm$ ratios respectively. Analytical errors in Sm/Nd are too small to be represented by error bars on Figures 4.2 and 4.3 and recalculation of epsilon$_{Nd}$ for all samples based on maximum analytical errors produced no change in the calculated epsilon$_{Nd}$. For six samples, the Sm/Nd ratio was measured by ICP-MS at Memorial University of Newfoundland. Analytical uncertainty quoted by the analyst based on count statistics and repeated measurement of standard materials is ±2% for concentrations above 5 x chondritic although errors may be much higher near the detection limits. These errors are large enough to be shown on Figures 4.2 and 4.3 and are represented by horizontal error bars. As a check on accuracy and precision, 6 samples were measured for which ID data are also available. These are reported in Table A10.4 and are consistent with quoted accuracy. Note that the most depleted samples have uncertainties in the ±5% range. This is the error bar used for depleted unknown sample 2140526 and the uncertainty in epsilon$_{Nd}$ is calculated from this error.

Table A10.3: Analyses of Nd and Sm blanks prepared at the same time as the whole rocks for Nd isotope analysis reported in Chapter 4.

Sample No.	total Nd (picograms)	total Sm (picograms)
BJF-BI-10	230	107
HSS-BI-1	97	64

The blanks were overspiked which particularly affects the precision of the Sm results. The reported absolute values for Sm should, therefore, be regarded as approximate. Irrespective of this, total Nd and Sm in the blanks is negligible compared to amounts analysed in the whole rock powders.

Table A10.4: Comparison of analyses of Sm / Nd ratios by isotope dilution and ICP-MS

Sample. No.	Nd (ppm)	147Sm / 144Nd	
		ID	ICP-MS
2140457	31.1	0.132	0.136
2140467	18.8	0.151	0.150
2140473	0.9	0.242	0.265
2140476	1.3	0.266	0.272
2140503	7.4	0.184	0.192
2140512	12.4	0.151	0.151

RE DAME BAY

Leading Tickles

Leading
Tickles
South

SEAL BAY
HEAD

VC

SBH
80

WILD
BIGHT

BB

VC

49

VC

VC

76

GHp

36

GHp

VC

LOCKPORT

Glovers
Hbr

60

LOCKS
HBR

GH

VC

VC

68

G

50

65

NOTRE DAME BAY

ISLAND Jim's Cv.

Card's Hbr.

SEAL BAY HEAD

VC

SBH PD

WILD BIGHT

G

G E R

BAY

LITTLE CV.

G)

VC

36

LOCKPORT

LOCKS HBR

CH.

7

68

50

G

NEW
BAY

Leading Tickles

SA

Leading
Tickles
South

VC

WILD

BIGHT

NB

VC

81

65

VC

70

49
M

BH

VC

GHp

76

GHp

VC

b
T

VC

Glovers
Hbr

60

85

GHry

VC

VC

ARM

OSMONTON

65

SA

BADGER

BAY

Geological map of the Seal Bay area showing various rock units and structural features including the Winterhouse Cove Fault, Osmonton Arm Fault, and Seal Bay Brook.

Map labels (as they appear on the figure):

54

35

G

PTL

VC

64

SEAL BAY BROOK FAULT

VC

VC

85

OP

SBB

SBB

VC

VC

SHp

SHr

BLL

PT
LEAMINGTON

49

49

VC

VC

BLL

SA

BIG
LEWIS
LAKE

FROZEN OCEAN LAKE FAULT

PHH

LEGEND

JURASSIC

BH   Budgells Harbour stock, dominantly alkali gabbro

DEVONIAN OR OLDER

mafic to felsic plutonic rocks: PTW - Twin Lakes Complex: mainly diorite,
granodiorite, lesser granite; PHH - Hodges Hill Granite: mainly granite, lesser
mafic phases PN - New Bay River Pluton: diabase, fine-grained gabbro

Complex: gabbro, dunite, granodiorite. May be in part

VC

LONG PD.

LONG PD.

SEAL BAY

SBB

OP

SBB

SBB

OP

G

SBB

(G)

G

43

VC

VC

VC

SEAL BAY BROOK FAULT

64

85

VC

LP T I

LP T II

LP₀ I

LP C

VC

VC

VC

VC

VC

G

VC

LONG POND FAULT

WEST ARM BROOK

SH p

SH r

PT.
LEAMINGTON

49

BLL

VC

BLL

79

VC

ENIS

AKE

VC

79

SL

VC

695

BLL

FOUR MILE LAKE FAULT

N

BIG
LEWIS
LAKE

SA

FROZEN OCEAN LAKE FAULT

SA

76

BLL

VC

SA

x: mainly diorite,
mainly granite, lesser
grained gabbro

Point Leamington

SLIC

350

POUR MILE LK

LIC

VC

70

NBL r

85

SA

VC

NBL D

82

NANNY BAG LAKE

85

NA

SA

PN

NEW BAY RIVER

75

LEGEND

JURASSIC

[BH] Budgells Harbour stock dominantly alkali gabbro

DEVONIAN OR OLDER

[ ] mafic to felsic plutonic rocks PTW - Twin Lakes Complex: mainly diorite, granodiorite, lesser granite; PHH - Hodges Hill Granite: mainly granite, lesser mafic phases; PN - New Bay River Pluton: diabase, fine-grained gabbro

[SLIC] South Lake Igneous Complex gabbro, diorite, granodiorite. May be in part ophiolitic

MIDDLE ORDOVICIAN

[ ] Shoal Arm Formation: carbonaceous argillite, ferruginous argillite, chert

EARLY TO MIDDLE ORDOVICIAN

WILD BIGHT GROUP

[G] Subvolcanic intrusive rocks, gabbro, diabase

[BLL] Big Lewis Lake basalt; dominantly pillow breccia, lesser pillow lava

[NA] Northern Arm basalt, mainly pillow lava

[BB] Badger Bay basalt, dominantly pillow breccia, lesser pillow lava

[NB] New Bay basalt, pillow lava

[SBH] Seal Bay Head basalt, pillow lava

Side Harbour volcanic unit,
   [SHp] pillow lava
   [SHr] quartz- feldspar porphyritic rhyolite and rhyolitic crystal tuff

Long Pond volcanic unit;
   [LPp] pillow lava
   [LPr] quartz- feldspar porphyritic rhyolite and rhyolitic crystal tuff
   [LPc] green to black argillite, ferruginous argillite and chert

Nanny Bag Lake volcanic unit;
   [NBLp] pillow lava
   [NBLr] quartz- feldspar porphyritic rhyolite and rhyolitic crystal tuff

Glover's Harbour volcanic unit,
   [GHp] pillow lava
   [GHr] quartz- feldspar porphyritic rhyolite and rhyolitic crystal tuff

Indian Cove volcanic unit.
   [ICp] pillow lava
   [ICr] quartz- feldspar porphyritic rhyolite and rhyolitic crystal tuff
   [ICx] felsic to intermediate pyroclastic rocks
   [ICc] green to black argillite, ferruginous argillite and chert

[SBB] Seal Bay Bottom basalt, pillow lava

[VC] Epiclastic rocks; dominantly sandstone and siltstone turbidites, polymictic conglomerate, lesser argillite, chert

FIGURE 2.2: GEOLOGY
EASTERN PARTS OF T

0   1000

METERS

Geology after Dean and Strong (1976) wi

SYMBOLS

Geological contact; defined, appro
Fault; defined, approximate, assum
bedding attitude (tops known); incli
bedding attitude (tops unknown); ir
cleavage; inclined, vertical
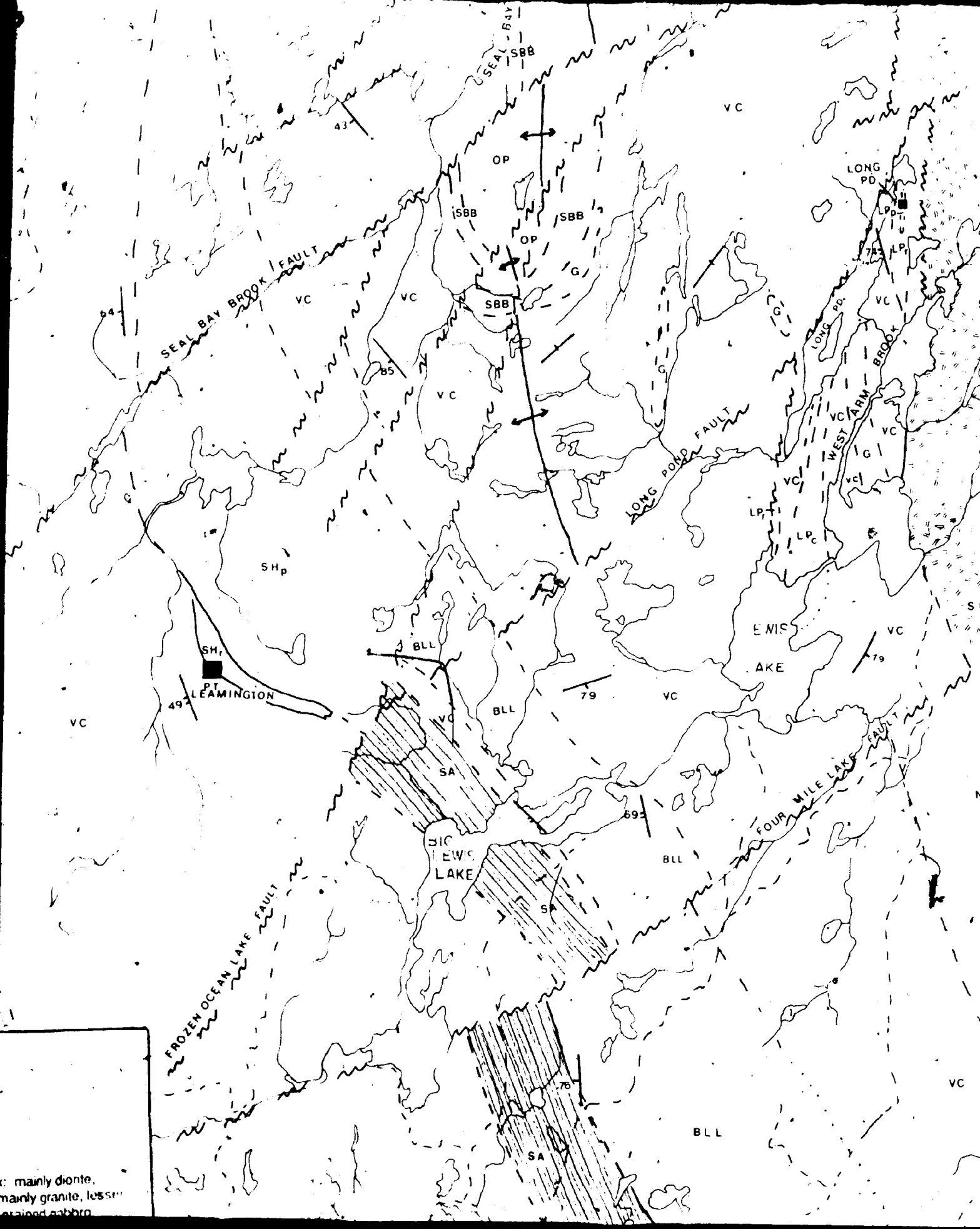fold axis; anticline, syncline
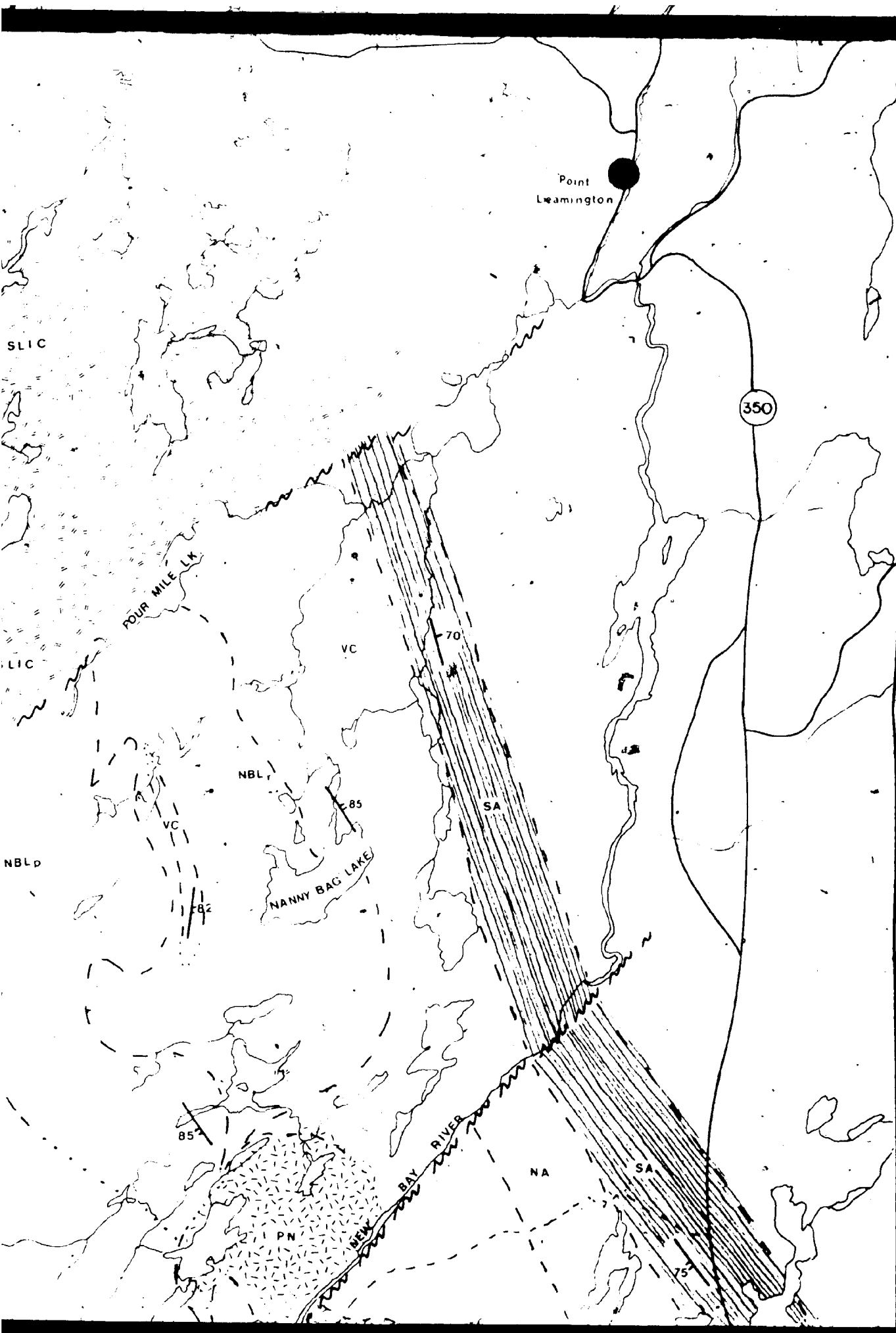volcanogenic sulphide deposit
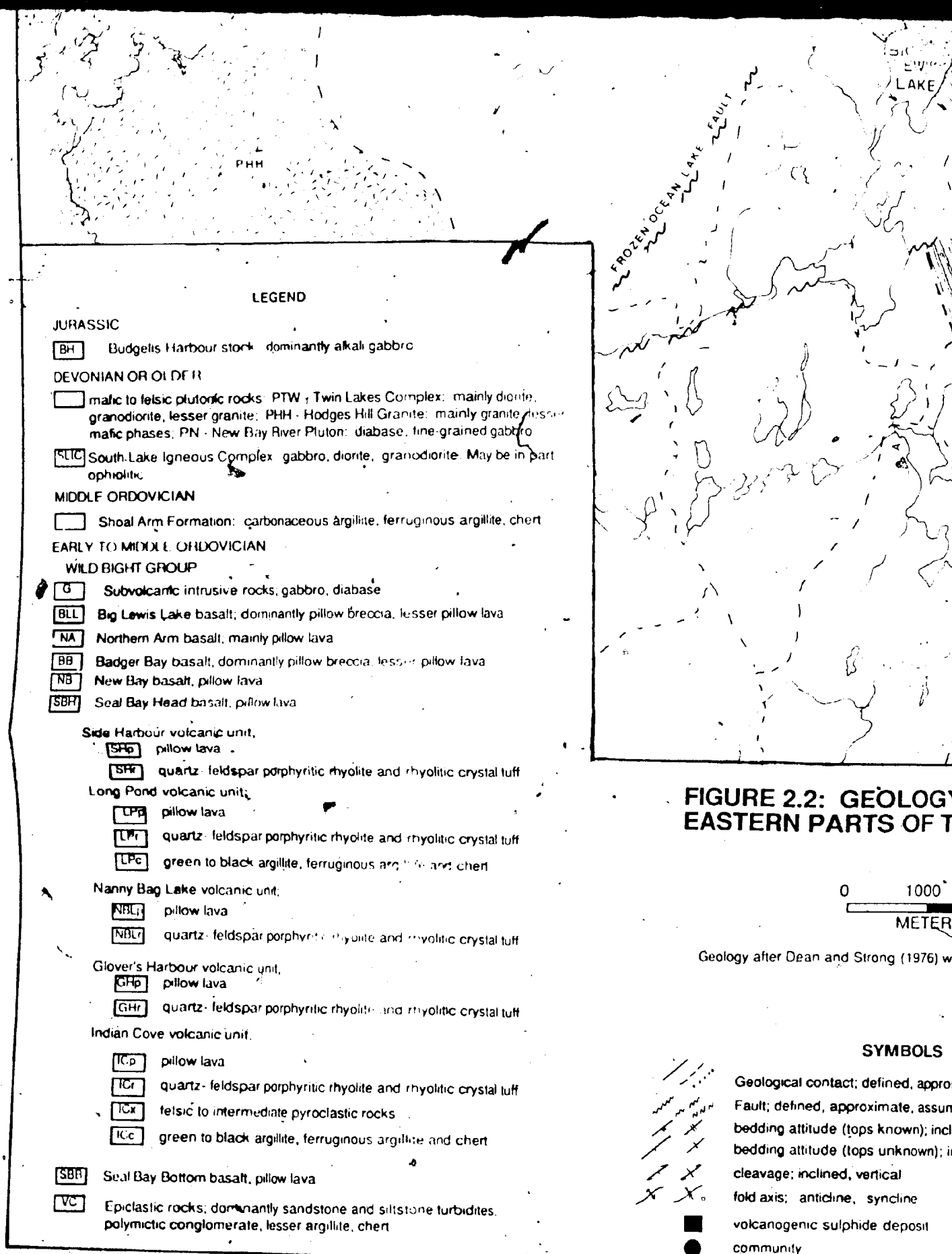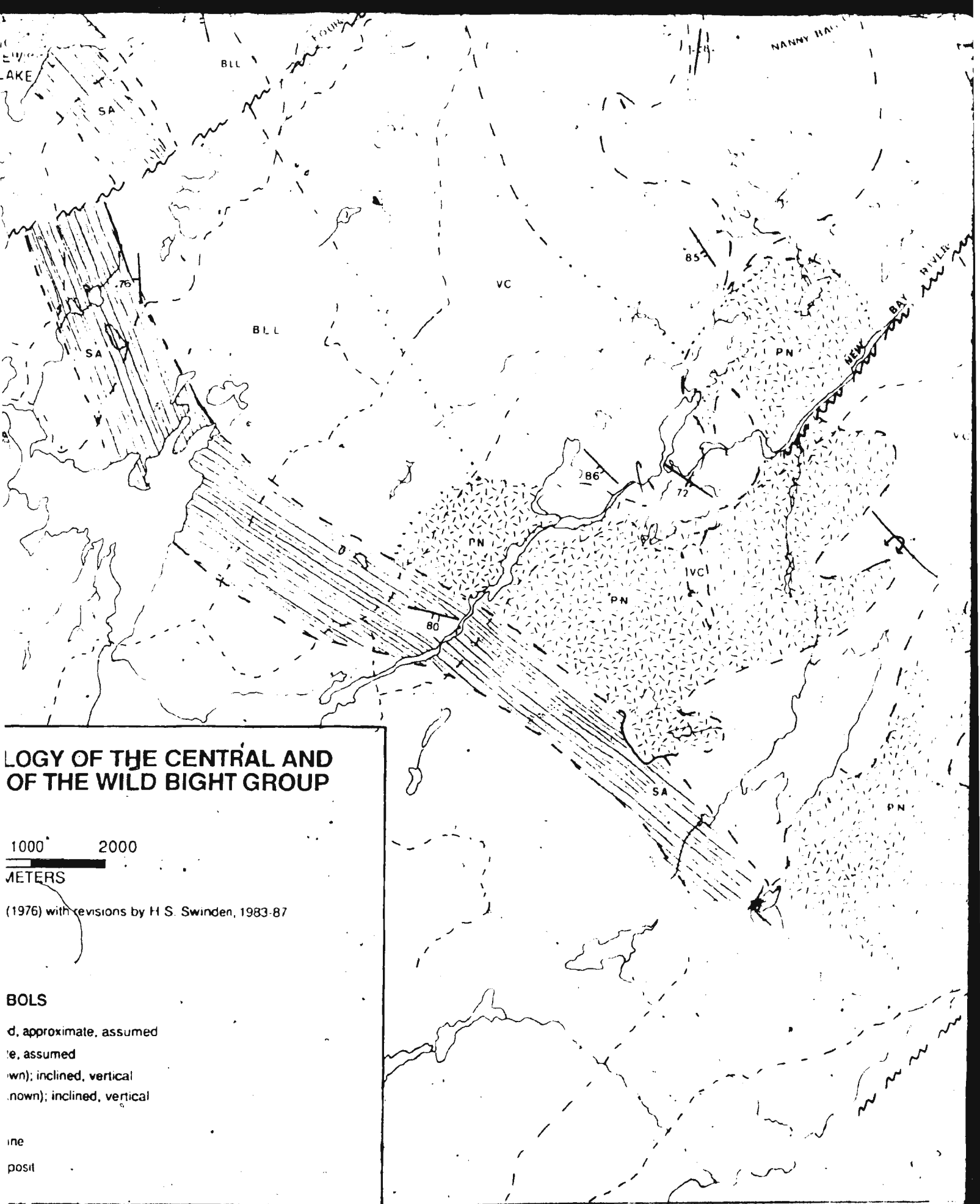community

LOGY OF THE CENTRAL AND
OF THE WILD BIGHT GROUP

1000   2000

ᴍETERS
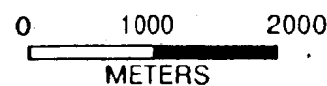
(1976) with revisions by H S. Swinden, 1983-87

BOLS

d, approximate, assumed

te, assumed

wn); inclined, vertical

nown); inclined, vertical

ine

posit

FIGURE 2.2: GEOLOGY OF THE CENTRAL AND EASTERN PARTS OF THE WILD BIGHT GROUP

```
0        1000      2000
   ▭▭▭▭▭▬▬▬▬▬
         METERS
```

Geology after Dean and Strong (1976) with revisions by H.S. Swinden, 1983-87.

SYMBOLS

Geological contact; defined, approximate, assumed
Fault; defined, approximate, assumed
bedding attitude (tops known); inclined, vertical
bedding attitude (tops unknown); inclined, vertical
cleavage; inclined, vertical
fold axis; anticline, syncline
■ volcanogenic sulphide deposit
● community

mainly diorite,
unly granite,
grained gabbro
rite May be in part

us argillite, chert

pillow lava

low lava

litic crystal tuff

olitic crystal tuff

chert

altic crystal tuff

olitic crystal tuff

olitic crystal tuff

and chert

ne turbidites.